frontiers | Research Topics

Protein post-translational modifications in the nervous system: from development to disease and ageing

Edited by
Beatriz Alvarez, Judit Symmank, Miguel Diaz-Hernandez and Geraldine Zimmer-Bensch

Coordinated by
Patricia Franzka

Published in
Frontiers in Molecular Neuroscience

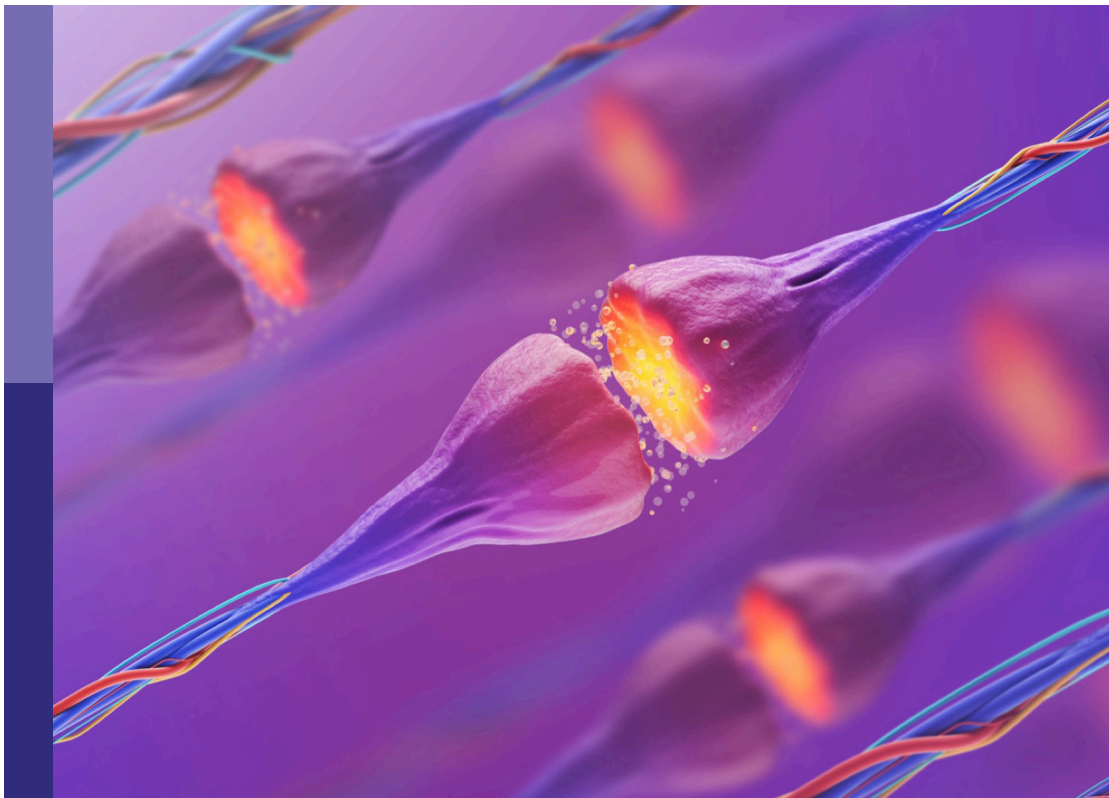

ISSN 1664-8714
ISBN 978-2-8325-5619-1
DOI 10.3389/978-2-8325-5619-1

About Frontiers

Frontiers is more than just an open access publisher of scholarly articles: it is a pioneering approach to the world of academia, radically improving the way scholarly research is managed. The grand vision of Frontiers is a world where all people have an equal opportunity to seek, share and generate knowledge. Frontiers provides immediate and permanent online open access to all its publications, but this alone is not enough to realize our grand goals.

Frontiers journal series

The Frontiers journal series is a multi-tier and interdisciplinary set of open-access, online journals, promising a paradigm shift from the current review, selection and dissemination processes in academic publishing. All Frontiers journals are driven by researchers for researchers; therefore, they constitute a service to the scholarly community. At the same time, the *Frontiers journal series* operates on a revolutionary invention, the tiered publishing system, initially addressing specific communities of scholars, and gradually climbing up to broader public understanding, thus serving the interests of the lay society, too.

Dedication to quality

Each Frontiers article is a landmark of the highest quality, thanks to genuinely collaborative interactions between authors and review editors, who include some of the world's best academicians. Research must be certified by peers before entering a stream of knowledge that may eventually reach the public - and shape society; therefore, Frontiers only applies the most rigorous and unbiased reviews. Frontiers revolutionizes research publishing by freely delivering the most outstanding research, evaluated with no bias from both the academic and social point of view. By applying the most advanced information technologies, Frontiers is catapulting scholarly publishing into a new generation.

What are Frontiers Research Topics?

Frontiers Research Topics are very popular trademarks of the *Frontiers journals series*: they are collections of at least ten articles, all centered on a particular subject. With their unique mix of varied contributions from Original Research to Review Articles, Frontiers Research Topics unify the most influential researchers, the latest key findings and historical advances in a hot research area.

Find out more on how to host your own Frontiers Research Topic or contribute to one as an author by contacting the Frontiers editorial office: frontiersin.org/about/contact

Protein post-translational modifications in the nervous system: from development to disease and ageing

Topic editors

Beatriz Alvarez — Complutense University of Madrid, Spain
Judit Symmank — University Hospital Jena, Germany
Miguel Diaz-Hernandez — Complutense University of Madrid, Spain
Geraldine Zimmer-Bensch — RWTH Aachen University, Germany

Topic coordinator

Patricia Franzka — University Hospital Jena, Germany

Citation

Alvarez, B., Symmank, J., Diaz-Hernandez, M., Zimmer-Bensch, G., Franzka, P., eds. (2024). *Protein post-translational modifications in the nervous system: from development to disease and ageing*. Lausanne: Frontiers Media SA.
doi: 10.3389/978-2-8325-5619-1

Table of contents

frontiers | Frontiers in Molecular Neuroscience

TYPE Editorial
PUBLISHED 18 October 2024
DOI 10.3389/fnmol.2024.1501719

OPEN ACCESS

EDITED AND REVIEWED BY
Jean-Marc Taymans,
Institut National de la Santé et de la Recherche Médicale (INSERM), France

*CORRESPONDENCE
Patricia Franzka
✉ Patricia.Franzka@med.uni-jena.de

RECEIVED 25 September 2024
ACCEPTED 01 October 2024
PUBLISHED 18 October 2024

CITATION
Alvarez B, Symmank J, Zimmer-Bensch G, Diaz-Hernandez M and Franzka P (2024) Editorial: Protein post-translational modifications in the nervous system: from development to disease and ageing. *Front. Mol. Neurosci.* 17:1501719. doi: 10.3389/fnmol.2024.1501719

Editorial: Protein post-translational modifications in the nervous system: from development to disease and ageing

Beatriz Alvarez[1,2], Judit Symmank[3], Geraldine Zimmer-Bensch[4], Miguel Diaz-Hernandez[1,2] and Patricia Franzka[5]*

[1]Department of Biochemistry and Molecular Biology, Veterinary School, Complutense University of Madrid, Madrid, Spain, [2]Instituto de Investigación Sanitaria del Hospital Clínico San Carlos (IdISSC), Madrid, Spain, [3]Department of Orthodontics, University Hospital Jena, Jena, Germany, [4]Division of Neuroepigenetics, Institute for Biology II, Rhenish-Westphalian Technical Aachen University (RWTH), Aachen, Germany, [5]Institute of Human Genetics, Jena University Hospital, Friedrich Schiller University, Jena, Germany

KEYWORDS

protein post-translational modifications (PTMs), aging, muscle, brain, development, disease, nervous system

Editorial on the Research Topic
Protein post-translational modifications in the nervous system: from development to disease and ageing

Post-translational modifications (PTMs) increase the functional diversity of the proteome by reversibly or irreversibly modifying proteins during or after their synthesis. Thereby, they contribute to the structural and functional variety of proteins, conveying a complexity to the proteome that is significantly higher than the coding capacity of the genome. Moreover, providing another level of epigenetic regulation, PTMs of histone proteins in particular contribute to the modulation of gene accessibility and specific cell expression profiles. This Frontiers Research Topic entitled "*Protein post-translational modifications in the nervous system: from development to disease and ageing*" has collected 10 contributions from experts giving new insights into our understanding of protein post-translational modifications and their involvement in disease progression, development and aging.

Three articles assessed the neurodegenerative diseases Alzheimer (AD) and Parkinson (PD) as well as key regulators of aging. Varshavskaya et al. investigated how PTMs of β-amyloid (Aβ) may affect AD. In AD, Aβ plaques accumulate within the brain and hence serve as a biomarker for this disorder. The authors provided evidence for phosphorylated $A\beta_{42}$ as well as isomerized $A\beta_{42}$ to cross an *in-vitro* blood-brain barrier more efficiently than unmodified $A\beta_{42}$, and reported a different mechanism of transport. These findings could be significant for understanding AD pathogenesis and treatment, and may prove valuable in the search for biomarkers. Jonischkies et al. stressed the nuclear DBF2-related (NDR) family of serine-threonine AGC kinases as essential regulators of aging by underlining their functions, such as autophagy and inflammatory cytokine regulation, nutrient, AMPK or insulin signaling, and dysfunctions in the context of aging. Luo et al. highlighted recent findings on major PTMs, such

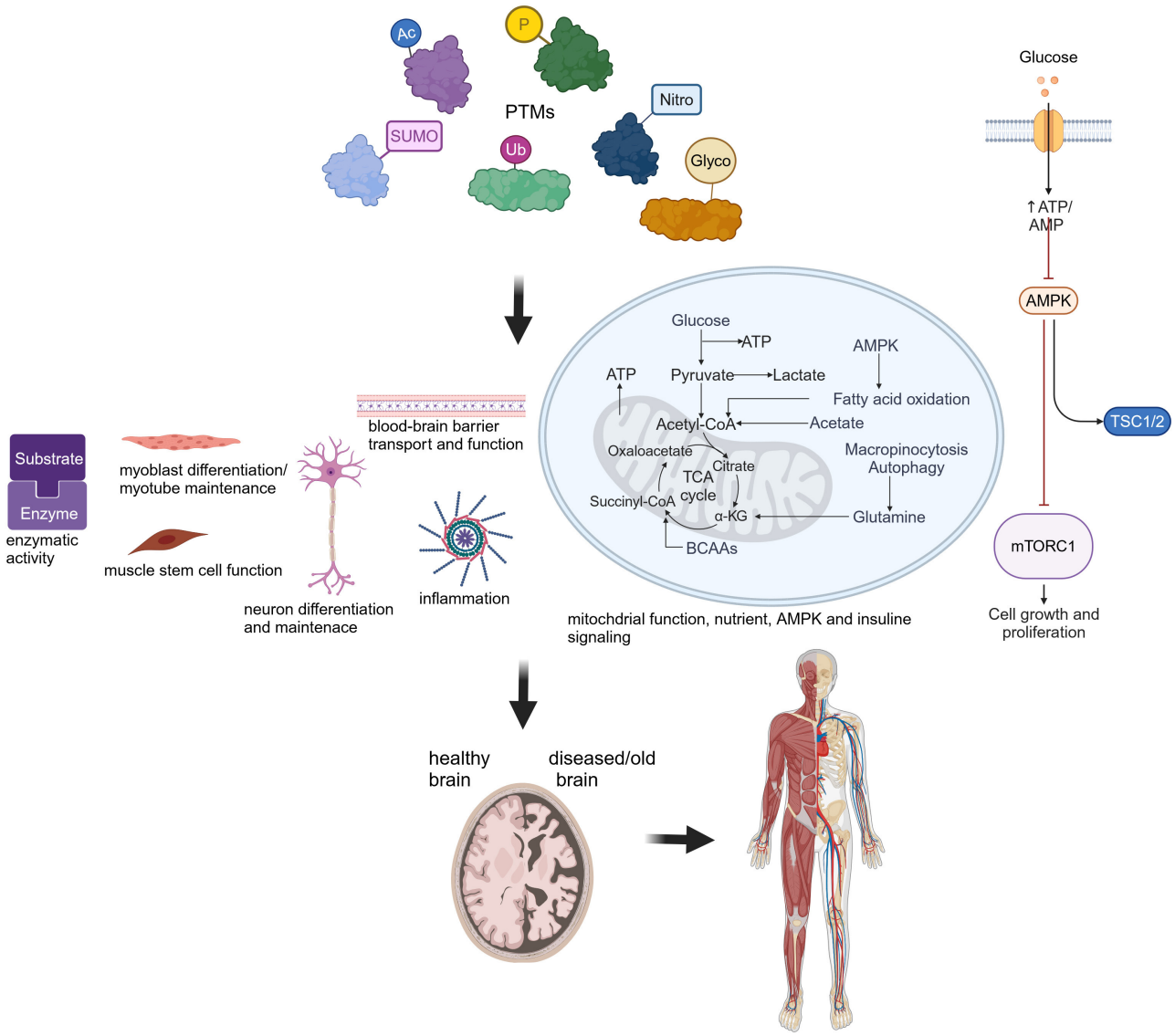

GRAPHICAL ABSTRACT
PTMs are crucial for biological processes contributing to healthy organ function. Protein post-translational modifications (PTMs), such as phosphorylation (P), acetylation (Ac), SUMOylation (SUMO), S-nitrosylation (Nitro), ubiquitination (Ub) and glycosylation (Glyco), affect a wide range of cellular and biological functions as depicted in this cartoon. Perturbations lead to severe consequences for the normal function of the brain and other organs, such as muscle. Created in BioRender. Hübner (2024) BioRender.com/j49w898.

as ubiquitination, phosphorylation, SUMOylation, acetylation, or S-nitrosylation, on mitochondrial dysfunction, a central factor in PD pathogenesis. Moreover, they discussed the potential of proteins harboring PTM sites, such as α-synuclein or VPS35, as biomarkers for PD.

In agreement with mitochondrial changes upon PTM alterations, Liu et al. showed that chronic intermittent hypoxia (CHI) alters hippocampal protein acetylation in mice. The majority of the affected proteins were involved in mitochondrial processes including oxidative phosphorylation, and the tricarboxylic acid (TCA) cycle. Mice under CHI treatment showed cognitive impairment, hippocampal lesions, glial cell activation, inhibited neurogenesis and induced inflammation.

Similarly, hippocampal lesions, plaques, and astrocytic gliosis are observed in prion disease. Bizingre et al. discussed recent findings on the impact of altered PTMs on the prion protein (PrPC), its function, and its conversion into the pathogenic variant. They also explored prion-related downstream factors as potential drug targets.

Two articles assessed the role of ubiquitination for protein function and stability in the context of neuronal development. Day et al. revealed that the Anaphase Promoting Complex (APC/C), an E3 ubiquitin ligase, regulates primary neurite formation and protein levels of the deubiquitinase ubiquitin specific peptidase 1 (USP1). Notably, SUMOylation of APC/C did not affect USP1 levels and neuron morphology.

Franzka et al. assessed ubiquitination of GDP-mannose pyrophosphorylase B (GMPPB). GMPPB is important for generating GDP-mannose, which serves as a mannose donor for glycosylation. The authors showed that ubiquitination of GMPPB neither affects its stability nor its interaction with GMPPA, but modulates its enzymatic activity. Moreover, they disclosed that patient mutations could alter GMPPB ubiquitination. Thus, ubiquitination provides another level to regulate GMPPB activity and mannosylation. Notably, loss of GMPPB results in embryonic lethality as shown by Schurig et al.. Knockdown of GMPPB disrupted myoblast differentiation leading to myotube degeneration, and impaired neuron-like differentiation in N2A cells. In accordance, the authors reported that GMPPB protein abundance increased during brain and skeletal muscle development, which was accompanied by an increase in overall protein mannosylation. Another protein implicated in glycosylation disorders is the Inositol polyphosphate 5-phosphatase K (INPP5K), a phosphatase of phosphoinositides (PIs). Manzolillo et al. demonstrated that INPP5K expression increases during brain development, and its knockdown impaired neuronal-like differentiation of N2A cells, while disrupting protein glycosylation.

The final article in this Research Topic, by Majchrzak et al., explored the interactions between muscle stem cells and their immediate niche, the regulatory role of post-translational modifications (PTMs), and how these factors influence quiescence, activation, and self-renewal, particularly in the context of aging and disease.

In summary, this Research Topic highlighted the critical role of PTMs for nervous system and muscle function, as well as their interconnection during development, disease and aging.

Author contributions

BA: Writing – original draft, Writing – review & editing. JS: Writing – original draft, Writing – review & editing. GZ-B: Writing – original draft, Writing – review & editing. MD-H: Writing – original draft, Writing – review & editing. PF: Conceptualization, Visualization, Writing – original draft, Writing – review & editing.

Conflict of interest

The authors declare that the research was conducted in the absence of any commercial or financial relationships that could be construed as a potential conflict of interest.

The author(s) declared that they were an editorial board member of Frontiers, at the time of submission. This had no impact on the peer review process and the final decision.

Publisher's note

frontiers | Frontiers in Molecular Neuroscience

TYPE Review
PUBLISHED 11 January 2024
DOI 10.3389/fnmol.2023.1329554

OPEN ACCESS

EDITED BY
Judit Symmank,
University Hospital Jena, Germany

REVIEWED BY
Claudia Crosio,
University of Sassari, Italy
Mariaelena Repici,
Aston University, United Kingdom

*CORRESPONDENCE
Zhuohua Zhang
✉ zhangzhuohua@sklmg.edu.cn
Danling Wang
✉ danlingwang@usc.edu.cn

RECEIVED 29 October 2023
ACCEPTED 21 December 2023
PUBLISHED 11 January 2024

CITATION
Luo S, Wang D and Zhang Z (2024) Post-translational modification and mitochondrial function in Parkinson's disease.
Front. Mol. Neurosci. 16:1329554.
doi: 10.3389/fnmol.2023.1329554

Post-translational modification and mitochondrial function in Parkinson's disease

Shishi Luo[1,2,3], Danling Wang[1,2,3]* and Zhuohua Zhang[1,2,4]*

[1]Institute for Future Sciences, Hengyang Medical School, University of South China, Hengyang, Hunan, China, [2]Key Laboratory of Rare Pediatric Diseases, Ministry of Education, Hengyang, Hunan, China, [3]The Affiliated Changsha Central Hospital, Hengyang Medical School, University of South China, Changsha, Hunan, China, [4]Institute of Molecular Precision Medicine, Xiangya Hospital, Key Laboratory of Molecular Precision Medicine of Hunan Province and Center for Medical Genetics, Hunan Key Laboratory of Medical Genetics, Central South University, Changsha, Hunan, China

Parkinson's disease (PD) is the second most common neurodegenerative disease with currently no cure. Most PD cases are sporadic, and about 5–10% of PD cases present a monogenic inheritance pattern. Mutations in more than 20 genes are associated with genetic forms of PD. Mitochondrial dysfunction is considered a prominent player in PD pathogenesis. Post-translational modifications (PTMs) allow rapid switching of protein functions and therefore impact various cellular functions including those related to mitochondria. Among the PD-associated genes, *Parkin*, *PINK1*, and *LRRK2* encode enzymes that directly involved in catalyzing PTM modifications of target proteins, while others like α-synuclein, FBXO7, HTRA2, VPS35, CHCHD2, and DJ-1, undergo substantial PTM modification, subsequently altering mitochondrial functions. Here, we summarize recent findings on major PTMs associated with PD-related proteins, as enzymes or substrates, that are shown to regulate important mitochondrial functions and discuss their involvement in PD pathogenesis. We will further highlight the significance of PTM-regulated mitochondrial functions in understanding PD etiology. Furthermore, we emphasize the potential for developing important biomarkers for PD through extensive research into PTMs.

KEYWORDS

Parkinson's disease, post-translational modification (PTM), mitochondrial function, ubiquitination, phosphorylation, acetylation, SUMOylation, s-nitrosylation

1 Introduction

Parkinson's disease (PD) is the most common neurodegenerative movement disease, affecting more than 10 million people worldwide (Kalia and Lang, 2015). Pathologically, PD is characterized by the progressive loss of dopaminergic (DA) neurons in the substantia nigra pars compacta (SNpc) and the accumulation of aggregated α-synuclein in the form of intracellular inclusion called Lewy Body (LB) (Tanner, 1992). The manifestations of PD are chronic and progressive, with the main symptoms involving movement dysfunctions such as tremor, tonicity, bradykinesia, and postural instability. Many patients also experience prodromal symptoms, including non-motor disturbances such as constipation, hyposmia, and mood disorders (Martinez-Martin et al., 2007; Lajoie et al., 2021). Currently, there is

no cure for PD. The available treatments only alleviate the movement symptoms with little effects on disease progression.

Most PD cases are sporadic, or idiopathic, with age and environmental exposures (such as pesticides, herbicides, heavy metal, and head injury) being the main known risk factors (Goldman, 2014; Ascherio and Schwarzschild, 2016). About 15% PD cases have a familial history, and about 5–10% of PD patients present a monogenic inheritance pattern (Hernandez et al., 2016). Mutations in at least 20 genes are identified to be linked with familiar PD (**Table 1**). From which, dominantly associated genes such as *SNCA* (α-*synuclein*), *LRRK2*, and *VPS35*, as well as recessively associated genes like *PRKN* (*Parkin*), *DJ-1*, *GBA*, *PINK1*, *ATP13A2*, and *FBXO7*, are identified (Polymeropoulos et al., 1997; Kitada et al., 1998; Bonifati et al., 2003; Lwin et al., 2004; Valente et al., 2004; Gilks et al., 2005; Ramirez et al., 2006; Di Fonzo et al., 2009; Vilarino-Guell et al., 2011; Funayama et al., 2015). More than additional 90 genetic risk loci are shown to be associated with idiopathic PD (Bekris et al., 2010; Nalls et al., 2019). Individuals with genetic changes of those genes likely predispose to PD.

Human genetics have significantly contributed to our understanding of the molecular mechanisms of PD pathogenesis. Several key pathways, including those related to protein misfolding and aggregation, the ubiquitin-proteasomal system, autophagy, mitochondrial dysfunction, lysosomal abnormality, and vesicle trafficking, are revealed to PD (Henchcliffe and Beal, 2008; Meredith et al., 2009; Ebrahimi-Fakhari et al., 2012; Hunn et al., 2015; De Virgilio et al., 2016; Blumenreich et al., 2020). Of particular, mitochondrial dysfunction has long been implied in PD pathogenesis. Methyl-4-phenyl-1,2,3,4-tetrahydropyridine (MPTP), a mitochondrial complex I inhibitor, induces Parkinsonism in both human and animals (Langston et al., 1983). Multiple pesticides and herbicides are shown to induce parkinsonism via mitochondria-mediated mechanisms (Chen et al., 2017). A number of PD pathogenic monogenetic genes either encode mitochondrial proteins or regulate mitochondrial functions (Nicoletti et al., 2021). Genome-wide association studies (GWAS) also indicate that mitochondria-related processes are involved in both familiar and sporadic forms of PD (Billingsley et al., 2019).

Post-translational modifications (PTMs) refer to covalent chemical alterations of a protein after its synthesis. More than 400 types of PTMs are identified (Khoury et al., 2011). Some widely studied PTMs include phosphorylation, ubiquitination, methylation, acetylation, SUMOylation, etc. PTMs increase functional diversity of the modified protein, therefore modulate almost every aspect of cellular processes, including mitochondrial functions (Karve and Cheema, 2011; Stram and Payne, 2016). Among the PD-associated genes, *Parkin*, *PINK1*, and *LRRK2* encode enzymes that directly catalyze the PTM of target proteins while they are PTM modified themselves (Trempe et al., 2013; Eiyama and Okamoto, 2015; Taylor and Alessi, 2020). PD-related proteins like α-synuclein, FBXO7, HTRA2, VPS35, CHCHD2, and DJ-1 either participate in or are heavily modified by PTMs (Mitsumoto et al., 2001; Plun-Favreau et al., 2007; Kang et al., 2012; Burchell et al., 2013; Tang et al., 2015; Meng et al., 2017). In this review, we aim to summarize the recent findings on major PTMs associated with PD-related proteins, either as enzymes or substrates, that have been shown to play significant roles in various mitochondrial functions, hence, PD pathogenesis.

2 Ubiquitination: regulating mitochondrial functions in Parkinson's disease

Ubiquitination is a PTM characterized by the covalent binding of ubiquitin (Ub) molecule to a specific target protein. This essential PTM primarily determines protein stability by marking the target protein for proteasomal degradation. However, it has also been reported to be able to enhance protein stability and regulate protein activities. Ubiquitination plays an essential role in maintaining normal mitochondrial functions. Dysregulated ubiquitination can cause mitochondrial dysfunctions. While the accumulation of misfolded and ubiquitinated α-synuclein has long been recognized as the toxic factor in PD brain pathology, evidence implicating the direct involvement of ubiquitination dysregulation in mitochondrial dysfunction and thus PD pathology emerged from the intensive study of PD associated Parkin and PINK1. As non-mitochondrial proteins, other PD-related proteins, such as VPS35, FBXO7, and LRRKs, are found to regulate mitochondrial functions by modifying ubiquitination process (**Table 2**).

2.1 Parkin-mediated ubiquitination and mitophagy

Mutations in *Parkin* gene are the most common genetic cause of juvenile-onset and early-onset PD (EOPD), defined by the appearance of PD symptoms in teens and before the age of 60 (Kitada et al., 1998). The *Parkin* gene encodes Parkin, an E3 ubiquitin ligase belonging to the RING-between-RING (RBR) family, which accepts Ub from the E2 enzyme and transfers it onto the target protein (Imai et al., 2000; Shimura et al., 2000; Zhang et al., 2000). By ubiquitinating various substrates, Parkin plays a central role in maintaining mitochondrial function and homeostasis (Palacino et al., 2004; Narendra et al., 2008).

The groundbreaking study illustrating Parkin's role in mitophagy, the biological pathway that selectively eliminates defective mitochondria, was conducted by the Youle laboratory (Narendra et al., 2008). Later studies collectively reveal that Parkin-mediated mitophagy consists of three major steps: (1) initiation, the activation and translocation of Parkin onto the damaged mitochondria (Narendra et al., 2008; Matsuda et al., 2010); (2) priming, the cascade ubiquitination of various targets on the outer mitochondrial membrane (OMM) by Parkin (Tanaka et al., 2010; Chan et al., 2011; Sarraf et al., 2013); and (3) finishing, the lysosomal sequestration and degradation of heavily ubiquitinated mitochondria (Karbowski and Youle, 2011). Evidence suggests that the recruitment of Parkin to the damaged mitochondria is mediated by the binding of Parkin to the mitochondria-situated phosphorylated-Ub (phospho-Ub, pUb), which is formed by the kinase activity of PINK1 (PTEN-induced putative kinase 1) (Xiong et al., 2009; Kane et al., 2014; Sauve et al., 2015). During the priming stage, Parkin ubiquitinates multiple proteins, showing a preference for OMM proteins including Parkin itself, MFN1 and 2 (mitofusin 1 and 2), MIRO1 and 2 (mitochondrial Rho GTPase 1 and 2), VDAC1-3 (voltage-dependent anion channel 1–3), CISD1 (CDGSH iron-sulfur domain 1), and TOM 20, 40, and

TABLE 1 Genes associated with familiar PD.

	Gene	PARK locus	Alternative names	Inheritance	Type of parkinsonism
Widely validated	*SNCA*	*PARK1*, *PARK4*	*NCAP*	AD	Early/late onset, atypical
	PRKN	*PARK2*	*Parkin*	AR	Early onset, typical
	PINK1	*PARK6*	*BRPK*	AR	Early onset, typical
	DJ-1	*PARK7*	*GATD2*	AR	Early onset, typical
	LRRK2	*PARK8*	*ROCO2*, *RIPK7*	AD	Late onset, typical
	ATP13A2	*PARK9*	*HSA9947*, *CLN12*	AR	Juvenile onset, atypical
	PLA2G6	*PARK14*	*PNPLA9*, *IPLA2*	AR	Juvenile onset, atypical
	FBXO7	*PARK15*	*FBX7*	AR	Early onset, atypical
	VPS35	*PARK17*	*MEM3*	AD	Late onset, typical
	DNAJC6	*PARK19*	*KIAA0473*, *DJC6*	AR	Juvenile onset, atypical
	SYNJ1	*PARK20*	*INPP5G*	AR	Juvenile onset, atypical
	DNAJC13	*PARK21*	*KIAA0678*, *RME8*	AD	Late onset, typical
	VPS13C	*PARK23*	*KIAA1421*, *BLTP5C*	AR	Early onset, atypical
	POLG	-	*POLG1*, *POLGA*	AD	Early onset, atypical
Less validated	*UCHL1*	*PARK5*	*PGP9.5*	AD	Late onset, typical
	GIGYF2	*PARK11*	*TNRC15*, *PERQ2*, *GYF2*	AD	Late onset, typical
	HTRA2	*PARK13*	*OMI*	AD	Late onset, typical
	EIF4G1	*PARK18*	*P220*	AD	Late onset, typical
	CHCHD2	*PARK22*	*C7orf17*, *MIX17B*	AD	Late onset, typical
	PSAP	*PARK24*	*GLBA*, *SAP1*	AD	Late onset, typical

AD, autosomal dominant; AR, autosomal recessive; juvenile-onset, clinical symptom starting before 21 years; early-onset, clinical symptom starting between 20 and 60 years; late-onset, clinical symptom starting after 60 years; typical PD, PD cases presenting classical motor symptoms, with slow progression and good response to dopaminergic therapeutics; atypical PD, PD cases featuring prominent additional neurological signs, such as dementia, spasticity, dystonia, with or without abnormal ocular movements (Cherian and Vijayaraghavan, 2023); "-" means no answer.

70 (translocases of the outer membrane 20, 40, and 70) (Gegg et al., 2010; Lazarou et al., 2012; Sun et al., 2012; Ordureau et al., 2015; Liu et al., 2018; Lopez-Domenech et al., 2018). Ubiquitination of OMM proteins further promotes the recruitment of Ub-binding autophagy receptors such as P62/SQSTM1 (sequestosome 1), OPTN (optineurin), NDP52/CALCOCO2 (calcium-binding and coiled-coil domain-containing protein 2), and NBR1 (neighbor of Brca1). In turn, these receptors elicit the targeting of the damaged mitochondria to LC3-positive phagophores for lysosomal degradation (**Figure 1**; Heo et al., 2015; Ordureau et al., 2018; Padman et al., 2019).

Unlike many other E3 ligases that exhibit stringent substrate specificity, Parkin appears to be loose on substrate selectivity. In addition to the well-studied Parkin substrates, recent proteomic analyses have revealed that Parkin ubiquitinates an extensive large number of proteins (Rose et al., 2016; Martinez et al., 2017). After treatment with the mitochondrial uncoupler carbonyl cyanide m-chlorophenylhydrazone (CCCP) for extended hours, most OMM proteins are ubiquitinated without necessarily having functional consequences (Chan et al., 2011; Sarraf et al., 2013). In general, Parkin is activated by PINK1-mediated phosphorylation of its N-terminal ubiquitin-like domain. With the help of PINK1, ubiquitination on the OMM by Parkin leads to more pUb and consecutively greater Parkin recruitment and activation, creating a feed-forward loop to amplify the Parkin-mediated ubiquitination to the maximum (Ordureau et al., 2014). Using artificial mitochondria-targeted proteins, Koyano et al. (2019) have found that the substrate specificity of Parkin is not determined by the amino-acid sequence within the substrate, but rather by the presence of pUb on the target protein (Durcan et al., 2012).

Proteomic analyses of purified mitochondria have revealed that Parkin produces a mixture of canonical and non-canonical Ub chains on damaged mitochondria. In general, Ub chains can form through any of the seven lysine (K6, K11, K27, K29, K33, K48, and K63) and the N-terminal methionine (Met1) (Kulathu and Komander, 2012; Akutsu et al., 2016). *In vitro*, Parkin ubiquitinates mitochondrial proteins with K6-, K11-, K48-, and K63-linked Ub chains to signal damaged mitochondria for mitophagy (Ordureau et al., 2014). Canonical K48-linked Ub chains are crucial for the proteasomal targeting and degradation of modified proteins (Manohar et al., 2019), while K63-linked Ub chains activate the autophagic machinery through recruiting autophagy adaptors like HDAC6 (histone deacetylase 6) and P62 (Seibenhener et al., 2004; Olzmann et al., 2007). Intriguingly, Parkin catalyzes certain degrees of K6- and K11-linked Ub chains on OMM proteins. Activity of Parkin-mediated mitophagy is impaired when either K6 or K11 Ub-linkage was inhibited by the expression of mutant Ub K6R or K11R, suggesting that K6- and K11-linked Ub chains positively regulate the mitophagy process (Durcan et al., 2014; Cunningham et al., 2015). Therefore, Parkin is considered a rather promiscuous E3 ligase that, once activated, ubiquitinates a broad range of proteins with a wide spectrum of Ub chains and amplifies the Ub signals via

TABLE 2 Ubiquitination of PD-related proteins and mitochondrial dysfunction.

PD-related protein		Enzyme	Substrate	Regulated mitochondrial function	References
Parkin	Directly involved in PTM enzymatic reaction	Parkin	Parkin	Activates mitophagy	Zhang et al., 2000
		Parkin	OMM proteins	Activates mitophagy	Gegg et al., 2010; Lazarou et al., 2012; Sun et al., 2012; Ordureau et al., 2015; Liu et al., 2018; Lopez-Domenech et al., 2018
		Parkin	Tollip	Promotes MDVs transport	Ryan et al., 2020
		Parkin	SNX9	Inhibits immune-related-MDVs formation	Matheoud et al., 2016
		Parkin	DRP1	Inhibits mitochondrial fission	Wang H. et al., 2011
		Parkin	MFN1	Inhibits mitochondrial fusion	Gegg et al., 2010
		Parkin	MFN2	Inhibits mitochondrial fusion, increases mitochondria-ER contacts	Gegg et al., 2010; Basso et al., 2018
		Parkin	PARIS	Promotes mitochondrial biogenesis	Siddiqui et al., 2016
		Parkin	MICU1	Maintains calcium homeostasis	Matteucci et al., 2018
		Parkin	MIRO	Increases mitochondria-ER contacts	Wang X. et al., 2011
α-synuclein		SIAH-1	α-synuclein	Increases cytochrome c release	Lee et al., 2008
FBXO7		FBXO7	PINK1	Increases mitophagy	Liu et al., 2020
VPS35	Indirectly involved in PTM enzymatic reaction	MULAN	MFN2	Promotes mitochondrial fusion	Tang et al., 2015
LRRK2		PERK	MARCH5, MULAN, Parkin	Inhibits mitochondria-ER contacts	Toyofuku et al., 2020

Tollip, the endosomal adaptor Toll interacting protein; SNX9, sorting nexin 9; DRP1, dynamin-related protein 1; MFN1 and 2, mitofusin 1 and 2; PARIS, Parkin-interacting substrate; MICU1, mitochondrial calcium uptake 1; MIRO, mitochondrial Rho GTPase; PINK1, PTEN induced putative kinase 1; MULAN, mitochondrial E3 ubiquitin protein ligase 1; LRRK2, leucine-rich repeat kinase 2; MARCH5, membrane associated Ring-CH-type finger 5; ER, endoplasmic reticulum; MDV, mitochondrial-derived vesicle.

a positive-feedback manner to maximally ubiquitinated proteins on the damaged mitochondria.

Over 200 missense variants are identified in the *Parkin* gene, but only a small fraction has been clearly annotated to be pathogenic. Integrating clinical evidence with *in vitro* mitophagy activity, Yi et al. (2019) has conducted a systematic analysis of 51 Parkin variants, finding a correlation between the degree of mitophagy defect and the level of clinical manifestation. Among them, 13 Parkin variants are classified as pathogenic or likely pathogenic that all display severe mitophagy defects. Those variants designated as non-pathogenic show normal or near-normal mitophagy function (Yi et al., 2019). Likewise, Broadway et al. (2022) have investigated 10 rare Parkin mutants and found 7 with impaired mitophagy activity. These studies suggest that Parkin mediated mitophagy plays important roles in PD pathogenesis.

2.2 Parkin-mediated ubiquitination and mitochondrial-derived vesicles

In addition to mitophagy, an alternative mitochondrial quality control mechanism is via mitochondrial-derived vesicles (MDVs) (Cadete et al., 2016). With this, mitochondria transfer their defective mitochondrial contents to destination organelles, such as lysosomes, peroxisomes, and multivesicular bodies, for degradation via releasing vesicles with 70–150 nm in diameter (Futter et al., 1996; Soubannier et al., 2012a; Vasam et al., 2021; Rosina et al., 2022). Depending on the source of the mitochondrial stress, MDVs derive from the inner mitochondrial membrane (IMM) as a double-membrane structure or from the OMM as a single-membrane vesicle (Konig et al., 2021; Popov, 2022; Heyn et al., 2023). Whether Parkin plays a preferential role in the formation of MDVs remains to be elucidated. *In vitro*, the formation of MDVs carrying inner membrane marker PDH (pyruvate dehydrogenase) is dependent on Parkin activity (McLelland et al., 2014; Ge et al., 2020). Targeting of Parkin-dependent MDVs to the later endo-lysosomal compartments is mediated by the ternary SNARE protein complex composed of STX17 (syntaxin 17), SNAP29 (synaptosome associated protein 29), and VAMP7 (vesicle-associated membrane protein 7) (Soubannier et al., 2012a; Juhasz, 2016; McLelland et al., 2016). Unlike those PDH-positive MDVs, the presence of MDVs containing only OMM marker like Tom20 is not affected by loss-of-function Parkin mutants T240R or C431S, indicating the independence of Parkin E3 ligase activity (Soubannier et al., 2012b). However, Parkin was found to coordinate with Tollip (the endosomal adaptor Toll interacting protein) to facilitate the transport of these single-membrane MDVs to the endo-lysosomal compartment, with the help of the STX17-SNAP29-VAMP7 SNARE complex (**Figure 1**; Ryan et al., 2020). In contrast, Parkin seems to inhibit the formation of a subtype of MDVs that plays important roles in immune cells related mitochondrial antigen presentation (MitAP) through triggering ubiquitination and proteasomal degradation of SNX9 (sorting nexin 9) (Matheoud et al., 2016). Thus, Parkin-mediated ubiquitination potentially link between mitochondrial dysfunction and neuroinflammation in PD (Sliter et al., 2018). Consistently, Parkin-null mice show

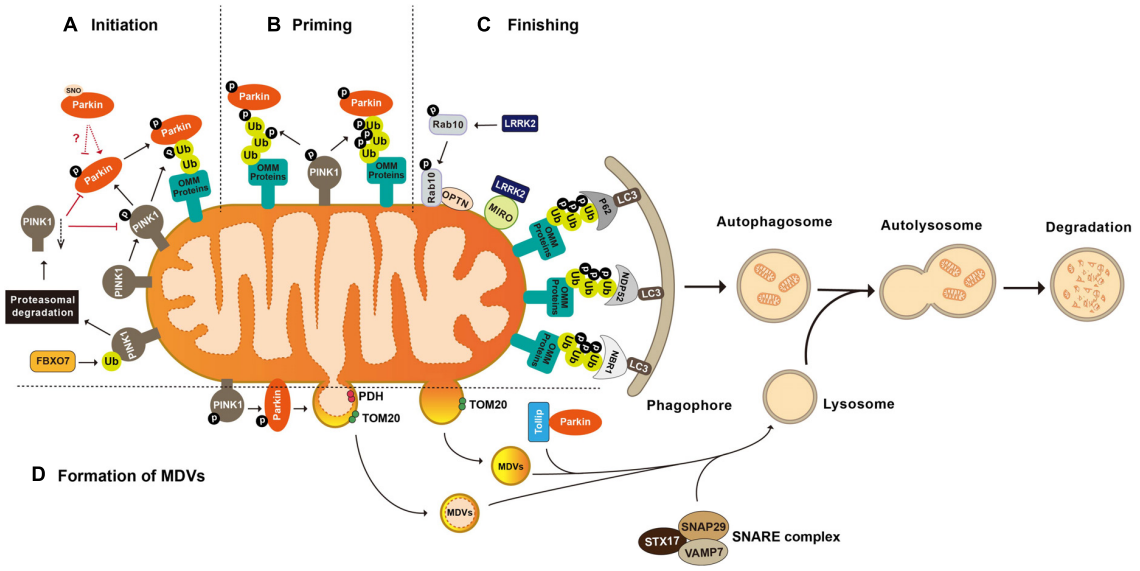

FIGURE 1
Post-translational modifications in the regulation of mitophagy and mitochondrial-derived vesicles formation. **(A)** Initiation of mitophagy. Parkin is activated and translocated onto the damaged mitochondria. PINK1 mediated phosphorylation of Parkin and mitochondria situated Ub is essential for Parkin activation. FBXO7 negatively regulates mitophagy activity by enhancing the ubiquitination of PINK1. **(B)** Priming of mitophagy. After activation, Parkin ubiquitinates a large number of mitochondrial proteins, resulting in increased Ub signal and successively increased pUb signals mediated by PINK1. **(C)** Finishing of mitophagy. Ubiquitination of OMM proteins further promotes the recruitment of Ub binding autophagy receptors such as P62/SQSTM1, OPTN, NDP52/CALCOCO2, and NBR1 to target the damaged mitochondria to LC3 positive phagophores for lysosomal degradation. LRRK2 mediated phosphorylation regulates mitophagy through its substrates MIRO and Rab10. **(D)** Formation of mitochondrial-derived vesicles (MDVs). Parkin mediated ubiquitination and PINK1 mediated phosphorylation are required by the formation of PDH+ MDVs. Parkin and Tollip facilitate the transport of TOM20+ MDVs to the endo lysosomal compartment with the help of the STX17 SNAP29 VAMP7 SNARE complex. FBXO7, F-box protein 7; PINK1, PTEN induced putative kinase 1; Ub, ubiquitin; P62/SQSTM 1, sequestosome 1; NDP52/CALCOCO2, calcium binding and coiled coil domain containing protein 2; NBR1, neighbor of Brca1; OPTN, optineurin; MIRO, mitochondrial Rho GTPase; LRRK2, leucine-rich repeat kinase 2; LC3, microtuble-associated protein light chain 3; PDH, pyruvate dehydrogenase; and TOM20, translocases of the outer membrane 20.

excessive inflammation due to STING-dependent (stimulator-of-interferon-genes dependent) pro-inflammation activity and increased vulnerability to inflammation-induced degeneration (Frank-Cannon et al., 2008; Sliter et al., 2018).

2.3 Parkin-mediated ubiquitination and other mitochondrial functions

2.3.1 Parkin-mediated ubiquitination and mitochondrial dynamics

Mitochondria undergo constant fission-and-fusion in reflection of their functional statuses (Lewis and Lewis, 1914; Chen and Chan, 2017; Kraus et al., 2021). Increased mitochondrial fission results in small and round mitochondria to probably facilitate the mitochondrial trafficking within cells, while enhanced mitochondrial fusion leads to elongated mitochondria for efficient ATP production (Martini and Passos, 2023). Certain mitochondrial damages promote fission activity leading to the separation of depolarized mitochondria to facilitate their later removal by mitophagy or other mitochondrial quality control mechanisms (Han et al., 2020; da Silva Rosa et al., 2021; Cai et al., 2022).

Parkin is responsible for the ubiquitination and proteasomal degradation of several bona fide players in mitochondrial fission-and-fusion pathways, including the fission mediator DRP1 (dynamin-related protein 1) and fusion mediators MFN1 and MFN2 (Narendra et al., 2008; Yamada et al., 2018, 2019; Ham et al., 2020). Parkin interacts with DRP1 through its second RING domain and subsequently ubiquitinates DRP1, leading to its proteasomal degradation. Both the deficiency of Parkin and expression of the PD-associated Parkin mutant C431F inhibit ubiquitination and degradation of DRP1, resulting in mitochondrial fragmentation (**Figure 2**; Lutz et al., 2009; Wang H. et al., 2011). In *Drosophila*, overexpression of DRP1 rescues muscle degeneration and mitochondrial abnormalities in *PINK1*$^{-/-}$ or *Parkin*$^{-/-}$ mutants (Deng et al., 2008). *In vitro*, Parkin also ubiquitinates MFN-1 and MFN-2. Ubiquitination of MFN-1 and MFN-2 is reduced in either cell lines with Parkin deficiency or fibroblasts derived from PD patients harboring *Parkin* mutations (Gegg et al., 2010; Rakovic et al., 2011). In *Drosophila*, accumulated Marf (*Drosophila* homolog of MFN), along with reduced ubiquitinated Marf and increased non-ubiquitinated Marf, is observed in Parkin mutant flies (Poole et al., 2010; Ziviani et al., 2010). Thus, Parkin participates in regulation of mitochondrial dynamics.

2.3.2 Parkin-mediated ubiquitination and mitochondrial biogenesis

Another mechanism cells employ to cope with mitochondrial damage is to generate new mitochondria, a process known as mitochondrial biogenesis (Ivankovic et al., 2016; Popov, 2020). Mitochondrial biogenesis is governed by the master regulator PGC1-α (peroxisome proliferator-activated receptor gamma coactivator 1-alpha). PGC1-α binds and actives nuclear

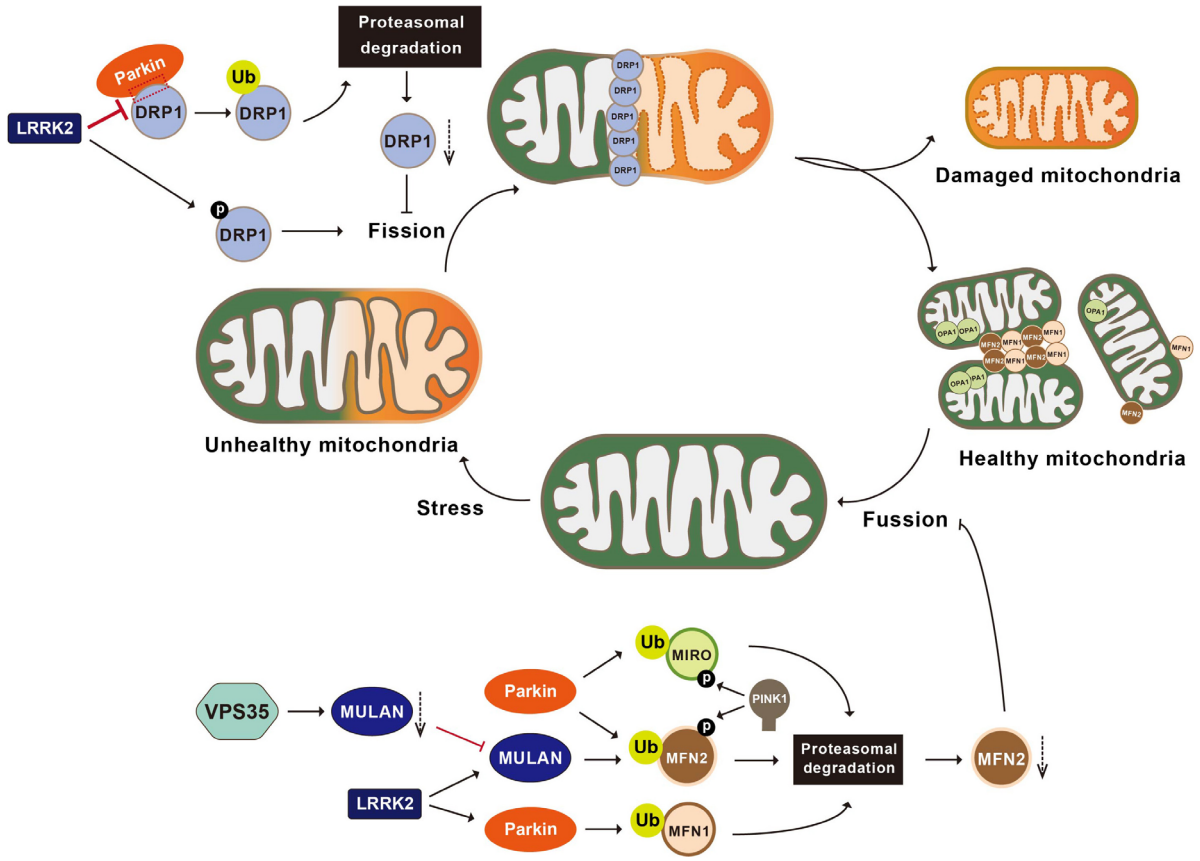

FIGURE 2
Post-translational modifications in the regulation of mitochondrial dynamics. Mitochondria undergo constant fusion (joining two mitochondria together with the help of MFN1, MFN2, and OPA1) and fission (separating one mitochondrion into two mitochondria with the help of DRP1). Parkin ubiquitinates DRP1, leading to the proteasomal degradation of DRP1 and inhibiting mitochondrial fragmentation. LRRK2 phosphorylates DRP1, impairs the interactions between Parkin and DRP1, and activates MULAN and Parkin's E3 ligase activities, therefore regulating mitochondrial fragmentation. VPS35 regulates the degradation of the MULAN, thereby inhibiting MUL1 mediated ubiquitination and degradation of MFN2 and promoting mitochondrial fusion. Parkin ubiquitinates MFN1, MFN2 and MIRO, leading to their degradation via the proteasomal system and inhibiting mitochondrial fusion. PINK1 phosphorylates MIRO and activates Parkin mediated ubiquitination and degradation of MIRO. MFN1, mitofusin 1; MFN2, mitofusin 2; OPA1, optic atrophy 1; LRRK2, leucine-rich repeat kinase 2; VPS35, vacuolar protein sorting 35; MULAN, mitochondrial E3 ubiquitin protein ligase; MIRO, mitochondrial Rho GTPase.

transcription factors NRF-1 and 2 (nuclear respiratory factor 1 and 2) to increase transcription and therefore expression of proteins for mitochondrial biogenesis (Scarpulla, 2008; Li et al., 2011, 2021). PARIS (Parkin-interacting substrate) is a zinc finger protein that binds to and represses PGC-1α. Parkin interacts with PARIS and tags it with Ub chains for proteasomal degradation (Shin et al., 2011; Siddiqui et al., 2015; Stevens et al., 2015; Lee et al., 2017). Parkin deficiency leads to accumulation of PARIS, downregulation of PGC-1α, and selective loss of SNpc DA neurons. All of these are rescued by PGC-1α expression (Shin et al., 2011; Stevens et al., 2015; Siddiqui et al., 2016). These observations suggest that Parkin-mediated ubiquitination plays an important regulatory role in the PGC-1α-mediated mitochondrial biogenesis by ubiquitinating PARIS (**Figure 3**).

2.3.3 Parkin-mediated ubiquitination and calcium homeostasis

Recent studies suggest that Parkin regulates calcium homeostasis by ubiquitinating a range of tethering proteins involved in mitochondria-endoplasmic reticulum contact sites (MERCs), such as MFN1, MFN2, MIRO1, and MICU (**Figure 4**). Parkin in calcium regulation was initially reported by Sandebring et al., 2009. With epidermal growth factor (EGF) stimulation, expression of both PD-associated Parkin mutants (R42P and G328E) or Parkin knockdown results in increased PLCγ1 (phospholipase C gamma1) and elevated basal cytosolic Ca^{2+} levels. These phenotypes are completely reversed with the treatment of PLC-inhibitor neomycin (Sandebring et al., 2009). A later study demonstrates that glutamate excitotoxicity in neuronal cells triggers Parkin accumulation on the ER and MERCs, suggesting a role of Parkin in the mitochondria-ER crosstalk (Van Laar et al., 2015). In Hela cells that do not express endogenous Parkin, overexpression of Parkin, but not the Parkin mutant lacking Ubl domain, enhances ER-mitochondrial tethering and increases agonist-induced Ca^{2+} transients (Cali et al., 2013). Conversely, Parkin knockdown impairs mitochondrial Ca^{2+} transfer and reduces mitochondria-ER contacts, suggesting that Parkin may enhance mitochondria-ER Ca^{2+} transfer by maintaining MERCs (Cali et al., 2013). However, confounding evidences are observed in fibroblasts derived from PD patients carrying *Parkin* mutations

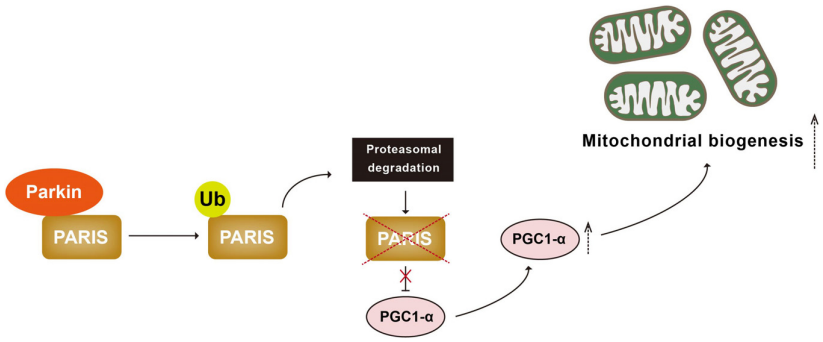

FIGURE 3
Parkin-mediated ubiquitination regulates mitochondrial biogenesis. PARIS binds to and represses PGC 1α, the master regulator of mitochondrial biogenesis. Parkin interacts with and ubiquitinated PARIS, leading to its proteasomal degradation and promoting mitochondrial biogenesis. PARIS, Parkin-interacting substrate; PGC 1α, peroxisome proliferator-activated receptor gamma coactivator 1-alpha.

and in *Parkin*$^{-/-}$ mice. Loss of Parkin results in close proximity between ER and mitochondria, leading to increased mitochondria-ER Ca^{2+} transfer, while overexpression of Parkin could restore the cytosolic Ca^{2+} transient to normal (Gautier et al., 2016).

Mitochondria take up Ca^{2+} through the mitochondrial calcium uniporter (MCU) complex that are composed of four core components, including the pore-forming subunit MCU, gatekeeping subunits MICU1 and 2 (mitochondrial calcium uptake 1 and 2), and the auxiliary subunit EMRE (essential mitochondrial regulator) (Sancak et al., 2013; Raffaello et al., 2013). MICU1 and 2, respectively, act as positive and negative regulators of the MCU complex (Plovanich et al., 2013). Under basal conditions, Parkin ubiquitinates MICU1, leading to its rapid degradation via the proteasomal system. Given that MICU2 stability is strictly dependent on MICU1, Parkin-mediated ubiquitination also indirectly regulates the amount of MICU2 (Matteucci et al., 2018). By maintaining appropriate levels of MICUs, Parkin plays a regulatory role in mitochondrial calcium homeostasis. Additionally, Parkin exerts its effects on ER-mitochondrial tethering via ubiquitinating of MFN2. ER located MFN2 forms a homotypic or heterotypic complex with either mitochondria-located MFN2 or mitochondria-located MFN1, thereby bridging mitochondria and ER (de Brito and Scorrano, 2008). Parkin ubiquitinates MFN2 on K416 in the HR1 domain, which in turn positively affects the physical and functional interactions between mitochondria and ER. Parkin-resistant MFN2 mutant K416R loses the ability to restore the decreased mitochondria-ER interactions in Parkin deficient cells and fibroblasts carrying PD-associated Parkin mutants (Basso et al., 2018). MIRO is another substrate of Parkin that regulates mitochondria-ER contacts. In yeast cells, yeast MIRO (Gem1p) deficiency leads to significant decrease of MERCs (**Figure 4**; Wang X. et al., 2011).

2.4 Ubiquitination of other PD-associated proteins and mitochondrial functions

2.4.1 Ubiquitination of α-synuclein and mitochondrial functions

α-Synuclein, a principal component of LB, is a key protein involved both genetically and pathologically in PD. Mutations in the *α-synuclein* gene cause familiar forms of PD. The polymorphisms of *α-synuclein* confer a relatively increased risk of developing idiopathic PD. Since 1997, point mutations and duplication of *α-synuclein* gene have been inventoried with autosomal dominant PD, suggesting a gain-of-function mechanism (Polymeropoulos et al., 1997; Fuchs et al., 2007; Elia et al., 2013).

α-Synuclein is predominantly found in the presynaptic terminals of the central nervous system and is implicated in regulating synaptic plasticity and neurotransmitter release (Burre et al., 2010; Venda et al., 2010). Compelling evidence suggests that mitochondrial functions, such as cytochrome c release, calcium homeostasis, ATP production, and mitochondrial fission-and-fusion balance, are also directly regulated by α-synuclein. Remarkably, α-synuclein is found in all mitochondrial compartments and can selectively be localized to mitochondria under stress conditions (Ulmer et al., 2005; Li et al., 2007; Parihar et al., 2008; Zhang et al., 2008; Devi and Anandatheerthavarada, 2010; Subramaniam et al., 2014). The N-terminal 32 amino-acid sequence of α-synuclein is critical for its mitochondrial translocation. α-Synuclein undergoes multiple PTMs, including ubiquitination. α-Synuclein is a target of Parkin upon mitochondrial stress. Under basal conditions, no interaction between α-synuclein and Parkin is detected. With the treatment of CCCP or rotenone, Parkin forms a complex with α-synuclein and catalyzes formation of K63-linked Ub chains to recruit Synphilin 1, a negative regulator of α-synuclein toxicity, to the α-synuclein-Parkin complex. Therefore, Parkin-mediated ubiquitination may negatively regulate α-synuclein's response to the mitochondrial stress (Norris et al., 2015). Consistently, α-synuclein is the substrate of RING-type E3 ligase SIAH-1 (seven *in absentia* homolog-1). SIAH-1 facilitates the mono- and poly-ubiquitination of α-synuclein to increase α-synuclein insolubility and exacerbate its aggregation-associated toxicity (**Figure 4**). Cells overexpressing WT α-synuclein or PD-associated mutant α-synuclein A53T show exacerbated cytochrome c release and apoptosis with increased of SIAH-1 activity (Lee et al., 2008).

Ubiquitinated α-synuclein is predominately found in LBs and has been demonstrated to contribute to the misfolding of α-synuclein, mitochondrial dysfunction, and neuronal death (Spillantini et al., 1997; Devi et al., 2008; Choubey et al., 2011). Despite these associations, efforts to establish α-synuclein as a

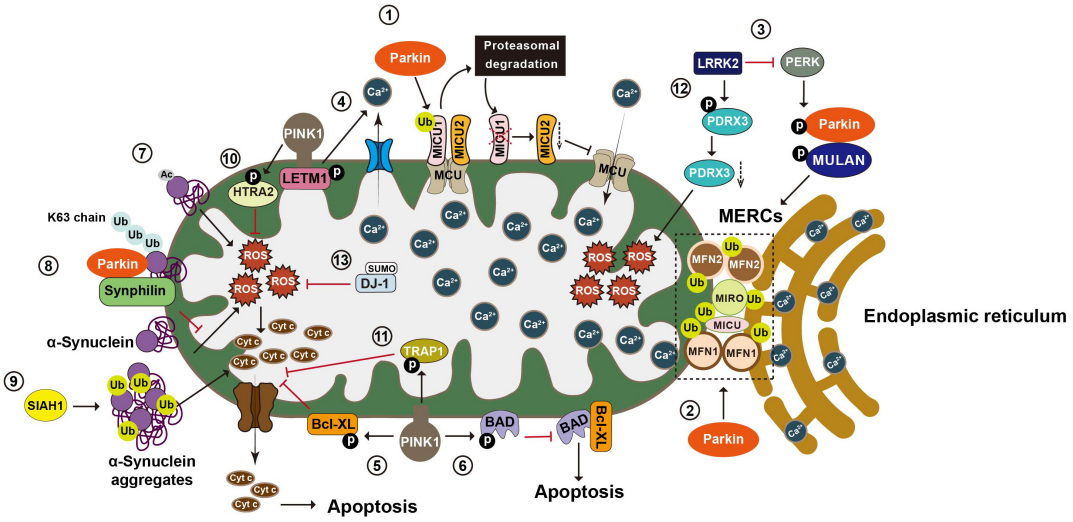

FIGURE 4
Post-translational modifications in the regulation of calcium homeostasis, oxidative stress, and apoptosis. Mitochondria play an essential role in maintaining Ca2+ homeostasis, regulating oxidative stress, and integrating apoptosis signals. (1) Mitochondria take up Ca2+ through the MCU complex, which is positively and negatively regulated by MICU1 and 2, respectively. Parkin regulates mitochondrial calcium homeostasis by directly ubiquitinating MICU1, leading to its proteasomal degradation, and indirectly affecting MICU2's protein level. (2) Parkin also regulates calcium homeostasis by ubiquitinating tethering proteins involved in mitochondria endoplasmic reticulum contact sites (MERCs), such as MFN1, MFN2, MIRO1, and MICU. (3) LRRK2 blocks PERK mediated phosphorylation and activation of Parkin and MULAN, causing increased degradation of MERCS tethering proteins and reduced ER mitochondrial contacts. (4) PINK1 phosphorylates LETM1, leading to increased calcium release and facilitating calcium transport in mitochondria. (5) PINK1 phosphorylates Bcl XL and prevents its pro apoptotic cleavage. (6) PINK1 also phosphorylates BAD and prevents the formation of pro apoptotic Bcl XL BAD complex. (7) N α acetylation of α synuclein induces mitochondrial dysfunction. (8) Parkin increases K63-linked Ub chains on α synuclein, leading to the recruitment of Synphilin 1 to inhibit α synuclein toxicity. (9) SIAH-1 facilitates ubiquitination of α synuclein, increasing α synuclein's insolubility and exacerbating its aggregation associated toxicity. (10) PINK1 mediated phosphorylation enhances the proteolytic activity of HTRA2 and protects cells against mitochondrial stress. (11) Phosphorylation of TRAP1 by PINK1 inhibits cytochrome c release and reduces cell death during oxidative stress. (12) LRRK2 phosphorylates PRDX3 and decreases its peroxidase activity. (13) SUMOylation of DJ 1 is crucial for of DJ 1's anti-ROS activity. MCU, mitochondrial calcium uniporter; MICU1, mitochondrial calcium uptake 1; MICU2, mitochondrial calcium uptake 2; MFN1, mitofusin 1; MFN2, mitofusin 2; MIRO1, mitochondrial Rho GTPase 1; LRRK2, leucine-rich repeat kinase 2; PERK, protein kinase RNA-like ER kinase; LETM1, leucine zipper-EF-hand-containing transmembrane protein 1; ER, endoplasmic reticulum; Bcl XL, B-cell lymphoma-extra large; BAD, BCL2 associated agonist of cell death; Ub, ubiquitin; SIAH-1, seven *in absentia* homolog-1; HTRA2, high-temperature requirement serine protease A2; TRAP1, TNF receptor-associated protein 1; PRDX3, peroxiredoxin 3; ROS, reactive oxygen species.

biomarker for PD diagnosis or prognosis primarily focus on three species of α-synuclein-total α-synuclein, phosphorylated α-synuclein, and the oligomeric form of α-synuclein-in tissues and fluids like blood components, CSF, saliva, and extracellular vesicle (EVs) (Hong et al., 2010; Tokuda et al., 2010; Mollenhauer et al., 2011, 2013; Foulds et al., 2012; Wang Y. et al., 2012; van Steenoven et al., 2018; Vivacqua et al., 2019; Stuendl et al., 2021). Monoubiquitinated and polyubiquitinated α-synuclein are able to be detected in plasma using a polyclonal anti-ubiquitin antibody (FL-76) (Foulds et al., 2011). It will of interest in studying whether this is useful for PD diagnosis.

2.4.2 FBXO7-regulated ubiquitination and mitochondrial functions

Mutations in *FBXO7* cause autosomal recessive EOPD (Shojaee et al., 2008). Being a F-box domain-containing protein, FBXO7 (F-box protein 7) acts as an adapter for Skp1-Cullin-F-box (SCF) type E3-ubiquitin ligase (Skowyra et al., 1997). Emerging evidence suggests that FBXO7 participates in the maintenance of mitochondrial homeostasis through facilitating ubiquitination modification of key proteins in the mitochondrial quality control pathways. Overexpression of FBXO7 enhances Parkin recruitment onto damaged mitochondria, suggesting a role of FBXO7 in mitophagy process (Burchell et al., 2013). It seems that FBXO7 negatively regulates mitophagy activity by enhancing the ubiquitination of PINK1, thereby, suppressing Parkin E3 ligase activity (**Figure 1**; Liu et al., 2020). Furthermore, ubiquitination of MFN1 was also found to be significantly reduced in both fibroblasts derived from patients harboring homozygous *FBXO7* R378G mutation and in SH-SY5Y cells with FBXO7 deficiency, which is restored by wild-type FBXO7. However, a recent study reports that FBXO7 is dispensable in the Parkin-mediated mitophagy process. Accumulation of pUb, recruitment of Parkin onto mitochondria, and mitophagy flux are all barely affected in *FBXO7*$^{-/-}$ cells. Moreover, increased pUb foci were detected in *FBXO7*$^{-/-}$ cells than that in control cells after treating with mitochondrial targeted HSP90 (heat shock protein 90) inhibitor Gamitrinib-TPP (Kraus et al., 2023). It is possible that FBXO7 regulates mitochondrial functions differentially depending on conditions. Nonetheless, the regulation is likely one via ubiquitination modification.

2.4.3 VPS35-regulated ubiquitination and mitochondrial functions

VPS35 (vacuolar protein sorting 35) is a critical component of the retromer complex that is important for the retrograde transport of transmembrane protein-cargo from endosomes to the trans-Golgi network (TGN) (Hierro et al., 2007). Mutations in *VPS35* have recently been identified as the cause of familiar PD.

A single missense mutation in *VPS35*, c.1858G > A (p.D620N), has been unambiguously identified to segregate with late-onset PD (LOPD) in an autosomal dominant manner (Zimprich et al., 2011). Studies suggest that VPS35 can indirectly participate in mitochondrial dynamics via the alteration of ubiquitination events. Using a transgenic mouse model, Tang et al. (2015) revealed that VPS35 regulates the trafficking and degradation of the MULAN (mitochondrial E3 ubiquitin protein ligase 1), thereby inhibiting MUL1-mediated ubiquitination and degradation of MFN2 and promoting mitochondrial fusion (**Figure 2**). Consistently, selective deletion of the VPS35 in DA neuron results in mitochondrial fragmentation and PD-relevant pathologies in $VPS35^{\pm}$ mice (Tang et al., 2015).

2.4.4 LRRK2-regulated ubiquitination and mitochondrial functions

Another PD-associated protein that indirectly participate in mitochondrial dynamics through ubiquitination modification is LRRK2 (leucine-rich repeat kinase 2). LRRK2, also known as dardarin (from the Basque word "dardara" that means trembling) and PARK8 (from early identified association with PD), is a large multifunctional kinase. Variants of this gene are associated with increased risk of PD and Crohn's disease (Funayama et al., 2002). LRRK2, through its N-terminal domain, interacts with mitochondrial membrane-binding E3 ubiquitin ligases MARCH5 (membrane associated Ring-CH-type finger 5), MULAN, and Parkin. The kinase activity of LRRK2 is required for activation of these E3 ligase (**Figure 2**). No evidence of direct phosphorylation of these E3 ligases by LRRK2 has been found in *in vitro* assays, but screening assay using siRNA library revealed that PERK (protein kinase RNA-like ER kinase) is the kinase that directly phosphorylates and activates these E3 ligases. Via binding to these E3 ligases, LRRK2 WT blocks the PERK-mediated phosphorylation and activation of these E3 ligases. PD-associated LRRK2 mutant G2019S has decreased binding activity to these E3 ligases, resulting in increased phosphorylation and activation of E3 ubiquitin ligases by PERK, which consequently causes increased degradation of MERCS tethering proteins and reduced ER-mitochondrial contacts (**Figure 4**; Toyofuku et al., 2020).

3 Regulation of mitochondrial functions by phosphorylation in Parkinson's disease

Protein phosphorylation, a prevalent PTM mediated by kinases, involves the covalent attachment of a phosphate group to an amino acid residue like serine (S), threonine (T), or tyrosine (Y). This dynamic modification offers a swift mechanism to alter protein function, thus playing crucial roles in regulation of various cellular pathways. Emerging evidence indicates that aberrant phosphorylation of proteins impacts mitochondrial functions, such as mitochondrial dynamics, mitophagy, MDV formation, mitochondrial respiratory activity, and calcium homeostasis. Notably, PD-associated kinase proteins, such as PINK1 and LRRK2, have been found to cause mitochondrial dysfunction through their dysregulated phosphorylation activity, ultimately leading to PD pathogenesis. Therefore, we aim to provide an overview elucidating how PINK1 and LRRK2 modulate a range of mitochondrial functions via their kinase activity, outlining their implications in the pathogenesis of PD through protein phosphorylation (**Table 3**).

3.1 PINK1-mediated phosphorylation and mitophagy

Mutations in *PINK1* are the second most common cause of EOPD, accounting for 1–9% PD patients. More than 300 PINK1 variants have been identified from PD patients (Ma et al., 2021; Vizziello et al., 2021). The *PINK1* gene encodes a 581 amino acid protein, which contains an N-terminal mitochondrial targeting sequence (MTS), a transmembrane domain (TMD), and a highly conserved S/T kinase domain (Cardona et al., 2011). Under normal conditions, PINK1 is targeted to mitochondria through its MTS via the TOM (translocase of the outer membrane) and TIM (translocase of the inner membrane) complexes (Lazarou et al., 2012). During the translocation process, PINK1 undergoes consecutive cleavages by MPP (mitochondrial processing peptidase) and PARL (presenilin-associated rhomboid-like protease) (Jin et al., 2010; Deas et al., 2011; Greene et al., 2012), and the cleaved 52-kDa PINK1 is retro-translocated into the cytosol and undergoes rapid turnover by the proteasome via the N-end rule pathway (Whitworth et al., 2008; Greene et al., 2012). Therefore, PINK1 is normally maintained at a very low steady-state level. With damaged mitochondria, PINK1's mitochondrial import is inhibited by the reduced mitochondrial membrane potential, which leads to the accumulation of full-length PINK1 on the OMM (Jin and Youle, 2013).

The landmark studies suggesting that both Parkin and PINK1 function through a common pathway to regulate mitochondrial function were from a series of *Drosophila* research (Greene et al., 2003; Clark et al., 2006; Park et al., 2006). Not only do $PINK1^{-/-}$ and $Parkin^{-/-}$ mutant flies exhibit similar degenerative phenotypes in neuron and muscle cells due to mitochondrial abnormalities, but overexpression of Parkin also rescues the $PINK1^{-/-}$ phenotype, not vice versa, suggesting PINK1 acts upstream of Parkin in a linear pathway (Yang et al., 2006). Later on, more studies gradually unveil the models of how PINK1 and Parkin work together to regulate various mitochondrial functions (Durcan and Fon, 2015; Mouton-Liger et al., 2017).

PINK1-mediated phosphorylation plays essential roles at multiple steps of the mitophagy process, largely interacting with Parkin-mediated ubiquitination modification (Ordureau et al., 2014). First, autophosphorylation of PINK1 is important for its own activation, coinciding with its accumulation on the OMM (Kondapalli C. et al., 2012). PINK1 activity is determined by autophosphorylation at residues S228, S230, T257, and S402 (Kondapalli C. et al., 2012; Okatsu et al., 2012b; Aerts et al., 2015; Rasool et al., 2022). Although conflicting results regarding the regulatory role of autophosphorylation residues in PINK1are reported, autophosphorylation at S228 is important for the subsequent phosphorylation of PINK1 substrates in cells (Okatsu et al., 2012a; Aerts et al., 2015; Kumar et al., 2017; Rasool et al., 2018). Furthermore, the equivalent site of human PINK1 S228 is confirmed to be autophosphorylated in multiple PINK1 homologs, including S346 of *Drosophila* PINK1, S205 of

TABLE 3 Phosphorylation of PD-related proteins and mitochondrial dysfunction.

PD-related protein	Enzyme	Substrate	Regulated mitochondrial function	Modification site (human)	References
PINK1	PINK1	PINK1	Activates PINK1	S228, S230, T257, S402	Kondapalli C. et al., 2012; Okatsu et al., 2012b; Aerts et al., 2015
	PINK1	Ub	Activates Parkin	S65	Kazlauskaite et al., 2014
	PINK1	Parkin	Promotes mitophagy, increases MDVs production	S65	Kazlauskaite et al., 2014
	PINK1	NDUFA10	Enhances CI activity	S250	Morais et al., 2014
	PINK1	Bcl-XL	Inhibits pro-apoptotic signal	S62	Arena et al., 2013
	PINK1	BAD	Prevents apoptosis	S112, S136	Wan et al., 2018
	PINK1	HTRA2	Reduces mitochondrial stress	S141	Plun-Favreau et al., 2007
	PINK1	TRAP1	Inhibits cytochrome c release	-	Pridgeon et al., 2007
	PINK1	LETM1	Maintains calcium homeostasis	T192	Huang et al., 2017
	MARK2	PINK1	Activates PINK1	T313	Matenia et al., 2012
LRRK2	LRRK2	Parkin	Inhibits mitophagy	-	Bonello et al., 2019
	LRRK2	MIRO	Inhibits mitophagy	-	Hsieh et al., 2016
	LRRK2	Rab10	Inhibits mitophagy	T73	Wauters et al., 2020
	LRRK2	BCL2	Increases mitophagy	T56	Su et al., 2015
	LRRK2	DRP1	Increases mitochondrial fragmentation	T595	Su and Qi, 2013
	LRRK2	4E-BP	Increases oxidative stress	T37, T46	Imai et al., 2008
	LRRK2	PRDX3	Increases oxidative stress	T146	Angeles et al., 2011
	LRRK2	unknown	Exacerbates mtDNA damage	-	Howlett et al., 2017; Gonzalez-Hunt et al., 2020

PINK1, PTEN induced putative kinase 1; Ub, ubiquitin; NDUFA10, NADH: ubiquinone oxidoreductase subunit A10; Bcl-XL, B-cell lymphoma-extra large; BAD, BCL2 associated agonist of cell eath; HTRA2, high-temperature requirement serine protease A2; TRAP1, TNF receptor-associated protein 1; LETM1, leucine zipper-EF-hand-containing transmembrane protein 1; MARK2, microtubule affinity-regulating kinase; LRRK2, leucine-rich repeat kinase 2; MIRO, mitochondrial Rho GTPase; BCL2, B-cell lymphoma 2; DRP1, dynamin-related protein 1; 4E-BP, 4E-binding protein; PRDX3, peroxiredoxin 3; MDV, mitochondrial-derived vesicle; CI, mitochondrial respiratory complex I; mtDNA, mitochondrial DNA; T, threonine; S, serine; "-" means no answer.

Tribolium PINK1, and S202 of *Pediculus* PINK1 (Rasool et al., 2018). *Drosophila* carrying the PINK1 S346A mutant displays similar mitochondrial defects to those observed in *PINK1*$^{-/-}$ mutant flies (Clark et al., 2006). Second, PINK1 phosphorylates Parkin at S65 of the ubiquitin domain to induce recruitment of Parkin to mitochondria and the release of Parkin E3 ligase activity. PINK1-mediated phosphorylation is essential for Parkin activation (Xiong et al., 2009; Kondapalli K. C. et al., 2012; Kane et al., 2014; Kazlauskaite et al., 2014; Koyano et al., 2014; Wauer et al., 2015a). In the absence of an activation signal, Parkin stays in the cytosol in an auto-inhibited structure due to the inhibitory intradomain contacts (Trempe and Gehring, 2023). PINK1 phosphorylates Ub on S65 (Kazlauskaite et al., 2014; Koyano et al., 2014; Wauer et al., 2015b). pUb serves as a receptor for Parkin to bind. Upon pUb binding, Parkin Ubl domain becomes more accessible by PINK1, leading to the subsequent phosphorylation of Ubl S65 (Durcan and Fon, 2015). Phosphorylation of Parkin by PINK1 further dissociates the inhibitory intradomain-contacting inside Parkin, resulting in the full activation of Parkin's enzymatic activity (Trempe and Gehring, 2023). Third, PINK1-mediated phosphorylation amplifies the Parkin-mediated ubiquitination signal. After activation, Parkin ubiquitinates a large number of mitochondrial proteins and thereby produces increased Ub substrates for PINK1 to generate pUb signals, which successively initiate more Parkin recruitment and greater Parkin activation, creating a feed-forward loop to reach a maximal of Parkin-mediated ubiquitination (**Figure 1**; Ordureau et al., 2015; Koyano et al., 2019). On a relevant note, MARK2 (microtubule affinity-regulating kinase) is identified as an activating kinase of PINK1. MARK2 phosphorylates PINK1 at residue T313 that coincidentally is a residue frequently mutated to a non-phosphorylatable form T313M in PD cases (Tang et al., 2006). The expression of PINK1 T313M causes severe toxicity and abnormal mitochondrial accumulation in cells, also suggesting the mitochondrial consequence of the PINK1 activity (Matenia et al., 2012).

PINK1-mediated phosphorylation is a potential biomarker for PD diagnosis (Chin and Li, 2016). An antibody designed for pS65 on Ub (pS65-Ub) reveals that a rapid accumulation of pS65-Ub signal in mitochondria following mitochondrial damage. The presence of pS65-Ub positive granule also increases in cells derived from aging individuals and sporadic PD cases (Fiesel et al., 2015). Furthermore, a patent filed by Geldenhuys et al. (2014) details the use of PINK1 T257 autophosphorylation and PINK1-mediated phosphorylation of Parkin at S56 in serum and CSF as diagnostic measures. Additional efforts will be required to evaluate their clinical applicability.

Of the reported PD-associated *PINK1* mutations, about 30 of them are defined as "pathogenic" or "likely pathogenic," causing similar clinical symptoms as in the cases caused by *Parkin* mutations (Richards et al., 2015; Ellard et al., 2020). Recently,

Ma et al. (2021) analyzed 50 PINK1 variants and found most these pathogenic variants cause a significant decrease in mitophagy activity. However, these consist of only a small fraction of identified pathogenic PINK1. Further investigation is still needed to understand PINK1-phosphorylation regulated mitophagy in PD pathogenesis (Lin and Kang, 2008).

3.2 PINK1-mediated phosphorylation and mitochondrial-derived vesicles

PINK1, along with Parkin, are identified as key regulators of the MDV pathways that plays important roles in the regulation of mitochondrial turnover and MitAP production (Matheoud et al., 2016). PINK1 was initially found to be required for the formation of MDVs that deliver damaged mitochondrial portion to the lysosome for degradation (Sugiura et al., 2014; Pickrell and Youle, 2015). Ramirez et al. (2022) have recently reported that cannabidiol (CBD) activates PINK1 and Parkin in a dose-dependent manner, leading to elevated production of MDVs. CBD causes PINK1 accumulation on the mitochondrial out membrane to activate Parkin to promote the generation of MDVs (**Figure 1**). However, detailed mechanism underlying PINK1-regulated MDV formation remains unknown. It is possible that PINK1 participates in recognition of damaged sites of mitochondria and promotes segregation of damaged part of mitochondria. Consistent with this notion, PINK1 is shown to phosphorylate DRP1at S616 to activate fission, a potential mechanism to separate damaged and health portion of a mitochondrion (Han et al., 2020).

3.3 PINK1-mediated phosphorylation and other mitochondrial functions

3.3.1 PINK1-mediated phosphorylation and mitochondrial dynamics

PINK1 is implicated in the phosphorylation of mitochondrial proteins that are important for the regulation of mitochondrial dynamics. First, PINK1 phosphorylates a group of key players in the mitochondrial dynamic pathways. The dynamin-related GTPase DRP1 is a crucial factor of the mitochondrial fission machinery, and its activity is regulated by phosphorylation (Yu et al., 2019; Han et al., 2020). Around 10 residues of DRP1 are able to be phosphorylated. Phosphorylation of S616 and S637 is extensively studied (Kim et al., 2016; Cha et al., 2021). After recruiting to the OMM, DRP1 is phosphorylated by PKA (protein kinase A) at S637, inhibiting DRP1 GTPase activity and suppressing its translocation to the mitochondria, and thereby impeding mitochondrial fission (Cereghetti et al., 2008). $DRP1^{S616}$ was initially found to be phosphorylated by Cdk1/cyclin B, resulting in mitochondrial fragmentation (Pryde et al., 2016). We recently demonstrate that PINK1 directly phosphorylate $DRP1^{S616}$ site to regulate mitochondrial fission that is independent of Parkin and autophagy activity (Han et al., 2020). MFN2 is also a substrate of PINK1. PINK1 phosphorylates MFN2 at residues T111 and S442, resulting in increased ubiquitination and proteasomal degradation of MFN2, leading to eventual mitochondrial fusion via Parkin mediated mechanism (Chen and Dorn, 2013; Tsai et al., 2014). Likewise, PINK1 phosphorylates MIRO1 at residue S156, in turn activates Parkin-mediated ubiquitination and degradation of MIRO1, therefore, inhibits axonal transport of mitochondria (**Figure 2**; Wang X. et al., 2011).

3.3.2 PINK1-mediated phosphorylation and mitochondrial respiratory activity

Both PINK1 deficiency and PD-associated PINK1 mutants impair functions of mitochondrial respiratory complex I (CI) (Morais et al., 2009, 2014). NDUFA10 (NADH: ubiquinone oxidoreductase subunit A10) is an auxiliary subunit of CI. Although it is still unclear whether PINK1 directly phosphorylates NDUFA10, phosphoproteomic analysis reveals abolished phosphorylation of NDUFA10 at residue S250 in PINK1 knockout (KO) mice. Furthermore, both WT NDUFA10 and the phosphomimetic NDUFA10 mutant (S250D) enhance CI activity and rescue PINK1 deficiency-induced mitochondrial damage in mouse and cellular models. In contrast, the phosphorylation deficient mutant NDUFA10 S250A fails to rescue the PINK1 deficiency-related phenotypes (Morais et al., 2014). These results suggest a crucial role of phosphorylated NDUFA10 in the regulation of mitochondrial bioenergetics. Consistently, NDUFA10 improves PINK1 knockdown (KD)-induced mitochondrial hyperfusion in *Drosophila* by increasing CI activity (Pogson et al., 2014).

3.3.3 PINK1-mediated phosphorylation and apoptosis

Mitochondria hold a central position in the apoptosis process. PINK1-mediated phosphorylation is found to prevent mitochondria-mediated cell death in multiple ways. PINK1 phosphorylates Bcl-XL (B-cell lymphoma-extra large) and prevents its pro-apoptotic cleavage. Bcl-XL has an anti-apoptotic activity by protecting the mitochondrial membrane potential ($\Delta\psi$) and preventing cytochrome c release via its binding to and inhibition of VDACs. The N-terminal BH4 domain of the Bcl-XL is essential for this apoptosis inhibition activity (Shimizu et al., 2000). Upon mitochondrial depolarization, PINK1 interacts with Bcl-XL and phosphorylates it at residue S62, leading to the resistance of Bcl-XL to the cleavage of its N-terminal and the reduction of pro-apoptotic signal (Arena et al., 2013). BAD (BCL2 associated agonist of cell death) is a BH3-only protein. Phosphorylation of BAD at residue S112 inhibits its ability to form pro-apoptotic complex with Bcl-XL on the OMM (Hirai and Wang, 2001). Upon CCCP treatment, PINK1 phosphorylates BAD at residues S112 and S136, preventing the formation of pro-apoptotic Bcl-XL-BAD complex, leading to cell survival (**Figure 4**; Wan et al., 2018).

HTRA2 (high-temperature requirement serine protease A2) is implicated in the pathogenesis of PD and other neurodegenerative conditions. Mutations in *HTRA2* are a risk factor for sporadic PD cases. As a mitochondrial serine protease, HTRA2 functions in mitochondrial quality control and apoptosis. During apoptosis, HTRA2 is released into the cytosol and facilitates apoptosis by antagonizing IAPs (inhibitors of apoptosis). Interestingly, HTRA2 activation is dependent on the direct phosphorylation of its S141 by PINK1. PINK1-mediated S141 phosphorylation enhances the proteolytic activity of HTRA2 and protects cells against

mitochondrial stress (**Figure 4**; Plun-Favreau et al., 2007). HTRA2 variants, A141S and P143A, identified in sporadic PD patients are in close proximity to the S142, suggesting they may contribute to PD by interfering with PINK1-mediated phosphorylation and HTRA2 activation (Strauss et al., 2005; Lin et al., 2011). Genetic studies in *Drosophila* further demonstrated the functional interaction between PINK1 and HTRA2. These studies collectively suggest that HTRA2, in parallel with Parkin, acts downstream of the PINK1 to maintain mitochondrial integrity (Whitworth et al., 2008; Tain et al., 2009). Consistently, reduced HTRA2 phosphorylation is observed in brains of PD patients carrying *PINK1* mutations (Plun-Favreau et al., 2007).

TRAP1 (TNF receptor-associated protein 1), also known as HSP75 (heat shock protein 75), is a mitochondrial chaperone protein. PINK1 binds to TRAP1 on mitochondria and phosphorylates TRAP1 in the mitochondrial intermembrane space (IMS). Phosphorylation of TRAP1 by PINK1 inhibits cytochrome c release and reduces cell death during oxidative stress. PD-associated PINK1 mutants G309D and L347P, both with reduced kinase activity, diminish the TRAP1 phosphorylation and result in increased apoptosis upon mitochondrial oxidative stress (Pridgeon et al., 2007). In *Drosophila*, TRAP1 deficiency results in mitochondrial dysfunction and vulnerability to various mitochondrial stress. Overexpression of human TRAP1 rescues PINK1-deficiency induced mitochondrial abnormalities (Costa et al., 2013; Zhang et al., 2013).

3.3.4 PINK1-mediated phosphorylation and calcium homeostasis

Mitochondria are both major effectors and essential regulators of intracellular Ca^{2+} levels. The amount of Ca^{2+} retained inside the mitochondrial matrix is regulated by mitochondrial Ca^{2+} transient, which includes Ca^{2+} influx mediated by MCU and mitochondrial Ca^{2+} efflux mediated by Na^{+}/Ca^{2+} and H^{+}/Ca^{2+} antiporters (Szabadkai et al., 2006). PINK1 deficiency leads to dysfunction of the Na^{+}/Ca^{2+} exchanger and causes mitochondrial calcium overload (Gandhi et al., 2009). Studies reveal that LETM1 (leucine zipper-EF-hand-containing transmembrane protein 1) is a mitochondrial H^{+}/Ca^{2+} antiporter situated on the IMM. PINK1 interacts with LETM1 and directly phosphorylates it at residue T192, leading to increased calcium release in liposomes and facilitating calcium transport in mitochondria (**Figure 4**). Both PINK1 deficiency and PD-associated mutant PINK1 Q456X significantly reduce LETM1 phosphorylation, causing mitochondrial calcium-transport dysfunction and neuronal death (Huang et al., 2017).

3.4 LRRK2-mediated phosphorylation and mitochondrial functions

3.4.1 LRRK2-mediated phosphorylation and mitophagy

Mutations in *LRRK2* are the most common cause of autosomal dominant LOPD (Zimprich et al., 2004). *LRRK2* encodes a 286-kDa protein containing multiple domains, including a leucine-rich repeat (LRR), a Ras of complex protein (ROC) GTPase domain, a mitogen-activated kinase domain, and WD40 domains. Therefore, LRRK2 is a bienzymatic protein with both GTPase and kinase activities. Six pathogenic mutations have been identified in *LRRK2*, including R1441C/G, N1437H, Y1699C, G2019S, and I2020T (Ross et al., 2011). The most common LRRK2 mutation, G2019S, is located right in the kinase domain. This mutation increases LRRK2 kinase activity toward itself and other substrates (Ross et al., 2011). Thus, the increased kinase activity of LRRK2 is considered important in the pathogenesis of PD.

While majority of LRRK2 is located at cytoplasm, a portion of LRRK2 is associated with the OMM (West et al., 2005; Biskup et al., 2006). iPSC-derived neural cells bearing LRRK2 G2019S and fibroblasts derived from PD patients carrying LRRK2 G2019S show mitochondrial impairment, suggesting that LRRK2 pathogenesis might involve mitochondrial dysfunction (Mortiboys et al., 2010; Sanders et al., 2014). *In vitro*, expression of LRRK2 increases mitochondrial clustering and reduced mitochondrial clearance upon CCCP treatment. In contrast, LRRK2 G2019S further exacerbated the damaging effects (Hsieh et al., 2016). Likewise, reduced mitochondrial autophagy in DA neurons and astrocytes in LRRK2 G2019S mouse brain that is rescued by treatment with LRRK2 kinase inhibitor GSK3357679A (Singh et al., 2021). Several possible mechanisms for the negative regulation of mitophagy by LRRK2 kinase activity are proposed: (1) LRRK2 impairs the interactions between Parkin and DRP1 and their mitochondrial targets in a kinase-dependent manner (Bonello et al., 2019); (2) LRRK2 interacts with MIRO, and the LRRK2 G2019S mutant prevents proteasomal degradation of MIRO, leading to delayed mitophagy (Hsieh et al., 2016); (3) LRRK2 phosphorylates Rab10 on the residue T73, and PD-associated LRRK2 mutants (G2019S and R1441C) impair Rab10 mitochondrial localization and disrupts its interaction with OPTN, resulting in impaired mitochondrial autophagy via a kinase activity related manner (**Figures 1**, **2**; Wauters et al., 2020). In contrast, a study suggests a positive regulation of mitophagy by LRRK2's kinase activity. LRRK2 G2019S phosphorylates BCL2 at residue T56, leading to the loss of $\Delta\psi$ and triggering excessive mitophagy via the recruitment of P62 to the mitochondria, (Su et al., 2015).

Recognizing the crucial role of elevated LRRK2 kinase activity in PD pathogenesis, multiple research groups have undertaken studies to quantitatively assess LRRK2-related phosphorylation across various tissues and biofluids, exploring their potential of being used as a PD diagnosis (Delbroek et al., 2013; Wang et al., 2017; Padmanabhan et al., 2020; Vissers et al., 2023). Collectively, the expressional level of total LRRK2 (tLRRK2), phosphorylation of LRRK2 at S1292 or S935 (pS1292-LRRK2 or pS935-LRRK2), and phosphorylation of the LRRK2 substrate Rab10 at T73 (pT73-Rab10) have been the focus of extensive study. The observed changes of tLRRK2 and LRRK2-associated phosphorylation in PD cases vary among brain regions, tissues, and cell types (Rideout et al., 2020). Increased tLRRK2 in the frontal cortex in sporadic PD cases, conflicting changes of tLRRK2 l in cerebrospinal fluid (CSF) in sporadic PD cases, elevated pS1292-LRRK2 in urinary EVs in but deceased pS935-LRRK2 in PBMCs among LRRK2-G2019S carriers, and increased pT73-Rab10 in neutrophils in idiopathic PD and LRRK2-G2019S carriers have been reported (Cho et al., 2013; Fraser et al., 2016; Fan et al., 2018; Mabrouk et al., 2020; Padmanabhan et al., 2020).

Remarkably, the highest expression of LRRK2 is not observed in neurons but in peripheral blood mononuclear cells (PBMCs) (Thevenet et al., 2011). Particularly, certain cell types in PMBCs show increased LRRK2 expression in PD patients compared to healthy controls, including B cells, T cells, CD16+ monocytes, neutrophiles, but not mixed PBMCs (Cook et al., 2017; Atashrazm et al., 2019). An LRRK2 inhibitor MLi2[25] significantly reduced pS935-LRRK2 and pT73-Rab10 in both neutrophils and mixed PBMC (Atashrazm et al., 2019). Although pS935-LRRK2 does not directly reflect LRRK2 kinase activity like pS1292-LRRK2, it is sensitive to dephosphorylation caused by LRRK2 kinase inhibitor (Delbroek et al., 2013; Lobbestael et al., 2013). Therefore, pS935-LRRK2 and pT73-Rab10 are considered potential pharmacodynamics marker in clinical trials of LRRK2 kinase inhibitors.

3.4.2 LRRK2-mediated phosphorylation and other mitochondrial functions

LRRK2 regulates mitochondrial dynamics via DRP1 in a kinase-dependent manner. In BV2 microglia cells and primary cultured microglia cells, treatment of lipopolysaccharide (LPS) activates microglia, resulting in enhanced mitochondrial fragmentation (Ho et al., 2018). Interestingly, LPS-induced mitochondrial fragmentation can be reversed by LRRK2 kinase inhibitor GSK2578215A. Results suggest an important role of LRRK2 kinase activity in regulating mitochondrial dynamics in microglia (Ho et al., 2018). Consistently, overexpression of WT LRRK2 or LRRK2 G2019S in cells results in apparent mitochondrial fragmentation, while overexpression of LRRK2 kinase-dead mutant D1994A does not cause such phenotype (Wang X. et al., 2012; Perez Carrion et al., 2018). LRRK2 directly interacts with and phosphorylates DRP1. PD-associated LRRK2 G2019S and R1441C mutants further enhance this interaction (Su and Qi, 2013; Stafa et al., 2014). LRRK2 G2019S phosphorylates DRP1 at residue T595 (Su and Qi, 2013). In fibroblasts derived from PD patients carrying LRRK2 G2019S, both the selective DRP1-inhibitor P110 or the expression of non-phosphorylatable mutant DRP1 T595A reverse the mitochondrial fragmentation and improve mitochondrial quality, indicating that LRRK2 G2019S-induced mitochondrial fragmentation is possible via a mechanism related to DRP1 T595 phosphorylation (**Figure 2**; Su and Qi, 2013).

Cells expressing PD associated LRRK2 mutants increase susceptibility to oxidative stress, suggesting that increased LRRK2 kinase activity might interfere antioxidant defense mechanism (Heo et al., 2010; Nguyen et al., 2011; Bahnassawy et al., 2013; Kim et al., 2019). LRRK2 phosphorylates 4E-BP (4E-binding protein) at residues T37/T46, both *in vitro* and *in vivo*. 4E-BP is a eukaryotic translation initiation factor regulating overall protein translation in cells that is crucial for cell survival under stress conditions (Haghighat et al., 1995; Tettweiler et al., 2005). *Drosophila* LRRK2 also phosphorylates 4E-BP, attenuating the resistance to oxidative stress via a 4E-BP phosphorylation-dependent manner (Imai et al., 2008). Therefore, LRRK2 kinase activity regulates cell response to oxidative stress through a 4E-BP mediated pathway. Studies also suggest that LRRK2 affects antioxidant defense mechanism through its phosphorylation of PRDX3 (peroxiredoxin 3). PRDX3 is a mitochondrial antioxidant of the thioredoxin-peroxidase family, efficiently scavenging peroxides and controlling the level of reactive oxygen species (ROS) in mitochondria (Fujii and Ikeda, 2002). *In vitro*, LRRK2 interacts with PRDX3 and potentially phosphorylates PRDX3 at residue T146. PD-associated mutant LRRK2 G2019S enhances its interaction with and causes decreased peroxidase activity of PRDX3 along with increased cell death (**Figure 4**; Angeles et al., 2011). Consistently, *Drosophila* expressing LRRK2 G2019S show reduced PRDX3 peroxidase activity and exacerbated oxidative stress (Angeles et al., 2014).

Furthermore, LRRK2 kinase activity is associated with increased mitochondrial DNA (mtDNA) damage. In various cellular models, including iPSC-derived neural cells, immune cells and fibroblasts, PD-associated mutant LRRK2 G2019S increases mtDNA damage that is abrogated by either gene editing to correct the G2019S mutation or by treatment with LRRK2 kinase inhibitors (Howlett et al., 2017; Gonzalez-Hunt et al., 2020).

Together, LRRK2-mediated phosphorylation regulates mitochondrial functions. Elevated LRRK2 kinase activity could contribute PD pathogenesis through impairing mitochondria.

4 Other post-translational-modifications: regulating mitochondrial functions in Parkinson's disease

In addition to ubiquitination and phosphorylation, multiple other PTMs regulates mitochondrial functions and is implicated in the PD pathogenesis. In this context, we will provide a summary of recent research findings on how PD-related proteins affect mitochondrial functions through SUMOylation, acetylation, or s-nitrosylation, to elucidate their involvement in the development of PD (**Table 4**).

4.1 SUMOylation-regulated mitochondrial function and Parkinson's disease

SUMOylation refers to the PTM that covalently attaches small ubiquitin-like modifier (SUMO) to lysine residues on the substrate protein. SUMOylation occurs through multiple steps of enzymatic reactions, very similar to those in the ubiquitination process but with different specific enzymes, causing biochemical and functional changes of the target protein. SUMOylation modifies a broad range of proteins and regulates a diversity of biological processes, such as chromatin remodeling, transcription, and mitochondrial dynamics. SUMOylation regulates mitochondrial dynamics through a number of proteins that are either directly encoded by or in close functional-relationship with PD-associated genes (Guerra de Souza et al., 2016).

Mutations in *DJ-1* cause autosomal recessive forms of PD. Being a peroxiredoxin-like peroxidase, DJ-1 helps maintain mitochondrial function during oxidative stress as a sensor of damage and a regulator of CI activity (Taira et al., 2004; Andres-Mateos et al., 2007). DJ-1 deficiency results in increased

TABLE 4 Other PTMs of PD-related proteins and mitochondrial dysfunction.

Type of PTM	PD-related protein	Enzyme	Substrate	Regulated mitochondrial function	Modification site (human)	References
SUMOylation	DJ-1	/	DJ-1	Inhibits ROS production	K130	Shinbo et al., 2006; Krebiehl et al., 2010
	Parkin	/	Parkin	Increases Parkin's ubiquitination	-	Um and Chung, 2006
Acetylation	PINK1	SIRT3	PINK1	Inhibits PINK1's acetylation	-	Wei et al., 2017
	Parkin	SIRT3	Parkin	Inhibits Parkin's acetylation	-	Wei et al., 2017
S-nitrosylation	Parkin	/	Parkin	Inhibits Parkin	-	Chung et al., 2004
	Parkin	/	Parkin	Activates Parkin	C323	Ozawa et al., 2013
	PINK1	/	PINK1	Inhibits PINK1	C568	Oh et al., 2017

PINK1, PTEN induced putative kinase 1; SIRT3, NAD-dependent protein deacetylase sirtuin-3; ROS, reactive oxygen species; C, cysteine; "-" means no answer.

production of ROS and decreased $\Delta\psi$ in cellular and mouse models (Krebiehl et al., 2010). SUMOylation plays important roles in regulating DJ-1 function. SUMOylation of DJ-1 K130 is crucial for the full activity of DJ-1 (**Figure 4**). The PD-associated DJ-1 L166P mutant becomes improperly SUMOylated and hence more insoluble, leading to its aggregation in mitochondria, ultimately suppresses its proteasomal degradation (Shinbo et al., 2006). DJ-1 is not only an effector of SUMOylation but also suppresses SUMOylating of other proteins at the global level through its interaction with key proteins of the SUMOylation machinery. For example, DJ-1 inhibits the SUMOylation of PSF (pyrimidine tract-binding protein-associated splicing factor), consequently reducing PSF-mediated apoptosis. The PD-associated pathogenic DJ-1 mutant L166P causes accumulation of high-molecular-weight SUMOylated PSF (Zhong et al., 2006). Together, these findings suggest that SUMOylation is involved in DJ-1's regulation on mitochondria-associated oxidative stress and apoptosis.

Several biomarker studies have aimed to identify and quantify different DJ-1 species levels in PD patients compared to healthy controls. Presently, these studies primarily concentrate on the measurement of total DJ-1 in CSF, DJ-1 isoforms in whole blood, or oxidized DJ-1 in blood or urine (Waragai et al., 2006; Hong et al., 2010; Lin et al., 2012; Gui et al., 2015; Saito, 2017; Jang et al., 2018). Until now, the reliable detection of SUMOylated DJ-1 in various tissues or biofluids, and its potential use as an indicator for PD disease progression, stays unexplored. Similar to the challenge faced in using ubiquitinated proteins as biomarkers, the obstacle here may also be attributed to the lack of specific antibodies targeting SUMOylated DJ-1 (Magalhaes and Lashuel, 2022).

It's noteworthy that not only is proper SUMOylation essential for the solubility and activity of DJ-1 protein, but also is the PKA induced phosphorylation at the T154 residue of DJ-1 (Ko et al., 2019). Currently, there is no evidence showing crosstalk between the T154 phosphorylation and the K130 SUMOylation of DJ-1. However, it is an intriguing question worth investigating.

Parkin has also been reported to selectively interact with SUMO-1 (small ubiquitin like modifier 1), both *in vitro* and *in vivo*, resulting in increased ubiquitination and nuclear translocation of Parkin. Therefore, SUMOylation might play a role in Parkin-mediated ubiquitination and its relevance to PD pathogenesis (Um and Chung, 2006). In agreement with this, DRP1 is a target of all SUMO isoforms with various functional-consequences. SUMOylation of DRP1 by SUMO-1 enhances its association with mitochondria, promotes mitochondrial fragmentation, and increases apoptosis (Wasiak et al., 2007). In contrast, SUMOylation of DRP1 by SUMO-2/3 decreases its mitochondrial localization and reduces apoptosis under stress conditions (Guo et al., 2013). Collectively, these studies underscore the significance of SUMO-regulated mitochondrial functions in the pathogenesis of PD.

4.2 Acetylation-regulated mitochondrial function and Parkinson's disease

Protein acetylation refers to the transfer of an acetyl group (CH_3CO) from acetyl-CoA to either the ε-amino group (NH_3^+) of lysine residues (ε-lysine acetylation) or to the N-terminal amino acid of a protein (*N*-α-acetylation). *N*-α-acetylation is an irreversible reaction catalyzed by N-terminal acetyltransferases (NATs), while l ε-lysine acetylation is a reversible modification tightly regulated by histone acetyltransferases (HATs) and histone deacetylases (HDACs) (Drazic et al., 2016). Recent evidence indicates that acetylation of PD-associated proteins might have important functional-consequences in mitochondria, although the detailed mechanism remains largely unknown.

In vitro, *N*-α-acetylation affects the secondary structure of α-synuclein, leading to the oligomeric form with a partial α-helical structure (Kang et al., 2012). *In vivo*, decreased $\Delta\psi$ and increased ROS level are detected in the mouse brain overexpressing predominantly N-terminally acetylated α-synuclein (Sarafian et al., 2013), suggesting that *N*-α-acetylation of α-synuclein cause mitochondrial dysfunction and have pathological implications in PD. Consistently, knockdown of deacetylase SIRT3 (NAD-dependent protein deacetylase sirtuin-3) in SH-SY5Y cells significantly increases rotenone-induced α-synuclein accumulation and reduces the activities of SOD (superoxide dismutase) and GSH (glutathione), leading to increased ROS generation and damaged mitochondria (Zhang et al., 2016). SIRT3 is also reported to be inversely related to the acetylation of Parkin and PINK1—acetylated PINK1 and Parkin are increased with knockdown of SIRT3 but decreased with overexpression of

SIRT3 (Wei et al., 2017). PKAN (pantothenate kinase-associated neurodegeneration) is the enzyme catalyzing the first and rate-limiting step of CoA synthesis (Leonardi et al., 2005). A recently study reported that Fbl (Fumble, *Drosophila* homolog of PANK2), functioning downstream of PINK1, regulates acetylation of Ref(2)P (*Drosophila* homolog of P62) and promotes mitophagy activity (Huang et al., 2022).

4.3 S-nitrosylation-regulated mitochondrial function and Parkinson's disease

S-nitrosylation involves the covalent attachment of a nitro oxide group (-NO) to the thiol side chain of a cysteine residue within a protein (Hess and Stamler, 2012). Like other PTMs, s-nitrosylation has emerged as an important regulator of various classes of proteins. S-nitrosylation plays a role in PD-related mitochondrial pathology through its modification of Parkin and PINK1. The initial two studies showing Parkin could be s-nitrosylated were both published in 2004, yielding contrary conclusions. Chung et al. (2004) reported that s-nitrosylation of Parkin inhibits its E3 ligase activity, resulting in decreased ubiquitination of Parkin substrates, including Parkin itself and Synphilin-1. While Yao et al. (2004) found that s-nitrosylation of Parkin stimulates its E3 ligase activity, leading to increased self-ubiquitination. Later on, Ozawa et al. (2013) reported that Parkin is predominantly s-nitrosylated at residue C323 resulting in activation of Parkin's E3 ligase activity and induces mitochondrial degradation. Interestingly, s-nitrosylation of Parkin is regulated by DJ-1, another PD-associated protein that has been found in the same complex with Parkin and PINK1 (Tang et al., 2006; Xiong et al., 2009). Loss-of-function of DJ-1 results in decreased s-nitrosylation of Parkin, along with increased mitochondrial depolarization and cell death (Ozawa et al., 2020), adding additional evidence for the long-observed functional interaction between Parkin, PINK1, and DJ-1. Intriguingly, s-nitrosylation has also been observed with PINK1 at residue C568 that negatively regulates PINK1 kinase activity, therefore reducing PINK1-dependent phosphorylation and activation of Parkin (Oh et al., 2017). However, the detailed mechanisms of how s-nitrosylation regulates Parkin and PINK1 mediated mitophagy, as well as whether DJ-1 is also required for PINK1's s-nitrosylation, remain unclear and require further study to elucidate.

5 Perspectives and conclusion

Mounting evidence indicates involvement of PTMs-regulated mitochondrial functions in the PD etiology. A major challenge in the field is to distinguish physiological functions from the pathological roles within these pathways implicated in PD. For example, understanding how PINK1/Parkin- and BNIP3-regulated mitophagy contributes to PD pathogenesis is crucial. It is well known that PINK1 and Parkin can function both collaboratively and independently regulating mitochondrial functions, but which function of PINK1 and Parkin is critical for PD? Moreover, since the deletion of PINK1, Parkin, or both does not result in significant DA neurodegeneration in mouse models, are there other factors important for DA neurodegeneration in patients carrying PINK1 and Parkin mutations?

Phosphorylated tau protein has recently been demonstrated as a valuable biomarker of Alzheimer's disease at a systemic level (Karikari et al., 2020; Teunissen et al., 2022). A deeper understanding of the PD-related, specific alterations of PTMs-especially those with significant consequences on mitochondrial functions—may lead to candidates for the long sought-after biomarkers for PD. However, the development of PD biomarkers based on PTMs is currently in its early stages.

Author contributions

SL: Writing – original draft, Writing – review & editing. DW: Writing – original draft, Writing – review & editing. ZZ: Conceptualization, Writing – review & editing.

Funding

The authors declare financial support was received for the research, authorship, and/or publication of this article. This work was supported by the National Natural Science Foundation of China (8171101313, 81842044, 31730036, 81429002, and 31330031), the Discipline Innovative Engineering Plan (111 Program) of China (B13036), the Department of Science and Technology of Hunan Province (2021SK1010, 2016TP1006, 2018SK1030, 2022WZ1027, and 2021SK1014), the Department of Science and Technology of Changsha City (KC1702038), and the Education Department Program of Hunan Province (HNJG-2020-0440).

Conflict of interest

The authors declare that the research was conducted in the absence of any commercial or financial relationships that could be construed as a potential conflict of interest.

Publisher's note

References

Aerts, L., Craessaerts, K., De Strooper, B., and Morais, V. A. (2015). PINK1 kinase catalytic activity is regulated by phosphorylation on serines 228 and 402. *J. Biol. Chem.* 290, 2798–2811. doi: 10.1074/jbc.M114.620906

Akutsu, M., Dikic, I., and Bremm, A. (2016). Ubiquitin chain diversity at a glance. *J. Cell Sci.* 129, 875–880. doi: 10.1242/jcs.183954

Andres-Mateos, E., Perier, C., Zhang, L., Blanchard-Fillion, B., Greco, T. M., Thomas, B., et al. (2007). DJ-1 gene deletion reveals that DJ-1 is an atypical peroxiredoxin-like peroxidase. *Proc. Natl. Acad. Sci. U.S.A.* 104, 14807–14812. doi: 10.1073/pnas.0703219104

Angeles, D. C., Gan, B. H., Onstead, L., Zhao, Y., Lim, K. L., Dachsel, J., et al. (2011). Mutations in LRRK2 increase phosphorylation of peroxiredoxin 3 exacerbating oxidative stress-induced neuronal death. *Hum. Mutat.* 32, 1390–1397. doi: 10.1002/humu.21582

Angeles, D. C., Ho, P., Chua, L. L., Wang, C., Yap, Y. W., Ng, C., et al. (2014). Thiol peroxidases ameliorate LRRK2 mutant-induced mitochondrial and dopaminergic neuronal degeneration in Drosophila. *Hum. Mol. Genet.* 23, 3157–3165. doi: 10.1093/hmg/ddu026

Arena, G., Gelmetti, V., Torosantucci, L., Vignone, D., Lamorte, G., De Rosa, P., et al. (2013). PINK1 protects against cell death induced by mitochondrial depolarization, by phosphorylating Bcl-xL and impairing its pro-apoptotic cleavage. *Cell Death Differ.* 20, 920–930. doi: 10.1038/cdd.2013.19

Ascherio, A., and Schwarzschild, M. A. (2016). The epidemiology of Parkinson's disease: Risk factors and prevention. *Lancet Neurol.* 15, 1257–1272. doi: 10.1016/S1474-4422(16)30230-7

Atashrazm, F., Hammond, D., Perera, G., Bolliger, M. F., Matar, E., Halliday, G. M., et al. (2019). LRRK2-mediated Rab10 phosphorylation in immune cells from Parkinson's disease patients. *Mov. Disord.* 34, 406–415. doi: 10.1002/mds.27601

Bahnassawy, L., Nicklas, S., Palm, T., Menzl, I., Birzele, F., Gillardon, F., et al. (2013). The parkinson's disease-associated LRRK2 mutation R1441G inhibits neuronal differentiation of neural stem cells. *Stem Cells Dev.* 22, 2487–2496. doi: 10.1089/scd.2013.0163

Basso, V., Marchesan, E., Peggion, C., Chakraborty, J., von Stockum, S., Giacomello, M., et al. (2018). Regulation of ER-mitochondria contacts by Parkin via Mfn2. *Pharmacol. Res.* 138, 43–56. doi: 10.1016/j.phrs.2018.09.006

Bekris, L. M. I, Mata, F., and Zabetian, C. P. (2010). The genetics of Parkinson disease. *J. Geriatr. Psychiatry Neurol.* 23, 228–242. doi: 10.1177/0891988710383572

Billingsley, K. J., Barbosa, I. A., Bandres-Ciga, S., Quinn, J. P., Bubb, V. J., Deshpande, C., et al. (2019). Mitochondria function associated genes contribute to Parkinson's disease risk and later age at onset. *NPJ Park. Dis.* 5:8. doi: 10.1038/s41531-019-0080-x

Biskup, S., Moore, D. J., Celsi, F., Higashi, S., West, A. B., Andrabi, S. A., et al. (2006). Localization of LRRK2 to membranous and vesicular structures in mammalian brain. *Ann. Neurol.* 60, 557–569. doi: 10.1002/ana.21019

Blumenreich, S., Barav, O. B., Jenkins, B. J., and Futerman, A. H. (2020). Lysosomal storage disorders shed light on lysosomal dysfunction in Parkinson's disease. *Int. J. Mol. Sci.* 21:4966. doi: 10.3390/ijms21144966

Bonello, F., Hassoun, S. M., Mouton-Liger, F., Shin, Y. S., Muscat, A., Tesson, C., et al. (2019). LRRK2 impairs PINK1/Parkin-dependent mitophagy via its kinase activity: Pathologic insights into Parkinson's disease. *Hum. Mol. Genet.* 28, 1645–1660. doi: 10.1093/hmg/ddz004

Bonifati, V., Rizzu, P., van Baren, M. J., Schaap, O., Breedveld, G. J., Krieger, E., et al. (2003). Mutations in the DJ-1 gene associated with autosomal recessive early-onset parkinsonism. *Science* 299, 256–259. doi: 10.1126/science.1077209

Broadway, B. J., Boneski, P. K., Bredenberg, J. M., Kolicheski, A., Hou, X., Soto-Beasley, A. I., et al. (2022). Systematic functional analysis of PINK1 and PRKN coding variants. *Cells* 11:2426. doi: 10.3390/cells11152426

Burchell, V. S., Nelson, D. E., Sanchez-Martinez, A., Delgado-Camprubi, M., Ivatt, R. M., Pogson, J. H., et al. (2013). The Parkinson's disease-linked proteins Fbxo7 and Parkin interact to mediate mitophagy. *Nat. Neurosci.* 16, 1257–1265. doi: 10.1038/nn.3489

Burre, J., Sharma, M., Tsetsenis, T., Buchman, V., Etherton, M. R., and Sudhof, T. C. (2010). Alpha-synuclein promotes SNARE-complex assembly in vivo and in vitro. *Science* 329, 1663–1667. doi: 10.1126/science.1195227

Cadete, V. J., Deschenes, S., Cuillerier, A., Brisebois, F., Sugiura, A., Vincent, A., et al. (2016). Formation of mitochondrial-derived vesicles is an active and physiologically relevant mitochondrial quality control process in the cardiac system. *J. Physiol.* 594, 5343–5362. doi: 10.1113/JP272703

Cai, C., Wu, F., He, J., Zhang, Y., Shi, N., Peng, X., et al. (2022). Mitochondrial quality control in diabetic cardiomyopathy: From molecular mechanisms to therapeutic strategies. *Int. J. Biol. Sci.* 18, 5276–5290. doi: 10.7150/ijbs.75402

Cali, T., Ottolini, D., Negro, A., and Brini, M. (2013). Enhanced parkin levels favor ER-mitochondria crosstalk and guarantee Ca(2+) transfer to sustain cell bioenergetics. *Biochim. Biophys. Acta* 1832, 495–508. doi: 10.1016/j.bbadis.2013.01.004

Cardona, F., Sanchez-Mut, J. V., Dopazo, H., and Perez-Tur, J. (2011). Phylogenetic and in silico structural analysis of the Parkinson disease-related kinase PINK1. *Hum. Mutat.* 32, 369–378. doi: 10.1002/humu.21444

Cereghetti, G. M., Stangherlin, A., Martins de Brito, O., Chang, C. R., Blackstone, C., Bernardi, P., et al. (2008). Dephosphorylation by calcineurin regulates translocation of Drp1 to mitochondria. *Proc. Natl. Acad. Sci. U.S.A.* 105, 15803–15808. doi: 10.1073/pnas.0808249105

Cha, Y., Kim, T., Jeon, J., Jang, Y., Kim, P. B., Lopes, C., et al. (2021). SIRT2 regulates mitochondrial dynamics and reprogramming via MEK1-ERK-DRP1 and AKT1-DRP1 axes. *Cell Rep.* 37:110155. doi: 10.1016/j.celrep.2021.110155

Chan, N. C., Salazar, A. M., Pham, A. H., Sweredoski, M. J., Kolawa, N. J., Graham, R. L., et al. (2011). Broad activation of the ubiquitin-proteasome system by Parkin is critical for mitophagy. *Hum. Mol. Genet.* 20, 1726–1737. doi: 10.1093/hmg/ddr048

Chen, H., and Chan, D. C. (2017). Mitochondrial dynamics in regulating the unique phenotypes of cancer and stem cells. *Cell Metab.* 26, 39–48. doi: 10.1016/j.cmet.2017.05.016

Chen, T., Tan, J., Wan, Z., Zou, Y., Afewerky, H. K., Zhang, Z., et al. (2017). Effects of commonly used pesticides in china on the mitochondria and ubiquitin-proteasome system in Parkinson's disease. *Int. J. Mol. Sci.* 18:2507. doi: 10.3390/ijms18122507

Chen, Y., and Dorn, G. W. II (2013). PINK1-phosphorylated mitofusin 2 is a Parkin receptor for culling damaged mitochondria. *Science* 340, 471–475. doi: 10.1126/science.1231031

Cherian, A., K, P. D., and Vijayaraghavan, A. (2023). Parkinson's disease - genetic cause. *Curr. Opin. Neurol.* 36, 292–301. doi: 10.1097/WCO.0000000000001167

Chin, L. S., and Li, L. (2016). Ubiquitin phosphorylation in Parkinson's disease: Implications for pathogenesis and treatment. *Transl. Neurodegener.* 5:1. doi: 10.1186/s40035-015-0049-6

Cho, H. J., Liu, G., Jin, S. M., Parisiadou, L., Xie, C., Yu, J., et al. (2013). MicroRNA-205 regulates the expression of Parkinson's disease-related leucine-rich repeat kinase 2 protein. *Hum. Mol. Genet.* 22, 608–620. doi: 10.1093/hmg/dds470

Choubey, V., Safiulina, D., Vaarmann, A., Cagalinec, M., Wareski, P., Kuum, M., et al. (2011). Mutant A53T alpha-synuclein induces neuronal death by increasing mitochondrial autophagy. *J. Biol. Chem.* 286, 10814–10824. doi: 10.1074/jbc.M110.132514

Chung, K. K., Thomas, B., Li, X., Pletnikova, O., Troncoso, J. C., Marsh, L., et al. (2004). S-nitrosylation of parkin regulates ubiquitination and compromises Parkin's protective function. *Science* 304, 1328–1331. doi: 10.1126/science.1093891

Clark, I. E., Dodson, M. W., Jiang, C., Cao, J. H., Huh, J. R., Seol, J. H., et al. (2006). Drosophila pink1 is required for mitochondrial function and interacts genetically with parkin. *Nature* 441, 1162–1166. doi: 10.1038/nature04779

Cook, D. A., Kannarkat, G. T., Cintron, A. F., Butkovich, L. M., Fraser, K. B., Chang, J., et al. (2017). LRRK2 levels in immune cells are increased in Parkinson's disease. *NPJ Park. Dis.* 3:11. doi: 10.1038/s41531-017-0010-8

Costa, A. C., Loh, S. H., and Martins, L. M. (2013). Drosophila Trap1 protects against mitochondrial dysfunction in a PINK1/parkin model of Parkinson's disease. *Cell Death Dis.* 4:e467. doi: 10.1038/cddis.2012.205

Cunningham, C. N., Baughman, J. M., Phu, L., Tea, J. S., Yu, C., Coons, M., et al. (2015). USP30 and parkin homeostatically regulate atypical ubiquitin chains on mitochondria. *Nat. Cell Biol.* 17, 160–169. doi: 10.1038/ncb3097

da Silva Rosa, S. C., Martens, M. D., Field, J. T., Nguyen, L., Kereliuk, S. M., Hai, Y., et al. (2021). BNIP3L/Nix-induced mitochondrial fission, mitophagy, and impaired myocyte glucose uptake are abrogated by PRKA/PKA phosphorylation. *Autophagy* 17, 2257–2272. doi: 10.1080/15548627.2020.1821548

de Brito, O. M., and Scorrano, L. (2008). Mitofusin 2 tethers endoplasmic reticulum to mitochondria. *Nature* 456, 605–610. doi: 10.1038/nature07534

De Virgilio, A., Greco, A., Fabbrini, G., Inghilleri, M., Rizzo, M. I., Gallo, A., et al. (2016). Parkinson's disease: Autoimmunity and neuroinflammation. *Autoimmun. Rev.* 15, 1005–1011. doi: 10.1016/j.autrev.2016.07.022

Deas, E., Plun-Favreau, H., Gandhi, S., Desmond, H., Kjaer, S., Loh, S. H., et al. (2011). PINK1 cleavage at position A103 by the mitochondrial protease PARL. *Hum. Mol. Genet.* 20, 867–879. doi: 10.1093/hmg/ddq526

Delbroek, L., Van Kolen, K., Steegmans, L., da Cunha, R., Mandemakers, W., Daneels, G., et al. (2013). Development of an enzyme-linked immunosorbent assay for detection of cellular and in vivo LRRK2 S935 phosphorylation. *J. Pharm. Biomed. Anal.* 76, 49–58. doi: 10.1016/j.jpba.2012.12.002

Deng, H., Dodson, M. W., Huang, H., and Guo, M. (2008). The Parkinson's disease genes pink1 and parkin promote mitochondrial fission and/or inhibit fusion in Drosophila. *Proc. Natl. Acad. Sci. U.S.A.* 105, 14503–14508. doi: 10.1073/pnas.0803998105

Devi, L., and Anandatheerthavarada, H. K. (2010). Mitochondrial trafficking of APP and alpha synuclein: Relevance to mitochondrial dysfunction in Alzheimer's and Parkinson's diseases. *Biochim. Biophys. Acta* 1802, 11–19. doi: 10.1016/j.bbadis.2009.07.007

Devi, L., Raghavendran, V., Prabhu, B. M., Avadhani, N. G., and Anandatheerthavarada, H. K. (2008). Mitochondrial import and accumulation of alpha-synuclein impair complex I in human dopaminergic neuronal cultures and Parkinson disease brain. *J. Biol. Chem.* 283, 9089–9100. doi: 10.1074/jbc.M710012200

Di Fonzo, A., Dekker, M. C., Montagna, P., Baruzzi, A., Yonova, E. H., Correia Guedes, L., et al. (2009). FBXO7 mutations cause autosomal recessive, early-onset parkinsonian-pyramidal syndrome. *Neurology* 72, 240–245. doi: 10.1212/01.wnl.0000338144.10967.2b

Drazic, A., Myklebust, L. M., Ree, R., and Arnesen, T. (2016). The world of protein acetylation. *Biochim. Biophys. Acta* 1864, 1372–1401. doi: 10.1016/j.bbapap.2016.06.007

Durcan, T. M., and Fon, E. A. (2015). The three 'P's of mitophagy: PARKIN, PINK1, and post-translational modifications. *Genes Dev.* 29, 989–999. doi: 10.1101/gad.262758.115

Durcan, T. M., Kontogiannea, M., Bedard, N., Wing, S. S., and Fon, E. A. (2012). Ataxin-3 deubiquitination is coupled to Parkin ubiquitination via E2 ubiquitin-conjugating enzyme. *J. Biol. Chem.* 287, 531–541. doi: 10.1074/jbc.M111.288449

Durcan, T. M., Tang, M. Y., Perusse, J. R., Dashti, E. A., Aguileta, M. A., McLelland, G. L., et al. (2014). USP8 regulates mitophagy by removing K6-linked ubiquitin conjugates from parkin. *EMBO J.* 33, 2473–2491. doi: 10.15252/embj.201489729

Ebrahimi-Fakhari, D., Wahlster, L., and McLean, P. J. (2012). Protein degradation pathways in Parkinson's disease: Curse or blessing. *Acta Neuropathol.* 124, 153–172. doi: 10.1007/s00401-012-1004-6

Eiyama, A., and Okamoto, K. (2015). PINK1/Parkin-mediated mitophagy in mammalian cells. *Curr. Opin. Cell Biol.* 33, 95–101. doi: 10.1016/j.ceb.2015.01.002

Elia, A. E., Petrucci, S., Fasano, A., Guidi, M., Valbonesi, S., Bernardini, L., et al. (2013). Alpha-synuclein gene duplication: Marked intrafamilial variability in two novel pedigrees. *Mov. Disord.* 28, 813–817. doi: 10.1002/mds.25518

Ellard, S., Colclough, K., Patel, K. A., and Hattersley, A. T. (2020). Prediction algorithms: Pitfalls in interpreting genetic variants of autosomal dominant monogenic diabetes. *J. Clin. Invest.* 130, 14–16. doi: 10.1172/JCI133516

Fan, Y., Howden, A. J. M., Sarhan, A. R., Lis, P., Ito, G., Martinez, T. N., et al. (2018). Interrogating Parkinson's disease LRRK2 kinase pathway activity by assessing Rab10 phosphorylation in human neutrophils. *Biochem. J.* 475, 23–44. doi: 10.1042/BCJ20170803

Fiesel, F. C., Ando, M., Hudec, R., Hill, A. R., Castanedes-Casey, M., Caulfield, T. R., et al. (2015). (Patho-)physiological relevance of PINK1-dependent ubiquitin phosphorylation. *EMBO Rep.* 16, 1114–1130. doi: 10.15252/embr.201540514

Foulds, P. G., Mitchell, J. D., Parker, A., Turner, R., Green, G., Diggle, P., et al. (2011). Phosphorylated alpha-synuclein can be detected in blood plasma and is potentially a useful biomarker for Parkinson's disease. *FASEB J.* 25, 4127–4137. doi: 10.1096/fj.10-179192

Foulds, P. G., Yokota, O., Thurston, A., Davidson, Y., Ahmed, Z., Holton, J., et al. (2012). Post mortem cerebrospinal fluid alpha-synuclein levels are raised in multiple system atrophy and distinguish this from the other alpha-synucleinopathies, Parkinson's disease and Dementia with Lewy bodies. *Neurobiol. Dis.* 45, 188–195. doi: 10.1016/j.nbd.2011.08.003

Frank-Cannon, T. C., Tran, T., Ruhn, K. A., Martinez, T. N., Hong, J., Marvin, M., et al. (2008). Parkin deficiency increases vulnerability to inflammation-related nigral degeneration. *J. Neurosci.* 28, 10825–10834. doi: 10.1523/JNEUROSCI.3001-08.2008

Fraser, K. B., Rawlins, A. B., Clark, R. G., Alcalay, R. N., Standaert, D. G., Liu, N., et al. (2016). Ser(P)-1292 LRRK2 in urinary exosomes is elevated in idiopathic Parkinson's disease. *Mov. Disord.* 31, 1543–1550. doi: 10.1002/mds.26686

Fuchs, J., Nilsson, C., Kachergus, J., Munz, M., Larsson, E. M., Schule, B., et al. (2007). Phenotypic variation in a large Swedish pedigree due to SNCA duplication and triplication. *Neurology* 68, 916–922. doi: 10.1212/01.wnl.0000254458.17630.c5

Fujii, J., and Ikeda, Y. (2002). Advances in our understanding of peroxiredoxin, a multifunctional, mammalian redox protein. *Redox Rep.* 7, 123–130. doi: 10.1179/135100002125000352

Funayama, M., Hasegawa, K., Kowa, H., Saito, M., Tsuji, S., and Obata, F. (2002). A new locus for Parkinson's disease (PARK8) maps to chromosome 12p11.2-q13.1. *Ann. Neurol.* 51, 296–301. doi: 10.1002/ana.10113

Funayama, M., Ohe, K., Amo, T., Furuya, N., Yamaguchi, J., Saiki, S., et al. (2015). CHCHD2 mutations in autosomal dominant late-onset Parkinson's disease: A genome-wide linkage and sequencing study. *Lancet Neurol.* 14, 274–282. doi: 10.1016/S1474-4422(14)70266-2

Futter, C. E., Pearse, A., Hewlett, L. J., and Hopkins, C. R. (1996). Multivesicular endosomes containing internalized EGF-EGF receptor complexes mature and then fuse directly with lysosomes. *J. Cell Biol.* 132, 1011–1023. doi: 10.1083/jcb.132.6.1011

Gandhi, S., Wood-Kaczmar, A., Yao, Z., Plun-Favreau, H., Deas, E., Klupsch, K., et al. (2009). PINK1-associated Parkinson's disease is caused by neuronal vulnerability to calcium-induced cell death. *Mol. Cell* 33, 627–638. doi: 10.1016/j.molcel.2009.02.013

Gautier, E. F., Ducamp, S., Leduc, M., Salnot, V., Guillonneau, F., Dussiot, M., et al. (2016). Comprehensive proteomic analysis of human erythropoiesis. *Cell Rep.* 16, 1470–1484. doi: 10.1016/j.celrep.2016.06.085

Ge, P., Dawson, V. L., and Dawson, T. M. (2020). PINK1 and Parkin mitochondrial quality control: A source of regional vulnerability in Parkinson's disease. *Mol. Neurodegener.* 15:20. doi: 10.1186/s13024-020-00367-7

Gegg, M. E., Cooper, J. M., Chau, K. Y., Rojo, M., Schapira, A. H., and Taanman, J. W. (2010). Mitofusin 1 and mitofusin 2 are ubiquitinated in a PINK1/parkin-dependent manner upon induction of mitophagy. *Hum. Mol. Genet.* 19, 4861–4870. doi: 10.1093/hmg/ddq419

Geldenhuys, W. J., Abdelmagid, S. M., Gallegos, P. J., and Safadi, F. F. (2014). Parkinson's disease biomarker: A patent evaluation of WO2013153386. *Expert Opin. Ther. Pat.* 24, 947–951. doi: 10.1517/13543776.2014.931375

Gilks, W. P., Abou-Sleiman, P. M., Gandhi, S., Jain, S., Singleton, A., Lees, A. J., et al. (2005). A common LRRK2 mutation in idiopathic Parkinson's disease. *Lancet* 365, 415–416. doi: 10.1016/S0140-6736(05)17830-1

Goldman, S. M. (2014). Environmental toxins and Parkinson's disease. *Annu. Rev. Pharmacol. Toxicol.* 54, 141–164. doi: 10.1146/annurev-pharmtox-011613-135937

Gonzalez-Hunt, C. P., Thacker, E. A., Toste, C. M., Boularand, S., Deprets, S., Dubois, L., et al. (2020). Mitochondrial DNA damage as a potential biomarker of LRRK2 kinase activity in LRRK2 Parkinson's disease. *Sci. Rep.* 10:17293. doi: 10.1038/s41598-020-74195-6

Greene, A. W., Grenier, K., Aguileta, M. A., Muise, S., Farazifard, R., Haque, M. E., et al. (2012). Mitochondrial processing peptidase regulates PINK1 processing, import and Parkin recruitment. *EMBO Rep.* 13, 378–385. doi: 10.1038/embor.2012.14

Greene, J. C., Whitworth, A. J., Kuo, I., Andrews, L. A., Feany, M. B., and Pallanck, L. J. (2003). Mitochondrial pathology and apoptotic muscle degeneration in Drosophila parkin mutants. *Proc. Natl. Acad. Sci. U.S.A.* 100, 4078–4083. doi: 10.1073/pnas.0737556100

Guerra de Souza, A. C., Prediger, R. D., and Cimarosti, H. (2016). SUMO-regulated mitochondrial function in Parkinson's disease. *J. Neurochem.* 137, 673–686. doi: 10.1111/jnc.13599

Gui, Y., Liu, H., Zhang, L., Lv, W., and Hu, X. (2015). Altered microRNA profiles in cerebrospinal fluid exosome in Parkinson disease and Alzheimer disease. *Oncotarget* 6, 37043–37053. doi: 10.18632/oncotarget.6158

Guo, C., Hildick, K. L., Luo, J., Dearden, L., Wilkinson, K. A., and Henley, J. M. (2013). SENP3-mediated deSUMOylation of dynamin-related protein 1 promotes cell death following ischaemia. *EMBO J.* 32, 1514–1528. doi: 10.1038/emboj.2013.65

Haghighat, A., Mader, S., Pause, A., and Sonenberg, N. (1995). Repression of cap-dependent translation by 4E-binding protein 1: Competition with p220 for binding to eukaryotic initiation factor-4E. *EMBO J.* 14, 5701–5709. doi: 10.1002/j.1460-2075.1995.tb00257.x

Ham, S. J., Lee, D., Yoo, H., Jun, K., Shin, H., and Chung, J. (2020). Decision between mitophagy and apoptosis by Parkin via VDAC1 ubiquitination. *Proc. Natl. Acad. Sci. U.S.A.* 117, 4281–4291. doi: 10.1073/pnas.1909814117

Han, H., Tan, J., Wang, R., Wan, H., He, Y., Yan, X., et al. (2020). PINK1 phosphorylates Drp1(S616) to regulate mitophagy-independent mitochondrial dynamics. *EMBO Rep.* 21:e48686. doi: 10.15252/embr.201948686

Henchcliffe, C., and Beal, M. F. (2008). Mitochondrial biology and oxidative stress in Parkinson disease pathogenesis. *Nat. Clin. Pract. Neurol.* 4, 600–609. doi: 10.1038/ncpneuro0924

Heo, H. Y., Park, J. M., Kim, C. H., Han, B. S., Kim, K. S., and Seol, W. (2010). LRRK2 enhances oxidative stress-induced neurotoxicity via its kinase activity. *Exp. Cell Res.* 316, 649–656. doi: 10.1016/j.yexcr.2009.09.014

Heo, J. M., Ordureau, A., Paulo, J. A., Rinehart, J., and Harper, J. W. (2015). The PINK1-PARKIN mitochondrial ubiquitylation pathway drives a program of OPTN/NDP52 recruitment and TBK1 activation to promote mitophagy. *Mol. Cell* 60, 7–20. doi: 10.1016/j.molcel.2015.08.016

Hernandez, D. G., Reed, X., and Singleton, A. B. (2016). Genetics in Parkinson disease: Mendelian versus non-Mendelian inheritance. *J. Neurochem.* 139 Suppl 1(Suppl. 1), 59–74. doi: 10.1111/jnc.13593

Hess, D. T., and Stamler, J. S. (2012). Regulation by S-nitrosylation of protein post-translational modification. *J. Biol. Chem.* 287, 4411–4418. doi: 10.1074/jbc.R111.285742

Heyn, J., Heuschkel, M. A., and Goettsch, C. (2023). Mitochondrial-derived vesicles-link to extracellular vesicles and implications in cardiovascular disease. *Int. J. Mol. Sci.* 24:2637. doi: 10.3390/ijms24032637

Hierro, A., Rojas, A. L., Rojas, R., Murthy, N., Effantin, G., Kajava, A. V., et al. (2007). Functional architecture of the retromer cargo-recognition complex. *Nature* 449, 1063–1067. doi: 10.1038/nature06216

Hirai, I., and Wang, H. G. (2001). Survival-factor-induced phosphorylation of Bad results in its dissociation from Bcl-x(L) but not Bcl-2. *Biochem J* 359(Pt. 2), 345–352. doi: 10.1042/0264-6021:3590345

Ho, D. H., Je, A. R., Lee, H., Son, I., Kweon, H. S., Kim, H. G., et al. (2018). LRRK2 kinase activity induces mitochondrial fission in microglia via Drp1 and modulates neuroinflammation. *Exp. Neurobiol.* 27, 171–180. doi: 10.5607/en.2018.27.3.171

Hong, Z., Shi, M., Chung, K. A., Quinn, J. F., Peskind, E. R., Galasko, D., et al. (2010). DJ-1 and alpha-synuclein in human cerebrospinal fluid as biomarkers of Parkinson's disease. *Brain* 133(Pt. 3), 713–726. doi: 10.1093/brain/awq008

Howlett, E. H., Jensen, N., Belmonte, F., Zafar, F., Hu, X., Kluss, J., et al. (2017). LRRK2 G2019S-induced mitochondrial DNA damage is LRRK2 kinase dependent and inhibition restores mtDNA integrity in Parkinson's disease. *Hum. Mol. Genet.* 26, 4340–4351. doi: 10.1093/hmg/ddx320

Hsieh, C. H., Shaltouki, A., Gonzalez, A. E., Bettencourt da Cruz, A., Burbulla, L. F., St Lawrence, E., et al. (2016). Functional impairment in miro degradation and mitophagy is a shared feature in familial and sporadic Parkinson's disease. *Cell Stem Cell* 19, 709–724. doi: 10.1016/j.stem.2016.08.002

Huang, E., Qu, D., Huang, T., Rizzi, N., Boonying, W., Krolak, D., et al. (2017). PINK1-mediated phosphorylation of LETM1 regulates mitochondrial calcium transport and protects neurons against mitochondrial stress. *Nat. Commun.* 8:1399. doi: 10.1038/s41467-017-01435-1

Huang, Y., Wan, Z., Tang, Y., Xu, J., Laboret, B., Nallamothu, S., et al. (2022). Pantothenate kinase 2 interacts with PINK1 to regulate mitochondrial quality control via acetyl-CoA metabolism. *Nat. Commun.* 13:2412. doi: 10.1038/s41467-022-30178-x

Hunn, B. H., Cragg, S. J., Bolam, J. P., Spillantini, M. G., and Wade-Martins, R. (2015). Impaired intracellular trafficking defines early Parkinson's disease. *Trends Neurosci.* 38, 178–188. doi: 10.1016/j.tins.2014.12.009

Imai, Y., Gehrke, S., Wang, H. Q., Takahashi, R., Hasegawa, K., Oota, E., et al. (2008). Phosphorylation of 4E-BP by LRRK2 affects the maintenance of dopaminergic neurons in Drosophila. *EMBO J.* 27, 2432–2443. doi: 10.1038/emboj.2008.163

Imai, Y., Soda, M., and Takahashi, R. (2000). Parkin suppresses unfolded protein stress-induced cell death through its E3 ubiquitin-protein ligase activity. *J. Biol. Chem.* 275, 35661–35664. doi: 10.1074/jbc.C000447200

Ivankovic, D., Chau, K. Y., Schapira, A. H., and Gegg, M. E. (2016). Mitochondrial and lysosomal biogenesis are activated following PINK1/parkin-mediated mitophagy. *J. Neurochem.* 136, 388–402. doi: 10.1111/jnc.13412

Jang, J., Jeong, S., Lee, S. I., Seol, W., Seo, H., Son, I., et al. (2018). Oxidized DJ-1 levels in urine samples as a putative biomarker for Parkinson's disease. *Park. Dis.* 2018:1241757. doi: 10.1155/2018/1241757

Jin, S. M., and Youle, R. J. (2013). The accumulation of misfolded proteins in the mitochondrial matrix is sensed by PINK1 to induce PARK2/Parkin-mediated mitophagy of polarized mitochondria. *Autophagy* 9, 1750–1757. doi: 10.4161/auto.26122

Jin, S. M., Lazarou, M., Wang, C., Kane, L. A., Narendra, D. P., and Youle, R. J. (2010). Mitochondrial membrane potential regulates PINK1 import and proteolytic destabilization by PARL. *J. Cell Biol.* 191, 933–942. doi: 10.1083/jcb.201008084

Juhasz, G. (2016). A mitochondrial-derived vesicle HOPS to endolysosomes using Syntaxin-17. *J. Cell Biol.* 214, 241–243. doi: 10.1083/jcb.201607024

Kalia, L. V., and Lang, A. E. (2015). Parkinson's disease. *Lancet* 386, 896–912. doi: 10.1016/S0140-6736(14)61393-3

Kane, L. A., Lazarou, M., Fogel, A. I., Li, Y., Yamano, K., Sarraf, S. A., et al. (2014). PINK1 phosphorylates ubiquitin to activate Parkin E3 ubiquitin ligase activity. *J. Cell Biol.* 205, 143–153. doi: 10.1083/jcb.201402104

Kang, L., Moriarty, G. M., Woods, L. A., Ashcroft, A. E., Radford, S. E., and Baum, J. (2012). N-terminal acetylation of alpha-synuclein induces increased transient helical propensity and decreased aggregation rates in the intrinsically disordered monomer. *Protein Sci.* 21, 911–917. doi: 10.1002/pro.2088

Karbowski, M., and Youle, R. J. (2011). Regulating mitochondrial outer membrane proteins by ubiquitination and proteasomal degradation. *Curr. Opin. Cell Biol.* 23, 476–482. doi: 10.1016/j.ceb.2011.05.007

Karikari, T. K., Pascoal, T. A., Ashton, N. J., Janelidze, S., Benedet, A. L., Rodriguez, J. L., et al. (2020). Blood phosphorylated tau 181 as a biomarker for Alzheimer's disease: A diagnostic performance and prediction modelling study using data from four prospective cohorts. *Lancet Neurol.* 19, 422–433. doi: 10.1016/S1474-4422(20)30071-5

Karve, T. M., and Cheema, A. K. (2011). Small changes huge impact: The role of protein posttranslational modifications in cellular homeostasis and disease. *J. Amino Acids* 2011:207691. doi: 10.4061/2011/207691

Kazlauskaite, A., Kondapalli, C., Gourlay, R., Campbell, D. G., Ritorto, M. S., Hofmann, K., et al. (2014). Parkin is activated by PINK1-dependent phosphorylation of ubiquitin at Ser65. *Biochem. J.* 460, 127–139. doi: 10.1042/BJ20140334

Khoury, G. A., Baliban, R. C., and Floudas, C. A. (2011). Proteome-wide post-translational modification statistics: Frequency analysis and curation of the swiss-prot database. *Sci. Rep.* 1:190. doi: 10.1038/srep00090

Kim, D. I., Lee, K. H., Gabr, A. A., Choi, G. E., Kim, J. S., Ko, S. H., et al. (2016). Abeta-Induced Drp1 phosphorylation through Akt activation promotes excessive mitochondrial fission leading to neuronal apoptosis. *Biochim. Biophys. Acta* 1863, 2820–2834. doi: 10.1016/j.bbamcr.2016.09.003

Kim, J., Pajarillo, E., Rizor, A., Son, D. S., Lee, J., Aschner, M., et al. (2019). LRRK2 kinase plays a critical role in manganese-induced inflammation and apoptosis in microglia. *PLoS One* 14:e0210248. doi: 10.1371/journal.pone.0210248

Kitada, T., Asakawa, S., Hattori, N., Matsumine, H., Yamamura, Y., Minoshima, S., et al. (1998). Mutations in the parkin gene cause autosomal recessive juvenile parkinsonism. *Nature* 392, 605–608. doi: 10.1038/33416

Ko, Y. U., Kim, S. J., Lee, J., Song, M. Y., Park, K. S., Park, J. B., et al. (2019). Protein kinase A-induced phosphorylation at the Thr154 affects stability of DJ-1. *Park. Relat. Disord.* 66, 143–150. doi: 10.1016/j.parkreldis.2019.07.029

Kondapalli, C., Kazlauskaite, A., Zhang, N., Woodroof, H. I., Campbell, D. G., Gourlay, R., et al. (2012). PINK1 is activated by mitochondrial membrane potential depolarization and stimulates Parkin E3 ligase activity by phosphorylating Serine 65. *Open Biol.* 2:120080. doi: 10.1098/rsob.120080

Kondapalli, K. C., Kallay, L. M., Muszelik, M., and Rao, R. (2012). Unconventional chemiosmotic coupling of NHA2, a mammalian Na+/H+ antiporter, to a plasma membrane H+ gradient. *J. Biol. Chem.* 287, 36239–36250. doi: 10.1074/jbc.M112.403550

Konig, T., Nolte, H., Aaltonen, M. J., Tatsuta, T., Krols, M., Stroh, T., et al. (2021). MIROs and DRP1 drive mitochondrial-derived vesicle biogenesis and promote quality control. *Nat. Cell Biol.* 23, 1271–1286. doi: 10.1038/s41556-021-00798-4

Koyano, F., Okatsu, K., Kosako, H., Tamura, Y., Go, E., Kimura, M., et al. (2014). Ubiquitin is phosphorylated by PINK1 to activate parkin. *Nature* 510, 162–166. doi: 10.1038/nature13392

Koyano, F., Yamano, K., Kosako, H., Tanaka, K., and Matsuda, N. (2019). Parkin recruitment to impaired mitochondria for nonselective ubiquitylation is facilitated by MITOL. *J. Biol. Chem.* 294, 10300–10314. doi: 10.1074/jbc.RA118.006302

Kraus, F., Goodall, E. A. I, Smith, R., Jiang, Y., Paoli, J. C., Adolf, F., et al. (2023). PARK15/FBXO7 is dispensable for PINK1/Parkin mitophagy in iNeurons and HeLa cell systems. *EMBO Rep.* 24:e56399. doi: 10.15252/embr.202256399

Kraus, F., Roy, K., Pucadyil, T. J., and Ryan, M. T. (2021). Function and regulation of the divisome for mitochondrial fission. *Nature* 590, 57–66. doi: 10.1038/s41586-021-03214-x

Krebiehl, G., Ruckerbauer, S., Burbulla, L. F., Kieper, N., Maurer, B., Waak, J., et al. (2010). Reduced basal autophagy and impaired mitochondrial dynamics due to loss of Parkinson's disease-associated protein DJ-1. *PLoS One* 5:e9367. doi: 10.1371/journal.pone.0009367

Kulathu, Y., and Komander, D. (2012). Atypical ubiquitylation - the unexplored world of polyubiquitin beyond Lys48 and Lys63 linkages. *Nat. Rev. Mol. Cell Biol.* 13, 508–523. doi: 10.1038/nrm3394

Kumar, A., Tamjar, J., Waddell, A. D., Woodroof, H. I., Raimi, O. G., Shaw, A. M., et al. (2017). Structure of PINK1 and mechanisms of Parkinson's disease-associated mutations. *Elife* 6:e29985. doi: 10.7554/eLife.29985

Lajoie, A. C., Lafontaine, A. L., and Kaminska, M. (2021). The spectrum of sleep disorders in Parkinson disease: A review. *Chest* 159, 818–827. doi: 10.1016/j.chest.2020.09.099

Langston, J. W., Ballard, P., Tetrud, J. W., and Irwin, I. (1983). Chronic parkinsonism in humans due to a product of meperidine-analog synthesis. *Science* 219, 979–980. doi: 10.1126/science.6823561

Lazarou, M., Jin, S. M., Kane, L. A., and Youle, R. J. (2012). Role of PINK1 binding to the TOM complex and alternate intracellular membranes in recruitment and activation of the E3 ligase Parkin. *Dev. Cell* 22, 320–333. doi: 10.1016/j.devcel.2011.12.014

Lee, J. T., Wheeler, T. C., Li, L., and Chin, L. S. (2008). Ubiquitination of alpha-synuclein by Siah-1 promotes alpha-synuclein aggregation and apoptotic cell death. *Hum. Mol. Genet.* 17, 906–917. doi: 10.1093/hmg/ddm363

Lee, Y., Stevens, D. A., Kang, S. U., Jiang, H., Lee, Y. I., Ko, H. S., et al. (2017). PINK1 primes parkin-mediated ubiquitination of PARIS in dopaminergic neuronal survival. *Cell Rep.* 18, 918–932. doi: 10.1016/j.celrep.2016.12.090

Leonardi, R., Zhang, Y. M., Rock, C. O., and Jackowski, S. (2005). Coenzyme A: Back in action. *Prog. Lipid Res.* 44, 125–153. doi: 10.1016/j.plipres.2005.04.001

Lewis, M. R., and Lewis, W. H. (1914). Mitochondria in tissue culture. *Science* 39, 330–333. doi: 10.1126/science.39.1000.330

Li, L., Muhlfeld, C., Niemann, B., Pan, R., Li, R., Hilfiker-Kleiner, D., et al. (2011). Mitochondrial biogenesis and PGC-1alpha deacetylation by chronic treadmill exercise: Differential response in cardiac and skeletal muscle. *Basic Res. Cardiol.* 106, 1221–1234. doi: 10.1007/s00395-011-0213-9

Li, W. W., Yang, R., Guo, J. C., Ren, H. M., Zha, X. L., Cheng, J. S., et al. (2007). Localization of alpha-synuclein to mitochondria within midbrain of mice. *Neuroreport* 18, 1543–1546. doi: 10.1097/WNR.0b013e3282f03db4

Li, Y., Feng, Y. F., Liu, X. T., Li, Y. C., Zhu, H. M., Sun, M. R., et al. (2021). Songorine promotes cardiac mitochondrial biogenesis via Nrf2 induction during sepsis. *Redox Biol.* 38:101771. doi: 10.1016/j.redox.2020.101771

Lin, C. H., Chen, M. L., Chen, G. S., Tai, C. H., and Wu, R. M. (2011). Novel variant Pro143Ala in HTRA2 contributes to Parkinson's disease by inducing hyperphosphorylation of HTRA2 protein in mitochondria. *Hum. Genet.* 130, 817–827. doi: 10.1007/s00439-011-1041-6

Lin, W., and Kang, U. J. (2008). Characterization of PINK1 processing, stability, and subcellular localization. *J. Neurochem.* 106, 464–474. doi: 10.1111/j.1471-4159.2008.05398.x

Lin, X., Cook, T. J., Zabetian, C. P., Leverenz, J. B., Peskind, E. R., Hu, S. C., et al. (2012). DJ-1 isoforms in whole blood as potential biomarkers of Parkinson disease. *Sci. Rep.* 2:954. doi: 10.1038/srep00954

Liu, W., Duan, X., Fang, X., Shang, W., and Tong, C. (2018). Mitochondrial protein import regulates cytosolic protein homeostasis and neuronal integrity. *Autophagy* 14, 1293–1309. doi: 10.1080/15548627.2018.1474991

Liu, Y., Lear, T. B., Verma, M., Wang, K. Z., Otero, P. A., McKelvey, A. C., et al. (2020). Chemical inhibition of FBXO7 reduces inflammation and confers neuroprotection by stabilizing the mitochondrial kinase PINK1. *JCI Insight* 5:e131834. doi: 10.1172/jci.insight.131834

Lobbestael, E., Zhao, J. I, Rudenko, N., Beylina, A., Gao, F., Wetter, J., et al. (2013). Identification of protein phosphatase 1 as a regulator of the LRRK2 phosphorylation cycle. *Biochem. J.* 456, 119–128. doi: 10.1042/BJ20121772

Lopez-Domenech, G., Covill-Cooke, C., Ivankovic, D., Halff, E. F., Sheehan, D. F., Norkett, R., et al. (2018). Miro proteins coordinate microtubule- and actin-dependent mitochondrial transport and distribution. *EMBO J.* 37, 321–336. doi: 10.15252/embj.201696380

Lutz, A. K., Exner, N., Fett, M. E., Schlehe, J. S., Kloos, K., Lammermann, K., et al. (2009). Loss of parkin or PINK1 function increases Drp1-dependent mitochondrial fragmentation. *J. Biol. Chem.* 284, 22938–22951. doi: 10.1074/jbc.M109.035774

Lwin, A., Orvisky, E., Goker-Alpan, O., LaMarca, M. E., and Sidransky, E. (2004). Glucocerebrosidase mutations in subjects with parkinsonism. *Mol. Genet. Metab.* 81, 70–73. doi: 10.1016/j.ymgme.2003.11.004

Ma, K. Y., Fokkens, M. R., van Laar, T., and Verbeek, D. S. (2021). Systematic analysis of PINK1 variants of unknown significance shows intact mitophagy function for most variants. *NPJ Park. Dis.* 7:113. doi: 10.1038/s41531-021-00258-8

Mabrouk, O. S., Chen, S., Edwards, A. L., Yang, M., Hirst, W. D., and Graham, D. L. (2020). Quantitative measurements of LRRK2 in human cerebrospinal fluid demonstrates increased levels in G2019S patients. *Front. Neurosci.* 14:526. doi: 10.3389/fnins.2020.00526

Magalhaes, P., and Lashuel, H. A. (2022). Opportunities and challenges of alpha-synuclein as a potential biomarker for Parkinson's disease and other synucleinopathies. *NPJ Park. Dis* 8:93. doi: 10.1038/s41531-022-00357-0

Manohar, S., Jacob, S., Wang, J., Wiechecki, K. A., Koh, H. W. L., Simoes, V., et al. (2019). polyubiquitin chains linked by lysine residue 48 (K48) selectively target oxidized proteins in vivo. *Antioxid. Redox Signal.* 31, 1133–1149. doi: 10.1089/ars.2019.7826

Martinez, A., Lectez, B., Ramirez, J., Popp, O., Sutherland, J. D., Urbe, S., et al. (2017). Quantitative proteomic analysis of Parkin substrates in Drosophila neurons. *Mol. Neurodegener.* 12:29. doi: 10.1186/s13024-017-0170-3

Martinez-Martin, P., Schapira, A. H., Stocchi, F., Sethi, K., Odin, P., MacPhee, G., et al. (2007). Prevalence of nonmotor symptoms in Parkinson's disease in an international setting; study using nonmotor symptoms questionnaire in 545 patients. *Mov. Disord.* 22, 1623–1629. doi: 10.1002/mds.21586

Martini, H., and Passos, J. F. (2023). Cellular senescence: All roads lead to mitochondria. *FEBS J.* 290, 1186–1202. doi: 10.1111/febs.16361

Matenia, D., Hempp, C., Timm, T., Eikhof, A., and Mandelkow, E. M. (2012). Microtubule affinity-regulating kinase 2 (MARK2) turns on phosphatase and tensin homolog (PTEN)-induced kinase 1 (PINK1) at Thr-313, a mutation site in Parkinson disease: Effects on mitochondrial transport. *J. Biol. Chem.* 287, 8174–8186. doi: 10.1074/jbc.M111.262287

Matheoud, D., Sugiura, A., Bellemare-Pelletier, A., Laplante, A., Rondeau, C., Chemali, M., et al. (2016). Parkinson's disease-related proteins PINK1 and parkin repress mitochondrial antigen presentation. *Cell* 166, 314–327. doi: 10.1016/j.cell.2016.05.039

Matsuda, N., Sato, S., Shiba, K., Okatsu, K., Saisho, K., Gautier, C. A., et al. (2010). PINK1 stabilized by mitochondrial depolarization recruits Parkin to damaged mitochondria and activates latent Parkin for mitophagy. *J. Cell Biol.* 189, 211–221. doi: 10.1083/jcb.200910140

Matteucci, A., Patron, M., Vecellio Reane, D., Gastaldello, S., Amoroso, S., Rizzuto, R., et al. (2018). Parkin-dependent regulation of the MCU complex component MICU1. *Sci. Rep.* 8:14199. doi: 10.1038/s41598-018-32551-7

McLelland, G. L., Lee, S. A., McBride, H. M., and Fon, E. A. (2016). Syntaxin-17 delivers PINK1/parkin-dependent mitochondrial vesicles to the endolysosomal system. *J. Cell Biol.* 214, 275–291. doi: 10.1083/jcb.201603105

McLelland, G. L., Soubannier, V., Chen, C. X., McBride, H. M., and Fon, E. A. (2014). Parkin and PINK1 function in a vesicular trafficking pathway regulating mitochondrial quality control. *EMBO J.* 33, 282–295. doi: 10.1002/embj.201385902

Meng, H., Yamashita, C., Shiba-Fukushima, K., Inoshita, T., Funayama, M., Sato, S., et al. (2017). Loss of Parkinson's disease-associated protein CHCHD2 affects mitochondrial crista structure and destabilizes cytochrome c. *Nat. Commun.* 8:15500. doi: 10.1038/ncomms15500

Meredith, G. E., Totterdell, S., Beales, M., and Meshul, C. K. (2009). Impaired glutamate homeostasis and programmed cell death in a chronic MPTP mouse model of Parkinson's disease. *Exp. Neurol.* 219, 334–340. doi: 10.1016/j.expneurol.2009.06.005

Mitsumoto, A., Nakagawa, Y., Takeuchi, A., Okawa, K., Iwamatsu, A., and Takanezawa, Y. (2001). Oxidized forms of peroxiredoxins and DJ-1 on two-dimensional gels increased in response to sublethal levels of paraquat. *Free Radic. Res.* 35, 301–310. doi: 10.1080/10715760100300831

Mollenhauer, B., Locascio, J. J., Schulz-Schaeffer, W., Sixel-Doring, F., Trenkwalder, C., and Schlossmacher, M. G. (2011). alpha-Synuclein and tau concentrations in cerebrospinal fluid of patients presenting with parkinsonism: A cohort study. *Lancet Neurol.* 10, 230–240. doi: 10.1016/S1474-4422(11)70014-X

Mollenhauer, B., Trautmann, E., Taylor, P., Manninger, P., Sixel-Doring, F., Ebentheuer, J., et al. (2013). Total CSF alpha-synuclein is lower in de novo Parkinson patients than in healthy subjects. *Neurosci. Lett.* 532, 44–48. doi: 10.1016/j.neulet.2012.11.004

Morais, V. A., Haddad, D., Craessaerts, K., De Bock, P. J., Swerts, J., Vilain, S., et al. (2014). PINK1 loss-of-function mutations affect mitochondrial complex I activity via NdufA10 ubiquinone uncoupling. *Science* 344, 203–207. doi: 10.1126/science.1249161

Morais, V. A., Verstreken, P., Roethig, A., Smet, J., Snellinx, A., Vanbrabant, M., et al. (2009). Parkinson's disease mutations in PINK1 result in decreased Complex I activity and deficient synaptic function. *EMBO Mol. Med.* 1, 99–111. doi: 10.1002/emmm.200900006

Mortiboys, H., Johansen, K. K., Aasly, J. O., and Bandmann, O. (2010). Mitochondrial impairment in patients with Parkinson disease with the G2019S mutation in LRRK2. *Neurology* 75, 2017–2020. doi: 10.1212/WNL.0b013e3181ff9685

Mouton-Liger, F., Jacoupy, M., Corvol, J. C., and Corti, O. (2017). PINK1/parkin-dependent mitochondrial surveillance: From pleiotropy to Parkinson's disease. *Front. Mol. Neurosci.* 10:120. doi: 10.3389/fnmol.2017.00120

Nalls, M. A., Blauwendraat, C., Vallerga, C. L., Heilbron, K., Bandres-Ciga, S., Chang, D., et al. (2019). Identification of novel risk loci, causal insights, and heritable risk for Parkinson's disease: A meta-analysis of genome-wide association studies. *Lancet Neurol.* 18, 1091–1102. doi: 10.1016/S1474-4422(19)30320-5

Narendra, D., Tanaka, A., Suen, D. F., and Youle, R. J. (2008). Parkin is recruited selectively to impaired mitochondria and promotes their autophagy. *J. Cell Biol.* 183, 795–803. doi: 10.1083/jcb.200809125

Nguyen, H. N., Byers, B., Cord, B., Shcheglovitov, A., Byrne, J., Gujar, P., et al. (2011). LRRK2 mutant iPSC-derived DA neurons demonstrate increased susceptibility to oxidative stress. *Cell Stem Cell* 8, 267–280. doi: 10.1016/j.stem.2011.01.013

Nicoletti, V., Palermo, G., Del Prete, E., Mancuso, M., and Ceravolo, R. (2021). Understanding the multiple role of mitochondria in Parkinson's disease and related disorders: Lesson from genetics and protein-interaction network. *Front. Cell Dev. Biol.* 9:636506. doi: 10.3389/fcell.2021.636506

Norris, K. L., Hao, R., Chen, L. F., Lai, C. H., Kapur, M., Shaughnessy, P. J., et al. (2015). Convergence of Parkin, PINK1, and alpha-Synuclein on Stress-induced Mitochondrial Morphological Remodeling. *J. Biol. Chem.* 290, 13862–13874. doi: 10.1074/jbc.M114.634063

Oh, C. K., Sultan, A., Platzer, J., Dolatabadi, N., Soldner, F., McClatchy, D. B., et al. (2017). S-Nitrosylation of PINK1 Attenuates PINK1/Parkin-Dependent Mitophagy in hiPSC-Based Parkinson's Disease Models. *Cell Rep.* 21, 2171–2182. doi: 10.1016/j.celrep.2017.10.068

Okatsu, K., Iemura, S., Koyano, F., Go, E., Kimura, M., Natsume, T., et al. (2012a). Mitochondrial hexokinase HKI is a novel substrate of the Parkin ubiquitin ligase. *Biochem. Biophys. Res. Commun.* 428, 197–202. doi: 10.1016/j.bbrc.2012.10.041

Okatsu, K., Oka, T., Iguchi, M., Imamura, K., Kosako, H., Tani, N., et al. (2012b). PINK1 autophosphorylation upon membrane potential dissipation is essential for Parkin recruitment to damaged mitochondria. *Nat. Commun.* 3:1016. doi: 10.1038/ncomms2016

Olzmann, J. A., Li, L., Chudaev, M. V., Chen, J., Perez, F. A., Palmiter, R. D., et al. (2007). Parkin-mediated K63-linked polyubiquitination targets misfolded DJ-1 to aggresomes via binding to HDAC6. *J. Cell Biol.* 178, 1025–1038. doi: 10.1083/jcb.200611128

Ordureau, A., Heo, J. M., Duda, D. M., Paulo, J. A., Olszewski, J. L., Yanishevski, D., et al. (2015). Defining roles of PARKIN and ubiquitin phosphorylation by PINK1 in mitochondrial quality control using a ubiquitin replacement strategy. *Proc. Natl. Acad. Sci. U.S.A.* 112, 6637–6642. doi: 10.1073/pnas.1506593112

Ordureau, A., Paulo, J. A., Zhang, W., Ahfeldt, T., Zhang, J., Cohn, E. F., et al. (2018). Dynamics of PARKIN-dependent mitochondrial ubiquitylation in induced neurons and model systems revealed by digital snapshot proteomics. *Mol. Cell* 70, 211–227e8. doi: 10.1016/j.molcel.2018.03.012

Ordureau, A., Sarraf, S. A., Duda, D. M., Heo, J. M., Jedrychowski, M. P., Sviderskiy, V. O., et al. (2014). Quantitative proteomics reveal a feedforward mechanism for

mitochondrial PARKIN translocation and ubiquitin chain synthesis. *Mol. Cell* 56, 360–375. doi: 10.1016/j.molcel.2014.09.007

Ozawa, K., Komatsubara, A. T., Nishimura, Y., Sawada, T., Kawafune, H., Tsumoto, H., et al. (2013). S-nitrosylation regulates mitochondrial quality control via activation of parkin. *Sci. Rep.* 3:2202. doi: 10.1038/srep02202

Ozawa, K., Tsumoto, H., Miura, Y., Yamaguchi, J., Iguchi-Ariga, S. M. M., Sakuma, T., et al. (2020). DJ-1 is indispensable for the S-nitrosylation of Parkin, which maintains function of mitochondria. *Sci. Rep.* 10:4377. doi: 10.1038/s41598-020-61287-6

Padman, B. S., Nguyen, T. N., Uoselis, L., Skulsuppaisarn, M., Nguyen, L. K., and Lazarou, M. (2019). LC3/GABARAPs drive ubiquitin-independent recruitment of Optineurin and NDP52 to amplify mitophagy. *Nat. Commun.* 10:408. doi: 10.1038/s41467-019-08335-6

Padmanabhan, S., Lanz, T. A., Gorman, D., Wolfe, M., Joyce, A., Cabrera, C., et al. (2020). An assessment of LRRK2 serine 935 phosphorylation in human peripheral blood mononuclear cells in idiopathic Parkinson's disease and G2019S LRRK2 cohorts. *J. Park. Dis.* 10, 623–629. doi: 10.3233/JPD-191786

Palacino, J. J., Sagi, D., Goldberg, M. S., Krauss, S., Motz, C., Wacker, M., et al. (2004). Mitochondrial dysfunction and oxidative damage in parkin-deficient mice. *J. Biol. Chem.* 279, 18614–18622. doi: 10.1074/jbc.M401135200

Parihar, M. S., Parihar, A., Fujita, M., Hashimoto, M., and Ghafourifar, P. (2008). Mitochondrial association of alpha-synuclein causes oxidative stress. *Cell Mol. Life Sci.* 65, 1272–1284. doi: 10.1007/s00018-008-7589-1

Park, J., Lee, S. B., Lee, S., Kim, Y., Song, S., Kim, S., et al. (2006). Mitochondrial dysfunction in Drosophila PINK1 mutants is complemented by parkin. *Nature* 441, 1157–1161. doi: 10.1038/nature04788

Perez Carrion, M., Pischedda, F., Biosa, A., Russo, I., Straniero, L., Civiero, L., et al. (2018). The LRRK2 variant E193K prevents mitochondrial fission upon MPP+ treatment by altering LRRK2 binding to DRP1. *Front. Mol. Neurosci.* 11:64. doi: 10.3389/fnmol.2018.00064

Pickrell, A. M., and Youle, R. J. (2015). The roles of PINK1, parkin, and mitochondrial fidelity in Parkinson's disease. *Neuron* 85, 257–273. doi: 10.1016/j.neuron.2014.12.007

Plovanich, M., Bogorad, R. L., Sancak, Y., Kamer, K. J., Strittmatter, L., Li, A. A., et al. (2013). MICU2, a paralog of MICU1, resides within the mitochondrial uniporter complex to regulate calcium handling. *PLoS One* 8:e55785. doi: 10.1371/journal.pone.0055785

Plun-Favreau, H., Klupsch, K., Moisoi, N., Gandhi, S., Kjaer, S., Frith, D., et al. (2007). The mitochondrial protease HtrA2 is regulated by Parkinson's disease-associated kinase PINK1. *Nat. Cell Biol.* 9, 1243–1252. doi: 10.1038/ncb1644

Pogson, J. H., Ivatt, R. M., Sanchez-Martinez, A., Tufi, R., Wilson, E., Mortiboys, H., et al. (2014). The complex I subunit NDUFA10 selectively rescues Drosophila pink1 mutants through a mechanism independent of mitophagy. *PLoS Genet.* 10:e1004815. doi: 10.1371/journal.pgen.1004815

Polymeropoulos, M. H., Lavedan, C., Leroy, E., Ide, S. E., Dehejia, A., Dutra, A., et al. (1997). Mutation in the alpha-synuclein gene identified in families with Parkinson's disease. *Science* 276, 2045–2047. doi: 10.1126/science.276.5321.2045

Poole, A. C., Thomas, R. E., Yu, S., Vincow, E. S., and Pallanck, L. (2010). The mitochondrial fusion-promoting factor mitofusin is a substrate of the PINK1/parkin pathway. *PLoS One* 5:e10054. doi: 10.1371/journal.pone.0010054

Popov, L. D. (2020). Mitochondrial biogenesis: An update. *J. Cell Mol. Med.* 24, 4892–4899. doi: 10.1111/jcmm.15194

Popov, L. D. (2022). Mitochondrial-derived vesicles: Recent insights. *J. Cell Mol. Med.* 26, 3323–3328. doi: 10.1111/jcmm.17391

Pridgeon, J. W., Olzmann, J. A., Chin, L. S., and Li, L. (2007). PINK1 protects against oxidative stress by phosphorylating mitochondrial chaperone TRAP1. *PLoS Biol.* 5:e172. doi: 10.1371/journal.pbio.0050172

Pryde, K. R., Smith, H. L., Chau, K. Y., and Schapira, A. H. (2016). PINK1 disables the anti-fission machinery to segregate damaged mitochondria for mitophagy. *J. Cell Biol.* 213, 163–171. doi: 10.1083/jcb.201509003

Raffaello, A., De Stefani, D., Sabbadin, D., Teardo, E., Merli, G., Picard, A., et al. (2013). The mitochondrial calcium uniporter is a multimer that can include a dominant-negative pore-forming subunit. *EMBO J.* 32, 2362–2376. doi: 10.1038/emboj.2013.157

Rakovic, A., Grunewald, A., Kottwitz, J., Bruggemann, N., Pramstaller, P. P., Lohmann, K., et al. (2011). Mutations in PINK1 and Parkin impair ubiquitination of Mitofusins in human fibroblasts. *PLoS One* 6:e16746. doi: 10.1371/journal.pone.0016746

Ramirez, A., Heimbach, A., Grundemann, J., Stiller, B., Hampshire, D., Cid, L. P., et al. (2006). Hereditary parkinsonism with dementia is caused by mutations in ATP13A2, encoding a lysosomal type 5 P-type ATPase. *Nat. Genet.* 38, 1184–1191. doi: 10.1038/ng1884

Ramirez, A., Old, W., Selwood, D. L., and Liu, X. (2022). Cannabidiol activates PINK1-Parkin-dependent mitophagy and mitochondrial-derived vesicles. *Eur. J. Cell Biol.* 101:151185. doi: 10.1016/j.ejcb.2021.151185

Rasool, S., Soya, N., Truong, L., Croteau, N., Lukacs, G. L., and Trempe, J. F. (2018). PINK1 autophosphorylation is required for ubiquitin recognition. *EMBO Rep.* 19:e44981. doi: 10.15252/embr.201744981

Rasool, S., Veyron, S., Soya, N., Eldeeb, M. A., Lukacs, G. L., Fon, E. A., et al. (2022). Mechanism of PINK1 activation by autophosphorylation and insights into assembly on the TOM complex. *Mol. Cell* 82, 44–59.e6. doi: 10.1016/j.molcel.2021.11.012

Richards, S., Aziz, N., Bale, S., Bick, D., Das, S., Gastier-Foster, J., et al. (2015). Standards and guidelines for the interpretation of sequence variants: A joint consensus recommendation of the American College of Medical Genetics and Genomics and the Association for Molecular Pathology. *Genet. Med.* 17, 405–424. doi: 10.1038/gim.2015.30

Rideout, H. J., Chartier-Harlin, M. C., Fell, M. J., Hirst, W. D., Huntwork-Rodriguez, S., Leyns, C. E. G., et al. (2020). The current state-of-the art of LRRK2-based biomarker assay development in Parkinson's disease. *Front. Neurosci.* 14:865. doi: 10.3389/fnins.2020.00865

Rose, C. M., Isasa, M., Ordureau, A., Prado, M. A., Beausoleil, S. A., Jedrychowski, M. P., et al. (2016). Highly multiplexed quantitative mass spectrometry analysis of ubiquitylomes. *Cell Syst.* 3, 395–403.e4. doi: 10.1016/j.cels.2016.08.009

Rosina, M., Ceci, V., Turchi, R., Chuan, L., Borcherding, N., Sciarretta, F., et al. (2022). Ejection of damaged mitochondria and their removal by macrophages ensure efficient thermogenesis in brown adipose tissue. *Cell Metab.* 34, 533–548.e12. doi: 10.1016/j.cmet.2022.02.016

Ross, O. A., Soto-Ortolaza, A. I., Heckman, M. G., Aasly, J. O., Abahuni, N., Annesi, G., et al. (2011). Association of LRRK2 exonic variants with susceptibility to Parkinson's disease: A case-control study. *Lancet Neurol.* 10, 898–908. doi: 10.1016/S1474-4422(11)70175-2

Ryan, T. A., Phillips, E. O., Collier, C. L., Jb Robinson, A., Routledge, D., Wood, R. E., et al. (2020). Tollip coordinates Parkin-dependent trafficking of mitochondrial-derived vesicles. *EMBO J.* 39:e102539. doi: 10.15252/embj.2019102539

Saito, Y. (2017). DJ-1 as a biomarker of Parkinson's disease. *Adv. Exp. Med. Biol.* 1037, 149–171. doi: 10.1007/978-981-10-6583-5_10

Sancak, Y., Markhard, A. L., Kitami, T., Kovacs-Bogdan, E., Kamer, K. J., Udeshi, N. D., et al. (2013). EMRE is an essential component of the mitochondrial calcium uniporter complex. *Science* 342, 1379–1382. doi: 10.1126/science.1242993

Sandebring, A., Dehvari, N., Perez-Manso, M., Thomas, K. J., Karpilovski, E., Cookson, M. R., et al. (2009). Parkin deficiency disrupts calcium homeostasis by modulating phospholipase C signalling. *FEBS J.* 276, 5041–5052. doi: 10.1111/j.1742-4658.2009.07201.x

Sanders, L. H., Laganiere, J., Cooper, O., Mak, S. K., Vu, B. J., Huang, Y. A., et al. (2014). LRRK2 mutations cause mitochondrial DNA damage in iPSC-derived neural cells from Parkinson's disease patients: Reversal by gene correction. *Neurobiol. Dis.* 62, 381–386. doi: 10.1016/j.nbd.2013.10.013

Sarafian, T. A., Ryan, C. M., Souda, P., Masliah, E., Kar, U. K., Vinters, H. V., et al. (2013). Impairment of mitochondria in adult mouse brain overexpressing predominantly full-length, N-terminally acetylated human alpha-synuclein. *PLoS One* 8:e63557. doi: 10.1371/journal.pone.0063557

Sarraf, S. A., Raman, M., Guarani-Pereira, V., Sowa, M. E., Huttlin, E. L., Gygi, S. P., et al. (2013). Landscape of the PARKIN-dependent ubiquitylome in response to mitochondrial depolarization. *Nature* 496, 372–376. doi: 10.1038/nature12043

Sauve, V., Lilov, A., Seirafi, M., Vranas, M., Rasool, S., Kozlov, G., et al. (2015). A Ubl/ubiquitin switch in the activation of Parkin. *EMBO J.* 34, 2492–2505. doi: 10.15252/embj.201592237

Scarpulla, R. C. (2008). Transcriptional paradigms in mammalian mitochondrial biogenesis and function. *Physiol. Rev.* 88, 611–638. doi: 10.1152/physrev.00025.2007

Seibenhener, M. L., Babu, J. R., Geetha, T., Wong, H. C., Krishna, N. R., and Wooten, M. W. (2004). Sequestosome 1/p62 is a polyubiquitin chain binding protein involved in ubiquitin proteasome degradation. *Mol. Cell Biol.* 24, 8055–8068. doi: 10.1128/MCB.24.18.8055-8068.2004

Shimizu, S., Konishi, A., Kodama, T., and Tsujimoto, Y. (2000). BH4 domain of antiapoptotic Bcl-2 family members closes voltage-dependent anion channel and inhibits apoptotic mitochondrial changes and cell death. *Proc. Natl. Acad. Sci. U.S.A.* 97, 3100–3105. doi: 10.1073/pnas.97.7.3100

Shimura, H., Hattori, N., Kubo, S., Mizuno, Y., Asakawa, S., Minoshima, S., et al. (2000). Familial Parkinson disease gene product, parkin, is a ubiquitin-protein ligase. *Nat. Genet.* 25, 302–305. doi: 10.1038/77060

Shin, J. H., Ko, H. S., Kang, H., Lee, Y., Lee, Y. I., Pletinkova, O., et al. (2011). PARIS (ZNF746) repression of PGC-1alpha contributes to neurodegeneration in Parkinson's disease. *Cell* 144, 689–702. doi: 10.1016/j.cell.2011.02.010

Shinbo, Y., Niki, T., Taira, T., Ooe, H., Takahashi-Niki, K., Maita, C., et al. (2006). Proper SUMO-1 conjugation is essential to DJ-1 to exert its full activities. *Cell Death Differ.* 13, 96–108. doi: 10.1038/sj.cdd.4401704

Shojaee, S., Sina, F., Banihosseini, S. S., Kazemi, M. H., Kalhor, R., Shahidi, G. A., et al. (2008). Genome-wide linkage analysis of a Parkinsonian-pyramidal syndrome pedigree by 500 K SNP arrays. *Am. J. Hum. Genet.* 82, 1375–1384. doi: 10.1016/j.ajhg.2008.05.005

Siddiqui, A., Bhaumik, D., Chinta, S. J., Rane, A., Rajagopalan, S., Lieu, C. A., et al. (2015). Mitochondrial quality control via the PGC1alpha-TFEB signaling pathway is compromised by Parkin Q311X mutation but independently restored by rapamycin. *J. Neurosci.* 35, 12833–12844. doi: 10.1523/JNEUROSCI.0109-15.2015

Siddiqui, A., Rane, A., Rajagopalan, S., Chinta, S. J., and Andersen, J. K. (2016). Detrimental effects of oxidative losses in parkin activity in a model of sporadic Parkinson's disease are attenuated by restoration of PGC1alpha. *Neurobiol. Dis.* 93, 115–120. doi: 10.1016/j.nbd.2016.05.009

Singh, F., Prescott, A. R., Rosewell, P., Ball, G., Reith, A. D., and Ganley, I. G. (2021). Pharmacological rescue of impaired mitophagy in Parkinson's disease-related LRRK2 G2019S knock-in mice. *Elife* 10:e67604. doi: 10.7554/eLife.67604

Skowyra, D., Craig, K. L., Tyers, M., Elledge, S. J., and Harper, J. W. (1997). F-box proteins are receptors that recruit phosphorylated substrates to the SCF ubiquitin-ligase complex. *Cell* 91, 209–219. doi: 10.1016/s0092-8674(00)80403-1

Sliter, D. A., Martinez, J., Hao, L., Chen, X., Sun, N., Fischer, T. D., et al. (2018). Parkin and PINK1 mitigate STING-induced inflammation. *Nature* 561, 258–262. doi: 10.1038/s41586-018-0448-9

Soubannier, V., McLelland, G. L., Zunino, R., Braschi, E., Rippstein, P., Fon, E. A., et al. (2012a). A vesicular transport pathway shuttles cargo from mitochondria to lysosomes. *Curr. Biol.* 22, 135–141. doi: 10.1016/j.cub.2011.11.057

Soubannier, V., Rippstein, P., Kaufman, B. A., Shoubridge, E. A., and McBride, H. M. (2012b). Reconstitution of mitochondria derived vesicle formation demonstrates selective enrichment of oxidized cargo. *PLoS One* 7:e52830. doi: 10.1371/journal.pone.0052830

Spillantini, M. G., Schmidt, M. L., Lee, V. M., Trojanowski, J. Q., Jakes, R., and Goedert, M. (1997). Alpha-synuclein in Lewy bodies. *Nature* 388, 839–840. doi: 10.1038/42166

Stafa, K., Tsika, E., Moser, R., Musso, A., Glauser, L., Jones, A., et al. (2014). Functional interaction of Parkinson's disease-associated LRRK2 with members of the dynamin GTPase superfamily. *Hum. Mol. Genet.* 23, 2055–2077. doi: 10.1093/hmg/ddt600

Stevens, D. A., Lee, Y., Kang, H. C., Lee, B. D., Lee, Y. I., Bower, A., et al. (2015). Parkin loss leads to PARIS-dependent declines in mitochondrial mass and respiration. *Proc. Natl. Acad. Sci. U.S.A.* 112, 11696–11701. doi: 10.1073/pnas.1500624112

Stram, A. R., and Payne, R. M. (2016). Post-translational modifications in mitochondria: Protein signaling in the powerhouse. *Cell Mol. Life Sci.* 73, 4063–4073. doi: 10.1007/s00018-016-2280-4

Strauss, K. M., Martins, L. M., Plun-Favreau, H., Marx, F. P., Kautzmann, S., Berg, D., et al. (2005). Loss of function mutations in the gene encoding Omi/HtrA2 in Parkinson's disease. *Hum. Mol. Genet.* 14, 2099–2111. doi: 10.1093/hmg/ddi215

Stuendl, A., Kraus, T., Chatterjee, M., Zapke, B., Sadowski, B., Moebius, W., et al. (2021). alpha-Synuclein in plasma-derived extracellular vesicles is a potential biomarker of Parkinson's disease. *Mov. Disord.* 36, 2508–2518. doi: 10.1002/mds.28639

Su, Y. C., and Qi, X. (2013). Inhibition of excessive mitochondrial fission reduced aberrant autophagy and neuronal damage caused by LRRK2 G2019S mutation. *Hum. Mol. Genet.* 22, 4545–4561. doi: 10.1093/hmg/ddt301

Su, Y. C., Guo, X., and Qi, X. (2015). Threonine 56 phosphorylation of Bcl-2 is required for LRRK2 G2019S-induced mitochondrial depolarization and autophagy. *Biochim. Biophys. Acta* 1852, 12–21. doi: 10.1016/j.bbadis.2014.11.009

Subramaniam, S. R., Vergnes, L., Franich, N. R., Reue, K., and Chesselet, M. F. (2014). Region specific mitochondrial impairment in mice with widespread overexpression of alpha-synuclein. *Neurobiol. Dis.* 70, 204–213. doi: 10.1016/j.nbd.2014.06.017

Sugiura, A., McLelland, G. L., Fon, E. A., and McBride, H. M. (2014). A new pathway for mitochondrial quality control: Mitochondrial-derived vesicles. *EMBO J.* 33, 2142–2156. doi: 10.15252/embj.201488104

Sun, Y., Vashisht, A. A., Tchieu, J., Wohlschlegel, J. A., and Dreier, L. (2012). Voltage-dependent anion channels (VDACs) recruit Parkin to defective mitochondria to promote mitochondrial autophagy. *J. Biol. Chem.* 287, 40652–40660. doi: 10.1074/jbc.M112.419721

Szabadkai, G., Simoni, A. M., Bianchi, K., De Stefani, D., Leo, S., Wieckowski, M. R., et al. (2006). Mitochondrial dynamics and Ca2+ signaling. *Biochim. Biophys. Acta* 1763, 442–449. doi: 10.1016/j.bbamcr.2006.04.002

Tain, L. S., Chowdhury, R. B., Tao, R. N., Plun-Favreau, H., Moisoi, N., Martins, L. M., et al. (2009). Drosophila HtrA2 is dispensable for apoptosis but acts downstream of PINK1 independently from Parkin. *Cell Death Differ.* 16, 1118–1125. doi: 10.1038/cdd.2009.23

Taira, T., Saito, Y., Niki, T., Iguchi-Ariga, S. M., Takahashi, K., and Ariga, H. (2004). DJ-1 has a role in antioxidative stress to prevent cell death. *EMBO Rep.* 5, 213–218. doi: 10.1038/sj.embor.7400074

Tanaka, A., Cleland, M. M., Xu, S., Narendra, D. P., Suen, D. F., Karbowski, M., et al. (2010). Proteasome and p97 mediate mitophagy and degradation of mitofusins induced by Parkin. *J. Cell Biol.* 191, 1367–1380. doi: 10.1083/jcb.201007013

Tang, B., Xiong, H., Sun, P., Zhang, Y., Wang, D., Hu, Z., et al. (2006). Association of PINK1 and DJ-1 confers digenic inheritance of early-onset Parkinson's disease. *Hum. Mol. Genet.* 15, 1816–1825. doi: 10.1093/hmg/ddl104

Tang, F. L., Liu, W., Hu, J. X., Erion, J. R., Ye, J., Mei, L., et al. (2015). VPS35 deficiency or mutation causes dopaminergic neuronal loss by impairing mitochondrial fusion and function. *Cell Rep.* 12, 1631–1643. doi: 10.1016/j.celrep.2015.08.001

Tanner, C. M. (1992). Occupational and environmental causes of parkinsonism. *Occup. Med.* 7, 503–513.

Taylor, M., and Alessi, D. R. (2020). Advances in elucidating the function of leucine-rich repeat protein kinase-2 in normal cells and Parkinson's disease. *Curr. Opin. Cell Biol.* 63, 102–113. doi: 10.1016/j.ceb.2020.01.001

Tettweiler, G., Miron, M., Jenkins, M., Sonenberg, N., and Lasko, P. F. (2005). Starvation and oxidative stress resistance in Drosophila are mediated through the eIF4E-binding protein, d4E-BP. *Genes Dev.* 19, 1840–1843. doi: 10.1101/gad.1311805

Teunissen, C. E. I, Verberk, M. W., Thijssen, E. H., Vermunt, L., Hansson, O., Zetterberg, H., et al. (2022). Blood-based biomarkers for Alzheimer's disease: Towards clinical implementation. *Lancet Neurol.* 21, 66–77. doi: 10.1016/S1474-4422(21)00361-6

Thevenet, J., Pescini Gobert, R., Hooft van Huijsduijnen, R., Wiessner, C., and Sagot, Y. J. (2011). Regulation of LRRK2 expression points to a functional role in human monocyte maturation. *PLoS One* 6:e21519. doi: 10.1371/journal.pone.0021519

Tokuda, T., Qureshi, M. M., Ardah, M. T., Varghese, S., Shehab, S. A., Kasai, T., et al. (2010). Detection of elevated levels of alpha-synuclein oligomers in CSF from patients with Parkinson disease. *Neurology* 75, 1766–1772. doi: 10.1212/WNL.0b013e3181fd613b

Toyofuku, T., Okamoto, Y., Ishikawa, T., Sasawatari, S., and Kumanogoh, A. (2020). LRRK2 regulates endoplasmic reticulum-mitochondrial tethering through the PERK-mediated ubiquitination pathway. *EMBO J.* 39:e100875. doi: 10.15252/embj.2018100875

Trempe, J. F., and Gehring, K. (2023). Structural mechanisms of mitochondrial quality control mediated by PINK1 and Parkin. *J. Mol. Biol.* 435:168090. doi: 10.1016/j.jmb.2023.168090

Trempe, J. F., Sauve, V., Grenier, K., Seirafi, M., Tang, M. Y., Menade, M., et al. (2013). Structure of parkin reveals mechanisms for ubiquitin ligase activation. *Science* 340, 1451–1455. doi: 10.1126/science.1237908

Tsai, P. I., Course, M. M., Lovas, J. R., Hsieh, C. H., Babic, M., Zinsmaier, K. E., et al. (2014). PINK1-mediated phosphorylation of Miro inhibits synaptic growth and protects dopaminergic neurons in Drosophila. *Sci. Rep.* 4:6962. doi: 10.1038/srep06962

Ulmer, T. S., Bax, A., Cole, N. B., and Nussbaum, R. L. (2005). Structure and dynamics of micelle-bound human alpha-synuclein. *J. Biol. Chem.* 280, 9595–9603. doi: 10.1074/jbc.M411805200

Um, J. W., and Chung, K. C. (2006). Functional modulation of parkin through physical interaction with SUMO-1. *J. Neurosci. Res.* 84, 1543–1554. doi: 10.1002/jnr.21041

Valente, E. M., Abou-Sleiman, P. M., Caputo, V., Muqit, M. M., Harvey, K., Gispert, S., et al. (2004). Hereditary early-onset Parkinson's disease caused by mutations in PINK1. *Science* 304, 1158–1160. doi: 10.1126/science.1096284

Van Laar, V. S., Roy, N., Liu, A., Rajprohat, S., Arnold, B., Dukes, A. A., et al. (2015). Glutamate excitotoxicity in neurons triggers mitochondrial and endoplasmic reticulum accumulation of Parkin, and, in the presence of N-acetyl cysteine, mitophagy. *Neurobiol. Dis.* 74, 180–193. doi: 10.1016/j.nbd.2014.11.015

van Steenoven, I., Majbour, N. K., Vaikath, N. N., Berendse, H. W., van der Flier, W. M., van de Berg, W. D. J., et al. (2018). alpha-Synuclein species as potential cerebrospinal fluid biomarkers for dementia with lewy bodies. *Mov. Disord.* 33, 1724–1733. doi: 10.1002/mds.111

Vasam, G., Nadeau, R., Cadete, V. J. J., Lavallee-Adam, M., Menzies, K. J., and Burelle, Y. (2021). Proteomics characterization of mitochondrial-derived vesicles under oxidative stress. *FASEB J.* 35:e21278. doi: 10.1096/fj.202002151R

Venda, L. L., Cragg, S. J., Buchman, V. L., and Wade-Martins, R. (2010). Alpha-Synuclein and dopamine at the crossroads of Parkinson's disease. *Trends Neurosci.* 33, 559–568. doi: 10.1016/j.tins.2010.09.004

Vilarino-Guell, C., Wider, C., Ross, O. A., Dachsel, J. C., Kachergus, J. M., Lincoln, S. J., et al. (2011). VPS35 mutations in Parkinson disease. *Am. J. Hum. Genet.* 89, 162–167. doi: 10.1016/j.ajhg.2011.06.001

Vissers, M., Troyer, M. D., Thijssen, E., Pereira, D. R., Heuberger, J. A., Groeneveld, G. J., et al. (2023). A leucine-rich repeat kinase 2 (LRRK2) pathway biomarker characterization study in patients with Parkinson's disease with and without LRRK2 mutations and healthy controls. *Clin. Transl. Sci.* 16, 1408–1420. doi: 10.1111/cts.13541

Vivacqua, G., Suppa, A., Mancinelli, R., Belvisi, D., Fabbrini, A., Costanzo, M., et al. (2019). Salivary alpha-synuclein in the diagnosis of Parkinson's disease and Progressive Supranuclear Palsy. *Park. Relat. Disord.* 63, 143–148. doi: 10.1016/j.parkreldis.2019.02.014

Vizziello, M., Borellini, L., Franco, G., and Ardolino, G. (2021). Disruption of mitochondrial homeostasis: The role of PINK1 in Parkinson's disease. *Cells* 10:3022. doi: 10.3390/cells10113022

Wan, H., Tang, B., Liao, X., Zeng, Q., Zhang, Z., and Liao, L. (2018). Analysis of neuronal phosphoproteome reveals PINK1 regulation of BAD function and cell death. *Cell Death Differ.* 25, 904–917. doi: 10.1038/s41418-017-0027-x

Wang, H., Song, P., Du, L., Tian, W., Yue, W., Liu, M., et al. (2011). Parkin ubiquitinates Drp1 for proteasome-dependent degradation: Implication of dysregulated mitochondrial dynamics in Parkinson disease. *J. Biol. Chem.* 286, 11649–11658. doi: 10.1074/jbc.M110.144238

Wang, S., Liu, Z., Ye, T., Mabrouk, O. S., Maltbie, T., Aasly, J., et al. (2017). Elevated LRRK2 autophosphorylation in brain-derived and peripheral exosomes in LRRK2 mutation carriers. *Acta Neuropathol. Commun.* 5:86. doi: 10.1186/s40478-017-0492-y

Wang, X., Winter, D., Ashrafi, G., Schlehe, J., Wong, Y. L., Selkoe, D., et al. (2011). PINK1 and Parkin target Miro for phosphorylation and degradation to arrest mitochondrial motility. *Cell* 147, 893–906. doi: 10.1016/j.cell.2011.10.018

Wang, X., Yan, M. H., Fujioka, H., Liu, J., Wilson-Delfosse, A., Chen, S. G., et al. (2012). LRRK2 regulates mitochondrial dynamics and function through direct interaction with DLP1. *Hum. Mol. Genet.* 21, 1931–1944. doi: 10.1093/hmg/dds003

Wang, Y., Shi, M., Chung, K. A., Zabetian, C. P., Leverenz, J. B., Berg, D., et al. (2012). Phosphorylated alpha-synuclein in Parkinson's disease. *Sci. Transl. Med.* 4:121ra20. doi: 10.1126/scitranslmed.3002566

Waragai, M., Wei, J., Fujita, M., Nakai, M., Ho, G. J., Masliah, E., et al. (2006). Increased level of DJ-1 in the cerebrospinal fluids of sporadic Parkinson's disease. *Biochem. Biophys. Res. Commun.* 345, 967–972. doi: 10.1016/j.bbrc.2006.05.011

Wasiak, S., Zunino, R., and McBride, H. M. (2007). Bax/Bak promote sumoylation of DRP1 and its stable association with mitochondria during apoptotic cell death. *J. Cell Biol.* 177, 439–450. doi: 10.1083/jcb.200610042

Wauer, T., Simicek, M., Schubert, A., and Komander, D. (2015a). Mechanism of phospho-ubiquitin-induced PARKIN activation. *Nature* 524, 370–374. doi: 10.1038/nature14879

Wauer, T., Swatek, K. N., Wagstaff, J. L., Gladkova, C., Pruneda, J. N., Michel, M. A., et al. (2015b). Ubiquitin Ser65 phosphorylation affects ubiquitin structure, chain assembly and hydrolysis. *EMBO J.* 34, 307–325. doi: 10.15252/embj.201489847

Wauters, F., Cornelissen, T., Imberechts, D., Martin, S., Koentjoro, B., Sue, C., et al. (2020). LRRK2 mutations impair depolarization-induced mitophagy through inhibition of mitochondrial accumulation of RAB10. *Autophagy* 16, 203–222. doi: 10.1080/15548627.2019.1603548

Wei, T., Huang, G., Gao, J., Huang, C., Sun, M., Wu, J., et al. (2017). Sirtuin 3 deficiency accelerates hypertensive cardiac remodeling by impairing angiogenesis. *J. Am. Heart Assoc.* 6:e006114. doi: 10.1161/JAHA.117.006114

West, A. B., Moore, D. J., Biskup, S., Bugayenko, A., Smith, W. W., Ross, C. A., et al. (2005). Parkinson's disease-associated mutations in leucine-rich repeat kinase 2 augment kinase activity. *Proc. Natl. Acad. Sci. U.S.A.* 102, 16842–16847. doi: 10.1073/pnas.0507360102

Whitworth, A. J., Lee, J. R., Ho, V. M., Flick, R., Chowdhury, R., and McQuibban, G. A. (2008). Rhomboid-7 and HtrA2/Omi act in a common pathway with the Parkinson's disease factors Pink1 and Parkin. *Dis. Model. Mech.* 1, 168–74; discussion 173. doi: 10.1242/dmm.000109

Xiong, H., Wang, D., Chen, L., Choo, Y. S., Ma, H., Tang, C., et al. (2009). Parkin, PINK1, and DJ-1 form a ubiquitin E3 ligase complex promoting unfolded protein degradation. *J. Clin. Invest.* 119, 650–660. doi: 10.1172/JCI37617

Yamada, T., Dawson, T. M., Yanagawa, T., Iijima, M., and Sesaki, H. (2019). SQSTM1/p62 promotes mitochondrial ubiquitination independently of PINK1 and PRKN/parkin in mitophagy. *Autophagy* 15, 2012–2018. doi: 10.1080/15548627.2019.1643185

Yamada, T., Murata, D., Adachi, Y., Itoh, K., Kameoka, S., Igarashi, A., et al. (2018). Mitochondrial stasis reveals p62-mediated ubiquitination in parkin-independent mitophagy and mitigates nonalcoholic fatty liver disease. *Cell Metab.* 28, 588–604.e5. doi: 10.1016/j.cmet.2018.06.014

Yang, Y., Kovacs, M., Sakamoto, T., Zhang, F., Kiehart, D. P., and Sellers, J. R. (2006). Dimerized Drosophila myosin VIIa: A processive motor. *Proc. Natl. Acad. Sci. U.S.A.* 103, 5746–5751. doi: 10.1073/pnas.0509935103

Yao, D., Gu, Z., Nakamura, T., Shi, Z. Q., Ma, Y., Gaston, B., et al. (2004). Nitrosative stress linked to sporadic Parkinson's disease: S-nitrosylation of parkin regulates its E3 ubiquitin ligase activity. *Proc. Natl. Acad. Sci. U.S.A.* 101, 10810–10814. doi: 10.1073/pnas.0404161101

Yi, W., MacDougall, E. J., Tang, M. Y., Krahn, A. I., Gan-Or, Z., Trempe, J. F., et al. (2019). The landscape of Parkin variants reveals pathogenic mechanisms and therapeutic targets in Parkinson's disease. *Hum. Mol. Genet.* 28, 2811–2825. doi: 10.1093/hmg/ddz080

Yu, R., Liu, T., Ning, C., Tan, F., Jin, S. B., Lendahl, U., et al. (2019). The phosphorylation status of Ser-637 in dynamin-related protein 1 (Drp1) does not determine Drp1 recruitment to mitochondria. *J. Biol. Chem.* 294, 17262–17277. doi: 10.1074/jbc.RA119.008202

Zhang, J. Y., Deng, Y. N., Zhang, M., Su, H., and Qu, Q. M. (2016). SIRT3 acts as a neuroprotective agent in rotenone-induced parkinson cell model. *Neurochem. Res.* 41, 1761–1773. doi: 10.1007/s11064-016-1892-2

Zhang, L., Karsten, P., Hamm, S., Pogson, J. H., Muller-Rischart, A. K., Exner, N., et al. (2013). TRAP1 rescues PINK1 loss-of-function phenotypes. *Hum. Mol. Genet.* 22, 2829–2841. doi: 10.1093/hmg/ddt132

Zhang, L., Zhang, C., Zhu, Y., Cai, Q., Chan, P., Uéda, K., et al. (2008). Semi-quantitative analysis of alpha-synuclein in subcellular pools of rat brain neurons: An immunogold electron microscopic study using a C-terminal specific monoclonal antibody. *Brain Res.* 1244, 40–52. doi: 10.1016/j.brainres.2008.08.067

Zhang, Y., Gao, J., Chung, K. K., Huang, H., Dawson, V. L., and Dawson, T. M. (2000). Parkin functions as an E2-dependent ubiquitin- protein ligase and promotes the degradation of the synaptic vesicle-associated protein, CDCrel-1. *Proc. Natl. Acad. Sci. U.S.A.* 97, 13354–13359. doi: 10.1073/pnas.240347797

Zhong, N., Kim, C. Y., Rizzu, P., Geula, C., Porter, D. R., Pothos, E. N., et al. (2006). DJ-1 transcriptionally up-regulates the human tyrosine hydroxylase by inhibiting the sumoylation of pyrimidine tract-binding protein-associated splicing factor. *J. Biol. Chem.* 281, 20940–20948. doi: 10.1074/jbc.M601935200

Zimprich, A., Benet-Pages, A., Struhal, W., Graf, E., Eck, S. H., Offman, M. N., et al. (2011). A mutation in VPS35, encoding a subunit of the retromer complex, causes late-onset Parkinson disease. *Am. J. Hum. Genet.* 89, 168–175. doi: 10.1016/j.ajhg.2011.06.008

Zimprich, A., Biskup, S., Leitner, P., Lichtner, P., Farrer, M., Lincoln, S., et al. (2004). Mutations in LRRK2 cause autosomal-dominant parkinsonism with pleomorphic pathology. *Neuron* 44, 601–607. doi: 10.1016/j.neuron.2004.11.005

Ziviani, E., Tao, R. N., and Whitworth, A. J. (2010). Drosophila parkin requires PINK1 for mitochondrial translocation and ubiquitinates mitofusin. *Proc. Natl. Acad. Sci. U.S.A.* 107, 5018–5023. doi: 10.1073/pnas.0913485107

frontiers | Frontiers in Molecular Neuroscience

TYPE Brief Research Report
PUBLISHED 14 February 2024
DOI 10.3389/fnmol.2024.1356326

OPEN ACCESS

EDITED BY
Beatriz Alvarez,
Complutense University of Madrid, Spain

REVIEWED BY
Maria Joana Guimarães Pinto,
Universidade do Porto, Portugal
Fumihito Ono,
Osaka Medical and Pharmaceutical University, Japan

*CORRESPONDENCE
Patricia Franzka
✉ patricia.franzka@med.uni-jena.de

†These authors have contributed equally to this work

RECEIVED 15 December 2023
ACCEPTED 30 January 2024
PUBLISHED 14 February 2024

CITATION
Schurig MK, Umeh O, Henze H, Jung MJ, Gresing L, Blanchard V, von Maltzahn J, Hübner CA and Franzka P (2024) Consequences of GMPPB deficiency for neuromuscular development and maintenance.
Front. Mol. Neurosci. 17:1356326.
doi: 10.3389/fnmol.2024.1356326

Consequences of GMPPB deficiency for neuromuscular development and maintenance

Mona K. Schurig[1], Obinna Umeh[2], Henriette Henze[3†], M. Juliane Jung[3†], Lennart Gresing[1], Véronique Blanchard[2,4], Julia von Maltzahn[3,5], Christian A. Hübner[1,6†] and Patricia Franzka[1*†]

[1]Institute of Human Genetics, Jena University Hospital, Friedrich Schiller University, Jena, Germany, [2]Institute of Diagnostic Laboratory Medicine, Clinical Chemistry and Pathobiochemistry, Charité-Universitätsmedizin Berlin, corporate member of Freie Universität Berlin, Humboldt-Universität zu Berlin, and Berlin Institute of Health, Berlin, Germany, [3]Leibniz Institute on Aging - Fritz Lipmann Institute, Jena, Germany, [4]Department of Human Medicine, Medical School Berlin, Berlin, Germany, [5]Stem Cell Biology of Aging, Faculty of Health Sciences, Brandenburg Technische Universität Cottbus-Senftenberg, Senftenberg, Germany, [6]Center of Rare Diseases, Jena University Hospital, Friedrich Schiller University Jena, Jena, Germany

Guanosine diphosphate-mannose pyrophosphorylase B (GMPPB) catalyzes the conversion of mannose-1-phosphate and GTP to GDP-mannose, which is required as a mannose donor for the biosynthesis of glycan structures necessary for proper cellular functions. Mutations in GMPPB have been associated with various neuromuscular disorders such as muscular dystrophy and myasthenic syndromes. Here, we report that GMPPB protein abundance increases during brain and skeletal muscle development, which is accompanied by an increase in overall protein mannosylation. To model the human disorder in mice, we generated heterozygous GMPPB KO mice using CIRSPR/Cas9. While we were able to obtain homozygous KO mice from heterozygous matings at the blastocyst stage, homozygous KO embryos were absent beyond embryonic day E8.5, suggesting that the homozygous loss of GMPPB results in early embryonic lethality. Since patients with GMPPB loss-of-function manifest with neuromuscular disorders, we investigated the role of GMPPB *in vitro*. Thereby, we found that the siRNA-mediated knockdown of *Gmppb* in either primary myoblasts or the myoblast cell line C2C12 impaired myoblast differentiation and resulted in myotube degeneration. siRNA-mediated knockdown of *Gmppb* also impaired the neuron-like differentiation of N2A cells. Taken together, our data highlight the essential role of GMPPB during development and differentiation, especially in myogenic and neuronal cell types.

KEYWORDS

glycosylation, mannosylation, GMPPB, skeletal muscle, nervous system, myogenesis, neurogenesis

Introduction

Glycosylation is one of the most common post-translational modifications of proteins and lipids, which can have important consequences for protein stability and conformation. It plays a prominent role in cell-to-cell communication, cell matrix interaction, adhesion, protein targeting and folding, viral or bacterial infection, progression of cancer and aging

(Varki et al., 2009; Breloy and Hanisch, 2018). Abnormal glycosylation of proteins can induce deleterious effects as observed in congenital disorders of glycosylation (CDGs), which often result in serious, sometimes fatal malfunctions of different organ systems such as brain and muscle (Péanne et al., 2018). A typical example are mutations in the gene encoding the enzyme GDP-mannose-pyrophosphorylase-B (GMPPB). GMPPB is crucial for the conversion of mannose-1-phosphate and guanosine triphosphate into GDP-mannose, which is required as a mannose donor for glycosylation (Ning and Elbein, 2000). Bi-allelic mutations in GMPPB are associated with variable disorders such as muscular dystrophy and other neurological symptoms including intellectual disability (Carss et al., 2013; Belaya et al., 2015; Liu et al., 2021). Additional symptoms such as cerebellar hypoplasia, seizures, or cardiac involvement are reported for some patients. The age at onset and disease progression varies from early infancy to adulthood (Belaya et al., 2015; Jensen et al., 2015; Rodriguez Cruz et al., 2016; Balcin et al., 2017; Luo et al., 2017; Sun et al., 2020; Chompoopong and Milone, 2023).

Previous morpholino-based knockdown studies in zebrafish suggested that GMPPB is required for the development of motor neurons and myofibers (Carss et al., 2013; Liu et al., 2021; Zheng et al., 2021). Here, we report that the KO of GMPPB in mice results in early embryonic lethality, suggesting that protein mannosylation is essential for embryonic development and that the loss of GMPPB to provide activated mannose cannot be compensated during early development. Being unable to study the consequences for neuronal and muscular differentiation *in vivo*, we studied the consequences of the knockdown of *Gmppb* on myoblasts or N2A cells. Both, differentiation and viability of the cells was severely compromised upon knockdown of *Gmppb* emphasizing the essential role of GMPPB.

Methods

All animal experiments were approved by the Thüringer Landesamt für Lebensmittelsicherheit und Verbraucherschutz (TLV). Experiments were performed in a C57BL/6 background. Mice were housed in a 12-hour light/12-hour dark cycle and had access to mouse chow *ad libitum*.

Cell culture

N2A (ATCC) cells were cultured in DMEM Glutamax (Sigma-Aldrich) supplemented with 10% [v/v] FBS (Gibco), 1% [v/v] penicillin/streptomycin (Gibco) at 37°C. For differentiation, cells were treated with differentiation medium [Neurobasal medium 1g/l glucose (Gibco) + 1X B-27 (Gibco) + 1X sodium pyruvate (Gibco) + 1X glutamine (Gibco) + 1% [v/v] penicillin/streptomycin (Gibco)].

Embryonic stem (ES) cells were cultured in DMEM with high glucose, no sodium pyruvate and 25 mM HEPES (Invitrogen) supplemented with 15% [v/v] FBS (PAA Gold), 1% [v/v] penicillin/streptomycin (Gibco), 1X NEAA (Invitrogen), 1X sodium pyruvate (Invitrogen), 1X glutamine (Invitrogen), 1X Nulceosidmix (Invitrogen), 2 × 2-mercaptoethanol (Invitrogen) and 1000 U/ml LIF (Merck) @37°C.

Primary myoblasts isolated from WT mice were cultured in growth medium [F10, 20% (v/v) FBS, 2% penicillin/streptomycin, 2.5 ng/mL basic fibroblast growth factor (bFGF); all from Gibco] at 37°C. For differentiation, primary myoblasts were incubated with differentiation medium [DMEM, Sigma-Aldrich; 5% (v/v) horse serum, Gibco; 2% penicillin/streptomycin, Gibco].

C2C12 cells (ATCC) were seeded in growth medium (DMEM, Sigma-Aldrich; 10% [v/v] FBS, Gibco; 2% [v/v] penicillin/streptomycin; Gibco) at 37°C. For differentiation, cells were incubated with differentiation medium (DMEM, Sigma-Aldrich; 2% horse serum, Gibco).

Targeted inactivation of the murine *Gmppb* gene

To disrupt GMPPB in mice, we targeted exon 4 of the murine *Gmppb* gene in embryonic stem cells (ES) by CRISPR/Cas9 with two sgRNAs (sgRNA1: gttgaacgaagaaagggt, sgRNA2: gtgcccgatgaaactgcacca) resulting in a 54 bp deletion. For this, ES cells were injected with a pSpCas9-(BB)-2A-Puro (PX459) vector (62988, Addgene) that contained both Cas9 and sgRNAs. Success of ES cell transfection was verified by polymerase chain reaction (PCR) using gcaaactttagggccagcaaa as forward primer and gaggtggagggtaccttag as reverse primer as well as by Western Blot and Sanger sequencing. Selected ES cells were then injected into foster mice and resulting chimeric mice were subsequently mated with C57BL/6 mice until reaching the fourth generation.

N2A cell differentiation experiments for microscopic analysis

N2A cells were seeded in a 12-well cell culture plate. The next day, cells were treated with differentiation medium and transfected with siRNA against either control (siScr) (Dharmacon) or *Gmppb* (si*Gmppb*) (Thermo Fischer) according to the manufacturer's protocol using lipofectamine 2000 (Invitrogen). After 4 days of differentiation, cells were fixed with 4% paraformaldehyde (PFA) and imaged in phosphate-buffered saline (PBS). Images were taken with a Keyence microscope BZ-X800E in the brightfield modus. N2A cell differentiation was morphologically evaluated by measuring the length and numbers of dendrite-like protrusions of first, second and third order protrusions. All single cells from at least eight images per condition and experiment were traced manually.

For measuring total protrusion numbers per neuron-like cell, all traced/visible protrusions per cell were counted for all single cells in at least eight images per condition and experiment. From these cells, the mean was determined for each condition/experiment.

For measuring the total protrusion length per cell, the length of all traced/visible projections per cell was measured for all single cells from at least eight images per condition and experiment. From these cells, the mean was quantified for each condition/experiment.

For assessing the mean protrusion length per order, the length of all traced/visible protrusions per respective protrusion order was

measured for each cell. Per projection order, the mean length was measured from all assessed cells for each condition/experiment.

N2A cell differentiation experiments for immunoblot analysis

N2A cells were seeded in 10 cm cell culture dishes (Greiner). The next day, cells were treated with differentiation medium and transfected with siRNA against either control (siScr) (Dharmacon) or *Gmppb* (si*Gmppb*) (Thermo Fischer) according to the manufacturer's protocol using lipofectamine 2000 (Invitrogen). After 3 days of differentiation, cells were harvested and lysed in RIPA buffer [50 mM Tris-HCl pH 7.4, 150 mM NaCl, 1% (v/v) NP-40, 1% (w/v) sodium deoxycholate, 0.1% (w/v) SDS, 1 mM EDTA] and complete protease inhibitor (Roche). Cell homogenates were centrifuged at 10,000 g and the protein concentration in the supernatant was determined using the BCA assay kit (Thermo Fischer). Samples were stored at −20°C until further use.

N2A neurite growth experiments for microscopic analysis

N2A cells were seeded in a 12-well cell culture plate. The next day, cells were treated with differentiation medium and allowed to differentiate for 3 days. Then, cells were transfected with siRNA against either control (siScr) (Dharmacon) or *Gmppb* (si*Gmppb*) (Thermo Fischer) according to the manufacturer's protocol using lipofectamine 2000 (Invitrogen). After 4 days of differentiation, cells were fixed and processed as described above.

Protein isolation from ES cells

ES cells were harvested and lysed in RIPA buffer [50 mM Tris-HCl pH 7.4, 150 mM NaCl, 1% (v/v) NP-40, 1% (w/v) sodium deoxycholate, 0.1% (w/v) SDS, 1 mM EDTA] and complete protease inhibitor (Roche). Cell homogenates were centrifuged at 10,000 g and the protein concentration in the supernatant was determined using the BCA assay kit (Thermo Fischer). Samples were stored at −20°C until further use.

Protein isolation from brain

Pregnant mother mice or pups were sacrificed and brain as well as skeletal muscle tissue (*musculus quadriceps femoris*) from embryos or pups was isolated. Tissue lysates were prepared as described previously (Franzka et al., 2022). Shortly, samples were homogenized with the Potter S tissue homogenizer (Sartorius) in RIPA buffer [50 mM Tris-HCl pH 7.4, 150 mM NaCl, 1% (v/v) NP-40, 1% (w/v) sodium deoxycholate, 0.1% (w/v) SDS, 1 mM EDTA] and complete protease inhibitor (Roche). After sonication, homogenates were spun down at 16,900 g to remove nuclei and insoluble debris. Protein concentration in the supernatant was determined using the BCA assay kit (Thermo Fischer) and then stored at −80°C until further use.

Western blot

Proteins were denatured at 90°C for 5 min in Laemmli buffer (4X Laemmli buffer: 50% glycerol, 5% SDS, 0.25% 1.5 M Tris pH 6.8, 30% β-mercaptoethanol, 0.001% bromophenol blue, ddH_2O). After separation by SDS-PAGE, proteins were transferred onto PVDF membranes (Whatman). Membranes were blocked in 2% BSA and incubated with primary antibodies at appropriate dilutions overnight at 4°C. The following primary antibodies were used: rabbit anti-GMPPB (Proteintech) 1:500, rabbit anti-GAPDH (Proteintech) 1:1000, biotin Con A (Biozol) 1:300. Primary antibodies were detected with HRP-conjugated secondary antibodies or HRP-conjugated streptavidin. Detection was performed with the Clarity Western ECL Substrate Kit (BioRad). The quantification of bands was done with ImageJ.

Immunofluorescence stainings of embryo sections

Pregnant mother mice were sacrificed and embryos at embryonal day 13.5 (E 13.5) isolated. Embryos were immediately frozen in Tissue Tek (Weckert Labortechnik) on dry ice and afterwards cryo-sectioned. Sections were dried, fixed in 4% PFA, permeabilized with 0.25% TritonX100, blocked in 5% normal goat serum (NGS) and stained over night at 4°C with primary antibodies or lectins followed by incubation with the corresponding secondary antibodies or streptavidin coupled to fluorophores (Invitrogen). Following primary antibodies/lectins were used: biotin Con A (Biozol) 1:100, rabbit anti-GMPPB (Proteintech) 1:100. Nuclei were stained with DAPI (10 μg/ml, Invitrogen). Images were taken with a Keyence microscope BZ-X800E.

In situ hybridization

Pregnant mother mice were sacrificed and embryos at embryonal day 13.5 (E 13.5) isolated. Embryos were immediately frozen in liquid nitrogen and afterwards cryo-sectioned. Sections were dried, fixed in 4% PFA, permeabilized with 0.2 M HCL, blocked and hybridized with digoxigenin-labeled antisense and sense RNA probes. The riboprobes covered exon 1-6 of the *Gmppb* transcript.

Myoblast and C2C12 differentiation experiments for microscopic analysis

All experiments were performed as described previously (Franzka et al., 2021). Primary myoblasts isolated from WT mice were seeded on collagen-coated culture dishes. Cells were treated with differentiation medium for 2 days. Then, cells were transfected with siRNAs against either control (siScr) (Dharmacon) or *Gmppb* (si*Gmppb*) (Thermo Fischer) according to the manufacturer's protocol using lipofectamine 2000 (Invitrogen). After 4 days of differentiation, cells were fixed with 2% PFA, permeabilized, blocked, and stained with antibodies directed against myogenin

(F5D, DSHB) 1:2 and myosin heavy chain (MF20, DSHB) 1:2 overnight at 4°C followed by an incubation with the corresponding secondary antibodies (Invitrogen). Nuclei were stained with DAPI (10°µg/mL, Invitrogen).

The fusion index was quantified as the number of nuclei inside myosin heavy chain (MYHC)-positive myotubes divided by the total number of nuclei per field of view.

The myotube diameter was assessed by measuring the maximal width of all MYHC-positive myotubes per field of view.

C2C12 cells were seeded and treated with differentiation medium and transfected with siRNAs against either control (siScr) (Dharmacon) or *Gmppb* (si*Gmppb*) (Thermo Fischer) according to the manufacturer's protocol using lipofectamine 2000 (Invitrogen). After 4 days of differentiation, cells were fixed and processed as described above.

Myoblast differentiation experiments for immunoblot analysis

Primary myoblasts isolated from WT mice were seeded and treated with differentiation medium for 2 days. Then, cells were transfected with siRNAs against either control (siScr) (Dharmacon) or *Gmppb* (si*Gmppb*) (Thermo Fischer) according to the manufacturer's protocol using lipofectamine 2000 (Invitrogen). After 4 days of differentiation, cells were harvested and lysed in RIPA buffer [50 mM Tris-HCl pH 7.4, 150 mM NaCl, 1% (v/v) NP-40, 1% (w/v) sodium deoxycholate, 0.1% (w/v) SDS, 1 mM EDTA] and complete protease inhibitor (Roche). Cell homogenates were centrifuged at 10,000 g and the protein concentration in the supernatant was determined using the BCA assay kit (Thermo Fischer). Samples were stored at −20°C until further use.

C2C12 maintenance experiments for microscopic analysis

C2C12 cells were seeded, treated with differentiation medium for 3 days and then transfected with siRNAs against either control (siScr) (Dharmacon) or *Gmppb* (si*Gmppb*) (Thermo Fischer) according to the manufacturer's protocol using lipofectamine 2000 (Invitrogen). After 4 days of differentiation, cells were fixed and processed as described above.

Blastocyst isolation and visualization

Heterozygous GMPPB KO mice were mated in a timed manner and blastocysts were flushed from the uteri of pregnant females on embryonic day E3.5. Single blastocysts were transferred into a 96-well plate using a mouth pipette. Blastocysts where then imaged with a Keyence BZ-X800E microscope.

After imaging, blastocysts were transferred into reaction vessels containing 5 ml of blastocyst lysis buffer [10 mM Tris pH 8.3, 50 mM KCl, 2.5 mM $MgCl_2$, 0.45% NP-40, 0.45% Tween 20 and 0.2 mg/ml proteinase K in ddH_2O] and lysed for 3 h at 55°C followed by inactivation at 85°C for 15 min. Blastocyst were genotyped via nested PCR. Following primer pairs were used: gagggatggatactgactg as forward primer and gaggtggagggtaccttag as revers primer for the first PCR as well as gaggtggagggtaccttag as forward primer and gcaaactttagggccagctc as revers primer for the second PCR.

Statistical analysis

For statistical analysis, raw data were analyzed for normal distribution with the Kolmogorov–Smirnov test or by graphical analysis using the Box-Plot and QQ-Plot in Graphpad prism 9. If appropriate, we either used 1-way ANOVA, 2-way ANOVA, or two-tailed Student's *t*-tests. * indicates $p < 0.05$, ** $p < 0.01$, and *** $p < 0.001$. For statistical analysis, we used Graphpad prism 9. For all data, means with standard error of the mean (SEM) and individual data points with SEM are shown.

Results

Expression of GMPPB increases during murine brain and muscle development

To analyze the expression pattern of GMPPB during embryonic mouse development, we performed *in situ* hybridizations of sagittal embryonic day 13.5 (E13.5) mouse sections with *Gmppb* specific probes (**Figure 1A**, **Supplementary Figure 1A**). Overall, the expression was very broad with a prominent labeling of the developing brain and skeletal muscles (**Figure 1A**, **Supplementary Figure 1A**). Staining of embryonic sections with an antibody directed against GMPPB confirmed a broad expression pattern (**Figure 1B**, **Supplementary Figure 1B**). The staining for GMPPB is in agreement with the Concanavalin A (Con A) staining, a lectin that specifically binds to mannose residues in glycan structures, broadly labelling E13.5 embryo sections (**Figure 1B**, **Supplementary Figure 1B**).

To study the expression of GMPPB at different stages of mouse development, we also assessed the abundance of GMPPB and the incorporation of mannose into glycan structures in embryonic and early postnatal (P) brain (**Figure 1C**) and skeletal muscle protein lysates (**Figure 1D**). GMPPB abundance strongly increased during embryonic as well as early postnatal development in both brain and skeletal muscles (**Figures 1C, D**). This upregulation was accompanied by an increase of mannose residues in glycan structures (**Figures 1C, D**). In summary, expression of GMPPB increases during murine brain and skeletal muscle development.

Loss of GMPPB leads to embryonic lethality in mice

To study the physiological role of GMPPB in mice we deleted 54 base pairs in exon 4 of *Gmppb* in mouse ES cells using CRISPR/Cas9, which inactivates the nucleotide transferase domain of GMPPB (Zheng et al., 2021; **Figure 2A**). The deletion was verified by PCR and Sanger sequencing (**Figure 2B**). Immunoblot analysis of protein lysates of wild-type (WT) and heterozygous (Het) ES cells using a polyclonal GMPPB antibody, which

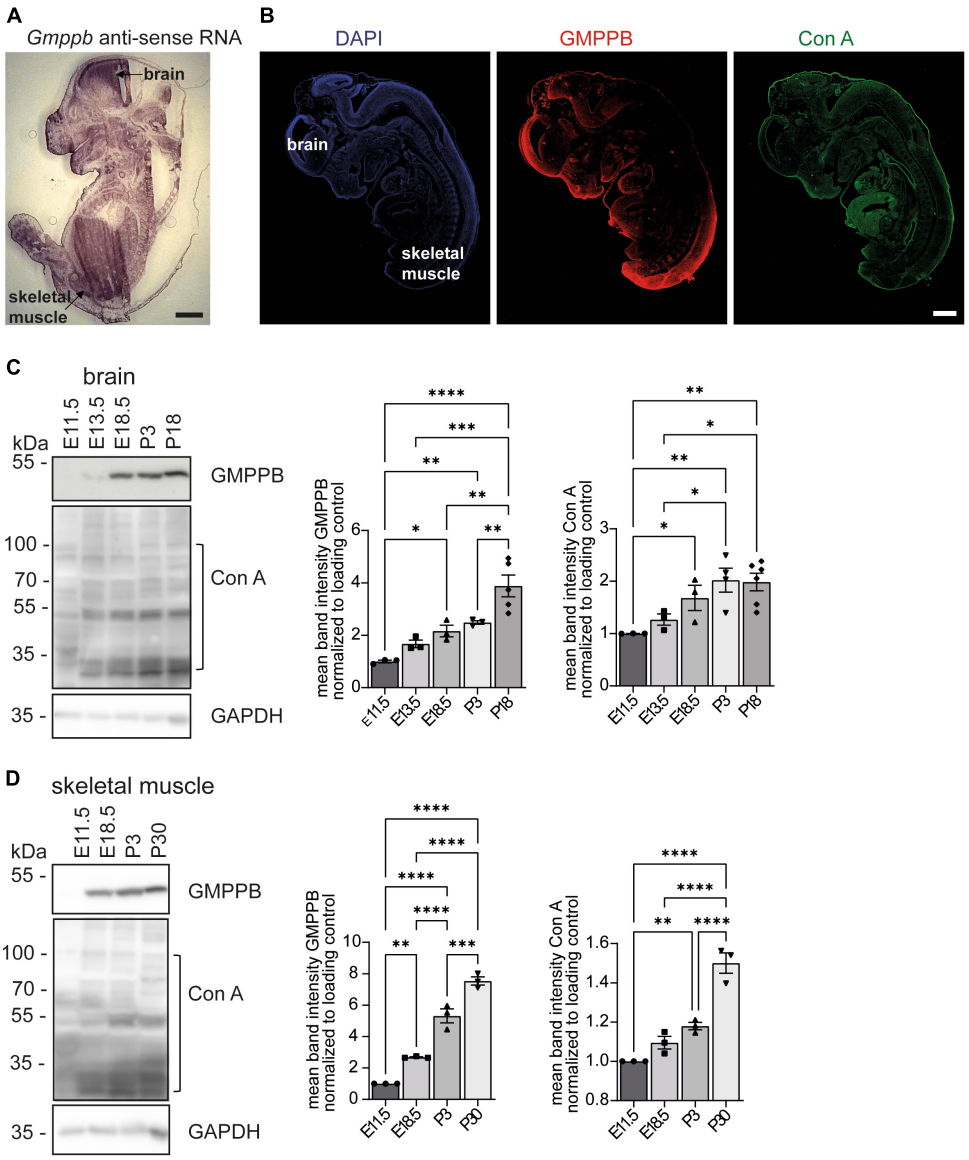

FIGURE 1
Expression of GMPPB increases during murine brain and skeletal muscle development. **(A)** *In situ* hybridization of an E13.5 murine embryo section with a *Gmppb*-specific antisense probe (scale bar: 500 μm). **(B)** Immunofluorescence labeling of nuclei (DAPI), GMPPB (red) and mannose residues in glycan structures (Con A, green). Scale bar: 500 μm. **(C)** Immunoblot analysis of brain tissues dissected at different time-points showing increasing signal intensities for GMPPB and Con A with increasing developmental stages. Black brackets indicate measured bands at indicated molecular weights. GAPDH served as loading control (n = 3–6 samples per developmental stage, 1-way-ANOVA with Fischer's LSD test). **(D)** Immunoblot analysis of skeletal muscle (*musculus quadriceps femoris*) dissected at different time-points showing increasing signal intensities for GMPPB and Con A with further development. Black brackets indicate measured bands at indicated molecular weights. GAPDH served as loading control (n = 3 samples per developmental stage, 1-way-ANOVA with Fischer's LSD test). Quantitative data are presented as mean ± SEM with individual data points. $^{*}P < 0.05$; $^{**}P < 0.01$; $^{***}P < 0.001$, $^{****}P < 0.0001$.

recognizes several epitopes in the protein, suggested a reduction in the abundance of GMPPB in Het cells (Figure 2B). Since no additional GMPPB-specific bands of lower size were detected in Het compared to WT cell lysates, it can be excluded that the deletion of 54 bp in exon 4 led to the expression of a variant truncated GMPPB protein. Concomitantly, mannosylation was reduced in Het cells (Figure 2B). Notably, we did not detect any homozygous deletions of the GMPPB allele in 384 analyzed individual ES cell clones (data not shown). Two independent heterozygous targeted ES cell clones were injected into blastocysts and transferred into foster mice. The resulting chimeric mice were subsequently mated with C57BL/6 mice for 3 generations. Heterozygous mice of the fourth generation were mated to obtain homozygous offspring. We did not detect any homozygous KO pups out of 113 genotyped newborn pups (Figure 2C). Analysis of embryos from terminated pregnancies from heterozygous matings at different embryonal time-points did not identify any homozygous KO embryos at E8.5 (35 genotyped embryos) or E12.5 (55 genotyped embryos) (Figure 2C). Only at E3.5, at the blastocyst stage, we were able to identify homozygous KO embryos. Overall, the structure and the size of blastocysts did not differ between genotypes (Figure 2D). Furthermore, the thickness of the zona

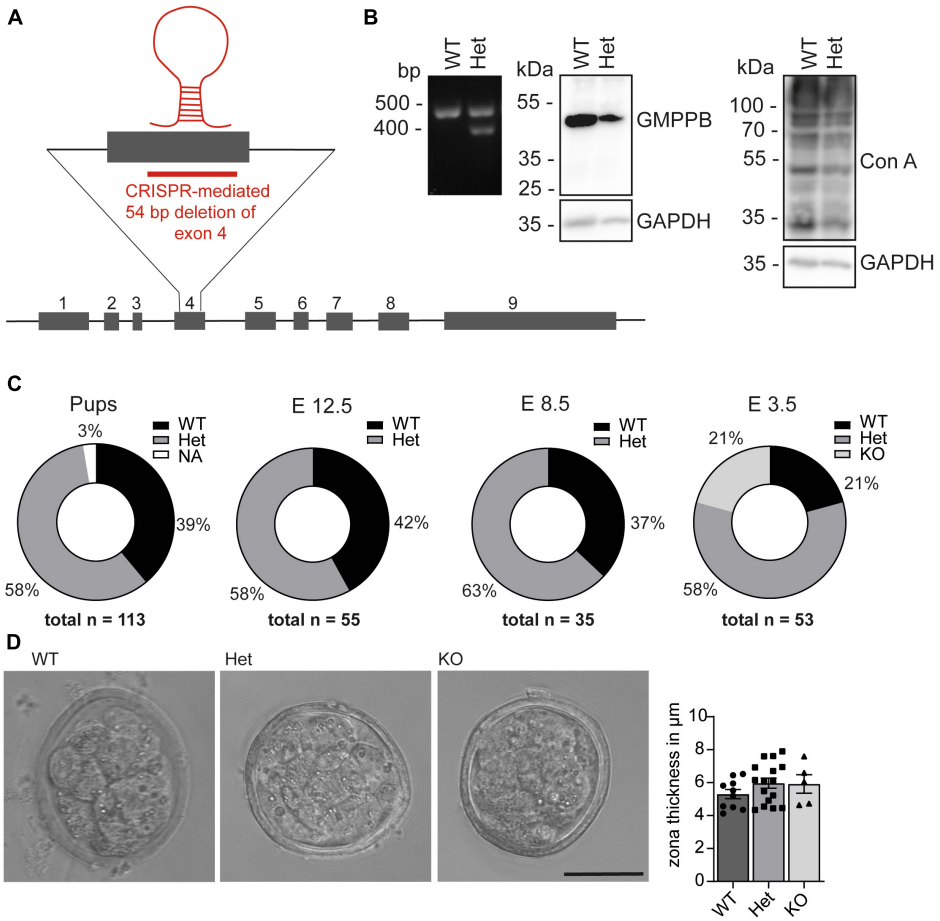

FIGURE 2
Loss of GMPPB leads to embryonic lethality in mice. **(A)** Genomic structure of the mouse *Gmppb* locus and the genome editing strategy. **(B)** Representative Ethidium bromide-stained agarose electrophoresis with the respective PCR products for GMPPB WT and Het ES cells. The immunoblot analysis suggests that the GMPPB protein abundance is reduced in Het compared to WT ES cells. In agreement, labeling for mannose residues in glycan structures was reduced. GAPDH served as loading control (n = 1). **(C)** Pie charts illustrating genotype percentages of WT, Het and KO GMPPB mice or embryos at different developmental stages [n (pups) = 113, n (E12.5) = 55, n (E8.5) = 35, n (E3.5) = 53]. **(D)** Representative images for WT, Het and KO blastocysts at E3.5 (scale bar: 50 µm) and quantification of the thickness of the zona pellucida (n = 5–16 blastocysts per genotype, 1-way-ANOVA with Fischer's LSD test). Quantitative data are presented as mean ± SEM with individual data points.

pellucida, which is built up of glycoproteins, did not differ between the different genotypes (Figure 2D). Taken together, loss of GMPPB leads to early embryonic lethality in mice, but does not affect the size and shape of blastocysts.

Knockdown of *Gmppb* affects N2A cell differentiation and growth

To assess the role of GMPPB for neurite differentiation and growth *in vitro*, we transfected N2A cells with siRNA to knockdown *Gmppb* and followed their neuronal-like differentiation upon serum deprivation. Knockdown of *Gmppb* was confirmed by immunoblot analysis 4 days after transfection (Figure 3A).

To assess the role of GMPPB in neurite differentiation, we transfected N2A cells with siRNA directed to *Gmppb*, or a scrambled control at induction of differentiation (Figure 3B). After 4 days of differentiation, cells were fixed and analyzed. Neurite differentiation was morphologically evaluated by measuring the length and numbers of dendrite-like projections of first, second and third order. Therefore, all visible single cells in at least eight images per condition and experiment were manually traced. While control cells showed prominent dendrite-like structures after 4 days of differentiation, the projection length was significantly decreased upon knockdown of *Gmppb* (Figure 3B).

To assess the role of GMPPB for the protrusion growth of differentiated N2A cells, we first differentiated N2A cells for 4 days, before transfection with siRNA directed against *Gmppb* (si*Gmppb*) or a control siRNA (siScr) (Figure 3C). After four additional days, cells were fixed and analyzed. While control cells maintained long primary dendrite-like protrusions with dendritic-like arborization of higher orders, cells with a knockdown of *Gmppb* showed primary dendrite-like protrusions with a significantly reduced length of primary and higher order protrusions indicating a lower cell complexity (Figure 3C). In summary, knockdown of *Gmppb* compromises N2A cell differentiation and growth of neurite-like protrusions.

10.3389/fnmol.2024.1356326

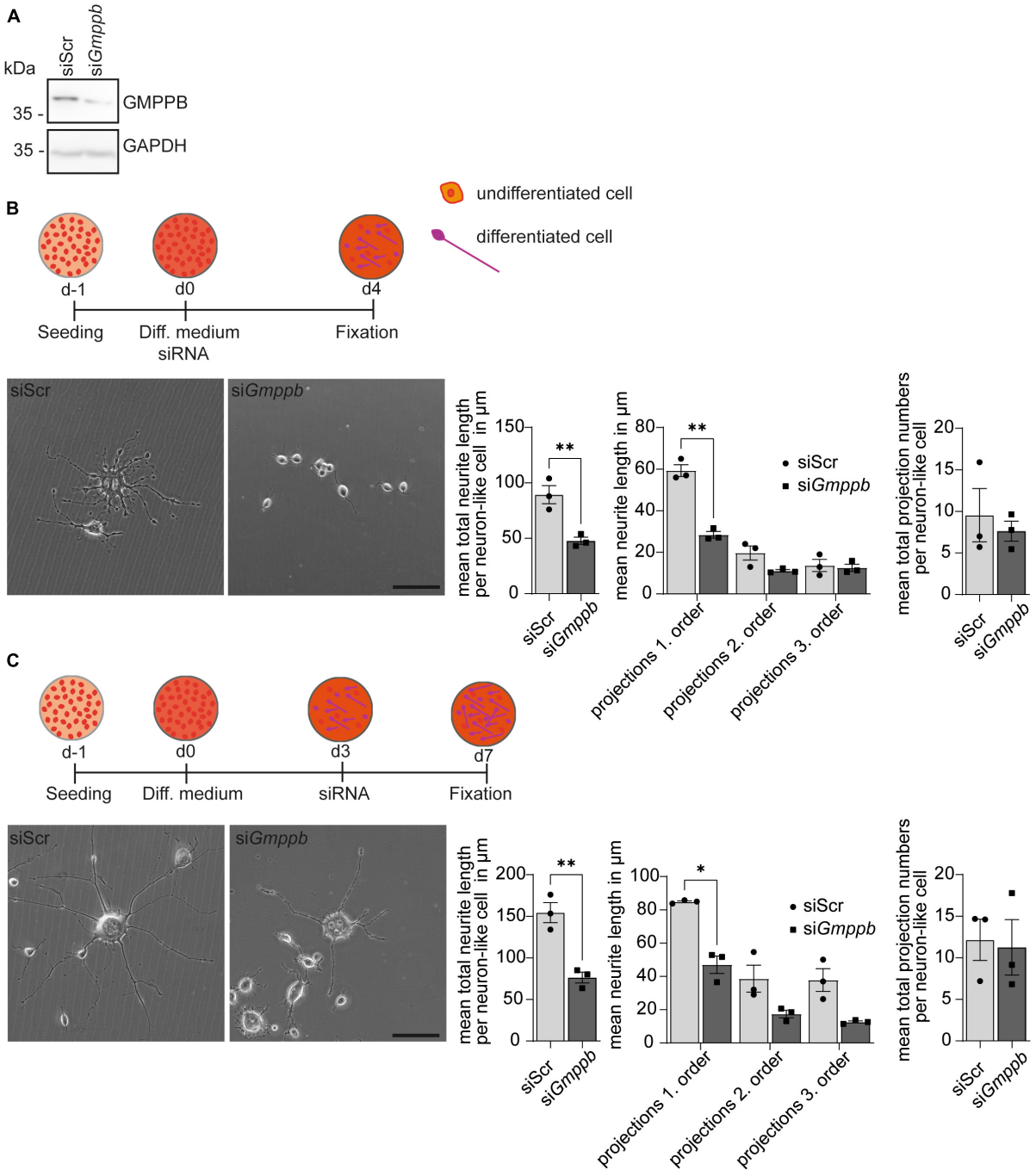

FIGURE 3
Knockdown of *Gmppb* affects N2A cell differentiation and neurite growth. **(A)** Immunoblot analysis confirming the knockdown of *Gmppb*. GAPDH served as loading control. **(B)** Experimental design, representative images of N2A cells (scale bar: 50 µm), and quantification of protrusion length and protrusion numbers (n = 3 experiments with 8–12 images per condition and experiment with 5–30 cells per image, Student's t-test or 1-way ANOVA with Fischer's LSD test). **(C)** Experimental design, representative images of N2A cells (scale bar: 50 µm), and quantification of protrusion lengths and numbers (n = 3 experiments with 8–12 images per condition and experiment with 1–15 cells per image, Student's t-test or 1-way ANOVA with Fischer's LSD test). Quantitative data are presented as mean ± SEM with individual data points. $^*P < 0.05$; $^{**}P < 0.01$.

Knockdown of *Gmppb* results in reduced myogenic differentiation and degeneration of myotubes

Because patients with GMPPB variants do not only show neurological disorders, but also myopathic symptoms, we performed knockdown experiments in primary murine myoblasts or the myoblast cell line C2C12 followed by differentiation into myotubes. Also here, knockdown of *Gmppb* was efficient as verified by immunoblot analysis (Figure 4A). To assess if loss of GMPPB affects myogenesis *per se*, we investigated whether knockdown of *Gmppb* in myoblasts interferes with myogenic

10.3389/fnmol.2024.1356326

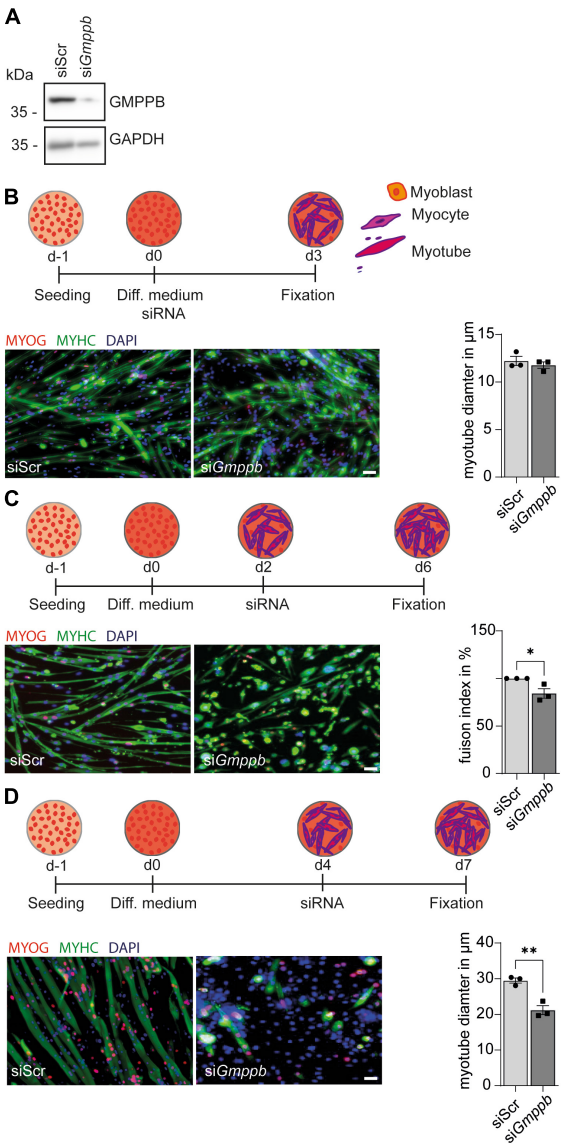

FIGURE 4
Knockdown of *Gmppb* results in reduced myogenic differentiation and degeneration of myotubes. **(A)** The knockdown of *Gmppb* in primary myoblasts was confirmed by immunoblot analysis. GAPDH served as loading control. **(B)** Experimental design and representative images of C2C12 cells stained for myogenin (MYOG) or myosin heavy chain (MYHC) (scale bar: 70 µm) and quantification of the myotube diameter (n = 3 experiments with 53–84 cells per condition and experiment, Student's t-test). **(C)** Experimental design and representative images of primary mouse myoblasts stained for myogenin (MYOG) or myosin heavy chain (MYHC) (scale bar: 70 µm) and quantification of the fusion index (=nuclei in MHC-positive /all nuclei per field of view) (n = 3 experiments with 53–84 cells per condition and experiment, Student's t-test). **(D)** Experimental design, representative images of C2C12 cells stained for myogenin (MYOG) or myosin heavy chain (MYHC) (scale bar: 70 µm), and quantification of the myotube diameter (n = 3 experiments with 53–84 cells per condition and experiment, Student's t-test). Quantitative data are presented as mean ± SEM with individual data points. $^{*}P < 0.05$; $^{**}P < 0.01$.

differentiation *in vitro*. Therefore, C2C12 cells were transfected with siRNA either targeting *Gmppb* or a scrambled control at the induction of myogenic differentiation (Figure 4B). Cells were stained for myogenin (MYOG), as marker for early myogenesis, namely myocytes, and myosin heavy chain (MYHC), a marker of terminally differentiated cells (myotubes). Notably, the myotube diameter was not affected by knockdown of *Gmppb* (Figure 4B) suggesting that induction of myogenic differentiation does not depend on GMPPB.

However, when mononucleated primary myocytes were transfected with a siRNA targeting *Gmppb*, we detected a decreased fusion index of myoblasts as a marker for myogenic differentiation (Figure 4C). This suggests that GMPPB is important for fusion of myoblasts with already existing myocytes or of myocytes with each other.

We next wondered whether differentiated myotubes are affected by loss of GMPPB as a measure of maintenance of myofibers *in vivo*. Therefore, we used C2C12 cells, a cell line derived from primary murine myoblasts, which are very similar to primary myoblasts but larger in size. To this end, C2C12 cells were differentiated into multinucleated myotubes, before they were transfected with a siRNA either targeting *Gmppb* or a scrambled control (Figure 4D). Thereby, we found that myotube diameter was significantly decreased after knock-down of *Gmppb* expression and that the number of myotubes was reduced in this condition (Figure 4D). These data suggest that the maintenance of differentiated myotubes depends on GMPPB. Taken together, loss of GMPPB affects fusion of myocytes and the size of late myotubes.

Discussion

Disease associated GMPPB variants include missense, nonsense and frameshift mutations (Astrea et al., 2018; Tian et al., 2019) and are considered to result in GMPPB loss-of-function. Functional studies reported decreased enzymatic activities of approximately up to 90% (Liu et al., 2021). Here, we show that the total loss of GMPPB activity by disrupting the catalytic nucleotide transferase domain results in embryonic lethality in mice suggesting a pivotal role of GMPPB activity for early development. In agreement with this finding, no patients homozygous for a *GMPPB* KO allele have been reported up to now. Notably, loss of other enzymes important for mannosylation, such as phosphomannomutase 2 (PMM2) or phosphomannose isomerase (PMI), also result in embryonic lethality (DeRossi et al., 2006; Schneider et al., 2011; Sharma et al., 2014) further highlighting the essential role for mannosylation during early development.

While homozygous GMPPB KO embryos were still found at E3.5 (blastocyst stage), they were absent at E8.5. The fertilized egg (1-cell stage, zygote) starts dividing within a protective shell provided by the zona pellucida until the blastocyst stage (early blastocyst: 32-cell stage, late blastocyst: <100-cell stage) is reached and the embryo is released from the zona pellucida to implant into the uterine mucosa (Mihajlović and Bruce, 2017). Since the zona pellucida is mainly composed of glycoproteins (Bleil and Wassarman, 1980) and defects of the zona pellucida often result in early embryonic lethality (Shi et al., 2014; Wassarman and Litscher, 2022), we quantified the thickness of the zona pellucida of WT and KO blastocysts. Because we neither detected differences in the thickness of the zona pellucida nor in the cell numbers of E3.5

blastocysts (data not shown), the development up to the blastocyst stage appears to be grossly intact. So far, we were not able to exactly resolve when and why KO embryos are lost between E3.5 and E8.5. Possibly, the release of the embryo from the zona pellucida, i.e., the hatching, its implantation or its gastrulation is affected by GMPPB loss-of-function, which will require further analysis.

Since external mannose supplementation rescued embryonic lethality in PMM2-deficient mice (Schneider et al., 2011), it is tempting to speculate that mannose supplementation might be beneficial for GMPPB KO mice as well.

In agreement with a previous report for zebrafish (Liu et al., 2021), GMPPB expression in mice increases during embryonal and postnatal development, which is accompanied by an increase in mannosylated glycans. Since GMPPB loss-of-function in humans manifests with variable muscular and neurological defects (Belaya et al., 2015; Jensen et al., 2015; Rodriguez Cruz et al., 2016; Balcin et al., 2017; Luo et al., 2017; Sun et al., 2020; Chompoopong and Milone, 2023), we assessed the consequences of the knockdown of *Gmppb* in myoblasts or N2A cells. Indeed, knockdown of *Gmppb* in N2A cells and myoblasts affected both the development of dendrite-like protrusions in N2A cells as well as the differentiation of myotubes. Moreover, the maintenance of dendrite-like protrusions and the diameter of myotubes decreased upon knockdown of *Gmppb*. These findings might explain why the nervous system and skeletal muscles are affected in patients harboring GMPPB mutations. Several case studies reported patients with intellectual disability, cerebellar hypoplasia and/or cortical hypoplasia, epilepsy as well as gait abnormalities, muscle weakness, decreased skeletal muscle fiber diameter with hypoglycosylation of alpha-dystroglycan and reduced nerve conductance. In most cases, one or more of the mentioned central nervous system (CNS) disorders are accompanied by skeletal muscle abnormalities, but not necessarily vice versa (Carss et al., 2013; Raphael et al., 2014; Belaya et al., 2015; Cabrera-Serrano et al., 2015; Rodriguez Cruz et al., 2016). Of note, alpha-dystroglycan is expressed in both skeletal muscle and in the brain. It has been shown that decreased expression or altered glycosylation of alpha-dystroglycan affects myogenic differentiation (Chen et al., 2012) and compromises the assembly of neuromuscular junctions (Jacobson et al., 2001). In the brain, a lack or altered glycosylation of alpha-dystroglycan affects extracellular matrix components thereby altering cortical development (Michele et al., 2002; Moore et al., 2002).

Notably, symptom severity correlates with enzymatic activity of mutated GMPPB: mutations in the N-terminal nucleotidyl-transferase domain of GMPPB seem to impair its activity more severely as mutations in its C-terminal beta-helix domain (Liu et al., 2021). Hence, mutations in the catalytic domain of GMPPB normally result in CNS and muscle involvement, whereas mutations in the C-terminal part of GMPPB affect mostly only skeletal muscles (Sun et al., 2020). Interestingly, the most common mutations in GMPPB are c.79G > C (p.Asp27His) in the N-terminal part and c.860G > A (p.Arg287Gln) in the C-terminal part. More than 50% of reported patients are compound heterozygous for one of these two mutations (Chompoopong and Milone, 2023). Additional suggested hotspots include mutations in the N-terminal part of GMPPB [c.95C > T (Pro32Leu), c.308C > T (Pro103Leu), c.553C > T (arg185Cys)] (Sarkozy et al., 2018).

In summary, our study highlights the essential role of mannosylation during early stages of development. These findings not only foster our knowledge regarding the molecular mechanisms underlying GMPPB-related disorders but also provide a striking example how perturbations in post-translational modification can affect early development and cellular differentiation.

Data availability statement

The raw data supporting the conclusions of this article will be made available by the authors, without undue reservation.

Ethics statement

The animal study was reviewed and approved by the Thüringer Landesamt für Lebensmittelsicherheit und Verbraucherschutz (TLV). The study was conducted in accordance with the local legislation and institutional requirements.

Author contributions

MS: Formal Analysis, Investigation, Writing – original draft. OU: Formal Analysis, Writing – original draft. HH: Investigation, Writing – original draft. MJ: Investigation, Writing – original draft. LG: Methodology, Writing – original draft. VB: Writing – original draft. JM: Investigation, Writing – original draft. CH: Conceptualization, Funding acquisition, Project administration, Supervision, Writing – original draft, Writing – review & editing. PF: Conceptualization, Formal Analysis, Funding acquisition, Investigation, Methodology, Project administration, Software, Supervision, Writing – original draft, Writing – review & editing.

Funding

The author(s) declare financial support was received for the research, authorship, and/or publication of this article. This study was funded by the DFG GRK 2155 ProMoAge and the DFG grant HU 800/15-1 to CH. OU is financially supported by the DFG (BL 1436/4-1). This study is supported by a Medical Scientist Award from the Interdisciplinary Center for Clinical Research (IZKF) at the Jena University Hospital (MSP13) and by IMPULSE funding (FKZ IP 2021-04) from the Friedrich-Schiller-University Jena to PF.

Acknowledgments

We gratefully acknowledge support from Katrin Schorr and Johanna Fischer.

Conflict of interest

The authors declare that the research was conducted in the absence of any commercial or financial relationships that could be construed as a potential conflict of interest.

Publisher's note

All claims expressed in this article are solely those of the authors and do not necessarily represent those of their affiliated organizations, or those of the publisher, the editors and the reviewers. Any product that may be evaluated in this article, or claim that may be made by its manufacturer, is not guaranteed or endorsed by the publisher.

Supplementary material

The Supplementary Material for this article can be found online at: https://www.frontiersin.org/articles/10.3389/fnmol.2024.1356326/full#supplementary-material

References

Astrea, G., Romano, A., Angelini, C., Antozzi, C. G., Barresi, R., Battini, R., et al. (2018). Broad phenotypic spectrum and genotype-phenotype correlations in GMPPB-related dystroglycanopathies: An Italian cross-sectional study. *Orphanet. J. Rare Dis.* 13:170. doi: 10.1186/s13023-018-0863-x

Balcin, H., Palmio, J., Penttilä, S., Nennesmo, I., Lindfors, M., Solders, G., et al. (2017). Late-onset limb-girdle muscular dystrophy caused by GMPPB mutations. *Neuromuscul. Disord.* 27, 627–630. doi: 10.1016/j.nmd.2017.04.006

Belaya, K., Rodriguez Cruz, P. M., Liu, W. W., Maxwell, S., McGowan, S., Farrugia, M. E., et al. (2015). Mutations in GMPPB cause congenital myasthenic syndrome and bridge myasthenic disorders with dystroglycanopathies. *Brain* 138(Pt. 9), 2493–2504. doi: 10.1093/brain/awv185

Bleil, J. D., and Wassarman, P. M. (1980). Synthesis of zona pellucida proteins by denuded and follicle-enclosed mouse oocytes during culture in vitro. *Proc. Natl. Acad. Sci. U.S.A.* 77, 1029–1033. doi: 10.1073/pnas.77.2.1029

Breloy, I., and Hanisch, F. G. (2018). Functional roles of O-glycosylation. *Molecules* 23:3063. doi: 10.3390/molecules23123063

Cabrera-Serrano, M., Ghaoui, R., Ravenscroft, G., Johnsen, R. D., Davis, M. R., Corbett, A., et al. (2015). Expanding the phenotype of GMPPB mutations. *Brain* 138(Pt. 4), 836–844. doi: 10.1093/brain/awv013

Carss, K. J., Stevens, E., Foley, A. R., Cirak, S., Riemersma, M., Torelli, S., et al. (2013). Mutations in GDP-mannose pyrophosphorylase B cause congenital and limb-girdle muscular dystrophies associated with hypoglycosylation of α-dystroglycan. *Am. J. Hum. Genet.* 93, 29–41. doi: 10.1016/j.ajhg.2013.05.009

Chen, F., Cao, J., Liu, Q., Qin, J., Kong, J., Wang, Y., et al. (2012). Comparative study of myocytes from normal and mdx mice iPS cells. *J. Cell Biochem.* 113, 678–684. doi: 10.1002/jcb.23397

Chompoopong, P., and Milone, M. (2023). GDP-mannose pyrophosphorylase B (*GMPPB*)-related disorders. *Genes.* 14:372. doi: 10.3390/genes14020372

DeRossi, C., Bode, L., Eklund, E. A., Zhang, F., Davis, J. A., Westphal, V., et al. (2006). Ablation of mouse phosphomannose isomerase (Mpi) causes mannose 6-phosphate accumulation, toxicity, and embryonic lethality. *J. Biol. Chem.* 281, 5916–5927. doi: 10.1074/jbc.M511982200

Franzka, P., Henze, H., Jung, M. J., Schüler, S. C., Mittag, S., Biskup, K., et al. (2021). GMPPA defects cause a neuromuscular disorder with α-dystroglycan hyperglycosylation. *J. Clin. Invest.* 131:e139076. doi: 10.1172/JCI139076

Franzka, P., Turecki, G., Cubillos, S., Kentache, T., Steiner, J., Walter, M., et al. (2022). Altered mannose metabolism in chronic stress and depression is rapidly reversed by vitamin B12. *Front. Nutr.* 9:981511. doi: 10.3389/fnut.2022.981511

Jacobson, C., Côté, P. D., Rossi, S. G., Rotundo, R. L., and Carbonetto, S. (2001). The dystroglycan complex is necessary for stabilization of acetylcholine receptor clusters at neuromuscular junctions and formation of the synaptic basement membrane. *J. Cell Biol.* 152, 435–450. doi: 10.1083/jcb.152.3.435

Jensen, B. S., Willer, T., Saade, D. N., Cox, M. O., Mozaffar, T., Scavina, M., et al. (2015). GMPPB-associated dystroglycanopathy: Emerging common variants with phenotype correlation. *Hum. Mutat.* 36, 1159–1163. doi: 10.1002/humu.22898

Liu, Z., Wang, Y., Yang, F., Yang, Q., Mo, X., Burstein, E., et al. (2021). GMPPB-congenital disorders of glycosylation associate with decreased enzymatic activity of GMPPB. *Mol. Biomed.* 2:13. doi: 10.1186/s43556-021-00027-2

Luo, S., Cai, S., Maxwell, S., Yue, D., Zhu, W., Qiao, K., et al. (2017). Novel mutations in the C-terminal region of GMPPB causing limb-girdle muscular dystrophy overlapping with congenital myasthenic syndrome. *Neuromuscul. Disord.* 27, 557–564. doi: 10.1016/j.nmd.2017.03.004

Michele, D. E., Barresi, R., Kanagawa, M., Saito, F., Cohn, R. D., Satz, J. S., et al. (2002). Post-translational disruption of dystroglycan-ligand interactions in congenital muscular dystrophies. *Nature* 418, 417–422. doi: 10.1038/nature00837

Mihajlović, A. I., and Bruce, A. W. (2017). The first cell-fate decision of mouse preimplantation embryo development: Integrating cell position and polarity. *Open Biol.* 7, 170210. doi: 10.1098/rsob.170210

Moore, S. A., Saito, F., Chen, J., Michele, D. E., Henry, M. D., Messing, A., et al. (2002). Deletion of brain dystroglycan recapitulates aspects of congenital muscular dystrophy. *Nature* 418, 422–425. doi: 10.1038/nature00838

Ning, B., and Elbein, A. D. (2000). Cloning, expression and characterization of the pig liver GDP-mannose pyrophosphorylase. Evidence that GDP-mannose and GDP-Glc pyrophosphorylases are different proteins. *Eur. J. Biochem.* 267, 6866–6874. doi: 10.1046/j.1432-1033.2000.01781.x

Péanne, R., De Lonlay, P., Foulquier, F., Kornak, U., Lefeber, D. J., Morava, E., et al. (2018). Congenital disorders of glycosylation (CDG): Quo vadis? *Eur. J. Med. Genet.* 61, 643–663. doi: 10.1016/j.ejmg.2017.10.012

Raphael, A. R., Couthouis, J., Sakamuri, S., Siskind, C., Vogel, H., Day, J. W., et al. (2014). Congenital muscular dystrophy and generalized epilepsy caused by GMPPB mutations. *Brain Res.* 1575, 66–71. doi: 10.1016/j.brainres.2014.04.028

Rodriguez Cruz, P. M., Belaya, K., Basiri, K., Sedghi, M. E., Farrugia, M., Holton, J. L., et al. (2016). Clinical features of the myasthenic syndrome arising from mutations in GMPPB. *J. Neurol. Neurosurg. Psychiatry* 87, 802–809. doi: 10.1136/jnnp-2016-313163

Sarkozy, A., Torelli, S., Mein, R., Henderson, M., Phadke, R., Feng, L., et al. (2018). Mobility shift of beta-dystroglycan as a marker of *GMPPB* gene-related muscular dystrophy. *J. Neurol. Neurosurg. Psychiatry* 89, 762–768. doi: 10.1136/jnnp-2017-316956

Schneider, A., Thiel, C., Rindermann, J., DeRossi, C., Popovici, D., Hoffmann, G. F., et al. (2011). Successful prenatal mannose treatment for congenital disorder of glycosylation-Ia in mice. *Nat. Med.* 18, 71–73. doi: 10.1038/nm.2548

Sharma, V., Nayak, J., DeRossi, C., Charbono, A., Ichikawa, M., Ng, B. G., et al. (2014). Mannose supplements induce embryonic lethality and blindness in phosphomannose isomerase hypomorphic mice. *FASEB J.* 28, 1854–1869. doi: 10.1096/fj.13-245514

Shi, W., Xu, B., Wu, L. M., Jin, R. T., Luan, H. B., Luo, L. H., et al. (2014). Oocytes with a dark zona pellucida demonstrate lower fertilization, implantation and clinical pregnancy rates in IVF/ICSI cycles. *PLoS One* 9:e89409. doi: 10.1371/journal.pone.0089409

Sun, L., Shen, D., Xiong, T., Zhou, Z., Lu, X., and Cui, F. (2020). Limb-girdle muscular dystrophy due to GMPPB mutations: A case report and comprehensive literature review. *Bosn. J. Basic Med. Sci.* 20, 275–280. doi: 10.17305/bjbms.2019.3992

Tian, W. T., Zhou, H. Y., Zhan, F. X., Zhu, Z. Y., Yang, J., Chen, S. D., et al. (2019). Lysosomal degradation of GMPPB is associated with limb-girdle muscular dystrophy type 2T. *Ann. Clin. Transl. Neurol.* 6, 1062–1071. doi: 10.1002/acn3.787

Varki, A., Cummings, R. D., Esko, J. D., Freeze, H. H., Stanley, P., Bertozzi, C. R., et al. (2009). *Essentials of Glycobiology*. Cold Spring Harbor, NY: Cold Spring Harbor Laboratory Press.

Wassarman, P. M., and Litscher, E. S. (2022). Female fertility and the zona pellucida. *Elife* 11:e76106. doi: 10.7554/eLife.76106

Zheng, L., Liu, Z., Wang, Y., Yang, F., Wang, J., Huang, W., et al. (2021). Cryo-EM structures of human GMPPA-GMPPB complex reveal how cells maintain GDP-mannose homeostasis. *Nat. Struct. Mol. Biol.* 28, 1–12. doi: 10.1038/s41594-021-00591-9

frontiers | Frontiers in Molecular Neuroscience

TYPE Original Research
PUBLISHED 22 February 2024
DOI 10.3389/fnmol.2024.1324458

OPEN ACCESS

EDITED BY
Miguel Diaz-Hernandez,
Complutense University of Madrid, Spain

REVIEWED BY
Matteo Spinelli,
University College London, United Kingdom
Maciej Maurycy Lalowski,
Adam Mickiewicz University, Poland

*CORRESPONDENCE
Shan Wang
✉ wsaquarius@sina.com
Ting Zhang
✉ zhangtingcv@126.com

RECEIVED 19 October 2023
ACCEPTED 08 February 2024
PUBLISHED 22 February 2024

CITATION
Liu F, Yan W, Chen C, Zeng Y, Kong Y, He X, Pei P, Wang S and Zhang T (2024) Acetylome analyses provide novel insights into the effects of chronic intermittent hypoxia on hippocampus-dependent cognitive impairment.
Front. Mol. Neurosci. 17:1324458.
doi: 10.3389/fnmol.2024.1324458

Acetylome analyses provide novel insights into the effects of chronic intermittent hypoxia on hippocampus-dependent cognitive impairment

Fan Liu[1,2,3], Weiheng Yan[1], Chen Chen[2], Yubing Zeng[1,2], Yaru Kong[1], Xuejia He[4], Pei Pei[2], Shan Wang[1,2,3,4]* and Ting Zhang[1,2,3,4]*

[1]Children's Hospital Capital Institute of Pediatrics, Chinese Academy of Medical Sciences and Peking Union Medical College, Beijing, China, [2]Beijing Municipal Key Laboratory of Child Development and Nutriomics, Capital Institute of Pediatrics, Beijing, China, [3]Graduate School of Peking Union Medical College, Beijing, China, [4]Beijing Municipal Key Laboratory of Child Development and Nutriomics, Capital Institute of Pediatrics-Peking University Teaching Hospital, Beijing, China

Introduction: Chronic intermittent hypoxia (CIH) can negatively affect hippocampal function through various molecular mechanisms. Protein acetylation, a frequently occurring modification, plays crucial roles in synaptic plasticity and cognitive processes. However, the global protein acetylation induced by CIH in the hippocampus and its specific effects on hippocampal function and behavior remain poorly understood.

Methods: To address this gap, we conducted a study using liquid chromatography-tandem mass spectrometry to analyze the lysine acetylome and proteome of the hippocampus in healthy adult mice exposed to intermittent hypoxia for 4 weeks (as a CIH model) compared to normoxic mice (as a control).

Results: We identified and quantified a total of 2,184 lysine acetylation sites in 1,007 proteins. Analysis of these acetylated proteins revealed disturbances primarily in oxidative phosphorylation, the tricarboxylic acid (TCA) cycle, and glycolysis, all of which are localized exclusively to mitochondria. Additionally, we observed significant changes in the abundance of 21 proteins, some of which are known to be associated with cognitive impairments.

Discussion: This study helps to elucidate the molecular mechanisms underlying CIH-induced changes in protein acetylation in the hippocampus. By providing valuable insights into the pathophysiological processes associated with CIH and their impacts on hippocampal function, our findings contribute to a better understanding of the consequences of CIH-induced changes in protein acetylation in the hippocampus and the potential role of CIH in cognitive impairment.

KEYWORDS

cognition, lysine acetylation, CIH, hippocampus, mitochondria

1 Introduction

Obstructive sleep apnoea (OSA) is a typical sleep disorder characterized by recurrent episodes of pharyngeal collapse during sleep. Moreover, OSA causes repetitive fluctuations in blood oxygen saturation and leads to chronic intermittent hypoxia (CIH). Over the past two decades, the prevalence of OSA has doubled (Bannow et al., 2022). Cognitive and behavioral scales have indicated OSA-induced abnormalities in learning, memory, and cognition (Hunter et al., 2016; Labarca et al., 2020; Osorio et al., 2022). In addition, brain MRI revealed OSA-associated reductions in the frontal cortex, anterior cingulate cortex, and hippocampus (Canessa et al., 2011; Zhao et al., 2016; Philby et al., 2017; Koo et al., 2020). Research has indicated that patients with OSA exhibit localized reductions in the volume of gray matter within the hippocampus (Canessa et al., 2011) and significant decreases in hippocampal neuronal functional connectivity (Zhou et al., 2020). The brain constitutes 20% of basal oxygen utilization, rendering it exceptionally susceptible to hypoxic conditions (Burtscher et al., 2021). OSA imposes brain risks through CIH and impairs cognitive performance. Although earlier studies have shown that OSA impacts adult hippocampal neurogenesis and cognitive processes (Anacker and Hen, 2017), the exact mechanism through which CIH affects hippocampal function, particularly learning and memory, remains unclear.

As neuroinflammation can influence cognitive functions, it may constitute a significant mechanism underlying the cognitive deficits induced by CIH. Cao et al. (2020, 2021) ascertained that aberrant autophagic activity within hippocampal neurons is associated with impaired cognitive function. Upon suppression of excessive autophagy, apoptosis of hippocampal neurons is ameliorated. Substantial astrogliosis within the cortical and hippocampal regions of rats subjected to IH has been documented (Aviles-Reyes et al., 2010). Microglia play key physiological roles, including synapse monitoring, debris clearance, and synaptic pruning. They impact cognition by modulating learning and memory via neuronal activity and synaptic plasticity (Ben Achour and Pascual, 2010; Yang et al., 2010). CIH triggers neurocognitive impairments in the hippocampus by enhancing neuroinflammation, neuroapoptosis, and oxidative stress (Zhou et al., 2016).

Posttranslational modifications (PTMs) are critical for regulating various cellular processes, including protein-protein interactions, enzyme activity, and gene expression. The eukaryotic proteome consists of hundreds of distinct PTMs. However, only a few proteins, such as those involved in phosphorylation, glycosylation, methylation, ubiquitylation, and acetylation, have been extensively investigated (Narita et al., 2019). Among the many types of PTMs that occur in proteins, lysine acetylation plays critical roles in regulating memory and the balance between neuroprotection and neurodegeneration (Schueller et al., 2020; Qian et al., 2022). Lysine acetylation is a reversible PTM that affects protein function through various mechanisms, including altering charge, structure, stability, and interactions with other molecules. Moreover, it has been shown to regulate numerous cellular processes, including gene expression, chromatin remodeling, metabolism, and mitochondrial function (Xiao et al., 2020). Recently, considerable focus has been directed toward the functions of hypoxia-induced PTMs in various pathological conditions. However, less is known about possible CIH-induced PTMs. Histone acetylation is involved in memory and long-term synaptic plasticity (Mews et al., 2017; Campbell and Wood, 2019). Spatial memory relies on changes in gene expression in the hippocampus, which are partly regulated by histone acetylation (Mews et al., 2017). Specifically, dysregulation of H3K9 acetylation has been associated with impaired establishment of epigenetic memory at genes involved in striatal plasticity (Alcalá-Vida et al., 2022). Additionally, inhibiting the histone deacetylase (HDAC) family with sodium butyrate (NaB) administration attenuated neurodegeneration and memory loss in hypobaric hypoxia-exposed rats (Kumar et al., 2021). Recently, non-histone acetylation has gained increased amounts of attention. SIRT1 ameliorated CIH-induced cognitive behaviour in mice by reducing NF-κB acetylation in the hippocampus (Fan et al., 2018). By deacetylating the RelA/p65 subunit of NF-κB at lysine 310, SIRT1 can suppress its transcriptional activity and reduce the expression of proinflammatory genes (Yeung et al., 2004). SIRT1 activation significantly promoted potent neuroprotection (Chen et al., 2005). SIRT1 deficiency in microglia leads to the upregulation of IL-1β, resulting in cognitive decline (Cho et al., 2015). Although acetylation is known to be associated with hippocampal cognitive function, the relationships between acetylation, especially non-histone acetylation, and hippocampal function in CIH patients have not been elucidated.

In this study, we employed liquid chromatography–tandem mass spectrometry (LC-MS/MS) to investigate whether CIH alters the hippocampal acetylation landscape. Quantitative analysis of the acetylome revealed the involvement of acetylated proteins in oxidative phosphorylation and the TCA cycle, primarily in mitochondria, linking CIH to cognitive function.

2 Materials and methods

2.1 Animals

This study utilized male C57BL/6J mice that were obtained from Sibeifu Biotechnology Co., Ltd. The mice were 6 weeks old and weighed between 20–22 g at the beginning of the experiment. To ensure their health and wellbeing, all mice used in the study were free from specific pathogens. Throughout the experimental period, the mice were housed in a controlled environment with a 12/12-h light/dark cycle. They were provided with *ad libitum* access to food and water. To maintain stable conditions, the temperature and humidity were strictly controlled. After being habituated to their new environment for 1 week, the mice were randomly assigned to either the CIH or control (CON) group. All procedures were carried out during the mice's inactive period and their body weight was monitored weekly. The Capital Institute of Pediatrics' Ethics Committee on Animal Care and Use approved the study on November 9, 2021 (approval No. DWLL2021016).

2.2 Establishment of chronic intermittent hypoxia model and supplementation of sodium butyrate

We followed an established CIH modeling method for gas control (Du et al., 2020; Hernández-Soto et al., 2021). Mice were kept in custom standard cages (Zhongshi Technology Co, Ltd). A gas control system managed room airflow (N_2 and O_2). Programs and flow regulators allowed manipulation of inspired O_2 fraction from 20.9 to 5.0% over 2 min, followed by rapid reoxygenation to normal air levels via a 100% O_2 burst in the next minute. Regarding the duration and timing of the CIH protocol, we have made improvements based on a previous CIH modeling method (Du et al., 2020; Hernández-Soto et al., 2021). Intermittent hypoxia events occurred cyclically for 8 h each day, from 9:00 am to 5:00 pm, during the light phase and lasted for 28 days. At other times, CIH animals were in a normoxic environment. Control animals were in a normoxic chamber for 28 days. The animals' weight and survival were monitored during this protocol. One day after chronic intermittent hypoxia modeling was completed, mice from both the CON and CIH groups was euthanized simultaneously to collect tissues for further experiments, including histological staining and omics sequencing analyses. The remaining mice were kept for behavioral experiments, including the Novel Object Recognition Test (NORT) and Y-maze test, with at least 1 day of rest between the two tests.

After the 28-day CIH protocol, half of the mice in the CIH group were randomly selected to receive treatment with NaB, forming the CIH+NaB group. The mice in this group were administered intraperitoneal injections of NaB (300 mg/kg, Sigma-303410) at a dosage of 100 μl once daily for a consecutive period of 14 days. On the 15th day, NORT tests or other types of analysis were performed.

2.3 Measures of metabolic parameters

For the locomotion assay, the animals were placed in an open box (50 × 50 × 35 cm, Beijing Zhongshi Dichuang Technology Development Co., Ltd) and allowed to freely move for 5 min after completing the 28-day CIH protocol (n = 12 mice/group). The distance traveled by each animal during this 5-min period was recorded using a camera. Food and water intake measurements were taken for a 16-h period immediately following the 28-day CIH exposure (Ciriello et al., 2021). For all analyses, the experimental unit used was mice, except for food/water consumption where the cage (with 4 mice per cage) served as the experimental unit. This was due to the inability to measure individual food and water consumption in standard individually ventilated cages.

2.4 Animal behavioral assessment

The cognition of the mice was evaluated using the NORT and open Y-maze after the CIH process. The mice were acclimated to the testing room and the apparatuses were cleaned before each test. A night vision camera recorded their activities and a blinded investigator carried out all assessments and data analyses. 12 mice in each group were chosen for the experiments. Inactive mice were excluded.

2.4.1 Novel object recognition test

Novel object recognition test (NORT) was performed in an open box (50 × 50 × 35 cm, Beijing Zhongshi Dichuang Technology Development Co., Ltd). During the adaptation stage, two objects with identical shape and material were positioned in the symmetrical area. In the open field test, each mouse was placed in the center of the open box and allowed to explore the two objects for 5 min while their behavior was recorded. Taking out the mice and detecting the recognition period after an interval of 1 h. In the recognition stage, we replaced one object (Green) with a new different object (Red), then repeat the procedure. The mice were again put into the open field to explore freely. The camera recorded the time exploring a new object (TN) and time exploring a familiar object (TF) of object A within 5 min, and the software (Beijing Zhongshi Dichuang Technology Development Co., Ltd) was used to track the mouse's trajectory. New thing identification index = [(TN-TF)/(TN+TF)] × 100%, the higher the index, the better the memory of mice.

2.4.2 Y-maze test

We utilized an experimental setup called the Y-maze, which consists of three identical arms measuring 300 × 200 × 60 mm each. The mice were placed in an arm and their movements were recorded while they explored for 8 min. To determine spontaneous alternation behavior, we counted the number of times a mouse consecutively entered all three arms of the maze. A higher percentage of spontaneous alternations indicates better spatial working memory performance. We calculated the percentage of spontaneous alternation using the formula [number of spontaneous alternations / (total arm entries–2)] × 100.

2.5 Hematoxylin–Eosin (HE) and Nissl staining

Six Mice from each group without undergoing behavior test were anesthetized with chloral hydrate and then sacrificed. To evaluate histological damage, mice were perfused with saline and paraformaldehyde. Their brains were removed, fixed in paraformaldehyde for 24 h, dehydrated in alcohol, and embedded in wax. The wax was trimmed and sectioned into 4 μm slices for staining with HE and Nissl. Then, the sections were dewaxed and dehydrated using xylene and ethanol solutions before being rinsed with tap water. For HE staining, they were stained with hematoxylin solution (Servicebio, G1003) and treated with differentiation and bluing solutions before being fixed with ethanol and stained with Eosin dye. The sections were then dehydrated and placed in xylene before being sealed with neutral gum. For Nissl Staining, they were stained with Nissl dye (Servicebio, G1036) and treated with a differentiation solution before being rinsed and sealed with neutral gum. The pathological changes in the hippocampus were observed under a light microscope. The Nissl-stained positive neurons in the hippocampal dentate gyrus (DG) region were counted under a light microscope. Besides, each section were visually counted in a blinded manner. The results show the

different number of surviving neurons in CIH group compared to the CON group in same regions (Chu et al., 2019; Ke et al., 2020).

2.6 Multiplex immunofluorescence staining

Each group (n = 6 mice/group) without undergoing behavior test were anesthetized with chloral hydrate and then sacrificed. To prepare the tissue sections for immunohistochemistry, we treated them with a 0.3% hydrogen peroxide solution and then used microwave treatment to enhance antigen retrieval. We blocked the sections in 5% BSA before incubating them overnight at 4°C with the primary antibody GFAP (diluted to 1:100, Cell Signal Technology). The next day, we performed secondary antibody detection using HRP-conjugated anti-rabbit IgG (ZSGB-Bio, Beijing, China) at room temperature for 1 h. We utilized TSA reaction of AlexaFluor FITC-Conjugated TSA (1:50, Akoya) to visualize immunoreactivity, followed by microwave treatment for 15 min and cooling. Subsequently, we performed immunostaining with the primary antibodies Neun (diluted to 1:1000, Cell Signal Technology), Iba-1 (diluted to 1:200, Cell Signal Technology), and DCX (diluted to 1:200, Cell Signal Technology) successively on the same section. Corresponding secondary detections were performed with AlexaFluor CY3- and CY5-Conjugated TSA (1:50, Akoya). For image capture, a fluorescence microscope (Olympus BX43 microscope) was used under uniform exposure settings and conditions for all samples. Subsequently, the acquired images were processed using ImageJ software[1] in a blind manner. To assess the staining intensity of Neun, GFAP, Iba-1, and DCX, we measured the integrated density (IntDen). Utilizing ImageJ software, positive staining was quantified in terms of pixels, and then IntDen (calculated as the area multiplied by the mean gray value) (Mela et al., 2022), was determined as an indirect indicator of protein level.

2.7 Cytokine and chemokine assays

In the central nervous system (CNS), glial cells could mediate the neuroinflammation by releasing potentially neurotoxic mediators including cytokines, chemokines. In order to analyze these inflammatory cytokines, we performed luminex liquid suspension chip assay by Wayen Biotechnologies (Shanghai, China), including interleukin (IL)-4, IL-6, IL-10, and tumor necrosis factor (TNF)-alpha. Briefly, we obtained hippocampus tissue samples from the CIH and CON groups (3 mice per group). We lysed and centrifuged the samples at 13,200 rpm for 15 min. After measuring the protein concentrations, we diluted 45 μg total protein in 50 μl solution to ensure equal protein quantity and equal buffer volume for each sample. After incubating the samples in 96-well plates with embedded microbeads for 1 h, we added detection antibodies (anti-mouse 31 cytokines, as instructed in the Luminex 200 kit manual) and incubated them for an additional 30 min. Subsequently, we introduced streptavidin-PE to each well and incubated the mixture at 850 rpm for 10 min. These samples were then incubated in 96-well plates embedded with microbeads for 1 h. Subsequently, detection antibodies (anti-mouse 31 cytokines, according to the manual of the Luminex 200 kit) were added and incubated for an additional 30 min. Finally, streptavidin-PE was added to each well and incubated at 850 rpm for 10 min. The values were measured using the Bio-Rad Luminex Bio-Plex 200 System.

2.8 Sample collection, protein extraction, and trypsin digestion

After the CIH procedure, the mice were euthanized, and their brains were extracted. Six mice were used for the CON group and another six mice for the CIH group. Due to the relatively small volume of the hippocampus, a strategy was employed to pool the hippocampi from two mice together as one replicate, and three replicates were conducted for each group. Specifically, the hippocampi were isolated and quickly frozen using liquid nitrogen to limit degradation. To avoid the potential influence of circadian rhythms, tissue collection was conducted simultaneously, ensuring that all samples were obtained at the same time. The samples were then stored at −80°C until processed further. Subsequently, the cellular powder was treated with lysis buffer and a protease inhibitor, followed by sonication utilizing a high-intensity ultrasonic processor (Scientz). After removing debris through centrifugation at 12,000 g for 10 min at 4°C, the supernatant containing the protein solution was obtained and quantified for its protein concentration using BCA kit. The protein solution underwent treatment with 5 mM dithiothreitol at 56°C, followed by alkylation with 11 mM iodoacetamide at 25°C in the absence of light. To minimize the urea concentration to less than 2 M, 100 mM TEAB was added to dilute the protein sample. For the initial overnight digestion, trypsin was employed at a 1:50 ratio of trypsin-to-protein mass to initiate digestion, and peptides were desalted by C18 solid-phase extraction column. The method for extracting and breaking down proteins was identical for both the proteome and acetylome.

2.9 Acetylated peptide enrichment and LC-MS/MS analysis

To enrich acetylated peptides in the acetylome, we followed a similar protocol as described above for protein extraction and trypsin digestion. However, we included additional inhibitors (3 μM trichostatin and 50 mM nicotinamide) in the lysis buffer, and each sample utilized 2.5 mg of protein for trypsin digestion. Subsequently, we dissolved the peptides in NETN buffer (1 mM EDTA, 100 mM NaCl, 0.5% NP-40,50 mM Tris–HCl, pH 8.0) and incubated them overnight with anti-acetyllysine antibody-conjugated agarose beads. Once the beads were washed and the bound peptides were eluted using trifluoroacetic acid, we combined the eluted peptides, vacuum-dried them, desalted them, and prepared them for analysis. More specific formulations for the inhibitors and NETN buffer can be found elsewhere (Qian et al., 2022). LC-MS/MS analysis was conducted at PTM Biolab in

1 http://imagej.nih.gov/ij/

Hangzhou, China. We dissolved the desalted peptides in solvent A, which contained 0.1% formic acid in 2% acetonitrile. Using a reversed-phase analytical column and a gradient of solvent B (0.1% formic acid in 100% acetonitrile), we performed proteome analysis with a gradient ranging from 6 to 24% over 70 min, followed by an increase from 24 to 35% over 12 min, and finally reaching 80% over 4 min, holding at 80% for an additional 240 s, while maintaining a constant flow rate of 450 nL/min. For acetylome analysis, we used a gradient starting at 6% and increasing to 24% over 40 min. The TimsTOF Pro mass spectrometer from Bruker Daltonics was used to analyze the peptides.

To analyze the raw MS/MS data obtained from our proteomic analysis, we utilized the MaxQuant computational proteomics platform (version 1.6.15.0[2]). The MaxQuant platform implements the MaxLFQ algorithm, and the specific algorithmic rules have been previously reported (Cox et al., 2014). We compared the data against the Mus_musculus_10090_SP_ 20230103.fasta database (Uniprot, 17,132 entries, acquired on 2023.1.3), which includes common contaminants and a reverse decoy database. To ensure accuracy and reliability, we specified the cleavage enzyme as Trypsin/P with allowance for up to two missing cleavages and up to five modifications per peptide. A mass error of 20 ppm was set for both precursor ions in the searches. To maintain high confidence and reliability, we set the false discovery rate (FDR) thresholds below 1% for proteins, peptides, and acetylated sites.

2.10 Bioinformatic analysis

We employed the ClustVis tool[3] to conduct a principal components analysis (PCA) and characterize the CIH and CON groups. For differential expression analysis of acetylated proteins (DAPs), we applied strict criteria, including a p-value less than 0.05 and a fold change greater than 1.5 or less than 0.67, to identify DAPs. To analyze correlations of posttranslational modifications (PTMs) in our data, identify novel acetylation sites, and explore overlaps with other PTM types, we utilized the protein lysine modifications database (PLMD; version 3.0[4]) (Xu et al., 2017). Protein domains were analyzed using the InterPro database,[5] while subcellular distribution prediction was performed using the Wolf Psort tool (version 1.0[6]). For functional enrichment analysis, we utilized the UniProt-GOA and Kyoto Encyclopedia of Genes and Genomes (KEGG) databases.[7,8] To construct a protein-protein interaction (PPI) network, we used the STRING database (version 11.0[9]), and visualized the network in R using networkD3 (R package version 0.4). We selected interactions with a confidence score greater than 0.7 for DAPs. The MCODE plugin in Cytoscape software (version 3.6.1[10]) was utilized to identify the top five clusters with the highest degree of interconnectivity. We also examined the connections between DAPs and markers of gliosis (GFAP) and neurogenesis (DCX). To categorize acetylated sites based on their response to CIH, we employed a Gaussian mixture model. Furthermore, motif analysis of acetylated sites, considering the potential influence of neighboring conserved sequences on enzyme-substrate preference, was performed using the iceLogo tool (version 1.3.8[11]) (Colaert et al., 2009; Shen et al., 2022). We identified significant motifs within ± 6 amino acids surrounding lysine acetylation sites, using Mus musculus protein sequences as a reference. Additionally, prediction of secondary structure and surface accessibility was carried out using the NetSurfP tool (version 3.0[12]). The significance of both bioinformatic analyses was assessed using Fisher's exact test with a corrected p-value < 0.05.

2.11 Immunoprecipitation and western blotting

For immunoprecipitation assays, the proteins extracted from mouse hippocampus were lysed using immunoprecipitation buffer (NP-40, Beyotime Biotechnology). Then, the samples were incubated with anti-acetyllysine antibody conjugated agarose beads (PTM Biolab) at 4°C overnight. After three washes with immunoprecipitation buffer, the acetylated proteins were centrifugated to pelletize beads (4°C, 60 s). The bound acetylated proteins were eluted by boiling in SDS loading buffer for 5 min. Samples were collected after centrifugation (4°C, 10,000 g). For Western blot assays, the immunoprecipitated proteins or input were separated on 12% SDS-PAGE gel. And then, the samples were transferred onto polyvinylidene fluoride (PVDF) membrane (Millipore, United States). The membranes were blocked for 1 h with 5% milk in TBST, and then incubated with primary antibodies: VDAC rabbit monoclonal antibody (diluted to 1:1000, Cell Signal Technology), 14-3-3 protein zeta/delta (Ywhaz) rabbit monoclonal antibody (diluted to 1:1000, Cell Signal Technology), and Camk2a rabbit monoclonal antibody (diluted to 1:1000, Cell Signal Technology) at 4°C overnight. Following three washes with TBST, the membranes were further incubated with horseradish peroxidase-conjugated secondary antibodies [Horse anti-mouse (diluted to 1:1000) and Goat anti-rabbit (diluted to 1:1000), ZSGB-Bio, Beijing, China] for 90 min at room temperature. Finally, the membranes were visualized using ECL (Beyotime Biotechnology, China).

2.12 Immunohistochemistry

Brain tissue was cut into 5-μm sections, and then were performed immunohistochemistry with anti-acetyl-Histone H3 (Lys27) antibody (H3K27ac), and anti-acetyl-Histone H3 (Lys9) antibody (H3K9ac). The sections were incubated overnight with primary antibodies against H3K27ac (diluted to 1:100, PTM Biolab), and H3K9ac (diluted to 1:50, PTM Biolab) at

2 http://www.maxquant.org/
3 http://biit.cs.ut.ee/clustvis/
4 https://cplm.biocuckoo.cn/
5 https://www.ebi.ac.uk/interpro/
6 https://wolfpsort.hgc.jp/
7 http://www.ebi.ac.uk/GOA/
8 https://www.kegg.jp/
9 https://string-db.org/
10 https://www.cytoscape.org/
11 https://iomics.ugent.be/icelogoserver/
12 https://services.healthtech.dtu.dk/services/NetSurfP-3.0/

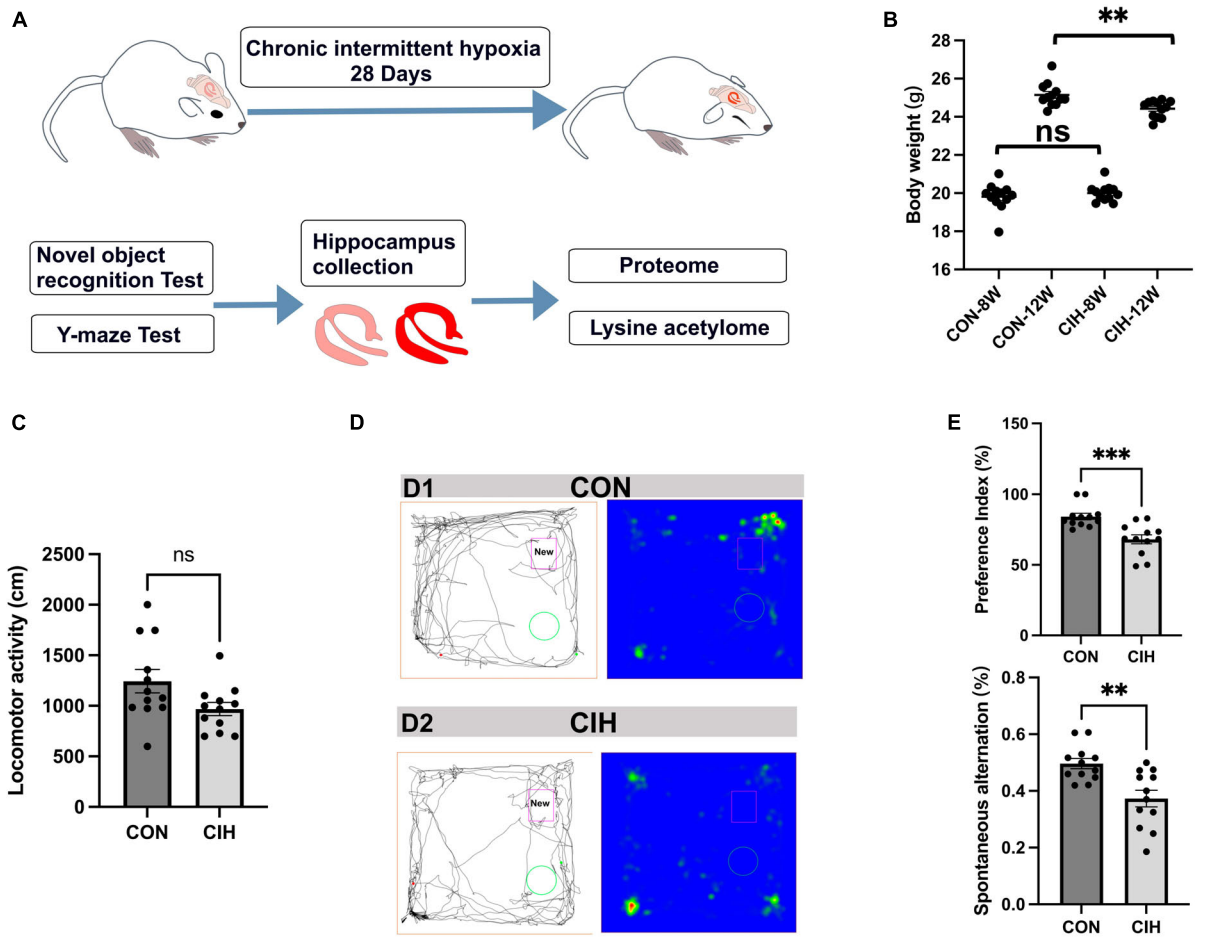

FIGURE 1
Decreased body weight, behavioral alterations, and hippocampal injury at 4 weeks post-CIH. **(A)** Experimental design. NORT, Novel object recognition test. **(B)** Statistical analysis for changes in body weights of the mice in CIH and CON groups upon 4 weeks of CIH intervention. Body weight was decreased during hypoxia (n = 12 mice/group). p = 0.0035 (unpaired t-test). **(C)** Bar charts shows locomotion after CIH or normoxia exposure. n = 12 for each group. Data are shown as mean ± SEM. ns: no significant. **(D,E)** Behavioral alterations were assessed by NORT and Y-Maze test (n = 12 mice/group). Typical movement tracks for CON (D1) and CIH (D2). Black lines indicate movement trajectories, whereas red hues denote the new object. Green circles indicate the old object. In the heatmap, areas with higher values of optical density indicate increased time spent by the mice in those regions. CIH significantly injured novel object recognition memory (p = 0.0005) and spatial working memory in the CIH group (p = 0.0017) when compared with the CON. Error bars represent mean ± SEM (n = 12 mice/group). ***p < 0.0001, **p < 0.005. ns: not significant; CON: Control; CIH: chronic intermittent hypoxia.

4°C. Subsequently, the sections were incubated with a biotin-conjugated secondary antibody (diluted to 1:600, Thermo Fisher), followed by staining using a diaminobenzidine solution. The stained tissue sections in the hippocampal dentate gyrus (DG) region were examined by a light microscope. The average integral optical density (IOD) of selected fields were analyzed by Image J software.

2.13 Statistics

We used GraphPad Prism 8 software to compare the CIH and CON groups, considering a p-value of less than 0.05 as statistically significant. We presented the data in the format of mean ± SEM. For the NORT, Y-maze test, and MS/MS data, we performed an unpaired t-test to calculate statistical significance. In bioinformatics analysis, which included protein domain, GO, and KEGG pathway analysis, we employed a two-way Fisher's exact test for calculation. To perform motif analysis, we utilized a binomial test, while we analyzed secondary structure distribution and surface accessibility through a Wilcoxon rank sum test.

3 Results

3.1 Hippocampal lesions and behavioral changes after chronic intermittent hypoxia

To characterize changes in cognition and lysine acetylation abundance specifically in the hippocampus in CIH mice, we treated male C57BL/6J mice with a gas control apparatus to simulate chronic intermittent hypoxia for 4 weeks (Figure 1A). Exposure to chronic intermittent hypoxia was found to influence the

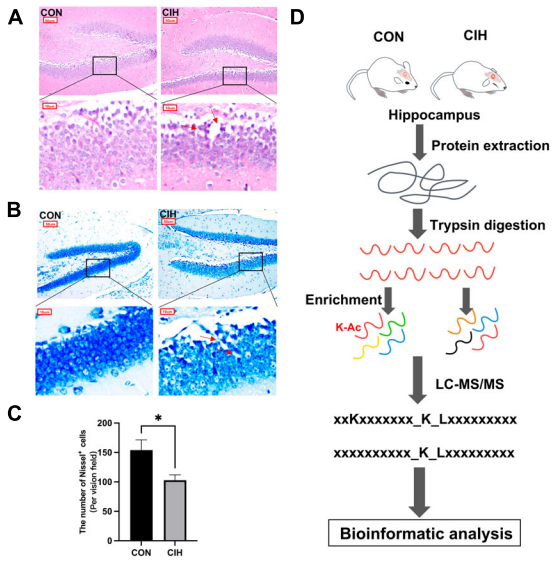

FIGURE 2
Pathological damage in CIH mice. HE staining **(A)** and Nissl staining **(B)** shows hippocampal morphological or structural abnormalities under CIH. The red arrow points to the damaged neuron body. Scale bar: 50 μm or 10 μm. **(C)** Quantification of the number of Nissl$^+$ cells (p = 0.0262). Data are expressed as mean ± SEM (n = 6 mice/group). *p < 0.05 (unpaired t-test). **(D)** Bioinformatic analysis of proteome and acetylome. CON: Control; CIH: chronic intermittent hypoxia.

progression of body weight (Figure 1B; Supplementary Table 1). After 4 weeks of CIH exposure, we observed a substantial reduction in the body weight of the CIH group (24.42 g ± 0.44) compared to that of the control group (25.14 g ± 0.63). To further investigate the cause of weight loss, we also measured the physical activity and dietary intake. In the 16 h after the last day of daily exposure, the CIH group consumed an average of 13.92 ± 1.04 g of food, which was significantly less than that of the CON group (15.78 ± 0.38 g of food; p = 0.044), while both groups drank the same amount of water (CIH, 26 ± 1.73 ml; CON, 22 ± 3.46 ml; p = 0.148) (Supplementary Table 1). Locomotor activity did not significantly change in the CIH group compared to the normoxic CON group (Figure 1C). The above results indicate that the reduction in food intake is a significant factor contributing to the weight loss observed in the CIH group. The above results indicate that a reduction in food intake was a significant factor contributing to the weight loss observed in the CIH group. The NORT and Y-maze (Figures 1D, E) tests revealed that cognitive ability, such as learning or memory, was significantly impaired following CIH exposure (Supplementary Table 1). Learning and memory ability are intimately associated with the structure and morphology of hippocampal neurons. Consequently, we used hematoxylin and eosin (HE) staining and Nissl staining to reveal damage in the hippocampi of the mice. HE staining (Figure 2A) and Nissl staining (Figure 2B) revealed that exposure to chronic intermittent hypoxia resulted in cytolysis and cytoplasmic vacuolation in the hippocampal DG region compared to the control group. In the CON group, neurons exhibited round or oval cell bodies with clearly visible nuclei, while in the CIH group, hippocampal neurons were damaged and lost (Figure 2C).

3.2 CIH promotes the activation of glial cells, inhibits neurogenesis, and induces inflammation

NeuN is a marker protein for neuronal cells, and Iba-1 and GFAP are marker proteins of microglia and astrocytes, respectively. In our study, we performed immunofluorescence staining in the DG region of the hippocampus using NeuN, GFAP, Iba-1 and DCX antibodies, as shown in Figures 3A–D. Compared with those in the CON group, the staining intensity level of GFAP and Iba-1 in the CIH group were increased, which indicated potential glial activation (Figures 3B, C, E). Conversely, NeuN was notably decreased in the CIH group, as demonstrated in Figures 3A, E. The downregulated NeuN suggested a potential detrimental effect of CIH on neuronal integrity, as a reduced level of NeuN is generally associated with neuronal loss or dysfunction. To explore the effects of chronic intermittent hypoxic conditioning on neurogenesis, we performed DCX immunofluorescence staining. Compared with that in the CON group, the number of DCX-positive cells in the hippocampus was significantly lower in the CIH group (Figures 3D, E), suggesting that CIH inhibits neurogenesis.

Microglia are innate immune cells that participate in immune surveillance within the CNS. Astrocytes also play an active role in the regulation of neuroinflammation. To assess the overall inflammatory status of the hippocampus, we next investigated the cytokine and chemokine levels in the hippocampi of mice in the CON and CIH groups via a Luminex assay. The levels of many cytokines and chemokines, including CXCL5, CXCL16, IL-4, IL-6, IL-10, and TNF-α, were increased in the CIH group compared with those in the CON group (Figure 3F). These results indicated that CIH induced neuroinflammation. In summary, above results underscore the potential detrimental effects of CIH on hippocampus function.

3.3 Changes in the hippocampal proteome

Despite the observed cognitive decline and neural damage resulting from CIH exposure, the specific mechanisms underlying the perturbation of the hippocampal proteome and acetylome remain elusive. To address this gap, we employed MS methods to examine the alterations in protein abundance and acetylation in mice subjected to CIH (Figure 2D). To identify changes in the protein abundance and biological processes (BP) associated with the CIH response, we carried out proteomic analysis (Figure 2D; Supplementary Table 2) using a CIH model. As shown by the PCA, our data clearly distinguished the CIH group from the CON group (Supplementary Figure 1A). We identified 5,729 proteins in the hippocampi of CIH and CON mice, 4,878 of which were quantified via proteomic spectrogram analysis (Supplementary Figure 1B). Although numerous proteins were identified, only 21 proteins exhibited significant differences (Supplementary Figure 1C). Specifically, as shown in Supplementary Figure 1D, Clic6 and Orai2 were significantly regulated in the CIH group and were tightly associated with cognitive changes (Xu et al., 2020; Ma et al., 2021). We specifically focused on the abundance of lysine acetyltransferases (KATs) and lysine deacetylases (KDACs) via

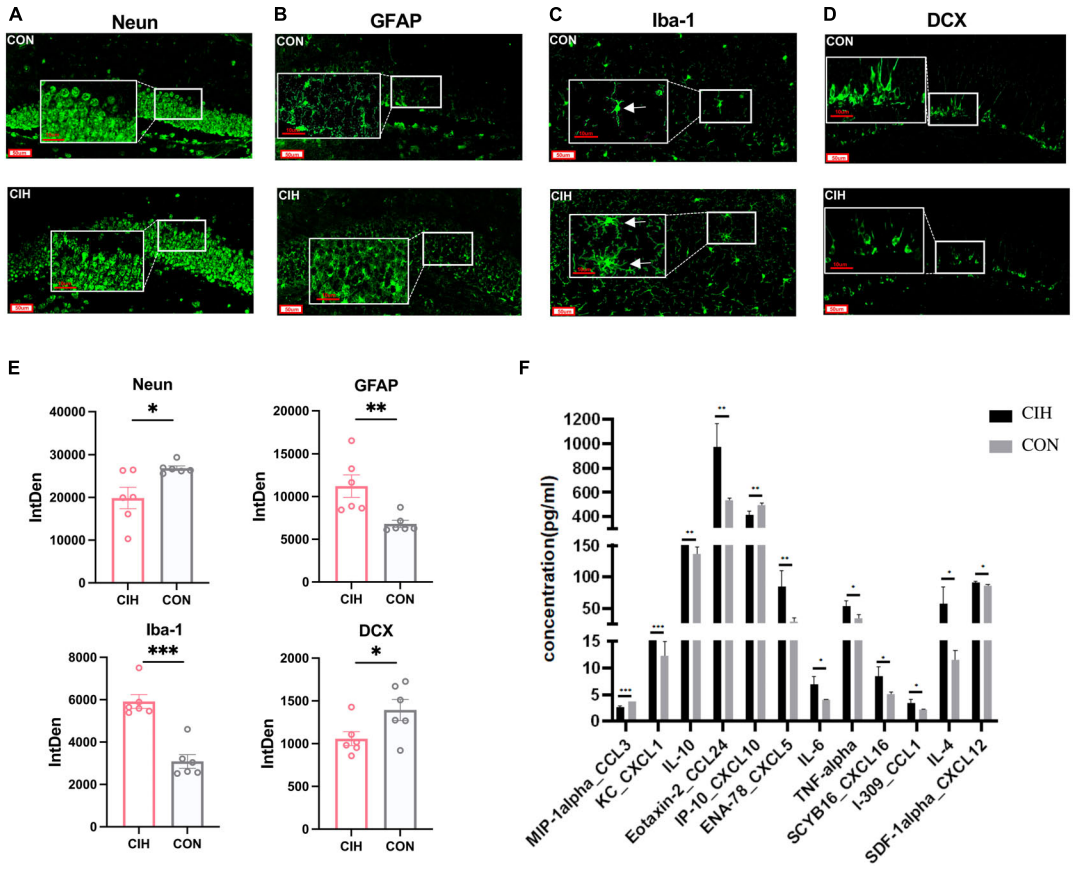

FIGURE 3
Representative immunofluorescence images. **(A–D)** Representative immunofluorescence images of Neun, GFAP, iba-1, and DCX for hippocampus when exposed to CIH. Scale bar: 50 μm or 10 μm. **(E)** Analysis of the immunofluorescence intensity of Neun, GFAP, iba-1, and DCX by measuring integrated density (IntDen) values. Data are expressed as mean ± SEM (n = 6 mice/group). **(F)** Cytokine and chemokine levels in the hippocampus of mice in the CON and CIH groups (n = 3 mice/group). Data are presented as means ± SEM. Statistical analysis was performed using student t-test, $^*p < 0.05$, $^{**}p < 0.01$, $^{***}p < 0.001$. CON: Control; CIH: chronic intermittent hypoxia.

proteomics analysis. The proteomic data encompassed several KDACs (Sirt2-3, Sirt5, Hdac1-2, Hdac4-6, Hdac11) and KATs (Acat1-2, Atat1, Chat, Crat, Crebbp, Dlat, Naa10, Naa15, Naa25, Naa30, Naa35, Naa50, Nat10, Nat14). Although there were more types of KATs and KDACs, no statistically significant differences in protein abundance were observed (**Supplementary Table 4**). In BP analysis, the majority of proteins were enriched in phagocytosis and immune response, especially in B cells (**Supplementary Figure 2A**; **Supplementary Table 3**). Furthermore, in the analysis of cellular components (CC), most of proteins showed enrichment in immunoglobulin complexes (**Supplementary Figure 2B**; **Supplementary Table 3**). Finally, in the analysis of molecular functions (MFs), a notable enrichment of these proteins in immunoglobulin receptor-binding activities was observed (**Supplementary Figure 2C**; **Supplementary Table 3**).

3.4 Identification of lysine acetylation proteins and sites in the hippocampus

Despite the limited number of differentially abundant proteins identified in the hippocampus, we observed substantial increases in the abundance of acetylated proteins and sites. Similarly, we evaluated the quality of MS data first. To ensure the reliability and relevance of our analysis, we applied strict filtering criteria to the data. Specifically, we used the significance criterion of $p < 0.05$ and a fold change threshold of at least 1.5 to narrow down the list of potentially relevant changes in lysine acetylation levels. We performed PCA to characterize the signatures of and distinguish the CIH and CON groups (**Figure 4A**). According to our identification, the lengths of all the acetylated peptides ranged from 7 to 27 amino acids, and most of them ranged from 7 to 16 amino acids (**Figure 4B**). Additionally, the number of lysine acetylation sites in each protein ranged from 1 to 19 and 55.8% of acetylated proteins had only one lysine acetylation site (**Figure 4C**). Mass errors in the lysine acetylome were highly accurate (**Figure 4D**; **Supplementary Table 5**). In total, we identified 2,184 acetylation sites distributed across 1,007 acetylated proteins. These findings highlighted that approximately 17.6% of all the modified proteins exhibited acetylations (**Figure 4E**, Top). Among the 1,672 acetylated sites quantified on 795 proteins, the upregulated DAPs and differential acetylated sites (DASs) were the majority (**Figure 4E**, Bottom). Interestingly, Qian et al. (2022) observed an increase in cognitive function in mice and found that the downregulated acetylation sites were predominant. It seems

that global changes in the hippocampal lysine acetylome could contribute to alterations in cognitive ability. Despite advances in the understanding of cognitive dysfunction, research exploring the impact of lysine acetylation on hippocampal models of cognitive changes is lacking. Additionally, those associated with mitochondria, such as Sptan1 (19 sites), Aco2 (18 sites), Cnp (15 sites), Idh2 (14 sites), and Got2 (13 sites), exhibited the most abundant acetylations. Furthermore, we predicted the subcellular distribution of DAPs upon CIH intervention; these proteins were localized mainly to mitochondria (35.75%), the cytoplasm (34.78%), and the nucleus (11.11%) (**Figure 4F**; **Supplementary Table 6**). Overall, these findings highlight the importance of acetylation in mitochondrial regulation and suggest their potential involvement in the cellular responses to CIH-induced damage. In addition, to further validate the reliability of our MS data, we performed Western blot analysis in this study (**Supplementary Figures 3A, B**). Western blot analysis conducted in our study also revealed that the levels of acetylated proteins (VDAC, Ywhaz, Camk2a) under CIH conditions were consistent with the results obtained from the MS data.

3.5 Posttranslational modification correlation analysis for acetylation sites

Determining novel lysine modification sites is crucial for expanding the understanding of PTMs, revealing new functionalities and regulatory mechanisms, and identifying potential therapeutic targets. By comparison with previously reported lysine modification sites in mice from the PLMD database, we identified 292 novel proteins and 977 newly discovered lysine acetylation sites (**Supplementary Table 7**). Furthermore, our analysis revealed the presence of various other types of PTMs at the identified lysine sites, including ubiquitination (920), succinylation (776), malonylation (604), and glutarylation (209) (**Supplementary Table 8**). Among them, the Ywhaz can undergo both acetylation and ubiquitination at sites K11, K120, and K138. Similarly, the Calcium/calmodulin-dependent protein kinase type II subunit delta (Camk2a) can be acetylated and ubiquitinated at sites K56, K136, K250, K258, K291, and K42 (**Supplementary Table 7**). Another example is fructose-bisphosphate aldolase (Aldoa), for which we newly discovered acetylation at the K208 site. These findings highlight the complexity of protein posttranslational modifications. Different types of modifications occurring at the same or adjacent sites on a protein can potentially result in crosstalk, which could contribute to the intricate nature of diseases.

3.6 CIH altered the characteristics of acetylation sites

To examine the patterns of identified acetylated sites following CIH treatment, we divided all acetylated sites into 3 categories: class I contained unregulated sites, class II mostly contained sites upregulated by CIH, and class III mostly contained downregulated sites (**Figure 5A**). We conducted motif analysis on each group to gain a better understanding of their physical properties (**Figure 5B**). We found that class II sites favored aspartic acid (D) at the −1 position, while class I sites favored glycine (G) at the −1 position. Furthermore, we observed that class III sites preferred isoleucine (I) at the +1 position, while leucine (L) was favored at both class I and II sites. Compared to non-modified lysine residues, DASs were significantly enriched in beta strands ($p = 4.45 \times 10^{-6}$; **Figure 5C**, left). Similarly, DASs exhibited greater accessibility to surface exposure (**Figure 5C**, right). These results suggest that DASs caused by chronic intermittent hypoxia in the hippocampus may impact protein function by changing preferences for neighboring amino acids, beta-strand secondary structure and surface accessibility.

3.7 Profiling the lysine acetylome in mouse models of CIH

To gain insight into the biological functions and networks associated with differentially acetylated lysine residues, we performed domain, GO/KEGG pathway, and subcellular localization analyses. Interestingly, we observed a significant increase in the number of upregulated DAPs localized to mitochondria compared to the number of downregulated DAPs when performing subcellular localization analysis separately for upregulated and downregulated proteins (**Figure 6A**, **Supplementary Table 6**). These findings further implies potential dysregulation of mitochondrial function in response to CIH. Such dysregulation may contribute to cognitive impairments. Next, we categorized the significantly changed acetylated sites into four groups (Q1-Q4) based on the degree of fold-change values observed (**Figure 6B**). For the KEGG pathways, DAPs in Q3 and Q4 were mainly enriched in TCA cycle, necroptosis, and neurodegeneration diseases (Parkinson's disease, Alzheimer's disease, and Huntington disease) (**Figure 6C**). For domain enrichment analysis (**Figure 6E**), DAPs in Q4 were mainly enriched in Acy-CoA dehydrogenase, while in Q3 they were mainly enriched in Biotin-requiring enzyme. The Acy-CoA dehydrogenase domain and the main KEGG pathways mentioned above are closely associated with mitochondria. Consistent with these above findings, GO enrichment analysis showed that the main biological process, molecular function, and cellular component were closely associated with mitochondrial activity. This includes GO:0032787 (monocarboxylic acid metabolic process), GO:0006090 (pyruvate metabolic process), and GO:0005759 (mitochondrial matrix) (**Figure 6D**). Both the subcellular localization analysis and functional pathway analyses consistently indicate that mitochondrial function is disrupted by CIH. The altered acetylation of proteins associated with mitochondrial function are likely significant contributors to the cognitive impairments observed in response to CIH.

3.8 Analysis of the functional enrichment of differentially acetylated mitochondrial proteins

Moreover, accumulating evidence has also demonstrated that mitochondrial dysfunction plays a pivotal role in the pathophysiology of cognitive impairment

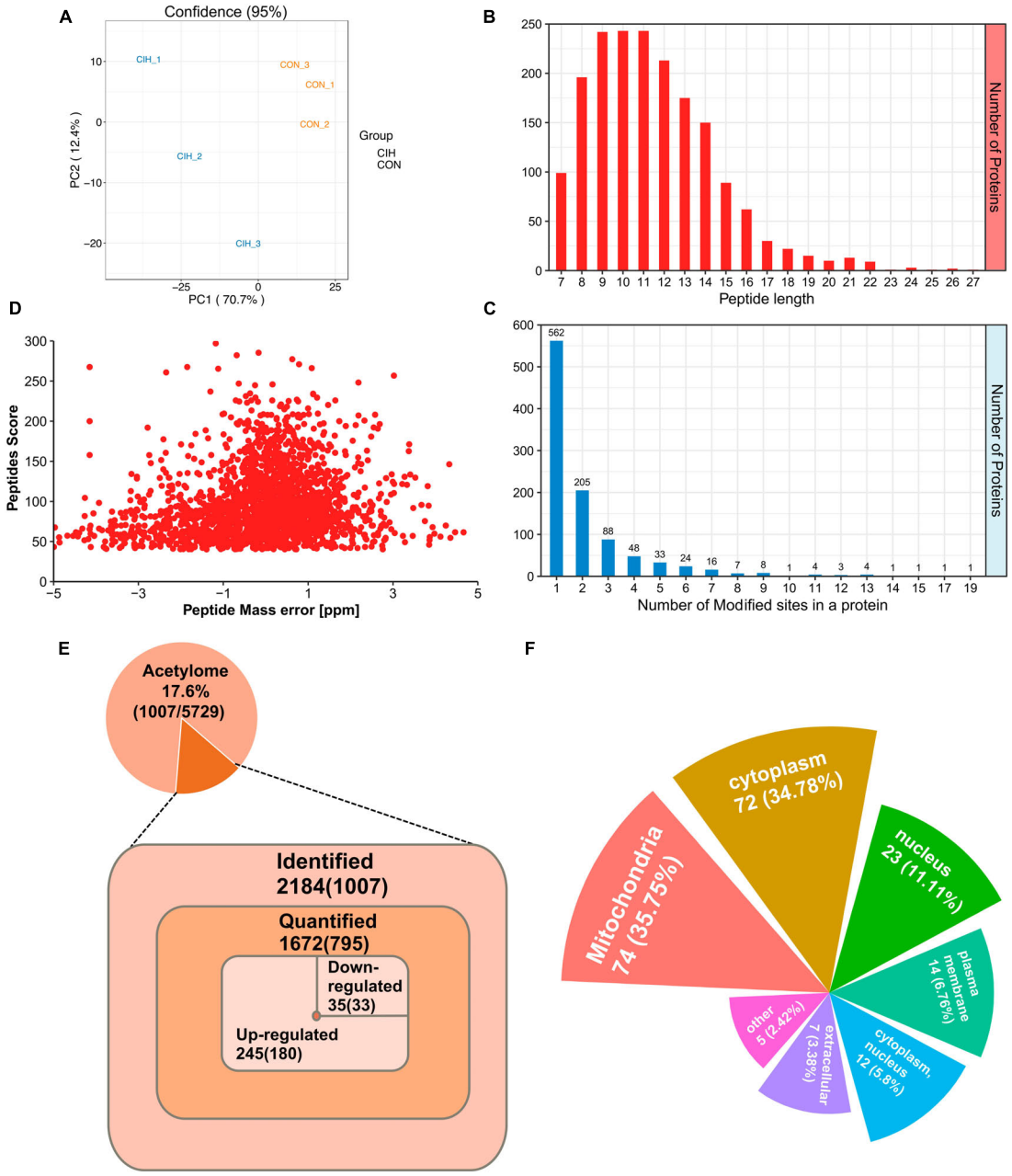

FIGURE 4
Profiling lysine acetylation proteome in the hippocampus. **(A)** Principal component analysis (PCA) of acetylome data generated from CIH and CON groups. **(B)** Distribution of peptide length of all identified acetylated peptides. **(C)** The number of acetylation sites within each modified protein. **(D)** Mass error distribution of all identified acetylated peptides. **(E)** The global view of the acetylated proteins and acetylation sites identified in the study (Top). The Venn diagram showed the number of acetylation sites and the corresponding proteins in brackets (Bottom). Significantly upregulated or downregulated proteins were defined as having a fold change > 1.5 or < 0.667 and $p < 0.05$. **(F)** Rose plots represent the cellular localization of significantly acetylated proteins after chronic intermittent hypoxia.

(Imai and Guarente, 2014; Bonkowski and Sinclair, 2016; Sorrentino et al., 2017; Song et al., 2021). Consistent with above evidence, we found that most acetylated sites were in mitochondrial proteins and were highly upregulated after chronic intermittent hypoxia (Figure 7A). Among the identified KEGG pathways (Figure 7B), the citrate cycle (TCA cycle) was the most highly enriched. The TCA cycle serves as a central hub in cellular metabolism due to its ability to accept multiple substrates. The metabolites of the TCA cycle are essential for protein synthesis. Furthermore, it is increasingly recognized that the metabolites of the TCA cycle also participate in regulating DNA methylation, histone modifications, and PTMs of proteins to modulate their function (Martínez-Reyes and Chandel, 2020). Taken together, the GO analysis of the DAPs revealed that these proteins are involved mainly in monocarboxylic acid catabolic processes, fatty acid beta-oxidation, and oxidoreductase activity, among other pathways (Figure 7B), consistent with the KEGG annotation results.

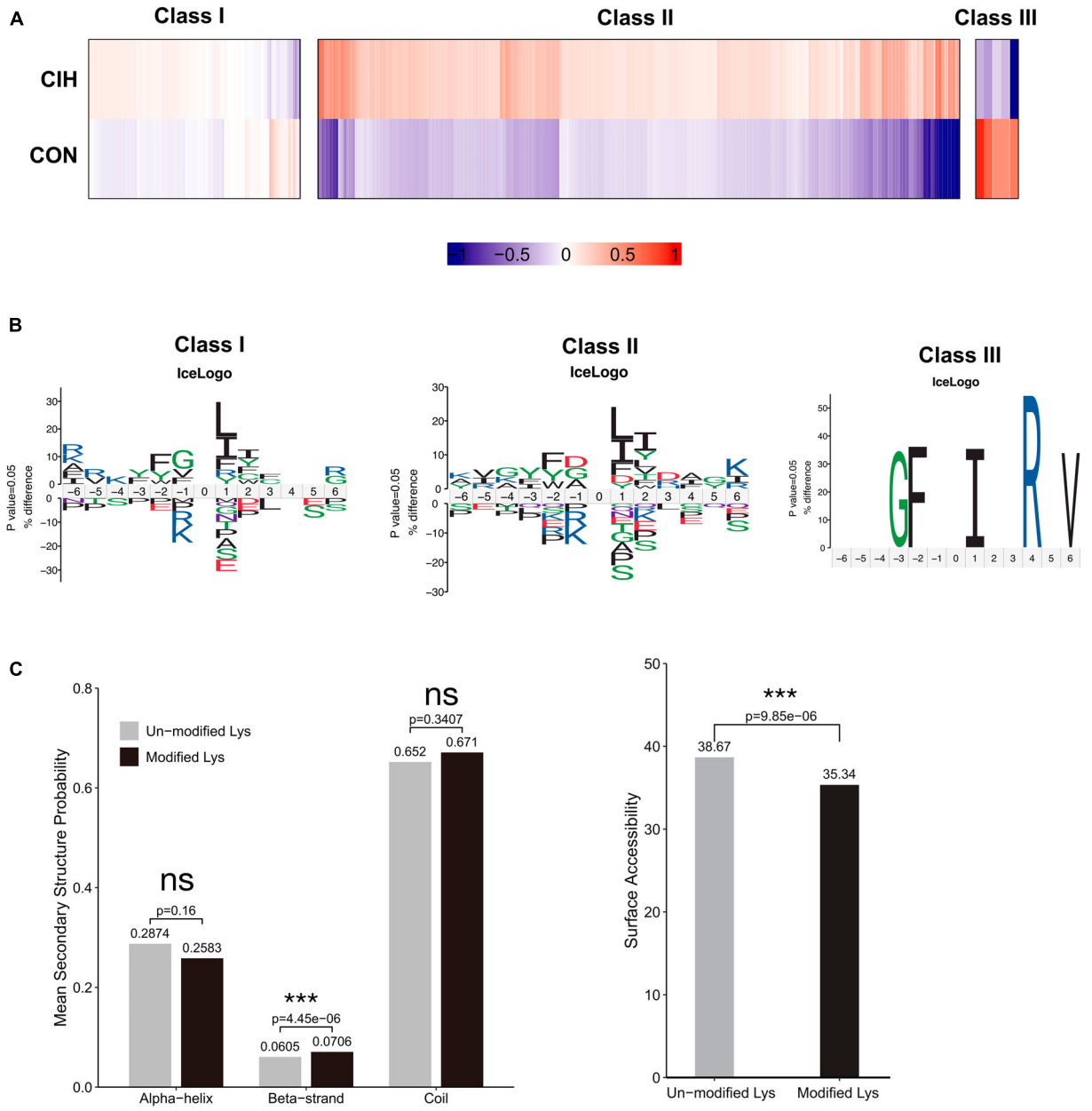

FIGURE 5
Motif analysis of all the identified sites. **(A)** Based on acetylated sites' overall trends between the CIH and normoxia conditions, we grouped 3 classes. Class I sites exhibited no significant change. Class II were upregulated, and Class III sites were downregulated. **(B)** Predicted amino acid motifs for each group identified using a binomial test ($p < 0.05$). The motif showed significant amino acids surrounding each site flanking position 0 lysine. **(C)** Conformational tendencies of all differentially acetylated sites were predicted by protein secondary structures (left) and surface accessibility (right). After chronic intermittent hypoxia, the differentially acetylated sites were significantly enriched in Beta-strand ($p = 4.45 \times 10^{-6}$) and showed a significant decrease in surface-exposed accessibility ($p = 9.85 \times 10^{-6}$) by the Wilcoxon Rank Sum test. ***$p < 0.001$. ns: not significant; CON: Control; CIH: chronic intermittent hypoxia.

3.9 Analysis of protein-protein interaction networks

Investigating protein-protein interactions (PPI) is a crucial step in uncovering the functions of proteins, enabling the study and manipulation of pivotal cellular processes. In order to gain a better understanding of the interactions among DAPs, we conducted a PPI network analysis to display the interconnections among 213 DAPs with high confidence (Figure 8A). In this analysis, highly clustered proteins often share similar or related functions. We identified the five most highly connected clusters: the TCA cycle, oxidative phosphorylation, fructose and mannose metabolism, the synaptic vesicle cycle, and antigen processing and presentation. In the TCA cycle cluster, Aco2, Ndufa10, Pdha1, and Ndufs1 were highly acetylated while their protein contents remained unchanged. In the fructose and mannose metabolism, we observed Voltage-dependent anion channel (Vdac)1–3 were highly acetylated. These proteins were documented to exhibit a

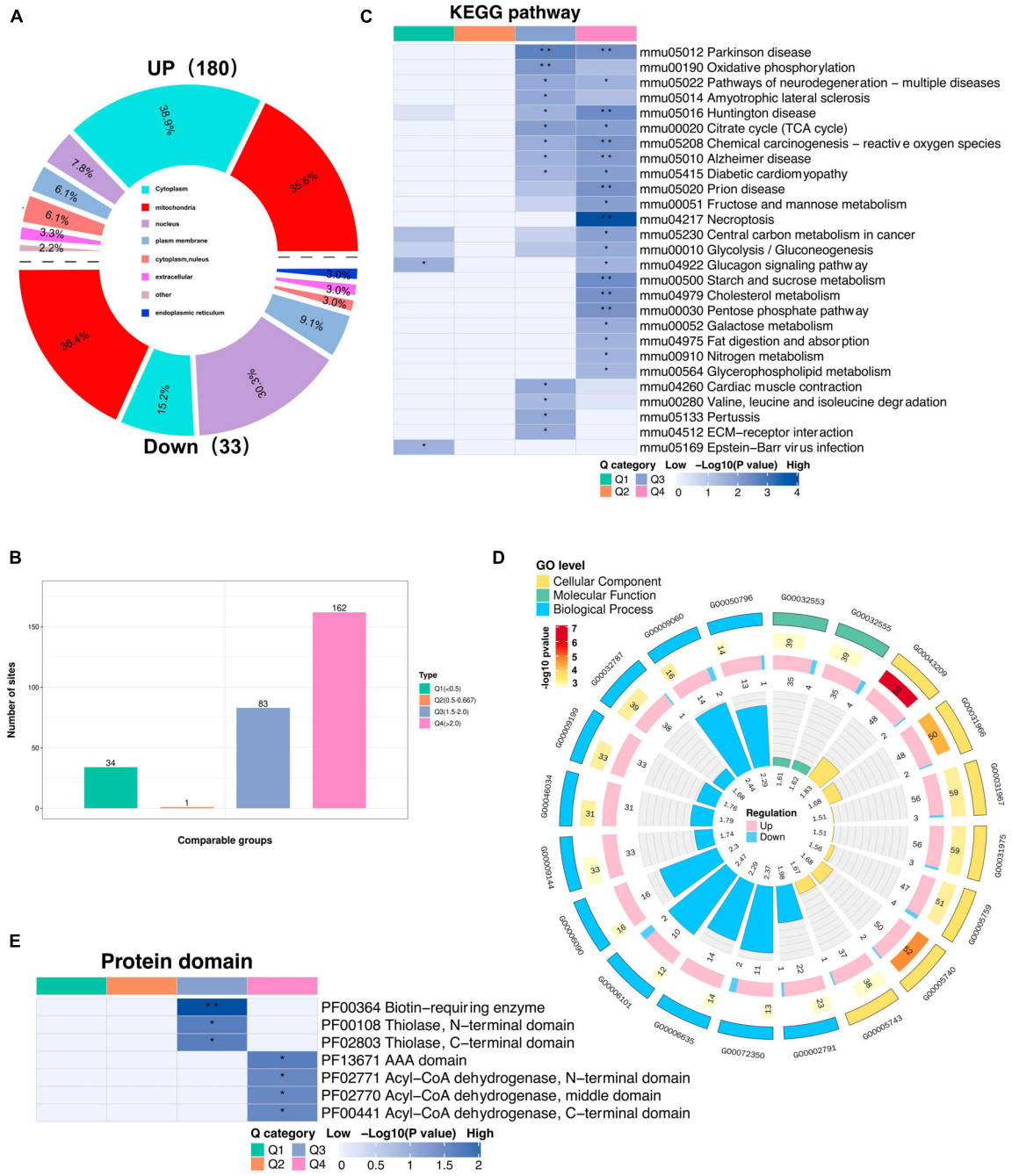

FIGURE 6
Subcellular location and KEGG/GO analysis of differentially expressed acetylated proteins. **(A)** Rose diagram showed the number of all different acetylated proteins in different subcellular structure species, and the corresponding subcellular structure information is shown in different colors. **(B)** The acetylated proteins were divided into four groups based on the fold-change values, respectively, named Q1 to Q4, and enriched with KEGG pathway and protein domain analysis, respectively. **(C)** The bar plot showed the major enriched KEGG pathways by acetylated proteins. **(D)** The Circular plot representing the GO enrichment of differentially acetylated proteins. Each circle means (from the outside to the inside): the First Circle: is the enriched GO function, with different colors representing different categories; the second circle: is the function that contains different acetylated protein numbers and significance *p*-value values, color represents the enrichment significance *p*-value after-Log10 transformation; the third circle: up and down-regulated differential acetylated protein number bar graph; the fourth circle: fold enrichment of each function after Log2 transformation. **(E)** The bar plot shows the major protein domains enriched by the acetylated proteins. $*p < 0.05$, $**p < 0.01$.

strong correlation with cognitive dysfunction (Akarsu et al., 2014; Mangialasche et al., 2015; Huang et al., 2021). Neurogenesis-glia interactions play an important role in hippocampal function (Kim et al., 2020). Based on our findings that CIH suppresses neurogenesis and enhances astrocyte activation, we further investigated the potential relationships between DAPs and GFAP or DCX (**Figure 8B**). The results showed that several DAPs were associated with DCX or GFAP, indicating that acetylation may have a significant impact on neurodevelopmental disorders during CIH.

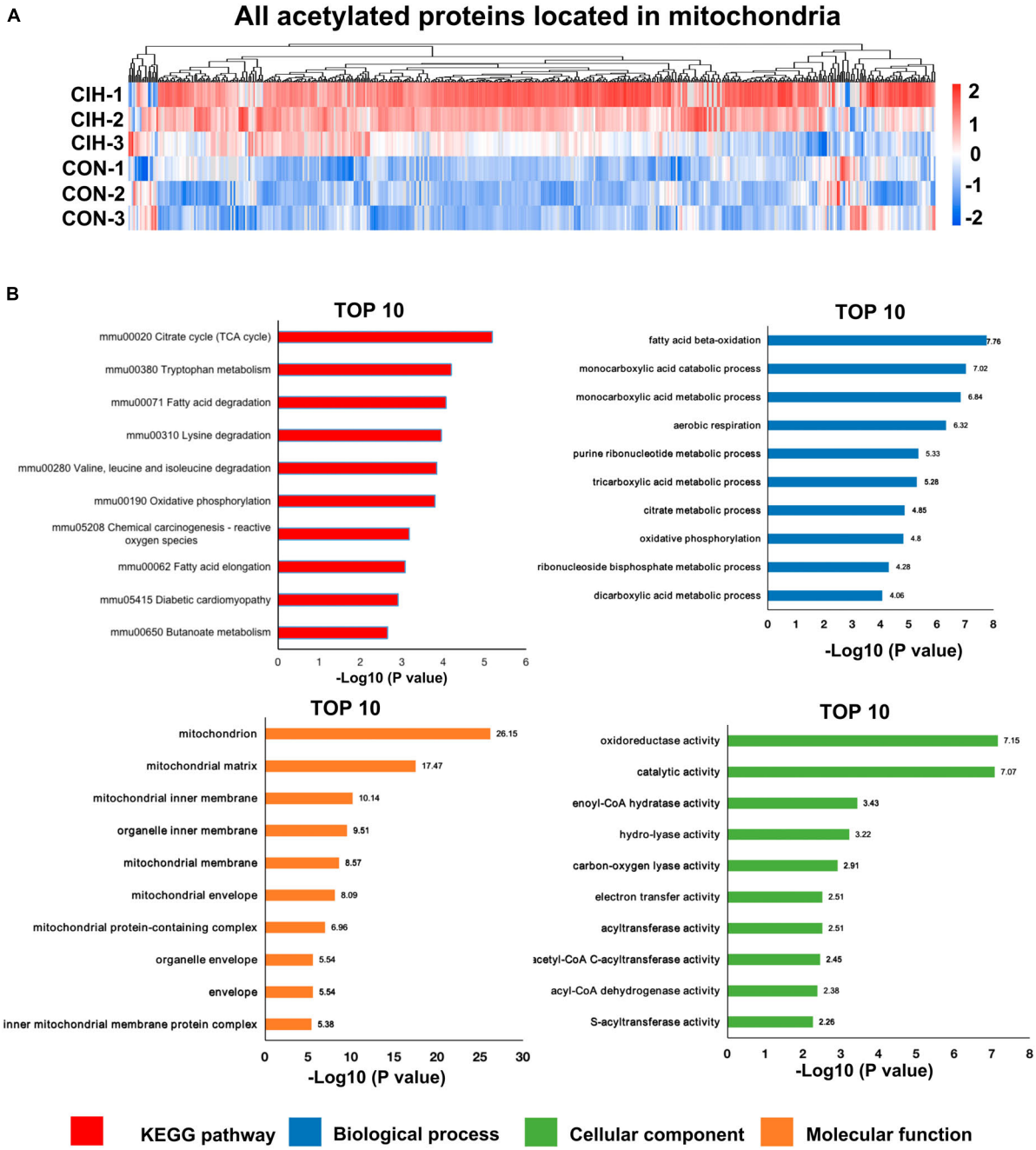

FIGURE 7
Functional pathway enrichment analysis of differentially regulated mitochondrial-localized proteins. **(A)** Heat map displaying differential acetylated proteins localized to mitochondria. The hippocampal samples were represented in rows, and the protein was delineated in columns. The color bar at the bottom of the figure showed that red indicated up-regulation and blue indicated down-regulation. **(B)** Bar plots are presented showing the KEGG pathways, as well as GO analysis results revealing biological processes, cellular components, and molecular functions of the differentially acetylated proteins localized to mitochondria.

3.10 Sodium butyrate regulates acetylation to ameliorate cognitive impairment

To enhance a connection between acetylation and CIH-induced hippocampal damage, we employed a histone deacetylase inhibitor, NaB, for intervention. NaB has recently been recognized as a potential neuroprotective agent for various neurodegenerative diseases (Sharma et al., 2015). After intraperitoneal injection of NaB (Supplementary Figure 3C), we observed an improvement in cognitive function in the CIH+NaB group compared to the CIH group, as assessed by the NORT (Supplementary Figure 3D). We hypothesized that histone acetylation may be linked to CIH hippocampus injury. We tested this hypothesis by examining the acetylation levels of H3K9 and H3K27 in hippocampus from the three groups. The results revealed that H3K9 and H3K27

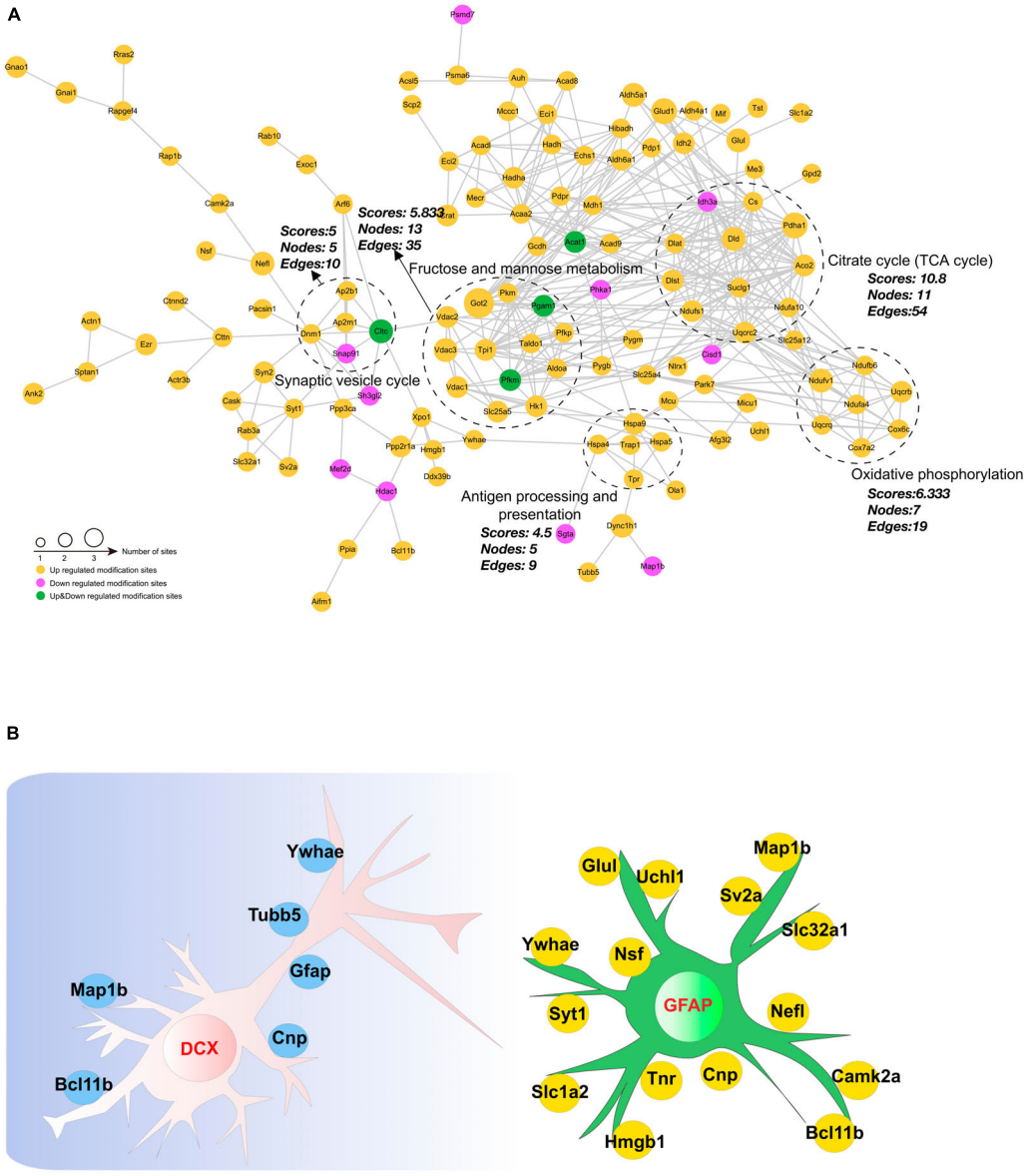

FIGURE 8
Interaction network encompassing the differentially acetylated proteins. **(A)** Network diagram of differentially acetylated proteins and their interactions. The five most highly connected subnetworks are circled for visualization. **(B)** Network methods relying on known protein-protein interactions identify proteins relating to GFAP and DCX (markers of adult gliosis and neurogenesis).

acetylation were suppressed in the CIH group, while treatment with NaB rescued its acetylation (Supplementary Figure 3E). These findings further confirm the role of acetylation in the cognitive impairment caused by CIH.

4 Discussion

Chronic intermittent hypoxia, a prominent characteristic of OSA, has been shown to induce cognitive decline in mice. However, the precise mechanisms responsible for this phenomenon are yet to be fully investigated. In this study, we investigated the changes in proteome and acetylome profiles in a CIH model. Proteome analysis revealed that only a few proteins, including Clic6 and Orai2, exhibited alterations (Supplementary Figure 1D), which were associated with cognition. However, no acetylations were identified on these two proteins, leading us to not delve into their discussion. Furthermore, our observations suggest that CIH resulted in a relatively limited number of global protein changes. In contrast, DAPs exhibited more significant and widespread alterations (Figure 4E). In recent years, there has been increasing research interest in the influence of PTMs, particularly acetylation, on cognitive function (Jaenisch and Bird, 2003; Perikleous et al., 2018). However, few studies have directly shown that PTM changes are responsible for long-lasting behavioral effects in CIH. Therefore, this study primarily focused on investigating and discussing the impact of acetylation on cognitive impairment induced by CIH (Figures 1A, 2D).

We identified 2,184 lysine acetylation sites on 1,007 proteins (**Figure 4E**). We further analyzed the quantified sites and proteins to identify those that were differentially regulated by CIH exposure. Our findings revealed that 280 of the identified acetylation sites located on 213 unique proteins were differentially regulated by CIH exposure. These results suggest that CIH exposure has significant effects on the acetylome profile of the hippocampus and may play a role in the pathogenesis of related cognitive impairments. We then conducted KEGG pathway analysis to gain insight into the potential molecular mechanisms underlying cognitive impairment induced by chronic intermittent hypoxia (CIH) exposure. Our analysis revealed that the pathways associated with the genes exhibiting the most enrichment were related to Parkinson's disease, necroptosis, and oxidative phosphorylation (**Figure 6C**). Further investigation of these pathways revealed significant alterations in neurodegeneration-related diseases such as Alzheimer's disease, Parkinson's disease, and Huntington's disease, as well as central carbon metabolism pathways including the TCA cycle, glycolysis/gluconeogenesis, and the pentose phosphate pathway. Additionally, we analyzed the protein domains enriched in the DAPs identified in our study, which revealed that the DAPs were primarily enriched in biotin-requiring enzymes and Acy-CoA dehydrogenase domains, further highlighting the potential role of lysine acetylation in regulating energy metabolism and cellular processes associated with cognitive function (**Figure 6E**). These findings provide novel insights into the complex molecular mechanisms underlying CIH-induced cognitive impairment and may have significant implications for the development of targeted interventions for related neurological disorders. However, further research is needed to validate these findings and identify specific protein targets for therapeutic intervention.

In addition to being involved in metabolic pathways, the necroptosis pathway was also significantly enriched in DAPs (**Figure 6C**), which are related to markers of neurogenesis (**Figure 8B**). Studies have suggested that necroptosis can be activated in response to ischemic brain injury, neuroinflammation, or neurodegenerative disorders such as Alzheimer's disease. In the hippocampi of CIH mice, we observed increases in the expression levels of inflammatory factors, including IL-4, IL-10, and TNF-a (**Figure 3F** and **Supplementary Table 9**). The involvement of the necroptosis pathway in the hippocampus might contribute to neuronal loss or dysfunction through neuroinflammation. Additionally, we observed acetylation of K250 in Camk2a protein within the necroptosis pathway. Camk2a plays crucial roles in synaptic plasticity, learning, and memory processes within the hippocampus. PTMs of the Camk2a protein have been implicated in various aspects of hippocampal function (Küry et al., 2017). Phosphorylation of the T286 residue in Camk2a has been demonstrated to be crucial for neuronal function and development (Küry et al., 2017). Camk2 activation is not only necessary but also sufficient for the induction of long-term potentiation (LTP) in the hippocampus. LTP is an index of hippocampal functional plasticity (Poggini et al., 2023). Additionally, the histidine residue at position 282 in Camk2a has been identified as an important inhibitory amino acid residue that effectively suppresses Camk2a activity (Smith et al., 1992). PTMs at specific sites in Camk2a are known to play crucial roles in neuronal plasticity. However, further investigations are needed to determine the specific impact of K250 acetylation on hippocampal synaptic plasticity in Camk2a protein. Additionally, it remains to be determined whether there is any cross-talk or interplay between these neighboring sites and whether different modifications occur at the same sites.

Increasing evidence has indicated that CIH damages cognitive function through mitochondrial dysfunction in the brain (Laouafa et al., 2019). Both subcellular localization and functional pathway analyses have consistently indicated that mitochondrial function is disrupted by CIH. Mitochondria are the main organelles in cells that consume oxygen for energy production and metabolism; therefore, oxidative phosphorylation is affected by a lack of oxygen (Scharping et al., 2021). Lysine acetylation is a common posttranslational modification observed in enzymes associated with intermediate metabolism. In our study, 35.75% of the DAPs were found in mitochondria (**Figure 4F**), and most of these DAPs were upregulated (**Figure 6A**). Moreover, significant enrichment of both the TCA cycle and oxidative phosphorylation pathways was observed (**Figure 7B**). Oxidative phosphorylation is the process by which ATP is generated through electron transfer via the electron transport chain, which includes complexes I, III, and IV (Vercellino and Sazanov, 2022). Interestingly, the acetylation levels of key proteins belonging to the electron transport chain, such as Cox6c, Cox7a2, and Ndufa4, were increased in our study (**Figure 8A**). In addition, several subunits of ATP synthase (Atp5pd, Atp5po, and Atp5f1a) were also increased in our study. Moreover, our study revealed that CIH induces the upregulation of multiple acetylation sites on Vdac1, which is involved in fructose and mannose metabolism (**Figure 8A**; **Supplementary Figure 3B**). Vdac1, the most abundant protein on the outer mitochondrial membrane, is a vital protein that regulates mitochondrial function. Increased levels of Vdac1 have been shown to be associated with the progression of diseases involving cognitive impairment, such as Alzheimer's disease and neonatal hypoxia–ischemia (Shoshan-Barmatz et al., 2010; Xue et al., 2021). Vdac1 undergoes PTMs due to oxidative stress, which is another critical pathological factor in Alzheimer's disease development. Oxidative damage in the brains of neurodegenerative patients caused by nitration and carbonylation of Vdac1 may impair channel function, promote the pathogenesis and progression of brain disease, and contribute to cognitive impairment (Shoshan-Barmatz et al., 2010). Changes in the phosphorylation state of Vdac have also been observed in neurons of patients with cognitive impairment; these changes disrupt glucose metabolism, promote mitochondrial dysfunction, and activate cell apoptosis (Verma et al., 2022). Dysregulation of Vdac1 and its PTMs are implicated in impaired energy metabolism, oxidative stress, and neurodegenerative processes associated with cognitive impairment. Understanding the role of these modifications in Vdac1 could offer insights into therapeutic strategies targeting mitochondrial function and oxidative stress in the neurogenesis process. Furthermore, our study revealed that, when exposed to CIH, Got2, a crucial enzyme involved in mitochondrial metabolism, undergoes acetylation at six lysine residues, K90, K82, K302, K309, K396, and K404. Our findings align with existing evidence that acetylation inhibits the activity of mitochondrial enzymes (Qian et al., 2022). Moreover, our findings suggest that chronic intermittent hypoxia (CIH)-induced lysine acetylation may have detrimental effects on the mitochondrial tricarboxylic acid (TCA) cycle and oxidative phosphorylation pathways within the hippocampus. This disruption may lead

to inefficient energy use, supporting the notion that CIH has damaging effects on cognitive function. By altering the activity of enzymes involved in these metabolic pathways, CIH-induced acetylation may decrease the efficiency of ATP production and contribute to mitochondrial dysfunction. This dysregulation can exacerbate oxidative stress and impair cellular processes crucial for normal brain function. Therefore, our findings provide new insights into the potential mechanisms underlying CIH-induced cognitive impairment and further highlight the importance of the proper regulation and maintenance of mitochondrial function in maintaining cognitive health.

Both animal and human studies have indicated that cognitive decline and memory problems are associated with low glucose metabolism in the brain (Ding et al., 2013; Zhang et al., 2021). Although this process occurs differently in different parts of the brain, it is mainly associated with regions that affect learning, memory, and behaviour (Pawlosky et al., 2017). Like in the TCA cycle and during oxidative phosphorylation, every enzyme in glycolysis is acetylated (Zhao et al., 2010). In accordance with the findings of a previous study, we observed increases in the acetylation of K783 and K819 on hexokinase (Hk1) and K208 on Aldoa and in K14 and K149 on triosephosphate isomerase (Tpi1) following CIH exposure. The increased acetylation of these critical glycolytic enzymes may inhibit their activity (Pei et al., 2022), further reducing glucose availability for energy production and contributing to cognitive impairment. Moreover, inflammatory activation of glial cells often leads to a metabolic shift from oxidative phosphorylation to aerobic glycolysis (Cheng et al., 2021). This metabolic switch may exacerbate the effects of CIH-induced glycolytic enzyme acetylation, further impairing cognitive function. Therefore, proper regulation of cellular metabolism is important for maintaining optimal cognitive health.

Hypoxia can also diminish cell viability in both glial cells and neurons (Wang et al., 2014). Effective communication between neurons, astrocytes, and microglia is crucial for the brain's functional organization (Lana et al., 2020). Dysregulation of energy metabolism in neurons and glial cells may contribute to the pathophysiology of neurodegeneration, particularly under conditions of hypoxia–ischemia. One study demonstrated that oligodendrocytes enhance axonal energy metabolism by delivering SIRT2 to deacetylate mitochondrial proteins (Chamberlain et al., 2021). Elevated HDAC2 modifies transcription in hippocampal neurons and impacts microglial activity during neuroinflammation-induced cognitive impairment (Sun et al., 2019). Our results showed that several DAPs, including Camk2a, Hgmb1, and Glul, were related to GFAP or DCX (**Figure 8B**). These findings suggested that acetylation may be crucial in neurodevelopmental disorders in individuals exposed to CIH and indicate that CIH has the potential to modulate various biological functions via alterations in the acetylation levels of pertinent proteins in neurons and glial cells, possibly helping the hippocampus adapt by reshaping its function.

Several recent studies have shown that memory can be modulated by manipulating histone modifications via the use of HDAC inhibitors during memory formation, consolidation, and reconsolidation (Vinarskaya et al., 2021). NaB is an HDAC inhibitor that affects various types of brain damage (Lee et al., 2019). Furthermore, NaB, which can cross the blood-brain barrier and affect the epigenetic machinery in the brain, has been shown to ameliorate reductions in novel object memory when administered intraperitoneally (Jung et al., 2016). In this study, we intraperitoneally administered NaB to CIH group mice. The results revealed an improvement in memory in the CIH group. Additionally, we observed significant fluctuations in the levels of H3K27ac and H3K9ac (**Supplementary Figure 3E**). These findings provide further evidence for the significant role of acetylation in the cognitive impairment associated with CIH.

The current study had certain limitations. First, the number of participants was limited due to budgetary and ethical reasons. Increasing the sample size would help decrease biological variability. Second, we used only male mice to establish the CIH model to perform the studies described here. However, to avoid potential sex bias, we will consider using both male and female mice in future studies. Additionally, studies focused on the mechanisms of key acetylated proteins are lacking. In the future, we plan to concentrate on functional studies.

In summary, our study aimed to uncover the molecular mechanisms responsible for cognitive dysfunction induced by CIH. To this end, we performed lysine acetylome profiling to create a comprehensive and detailed landscape of lysine acetylation in the hippocampus. We discovered 2,184 lysine acetylation sites across 1,007 proteins. CIH differentially regulated 280 acetylated sites on 213 proteins, 35.75% of which were acetylated in mitochondria. Our findings suggest that oxidative phosphorylation, the TCA cycle, and glycolysis, which are located primarily in mitochondria, may exacerbate cognitive impairment following CIH. Overall, investigating the mechanisms underlying CIH-induced changes in hippocampal acetylation can aid in the development of scientific prescriptions for cognitive decline caused by CIH.

Data availability statement

The data presented in the study are deposited in the ProteomeXchange repository, accession numbers PXD049225 and PXD049226.

Ethics statement

The animal study was approved by the Capital Institute of Pediatrics' Ethics Committee on Animal Care and Use. The study was conducted in accordance with the local legislation and institutional requirements.

Author contributions

FL: Data curation, Formal analysis, Investigation, Methodology, Writing—original draft. WY: Data curation, Methodology, Writing—original draft. CC: Data curation, Software, Writing—original draft. YZ: Methodology, Supervision,

Writing—original draft. YK: Methodology, Software, Writing—original draft. XH: Data curation, Methodology, Software, Writing—original draft. PP: Formal analysis, Validation, Writing—original draft. SW: Funding acquisition, Project administration, Resources, Visualization, Writing—review and editing. TZ: Resources, Supervision, Visualization, Writing—review and editing.

Funding

The author(s) declare financial support was received for the research, authorship, and/or publication of this article. This work was supported by grants from the Capital's Funds for Health Improvement and Research (2022-2-1132), the Beijing Hospitals Authority's Ascent Plan (DFL20221102), the Beijing Hospitals Authority Clinical Technology Innovation Program (XLMX 202110), the Public Service Development and Reform Pilot Project of Beijing Medical Research Institute (BMR2021-3), and the National Natural Science Foundation of China (82271193).

Conflict of interest

The authors declare that the research was conducted in the absence of any commercial or financial relationships that could be construed as a potential conflict of interest.

Publisher's note

Supplementary material

The Supplementary Material for this article can be found online at: https://www.frontiersin.org/articles/10.3389/fnmol.2024.1324458/full#supplementary-material

References

Akarsu, S., Torun, D., Bolu, A., Erdem, M., Kozan, S., Ak, M., et al. (2014). Mitochondrial complex I and III gene mRNA levels in schizophrenia, and their relationship with clinical features. *J. Mol. Psychiatry* 2:6. doi: 10.1186/s40303-014-0006-9

Alcalá-Vida, R., Lotz, C., Brulé, B., Seguin, J., Decraene, C., Awada, A., et al. (2022). Altered activity-regulated H3K9 acetylation at TGF-beta signaling genes during egocentric memory in Huntington's disease. *Progr. Neurobiol.* 219:102363. doi: 10.1016/j.pneurobio.2022.102363

Anacker, C., and Hen, R. (2017). Adult hippocampal neurogenesis and cognitive flexibility – linking memory and mood. *Nat. Rev. Neurosci.* 18, 335–346. doi: 10.1038/nrn.2017.45

Aviles-Reyes, R. X., Angelo, M. F., Villarreal, A., Rios, H., Lazarowski, A., and Ramos, A. J. (2010). Intermittent hypoxia during sleep induces reactive gliosis and limited neuronal death in rats: Implications for sleep apnea. *J. Neurochem.* 112, 854–869. doi: 10.1111/j.1471-4159.2009.06535.x

Bannow, L. I., Bonaterra, G. A., Bertoune, M., Maus, S., Schulz, R., Weissmann, N., et al. (2022). Effect of chronic intermittent hypoxia (CIH) on neuromuscular junctions and mitochondria in slow– and fast-twitch skeletal muscles of mice-the role of iNOS. *Skelet. Muscle* 12:6. doi: 10.1186/s13395-022-00288-7

Ben Achour, S., and Pascual, O. (2010). Glia: The many ways to modulate synaptic plasticity. *Neurochem. Int.* 57, 440–445.

Bonkowski, M. S., and Sinclair, D. A. (2016). Slowing ageing by design: The rise of NAD+ and sirtuin-activating compounds. *Nat. Rev. Mol. Cell Biol.* 17, 679–690. doi: 10.1038/nrm.2016.93

Burtscher, J., Mallet, R. T., Burtscher, M., and Millet, G. P. (2021). Hypoxia and brain aging: Neurodegeneration or neuroprotection? *Ageing Res. Rev.* 68:101343.

Campbell, R. R., and Wood, M. A. (2019). How the epigenome integrates information and reshapes the synapse. *Nat. Rev. Neurosci.* 20, 133–147. doi: 10.1038/s41583-019-0121-9

Canessa, N., Castronovo, V., Cappa, S. F., Aloia, M. S., Marelli, S., Falini, A., et al. (2011). Obstructive sleep apnea: Brain structural changes and neurocognitive function before and after treatment. *Am. J. Respir. Crit. Care Med.* 183, 1419–1426.

Cao, Y., Li, Q., Zhou, A., Ke, Z., Chen, S., Li, M., et al. (2021). Corrigendum: Notoginsenoside R1 reverses abnormal autophagy in hippocampal neurons of mice with sleep deprivation through melatonin receptor 1A. *Front. Pharmacol.* 12:832126. doi: 10.3389/fphar.2021.832126

Cao, Y., Yang, Y., Wu, H., Lu, Y., Wu, S., Liu, L., et al. (2020). Stem-leaf saponins from Panax notoginseng counteract aberrant autophagy and apoptosis in hippocampal neurons of mice with cognitive impairment induced by sleep deprivation. *J. Ginseng Res.* 44, 442–452. doi: 10.1016/j.jgr.2019.01.009

Chamberlain, K. A., Huang, N., Xie, Y., Licausi, F., Li, S., Li, Y., et al. (2021). Oligodendrocytes enhance axonal energy metabolism by deacetylation of mitochondrial proteins through transcellular delivery of SIRT2. *Neuron* 109:3456–3472.e8. doi: 10.1016/j.neuron.2021.08.011

Chen, J., Zhou, Y., Mueller-Steiner, S., Chen, L.-F., Kwon, H., Yi, S., et al. (2005). SIRT1 protects against microglia-dependent amyloid-beta toxicity through inhibiting NF-kappaB signaling. *J. Biol. Chem.* 280, 40364–40374. doi: 10.1074/jbc.M509329200

Cheng, J., Zhang, R., Xu, Z., Ke, Y., Sun, R., Yang, H., et al. (2021). Early glycolytic reprogramming controls microglial inflammatory activation. *J. Neuroinflammation* 18:129. doi: 10.1186/s12974-021-02187-y

Cho, S.-H., Chen, J. A., Sayed, F., Ward, M. E., Gao, F., Nguyen, T. A., et al. (2015). SIRT1 deficiency in microglia contributes to cognitive decline in aging and neurodegeneration via epigenetic regulation of IL-1β. *J. Neurosci.* 35, 807–818.

Chu, X., Cao, L., Yu, Z., Xin, D., Li, T., Ma, W., et al. (2019). Hydrogen-rich saline promotes microglia M2 polarization and complement-mediated synapse loss to restore behavioral deficits following hypoxia-ischemic in neonatal mice via AMPK activation. *J. Neuroinflammation* 16:104. doi: 10.1186/s12974-019-1488-2

Ciriello, J., Moreau, J. M., Caverson, M. M., and Moranis, R. (2021). Leptin: A potential link between obstructive sleep apnea and obesity. *Front. Physiol.* 12:767318. doi: 10.3389/fphys.2021.767318

Colaert, N., Helsens, K., Martens, L., Vandekerckhove, J., and Gevaert, K. (2009). Improved visualization of protein consensus sequences by iceLogo. *Nat. Methods* 6, 786–787. doi: 10.1038/nmeth1109-786

Cox, J., Hein, M. Y., Luber, C. A., Paron, I., Nagaraj, N., and Mann, M. (2014). Accurate proteome-wide label-free quantification by delayed normalization and maximal peptide ratio extraction, termed MaxLFQ. *Mol. Cell. Proteomics* 13, 2513–2526. doi: 10.1074/mcp.M113.031591

Ding, F., Yao, J., Rettberg, J. R., Chen, S., and Brinton, R. D. (2013). Early decline in glucose transport and metabolism precedes shift to ketogenic system in female aging and Alzheimer's mouse brain: Implication for bioenergetic intervention. *PLoS One* 8:e79977. doi: 10.1371/journal.pone.0079977

Du, Y., Wang, X., Li, L., Hao, W., Zhang, H., Li, Y., et al. (2020). miRNA-mediated suppression of a cardioprotective cardiokine as a novel mechanism exacerbating post-MI remodeling by sleep breathing disorders. *Circ. Res.* 126, 212–228.

Fan, J., Guang, H., Zhang, H., Chen, D., Ding, L., Fan, X., et al. (2018). SIRT1 mediates Apelin-13 in ameliorating chronic normobaric hypoxia-induced anxiety-like behavior by suppressing NF-κB pathway in mice hippocampus. *Neuroscience* 381, 22–34.

Hernández-Soto, R., Villasana-Salazar, B., Pinedo-Vargas, L., and Peña-Ortega, F. (2021). Chronic intermittent hypoxia alters main olfactory bulb activity and olfaction. *Exp. Neurol.* 340:113653. doi: 10.1016/j.expneurol.2021.113653

Huang, X., Yang, J., Huang, X., Zhang, Z., Liu, J., Zou, L., et al. (2021). Tetramethylpyrazine improves cognitive impairment and modifies the hippocampal proteome in two mouse models of Alzheimer's disease. *Front. Cell Dev. Biol.* 9:632843. doi: 10.3389/fcell.2021.632843

Hunter, S. J., Gozal, D., Smith, D. L., Philby, M. F., Kaylegian, J., and Kheirandish-Gozal, L. (2016). Effect of sleep-disordered breathing severity on cognitive performance measures in a large community cohort of young school-aged children. *Am. J. Respir. Crit. Care Med.* 194, 739–747. doi: 10.1164/rccm.201510-2099OC

Imai, S.-I., and Guarente, L. (2014). NAD+ and sirtuins in aging and disease. *Trends Cell Biol.* 24, 464–471.

Jaenisch, R., and Bird, A. (2003). Epigenetic regulation of gene expression: How the genome integrates intrinsic and environmental signals. *Nat. Genet.* 33, 245–254.

Jung, H. Y., Yoo, D. Y., Kim, J. W., Kim, D. W., Choi, J. H., Chung, J. Y., et al. (2016). Sirtuin-2 inhibition affects hippocampal functions and sodium butyrate ameliorates the reduction in novel object memory, cell proliferation, and neuroblast differentiation. *Lab. Anim. Res.* 32, 224–230. doi: 10.5625/lar.2016.32.4.224

Ke, H., Liu, D., Li, T., Chu, X., Xin, D., Han, M., et al. (2020). Hydrogen-rich saline regulates microglial phagocytosis and restores behavioral deficits following hypoxia-ischemia injury in neonatal mice via the Akt pathway. *Drug Des. Dev. Ther.* 14, 3827–3839. doi: 10.2147/DDDT.S264684

Kim, Y. S., Choi, J., and Yoon, B.-E. (2020). Neuron-glia interactions in neurodevelopmental disorders. *Cells* 9:2176.

Koo, D. L., Kim, H. R., Kim, H., Seong, J.-K., and Joo, E. Y. (2020). White matter tract-specific alterations in male patients with untreated obstructive sleep apnea are associated with worse cognitive function. *Sleep* 43:zsz247. doi: 10.1093/sleep/zsz247

Kumar, R., Jain, V., Kushwah, N., Dheer, A., Mishra, K. P., Prasad, D., et al. (2021). HDAC inhibition prevents hypobaric hypoxia-induced spatial memory impairment through PI3K/GSK3β/CREB pathway. *J. Cell. Physiol.* 236, 6754–6771.

Küry, S., Van Woerden, G. M., Besnard, T., Proietti Onori, M., Latypova, X., Towne, M. C., et al. (2017). De novo mutations in protein kinase genes CAMK2A and CAMK2B cause intellectual disability. *Am. J. Hum. Genet.* 101, 768–788. doi: 10.1016/j.ajhg.2017.10.003

Labarca, G., Saavedra, D., Dreyse, J., Jorquera, J., and Barbe, F. (2020). Efficacy of CPAP for improvements in sleepiness, cognition, mood, and quality of life in elderly patients with OSA: Systematic review and meta-analysis of randomized controlled trials. *Chest* 158, 751–764. doi: 10.1016/j.chest.2020.03.049

Lana, D., Ugolini, F., and Giovannini, M. G. (2020). An overview on the differential interplay among neurons-astrocytes-microglia in CA1 and CA3 hippocampus in hypoxia/ischemia. *Front. Cell. Neurosci.* 14:585833. doi: 10.3389/fncel.2020.585833

Laouafa, S., Roussel, D., Marcouiller, F., Soliz, J., Gozal, D., Bairam, A., et al. (2019). Roles of oestradiol receptor alpha and beta against hypertension and brain mitochondrial dysfunction under intermittent hypoxia in female rats. *Acta Physiol.* 226:e13255. doi: 10.1111/apha.13255

Lee, H. J., Son, Y., Lee, M., Moon, C., Kim, S. H., Shin, I. S., et al. (2019). Sodium butyrate prevents radiation-induced cognitive impairment by restoring pCREB/BDNF expression. *Neural Regen. Res.* 14, 1530–1535. doi: 10.4103/1673-5374.255974

Ma, Y., Dammer, E. B., Felsky, D., Duong, D. M., Klein, H.-U., White, C. C., et al. (2021). Atlas of RNA editing events affecting protein expression in aged and Alzheimer's disease human brain tissue. *Nat. Commun.* 12:7035. doi: 10.1038/s41467-021-27204-9

Mangialasche, F., Baglioni, M., Cecchetti, R., Kivipelto, M., Ruggiero, C., Piobbico, D., et al. (2015). Lymphocytic mitochondrial aconitase activity is reduced in Alzheimer's disease and mild cognitive impairment. *J. Alzheimers Dis.* 44, 649–660. doi: 10.3233/JAD-142052

Martínez-Reyes, I., and Chandel, N. S. (2020). Mitochondrial TCA cycle metabolites control physiology and disease. *Nat. Commun.* 11:102.

Mela, V., Sayd Gaban, A., O'neill, E., Bechet, S., Walsh, A., and Lynch, M. A. (2022). The modulatory effects of DMF on microglia in aged mice are sex-specific. *Cells* 11:729. doi: 10.3390/cells11040729

Mews, P., Donahue, G., Drake, A. M., Luczak, V., Abel, T., and Berger, S. L. (2017). Acetyl-CoA synthetase regulates histone acetylation and hippocampal memory. *Nature* 546, 381–386.

Narita, T., Weinert, B. T., and Choudhary, C. (2019). Functions and mechanisms of non-histone protein acetylation. *Nat. Rev. Mol. Cell Biol.* 20, 156–174.

Osorio, R. S., Martínez-García, M. Á, and Rapoport, D. M. (2022). Sleep apnoea in the elderly: A great challenge for the future. *Eur. Respir. J.* 59:2101649.

Pawlosky, R. J., Kemper, M. F., Kashiwaya, Y., King, M. T., Mattson, M. P., and Veech, R. L. (2017). Effects of a dietary ketone ester on hippocampal glycolytic and tricarboxylic acid cycle intermediates and amino acids in a 3xTgAD mouse model of Alzheimer's disease. *J. Neurochem.* 141, 195–207.

Pei, J., Yuan, Y., Tian, D., Huang, F., Zhang, C., Wang, C., et al. (2022). Comprehensive analysis of protein acetylation and glucose metabolism in mouse brains infected with rabies virus. *J. Virol.* 96:e0194221. doi: 10.1128/JVI.01942-21

Perikleous, E., Steiropoulos, P., Tzouvelekis, A., Nena, E., Koffa, M., and Paraskakis, E. (2018). DNA methylation in pediatric obstructive sleep apnea: An overview of preliminary findings. *Front. Pediatr.* 6:154. doi: 10.3389/fped.2018.00154

Philby, M. F., Macey, P. M., Ma, R. A., Kumar, R., Gozal, D., and Kheirandish-Gozal, L. (2017). Reduced regional grey matter volumes in pediatric obstructive sleep apnea. *Sci. Rep.*7:44566.

Poggini, S., Lopez, M. B., Albanese, N. C., Golia, M. T., Ibáñez, F. G., Limatola, C., et al. (2023). Minocycline treatment improves cognitive and functional plasticity in a preclinical mouse model of major depressive disorder. *Behav. Brain Res.* 441:114295. doi: 10.1016/j.bbr.2023.114295

Qian, P., Ma, F., Zhang, W., Cao, D., Li, L., Liu, Z., et al. (2022). Chronic exercise remodels the lysine acetylome in the mouse hippocampus. *Front. Mol. Neurosci.* 15:1023482. doi: 10.3389/fnmol.2022.1023482

Scharping, N. E., Rivadeneira, D. B., Menk, A. V., Vignali, P. D. A., Ford, B. R., Rittenhouse, N. L., et al. (2021). Mitochondrial stress induced by continuous stimulation under hypoxia rapidly drives T cell exhaustion. *Nat. Immunol.* 22, 205–215. doi: 10.1038/s41590-020-00834-9

Schueller, E., Paiva, I., Blanc, F., Wang, X.-L., Cassel, J.-C., Boutillier, A.-L., et al. (2020). Dysregulation of histone acetylation pathways in hippocampus and frontal cortex of Alzheimer's disease patients. *Eur. Neuropsychopharmacol.* 33, 101–116. doi: 10.1016/j.euroneuro.2020.01.015

Sharma, S., Taliyan, R., and Singh, S. (2015). Beneficial effects of sodium butyrate in 6-OHDA induced neurotoxicity and behavioral abnormalities: Modulation of histone deacetylase activity. *Behav. Brain Res.* 291, 306–314. doi: 10.1016/j.bbr.2015.05.052

Shen, M., Chen, Z., Ming, M., Cheng, Z., Sun, J., Liang, Q., et al. (2022). The acetylome of adult mouse sciatic nerve. *J. Neurochem.* 162, 262–275. doi: 10.1111/jnc.15648

Shoshan-Barmatz, V., De Pinto, V., Zweckstetter, M., Raviv, Z., Keinan, N., and Arbel, N. (2010). VDAC, a multi-functional mitochondrial protein regulating cell life and death. *Mol. Aspects Med.* 31, 227–285.

Smith, M. K., Colbran, R. J., Brickey, D. A., and Soderling, T. R. (1992). Functional determinants in the autoinhibitory domain of calcium/calmodulin-dependent protein kinase II. Role of His282 and multiple basic residues. *J. Biol. Chem.* 267, 1761–1768.

Song, T., Song, X., Zhu, C., Patrick, R., Skurla, M., Santangelo, I., et al. (2021). Mitochondrial dysfunction, oxidative stress, neuroinflammation, and metabolic alterations in the progression of Alzheimer's disease: A meta-analysis of in vivo magnetic resonance spectroscopy studies. *Ageing Res. Rev.* 72:101503. doi: 10.1016/j.arr.2021.101503

Sorrentino, V., Romani, M., Mouchiroud, L., Beck, J. S., Zhang, H., D'amico, D., et al. (2017). Enhancing mitochondrial proteostasis reduces amyloid-β proteotoxicity. *Nature* 552, 187–193.

Sun, X.-Y., Zheng, T., Yang, X., Liu, L., Gao, S.-S., Xu, H.-B., et al. (2019). HDAC2 hyperexpression alters hippocampal neuronal transcription and microglial activity in neuroinflammation-induced cognitive dysfunction. *J. Neuroinflammation* 16:249. doi: 10.1186/s12974-019-1640-z

Vercellino, I., and Sazanov, L. A. (2022). The assembly, regulation and function of the mitochondrial respiratory chain. *Nat. Rev. Mol. Cell Biol.* 23, 141–161.

Verma, A., Shteinfer-Kuzmine, A., Kamenetsky, N., Pittala, S., Paul, A., Nahon Crystal, E., et al. (2022). Targeting the overexpressed mitochondrial protein VDAC1 in a mouse model of Alzheimer's disease protects against mitochondrial dysfunction and mitigates brain pathology. *Transl. Neurodegener.* 11:58.

Vinarskaya, A. K., Balaban, P. M., Roshchin, M. V., and Zuzina, A. B. (2021). Sodium butyrate as a selective cognitive enhancer for weak or impaired memory. *Neurobiol. Learn. Mem.* 180:107414.

Wang, Q., Chao, D., Chen, T., Sandhu, H., and Xia, Y. (2014). δ-Opioid receptors and inflammatory cytokines in hypoxia: Differential regulation between glial and neuron-like cells. *Transl. Stroke Res.* 5, 476–483. doi: 10.1007/s12975-014-0342-1

Xiao, Q., Liu, Z., Zhao, X., and Xiong, H. (2020). Multiple site-specific one-pot synthesis of two proteins by the bio-orthogonal flexizyme system. *Front. Bioeng. Biotechnol.* 8:37. doi: 10.3389/fbioe.2020.00037

Xu, H., Zhou, J., Lin, S., Deng, W., Zhang, Y., and Xue, Y. (2017). PLMD: An updated data resource of protein lysine modifications. *J. Genet. Genomics* 44, 243–250.

Xu, Z., Lu, W., Miao, Y., Li, H., Xie, X., and Zhang, F. (2020). mRNA profiling reveals the potential mechanism of TIPE2 in attenuating cognitive deficits in APP/PS1 mice. *Int. Immunopharmacol.* 87:106792. doi: 10.1016/j.intimp.2020.106792

Xue, L.-L., Du, R.-L., Hu, Y., Xiong, L.-L., Su, Z.-Y., Ma, Z., et al. (2021). BDNF promotes neuronal survival after neonatal hypoxic-ischemic encephalopathy by up-regulating Stx1b and suppressing VDAC1. *Brain Res. Bull.* 174, 131–140.

Yang, I., Han, S. J., Kaur, G., Crane, C., and Parsa, A. T. (2010). The role of microglia in central nervous system immunity and glioma immunology. *J. Clin. Neurosci.* 17, 6–10.

Yeung, F., Hoberg, J. E., Ramsey, C. S., Keller, M. D., Jones, D. R., Frye, R. A., et al. (2004). Modulation of NF-kappaB-dependent transcription and cell survival by the SIRT1 deacetylase. *EMBO J.* 23, 2369–2380. doi: 10.1038/sj.emboj.7600244

Zhang, S., Lachance, B. B., Mattson, M. P., and Jia, X. (2021). Glucose metabolic crosstalk and regulation in brain function and diseases. *Progr. Neurobiol.* 204:102089.

Zhao, S., Xu, W., Jiang, W., Yu, W., Lin, Y., Zhang, T., et al. (2010). Regulation of cellular metabolism by protein lysine acetylation. *Science* 327, 1000–1004.

Zhao, Y.-N., Wang, H.-Y., Li, J.-M., Chen, B.-Y., Xia, G., Zhang, P.-P., et al. (2016). Hippocampal mitogen-activated protein kinase activation is associated with intermittent hypoxia in a rat model of obstructive sleep apnea syndrome. *Mol. Med. Rep.* 13, 137–145. doi: 10.3892/mmr.2015.4505

Zhou, L., Chen, P., Peng, Y., and Ouyang, R. (2016). Role of oxidative stress in the neurocognitive dysfunction of obstructive sleep apnea syndrome. *Oxid. Med. Cell. Longev.* 2016:9626831.

Zhou, L., Liu, G., Luo, H., Li, H., Peng, Y., Zong, D., et al. (2020). Aberrant hippocampal network connectivity is associated with neurocognitive dysfunction in patients with moderate and severe obstructive sleep apnea. *Front. Neurol.* 11:580408. doi: 10.3389/fneur.2020.580408

frontiers | Frontiers in Molecular Neuroscience

TYPE Original Research
PUBLISHED 07 March 2024
DOI 10.3389/fnmol.2024.1362581

OPEN ACCESS

EDITED BY
Geraldine Zimmer-Bensch,
RWTH Aachen University, Germany

REVIEWED BY
Sadaharu Miyazono,
Asahikawa Medical University, Japan
Homira Behbahani,
Karolinska Institutet (KI), Sweden

*CORRESPONDENCE
Vladimir A. Mitkevich
✉ mitkevich@gmail.com

RECEIVED 28 December 2023
ACCEPTED 21 February 2024
PUBLISHED 07 March 2024

CITATION
Varshavskaya KB, Petrushanko IY, Mitkevich VA, Barykin EP and Makarov AA (2024) Post-translational modifications of beta-amyloid alter its transport in the blood-brain barrier *in vitro* model. *Front. Mol. Neurosci.* 17:1362581. doi: 10.3389/fnmol.2024.1362581

Post-translational modifications of beta-amyloid alter its transport in the blood-brain barrier *in vitro* model

Kseniya B. Varshavskaya, Irina Yu Petrushanko, Vladimir A. Mitkevich*, Evgeny P. Barykin and Alexander A. Makarov

Engelhardt Institute of Molecular Biology, Moscow, Russia

One of the hallmarks of Alzheimer's disease (AD) is the accumulation of beta-amyloid peptide (Aβ) leading to formation of soluble neurotoxic Aβ oligomers and insoluble amyloid plaques in various parts of the brain. Aβ undergoes post-translational modifications that alter its pathogenic properties. Aβ is produced not only in brain, but also in the peripheral tissues. Such Aβ, including its post-translationally modified forms, can enter the brain from circulation by binding to RAGE and contribute to the pathology of AD. However, the transport of modified forms of Aβ across the blood–brain barrier (BBB) has not been investigated. Here, we used a transwell BBB model as a controlled environment for permeability studies. We found that $Aβ_{42}$ containing isomerized Asp7 residue (iso-$Aβ_{42}$) and $Aβ_{42}$ containing phosphorylated Ser8 residue (pS8-$Aβ_{42}$) crossed the BBB better than unmodified $Aβ_{42}$, which correlated with different contribution of endocytosis mechanisms to the transport of these isoforms. Using microscale thermophoresis, we observed that RAGE binds to iso-$Aβ_{42}$ an order of magnitude weaker than to $Aβ_{42}$. Thus, post-translational modifications of Aβ increase the rate of its transport across the BBB and modify the mechanisms of the transport, which may be important for AD pathology and treatment.

KEYWORDS

Alzheimer's disease, blood-brain barrier, beta-amyloid, post-translational modifications, rage, caveolin-dependent endocytosis, clathrin-dependent endocytosis

1 Introduction

Alzheimer's disease (AD) is the most common neurodegenerative disease, accounting for 60%–80% of all cases of dementia (Sonkusare et al., 2005). AD is characterized by various pathological markers in the brain, such as the accumulation of beta-amyloid peptide (Aβ), which can form senile plaques, intracellular accumulation of neurofibrillary tangles formed by hyperphosphorylated tau protein, and progressive loss of nerve cells (Scheltens et al., 2016). Most cases of AD are sporadic and aging is considered a major risk factor for AD, but the pathways through which aging triggers the development of the disease are still unclear. It has been suggested that aging may induce post-translational modifications of Aβ (PTMs), which enhance its pathogenic properties (Moro et al., 2018). Thus, Aβ is capable of undergoing various PTMs that are triggered by enzymes or low molecular weight substances,

as well as spontaneously (Barykin et al., 2017). Some of these modifications are isomerization of the aspartic acid residue at position 7 (iso-Aβ) and phosphorylation at serine 8 (pS8-Aβ). These modifications are located in the metal-binding domain of Aβ, which regulates its zinc-dependent oligomerization (Zirah et al., 2006; Barykin et al., 2018) and interaction with receptors (Barykin et al., 2018; Forest et al., 2018). In amyloid plaques, iso-Aβ was found to constitute more than 50% of all Aβ molecules (Mukherjee et al., 2021). Iso-Aβ has an increased ability to oligomerize (Shimizu et al., 2005), is more toxic (Mitkevich et al., 2013) and demonstrates resistance to proteolysis (Kummer and Heneka, 2014). At the same time, the level of iso-Aβ increases with age and in patients with AD (Moro et al., 2018). PS8-Aβ was detected in brain tissue of both patients with AD and AD model mice. It is localized both in amyloid plaques and in the cytoplasm of neurons, and compared to unmodified Aβ has increased neurotoxicity *in vitro* (Jamasbi et al., 2017) and higher resistance to degradation by an insulin-degrading enzyme (Kummer and Heneka, 2014). Thus, pS8-Aβ and iso-Aβ are important isoforms that differ significantly in properties from intact Aβ. The changes in the homeostasis of these isoforms may trigger pathological events contributing to development of AD.

Numerous studies have shown that AD is accompanied by a disruption of the blood-brain barrier (BBB), which occurs at an early stage of the disease (Nation et al., 2019; Barisano et al., 2022). The BBB controls the entry of Aβ from plasma into the brain via the RAGE receptor, as well as the clearance of Aβ from the brain into the peripheral circulation via the LRP-1 receptor (Zenaro et al., 2017). Disruption of these BBB functions can lead to pathological accumulation of Aβ in the brain and manifestation of AD symptoms. Increasing evidence indicates that Aβ from blood can enter the brain and serve as a trigger for the disease (Bu et al., 2018; Sun et al., 2021). Interestingly, peripheral injection of synthetic $Aβ_{42}$ into the bloodstream did not lead to the formation of amyloid plaques in the brains of mouse models of AD. However, intravenous injections of modified forms of Aβ altered the pathology of AD: the injection of iso-Aβ accelerated the amyloidogenesis (Kozin et al., 2013), while injection of pS8-Aβ reduced the number of amyloid plaques in the brain of transgenic mice (Barykin et al., 2018). This evidence suggests that pathogenic isoforms of Aβ may arise in the circulatory system, after which they penetrate the brain and contribute to AD pathology (Kozin and Makarov, 2019). However, the transport of modified forms of Aβ across the BBB has not been previously studied.

In this work, we compared the efficiency of transport of $Aβ_{42}$, pS8-$Aβ_{42}$, and iso-$Aβ_{42}$ through a monolayer of BBB endothelial cells, and also established the contribution of clathrin- and caveolin-dependent mechanisms to this process. It was also determined how modifications of Aβ affect its affinity for RAGE.

2 Materials and methods

2.1 Preparation of synthetic beta-amyloid peptides

Synthetic beta-amyloid peptides: $Aβ_{42}$ and iso-$Aβ_{42}$ were obtained from Lifetein (Somerset, NJ, USA). PS8-$Aβ_{42}$ and $Aβ_{1-16}$ were obtained from Biopeptide (San Diego, CA, USA). $Aβ_{17-42}$ was obtained from Verta (Saint-Petersburg, Russia). The amino acid sequence of the peptides is shown in Table 1.

Peptides were monomerized using hexafluoroisopropanol (Fluka), aliquoted and dried as described in Barykin et al. (2018). An aliquot of Aβ was dissolved in 10 μl of dimethyl sulfoxide (DMSO) (Sigma-Aldrich, St. Loius, MO, USA) at room temperature for an hour to obtain a 1.25 mM stock solution and then diluted to 1 μM using serum-free DMEM media for Aβ transport experiments.

2.2 Cell culture

Mouse brain endothelial cell line bEnd.3, obtained from the American Type Culture Collection, was cultured at 37°C in an atmosphere of 5% CO_2 in Dulbecco's Modified Eagles Medium (DMEM; Gibco, ThermoFisher Scientific, Waltham, MA, USA) containing 4.5 g/l glucose, 1% GlutaMax (Gibco, ThermoFisher Scientific, Waltham, MA, USA), 100 units/mL penicillin, 100 μg/mL streptomycin (Sigma, St. Louis, MO, USA) with the addition of 10% fetal bovine serum (FBS; Gibco, USA).

2.3 *In vitro* model of the BBB

2.3.1 Cell cultivation on transwell membrane

To simulate the BBB, a mono-cultured model based on bEnd.3 cells was used. BEnd.3 cells were cultured in transwell inserts (Greiner Bio-One, pore diameter 0.4 μm) submerged in the wells of a 12-well plate (Greiner Bio-One). BEnd.3 cells were seeded on the upper surface of the transwell membrane in an amount of 70 thousand per well and cultured for 7 days until confluence. The volume of DMEM medium (10% FBS) in the upper (luminal) compartment was 750 μl, in the lower (abluminal) compartment – 1 ml. Cell counting before seeding was carried out in a Goryaev chamber with preliminary staining of cells with damaged membranes with trypan blue (Invitrogen).

2.3.2 Measuring the passage of Aβ isoforms through a monolayer of bEnd.3 cells

The transport of Aβ and its isoforms was studied in the transwell model. Aβ is able to bind albumin and other serum proteins (Biere et al., 1996). Therefore, before the experiment, the upper and lower sections of the transwell were washed with 500 and 1000 μL of serum-free DMEM, respectively. To study the transfer of Aβ from the luminal to abluminal compartment (modeling transport from the blood to the brain), the upper part of the transwell was filled with 300 μl of DMEM containing 1 μM Aβ. An appropriate amount of DMSO (0.08% DMSO) was added to control samples. The lower compartment was filled with 750 μl of DMEM. After adding the peptide, samples were taken from the lower part of the transwell in a volume of 200 μl after 2, 6, and 24 h. Each time after sampling, 200 μl of DMEM medium was added to the lower compartment. After 6 h of incubation, FBS was added to the upper compartment of each well to a final concentration of 5%.

TABLE 1 Amino acid sequence of Aβ and its isoforms.

Peptide	Sequence
$Aβ_{42}$	[H2N]-DAEFRHDSGYEVHHQKLVFFAEDVGSNKGAIIGLMVGGVVIA-[COOH]
iso-$Aβ_{42}$	[H2N]-DAEFRH[isoD]SGYEVHHQKLVFFAEDVGSNKGAIIGLMVGGVVIA-[COOH]
pS8-$Aβ_{42}$	[H2N]-DAEFRHD[pS]GYEVHHQKLVFFAEDVGSNKGAIIGLMVGGVVIA-[COOH]
$Aβ_{1-16}$	[H2N]-DAEFRHDSGYEVHHQK-[COOH]
$Aβ_{17-42}$	[H2N]-LVFFAEDVGSNKGAIIGLMVGGVVIA-[COOH]

The concentration of Aβ in the samples was determined by enzyme-linked immunosorbent assay (ELISA). To account for dilution due to sampling and addition of DMEM medium, the concentration of Aβ was corrected using the following equation:

$$C_t' = C_t + \left(\frac{V}{V_{total}} \times C_{t-1} f\right)$$

where C_t' is the concentration of Aβ at time t, taking into account dilution; C_t is the concentration of Aβ measured with ELISA at time t; C_{t-1} - concentration of Aβ measured at the previous time point; V is the volume added to the lower compartment after sampling; V_{total} is the total volume in the lower compartment.

The permeability coefficients obtained by incubating cells with 1 μM and 100 nM Aβ are presented in the Supplementary Figure 1.

After each experiment, BBB permeability was assessed as described in section 2.3.3 to ensure that the cell monolayer was not disrupted by incubation with Aβ.

2.3.3 Endothelial permeability measurement

To assess paracellular permeability of the endothelium, the fluorescent label sodium fluorescein (Sigma-Aldrich) was used. The lower and upper compartments of the transwell were washed with PBS (Gibco) and filled with HBSS buffer (Gibco): 250 and 750 μl in the upper and lower compartments, respectively. Then, 50 μl of 60 μg/ml sodium fluorescein dissolved in HBSS was added to the upper compartment to a final concentration of 10 μg/ml. Samples (100 μl) were taken from the lower compartment at 0, 15, 30, 45, and 60 min after the addition of the fluorescent label. Each time after sampling, 100 μl of HBSS was added to the lower compartment. The fluorescence intensity in the samples was measured on a SPARK plate reader (Tecan, Switzerland) with an excitation wavelength of 485 nm and a fluorescence recording wavelength of 535 nm. Dilution of sodium fluorescein at each sampling step was taking into account using the following equation:

$$I_t' = I_t + \left(\frac{V}{V_{total}} \times I_{t-1}\right)$$

where I_t' is the fluorescence intensity at time t after dilution correction; I_t is the fluorescence intensity measured at time t; I_{t-1} is fluorescence intensity measured at the previous time point; V is the volume added to the lower compartment after sampling; V_{total} is the total volume in the lower compartment.

2.3.4 Study of the transport mechanisms of beta-amyloid and its isoforms

Various inhibitors were used to study the transport mechanisms of Aβ and its isoforms. The contribution of RAGE to the transport of Aβ across the endothelial monolayer was assessed using the antagonist of this receptor FPS-ZM1 (Sigma) at a concentration of 20 μM (to obtain a stock solution, FPS-ZM1 was dissolved in DMSO to a concentration of 305 mM). To study the caveolin-dependent transport of Aβ isoforms, the inhibitor filipin (Sigma) was used at a concentration of 3 μg/ml (to obtain a stock solution, filipin was dissolved in DMSO to a concentration of 5 mg/ml). An equivalent amount of DMSO was added to the control samples. The contribution of clathrin-dependent endocytosis was assessed using chlorpromazine (Merck) at a concentration of 5 μg/ml (to obtain a stock solution, chlorpromazine was dissolved in DMEM). These concentrations were selected based on literature data and tested for toxicity to bEnd.3 cells using MTT (Filipin) and WST (FPS-ZM1 and chlorpromazine) assays according to the manufacturer's protocol (Supplementary Figure 2). Before experiments, cells were preincubated with inhibitors added to the upper transwell compartment for 1 h, after which they were filled with solutions containing the inhibitor and 1 μM Aβ, and samples were taken from the lower compartment after 2, 6 and 24 h.

2.4 ELISA

The concentration of Aβ and its isoforms was measured using sandwich ELISA. BAM113cc antibodies (HyTest), which recognize the C-terminus of Aβ, were added to a 96-well ELISA plate (NEST) in a volume of 100 μl (0.5 ng/μl) and incubated overnight at +4°C. The wells of the plate were washed 2 times with 200 μl of PBST (0.05% Tween20) and blocked in 1% BSA (Dia-m) in PBST at room temperature and shaking for 3–4 h. Then the plate was washed 2 times with 200 μl of PBST. BAM7cc antibodies (HyTest) conjugated to HRP were added (50 μl per well, 2 ng/μl), then standards and experimental samples were added (50 μl per well). Samples were incubated overnight at +4°C, washed 6 times with 200 μl PBST and analyzed using TMB (Merck). Absorbance was measured at 450 nm using a Multiskan FC Microplate Photometer (Thermo

Fisher Scientific). The calibration curves are presented in the Supplementary Figure 3).

2.5 Determination of parameters of interaction of Aβ and its isoforms with RAGE

The His-tag-containing sRAGE protein (Abcam) was stained with a fluorescent dye using the second-generation Monolith His-Tag Labeling Kit RED-tris-NTA according to the manufacturer's protocol. Aliquots of $A\beta_{42}$, pS8-$A\beta_{42}$, iso-$A\beta_{42}$, and $A\beta_{17-42}$ were dissolved in DMSO to a concentration of 5 mM, after which a series of dilutions were prepared to obtain solutions with Aβ concentrations from 6.1 nM to 200 μM. Aliquots of $A\beta_{1-16}$ were dissolved in PBS to a concentration of 2.5 mM, after which a series of dilutions were prepared (the final concentration of $A\beta_{1-16}$ in the samples varied from 38.1 nM to 1.25 mM). Samples were loaded into Monolith NT.115 Premium capillaries. The concentration of RED-tris-NTA-labeled sRAGE was constant (50 nM). All samples contained 4% DMSO and 20% glycerol. Microthermophoresis was performed using a Monolith NT.115 system (Nano Temper Technologies GmbH). Data analysis was performed using MO. Affinity Analysis v.2.3 software (Nano Temper Technologies GmbH).

2.6 Measurement of intracellular concentrations of Aβ and its isoforms

BEnd.3 cells were seeded into a 12-well plate (Greiner Bio-One) at 35 thousand per well and cultured for a week in DMEM (10% FBS), after which they were incubated with 1 μM $A\beta_{42}$, pS8-$A\beta_{42}$ or iso-$A\beta_{42}$ within 24 h in serum-free DMEM. Cells were washed three times with PBS, frozen in liquid nitrogen, and stored at −80°C overnight. Cells were lyzed on ice for 15 min with 250 μl of IP Lysis Buffer (Pierce) containing protease and phosphatase inhibitors (Roche) per well. The cells were removed using a scraper and placed in tubes, after which the cells were lysed for 1 h at +4°C with shaking. The cell lysate was centrifuged for 10 min at 16000 g, +4°C, and the supernatant was collected. The amount of protein in the lysates was determined using a BCA assay kit (Sigma) according to the manufacturer's protocol. The concentration of Aβ and its isoforms in cell lysates was measured using ELISA as described above.

2.7 Statistical data processing

Experimental data are presented as the mean of independent experiments ± standard deviations (SD) or as a boxplot showing the median, lower and upper quartiles, minimum and maximum values of the sample. The number of independent experiments is indicated in the figure legends. The normality of the distribution was checked using the Kolmogorov-Smirnov test, and outliers were analyzed using the Q-test. Statistical differences between experimental groups for normally distributed samples were determined using Student's t test (when comparing two groups) or One-way ANOVA (when comparing multiple groups) using Tukey's test for multiple comparisons. Differences were considered statistically significant at $p<0.05$. Statistical analysis was performed using GraphPad Prism 8.0.2 software.

3 Results

3.1 Isomerized and phosphorylated Aβ pass through the BBB model more efficiently than unmodified Aβ

The passage of $A\beta_{42}$, pS8-$A\beta_{42}$ and iso-$A\beta_{42}$ across the BBB was measured in a transwell system. It was found that pS8-$A\beta_{42}$ and iso-$A\beta_{42}$ are transported by endothelial cells from the luminal (upper) transwell compartment to the abluminal (lower) compartment more efficiently than $A\beta_{42}$ (Figure 1). Thus, the transport efficiency of pS8-$A\beta_{42}$ was 1.8, 1.7 and 1.4 times higher than that of the unmodified peptide after 2, 6 and 24 h of incubation, respectively. Transport of iso-$A\beta_{42}$ through the endothelium was 1.9, 1.8 times (at 2 and 6 h, respectively) and 1.4 times (at 24 h) more efficient than $A\beta_{42}$ transport. It can be seen that the transport rate is lower after 24 h of incubation compared to 2 and 6 h. A possible reason for this is that prolonged incubation can lead to degradation or aggregation of Aβ.

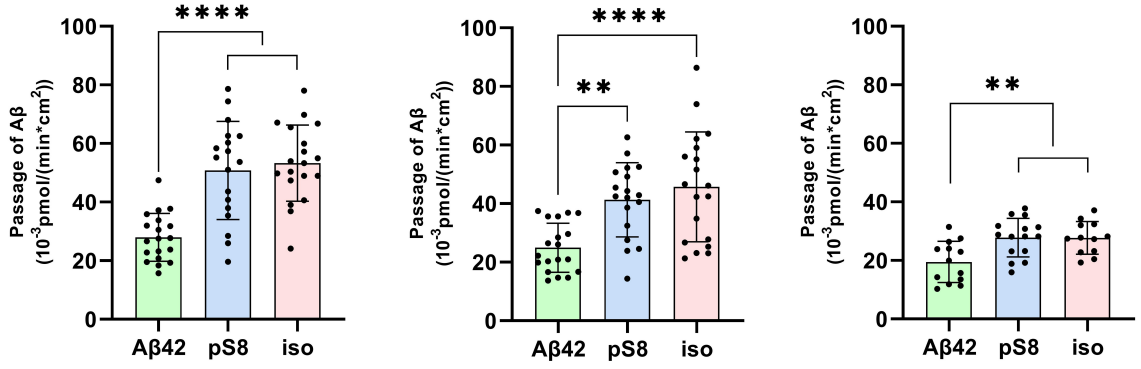

FIGURE 1
Passage of 1 μM $A\beta_{42}$, pS8-$A\beta_{42}$ and iso-$A\beta_{42}$ through a monolayer of bEnd.3 cells from the upper transwell compartment to the lower compartment at 2, 6 and 24 hours. The amounts (pmol) of $A\beta_{42}$, pS8-$A\beta_{42}$ and iso-$A\beta_{42}$ in the lower compartment measured by sandwich ELISA normalized by incubation time (min) and transwell area (cm^2) are presented. Number of values in each group $n = 15–19$ representing 6 independent experiments. $^{**}p < 0.01$, $^{****}p < 0.0001$.

After the experiment, the integrity of the endothelium was checked using sodium fluorescein (Figure 2). The permeability of cell monolayer to sodium fluorescein did not differ between control cells and cells treated with amyloid peptides. This indicates that incubation with amyloid peptides did not affect the integrity of the bEnd.3 cell monolayer.

3.2 The mechanism of transport of Aβ$_{42}$, pS8-Aβ$_{42}$ and iso-Aβ$_{42}$ across the BBB is different

The different efficiency of passage of Aβ isoforms through the BBB model may indicate differences in the mechanisms of their transcellular transport. It is known that Aβ$_{42}$ enters the brain from the blood through the mechanism of caveolin-dependent endocytosis, binding to RAGE, and Aβ$_{42}$ is cleared from the brain to the blood mainly through the LRP-1 receptor via clathrin-dependent endocytosis (Zhu et al., 2018) (Figure 3). In order to study the contribution of various mechanisms to the transport of Aβ and its isoforms, an inhibitor of caveolin-dependent endocytosis, filipin, and an inhibitor of clathrin-dependent endocytosis, chlorpromazine, were used.

It was found that filipin inhibits not only the transport of Aβ$_{42}$, as reported previously (Zhu et al., 2018), but also the passage of pS8-Aβ$_{42}$ and iso-Aβ$_{42}$ (Figures 4A–C). The degree of inhibition for all of the isoforms was about 75% (Figure 4D).

Chlorpromazine inhibited the transport of Aβ$_{42}$ and pS8-Aβ$_{42}$ by 30% (Figures 5A, B). Surprisingly, the efficiency of iso-Aβ$_{42}$ passage through the endothelium in the presence of chlorpromazine decreased by about 75% (Figure 5C). The degree of inhibition for iso-Aβ$_{42}$ was different from other isoforms (Figure 5D). This indicates a difference in the contribution of clathrin and caveolin-dependent endocytosis to the transfer of Aβ isoforms across the endothelium in BBB model.

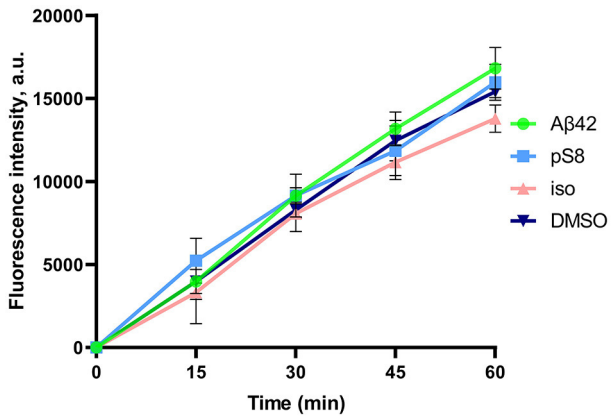

FIGURE 2
Efficiency of sodium fluorescein passage through a monolayer of bEnd.3 cells. Prior to the measurement, the cells were incubated with 0.08% DMSO, or with 1 μM Aβ$_{42}$, pS8-Aβ$_{42}$, or iso-Aβ$_{42}$ for 24 h. Fluorescence intensity values in the lower transwell compartment are shown. Number of independent replicates $n = 3$.

3.3 Aβ modifications affect the interaction with RAGE

Differences in the efficiency of passage of Aβ$_{42}$, pS8-Aβ$_{42}$, and iso-Aβ$_{42}$ through the BBB endothelium may be a result of the differences in interaction with RAGE. To study RAGE/Aβ interaction in our BBB model, inhibitor FPS-ZM1, which blocks the binding of Aβ$_{42}$ to the V domain of the receptor (Deane et al., 2012), was used. FPS-ZM1 was found to significantly reduce the efficiency of transport of all Aβ isoforms through a monolayer of bEnd.3 cells (Figure 6). However, FPS-ZM1 inhibited the passage

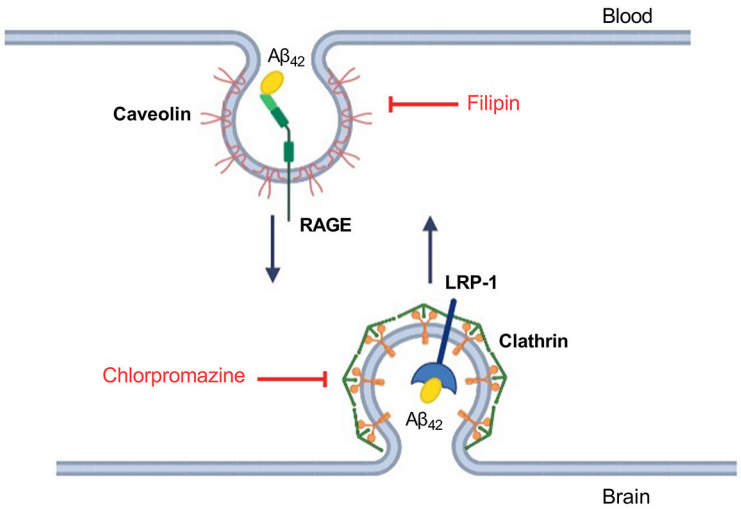

FIGURE 3
Schematic representation of Aβ$_{42}$ transport through the endothelium of the BBB and the underlying molecular mechanisms. Inhibitors affecting caveolin- and clathrin-dependent endocytosis are indicated in red. Filipin binds cholesterol in the membrane and interferes with caveolae formation (Abulrob et al., 2005). Chlorpromazine affects the complex of adapter proteins AP-2 involved in clathrin-dependent endocytosis (Daniel et al., 2015).

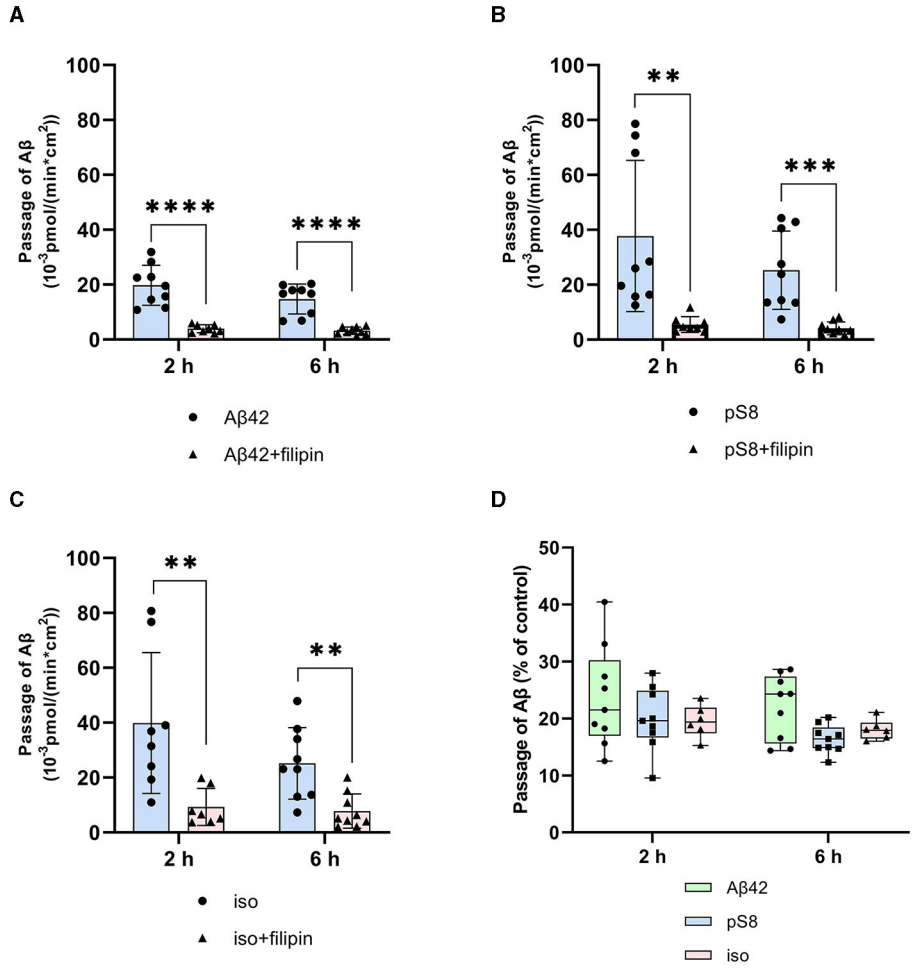

FIGURE 4
Effects of filipin on the efficiency of $A\beta_{42}$ **(A)**, pS8-$A\beta_{42}$ **(B)** and iso-$A\beta_{42}$ **(C)** transport through a monolayer of bEnd.3 cells in the transwell model. The amounts (pmol) of $A\beta_{42}$, pS8-$A\beta_{42}$ and iso-$A\beta_{42}$ in the lower compartment normalized by incubation time (min) and transwell area (cm^2) after 2 and 6 hours of incubation with amyloid peptides in the absence or presence of filipin are shown. **(D)** Comparison of the degree of inhibition of filipin $A\beta_{42}$, pS8-$A\beta_{42}$ and iso-$A\beta_{42}$, where transport of the peptides in the absence of the inhibitor was taken as 100% (not shown). Summarized data from three independent experiments are presented, the number of values in each group $n = 6–9$, $^{**}p < 0.01$, $^{***}p < 0.001$, $^{****}p < 0.0001$.

of $A\beta_{42}$ and iso-$A\beta_{42}$ more efficiently than that of pS8-$A\beta_{42}$ for 2 and 24 h of incubation (Figure 6D).

The dissociation constants (Kd) of $A\beta_{42}$, pS8-$A\beta_{42}$ and iso-$A\beta_{42}$ with the soluble extracellular part of RAGE (sRAGE), determined using microscale thermophoresis (MST), were 1.0 ± 0.2 μM, 7 ± 2 μM and 23 ± 4 μM, respectively (Figure 7). In addition, it was found that the C-terminal domain of $A\beta_{17–42}$ forms a complex with sRAGE with Kd = 10 ± 5 μM (Figure 8). The interaction of sRAGE with the N-terminal domain of $A\beta_{1–16}$ was not detected. Thus, C-terminal domain is the main factor in the interaction of amyloid peptides with sRAGE, and the N-terminal domain modulates this interaction.

3.4 $A\beta_{42}$, pS8-$A\beta_{42}$ and iso-$A\beta_{42}$ accumulate differently in bEnd.3 cells

The reduced affinity of pS8-$A\beta_{42}$ and iso-$A\beta_{42}$ for RAGE compared to $A\beta_{42}$ may cause lesser accumulation of these peptides inside cells and a more efficient transport to the abluminal side. To test this hypothesis, the intracellular levels of $A\beta_{42}$, pS8-$A\beta_{42}$, and iso-$A\beta_{42}$ were measured after incubating cells with 1 μM of these peptides for 24 h (Figure 9). It was shown that intact $A\beta_{42}$ accumulates better inside cells, while the level of accumulation of iso-$A\beta_{42}$ is minimal compared to other peptides.

4 Discussion

It is known that Aβ is expressed not only in the brain, but also in cells of other organs and tissues: kidneys and adrenal glands, heart, liver, spleen, pancreas, as well as in muscles, blood cells and endothelium (Roher et al., 2009). Significant amounts of Aβ have been found in human red blood cells, and the $A\beta_{42}/A\beta_{40}$ ratio in red blood cells is higher than in plasma (Kiko et al., 2012). Platelets also express large amounts of amyloid precursor protein (APP) and release beta-amyloid. Once activated, for example by bleeding, platelets can secrete significant amounts of Aβ into the blood (Humpel, 2017; Carbone et al., 2021). Several studies have shown that platelets from people with AD may have a greater

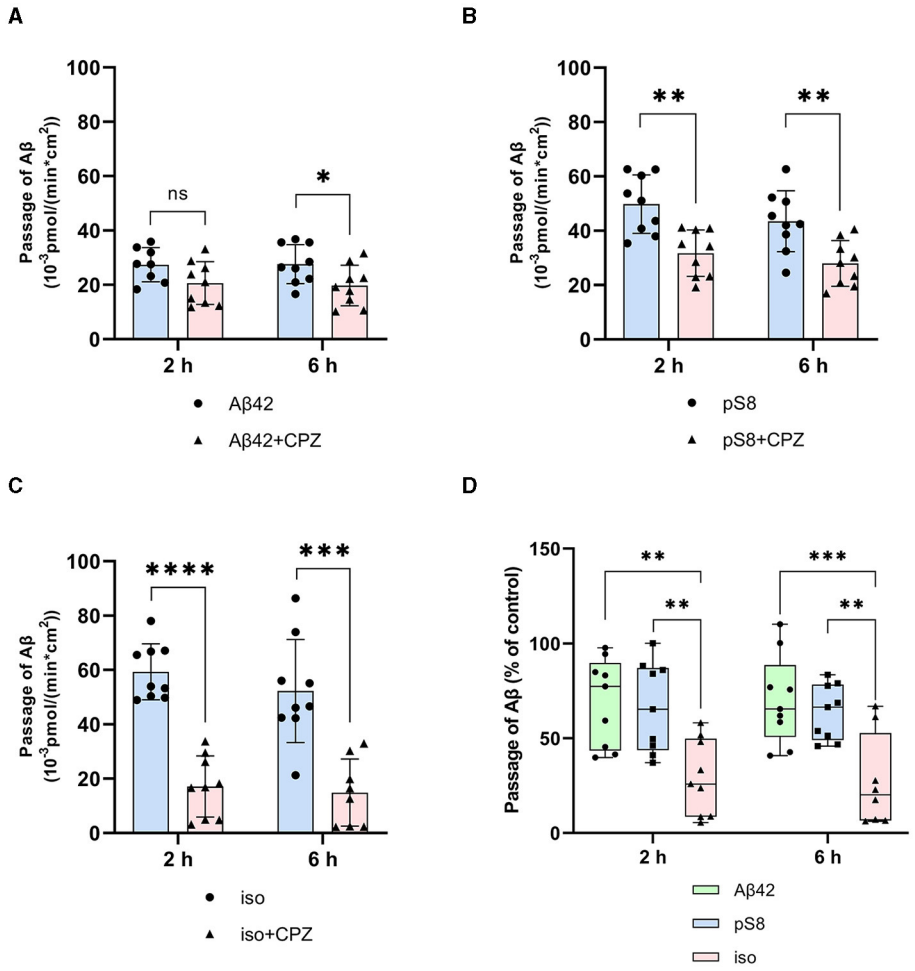

FIGURE 5
Effects chlorpromazine (CPZ) on the efficiency of $A\beta_{42}$ **(A)**, pS8-$A\beta_{42}$ **(B)** and iso-$A\beta_{42}$ **(C)** transport through a monolayer of bEnd.3 cells in the transwell model. The amounts (pmol) of $A\beta_{42}$, pS8-$A\beta_{42}$ and iso-$A\beta_{42}$ in the lower compartment normalized by incubation time (min) and transwell area (cm^2) after 2 and 6 h of incubation with amyloid peptides in the absence or presence of CPZ are shown. **(D)** Comparison of the degree of inhibition of CPZ $A\beta_{42}$, pS8-$A\beta_{42}$ and iso-$A\beta_{42}$, where transport of the peptides in the absence of the inhibitor was taken as 100% (not shown). Summarized data from three independent experiments are presented, the number of values in each group $n = 6–9$, ns - not significant, $*p < 0.05$, $**p < 0.01$, $***p < 0.001$, $****p < 0.0001$.

tendency to become activated and therefore release Aβ into the blood (Carbone et al., 2021).

Increasing evidence indicates that peripheral Aβ can penetrate into the brain and play a significant role in the pathogenesis of AD. Thus, peripheral inoculation of brain extracts containing Aβ led to amyloidosis in the brain of mice (Eisele et al., 2010, 2014; Burwinkel et al., 2018). It has also been shown that increasing the concentration of peripheral Aβ significantly reduces its removal from the brain (Marques et al., 2009). Inhibition of RAGE-ligand interaction suppressed brain Aβ accumulation in a transgenic mouse model (Deane et al., 2003). The important role of peripheral Aβ and its ability to enter the brain and trigger AD pathology was further highlighted in a parabiosis model in which the circulatory systems of a transgenic mouse with AD-like pathology and a wild-type mouse were connected. Using this model, the researchers demonstrated that human Aβ derived from a transgenic animal entered the wild-type mouse brain and initiated AD-like pathology, including tau hyperphosphorylation, neurodegeneration, neuroinflammation, impaired hippocampal long-term potentiation, and amyloid plaque formation (Bu et al., 2018). Another study demonstrated the contribution of Aβ produced by blood cells to the pathogenesis of AD: when bone marrow was transplanted from transgenic mice to wild-type mice, the latter showed signs of AD pathology (Sun et al., 2021). A number of data indicate that induction of AD requires not just an increase in the concentration of $A\beta_{42}$, but the appearance of pathogenic forms carrying post-translational modifications (Kummer and Heneka, 2014; Barykin et al., 2017). Thus, intravenous administration of iso-$A\beta_{42}$ accelerates amyloidogenesis in the brain of transgenic mice modeling AD (Kozin et al., 2013), and introduction of pS8-$A\beta_{42}$ into the blood, on the contrary, reduces the number of amyloid plaques (Barykin et al., 2018). At the same time, intravenous administration of the unmodified peptide does not affect the formation of amyloid plaques in the brain of model mice. It is possible that modified forms of Aβ arise in the circulatory system, after which they enter

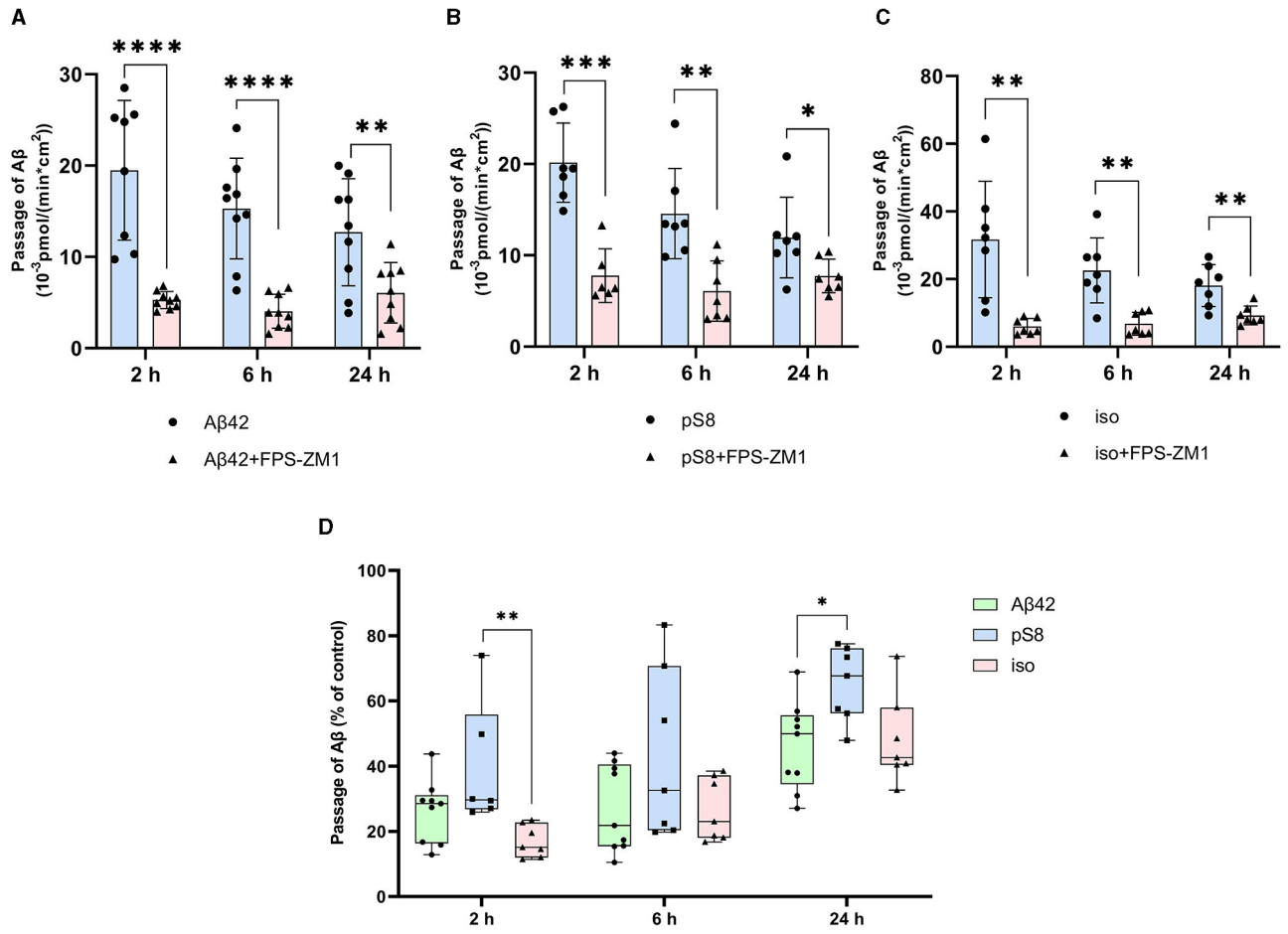

FIGURE 6
Effect of the RAGE antagonist FPS-ZM1 on the efficiency of transport of $A\beta_{42}$ **(A)**, pS8-$A\beta_{42}$ **(B)** and iso-$A\beta_{42}$ **(C)** through a monolayer of bEnd.3 cells in the transwell model. The amounts (pmol) of $A\beta_{42}$, pS8-$A\beta_{42}$ and iso-$A\beta_{42}$ in the lower compartment normalized by incubation time (min) and transwell area (cm^2) after 2, 6 and 24 hours of incubation with amyloid peptides in the absence or presence of FPS-ZM1 are shown. **(D)** Comparison of the degree of inhibition of FPS-ZM1 $A\beta_{42}$, pS8-$A\beta_{42}$ and iso-$A\beta_{42}$, where transport of the peptides in the absence of the inhibitor was taken as 100% (not shown). Summarized data from three independent experiments are presented, the number of values in each group $n = 6–9$, $^*p < 0.05$, $^{**}p < 0.01$, $^{***}p < 0.001$, $^{****}p < 0.0001$.

the brain and contribute to AD pathology (Kozin and Makarov, 2019).

In this work, we compared the efficiency of transport of Aβ isoforms in an *in vitro* model of the BBB, and also determined the contribution of different mechanisms of endocytosis to the passage of $A\beta_{42}$, pS8-$A\beta_{42}$ and iso-$A\beta_{42}$ through the endothelium. It was found that pS8-$A\beta_{42}$ and iso-$A\beta_{42}$ are better transported by BBB endothelial cells than $A\beta_{42}$ (Figure 1), which may be one of the factors determining the ability of modified forms of Aβ to influence cerebral amyloidogenesis when administered intravenously (Kozin et al., 2013; Barykin et al., 2018).

The main mechanism of transport of Aβ from the bloodstream to the brain is caveolin-dependent endocytosis (Zhu et al., 2018). Indeed, the inhibitor of this form of endocytosis, filipin, suppressed the transport of $A\beta_{42}$, pS8-$A\beta_{42}$, and iso-$A\beta_{42}$ from the upper to lower compartment to the same extent (Figure 4D). Strikingly, the addition of chlorpromazine, which is an inhibitor of clathrin-dependent endocytosis, significantly suppressed the transport of iso-$A\beta_{42}$ (Figure 5D). Thus, the transport of iso-$A\beta_{42}$ may also be dependent on clathrin endocytosis. Also, the contribution of clathrin endocytosis was found for $A\beta_{42}$ and pS8-$A\beta_{42}$, but less pronounced than for iso-$A\beta_{42}$. The involvement of clathrin-dependent endocytosis in transport of proteins from the bloodstream to the brain was previously shown for transferrin and insulin receptors (Roberts et al., 1992; Goulatis and Shusta, 2017; Ayloo and Gu, 2019; Pemberton et al., 2022), but not for beta-amyloid peptides. There is also evidence that LRP-1 can mediate Aβ transport in both directions (Pflanzner et al., 2011). It is possible that in the bEnd.3 cell line some part of the molecules of this receptor is present on the luminal side, which could explain the slight effect of the inhibitor on the transport of $A\beta_{42}$ and pS8-$A\beta_{42}$.

It is assumed that RAGE plays a major role in the transfer of Aβ from the circulatory system to the brain. It was previously shown that in cells expressing RAGE an inhibitor of this receptor, FPS-ZM1, prevented oxidative stress induced by $A\beta_{40}$ and $A\beta_{42}$ (Deane et al., 2012). However, the effect of FPS-ZM1 on the transport of Aβ and its isoforms across the BBB endothelium *in vitro* has not been studied. We found that FPS-ZM1 reduced the

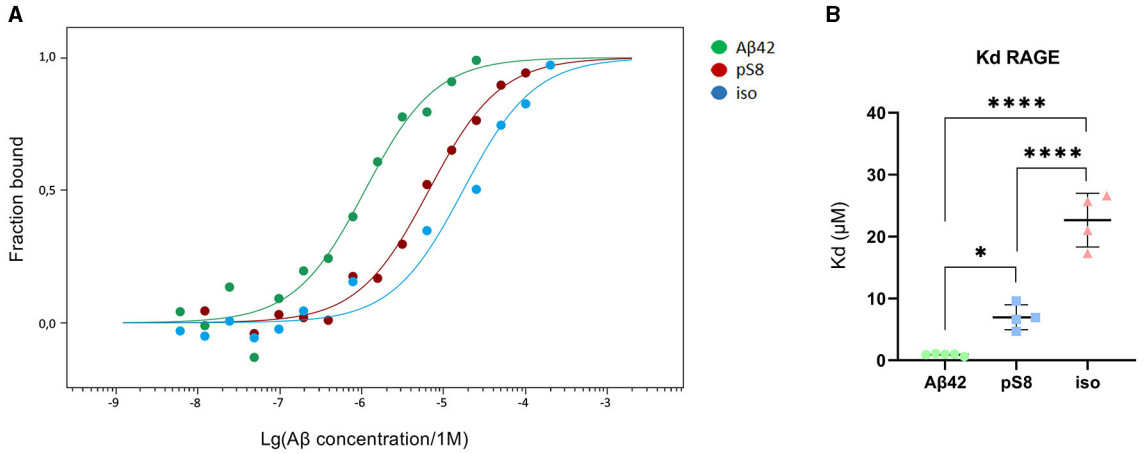

FIGURE 7
Interaction of Aβ isoforms with sRAGE. **(A)** MST curves showing the fraction of RAGE which is in the complex with the peptide at different concentrations of Aβ and its isoforms. **(B)** Values of dissociation constants (Kd) for complexes of Aβ isoforms with sRAGE. Number of replicates in each group $n = 4–5$, $*p < 0.05$, $****p < 0.0001$.

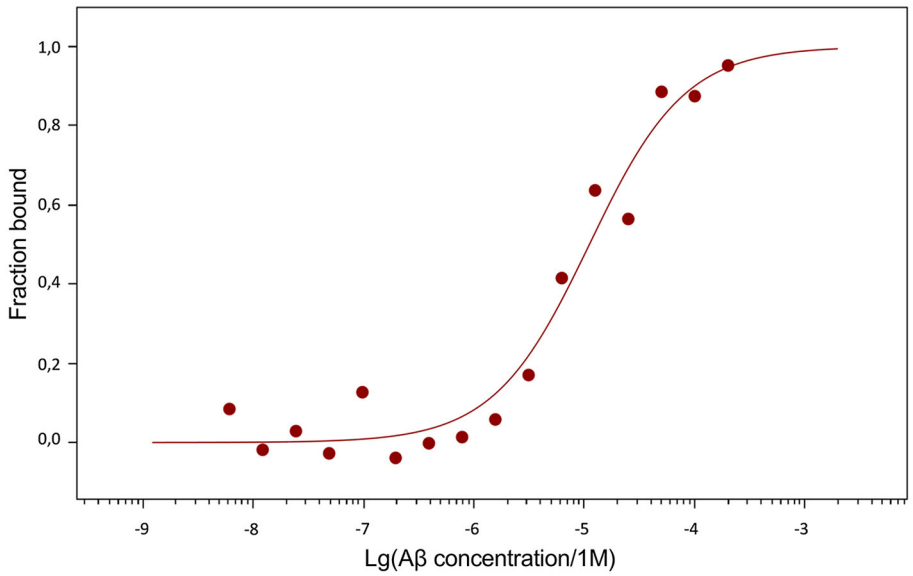

FIGURE 8
MST curve illustrating the interaction of $Aβ_{17–42}$ with sRAGE.

passage of $Aβ_{42}$ through the endothelium of the BBB (Figure 6), which correlates well with data obtained previously for $Aβ_{42}$ *in vivo* (Deane et al., 2003, 2012). FPS-ZM1 also inhibited the transport of pS8-$Aβ_{42}$ and iso-$Aβ_{42}$, but the effect of this inhibitor on the passage of pS8-$Aβ_{42}$ was less pronounced than for other isoforms (Figure 6D). Thus, it appears that RAGE is the major receptor in the transport of both Aβ and its modified forms across the BBB.

Since $Aβ_{42}$, pS8-$Aβ_{42}$, and iso-$Aβ_{42}$ differed in their ability to penetrate the cell monolayer, we decided to compare the ability of these isoforms to interact with RAGE. There is relatively little data in the literature on the interaction parameters of Aβ with RAGE. Thus, in cell cultures, the dissociation constants of RAGE with $Aβ_{40}$ and $Aβ_{42}$ were 75 ± 5 nM (Deane et al., 2012) and 92 ± 40 nM (Chellappa et al., 2021), respectively. For purified RAGE, a dissociation constant with $Aβ_{40}$ was shown to be 57 ± 14 nM (Yan et al., 1998). Using the surface plasmon resonance method, it was revealed that sRAGE binds $Aβ_{42}$ oligomers with a Kd of 17 nM (Chen et al., 2007), and the Kd for endogenous soluble RAGE (esRAGE) and $Aβ_{42}$ was 44.9 nM (Sugihara et al., 2012). Thus, direct measurements of the interaction of $Aβ_{42}$ monomers and its isoforms with RAGE have not been previously carried out. The interaction constants obtained for $Aβ_{42}$ are an order of magnitude higher compared to constants estimated in other systems. This may be due to the fact that in our experiments

stabilizing agents and other additives that are far from physiological were used, which could affect the obtained constants. Nevertheless, this model allowed us to compare the binding of different isoforms with RAGE in the same conditions. Across the three $A\beta_{42}$ isoforms, we found that RAGE demonstrates the highest affinity to $A\beta_{42}$ and the lowest to iso-$A\beta_{42}$ (Figure 7). These data are in good agreement with the results of computer modeling that we obtained earlier, according to which sRAGE has the lowest calculated Kd value with $A\beta_{42}$ and the highest with iso-$A\beta_{42}$ (Tolstova et al., 2022). The obtained Kd values correlate with the accumulation of amyloid peptides inside cells (Figure 9). We also found that RAGE interacts with $A\beta_{17-42}$, but not with $A\beta_{1-16}$, and the binding constant of the receptor with $A\beta_{17-42}$ was an order of magnitude smaller than the binding constant with the full-length $A\beta_{42}$ peptide. Previously, we observed a similar pattern in the interaction of Aβ with Na^+/K^+-ATPase: binding to the enzyme was detected for $A\beta_{17-42}$, but not for $A\beta_{1-16}$ (Barykin et al., 2018). Probably, the hydrophobic C-terminal fragment $A\beta_{17-42}$ makes a major contribution to the binding of $A\beta_{42}$ to various protein molecules, while $A\beta_{1-16}$ modulates this interaction.

Apparently, the high affinity of $A\beta_{42}$ for RAGE is the reason for its accumulation in cells and lower transport efficiency compared to other isoforms, while the isoforms with lower affinity for the receptor are more easily transported across the endothelial cell and are able to dissociate from the receptor on the abluminal side. This mechanism was previously shown for the passage of antibodies to the transferrin receptor across the BBB (Yu et al., 2011; Goulatis and Shusta, 2017). High-affinity antibodies against the transferrin receptor cause the antibody-receptor complex to be mainly directed to lysosomes, and those that undergo transcytosis remain associated with the receptor on the abluminal side. Low-affinity antibodies undergo transcytosis and dissociate on the abluminal side to a greater extent (Yu et al., 2011; Goulatis and Shusta, 2017). Similar studies focusing on drug delivery to the brain showed that transferrin-containing nanoparticles with high avidity for the transferrin receptor remained tightly associated with endothelial cells, whereas low avidity nanoparticles dissociated from the receptor after transcytosis (Wiley et al., 2013). In bEnd.3 cells, it was shown that strong binding of ligands to LRP-1 triggers internalization leading to endo-lysosomal sorting and degradation of ligand-receptor complex, while ligands with moderate binding strength to the receptor were transported across the endothelium (Tian et al., 2020). Thus, the stronger binding of $A\beta_{42}$ to RAGE may be the reason for its lowest transport efficiency of all isoforms across the bEnd.3 cell monolayer. Another factor influencing Aβ transport across the BBB may be different degrees of enzymatic degradation of Aβ isoforms. Thus, isomerization of the aspartate residue in Aβ has been shown to prevent its proteolysis in lysosomes (Lambeth et al., 2019). PS8-Aβ is resistant to degradation by insulin degrading enzyme, unlike unmodified Aβ (Kummer and Heneka, 2014). We found different affinities of Aβ isoforms for RAGE, which may affect enzymatic degradation.

Once Aβ enters the brain, it exerts multiple effects on its neuronal and glial targets (Mroczko et al., 2018). Phosphorylated and isomerized isoforms of Aβ act differently; as such, iso-Aβ is likely more toxic to cholinergic neurons bearing certain receptor types, such as alpha7 nicotinic acetylcholine receptor (Barykin et al., 2019), and pS8-Aβ is less prone to inhibit Na,K-ATPase (Barykin et al., 2018). Together with different transport rates of these isoforms, a complex interaction emerges. $A\beta_{42}$ has also been shown to bind to pyramidal neurons after administration into the blood (Clifford et al., 2007). However, the distribution of blood-derived Aβ isoforms in the brain is a subject for future research.

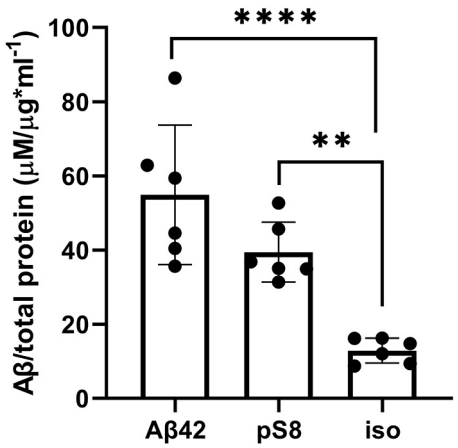

FIGURE 9
Levels of $A\beta_{42}$, pS8-$A\beta_{42}$ and iso-$A\beta_{42}$ in bEnd.3 cells after 24 h of incubation with these peptides (1 μM). The data were obtained on cell lysates using ELISA. The concentrations of peptides normalized to the total protein (μg) in the samples are presented. Number of replicates in each group $n = 6$, $^{**}p < 0.01$, $^{****}p < 0.0001$.

Aging may cause the appearance of modified Aβ isoforms (Moro et al., 2018). Thus, with age, isomerized and deaminated proteins accumulate, and the balance of phosphorylation/dephosphorylation is disrupted (Barykin et al., 2017). Pathogenic forms of Aβ carrying post-translational modifications can arise in the blood and then penetrate the brain, induce aggregation of endogenous beta-amyloid and cause AD pathology. Thus, the appearance of modified forms may precede the formation of plaques and occur in the early stages of the disease. We hypothesize that PTMs are more relevant to sporadic Alzheimer's disease than to familial Alzheimer's disease. However, genetic mutations can also lead to disruption of the PTM process if these mutations affect Aβ-modifying enzymes.

According to our data, phosphorylated and isomerized Aβ are transported more efficiently across the endothelium of the BBB than the unmodified peptide. The RAGE receptor was found to be essential for the transport of both $A\beta_{42}$ and its isoforms across the BBB. Differences in the transport of $A\beta_{42}$, pS8-$A\beta_{42}$, and iso-$A\beta_{42}$ may be due to different mechanisms of endocytosis or different affinities of these isoforms for the RAGE receptor. The mechanisms of transport of $A\beta_{42}$, pS8-$A\beta_{42}$ and iso-$A\beta_{42}$ across the BBB should be taken into account when developing agents for the treatment of AD. Thus, the data obtained may contribute to understanding the causes of the disease, as well as to the search for new drugs that prevent the accumulation of pathogenic Aβ isoforms in the brain.

Limitations: The use of higher than physiological concentrations of Aβ (1 μM) to study its transport is a limitation of this article. However, no saturation transport occurs at 1 μM (Supplementary Figure 1), which justifies the use of this concentration in our study. There are also a number of studies that use high concentrations of Aβ to study its transport across the BBB (Shackleton et al., 2016; Dal Magro et al., 2019; Shubbar and Penny, 2020; Zinchenko et al., 2020). Last, our study is the first to measure all isoforms of Aβ using single ELISA, and the sensitivity of our assay does not allow to measure lower concentrations.

Data availability statement

The original contributions presented in the study are included in the article/Supplementary material, further inquiries can be directed to the corresponding author.

Author contributions

KV: Formal analysis, Investigation, Methodology, Writing – original draft. IP: Conceptualization, Investigation, Methodology, Supervision, Writing – review & editing. VM: Conceptualization, Funding acquisition, Project administration, Resources, Supervision, Validation, Writing – review & editing. EB: Conceptualization, Formal analysis, Investigation, Methodology, Writing – original draft. AM: Conceptualization, Funding acquisition, Project administration, Resources, Supervision, Writing – review & editing.

Funding

The author(s) declare that financial support was received for the research, authorship, and/or publication of this article. This research was funded by the Ministry of Science and Higher Education of the Russian Federation (grant agreement no. 075-15-2020-795, state contract no. 13.1902.21.0027 of 29 September 2020, unique project ID: RF-190220X0027).

Conflict of interest

The authors declare that the research was conducted in the absence of any commercial or financial relationships that could be construed as a potential conflict of interest.

Publisher's note

All claims expressed in this article are solely those of the authors and do not necessarily represent those of their affiliated organizations, or those of the publisher, the editors and the reviewers. Any product that may be evaluated in this article, or claim that may be made by its manufacturer, is not guaranteed or endorsed by the publisher.

Supplementary material

The Supplementary Material for this article can be found online at: https://www.frontiersin.org/articles/10.3389/fnmol.2024.1362581/full#supplementary-material

References

Abulrob, A., Sprong, H., Van Bergen en Henegouwen, P., and Stanimirovic, D. (2005). The blood-brain barrier transmigrating single domain antibody: mechanisms of transport and antigenic epitopes in human brain endothelial cells. *J. Neurochem.* 95, 1201–1214. doi: 10.1111/j.1471-4159.2005.03463.x

Ayloo, S., and Gu, C. (2019). Transcytosis at the blood–brain barrier. *Curr. Opin. Neurobiol.* 57, 32–38. doi: 10.1016/j.conb.2018.12.014

Barisano, G., Montagne, A., Kisler, K., Schneider, J. A., Wardlaw, J. M., Zlokovic, B. V., et al. (2022). Blood–brain barrier link to human cognitive impairment and Alzheimer's disease. *Nat. Cardiovasc. Res.* 1, 108–115. doi: 10.1038/s44161-021-00014-4

Barykin, E. P., Garifulina, A. I., Kruykova, E. V., Spirova, E. N., Anashkina, A. A., Adzhubei, A. A., et al. (2019). Isomerization of Asp7 in beta-amyloid enhances inhibition of the α7 nicotinic receptor and promotes neurotoxicity. *Cells* 8:771. doi: 10.3390/cells8080771

Barykin, E. P., Mitkevich, V. A., Kozin, S. A., and Makarov, A. A. (2017). Amyloid β modification: a key to the sporadic Alzheimer's disease? *Front. Genet.* 8:58. doi: 10.3389/fgene.2017.00058

Barykin, E. P., Petrushanko, I. Y., Kozin, S. A., Telegin, G. B., Chernov, A. S., Lopina, O. D., et al. (2018). Phosphorylation of the amyloid-beta peptide inhibits zinc-dependent aggregation, prevents Na,K-ATPase inhibition, and reduces cerebral plaque deposition. *Front. Mol. Neurosci.* 11:302. doi: 10.3389/fnmol.2018.00302

Biere, A. L., Ostaszewski, B., Stimson, E. R., Hyman, B. T., Maggio, J. E., Selkoe, D. J., et al. (1996). Amyloid beta-peptide is transported on lipoproteins and albumin in human plasma. *J. Biol. Chem.* 271, 32916–32922. doi: 10.1074/jbc.271.51.32916

Bu, X. L., Xiang, Y., Jin, W. S., Wang, J., Shen, L. L., Huang, Z. L., et al. (2018). Blood-derived amyloid-β protein induces Alzheimer's disease pathologies. *Mol. Psychiatr.* 23, 1948–1956. doi: 10.1038/mp.2017.204

Burwinkel, M., Lutzenberger, M., Heppner, F. L., Schulz-Schaeffer, W., and Baier, M. (2018). Intravenous injection of beta-amyloid seeds promotes cerebral amyloid angiopathy (CAA). *Acta Neuropathol. Commun.* 6:23. doi: 10.1186/s40478-018-0511-7

Carbone, M. G., Pagni, G., Tagliarini, C., Imbimbo, B. P., and Pomara, N. (2021). Can platelet activation result in increased plasma Aβ levels and contribute to the pathogenesis of Alzheimer's disease? *Ageing Res. Rev.* 71:101420. doi: 10.1016/j.arr.2021.101420

Chellappa, R. C., Lukose, B., and Rani, P. (2021). Correction: G82S RAGE polymorphism influences amyloid-RAGE interactions relevant in Alzheimer's disease pathology. *PLoS ONE* 16:e0248252. doi: 10.1371/journal.pone.0248252

Chen, X., Walker, D. G., Schmidt, A. M., Arancio, O., Lue, L. F., Yan, S. D., et al. (2007). RAGE: a potential target for Abeta-mediated cellular perturbation in Alzheimer's disease. *Curr. Mol. Med.* 7, 735–742. doi: 10.2174/156652407783220741

Clifford, P. M., Zarrabi, S., Siu, G., Kinsler, K. J., Kosciuk, M. C., Venkataraman, V., et al. (2007). Aβ peptides can enter the brain through a defective blood–brain barrier and bind selectively to neurons. *Brain Res.* 1142, 223–236. doi: 10.1016/j.brainres.2007.01.070

Dal Magro, R., Simonelli, S., Cox, A., Formicola, B., Corti, R., Cassina, V., et al. (2019). The extent of human apolipoprotein A-I lipidation strongly affects the β-amyloid efflux across the blood-brain barrier in vitro. *Front. Neurosci.* 13:419. doi: 10.3389/fnins.2019.00419

Daniel, J. A., Chau, N., Abdel-Hamid, M. K., Hu, L., von Kleist, L., Whiting, A., et al. (2015). Phenothiazine-derived antipsychotic drugs inhibit dynamin and clathrin-mediated endocytosis. *Traffic* 16, 635–654. doi: 10.1111/tra.12272

Deane, R., Du Yan, S., Submamaryan, R. K., LaRue, B., Jovanovic, S., Hogg, E., et al. (2003). RAGE mediates amyloid-beta peptide transport across the blood-brain barrier and accumulation in brain. *Nat. Med.* 9, 907–913. doi: 10.1038/nm890

Deane, R., Singh, I., Sagare, A. P., Bell, R. D., Ross, N. T., LaRue, B., et al. (2012). A multimodal RAGE-specific inhibitor reduces amyloid β-mediated brain disorder in a mouse model of Alzheimer disease. *J. Clin. Invest.* 122, 1377–1392. doi: 10.1172/JCI58642

Eisele, Y. S., Fritschi, S. K., Hamaguchi, T., Obermüller, U., Füger, P., Skodras, A., et al. (2014). Multiple factors contribute to the peripheral induction of cerebral β-amyloidosis. *J. Neurosci.* 34, 10264–10273. doi: 10.1523/JNEUROSCI.1608-14.2014

Eisele, Y. S., Obermüller, U., Heilbronner, G., Baumann, F., Kaeser, S. A., Wolburg, H., et al. (2010). Peripherally applied Abeta-containing inoculates induce cerebral beta-amyloidosis. *Science* 330, 980–982. doi: 10.1126/science.1194516

Forest, K. H., Alfulaij, N., Arora, K., Taketa, R., Sherrin, T., Todorovic, C., et al. (2018). Protection against β-amyloid neurotoxicity by a non-toxic endogenous N-terminal β-amyloid fragment and its active hexapeptide core sequence. *J. Neurochem.* 144, 201–217. doi: 10.1111/jnc.14257

Goulatis, L. I., and Shusta, E. V. (2017). Protein engineering approaches for regulating blood–brain barrier transcytosis. *Curr. Opin. Struc. Biol.* 45, 109–115. doi: 10.1016/j.sbi.2016.12.005

Humpel, C. (2017). Platelets: their potential contribution to the generation of beta-amyloid plaques in Alzheimer's disease. *Curr. Neurovasc. Res.* 14, 290–298. doi: 10.2174/1567202614666170705150535

Jamasbi, E., Separovic, F., Hossain, M. A., and Ciccotosto, G. D. (2017). Phosphorylation of a full length amyloid-β peptide modulates its amyloid aggregation, cell binding and neurotoxic properties. *Mol. Biosyst.* 13, 1545–1551. doi: 10.1039/C7MB00249A

Kiko, T., Nakagawa, K., Satoh, A., Tsuduki, T., Furukawa, K., Arai, H., et al. (2012). Amyloid β levels in human red blood cells. *PLoS ONE* 7:e49620. doi: 10.1371/journal.pone.0049620

Kozin, S. A., Cheglakov, I. B., Ovsepyan, A. A., Telegin, G. B., Tsvetkov, P. O., Lisitsa, A. V., et al. (2013). Peripherally applied synthetic peptide isoAsp7-Aβ(1-42) triggers cerebral β-amyloidosis. *Neurotox. Res.* 24, 370–376. doi: 10.1007/s12640-013-9399-y

Kozin, S. A., and Makarov, A. A. (2019). The convergence of Alzheimer's disease pathogenesis concepts. *Mol. Biol.* 53, 896–903. doi: 10.1134/S0026893319060104

Kummer, M. P., and Heneka, M. T. (2014). Truncated and modified amyloid-beta species. *Alz. Res. Therapy* 6:28. doi: 10.1186/alzrt258

Lambeth, T. R., Riggs, D. L., Talbert, L. E., Tang, J., Coburn, E., Kang, A. S., et al. (2019). Spontaneous isomerization of long-lived proteins provides a molecular mechanism for the lysosomal failure observed in Alzheimer's disease. *Acscents Sci.* 12:605626. doi: 10.1021/acscentsci.9b00369

Marques, M. A., Kulstad, J. J., Savard, C. E., Green, P. S., Lee, S. P., Craft, S., et al. (2009). Peripheral amyloid-beta levels regulate amyloid-beta clearance from the central nervous system. *J. Alzheimers. Dis.* 16, 325–329. doi: 10.3233/JAD-2009-0964

Mitkevich, V. A., Petrushanko, I. Y., Yegorov, Y. E., Simonenko, O. V., Vishnyakova, K. S., Kulikova, A. A., et al. (2013). Isomerization of Asp7 leads to increased toxic effect of amyloid-β42 on human neuronal cells. *Cell Death Dis* 4, e939–e939. doi: 10.1038/cddis.2013.492

Moro, M. L., Phillips, A. S., Gaimster, K., Paul, C., Mudher, A., Nicoll, J. A. R., et al. (2018). Pyroglutamate and isoaspartate modified amyloid-beta in ageing and Alzheimer's disease. *Acta Neuropathol. Commun.* 6, 3. doi: 10.1186/s40478-017-0505-x

Mroczko, B., Groblewska, M., Litman-Zawadzka, A., Kornhuber, J., and Lewczuk, P. (2018). Cellular receptors of amyloid β oligomers (AβOs) in Alzheimer's disease. *Int. J. Mol. Sci.* 19:1884. doi: 10.3390/ijms19071884

Mukherjee, S., Perez, K. A., Lago, L. C., Klatt, S., McLean, C. A., Birchall, I. E., et al. (2021). Quantification of N-terminal amyloid-β isoforms reveals isomers are the most abundant form of the amyloid-β peptide in sporadic Alzheimer's disease. *Brain Commun.* 3:fcab028. doi: 10.1093/braincomms/fcab028

Nation, D. A., Sweeney, M. D., Montagne, A., Sagare, A. P., D'Orazio, L. M., Pachicano, M., et al. (2019). Blood-brain barrier breakdown is an early biomarker of human cognitive dysfunction. *Nat. Med.* 25, 270–276. doi: 10.1038/s41591-018-0297-y

Pemberton, S., Galindo, D. C., Schwartz, M. W., Banks, W. A., and Rhea, E. M. (2022). Endocytosis of insulin at the blood-brain barrier. *Front. Drug Deliv.* 2:1062366. doi: 10.3389/fddev.2022.1062366

Pflanzner, T., Janko, M. C., André-Dohmen, B., Reuss, S., Weggen, S., Roebroek, A. J. M., et al. (2011). LRP1 mediates bidirectional transcytosis of amyloid-β across the blood-brain barrier. *Neurobiol. Aging* 32, e1–e11. doi: 10.1016/j.neurobiolaging.2010.05.025

Roberts, R., Sandra, A., Siek, G. C., Lucas, J. J., and Fine, R. E. (1992). Studies of the mechanism of iron transport across the blood-brain barrier. *Annal. Neurol.* 32, S43–S50. doi: 10.1002/ana.410320709

Roher, A. E., Esh, C. L., Kokjohn, T. A., Castaño, E. M., Van Vickle, G. D., Kalback, W. M., et al. (2009). Amyloid beta peptides in human plasma and tissues and their significance for Alzheimer's disease. *Alzheimer's Dem.* 5, 18–29. doi: 10.1016/j.jalz.2008.10.004

Scheltens, P., Blennow, K., Breteler, M. M. B., de Strooper, S., Frisoni, B., Salloway, G. B., et al. (2016). Alzheimer's disease. *The Lancet* 388, 505–517. doi: 10.1016/S0140-6736(15)01124-1

Shackleton, B., Crawford, F., and Bachmeier, C. (2016). Inhibition of ADAM10 promotes the clearance of Aβ across the BBB by reducing LRP1 ectodomain shedding. *Fluids Barriers CNS* 13, 14. doi: 10.1186/s12987-016-0038-x

Shimizu, T., Matsuoka, Y., and Shirasawa, T. (2005). Biological significance of isoaspartate and its repair system. *Biol. Pharm. Bull.* 28, 1590–1596. doi: 10.1248/bpb.28.1590

Shubbar, M. H., and Penny, J. I. (2020). Therapeutic drugs modulate ATP-Binding cassette transporter-mediated transport of amyloid beta(1–42) in brain microvascular endothelial cells. *Eur. J. Pharmacol.* 874, 173009. doi: 10.1016/j.ejphar.2020.173009

Sonkusare, S. K., Kaul, C. L., and Ramarao, P. (2005). Dementia of Alzheimer's disease and other neurodegenerative disorders–memantine, a new hope. *Pharmacol. Res.* 51, 1–17. doi: 10.1016/j.phrs.2004.05.005

Sugihara, T., Munesue, S., Yamamoto, Y., Sakurai, S., Akhter, N., Kitamura, Y., et al. (2012). Endogenous secretory receptor for advanced glycation end-products inhibits Amyloid-β 1-42 uptake into mouse brain. *J. Alzheimer's Dis.* 28, 709–720. doi: 10.3233/JAD-2011-110776

Sun, H. L., Chen, S. H., Yu, Z. Y., Cheng, Y., Tian, D. Y., Fan, D. Y., et al. (2021). Blood cell-produced amyloid-β induces cerebral Alzheimer-type pathologies and behavioral deficits. *Mol. Psychiatr.* 26, 5568–5577. doi: 10.1038/s41380-020-0842-1

Tian, X., Leite, D. M., Scarpa, E., Nyberg, S., Fullstone, G., Forth, J., et al. (2020). On the shuttling across the blood-brain barrier via tubule formation: Mechanism and cargo avidity bias. *Sci. Adv.* 6, eabc4397. doi: 10.1126/sciadv.abc4397

Tolstova, A. P., Adzhubei, A. A., Mitkevich, V. A., Petrushanko, I. Y., and Makarov, A. A. (2022). Docking and molecular dynamics-based identification of interaction between various beta-amyloid isoforms and RAGE receptor. *Int. J. Mol. Sci.* 23, 11816. doi: 10.3390/ijms231911816

Wiley, D. T., Webster, P., Gale, A., and Davis, M. E. (2013). Transcytosis and brain uptake of transferrin-containing nanoparticles by tuning avidity to transferrin receptor. *Proc. Nat. Acad. Sci.* 110, 8662–8667. doi: 10.1073/pnas.1307152110

Yan, S. D., Stern, D., Kane, M. D., Kuo, Y. M., Lampert, H. C., Roher, A. E., et al. (1998). RAGE-Abeta interactions in the pathophysiology of Alzheimer's disease. *Restor. Neurol. Neurosci.* 12, 167–173.

Yu, Y. J., Zhang, Y., Kenrick, M., Hoyte, K., Luk, W., Lu, Y., et al. (2011). Boosting brain uptake of a therapeutic antibody by reducing its affinity for a transcytosis target. *Sci. Transl. Med.* 3:84ra44. doi: 10.1126/scitranslmed.3002230

Zenaro, E., Piacentino, G., and Constantin, G. (2017). The blood-brain barrier in Alzheimer's disease. *Neurobiol. Dis.* 107, 41–56. doi: 10.1016/j.nbd.2016.07.007

Zhu, D., Su, Y., Fu, B., and Xu, H. (2018). Magnesium reduces blood-brain barrier permeability and regulates amyloid-β transcytosis. *Mol. Neurobiol.* 55, 7118–7131. doi: 10.1007/s12035-018-0896-0

Zinchenko, E., Klimova, M., Mamedova, A., Agranovich, I., Blokhina, I., Antonova, T., et al. (2020). Photostimulation of extravasation of beta-amyloid through the model of blood-brain barrier. *Electronics* 9:1056. doi: 10.3390/electronics9061056

Zirah, S., Kozin, S. A., Mazur, A. K., Blond, A., Cheminant, M., Segalas-Milazzo, I., et al. (2006). Structural changes of region 1-16 of the Alzheimer disease amyloid beta-peptide upon zinc binding and in vitro aging. *J. Biol. Chem.* 281, 2151–2161. doi: 10.1074/jbc.M504454200

frontiers | Frontiers in Molecular Neuroscience

TYPE Brief Research Report
PUBLISHED 15 March 2024
DOI 10.3389/fnmol.2024.1356343

OPEN ACCESS

EDITED BY
Mohammed Akaaboune,
University of Michigan, United States

REVIEWED BY
Paul Smolen,
University of Texas Health Science Center at Houston, United States
Jana Alonso,
Spanish National Research Council (CSIC), Spain

*CORRESPONDENCE
Patricia Franzka
patricia.franzka@med.uni-jena.de

RECEIVED 15 December 2023
ACCEPTED 27 February 2024
PUBLISHED 15 March 2024

CITATION
Manzolillo A, Gresing L, Hübner CA and Franzka P (2024) Knockdown of INPP5K compromises the differentiation of N2A cells. *Front. Mol. Neurosci.* 17:1356343. doi: 10.3389/fnmol.2024.1356343

Knockdown of INPP5K compromises the differentiation of N2A cells

Annamaria Manzolillo[1], Lennart Gresing[1], Christian A. Hübner[1,2] and Patricia Franzka[1]*

[1]Institute of Human Genetics, Jena University Hospital, Friedrich Schiller University, Jena, Germany, [2]Center of Rare Diseases, Jena University Hospital, Friedrich Schiller University Jena, Jena, Germany

Inositol polyphosphate 5-phosphatase K (INPP5K), also known as SKIP (skeletal muscle and kidney-enriched inositol phosphatase), is a cytoplasmic enzyme with 5-phosphatase activity toward phosphoinositides (PIs). Mutations in INPP5K are associated with autosomal recessive congenital muscular dystrophy with cataracts and intellectual disability (MDCCAID). Notably, muscular dystrophy is characterized by the hypoglycosylation of dystroglycan. Thus, far, the underlying mechanisms are only partially understood. In this study, we show that INPP5K expression increases during brain development. Knockdown of INPP5K in the neuroblastoma-derived cell line N2A impaired their neuronal-like differentiation and interfered with protein glycosylation.

KEYWORDS

INPP5K, brain, development, endoplasmic reticulum, glycosylation

Introduction

Phosphoinositides (PIs) are signaling lipids derived from phosphatidylinositol, a ubiquitous phospholipid within the cytoplasmic leaflet of cellular membranes. Their intracellular levels are strictly regulated by specific PI kinases, phosphatases, and phospholipases. They act as integrators of membrane dynamics with a broad impact on all aspects of cell physiology, such as cytoskeleton organization, mitosis, transport processes, cell polarity, migration, and autophagy (Balla, 2013; Raghu et al., 2019; Posor et al., 2022). Recent discoveries indicate that dysfunctions in the control of their levels can result in different pathologies (Pendaries et al., 2003; Raghu et al., 2019). Mutations in INPP5K, the enzyme with 5-phosphatase activity toward PIs (Ijuin et al., 2000; Vandeput et al., 2006), were reported in patients suffering from congenital muscular dystrophy with cataracts and intellectual disability (MDCCAID) and short stature (Osborn et al., 2017; Wiessner et al., 2017). The morpholino knockdown in zebrafish embryos resulted in curled and shortened tails, impaired swimming and touch-evoked escape responses, smaller eyes, and altered skeletal muscle morphology (Osborn et al., 2017; Wiessner et al., 2017). Moreover, complete loss of INPP5K resulted in embryonic lethality in mice (Ijuin et al., 2008). In agreement with the phenotypes associated with INPP5K loss-of-function, INPP5K is highly expressed in the developing and adult brain, eye, and skeletal muscle (Ijuin et al., 2000). Notably, the overexpression of INPP5K in E17.5 cortical neurons promoted neurite outgrowth and increased the number of processes and branches per neuron (Fink et al., 2017; Kauer et al., 2022).

In this study, we show that INPP5K expression increases during brain development. siRNA-mediated knockdown of INPP5K impaired neuron-like differentiation in N2A cells and interfered with protein glycosylation.

Methods

All animal experiments were approved by the Thüringer Landesamt für Lebensmittelsicherheit und Verbraucherschutz (TLLV). The experiments were performed on a C57BL/6 background. Mice were housed in a 12-h light/12-h dark cycle and had access to mouse chow *ad libitum*.

N2A cell differentiation experiments for microscopic analysis

N2A (ATCC) cells were cultured in DMEM GlutaMAX (Sigma-Aldrich) supplemented with 10% [v/v] FBS (Biowest) and 1% [v/v] penicillin/streptomycin (Gibco) at 37°C. The N2A cells were seeded on poly-D-lysine (Thermo Fisher)-coated coverslips. The following day, the cells were treated with differentiation medium [Neurobasal medium 1 g/l glucose (Gibco) + 1X B-27 (Gibco) + 1X sodium pyruvate (Gibco) + 1X glutamine (Gibco) + 1% [v/v] penicillin/streptomycin (Gibco)] and transfected with siRNA against either control (siScr; Dharmacon) or INPP5K (si*Inpp5k*; Thermo Fisher) according to the manufacturer's protocol using Lipofectamine 2000 (Invitrogen). After 4 days of differentiation, the cells were fixed with 100% ice-cold methanol, permeabilized with 0.25% TritonX100, blocked in 5% normal donkey serum (NDS), and stained overnight with primary antibodies at 4°C, followed by incubation with the corresponding secondary antibodies or streptavidin coupled to fluorophores (Invitrogen). The following primary antibodies/lectins were used: biotin WGA (Biozol) 1:50, rabbit anti-INPP5K (Proteintech) 1:100, and mouse anti-PDI (Enzo) 1:300. Nuclei were stained with DAPI (10 µg/ml, Invitrogen). Images were taken with a Keyence microscope (BZ-X800E). Brightfield pictures were used for protrusion analysis, while fluorescence pictures were used for ER and glycosylation analysis. The experiments were performed three times. N2A cell differentiation was morphologically evaluated by measuring the length and numbers of dendrite-like protrusions of first-order, second-order, and third-order protrusions. The length and number of protrusions were measured by tracing protrusions manually with the tool "segmented line" in ImageJ. The length was measured in micrometers with the option "measure." All single cells from at least five to seven images per condition and experiment were traced manually.

For measuring the total protrusion numbers of individual N2A cells, all traced/visible protrusions per cell were counted for all single cells in at least five to seven images per condition and experiment, and the mean per cell was calculated for each condition.

For measuring the total protrusion length per cell, the length of all traced/visible projections per cell was measured for all single cells from at least five to seven images per condition and experiment, and the mean per cell was calculated for each condition.

To determine the mean protrusion length per order, the length of all traced/visible protrusions per respective protrusion order was measured for each cell and each condition.

Differentiation of N2A cells upon knockdown of INPP5K

N2A (ATCC) cells were cultured in DMEM GlutaMAX (Sigma-Aldrich) supplemented with 10% [v/v] FBS (Biowest) and 1% [v/v] penicillin/streptomycin (Gibco) at 37°C. The N2A cells were seeded in 10-cm cell culture dishes (Greiner). The following day, the cells were treated with differentiation medium [Neurobasal medium 1 g/L glucose (Gibco) + 1X B-27 (Gibco) + 1X sodium pyruvate (Gibco) + 1X glutamine (Gibco) + 1% [v/v] penicillin/streptomycin (Gibco)] and at the same time transfected with siRNA against either control (siScr; Dharmacon) or INPP5K (si*Inpp5k*; Thermo Fisher) according to the manufacturer's protocol using Lipofectamine 2000 (Invitrogen). After 3 days of differentiation, the cells were harvested and lysed in RIPA buffer [50 mM Tris-HCl pH 7.4, 150 mM NaCl, 1% [v/v] NP-40, 1% [w/v] sodium deoxycholate, 0.1% [w/v] SDS, 1 mM EDTA] and a complete protease inhibitor (Roche). Cell homogenates were centrifuged at 10,000 *g*, and the protein concentration in the supernatant was determined using the BCA assay kit (Thermo Fisher). Samples were stored at −20°C until further use. The experiments were performed three times.

Knockdown of INPP5K in differentiated N2A cells

N2A (ATCC) cells were cultured in DMEM GlutaMAX (Sigma-Aldrich) supplemented with 10% [v/v] FBS (Biowest), 1% [v/v] penicillin/streptomycin (Gibco) at 37°C. The N2A cells were seeded on poly-D-lysine (Thermo Fisher) coated coverslips. The following day, the cells were treated with differentiation medium [Neurobasal medium 1 g/L glucose (Gibco) + 1X B-27 (Gibco) + 1X sodium pyruvate (Gibco) + 1X glutamine (Gibco) + 1% [v/v] penicillin/streptomycin (Gibco)] and allowed to differentiate for 3 days. Then, the cells were transfected with siRNA against either control (siScr; Dharmacon) or INPP5K (si*Inpp5k*; Thermo Fisher) according to the manufacturer's protocol using Lipofectamine 2000 (Invitrogen). After 4 days of differentiation, cells were fixed and processed as described above. The experiments were performed three times.

Protein isolation from the brain

Pregnant mice or pups were sacrificed, and the brain tissues were dissected. The brain tissue was obtained from 3 E11.5 and 3 E18.5 embryos as well as from 3 postnatal day (P) 3 and 3 P18 pups. Tissue lysates were prepared as previously described (Franzka et al., 2022). Briefly, samples were homogenized with the Potter S tissue homogenizer (Sartorius) in RIPA buffer [50 mM Tris-HCl pH 7.4, 150 mM NaCl, 1% [v/v] NP-40, 1% [w/v] sodium deoxycholate, 0.1% [w/v] SDS, 1 mM EDTA] and a complete protease inhibitor (Roche). After sonication, homogenates were spun down at 16,900 *g* to remove nuclei and insoluble debris. Protein concentration in the supernatant was determined using the BCA assay kit (Thermo Fisher) and then stored at −80°C until further use.

Western blot

Proteins isolated from three embryos/pups at the indicated developmental stages or from N2A cells (transfected with siRNA against either control or INPP5K) from three individual experiments were denatured at 90°C for 5 min in Laemmli buffer (4X Laemmli buffer: 50% glycerol, 5% SDS, 0.25% 1.5 M Tris pH 6.8, 30% β-mercaptoethanol, and 0.001% bromophenol blue, ddH_2O). After separation by SDS-PAGE, proteins were transferred onto PVDF membranes (Whatman). Membranes were blocked in 2% BSA and incubated with primary antibodies at appropriate dilutions overnight at 4°C. The following primary antibodies or lectins were used: rabbit anti-INPPK (Proteintech) 1:500, rabbit anti-GAPDH (Proteintech) 1:1,000, biotin WGA (Biozol) 1:300, biotin PNA (Bioworld) 1:300, biotin SNL (Biozol) 1:300, biotin RCAI (Biozol) 1:300, biotin Con A (Biozol) 1:300, biotin LCH (Ey Laboratories) 1:300, and biotin MAL (Biomol) 1:300. Primary antibodies or lectins were detected with HRP-conjugated secondary antibodies or HRP-conjugated streptavidin. Detection was performed using the Clarity Western ECL Substrate Kit (BioRad). The quantification of bands was performed using ImageJ.

Coomassie blue staining of PVDF membranes was performed as described previously (Franzka et al., 2021). For Coomassie blue staining of transferred proteins, PVDF membranes were fixed for 3 min (10% acetic acid, 40% EtOH), stained in Coomassie blue solution (0.1% Brilliant Blue R (Serva), 45% EtOH, 10% acetic acid) for 5 min, destained (10% acetic acid, 20–40% EtOH), rinsed in H_2O, and imaged.

Immunofluorescence analysis of embryo sections

Pregnant mice or pups were sacrificed, and whole embryos or brain tissues were dissected. Tissue was obtained from each of the three E11.5, E13.5, and E18.5 embryos, as well as from the three postnatal day (P) 3 and P18 pups. The tissues were frozen in TissueTek (company) on dry ice and cryo-sectioned. Sections were dried, fixed in 4% paraformaldehyde (PFA), permeabilized with 0.25% TritonX100, blocked in 5% normal goat serum (NGS), and stained overnight at 4°C with primary antibodies or lectins, followed by incubation with the corresponding secondary antibodies or streptavidin coupled to fluorophores (Invitrogen). The following primary antibodies or lectins were used: biotin WGA (Biozol) 1:100, rabbit anti-INPP5K (Proteintech) 1:100, and biotin PNA (Bioworld) 1:100. Nuclei were stained with DAPI (10 μg/ml, Invitrogen). Images were taken using a Keyence microscope BZ-X800E.

Statistical analysis

For statistical analysis, raw data were analyzed for normal distribution with the Kolmogorov–Smirnov test or by graphical analysis using the Box-Plot and QQ-Plot in GraphPad Prism 9. If appropriate, we either used a one-way ANOVA, a two-way ANOVA, or a two-tailed Student's *t*-test. $^{*}p < 0.05$, $^{**}p < 0.01$, $^{***}p < 0.001$, $^{****}p < 0.0001$, and ns, not significant. For statistical analysis, we used GraphPad Prism 9. For all data, means with the standard error of the mean (SEM) and individual data points with the SEM are shown.

Results

INPP5K expression increases in the developing mouse brain

To analyze the expression pattern of INPP5K during mouse development, we stained sagittal whole embryo or brain sections of different developmental stages with an antibody directed against INPP5K (Figure 1A, Supplementary Figures 2, 3). Prominent INPP5K signals were found in developing skeletal muscles and in the central nervous system (Figure 1A, Supplementary Figures 2, 3). In the brain, INPP5K expression was detected in various regions, especially in the hippocampus, the cortex, and Purkinje cells (Figure 1B). Excluding the unspecific binding of secondary antibodies, no signals were observed when the primary antibody was omitted (Supplementary Figure 4).

We next assessed the abundance of INPP5K in protein lysates from mouse brains isolated at different time points of embryonic development. Notably, INPP5K levels increased dramatically during embryonic as well as early postnatal (P) brain development (Figure 1C, Supplementary Figure 5).

Taken together, these findings suggest a pivotal role for INPP5K in the brain.

INPP5K knockdown impairs the differentiation of N2A cells upon serum starvation

To assess whether INPP5K is relevant for cell differentiation, we transfected N2A cells with siRNAs directed against INPP5K (si*Inpp5k*) or a scrambled control siRNA (siScr; Figure 2A, Supplementary Figure 5). We then serum-deprived the transfected N2A cells to induce neuronal-like differentiation and measured the numbers and length of first-, second-, and third-order protrusions 4 days later. While the number of protrusions did not differ from controls, the length of first-order dendrites was significantly decreased after the siRNA-mediated knockdown of INPP5K (Figure 2B, Supplementary Figure 1A). Dendrite numbers did not differ between conditions (Figure 2B, Supplementary Figure 1A).

To assess whether INPP5K is required for the maintenance of differentiated N2A cells, we induced differentiation for 4 days before we knocked down INPP5K. The number and length of the protrusions were evaluated 4 days later. While control cells maintained long primary protrusions, the length of primary protrusions was significantly reduced after siRNA-mediated knockdown of INPP5K in differentiated N2A cells (Figure 2C, Supplementary Figure 1B).

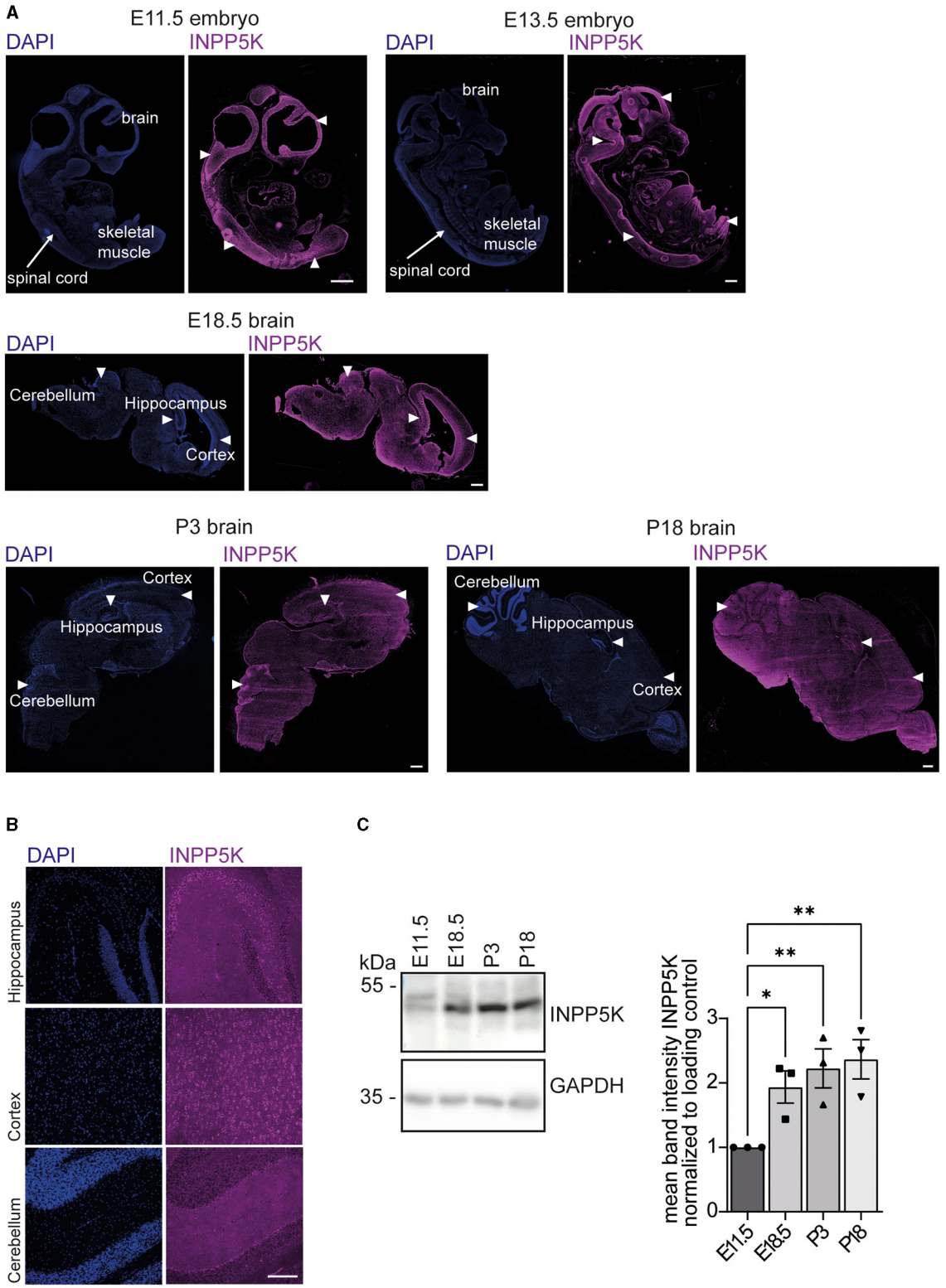

FIGURE 1
INPP5K expression increases in the developing mouse brain. **(A)** Immunofluorescence of sagittal whole embryo and brain sections at indicated time points stained for INPP5K (scale bar: 500 μm). Nuclei were labeled with DAPI. White arrowheads indicate prominent labeling of INPP5K in whole embryo sections. In E18.5 and P3 brain sections, arrowheads mark the hippocampus, the cortex, and the cerebellum. **(B)** Immunolabeling of INPP5K expression in a magnification of the hippocampus, cortex, and cerebellum of sagittal brain sections from P18 mice (scale bar: 100 μm). **(C)** Immunoblot analysis of brain tissue lysates at the indicated time points showed a strong increase in INPP5K abundance during brain development. GAPDH served as a loading control ($n = 3$ samples per time point, one-way ANOVA with Fisher's LSD test). Quantitative data are presented as mean ± SEM with individual data points. *$p < 0.05$, **$p < 0.01$.

10.3389/fnmol.2024.1356343

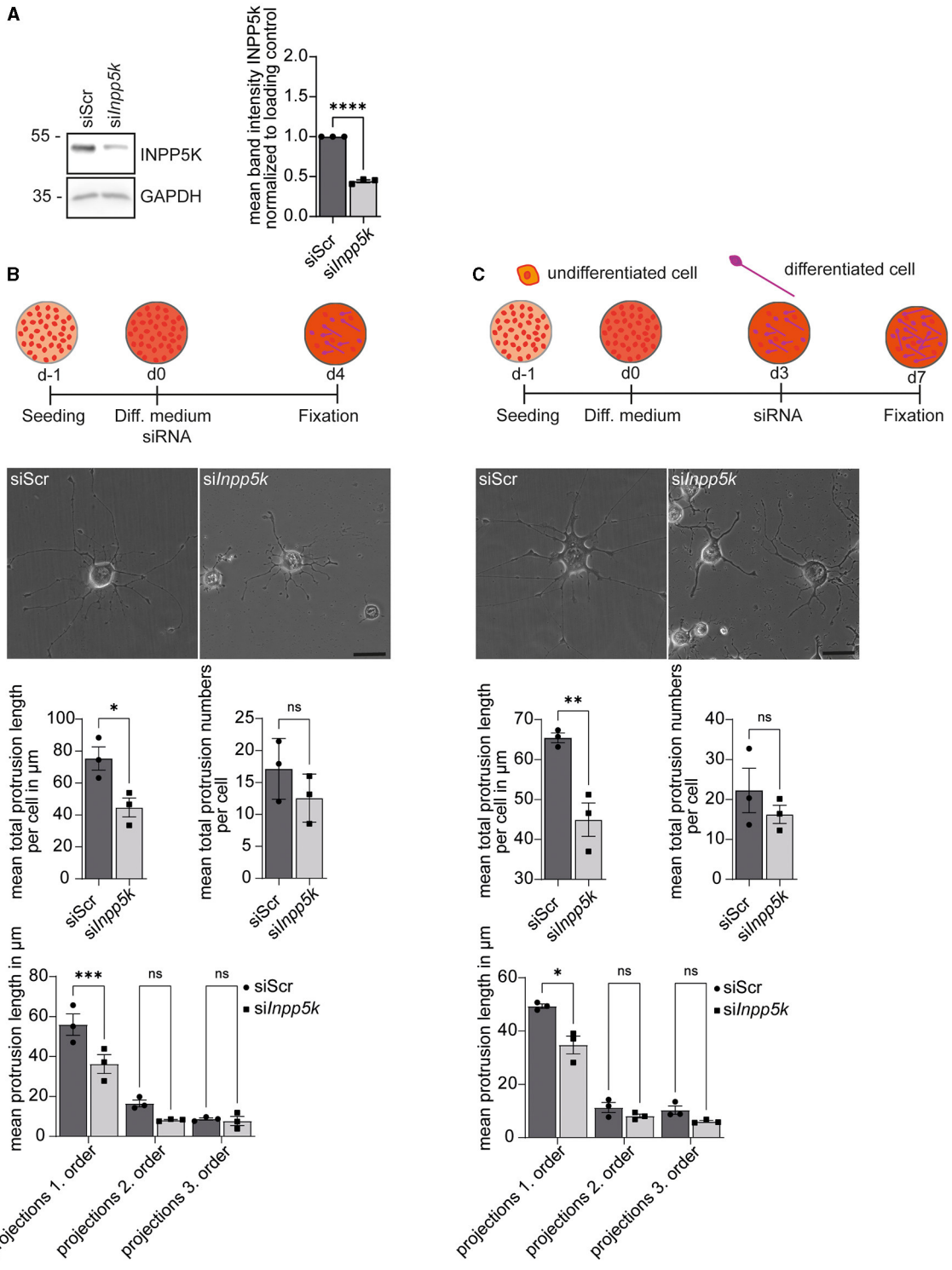

FIGURE 2
INPP5K knockdown impairs the differentiation of N2A cells upon serum starvation. **(A)** Immunoblot analyses confirmed the efficient knockdown of INPP5K. GAPDH served as a loading control. **(B)** Experimental design and representative images of N2A cells (scale bar: 50 µm) and the quantification of the length and numbers of protrusions [$n = 3$ experiments with 5–7 pictures per condition and experiment with 5–15 cells per picture (35–75 cells per experiment)], Student's *t*-test or one-way ANOVA with Fisher's LSD test. **(C)** Experimental design and representative images of N2A cells (scale bar: 50 µm) and quantification of the length and number of protrusions [$n = 3$ experiments with 5–7 pictures per condition and experiment with 5–15 cells per picture (35–75 cells per experiment)], Student's *t*-test or one-way ANOVA with Fisher's LSD test. Quantitative data are presented as mean ± SEM with individual data points. *$p < 0.05$, **$p < 0.01$, ***$p < 0.001$, ****$p < 0.0001$; ns, not significant.

10.3389/fnmol.2024.1356343

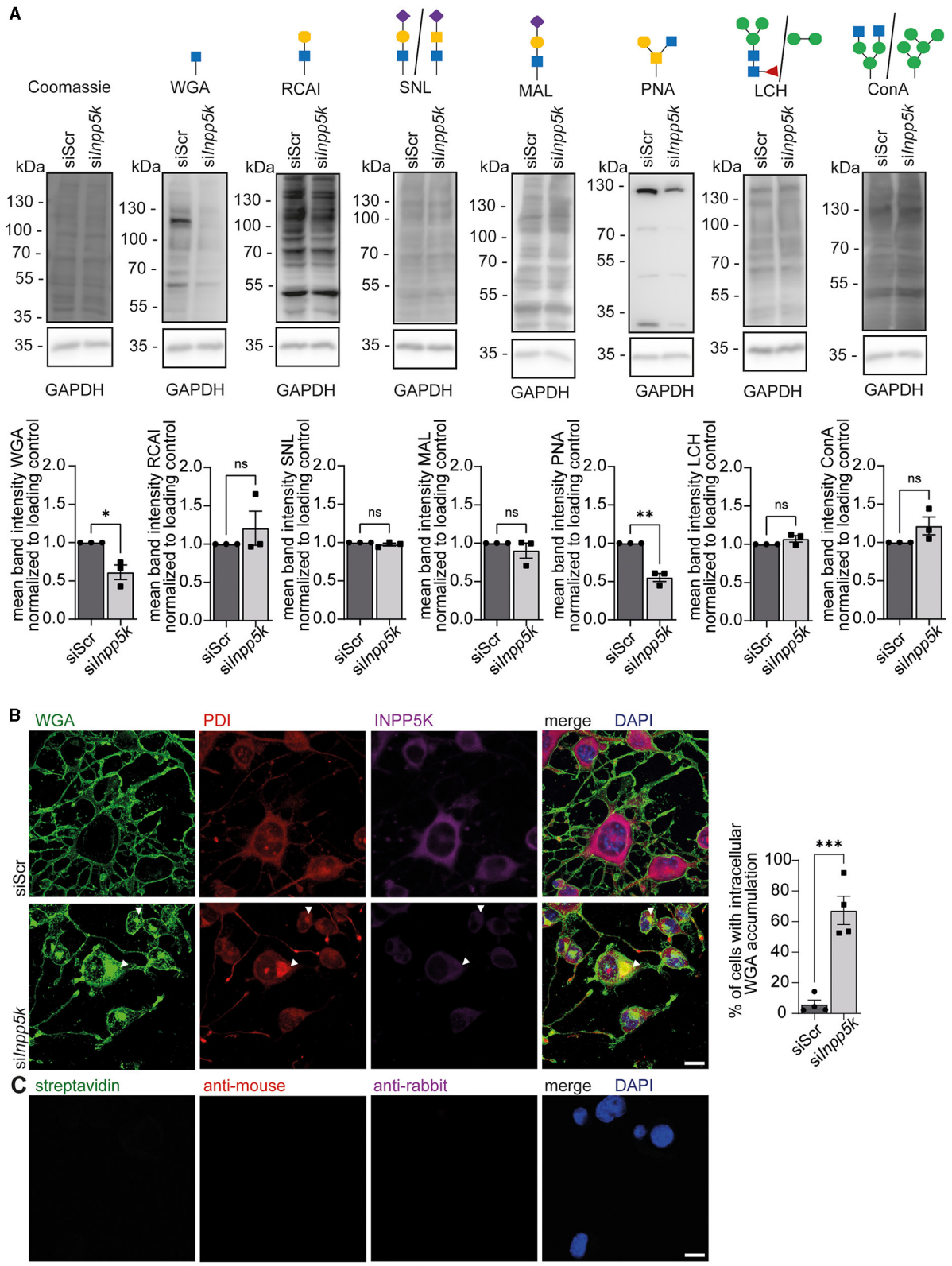

FIGURE 3
Knockdown of INPP5K in N2A cells interferes with protein glycosylation. **(A)** Representative Coomassie stained membranes and membranes probed with different biotinylated lectins, i.e., WGA, RCAI, SNL, MAL, PNA, LCH, and Con A, and the respective quantifications. GAPDH and Coomassie staining served as a loading control. Green circle = mannose, yellow circle = galactose, blue square = *N*-acetylglucosamine, yellow square = *N*-acetylgalactosamine, violet diamond = N-glycolylneuraminic acid, and red triangle = fucose. Lectin signals were normalized to GAPDH. N2A cells were transfected with either scRNA or siRNA to knock down INPP5K, harvested, and the respective protein lysates separated by SDS-PAGE and transferred to membranes ($n = 3$ experiments, Student's *t*-test). **(B)** Staining of N2A cells transfected with either scRNA or siRNA to knock down

(Continued)

FIGURE 3 (Continued)
INPP5K with WGA, anti-PDI, anti-INPP5K, and DAPI to label nuclei (scale bar 10 μm, $n = 4$ experiments with 200–5,000 cells per condition and experiment, Student's *t*-test). White arrowheads indicate examples of cells with WGA-positive deposits co-labeling with the ER marker PDI. Cells with intracellular deposits labeled by WGA were quantified. **(C)** As a control, we also incubated N2A cells with either secondary antibodies alone or fluorophore-coupled streptavidin, which was used to detect biotinylated WGA (scale bar 10 μm). Quantitative data are presented as mean ± SEM with individual data points. *$p < 0.05$, **$p < 0.01$, ***$p < 0.001$; ns, not significant.

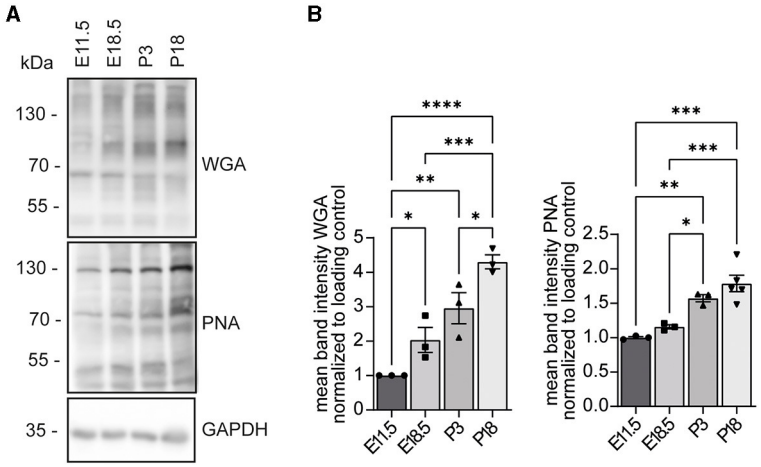

FIGURE 4
WGA and PNA reactivities increase during mouse brain development. **(A)** Protein lysates of mouse brains at the indicated developmental stages were separated by SDS-PAGE, blotted, and probed with either WGA or PNA. GAPDH served as a loading control. **(B)** Analysis of WGA and PNA signals shown in **(A)** ($n = 3$ samples per time point, one-way ANOVA with Fisher's LSD test). Quantitative data are presented as mean ± SEM with individual data points. *$p < 0.05$, **$p < 0.01$, ***$p < 0.001$, ****$p < 0.0001$.

Knockdown of INPP5K in N2A cells interferes with protein glycosylation

Patients with MDCCAID suffer from congenital muscular dystrophy with hypoglycosylation of dystroglycan (Osborn et al., 2017; Wiessner et al., 2017). To study whether the knockdown of INPP5K in N2A cells alters protein glycosylation, we isolated protein lysates of differentiated N2A cells transfected with either scRNA or siRNAs to knock down INPP5K upon the induction of differentiation. After separation by SDS-PAGE and blotting, membranes were incubated with different lectins to detect specific glycan structures. Upon knockdown of INPP5K, signals were diminished for wheat germ agglutinin (WGA), which detects *N*-acetylglucosamine residues, and for peanut agglutinin (PNA), which recognizes non-sialylated β(1–3)-linked galactose on *N*-acetylgalactosamine residues (Figure 3A, Supplementary Figure 5). No differences were found in non-sialylated/sialylated galactose/glucosamine on *N*-acetylglucosamine residues, as detected by ricinus communis agglutinin I (RCAI), sambucus nigra lectin (SNL) or maackia amurensis lectin (MAL). Similarly, no differences were found in fucosylated/mannose-carrying residues, as detected by the lens culinaris lectin (LCH) or concanavalin A (Con A; Figure 3A, Supplementary Figure 5).

We then fixed N2A cells either transfected with the scRNA or the siRNAs directed against INPP5K at the same time as the induction of differentiation and co-stained for *N*-acetylglucosamine residues and the luminal ER protein phosphodiesterase (PDI; Figures 3B, C). Consistent with our immunoblots, INPP5K signals were diminished upon knockdown of INPP5K. Notably, cells showing reduced INPP5K signals showed a prominent intracellular accumulation of WGA and a co-localization of PDI with WGA signals, suggesting that glycoproteins were retained within the ER (Figure 3B).

In summary, the knockdown of INPP5K in N2A cells affects protein glycosylation.

WGA and PNA reactivities increase during mouse brain development

Because WGA and PNA reactivities were diminished in protein lysates of cells transfected with siRNAs to knock down INPP5K (Figure 3), we wondered about the developmental profile for *N*-acetylglucosamine residues detected by WGA and non-sialylated β(1–3)-linked galactose on *N*-acetylgalactosamine residues detected by peanut agglutinin (PNA).

We assessed the abundance of *N*-acetylglucosamine residues and non-sialylated β(1–3)-linked galactose on *N*-acetylgalactosamine residues in mouse brains isolated at different time points of embryonic and postnatal development. The respective protein lysates were separated by SDS-PAGE and blotted. For both glycan structures, we observed a strong increase between E11.5 and P18 (Figure 4, Supplementary Figures 2–5).

Discussion

Mutations that decrease the enzymatic activity of INPP5K are associated with an autosomal recessive human disorder characterized by congenital muscular dystrophy with hypoglycosylation of dystroglycan in combination with cataracts, intellectual disability, and short stature (Osborn et al., 2017; Wiessner et al., 2017), while some polymorphisms in INPP5K have been associated with Parkinson's disease (Zhu et al., 2018). Remarkably, the total knockout caused embryonic lethality in mice (Ijuin et al., 2008). In agreement with the phenotype of patients and confirming previous reports (Ijuin et al., 2000), INPP5K is strongly expressed in the developing brain and skeletal muscles of the mouse and further increases with embryonic and postnatal brain development. Suggesting a major role in neuronal differentiation, the overexpression of INPP5K in E17.5 cortical neurons promoted neurite outgrowth and increased the number of processes and branches per neuron (Fink et al., 2017; Kauer et al., 2022). Here, we assessed the consequences of its siRNA-mediated knockdown in neuroblastoma-derived N2A cells. Under serum starvation, N2A cells can be differentiated into cells with complex protrusions resembling dendrites (Evangelopoulos et al., 2005). Remarkably, the knockdown of INPP5K impaired the outgrowth and the maintenance of dendrite-like protrusions in N2A cells, which may relate to the observation that patients with INPP5K loss-of-function show intellectual disability and brain abnormalities, especially cerebellar or global brain atrophy (Osborn et al., 2017; Wiessner et al., 2017; D'Amico et al., 2020; Hathazi et al., 2021).

The subcellular localization of INPP5K can vary depending on the specific cellular requirements. While a large pool localizes to the ER, INPP5K can be recruited to the plasma membrane to downregulate PI(3,4,5)P_3 signaling upon growth factor stimulation (Gurung et al., 2003). In *Caenorhabditis elegans*, INPP5K together with atlastin-1 was shown to be involved in maintaining the non-uniform, somatodendritic enrichment of neuronal ER/plasma membrane contacts in their soma and dendrites, which are mostly absent in axons (Loncke et al., 2023). The hypoglycosylation of dystroglycan in patients with INPP5K loss-of-function further connects INPP5K with ER and Golgi functions. In agreement, the knockdown of INPP5K in N2A cells clearly affected the glycosylation of proteins, as evidenced by reduced signal intensities for *N*-acetylglucosamine residues or non-sialylated β(1–3)–linked galactose. Because *N*-acetylglucosamine is the first sugar residue attached to the amide group for *N*-glycosylation of proteins (Varki et al., 2009; Breloy and Hanisch, 2018), loss of INPP5K can have important consequences for glycoproteins, such as α-dystroglycan or PDI, carrying *N*-glycosylated sugar residues. Aberrant protein glycosylation can interfere with proper protein folding and may thus explain the accumulation of glycoproteins carrying *N*-acetylglucosamine within the ER upon knockdown of INPP5K.

Data availability statement

The raw data supporting the conclusions of this article will be made available by the authors, without undue reservation.

Ethics statement

The animal study was reviewed and approved by the Thüringer Landesamt für Lebensmittelsicherheit und Verbraucherschutz (TLLV). The study was conducted in accordance with the local legislation and institutional requirements.

Author contributions

AM: Writing – original draft, Formal analysis. LG: Writing – original draft, Methodology. PF: Writing – review & editing, Writing – original draft, Supervision, Project administration, Methodology, Investigation, Funding acquisition, Conceptualization. CH: Writing – original draft, Writing – review & editing, Funding acquisition.

Funding

The author(s) declare financial support was received for the research, authorship, and/or publication of this article. This study was funded by the DFG GRK 2155 ProMoAge to CH. This study was supported by a Medical Scientist Award from the Interdisciplinary Center for Clinical Research (IZKF) at the Jena University Hospital (MSP13) and by IMPULSE funding (FKZ IP 2021-04) from the Friedrich-Schiller-University Jena to PF.

Acknowledgments

The authors gratefully acknowledge support from Katrin Schorr and Johanna Fischer.

Conflict of interest

The authors declare that the research was conducted in the absence of any commercial or financial relationships that could be construed as a potential conflict of interest.

Publisher's note

Supplementary material

The Supplementary Material for this article can be found online at: https://www.frontiersin.org/articles/10.3389/fnmol.2024.1356343/full#supplementary-material

References

Balla, T. (2013). Phosphoinositides: tiny lipids with giant impact on cell regulation. *Physiol. Rev*. 93, 1019–1137. doi: 10.1152/physrev.00028.2012

Breloy, I., and Hanisch, F.-G. (2018). Functional roles of O-glycosylation. *Molecules* 23:3063. doi: 10.3390/molecules23123063

D'Amico, A., Fattori, F., Nicita, F., Barresi, S., Tasca, G., Verardo, M., et al. (2020). A recurrent pathogenic variant of INPP5K underlies autosomal recessive congenital muscular dystrophy with cataracts and intellectual disability: evidence for a founder effect in Southern Italy. *Front. Genet*. 11:565868. doi: 10.3389/fgene.2020.565868

Evangelopoulos, M. E., Weis, J., and Krüttgen, A. (2005). Signalling pathways leading to neuroblastoma differentiation after serum withdrawal: HDL blocks neuroblastoma differentiation by inhibition of EGFR. *Oncogene* 24, 3309–3318. doi: 10.1038/sj.onc.1208494

Fink, K. L., López-Giráldez, F., Kim, I. J., Strittmatter, S. M., and Cafferty, W. B. J. (2017). Identification of intrinsic axon growth modulators for intact CNS neurons after injury. *Cell Rep*. 18, 2687–2701. doi: 10.1016/j.celrep.2017.02.058

Franzka, P., Krüger, L., Schurig, M. K., Olecka, M., Hoffmann, S., Blanchard, V., et al. (2021). Altered glycosylation in the aging heart. *Front. Mol. Biosci*. 8:673044. doi: 10.3389/fmolb.2021.673044

Franzka, P., Turecki, G., Cubillos, S., Kentache, T., Steiner, J., Walter, M., et al. (2022). Altered mannose metabolism in chronic stress and depression is rapidly reversed by vitamin B12. *Front. Nutr*. 9:981511. doi: 10.3389/fnut.2022.981511

Gurung, R., Tan, A., Ooms, L. M., McGrath, M. J., Huysmans, R. D., Munday, A. D., et al. (2003). Identification of a novel domain in two mammalian inositol-polyphosphate 5-phosphatases that mediates membrane ruffle localization. *J. Biol. Chem*. 278, 11376–11385. doi: 10.1074/jbc.M209991200

Hathazi, D., Cox, D., D'Amico, A., Tasca, G., Charlton, R., Carlier, R. Y., et al. (2021). INPP5K and SIL1 associated pathologies with overlapping clinical phenotypes converge through dysregulation of PHGDH. *Brain* 144, 2427–2442. doi: 10.1093/brain/awab133

Ijuin, T., Mochizuki, Y., Fukami, K., Funaki, M., Asano, T., and Takenawa, T. (2000). Identification and characterization of a novel inositol polyphosphate 5-phosphatase. *J. Biol. Chem*. 275, 10870–10875. doi: 10.1074/jbc.275.15.10870

Ijuin, T., Yu, Y. E., Mizutani, K., Pao, A., Tateya, S., Tamori, Y., et al. (2008). Increased insulin action in SKIP heterozygous knockout mice. *Mol. Cell. Biol*. 28, 5184–5195. doi: 10.1128/MCB.01990-06

Kauer, S. D., Fink, K. L., Li, E. H. F., Evans, B. P., Golan, N., and Cafferty, W. B. J. (2022). Inositol polyphosphate-5-phosphatase k (INPP5K) enhances sprouting of corticospinal tract axons after CNS trauma. *J. Neurosci*. 42, 2190–2204. doi: 10.1523/JNEUROSCI.0897-21.2022

Loncke, J., Luyten, T., Ramos, A. R., Erneux, C., and Bultynck, G. (2023). Loss of INPP5K attenuates IP3-induced Ca^{2+} responses in the glioblastoma cell line U-251 MG cells. *BBA Adv*. 4:100105. doi: 10.1016/j.bbadva.2023.100105

Osborn, D. P. S., Pond, H. L., Mazaheri, N., Dejardin, J., Munn, C. J., Mushref, K., et al. (2017). Mutations in INPP5K cause a form of congenital muscular dystrophy overlapping Marinesco-Sjögren syndrome and dystroglycanopathy. *Am. J. Hum. Genet*. 100, 537–545. doi: 10.1016/j.ajhg.2017.01.019

Pendaries, C., Tronchère, H., Plantavid, M., and Payrastre, B. (2003). Phosphoinositide signaling disorders in human diseases. *FEBS Lett*. 546, 25–31. doi: 10.1016/S0014-5793(03)00437-X

Posor, Y., Jang, W., and Haucke, V. (2022). Phosphoinositides as membrane organizers. *Nat. Rev. Mol. Cell Biol*. 23, 797–816. doi: 10.1038/s41580-022-00490-x

Raghu, P., Joseph, A., Krishnan, H., Singh, P., and Saha, S. (2019). Phosphoinositides: regulators of nervous system function in health and disease. *Front. Mol. Neurosci*. 12:208. doi: 10.3389/fnmol.2019.00208

Vandeput, F., Backers, K., Villeret, V., Pesesse, X., and Erneux, C. (2006). The influence of anionic lipids on SHIP2 phosphatidylinositol 3,4,5-trisphosphate 5-phosphatase activity. *Cell. Signal*. 18, 2193–2199. doi: 10.1016/j.cellsig.2006.05.010

Varki, A., Cummings, R. D., Esko, J. D., Freeze, H. H., Stanley, P., Bertozzi, C. R., et al. (2009). *Essentials of Glycobiology, 2nd Edn*. Cold Spring Harbor, NY: Cold Spring Harbor Laboratory Press.

Wiessner, M., Roos, A., Munn, C. J., Viswanathan, R., Whyte, T., Cox, D., et al. (2017). Mutations in INPP5K, encoding a phosphoinositide 5-phosphatase, cause congenital muscular dystrophy with cataracts and mild cognitive impairment. *Am. J. Hum. Genet*. 100, 523–536. doi: 10.1016/j.ajhg.2017.01.024

Zhu, W., Luo, X., Adnan, A., Yu, P., Zhang, S., Huo, Z., et al. (2018). Association analysis of NUCKS1 and INPP5K polymorphism with Parkinson's disease. *Genes Genet. Syst*. 93, 59–64. doi: 10.1266/ggs.17-00038

frontiers | Frontiers in Molecular Neuroscience

TYPE Review
PUBLISHED 13 May 2024
DOI 10.3389/fnmol.2024.1371086

OPEN ACCESS

EDITED BY
Judit Symmank,
University Hospital Jena, Germany

REVIEWED BY
Shuaipeng Ma,
University of Texas Southwestern Medical Center, United States
Terrence J. Piva,
RMIT University, Australia

*CORRESPONDENCE
Miguel del Angel
✉ delangel@ovgu.de
Kevin Jonischkies
✉ kevin.jonischkies@st.ovgu.de

†These authors have contributed equally to this work

RECEIVED 15 January 2024
ACCEPTED 22 April 2024
PUBLISHED 13 May 2024

CITATION
Jonischkies K, del Angel M, Demiray YE, Loaiza Zambrano A and Stork O (2024) The NDR family of kinases: essential regulators of aging. *Front. Mol. Neurosci.* 17:1371086. doi: 10.3389/fnmol.2024.1371086

The NDR family of kinases: essential regulators of aging

Kevin Jonischkies[1*†], Miguel del Angel[1*†], Yunus Emre Demiray[1], Allison Loaiza Zambrano[1] and Oliver Stork[1,2,3,4]

[1]Department of Genetics and Molecular Neurobiology, Institute of Biology, Otto-von-Guericke University Magdeburg, Magdeburg, Germany, [2]Center for Behavioral Brain Science, Magdeburg, Germany, [3]Center for Intervention and Research on Adaptive and Maladaptive Brain Circuits Underlying Mental Health (C-I-R-C), Jena-Magdeburg-Halle, Germany, [4]German Center for Mental Health (DZPG), Jena-Magdeburg-Halle, Germany

Aging is defined as a progressive decline of cognitive and physiological functions over lifetime. Since the definition of the nine hallmarks of aging in 2013 by López-Otin, numerous studies have attempted to identify the main regulators and contributors in the aging process. One interesting group of proteins whose participation has been implicated in several aging hallmarks are the nuclear DBF2-related (NDR) family of serine-threonine AGC kinases. They are one of the core components of the Hippo signaling pathway and include NDR1, NDR2, LATS1 and LATS2 in mammals, along with its highly conserved metazoan orthologs; Trc in *Drosophila melanogaster*, SAX-1 in *Caenorhabditis elegans*, CBK1, DBF20 in *Saccharomyces cerevisiae* and orb6 in *Saccharomyces pombe*. These kinases have been independently linked to the regulation of widely diverse cellular processes disrupted during aging such as the cell cycle progression, transcription, intercellular communication, nutrient homeostasis, autophagy, apoptosis, and stem cell differentiation. However, a comprehensive overview of the state-of-the-art knowledge regarding the post-translational modifications of and by NDR kinases in aging has not been conducted. In this review, we summarize the current understanding of the NDR family of kinases, focusing on their relevance to various aging hallmarks, and emphasize the growing body of evidence that suggests NDR kinases are essential regulators of aging across species.

KEYWORDS

nuclear Dbf2-related (NDR) kinases, aging, cellular senescence, autophagy, brain aging, neuroinflammation, nutrient sensing and signaling, DNA repair

Introduction

Aging is broadly characterized as the time-dependent decline in organism fitness, leading to an elevated risk of intrinsic mortality associated with diseases such as coronary heart disease, cancer, or neurodegenerative diseases, among many others. Based on the growing body of aging research, nine hallmarks of aging were proposed in 2013 regarding the molecular and cellular aspects underlying aging mechanisms. Each hallmark inherently manifests in physiological aging, and their experimental impairment accelerates the aging process, while experimental amelioration delays aging and increases lifespan. These criteria collectively define and highlight the key features that contribute to the complex phenomenon of aging (López-Otín et al., 2013).

The original nine aging hallmarks included Cellular senescence, deregulated nutrient signaling, loss of proteostasis, mitochondrial dysfunction genomic instability, epigenetic alterations, altered intracellular communication, telomere attrition and stem cell exhaustion. After a decade of intense aging research, three additional hallmarks were

proposed: chronic inflammation, impairment in macroautophagy and dysbiosis (López-Otín et al., 2023). It is important to emphasize that the hallmarks of aging do not exist as discrete biological entities; instead, they form a network of interconnected processes that frequently interact with each other. This interconnectedness is largely attributed to central signaling pathways that overlap across the aging hallmarks. Consequently, there is a significant interest in comprehending such pathways and identifying novel regulators that could serve as potential targets for anti-aging interventions.

The Nuclear Dbf2-related kinases (NDR) are part of the NDR/LATS (large-tumor-suppressor) subfamily of AGC (protein kinase A/G/C PKA/PKG/PKC-like). They are evolutionarily conserved from plants to mammals, and they were first described as core components of the Hippo signaling pathway (Hergovich, 2016). While four NDR-kinases are known to exist in vertebrates, four homologs have been described in invertebrates and more than 10 kinases are present in fungi, yeasts and plants (Table 1). As part of the Hippo pathway, NDR Kinases have an important function in the regulation of growth and organ size across tissues and species (Ma et al., 2019). In mammals, NDR1/2 and LATS1/2, together with their upstream activators mammalian sterile 20-like kinases (MST) 1 and 2 form the core cascade of the Hippo pathway (Chan et al., 2005; Hergovich et al., 2006; Praskova et al., 2008; Du et al., 2015; Tang et al., 2015; Gundogdu and Hergovich, 2016; Liu et al., 2016; Kurz et al., 2018). Activated LATS1/2 and NDR1/2 together with their co-activator MPS1-binder-related (MOB)-1 can directly phosphorylate the downstream transcription factors Yes-associated-protein (YAP) and WW domain–containing transcription regulator protein 1 (TAZ), leading to their cytosolic retention and degradation (Zhao et al., 2007, 2010; Liu et al., 2010). When unphosphorylated, YAP/TAZ shuttles to the nucleus and binds to the transcriptionally enhanced associate domains (TEAD) causing transcription of its downstream genes. Similarly, in *D. melanogaster*, the NDR1/2 homolog Tricornered (Trc) and LATS1/2 homolog Warts (Wts), are activated by the MST1/2-homolog Hippo and cause downstream phosphorylation and proteasomal degradation of the YAP homolog Yorkie (Yki) (Staley and Irvine, 2012).

The roles of NDR kinases have been extensively characterized across various species, implicating them in the regulation of diverse cellular processes. These kinases play key roles in controlling size, migration, cell cycle, inflammation, cell signaling, proteostasis, transcription, trafficking, apoptosis, and, more recently, have emerged as critical components in neuronal differentiation, plasticity, synaptogenesis, and cognition (Zallen et al., 2000; Stork et al., 2004; Demiray et al., 2018; Léger et al., 2018; Madencioglu Kul, 2019; Madencioglu et al., 2021), underscoring their role as important regulators of neuronal biology. On the other hand, numerous studies show how NDR kinases can play a maladaptive role in disease, particularly in cancer and inflammation and evidence points out that they might contribute to neurodegeneration as well (Tacutu et al., 2011). While the precise role of NDR kinases in aging remains to be fully understood, there is ample evidence in the literature that strongly suggests their significance in the biology of aging. Furthermore, despite the increasing research linking NDR kinases to essential processes crucial for survival, and in the brain, that relate to cognition and memory, studies investigating the role of NDR kinases on biological fitness and longevity are still lacking.

TABLE 1 List of known and predicted NDR kinases.

Protein	Gene	Taxonomy
NDR1	*STK38/Stk38*	Mammals
NDR2	*STK38L/Stk38l*	Mammals
LATS1	*LATS1/Lats1*	Mammals
LATS2	*LATS2/Lats2*	Mammals
Trc	*trc*	*D. melanogaster*
Warts	*wts*	*D. melanogaster*
SAX-1	*sax-1*	*C. elegans*
WARTS	*wts-1*	*C. elegans*
CBK1	*CBK1*	*S. cerevisiae*
DBF20	*DBF20*	*S. cerevisiae*
DBF2	*DBF2*	*S. cerevisiae*
orb6	*orb6*	*Schizosaccharomyces pombe*
sid2	*sid2*	*Schizosaccharomyces pombe*
COT1	*cot-1*	*Neurospora crassa*
*CpCot1	*cot1*	*Claviceps purpurea*
*TB3	*TB3*	*Colletotrichum trifolii*
*TBPK50	Unknown	*Trypanosoma brucei*
Ukc1	*ukc1*	*Ustilago maydis*

*Predicted by homology.
NDR1, NDR2, LATS1, and LATS2 are the main mammalian NDR kinases. NDR1/2 is the ortholog of Trc and SAX1, and together they are the homologs of the LATS family of proteins that also includes Warts/WARTS. The evolutionary relationship with the other NDR kinases is still under debate, but it is accepted that CBK1, orb6, Ukc1, COT1 and their protein orthologs constitute the sister group of NDR1/2, SAX-1 and Warts/WARTS, and that DBF2 and DBF20 are the most distantly related kinases (Tamaskovic et al., 2003).

Cellular senescence and chronic inflammation

Perhaps the most widely characterized process, and one of the earliest pieces of evidence that linked NDR kinase function to aging, relates to inflammation. In the first iteration of the Hallmarks of aging, increased inflammation was considered a feature of altered intercellular communication (López-Otín et al., 2013). A more updated understanding of the inflammatory processes that occur during aging "inflammageing" makes it clear that altered communication by increased inflammation is not the only contributor to aging, but rather that there exists chronic inflammation which is the result of many intersecting pathways that integrate altered signals from other hallmarks processes like loss of proteostasis, genomic instability, mitochondrial dysfunction, and others, but particularly from cellular senescence (López-Otín et al., 2023). Mechanistically, the literature suggests that the way

in which NDR kinases participate in inflammation overlaps with the regulation of inflammation through the Senescence-associated-secretory phenotype (SASP), hence, in this review, we address these two hallmarks in the same chapter.

Cellular senescence was first described as a replicative limit that most eukaryotic cell types can acquire irreversibly. Further research thoroughly demonstrated that senescence is a response to several signals, often related to stress, such as the shortening of the telomeres and accumulation of DNA damage after many replication cycles (Funayama and Ishikawa, 2007). Although the phenotype varies from cell to cell, some commonalities can be found among senescent cells. One of the main characteristics is that cells undergo a permanent cell cycle arrest mainly in the G_1/S phase progression, though there is plenty of evidence demonstrating that senescence can also permanently arrest the cells in the G_2/M transition (Chien et al., 2011). Overall, it has been widely demonstrated that prolonged arrest by activation of cell cycle regulators leads to cellular senescence (Alcorta et al., 1996; Stein et al., 1999; Shtutman et al., 2017; Safwan-Zaiter et al., 2022), supporting the idea that pathways that play a role in the regulation of the cell cycle are central to the regulation of aging and lifespan (Dottermusch et al., 2016; Seim et al., 2016; Campos et al., 2018). The other main characteristic is that although replication stops, senescent cells are highly active and acquire a SASP that includes secretion of mainly, but not exclusively, proinflammatory molecules, chemokines proteases and growth factors (Coppé et al., 2010). Cellular senescence, as well as other hallmarks of aging, display antagonistic pleiotropic features, it is considered to have evolved as a mechanism to assist in wound healing, tissue remodeling, and the prevention of malignant cellular transformation; senescent cells accumulate and evade clearance by the immune system through a not-yet-understood mechanism in aging organisms. Consequently, via the SASP, these cells become the primary contributors to chronic tissue inflammation and damage. Even though the regulation of the cell cycle progression and cellular senescence are intrinsically connected, it has been demonstrated that post-mitotic cells such as neurons can also become senescent and contribute to disease progression (Musi et al., 2018; Dehkordi et al., 2021; Herdy et al., 2022). A final but very important feature of senescent cells is that they are highly resistant to apoptosis, which is achieved partially by the upregulation of anti-apoptotic proteins such as B-cell lymphoma 2 (BCL-2) or B-cell-lymphoma-extra large (BCL-xL) (Hu et al., 2022).

NDR kinases regulate the cell cycle progression

The mammalian NDR kinases are known regulators of the cell cycle, which implicates them directly in a key aspect of cellular senescence. *In vitro,* both NDR1 and NDR2 interact with the CyclinD1/CDK4 complex, which drives cell cycle progression. Mechanistically, CyclinD1 has been shown to increase the kinase activity of NDR1/2 by reducing its autoinhibition and promoting the G_1/S cell cycle progression (Du et al., 2013). It is known that in the canonical Hippo pathway, NDR1/2 is activated by phosphorylation in the Thr444/Thr442-residue by the MST1/2 kinases. Moreover, *in vitro* work shows that NDR1/2 can also become phosphorylated by MST3 exclusively in the G_1 phase. This phosphorylation controls the NDR1/2 kinase activity on p21 during the cell cycle, as it was demonstrated that depletion of NDR1/2 increased p21 stability and induced G_1 arrest (Cornils et al., 2011).

The other mammalian NDR kinases, LATS1 and LATS2, have also been found to participate in the cell cycle transition. It was shown that, independently of its kinase activity, LATS1/2 can inhibit human cancer cell proliferation and induce a G_2/M arrest. The mechanism by which this occurs is yet not completely understood, but research suggests that LATS1 and LATS2 act independently in distinct pathways in cell cycle progression. LATS1 binds to Cell division control protein 2 (CDC2) and inhibits the kinase activity of both Cyclin A/CDK1 and Cyclin B/CDK1 protein complexes. On the other hand, LATS2 decreases the kinase activity of the Cyclin B/CDK1 and the Cyclin E/CDK2 complex exclusively. The consequence is that overexpression of LATS1/2 can prevent the G_2/M transition (Yang et al., 2001) and act as a negative regulator of the cell cycle progression. A finding that could seem contradictory was later revealed in a model of replicative senescence of human fibroblasts, which shows an increase in AMP-activated protein kinase 5 activity, and the subsequent phosphorylation of LATS1 at the S464, decreases LATS1 stability. Accordingly, inhibition of LATS1 activity accelerated replicative senescence (Humbert et al., 2010). This suggests that there are several pathways in which LATS1 might exert their role in the regulation of the cell cycle. A strong indication of this comes from the fact that overexpression of AMPK5 did not affect p53 activity, thus it is likely that the p53-p21 axis is not involved in this pathway. Arguably p16, a selective inhibitor of CDK4 and CDK6 kinases, is the most well-characterized CDK inhibitor that participates in the cell cycle arrest of senescent cells, mainly in the G_1/S transition. This is achieved by maintaining the CDK4/6 downstream target, the retinoblastoma protein (pRB) in a hypophosphorylated state (Safwan-Zaiter et al., 2022).

Even in a mouse neuronal cell line, p16 expression has been associated with resistance to apoptosis when cell cycle regulators like Cyclin D1 are overexpressed in terminally differentiated cells (Kranenburg et al., 1996). Besides the inactivation of the pRB, it has been shown that in human fibroblasts, p16 activation leads to an increase of reactive oxygen species (ROS) mediated by a positive feedback loop that involves the downstream activation of the protein kinase C delta and downregulation of LATS1, in a mechanism that irreversibly blocks the cell cycle progression (Takahashi et al., 2006). In this same direction, it was reported that LATS2 participates in the repression of E2F genes in cellular senescence after expression of pRB, particularly from the dimerization partner, RB-like, E2F and multi-vulval class B (DREAM)-repressor complex, and the formation of the senescence-associated histone foci (SAHF) and the increased beta-galactosidase activity, characteristic of senescent cells. Remarkably, it was also found that both *RB*1 and *LATS1* loci are mapped in close proximity to the 13q locus, which is often lost in tumourigenic cell lines and can impair the induction of cell cycle arrest (Tschöp

et al., 2011). Finally, another key piece of evidence that links NDR kinases in the permanent arrest of the cell cycle in senescent cells comes from a series of papers published by Aylon et al., in which they use multiple murine and human cell lines to investigate and describe a pathway that involves the translocation of LATS2 from the centrosomes to the nucleus in the context of mitotic stress, where it binds to Mouse double minute 2 homolog (MDM2), thus increasing p53 stability and transcription of downstream targets such as *CDKN1A* (p21) and *LATS2,* creating a positive feedback loop that helps to maintain the cell cycle arrest (Aylon et al., 2006). Moreover, they showed that LATS2 deficiency allows cells to escape oncogene-induced senescence (OIS) by HRAS (Aylon et al., 2009). The malignant transformation of cells is often linked to intrinsic causes, such as mutations in the DNA, and among them, mutations in *RAS* genes are one of the most aggressive and main risk factors of cancer. Interestingly, the expression of KRAS is sufficient to increase the NDR1 protein levels, and inhibition of NDR1 induces apoptosis and also increases p21 and LATS2 levels, possibly as a compensatory mechanism.

These data together suggest that although NDR kinases might have distinct roles within the pathways, there is a wide overlap of functions. It has also been shown that *NDR2* mRNA levels are increased in pancreatic cancer patients which allows for malignancy of transformed cells (Grant et al., 2017). Although this observation is contradictory to the role of NDR kinases in inducing cell cycle arrest in cellular senescence, it suggests that in cells that escape the cell cycle arrest, NDR kinases might allow for survival and an increase in the malignity of the tumors by hyperactivation of growth and facilitating migration possibly through MOB-mediated pathways and Hippo signaling. For example, it was shown that human MOB2 competes with MOB1 for binding to NDR1/2 as a negative regulator (Kohler et al., 2010) in a model of DNA damage and that independently of NDR1/2, MOB2 promotes survival and the cell cycle progression in human cells through inhibition of p21 and p53 (Gomez et al., 2015). Supporting this idea, it was shown that, unlike MOB1 or MOB2, MOB3 inhibits LATS1/2 signaling within the Hippo pathway and allows for continued proliferation of cells even after OIS (Dutchak et al., 2022), potentially contributing to cancer progression. This is consistent with the observation that LATS2 enforces cell cycle arrest during OIS by engaging with pRB and promoting the silencing of E2F genes (Tschöp et al., 2011). In summary, it is evident that NDR kinases play a significant role in cell cycle regulation through various mechanisms across different species. While their direct involvement in the permanent cell cycle regulation of cellular senescence has not been directly addressed, we suggest that they could be crucial components of the machinery enforcing the cell cycle arrest in senescent cells.

NDR kinases might facilitate resistance to apoptosis in senescent cells

Many studies have examined the complementary and yet contradictory relationship between cellular senescence and apoptosis mechanism during aging. The current consensus in the field is that both mechanisms have evolved as a regulatory process for tissue modeling and to prevent the malignant transformation of cells (Campisi, 2013), thus many of the molecular mechanisms that induce apoptosis, cellular senescence or apoptosis resistance in senescent cells overlap and are governed by the same proteins such as p53, BCL-2 or extracellular-signal-regulated kinases (ERK) signaling (Childs et al., 2014). It has been hypothesized that one main factor that determines whether the cell will enter senescence or apoptosis relates to cellular stress levels. Extreme cellular stress resulting from various factors such as irreversible DNA damage, exposure to UV irradiation, oncogenic activation, or withdrawal of growth factors triggers the intrinsic apoptotic pathway (Visser and Yang, 2010). It has been shown that both human LATS1 and LATS2 participate in parallel but independent apoptosis mechanisms, one in which LATS1 engages p53 independently of BAX which increases caspase 3 activity (Yang et al., 2001), and the other in which LATS2 overexpression downregulates BCL-2 and BCL-xL, resulting in a cascade that increases caspase 9 processing (Ke et al., 2004).

Other additional pathways in which LATS1/2 has been shown to be involved in the intrinsic apoptotic pathway are the upregulation of LATS2 by Checkpoint kinase 1 (CHEK1) upon activation of the DNA Damage Response (DDR) (Aylon et al., 2009), and the activation of the protease OMI/HTRA2 by LATS1, which is required for caspase cascade activation upon mitochondrial permeabilization (Kuninaka et al., 2005). Except for the case of excitotoxicity, aging neurons are highly resistant to stress and apoptosis (Kole et al., 2013), probably as a consequence of some of them becoming senescent (Si et al., 2021). Activating Transcription Factor 4 (ATF4) plays an important role in neuronal apoptosis and it is known that it induces the transcription of the C/EBP homologous protein, which activates the protein p53 Upregulated Modulator of Apoptosis (PUMA) in mouse cortical neurons (Galehdar et al., 2010). Additionally, it was shown both in mouse and human cell lines that EI2F-α promotes the translation of ATF4 and subsequent stabilization of LATS1 which increases cell death after oxidative stress (Rajesh et al., 2016). A downregulation on this pathway has yet to be demonstrated as a possible link between NDR kinases and the resistance of apoptosis in aging neurons.

NDR kinases might participate in the regulation of inflammatory cytokines of the SASP

SASP is a senescence state characterized by the secretion of a diverse array of molecules, ranging from pro-inflammatory cytokines to growth factors. While research on neuronal SASP is limited, compelling *in vitro* evidence from rat primary neurons suggests that senescent neurons also undergo SASP, a process driven by the transcription factor GATA Binding Protein 4 (GATA4) and impaired autophagic flux (Moreno-Blas et al., 2019). The potential involvement of NDR kinases in the regulation and secretion of SASP remains largely unexplored. However, NDR kinases have been associated with the regulation of established SASP components, such as Tumor necrosis factor-alpha (TNF-α) which has been implicated in the heightened neuroinflammatory response and cognitive impairment during aging (Habbas et al.,

2015; Probert, 2015). It has also been shown that murine NDR1 positively regulates the production of TNF-α and Interleukin 6 (IL-6) by directly binding to Smad ubiquitination regulatory factor 1 (SMURF 1) which leads to ubiquitination and degradation of mitogen-activated protein kinase 2 (MEKK2) and reducing the transcription of its downstream targets (Wen et al., 2015). Besides NDR2, another study reported that NDR1 activity also increases TNF-α dependent activation of the transcription factor nuclear factor "kappa-light-chain-enhancer" of activated B-cells (NF-κB) in various human tumor cell lines (Shi et al., 2012), supporting the important role of NDR1/2 in the regulation of TNF-α activity. Interestingly, Braitsch et al. (2019) found an opposing role for LATS1/2 in NF-κB regulation and reported that *LATS1/2* KO increases NFκB activation and *vanin1* expression, which favors epithelial-mesenchymal transition. NFκB is one of the main transcription factors that accumulate in the chromatin of senescent cells and controls the expression of SASP genes (Chien et al., 2011; Freund et al., 2011), suggesting an important link between NDR kinases and the control of the SASP.

In summary, NDR kinases serve as crucial regulators of the cell cycle. While not directly addressed, the existing literature strongly points out their involvement in enforcing cell cycle arrest in senescent cells. When this effect is circumvented, the expression of NDR kinases can have deleterious consequences, aiding cells in survival and migration, particularly through their role in the Hippo pathway. Additionally, it is plausible that NDR kinases participate in the pathways dictating whether a cell enters senescence or undergoes apoptosis and eventually providing senescent cells with resistance to apoptosis. A maladaptive feature of this role is that increased NDR expression is often observed in transformed cells due to its pro-survival effect, facilitating tumor progression and malignancy. Finally, it is well-known that mechanistically, NDR kinases can participate in the increased inflammatory activity during aging, and possibly in the control of SASP. As documented in the previous literature, functions of NDR1/2 and LATS1/2 have been associated with contradictory roles, which is compounded by a general lack of insight into their essential role as regulators of aging, a point that is highlighted throughout this review.

Nutrient signaling

Some of the most evolutionarily conserved pathways across species are associated with how cells perceive the presence or absence of nutrients and regulate intracellular metabolism. These pathways collectively have profound connections with the regulation of lifespan and are notably recognized for their extensive crosstalk among the hallmarks of aging. Among these, four major pathways have been extensively investigated: the Insulin and Insulin growth factor 1 signaling (IIS) pathway, the mammalian target of rapamycin (mTOR) pathway, the AMPK pathway (Stallone et al., 2019), and, notably in the brain, the sirtuin (SIRT) signaling. Importantly, NDR kinases emerge as a significant upstream regulator of nutrient sensing mechanisms, given the growing body of research that demonstrated their significant roles across all four major pathways. Moreover, there is also evidence in the literature which shows that NDR kinases interact with known anti-aging proteins that also exercise their function within the nutrient signaling pathways like Klotho and SIRT1. In the following chapter, the known molecular interactions of NDR within the four nutrient-sensing pathways are summarized.

NDR kinases participate in AMPK-signaling

There is enough evidence in the literature that links NDR kinases to AMPK signaling, which is required for the proper function of AMPK signaling, one of the main pathways that cells have to respond to nutrient deprivation. Moreover, NDR activity within the pathway has also been shown to play a maladaptive role, particularly by promoting age-related diseases such as metabolic syndrome. Besides nutrient sensing, activation of the AMPK pathway with metformin prolongs lifespan across species (Novelle et al., 2016), counteracts the development of neurodegenerative diseases (Rotermund et al., 2018) and in middle-aged mice improves cognitive performance by increasing autophagy of the hippocampus (Kodali et al., 2021). Additionally, clinical studies suggest that metformin treatment inhibits memory loss in diabetic adults (Ng et al., 2014). *In vitro,* evidence shows that the activation of the AMPK pathway by nutrient starvation, metformin treatment, or its more potent analog phenformin increases the phosphorylation and degradation of the NDR kinase downstream target YAP, either by direct phosphorylation of YAP on its Ser-94 residue and thus disruption of its interactions with TEAD or indirectly through increase of LATS1/2 activity (DeRan et al., 2014; Mo et al., 2015). In this line, it was also reported that silencing of LATS1/2 is sufficient to ablate the effect of energy stressors on AMPK-dependent YAP phosphorylation (DeRan et al., 2014). Interestingly LATS1/2 is not always essential for the activation of YAP via AMPK signaling since it was shown that AMPK can inhibit the oncogenic transformation of LATS-null mouse embryonic fibroblasts by directly inhibiting YAP activity (Mo et al., 2015).

Similarly, in *Drosophila melanogaster* larval central brain and ventral nerve cord, it has been shown that AMPK together with the AMPK upstream regulator liver kinase B1 (Lkb1), can inactivate Yki independent of the NDR Kinases (Gailite et al., 2015). AMPK signaling also seems to play a role in the shuttling of human YAP. A signaling cascade that involves AMPK, LK1B and LATS1/2, promotes the interaction of YAP with the WNT signaling protein Disheveled, and its eventual nuclear export (Lee et al., 2018). The mechanism involves the activation of AMPK, the downstream increase of SCRIB (Liu et al., 2020), Angiomiotin-like protein 1 and 2 (AMOTL1/2) and Angiomotin (AMOT) (DeRan et al., 2014) protein levels, which are involved in LATS1/2 stabilization and therefore AMPK-dependent YAP degradation. Furthermore, another study showed that Klotho$^{\pm}$ mice, a widely used knockout mouse model in aging research that displays extremely short life span and premature aging (Kuro-o et al., 1997) display a weaker AMPK-LATS1 interaction as well as decreased AMPK-dependent phosphorylation of YAP (Luo et al., 2023). Although the exact mechanism has not been described yet, these data suggest that there is a direct interaction between AMPK and LATS1 which might be facilitated by the anti-aging protein Klotho.

The other mammalian NDR kinases have also been linked to AMPK signaling. Overexpression of NDR1 in mice

decreases AMPK and the downstream Acetyl-CoA-carboxylase phosphorylation, which leads to enhanced *de novo* lipogenesis and increased incidence of non-alcoholic fatty liver diseases (NAFLD). In accordance, NDR1 overexpression alone is sufficient to cause NAFLD and increase inflammation in the liver under a regular diet. Interestingly, NDR1 exhibits a deleterious effect on the disease. A liver-specific KO of *Stk38* ameliorated high-fat-died (HFD) induced insulin resistance, hepatic inflammation, and lipid accumulation, as well as can reduce the cholesterol and triacylglycerol (TAG) levels (Rawat et al., 2023), which are major indicators of metabolic syndrome. Moreover, besides a systemic effect, NAFLD has been linked to reduced cognitive functions in adults (Bertolotti, 2014; Seo et al., 2016; Takahashi et al., 2017; Weinstein et al., 2018, 2019) and in mice, HFD has been shown to impair amygdala and hippocampus-dependent memory consolidation and cause neuroinflammation during aging (Spencer et al., 2017). Additionally changes in cholesterol as well as TAG levels have been linked to the neuronal aging process and the etiology of various age-related diseases including Alzheimer's (AD), Parkinson's (PD) and Huntington's disease (Spitler and Davies, 2020; Nunes et al., 2022). It has been extensively demonstrated that the responsiveness of rodent AMPK to nutrient deprivation decreases during aging (Salminen and Kaarniranta, 2012). Based on previous studies demonstrating the significant interactions of AMPK and NDR signaling, we suggest that the age-related reduction of AMPK signaling might involve a decreased downstream inhibition of YAP by NDR-kinases and increased lipid accumulation and higher incidence of NAFLD observed during aging.

NDR kinases display extensive crosstalk with mTOR signaling

The complex intercommunication between mTOR signaling and NDR kinases has been intensively studied both in Drosophila and in mammals. The first study that linked NDR-Kinases to mTOR showed that *Drosophila* salivary gland-specific KO of *wts* leads to decreased cell death, caspase activity and autophagy, while the expression of a dominant negative form of *Drosophila* Tor, abolished the effect of the *wts* KO (Dutta and Baehrecke, 2008). Furthermore, a substantial body of evidence indicates a two-way communication between NDR kinases and TOR signaling, with particular relevance for neuronal function.

In *Drosophila* Trc phosphorylation at T449 was shown to be dependent on TorC2 in class IV sensory neurons and required for the regulation of dendritic tilting (Koike-Kumagai et al., 2009). Along those lines, it is known that semaphorins promote neuronal substance adhesion in *Drosophila* by blocking dendrite crossing in a signaling cascade that involves the semaphorin receptor Sema-2B, TorC2, the β-integrin-subunit myospheroid (Mys), and Trc (Meltzer et al., 2016). Additionally, *trc* KO displays increased synaptic boutons number in the neuromuscular junction (NMJ), and a decrease in Yki phosphorylation therefore increasing Yki-dependent transcription of the Wiskott-Aldrich Syndrome Protein (Wasp) (Natarajan et al., 2015). It is well-known that Wasp regulates the synapse development in the neuromuscular juntion (Coyle et al., 2004; Khuong et al., 2010; Nahm et al., 2010)through actin polymerization (Stradal et al., 2004), hence a model was proposed where Trc acts downstream of TorC2 and regulates Wasp levels and modulates actin polymerization and synapse formation (Natarajan et al., 2015). In that regard, an accumulation of filamentous actin (F-actin) in the *Drosophila* brain has recently been suggested to occur during aging and disruption of actin polymerization in aged animals rescues autophagy levels, restores the youthful neuronal cell phenotype, and slows brain aging (Schmid et al., 2023). Besides their role as essential regulators of development in mammals (Kramer et al., 2022), the *Drosophila* Wasp homolog has been implicated in the increase of neuronal F-actin during aging in the brain, which suggests that their activity could be related to the pathological loss of proteostasis and deregulated nutrient sensing.

Another interesting role of NDR kinases in mTOR signaling is that NDR1 has been shown to increase mTOR-Complex 1 (mTORC1) activity and Rabin8 phosphorylation, leading to autophagy inhibition (Amagai et al., 2015), while on the other hand, LATS2 participates in the suppression of mTORC1 activity (Gan et al., 2020), which is implicated in pancreatic β-cell apoptosis and autophagic cell death under diabetic conditions. Additionally, the same study found that *Lats2* KO rescues high fat-died induced phosphorylation of the ribosomal S6 protein and p62 accumulation, which stems from increased mTORC1 signaling and impaired autophagic flux, respectively. Besides mediating autophagy-dependent effects under diabetic conditions, LATS2 is also colocalized with autophagosomes and accumulates upon treatment with bafilomycin or chloroquine, which are commonly used inhibitors of lysosomal function, suggesting that LATS2 is degraded by the autophagosome-lysosomal machinery (Yuan et al., 2021). Although not fully characterized, these data suggest an evolutionary conserved regulatory axis of NDR kinases by Tor/mTOR that participates in neuronal function and disease.

NDR kinases in insulin signaling

The IIS is one of the major nutritional signaling pathways and has been thoroughly implicated in lifespan control, aging and age-related pathologies across several species (Altintas et al., 2016; Mathew et al., 2017; Zia et al., 2021). The canonical activation of IIS commences with the binding of either insulin or IGF1 to the insulin receptor, leading to autophosphorylation of its cytoplasmic tyrosine residues. Subsequently, adapter proteins such as Insulin-receptor-substrates (IRS) bind to the phosphorylated residues, initiating the activation of the Phosphoinositide 3-kinases (PI3K), Protein kinases B (PKB/AKT, hereafter referred to as AKT), and mTOR cascade which results in the downregulation of forkhead box O (FOXO) transcription factors. This constitutes one of the best-defined regulatory networks central to the control of lifespan and longevity (Wang et al., 2014; Webb and Brunet, 2014; Klotz et al., 2015; Martins et al., 2016). The IIS has been shown to play a neuroprotective role during mammalian brain aging, and low levels of IGF1 are linked to several age-related diseases (Zia et al., 2021).

Within this regulatory axis, the activation of AKT has been demonstrated to reduce MST1 and LATS1 activity. Similarly,

inhibition of the PI3K-AKT pathway leads to an increase in MST1 and LATS1 phosphorylation that enforces cytosolic localization and degradation of YAP. Intriguingly, in a non-phosphorylated state, YAP remains in the nucleus and downregulates the phosphatase and tensin homolog (PTEN), a negative regulator of the PI3K-AKT pathway. This intricate interplay forms a positive feedback loop that illustrates the complex and nuanced regulation within this signaling network (Qian et al., 2021). AKT activation and its downstream effect on NDR-Kinases seem to be dependent on the DNA-double-strand-break-repairing protein DNA-dependent protein kinase, catalytic subunit (DNA-PKcs), as suggested by experiments in human glioblastoma cell lines. Inhibition of DNA-PKcs decreases AKT phosphorylation at its S473 residue and NDR1 activation upon glucose deprivation. Additionally, AKT and DNA-PKcs-dependent activation of MST1 in these conditions increases phosphorylation of NDR1 at S281 and T282 (Shiga et al., 2020). Supporting the role of NDR kinases in enforcing a positive feedback loop on AKT signaling, adenoviral overexpression of NDR1 in mice was shown to reduce the activation of AKT by phosphorylation at S473 and T308. This resulted in impairment in glucose-dependent Insulin signaling and increased inflammation, demonstrated by higher levels of Interleukin-6 and TNF- α (Rawat et al., 2023).

Even though it has not been demonstrated yet, this could mean that an increase or impairment in the function of NDR kinases during aging might have a maladaptive role which promotes the age-related loss of cognitive function through an increase in ISS.

NDR2 kinases and Sirtuins

Sirtuins are nicotinamide adenine dinucleotide (NAD^+) dependent protein deacetylases that have been thoroughly implicated in the regulation of aging and lifespan. It has been demonstrated in models ranging from *C. elegans* to humans that SIRT1 function and protein levels decrease with age and that overexpressing or reconstituting SIRT1 function can increase lifespan and delay aging (Satoh et al., 2013; Kilic et al., 2015). Moreover, the age-related alteration of autophagy has been linked to a decrease in SIRT1 (Xu et al., 2020), and the other way around, SIRT1 plays an essential role in the regulation of mammalian autophagy through the regulation of several key steps of the autophagic pathway (Kitada et al., 2016). In the brain, SIRT1 is predominantly expressed in neurons within the hippocampus and plays a crucial role in memory and plasticity (Michán et al., 2010). In human cell lines, it was shown that the acetyltransferases p300 and CREB-Binding Protein (CBP) can specifically acetylate NDR2 at K463, while SIRT1 is the major deacetylate of NDR2 (Tang and Yu, 2019). A similar study showed that LATS1 is also under the regulation of Sirtuins. Like NDR2, LATS1 can be acetylated by p300, but deacetylation takes place by distinct Sirtuins, namely SIRT3 and SIRT4 (Yang S. et al., 2022). Further, SIRT7 deacetylates the DNA damage-binding protein 1 (DDB1), which under acetylated conditions is involved in ubiquitination and degradation of LATS1 (Mo et al., 2017). While the evidence linking NDR kinases to Sirtuins is still limited, it underscores an entirely novel regulatory mechanism of NDR kinases that positions them within the central regulatory network of lifespan and longevity.

Other functions of NDR-kinases in nutrient signaling

Lastly, in human tumor cells with high glucose uptake, the O-GlcNAc transferase (OGT) has been shown to O-GlcNacylate YAP and disrupt its interaction with LATS, decreasing YAP-phosphorylation and degradation, therefore increasing YAP-dependent transcription in an AMPK-independent manner. Interestingly OGT is under YAP-dependent transcription, forming another feedback loop with the involvement of NDR-kinases in nutrient signaling pathways (Peng et al., 2017).

One consequence of the increased metabolic activity of senescent cells is elevated glycogenesis through a mechanism that involves the activation of glycogen synthase, downregulation of Glycogen synthase kinase 3 beta (GSK-3β) and an increase in reactive oxygen species (ROS) (Seo et al., 2008). It has been shown that GSK-3 β signaling is altered also in the murine brain during aging, particularly in the hippocampus (Drulis-Fajdasz et al., 2018). Interestingly, *in vitro* it has been shown that GSK-3β also inhibits NDR1 activation, emphasizing the protective role of NDR1 in preventing cell death under increased oxidative stress (Enomoto et al., 2012). Similarly, in human melanoma cells, LATS1 has also been implicated in the regulation of ROS, and *LATS1* knockdown results in increased oxidative stress (Kazimierczak et al., 2021).

Loss of proteostasis and disabled macroautophagy

A balance between protein synthesis and degradation is fundamental for the cell's functional integrity, a concept encapsulated in the term "proteostasis". Proteostasis represents the intricate regulatory mechanisms that ensure the proper handling of proteins within a cellular environment. This equilibrium involves the coordinated orchestration of protein synthesis by the ribosomal machinery, folding and transport assisted by chaperones, and eventual degradation mainly by the proteasome and the lysosomal pathway (Mizushima et al., 2008; Hartl et al., 2011; Koga et al., 2011). Maintaining proteostasis is essential for cellular health, and disruptions in this delicate balance are at the core of several diseases such as myopathy, metabolic disorders, cardiovascular disease, ataxia, cataracts or persistent nephrotic syndrome. The importance of proteostasis becomes even more evident during aging and in neurodegenerative disorders, like AD, PD or amyotrophic lateral sclerosis (ALS) which are characterized by the accumulation of misfolded proteins (Labbadia and Morimoto, 2015). Autophagy involves a series of networks that ensure the delivery and degradation of biomolecules and organelles through the lysosome and is one of the main mechanisms that controls proteostasis which is prone to be altered during aging. Macroautophagy is the most well-characterized form of autophagy and since the original paper by López-Otín et al. (2023) postulated its decline as an aging hallmark a decade ago, disruption in macroautophagy has drawn great attention as a main contributor to aging and disease, that now it is considered to be a hallmark of its own, given that macroautophagy participates not only in proteolysis, but also in cell-to-cell communication, antigen presentation, cell growth,

nutrient sensing, and many more (Nieto-Torres, 2021; Münz, 2022; Piletic et al., 2023). Here we summarize the role of NDR kinases both in the regulation of autophagy and proteostasis, highlighting how their maladaptive function during aging promotes disease, leaving the involvement in other features related to autophagy for the following chapters.

NDR kinases positively regulate autophagy

NDR kinases seem to play a major role in the regulation of (macro) autophagy. Some early evidence pointed out that a loss-of-function mutation of Wts impaired autophagy and contributed to tissue degeneration. Interestingly, overexpression of the downstream effectors of Wts, Yki and scalloped (Sd), failed to rescue the effect, and that the activation of PI3K-Akt-Tor-pathway was essential for the phenotype in mutant flies (Dutta and Baehrecke, 2008), which indicated that Wts participated in autophagy regulation independently of the core Hippo signaling, through Tor signaling. Wts also plays a crucial role in autophagy-mediated cholesterol trafficking and subsequent steroid production in *Drosophila*. Yki-dependent transcription of the miRNA bantam enhances Tor activation and inhibits ecdysone receptor signaling, a potent inducer of autophagy in *Drosophila*. This process results in diminished mobilization and trafficking of cholesterol (Texada et al., 2019). In mammals, NDR1/2 enhances the inhibitory impact of the guanine nucleotide-exchange factor Rabin8 on autophagy. This effect was shown to be independent of Rabin8ʹs guanine-exchange-factor activity toward its downstream target RAB8 or others like SEC15 and Mammalian TRAPPII-specific subunit 130 (mTRS130) (Amagai et al., 2015). In the same study, it was observed that the silencing of NDR1/2 leads to a reduction in mTORC1 activity, but silencing Rabin8 did not have an impact on it. These observations suggest that besides Rabin8, additional mechanisms through which NDR1/2 inhibits autophagy exist, for instance by activating mTORC1 (Coyle et al., 2004; Joffre et al., 2015).

More direct recent evidence supporting the pleiotropic role of NDR kinases in the regulation of autophagy is that NDR1 interacts with BECLIN1 and other proteins that are part of the same complex required for early autophagosome formation, and silencing NDR1 in human cell lines or its homolog Trc in *Drosophila* impaired autophagy (Joffre et al., 2015). Interestingly, NDR1 has been demonstrated to phosphorylate the nuclear exit protein exportin1 (XPO1) at S1055, thereby influencing the nuclear exit of BECLIN1, YAP and itself (Martin et al., 2019). This discovery showcases the idea that the NDR family of kinases have multiple and sometimes opposing roles, in this case, in the regulation of autophagy. A different mechanism has been proposed for the role of NDR2 in autophagy. Under conditions of nutrient starvation, the E3-ubiquitin ligase Tripartite Motif Containing 27 (TRIM27) ubiquitinates NDR2 at L6 and L11 which enhances NDR2 activity, resulting in the downstream phosphorylation of Unc-51-like kinase 1 (ULK1) at S495. Notably, this ULK1 phosphorylation leads to increased binding of ULK1 to TRIM27 and ULK1 polyubiquitination. Consequently, this polyubiquitination promotes the enhanced proteasomal turnover of ULK1, suggesting an inhibitory role for NDR2 in autophagy initiation. Intriguingly, the frequent presence of TRIM27 overexpression in breast cancer (BC) patients is associated with tumorigenesis, potentially through the inhibition of ULK1-mediated autophagy (Yang Y. et al., 2022).

Due to its high level of similitude, it is usually assumed that NDR1 and NDR2 have complementary and sometimes overlapping functions. A notable exception is in the CNS, as it has been suggested that NDR1 expression decreases postnatally and that NDR2 is the main functional kinase of them in the adult rodent brain (Zallen et al., 2000). Recently, a double KO of *Stk38* and *Stk38l* in mice has been linked to neurodegeneration in both adult and prenatal mice. This neurodegeneration is associated with impaired autophagy and the mechanism appears to involve the absence of NDR1/2-dependent phosphorylation of the endocytosis protein RAPH1. This deficiency leads to impaired endocytosis of the autophagy protein Autophagy-related protein (ATG) 9A at the presynapse, subsequently resulting in reduced axonal trafficking (Roșianu et al., 2023). Lastly, one notable interaction of NDR kinases and autophagy is that of the *Drosophila* Trc with Atg8 (Tsapras et al., 2022), which is the homolog of the Microtubule-associated proteins 1A/1B light chain 3 (LC3A/B). Although this interaction has not been described in mammals so far, it indicates that the NDR kinases are tightly associated with the regulation of autophagy and have to be considered one of the main regulators of macroautophagy. With respect to other types of autophagy, it is known that NDR1 is needed for mitochondrial clearance through mitophagy upon Extracellular matrix (ECM) detachment of Ras-transformed cells. NDR1 also participates in chaperone-assisted selective autophagy (CASA), a type of chaperone-mediated autophagy (Carra et al., 2008; Gamerdinger et al., 2009; Arndt et al., 2010; Klimek et al., 2017), by binding and inhibiting the function of the cochaperone BCL-2-associated athanogene 3 (BAG3) (Klimek et al., 2019) in tension-dependent degradation of filamins (Arndt et al., 2005, 2010). It is important to note that BAG3-mediated protein clearance is critical for the disposal of proteins associated with neurodegeneration like the AD-related protein TAU (Ji et al., 2019), Huntingtin (Klimek et al., 2017) and ALS-related Superoxide dismutase 1 (SOD1) (Crippa et al., 2010; Gamerdinger et al., 2011). This function of NDR kinases is already being explored for the treatment of age-related diseases. For instance, activating LATS1 in mice, either through the use of the traditional Chinese medicine compound Paris saponin VII or Long non-coding RNAs (lncRNAs) like RP1-59D14.5, can effectively reduce the growth of BC or prostate cancer cells in mice. This reduction is attributed to the induction of autophagy in breast and prostate cancer cells, respectively (Xiang et al., 2022; Zhong et al., 2022). Finally, the extract of the plant *Radix scrophulariae* has recently been shown to inhibit thyroid growth in a rat-hyperthyroidism model, through MST-LATS1-dependent autophagy activation (Zhang et al., 2023).

NDR kinases participate in correct protein folding

NDR kinases also seem to participate in protein folding by interacting with the chaperone HSP (Heat shock protein) 90, which is one of the two main chaperones involved in

maintaining proteostasis through the regulation of protein folding and stabilization, particularly in the CNS. *In vitro work* shows, that when HSP90 is inhibited, there is a notable decrease in the levels and activity of LATS1/2 (Huntoon et al., 2010) and NDR1 (Enomoto et al., 2013). From a mechanistic standpoint, it has been proposed that the HSP90 isoform HSP90β plays a role in inhibiting the proteasomal degradation of LATS mediated by SMURF1 (Qu et al., 2023). Furthermore, the build-up of methylglyoxal (MG) in tumor cells results in increased glycation of HSP90. This glycation, in turn, disrupts the interaction between HSP90 and LATS1, causing impairments in Hippo signaling. Consequently, this disruption is associated with heightened cellular growth and an increased potential for metastasis (Nokin et al., 2016). HSP90 also plays a crucial role in the disassociation and reactivation of LATS2 protein aggregates that form during heat shock. These aggregates, in turn, induce protein-phosphatase-1-dependent dephosphorylation of LATS2, highlighting the indispensable function of HSP90 in the dynamic regulation of LATS2 in response to protein stress (Jiang et al., 2021). It is also worth noting that in yeast, the LATS1/2 homolog CBK1 has been demonstrated to modulate HSP70 and inhibit the nuclear toxicity associated with huntingtin protein aggregates (Wolfe et al., 2014). Mirroring this pro-survival mechanism, HSP70 in mammals can form a complex with BAG3 that regulates the early aggresome formation in response to the accumulation of abnormal polypeptides in a LATS1-dependent manner (Meriin et al., 2018).

In summary, it is evident that NDR kinases play a crucial role in regulating proteostasis, specifically in governing protein stability through interaction with HSP90 or HSP70, and also the eventual protein degradation through autophagy. These kinases contribute to various points in the autophagic pathway, and it is crucial to underscore that their global impact on autophagy is highly complex; depending on the specific level of the pathway at which they participate, the distinct stress conditions inducing autophagy, and the particular cell type involved. Remarkably, their importance is especially evident in neuronal proteostasis, and the disturbance of NDR kinases during aging could potentially signify a previously unrecognized aspect of age-related neurodegenerative diseases. Finally, considering the crucial role of autophagy in memory maintenance during aging (Glatigny et al., 2019), this dysregulation may contribute to cognitive decline and needs to be further explored.

Mitochondrial dysfunction

For nearly 80 years, researchers have theorized that mitochondria play a critical role in the regulation of lifespan, dating back to the proposal of the mitochondrial theory of aging. Even though it is considered an outdated theory, it is clear that mitochondrial function plays a very important role in the regulation of lifespan and aging, not only by producing free radicals that damage cells over time but by impairing energy metabolism, homeostasis, creating oxidative stress and dysregulating apoptosis (Lima et al., 2022). NDR kinases also seem to have a pivotal role in mitochondrial biology, particularly in mitochondrial quality control (MQC), which is a system that involves the activation of several signaling pathways that ensure mitochondrial homeostasis. One of the main functions of the MQC is the clearance of damaged mitochondria through mitophagy and mitochondrial biogenesis through the transcription of mitochondrial genes. The PTEN-induced kinase 1 (PINK1)/PARKIN signaling pathways is one of the main effectors of MQC. It was shown that in *Drosophila* upon mitochondrial damage by increased ROS production through rotenone administration, Pink1 promotes the localization of Trc to mitochondria by the phosphorylation at the T453 in a Torc2-dependent manner, and by increasing the Trc phosphorylation at S292 via an unidentified signaling pathway (Wu et al., 2013). The mechanism by which the NDR kinases might be involved in mitochondrial clearance was explored further and it was demonstrated that phosphorylated Trc in the mitochondria interacts with Atg1, ortholog of mammalian ULK1/2, the mitochondrial transporter protein Miro and leads to Parkin phosphorylation which promotes the activation of pathways involved in MQC. Moreover, the mammalian ortholog NDR1 also localizes to the outer membrane of mitochondria and *Stk38* knockdown leads to the accumulation of damaged mitochondria due to dysfunctional PINK1/PARKIN pathway (Wu et al., 2013). Another study demonstrated that the mechanism behind the accumulation of damaged mitochondria in *Stk38* KO cells involves PINK1/PARKIN mediated mitophagy and NDR1 deficiency decreases the cell survival of the transformed cells after ECM detachment (Bettoun et al., 2016), hinting that a common maladaptive feature of NDR kinases is tumor metastasis. In neurons, a potential role of NDR1/2 in MQC has been implicated by the finding that murine neurons lacking NDR1/2 display fragmented and rounded mitochondria (Roșianu et al., 2023), a mitochondrial phenotype also observed in neurodegenerative conditions (Su et al., 2010). Interestingly, yeast of the species *Neurospora crassa* with mutations in COT-1 exhibit a higher prevalence of mitochondria with irregular shapes (Gorovits et al., 2000), suggesting an evolutionarily conserved feature of NDR kinases in mitochondrial biology.

Even though NDR kinases have been linked directly to the regulation of MQC through one of the most important pathways involving PINK1/PARKIN, direct evidence is still missing that demonstrates the role of this family of kinases in energy metabolism, oxidative phosphorylation and related processes that are a consequence of mitochondrial activity. Some indirect evidence comes from observations related to the other mammalian NDR kinases LATS1 and LATS2. Cells that are actively dividing rely on glutamine as a metabolic source to support the building of molecules needed for growth and to replenish the carbon pool within the mitochondria. Increased ROS production after glutaminolysis inhibition activates RAS homolog family member A (RhoA), which suppresses LATS1 phosphorylation. This event prevents the phosphorylation of YAP1 resulting in its nuclear transport and transcription of downstream targets such as Sestrin 2, which leads to suppression of mTORC1 and activates survival mechanisms such as autophagy (Kim et al., 2023). Another pathway involves SMAC (second mitochondria-derived activator of caspases), where LATS1 interacts with SMAC and promotes the ubiquitination of apoptosis inhibitor proteins such as X-linked inhibitor of apoptosis (XIAP) (García-Gutiérrez et al., 2022) that

participate in mitochondrial permeabilization and cytochrome c release (Zhao et al., 2020).

Genomic instability

It is commonly accepted that as organisms age, an interplay of the elevated rate of genetic mutations with the decline in DNA repair efficiency leads to genomic instability (Gorbunova et al., 2007). Accumulation of various DNA damage exposures, both from environmental and endogenous factors such as ROS and replication errors, are the main threats to genomic integrity. Particularly, the brain has a very high oxygen demand and is enriched with copper and iron molecules that actively participate in ROS generation, which results in substantial ROS-mediated oxidative stress on the genome (Singh et al., 2019). Neurons are one of the longest-lived cells in the body and have a high metabolic activity, thus, strongly depend on DNA repair mechanisms to sustain proper genomic function (Reid et al., 2021).

NDR kinases have been shown to regulate key processes that are involved in regulating DNA repair pathways. It has been demonstrated that NDR1 can be activated by hydrogen peroxide, an oxidative agent that can trigger DNA damage, and modulate metabolic pathways involved in oxidative stress response (Enomoto et al., 2012). Double-strand breaks (DSBs) induced by mutagenic agents represent the most deleterious DNA damage. Ataxia-telangiectasia mutated (ATM) is one of the main proteins involved in the orchestration of the DDR, along with the ATM-Rad3-related (ATR) kinases and the ubiquitin-like UFMylation pathway (Fang and Pan, 2019). Importantly, ATM kinases are also implicated in the sustained DDR in senescent cells, suggesting their potential as pharmacological targets for mitigating the effects of aging (Zhao et al., 2020). Notably, both NDR1 and NDR2 harbor binding motifs for Ubiquitin-fold modifier 1 (UFM1), the main effector of UFMylation, and research using human cell lines has shown that NDR1 is recruited to DSBs in response to DNA damage (Qin et al., 2020), and that loss of NDR1 strongly sensitizes the DNA to damage induced by ionizing radiation. Furthermore, it was shown that NDR1-mediated ATM activation is crucial for DNA repair (Qin et al., 2020). A parallel study validated this observation and noted that, although primarily localized in the cytoplasm, NDR1 accumulates in the nucleus following UV irradiation and confirmed that silencing of NDR1 diminishes the activity of ATR-mediated DNA repair (Park et al., 2015). It has also been shown that NDR1 promoter activity can be controlled by specificity protein 1 (SP1) (Enomoto et al., 2013), a transcription factor that is degraded by DNA damage-induced ATM activity (Swift and Azizkhan-Clifford, 2022), which might provide the potential feedback mechanism for the repair machinery. Along with ATM and ATR, the DNA-PKc, are the most important mediators of the complex DDR network (Menolfi and Zha, 2002). It should be noted that DNA-PKc plays a pivotal role in the non-homologous-end-joining (NHEJ) repair mechanism which is the primary pathway for repairing DSBs in non-dividing cells such as neurons (Yue et al., 2020). It has been further demonstrated that NHEJ efficiency decreases in both neurons as well as astrocytes during aging and contributes to genomic instability in rats and mice, respectively (Vyjayanti and Rao, 2006; Vaidya et al., 2014). Interestingly, DNA-PKc has been shown to activate NDR1 in human glioblastoma cells (Shiga et al., 2020). Given that NDR2 is the main NDR kinase in the adult brain, we suggest that NDR2 might play a very important role in maintaining genomic stability in aging neurons that has not been explored up to this date. Along this line, a large-scale analysis of the phospho-proteome after the activation of the DNA damage response revealed that the mouse NDR2 kinase is one of the substrates of DNA-damage-induced ATM/ATR activity (Matsuoka et al., 2007).

Another finding implicates NDR2 in the Ribosomal DNA (rDNA) integrity, which as one of the most active parts of the eukaryotic genome, is highly susceptible to damage during aging (Kasselimi et al., 2022). RASSF1A is one of the main mediators of rDNA repair that is recruited to rDNA breaks and mediates ATM signaling (Tsaridou et al., 2022). Interestingly, it is known that in the context of DDR, RASSF1A recruits LATS1 (Pefani et al., 2014), and furthermore, RASSF1A can interact and inhibit NDR2 in transformed cells (Keller et al., 2019). NHEJ is also crucial to maintain efficient neurogenesis throughout the lifespan and to ensure the seamless integration of adult-born neurons into the circuitry. Previous studies have shown that neurogenesis decreases notably during aging and this impairment is well-linked to the aging-associated cognitive decline (Lupo et al., 2019; Navarro Negredo et al., 2020). Cell cycle checkpoints are crucial for controlling genomic stability during cell division since they ensure the accuracy of the genome and can trigger DNA repair mechanisms in case of genomic instability. As established before, NDR kinases serve critical roles in the cell cycle progression and the physical segregation of chromosomes after replication as a key factor for the cell cycle and genomic integrity. In this context, it is known that human NDR2 is translocated to the centrosomes in mitosis progression and modulating NDR2 expression results in over or under-duplication of centrosomes (Hergovich et al., 2007). *Lats1* KO mice display increased centrosome overduplication, chromosomal misalignment and deficiency in cytokinesis (Yabuta et al., 2013). NDR1 is also implicated in the mitotic spindle formation and its activity is strictly regulated during kinetochore-microtubule interactions (Yan et al., 2015). Lastly, it has been reported that LATS can inhibit MDM2, which is required for p53 regulation in chromosome number maintenance during mitosis (Aylon et al., 2006).

Overall, the NDR kinases seem to be very important contributors to genome stability and are deeply connected to the DDR network mainly by ATM and DNAPKc-dependent pathways. They also participate in genomic stability by regulating the cell cycle, and more directly, in the segregation of the chromosomes. In the context of neuronal aging, cognitive decline in the human brain is notably associated with a significant downregulation of genes related to learning, memory and synaptic plasticity as well as an increase in DNA damage and corresponding reduction of repair mechanisms (Lu et al., 2004). Taken together, further exploration of the NDR kinases in the maintenance of genomic stability with a particular focus on DDR in neuronal aging is a compelling avenue for future research.

Epigenetic alterations

One of the consequences of aging on the genome is loss of epigenetic information over the lifespan due to several mechanisms that include alterations in chromatin remodeling, post-translational modification of histones like H3K56ac, H4K16ac, H3K4me3, H3K9me3, and H3K27me3, DNA methylation patterns and regulation of non-coding RNAs (ncRNAs) across different species (Yang et al., 2023). The exact roles of NDR kinases in epigenetic remodeling are still scarce, however, it was shown that In HeLa Cells LATS2 binds to the Polycomb Repressive Complex 2 (PRC2) and increases its histone-methyltransferase activity through phosphorylation, causing an increase in H3K27me3 (Torigata et al., 2016), emphasizing the role of NDR kinases in the control of the epigenetic architecture. H3K27me3 is a modification that participates in gene silencing and interestingly, age-related decrease of H3K27me3 is regarded as one of the main age-related features of histone modification and has been observed in several animal models and yeast (Wang et al., 2022). Moreover, cells taken from Hutchinson-Gilford Progeria Syndrome (HGPS) patients, characterized by rapid aging, display a similar H3K27me3 decrease (Shumaker et al., 2006). Although an alteration in LATS2-PRC2 interaction during aging has not been experimentally confirmed, this evidence hints that further studies are necessary to explore the role of LATS2 in histone methylation in aging. On the other hand, increased H3K27me3 causes a loss of function in mammalian mesenchymal stem cells and muscle satellite cells during aging (Noer et al., 2009) and has been linked to aging in killifish and mouse brain (Baumgart et al., 2014). Overall, this suggests that the effect of LATS2 through histone-methylation could be complex, species and tissue-specific but might accelerate aging in neuronal tissue.

Altered intracellular communication

The complex function of the nervous system heavily depends on communication between neurons, collaborative support provided by non-neuronal cells and the interaction of neurons and glia with their extracellular environment. During aging, significant alterations of these intercellular communication pathways have been demonstrated, ranging from an aberrant secretion of inflammatory response (Ransohoff, 2016) to alterations in the mechanical properties of the brain (Elkin et al., 2010) such as increased stiffening. There is evidence that hints that as important mediators of the immune response and central players in the mechanosensing via the Hippo pathway, NDR kinases may have maladaptive features that impair brain function during aging.

TNF-α is an upstream ligand of NF-κB signaling for the inflammatory response and has been shown to accumulate during aging (Bruunsgaard, 1999). It has been reported that the deficiency of NDR1 inhibits TNF-α-mediated transcriptional responses (Ma et al., 2017). Notably, TNF-α can activate both NDR1 and NDR2, and silencing of *Stk38* and *Stk38l* significantly reduces TNF-α-mediated cellular effects, including apoptosis (Vichalkovski et al., 2008). Interestingly, *Stk38* KO mice display increased TNF-α and interleukin production, which suggests that NDR kinases are also a limiting factor for inflammation response (Wen et al., 2015). In addition to TNF-α, several other interleukins, such as Interleukin-17 (IL-17) whose receptors exhibit a high expression in the brain (Das Sarma et al., 2009), show a significant increase in the aging murine brain (Porcher et al., 2021). Conversely, while NDR1 facilitates IL-17 signaling by disinhibiting the IL-17 receptors (Ma et al., 2017); NDR2 has been shown to block the IL-17 pathway and silencing of NDR2 enhances IL-17-induced inflammatory response (Vichalkovski et al., 2008). The brain is highly susceptible to blood-circulating cytokines such as Interferon-1 (IFN1), particularly at the choroid plexus which serves as an interface between the periphery and central nervous system. Studies have shown that blocking the exaggerated IFN1 response in aged mouse brains can potentially restore cognitive impairments and neurogenesis defects associated with aging (Baruch et al., 2014). Regarding the other mammalian kinases, LATS1 is a previously recognized important player in the IFN1 response. LATS1 is recruited to IFN1 receptors, undergoes rapid activation upon IFN1 binding, and plays a pivotal role in mediating downstream transcriptional signaling (Zuo et al., 2022). Besides cell-to-cell inflammatory communication, alterations in growth signal transductions such as IGF (Wrigley et al., 2017) and vascular endothelial growth factor (VEGF) (Grunewald et al., 2021) are commonly observed in aging organisms. A study demonstrated that NDR2 is activated following IGF stimulation and that a hyperactive NDR2 mutant can initiate downstream cell survival pathways even in the absence of the IGF ligand (Suzuki et al., 2006). Moreover, it has been reported that in multiple cell lines, LATS1/2 kinase activity is inhibited by VEGF signaling and the PI3K pathway, which is required for the VEGF effects on the modulation of the Hippo pathway (Azad et al., 2018).

NDR kinases control extracellular matrix communication

Several studies have reported that the stiffness of the brain tissue changes throughout aging (Gefen et al., 2003; Sack et al., 2009; Elkin et al., 2010). This altered mechanical signaling from the extracellular space can be sensed via integrin receptors on the membrane and Hippo pathway and consequently triggers cytoskeleton remodeling as a response (Cai et al., 2021). Increased stiffness of brain tissue may cause age-related alterations such as loss of function of progenitor cells over time (Segel et al., 2019) or modulation of neuronal morphology (Si et al., 2023). The relationship between NDR kinases and ECM is tightly conserved across species. The LATS kinase homolog DBF2 in *S. cerevisiae* phosphorylates and activates both chitin synthase CHS2 and CYK3 during cell division. The localization of CYK3 is dependent on DBF2, setting up a mechanism for the direct control of the primary septum remodeling during the cell cycle, which is equivalent to the metazoan ECM (Oh et al., 2012). NDR kinases contribute to these processes both through the Hippo pathway and as critical regulators of integrin-mediated intracellular signaling. In this line, we have previously shown that NDR2 can modulate integrin receptor trafficking and activity in T cells (Waldt et al., 2018) and murine neurons (Rehberg et al., 2014). Furthermore, NDR kinases regulate the arborization of dendrites and axons as well as spine development and synaptic function in mammalian neurons

(Ultanir et al., 2012; Rehberg et al., 2014). We showed that NDR2 controls substrate selectivity by regulating integrin subunit availability in growth cones during neurite growth (Demiray et al., 2018). Notably, integrin receptor regulation is also addressed in aging-associated pathologies, as enhancing integrin signaling holds promise in alleviating impairments in blood-brain barrier integrity in rats (Halder et al., 2023) and promoting cellular regeneration (Rozo et al., 2016; Ojha et al., 2022).

Moreover, functioning as a scaffold, the ECM supports cells, allowing them to perceive external forces and maintain their shape (Hynes, 2009) by transducing mechanical cues from the environment to the cells (Humphrey et al., 2014). Along this line, previous studies revealed a functional link between the ECM mechanotransducer glycoprotein AGRIN and Hippo pathway mediator YAP. AGRIN, as a sensor of ECM stiffness, increases the stability of YAP by the focal adhesion and LRP4/MUSK receptor pathways. AGRIN inhibits the focal adhesion assembly of Hippo pathway proteins by promoting ILK-PAK1 signaling and decreasing MERLIN and LATS1/2 interaction (Chakraborty et al., 2017). AGRIN also plays a role in supporting murine adult hippocampal neurogenesis (Zhang et al., 2019), facilitating synaptogenesis in developmental stages in a rat model of post-exercise stroke (Zhang et al., 2020), maintaining murine adult NMJs (Samuel et al., 2012), and is implicated in the pathogenesis of AD (Donahue et al., 1999; Verbeek et al., 1999). Altogether, NDR kinases could potentially be involved in AGRIN function of the developing and aging brain.

Beyond its mechanical function and role in transduction, ECM serves as a cohesive substrate for cell movement. This adhesive property is critical during cell migration and in processes such as development, wound healing, and regeneration (Rolfe and Grobbelaar, 2012; Kular et al., 2014). Fibronectin (FN), an important member of brain ECM, has a neuroprotective function in axonal regeneration and neurite outgrowth of cortical and hippocampal adult mice neurons (Tonge et al., 2012) and it diminishes during aging in the brain (Wang et al., 2011). Interestingly, it has been shown that FN adhesion increases the accumulation of YAP in the nucleus. Mechanistically, FN activates the focal adhesion kinase (FAK), which negatively regulates LATS1/2 via PI3K signaling. Reduction of LATS1/2 activity leads to YAP nuclear accumulation and transcriptional response in response to FN adhesion (Kim and Gumbiner, 2015). Notably, integrin receptors on the membrane recognize the FN in ECM and their activity can be modulated by NDR2 kinase activity (Rehberg et al., 2014), indicating the potential role of NDR Kinases in the neuroprotective functions of FN. Furthermore, cytoskeleton remodeling is a key downstream target of ECM signals and alterations in cytoskeletal dynamics have been closely associated with aging (Starodubtseva, 2011; Zahn et al., 2011; Lai and Wong, 2020). Along this line, *in vitro* experiments using human cell lines have shown that disturbance of microtubules with nocodazole reduces the activity of LATS1/2, while the disruption of the actin cytoskeleton with latrunculin B activates LATS1/2 (Zhao et al., 2012), implying the involvement of the cytoskeleton in the LATS-dependent regulation of YAP activity.

Taken together, the modulation of immune signaling between cells, regulation of neuronal shape and synaptic signaling, and the transduction of mechanosignalling driven by the extracellular matrix underscore the crucial role of NDR kinases in governing intercellular communication within the brain. However, further studies are necessary to specifically address the role of NDR kinases in the context of age-associated alterations in cellular communication in the nervous system.

Closing remarks

There is abundant evidence supporting the crucial involvement of NDR-Kinases in diverse cellular processes underlying aging. This review summarizes their key roles in a comprehensive way so that it reflects the hallmarks of aging, particularly in cellular senescence, chronic inflammation, deregulated nutrient sensing, loss of proteostasis, impaired macroautophagy, and to a lesser extent, altered intracellular communication, mitochondrial dysfunction, genomic instability, and epigenetic alterations, with an increased focus on neuronal biology (Figure 1).

In summary, NDR kinases seem to be key components of the complex changes observed in senescent cells. They might contribute to the arrest of proliferation, chronic inflammation through the regulation of constituents of the SASP such as TNF-α, IL-6, and NF-κB, and the resistance of senescent cells to apoptosis. Interestingly, NDR1/2 and LATS1/2 often seem to have opposed roles in these processes which shows that understanding the molecular mechanisms that maintain a balance between their activity is a promising target to understand the nuances of the regulatory network in senescent cells. Another avenue that still needs further exploration is their involvement in neuronal senescence, which has only recently gained recognition as a feature of aging neurons. Another consequence is that by modulation of interleukins, IGF, VGEF, integrin signaling or mechanosensing through the ECM, which is sensitive to ECM proteases present in the SASP, NDR kinases could participate in altered intercellular communication during aging. Besides, it is plausible to assume that NDR-Kinases play an important role in age-dependent stem cell exhaustion as essential regulators of cell cycle progression and previously shown players in stem cell function (Mo et al., 2014).

In the context of nutrient sensing, NDR Kinases play an important role in insulin, mTOR, and AMPK signaling. These pathways, including SIRT1, have been demonstrated to be the central metabolic pathways that dictate lifespan and the rate of aging across all eukaryotes. While NDR kinases have a complex intercommunication with mTOR and AMPK signaling that can result in both inhibition or activation of the pathways; increased insulin signaling often leads to activation of NDR kinases. There is a substantial body of evidence that indicates NDR kinases as master regulators of autophagy, supported by their involvement in macroautophagy, CASA, and mitophagy. NDR kinases actively contribute to DNA repair through the orchestration of the DDR and NHEJ in neurons. Together with their functions in chromosomal alignment and maintenance, NDR kinases demonstrate their importance as components of the cellular machinery that maintains genomic stability under stress and replication. There is also some evidence that points out their role in epigenetic regulation, particularly by increasing H3K27me

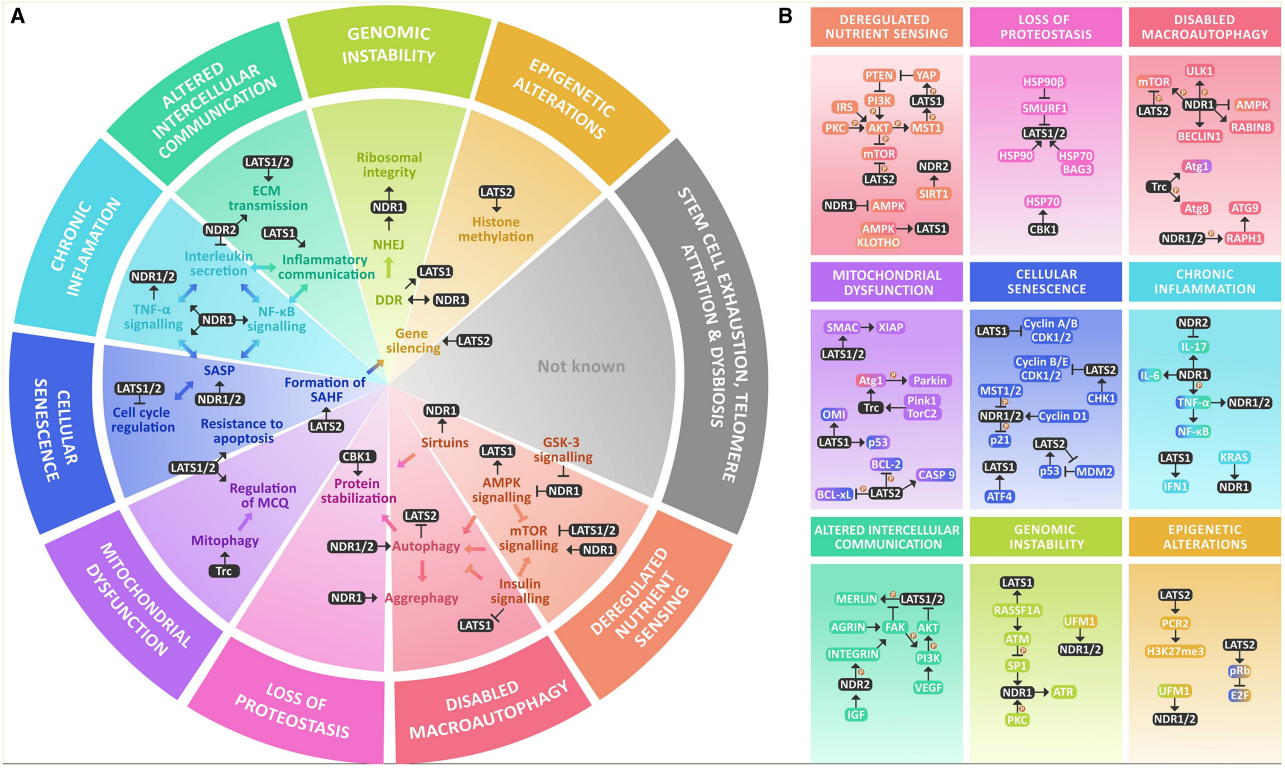

FIGURE 1
NDR kinases within the hallmarks of aging at a glance. **(A)** NDR kinases are involved in various key processes that are altered within the hallmarks of aging. They are known to regulate AMPK and mTOR signaling and are modulated by GSK-3 and Sirtuins. NDR1/2 kinases play a crucial role in regulating autophagy and integrating growth signals from AMPK, mTOR, and insulin signaling. They also participate in protein stabilization through chaperones. In mitochondrial dysfunction, NDR kinases participate in mitophagy and MQC. They have a significant role in inflammation and cellular senescence by participating in the formation of SAHF, regulating the cell cycle, resistance to apoptosis, and increasing inflammation through SASP, TNF-α, NF-κB, and interleukin secretion. NDR kinases also participate in intercellular communication by modulating ECM transmission and regulating inflammatory communication, in genomic instability mainly through NHEJ and DDR, and in epigenetic alterations by gene silencing through histone methylation. However, their roles in stem cell exhaustion, telomere attrition, or dysbiosis are not yet reported. **(B)** NDR kinases participate in nutrient signaling through a complex interplay between the major nutrient sensing pathways: AMPK, mTOR & Insulin signaling, and though the functional outcome is not known yet, they are also deacetylated by SIRT1. For their role in the loss of proteostasis, they participate in protein stability by regulating molecular chaperones like HSP70 and are in turn stabilized by it as well as HSP90. NDR kinases are regulators of macroautophagy (mTOR, ULK1, AMPK, BECLIN1, Atg1, Atg8, and Atg3). Within mitochondrial dysfunction, they are known regulators of MQC and mitophagy by a Pink1/Parkin-dependent mechanism that involves Atg1. NDR kinases participate in cellular senescence by regulating the cell cycle, mainly regulating Cyclin A/B or Cyclin B/E and CDK protein complexes and modulation of E2F through pRB. Additionally, they regulate p21 and p53 signaling. LATS1 is also a downstream target of ATF4. They also provide resistance to apoptosis through the same mechanism and interact with BCL-2, BCL-xL, and BAX in parallel with SMAC and XIAP. They might be involved in regulating SASP and Chronic inflammation, mainly by increasing TNF-α and NF-κB activation and proinflammatory interleukin secretion, mainly IL-6, as well as IFN1For altered intercellular communication, they participate as signal transducers of growth factors like VEGF and IGF. They participate in inflammatory communication through TNF-α, NF-κB, and IL-17 and regulate ECM signaling through activation of the integrins. They might participate in genomic instability by regulating DDR and rDNA integrity by coordinating the response of ATM, ATR, and DNA PKc. Finally, there is evidence that links NDR kinases to the regulation of the epigenome by increasing the methylation of the Polycomb repressive complex 2.

through the methyltransferase activity of PRC2. Although there is no evidence indicating that NDR kinases play a role in the maintenance of telomeres, given their close involvement in DNA biology, the possibility of their involvement cannot be entirely dismissed and warrants further attention. One last hallmark of aging that remains to be addressed is dysbiosis. The paracrine effect that the microbiome exerts over other cells has been explored only in recent years as a mechanism that regulates lifespan and aging, and it isn't surprising that there is no evidence linking NDR kinases to dysbiosis, given there are no prokaryotic analogs of the NDR kinases. The mechanism by which the microbiome regulates lifespan remains poorly understood, therefore an intriguing area of exploration relates to the signals originating from the microbiome and the mechanisms of how cells perceive them. It is known that the primary receptors for microbiome signals are the immune system and the CNS (Zheng et al., 2020; Park and Kim, 2021), both of which have an active participation of NDR kinases. These observations raise the possibility that NDR kinases might participate in the transduction of gut microbiota alterations during aging.

It is evident that NDR kinases have an intricate connection to many of the cellular and molecular processes that are considered to be the cause of aging by our current understanding. The functional outcomes of many of the interactions described in this review are not always clear, with the existence of much contradictory evidence. For instance, while NDR kinases are required for proper cell

function, they also participate in cancer and disease development. They promote cell cycle progression, but in some contexts, they also induce apoptosis and cellular arrest. NDR kinases both seem to activate and inhibit central metabolic cascades or promote and downregulate inflammatory signals. As a final remark, we want to propose that many of the observed contradictions in the literature regarding the function of NDR kinases arise from the fact that they might have evolved having antagonistic pleiotropic functions in aging. The current paradigm of the evolution of aging suggests that aging occurs by the accumulation by natural selection of genes that have antagonistic pleiotropic features that increase fitness during a young age, but that also show maladaptive features during aging, favoring a trade-off between reproduction and lifespan (Chistyakov and Denisenko, 2019). The evidence presented so far indicates that NDR kinases display these classic antagonistic pleiotropic functions that contribute to the loss of fitness during aging. If they are studied within this new perspective, many of the opposite roles that they exhibit can be easily understood, paving the way for further comprehending the interconnectivity that exists among the hallmarks of aging and given their importance in neuronal biology, also understanding more about the mechanisms that lead to age-related loss of cognitive function.

Author contributions

KJ: Data curation, Investigation, Writing – original draft, Conceptualization. MA: Conceptualization, Data curation, Investigation, Supervision, Writing – original draft, Writing – review & editing. YD: Investigation, Writing – original draft, Data curation, Writing – review & editing. AL: Investigation, Writing – original draft. OS: Funding acquisition, Project administration, Resources, Supervision, Validation, Writing – review & editing.

Funding

The author(s) declare financial support was received for the research, authorship, and/or publication of this article. This work was supported by grants from the German Research Foundation (362321501/RTG 2413 SynAGE and STO 488/8 to OS).

Conflict of interest

The authors declare that the research was conducted in the absence of any commercial or financial relationships that could be construed as a potential conflict of interest.

The author(s) declared that they were an editorial board member of Frontiers, at the time of submission. This had no impact on the peer review process and the final decision.

Publisher's note

References

Alcorta, D. A., Xiong, Y., Phelps, D., Hannon, G., Beach, D., and Barrett, J. C. (1996). Involvement of the cyclin-dependent kinase inhibitor p16 (INK4a) in replicative senescence of normal human fibroblasts. *Biochemistry* 93, 13742–13747. doi: 10.1073/pnas.93.24.13742

Altintas, O., Park, S., and Lee, S-., J. V. (2016). The role of insulin/IGF-1 signaling in the longevity of model invertebrates, *C. elegans* and *D. melanogaster*. *BMB Rep.* 49, 81–92. doi: 10.5483/BMBRep.2016.49.2.261

Amagai, Y., Itoh, T., Fukuda, M., and Mizuno, K. (2015). Rabin8 suppresses autophagosome formation independently of its guanine nucleotide-exchange activity towards Rab8. *J. Biochem.* 158, 139–153. doi: 10.1093/jb/mvv032

Arndt, V., Daniel, C., Nastainczyk, W., Alberti, S., and Höhfeld, J. (2005). BAG-2 acts as an inhibitor of the chaperone-associated ubiquitin ligase CHIP. *Mol. Biol. Cell* 16, 5891–5900. doi: 10.1091/mbc.e05-07-0660

Arndt, V., Dick, N., Tawo, R., Dreiseidler, M., Wenzel, D., and Hesse, M. (2010). Chaperone-assisted selective autophagy is essential for muscle maintenance. *Curr. Biol.* 20, 143–148. doi: 10.1016/j.cub.2009.11.022

Aylon, Y., Michael, D., Shmueli, A., Yabuta, N., Nojima, H., and Oren, M. (2006). A positive feedback loop between the p53 and Lats2 tumor suppressors prevents tetraploidization. *Genes Dev.* 20, 2687–2700. doi: 10.1101/gad.1447006

Aylon, Y., Yabuta, N., Besserglick, H., Buganim, Y., Rotter, V., Nojima, H., et al. (2009). Silencing of the lats2 tumor suppressor overrides a p53-dependent oncogenic stress checkpoint and enables mutant H-Ras-driven cell transformation. *Oncogene* 28, 4469–4479. doi: 10.1038/onc.2009.270

Azad, T., van Rensburg, H. J. J., Lightbody, E. D., Neveu, B., Champagne, A., Ghaffari, A., et al. (2018). A LATS biosensor screen identifies VEGFR as a regulator of the Hippo pathway in angiogenesis. *Nat. Commun.* 9:1061. doi: 10.1038/s41467-018-03278-w

Baruch, K., Deczkowska, A., David, E., Castellano, J. M., Miller, O., Kertser, A., et al. (2014). Aging. Aging-induced type I interferon response at the choroid plexus negatively affects brain function. *Science* 346, 89–93. doi: 10.1126/science.1252945

Baumgart, M., Groth, M., Priebe, S., Savino, A., Testa, G., Dix, A., et al. (2014). RNA-seq of the aging brain in the short-lived fish *N. furzeri* - conserved pathways and novel genes associated with neurogenesis. *Aging Cell* 13, 965–974. doi: 10.1111/acel.12257

Bertolotti, M. (2014). Nonalcoholic fatty liver disease and aging: epidemiology to management. *World J. Gastroenterol.* 20:14185. doi: 10.3748/wjg.v20.i39.14185

Bettoun, A., Joffre, C., Zago, G., Surdez, D., Vallerand, D., Gundogdu, R., et al. (2016). Mitochondrial clearance by the STK38 kinase supports oncogenic Ras-induced cell transformation. *Oncotarget* 7, 44142–44160. doi: 10.18632/oncotarget.9875

Braitsch, C. M., Azizoglu, D. B., Htike, Y., Barlow, H. R., Schnell, U., Chaney, C. P., et al. (2019). LATS1/2 suppress NFκB and aberrant EMT initiation to permit pancreatic progenitor differentiation. *PLoS Biol.* 17:e3000382. doi: 10.1371/journal.pbio.3000382

Bruunsgaard, H. (1999). A high plasma concentration of tnf-α is associated with dementia in centenarians. *J. Gerontol. Ser. A Biol. Sci. Med. Sci.* 54, 357–364. doi: 10.1093/gerona/54.7.M357

Cai, X., Wang, K. C., and Meng, Z. (2021). Mechanoregulation of YAP and TAZ in cellular homeostasis and disease progression. *Front. Cell. Dev. Biol.* 9, 1–12. doi: 10.3389/fcell.2021.673599

Campisi, J. (2013). Aging, cellular senescence, and cancer. *Annu. Rev. Physiol.* 75, 685–705. doi: 10.1146/annurev-physiol-030212-183653

Campos, S. E., Avelar-Rivas, J. A., Garay, E., Juárez-Reyes, A., and DeLuna, A. (2018). Genomewide mechanisms of chronological longevity by dietary restriction in budding yeast. *Aging Cell* 17:e12749. doi: 10.1111/acel.12749

Carra, S., Seguin, S. J., Lambert, H., and Landry, J. (2008). HspB8 chaperone activity toward poly(Q)-containing proteins depends on its association with Bag3, a stimulator of macroautophagy. *J. Biol. Chem.* 283, 1437–1444. doi: 10.1074/jbc.M706304200

Chakraborty, S., Njah, K., Pobbati, A. V., Lim, Y. B., Raju, A., Lakshmanan, M., et al. (2017). Agrin as a mechanotransduction signal regulating YAP through the Hippo pathway. *Cell Rep.* 18, 2464–2479. doi: 10.1016/j.celrep.2017.02.041

Chan, E. H. Y., Nousiainen, M., Chalamalasetty, R. B., Schäfer, A., Nigg, E. A., and Silljé, H. H. (2005). The Ste20-like kinase Mst2 activates the human large tumor suppressor kinase Lats1. *Oncogene* 24, 2076–2086. doi: 10.1038/sj.onc.1208445

Chien, Y., Scuoppo, C., Wang, X., Fang, X., Balgley, B., Bolden, J. E., et al. (2011). Control of the senescence-associated secretory phenotype by NF-κB promotes senescence and enhances chemosensitivity. *Genes Dev.* 25, 2125–2136. doi: 10.1101/gad.17276711

Childs, B. G., Baker, D. J., Kirkland, J. L., Campisi, J., and van Deursen, J. M. (2014). Senescence and apoptosis: dueling or complementary cell fates? *EMBO Rep.* 15, 1139–1153. doi: 10.15252/embr.201439245

Chistyakov, V. A., and Denisenko, Y. V. (2019). "Antagonistic pleiotropy aging theory," in *Encyclopedia of Gerontology and Population Aging*, eds. D. Gu and M. E. Dupre (Cham: Springer), 473–479.

Coppé, J. P., Desprez, P. Y., and Krtolica, A. C. (2010). The senescence-associated secretory phenotype: the dark side of tumor suppression. *Ann. Rev. Pathol. Mech. Dis.* 5, 99–118. doi: 10.1146/annurev-pathol-121808-102144

Cornils, H., Kohler, R. S., Hergovich, A., and Hemmings, B. A. (2011). Human NDR kinases control G 1 /S cell cycle transition by directly regulating p21 stability. *Mol. Cell. Biol.* 31, 1382–1395. doi: 10.1128/MCB.01216-10

Coyle, I. P., Koh, Y-H., Lee, W-C. M., Slind, J., Fergestad, T., Littleton, J. T., et al. (2004). Nervous wreck, an SH3 adaptor protein that interacts with Wsp, regulates synaptic growth in *Drosophila*. *Neuron* 41, 521–534. doi: 10.1016/S0896-6273(04)00016-9

Crippa, V., Sau, D., Rusmini, P., Boncoraglio, A., Onesto, E., Bolzoni, E., et al. (2010). The small heat shock protein B8 (HspB8) promotes autophagic removal of misfolded proteins involved in amyotrophic lateral sclerosis (ALS). *Hum. Mol. Genet.* 19, 3440–3456. doi: 10.1093/hmg/ddq257

Das Sarma, J., Ciric, B., Marek, R., Sadhukhan, S., Caruso, M. L., Shafagh, J., et al. (2009). Functional interleukin-17 receptor A is expressed in central nervous system glia and upregulated in experimental autoimmune encephalomyelitis. *J. Neuroinflamm.* 6, 1–12. doi: 10.1186/1742-2094-6-14

Dehkordi, S. K., Walker, J., Sah, E., Bennett, E., Atrian, F., Frost, B., et al. (2021). Profiling senescent cells in human brains reveals neurons with CDKN2D/p19 and tau neuropathology. *Nat. Aging* 1, 1107–1116. doi: 10.1038/s43587-021-00142-3

Demiray, Y. E., Rehberg, K., Kliche, S., and Stork, O. (2018). Ndr2 kinase controls neurite outgrowth and dendritic branching through α1 integrin expression. *Front. Mol. Neurosci.* 11:66. doi: 10.3389/fnmol.2018.00066

DeRan, M., Yang, J., Shen, C-H., Peters, E. C., Fitamant, J., Chan, P., et al. (2014). Energy stress regulates Hippo-YAP signaling involving AMPK-mediated regulation of angiomotin-like 1 protein. *Cell Rep.* 9, 495–503. doi: 10.1016/j.celrep.2014.09.036

Donahue, J. E., Berzin, T. M., Rafii, M. S., Glass, D. J., Yancopoulos, G. D., Fallon, J. R., et al. (1999). Agrin in Alzheimer's disease: altered solubility and abnormal distribution within microvasculature and brain parenchyma. *Proc. Nat. Acad. Sci. U. S. A.* 96, 6468–6472. doi: 10.1073/pnas.96.11.6468

Dottermusch, M., Lakner, T., Peyman, T., Klein, M., Walz, G., Neumann-Haefelin, E., et al. (2016). Cell cycle controls stress response and longevity in *C. elegans*. *Aging* 8:2100. doi: 10.18632/aging.101052

Drulis-Fajdasz, D., Rakus, D., Wiśniewski, J. R., McCubrey, J. A., and Gizak, A. (2018). Systematic analysis of GSK-3 signaling pathways in aging of cerebral tissue. *Adv. Biol. Regul.* 69, 35–42. doi: 10.1016/j.jbior.2018.06.001

Du, X., Yu, A., and Tao, W. (2015). The non-canonical Hippo/Mst pathway in lymphocyte development and functions. *Acta Biochim. Biophys. Sin.* 47, 60–64. doi: 10.1093/abbs/gmu112

Du, Z., Tong, X., and Ye, X. (2013). Cyclin D1 promotes cell cycle progression through enhancing NDR1/2 kinase activity independent of cyclin-dependent kinase. *J. Biol. Chem.* 288, 26678–26687. doi: 10.1074/jbc.M113.466433

Dutchak, K., Garnett, S., Nicoll, M., de Bruyns, A., and Dankort, D. (2022). MOB3A bypasses BRAF and RAS oncogene-induced senescence by engaging the Hippo pathway. *Mol. Cancer Res.* 20, 770–781. doi: 10.1158/1541-7786.MCR-21-0767

Dutta, S., and Baehrecke, E. H. (2008). Warts is required for PI3K-regulated growth arrest, autophagy, and autophagic cell death in *Drosophila*. *Curr. Biol.* 18, 1466–1475. doi: 10.1016/j.cub.2008.08.052

Elkin, B. S., Ilankovan, A., and Morrison, B. (2010). Age-dependent regional mechanical properties of the rat hippocampus and cortex. *J. Biomech. Eng.* 132, 1–10. doi: 10.1115/1.4000164

Enomoto, A., Fukasawa, T., Takamatsu, N., Ito, M., Morita, A., Hosoi, Y., et al. (2013). The HSP90 inhibitor 17-allylamino-17-demethoxygeldanamycin modulates radiosensitivity by downregulating serine/threonine kinase 38 via Sp1 inhibition. *Eur. J. Cancer* 49, 3547–3558. doi: 10.1016/j.ejca.2013.06.034

Enomoto, A., Kido, N., Ito, M., Takamatsu, N., and Miyagawa, K. (2012). Serine-Threonine Kinase 38 is regulated by Glycogen Synthase Kinase-3 and modulates oxidative stress-induced cell death. *Free Radic. Biol. Med.* 52, 507–515. doi: 10.1016/j.freeradbiomed.2011.11.006

Fang, Z., and Pan, Z. (2019). Essential role of ubiquitin-fold modifier 1 conjugation in DNA damage response. *DNA Cell Biol.* 38, 1030–1039. doi: 10.1089/dna.2019.4861

Freund, A., Patil, C. K., and Campisi, J. (2011). P38MAPK is a novel DNA damage response-independent regulator of the senescence-associated secretory phenotype. *EMBO J.* 30, 1536–1548. doi: 10.1038/emboj.2011.69

Funayama, R., and Ishikawa, F. (2007). Cellular senescence and chromatin structure. *Chromosoma* 116, 431–440. doi: 10.1007/s00412-007-0115-7

Gailite, I., Aerne, B. L., and Tapon, N. (2015). Differential control of Yorkie activity by LKB1/AMPK and the Hippo/Warts cascade in the central nervous system. *Proc. Nat. Acad. Sci. U. S. A.* 112, E5169–E5178. doi: 10.1073/pnas.1505512112

Galehdar, Z., Swan, P., Fuerth, B., Callaghan, S. M., Park, D. S., and Cregan, S. P. (2010). Neuronal apoptosis induced by endoplasmic reticulum stress is regulated by ATF4-CHOP-mediated induction of the Bcl-2 homology 3-only member PUMA. *J. Neurosci.* 30, 16938–16948. doi: 10.1523/JNEUROSCI.1598-10.2010

Gamerdinger, M., Hajieva, P., Kaya, A. M., Wolfrum, U., Hartl, F. U., and Behl, C. (2009). Protein quality control during aging involves recruitment of the macroautophagy pathway by BAG3. *EMBO J.* 28, 889–901. doi: 10.1038/emboj.2009.29

Gamerdinger, M., Kaya, A. M., Wolfrum, U., Clement, A. M., and Behl, C. (2011). BAG3 mediates chaperone-based aggresome-targeting and selective autophagy of misfolded proteins. *EMBO Rep.* 12, 149–156. doi: 10.1038/embor.2010.203

Gan, W., Dai, X., Dai, X., Xie, J., Yin, S., Zhu, J., et al. (2020). LATS suppresses mTORC1 activity to directly coordinate Hippo and mTORC1 pathways in growth control. *Nat. Cell Biol.* 22, 246–256. doi: 10.1038/s41556-020-0463-6

García-Gutiérrez, L., Fallahi, E., Aboud, N., Quinn, N., and Matallanas, D. (2022). Interaction of LATS1 with SMAC links the MST2/Hippo pathway with apoptosis in an IAP-dependent manner. *Cell Death Dis.* 13:692. doi: 10.1038/s41419-022-05147-3

Gefen, A., Gefen, N., Zhu, Q., Raghupathi, R., and Margulies, S. S. (2003). Age-dependent changes in material properties of the brain and braincase of the rat. *J. Neurotrauma* 20, 1163–1177. doi: 10.1089/089771503770802853

Glatigny, M., Moriceau, S., Rivagorda, M., Ramos-Brossier, M., Nascimbeni, A. C., Lante, F., et al. (2019). Autophagy is required for memory formation and reverses age-related memory decline. *Curr. Biol.* 29, 435–448.e8. doi: 10.1016/j.cub.2018.12.021

Gomez, V., Gundogdu, R., Gomez, M., Hoa, L., Panchal, N., O'Driscoll, M., et al. (2015). Regulation of DNA damage responses and cell cycle progression by hMOB2. *Cell. Signal.* 27, 326–339. doi: 10.1016/j.cellsig.2014.11.016

Gorbunova, V., Seluanov, A., Mao, Z., and Hine, C. (2007). Changes in DNA repair during aging. *Nucl. Acids Res.* 35, 7466–7474. doi: 10.1093/nar/gkm756

Gorovits, R., Sjollema, K. A., Sietsma, J. H., and Yarden, O. (2000). Cellular distribution of COT1 kinase in *Neurospora crassa*. *Fungal Genet. Biol.* 30, 63–70. doi: 10.1006/fgbi.2000.1198

Grant, T. J., Mehta, A. K., Gupta, A., Sharif, A. A. D., Arora, K. S., Deshpande, V., et al. (2017). STK38L kinase ablation promotes loss of cell viability in a subset of KRAS-dependent pancreatic cancer cell lines. *Oncotarget* 8:78556. doi: 10.18632/oncotarget.20833

Grunewald, M., Kumar, S., Sharife, H., Volinsky, E., Gileles-Hillel, A., Licht, T., et al. (2021). Counteracting age-related VEGF signaling insufficiency promotes healthy aging and extends life span. *Science* 373:eabc8479. doi: 10.1126/science.abc8479

Gundogdu, R., and Hergovich, A. (2016). The possible crosstalk of MOB2 with NDR1/2 kinases in cell cycle and DNA damage signaling. *J. Cell Signal* 1:125. doi: 10.4172/2576-1471.1000125

Habbas, S., Santello, M., Becker, D., Stubbe, H., Zappia, G., Liaudet, N., et al. (2015). Neuroinflammatory TNFα impairs memory via astrocyte signaling. *Cell* 163, 1730–1741. doi: 10.1016/j.cell.2015.11.023

Halder, S. K., Delorme-Walker, V. D., and Milner, R. (2023). β1 integrin is essential for blood–brain barrier integrity under stable and vascular remodelling conditions; effects differ with age. *Fluids Barr. CNS* 20, 1–16. doi: 10.1186/s12987-023-00453-0

Hartl, F. U., Bracher, A., and Hayer-Hartl, M. (2011). Molecular chaperones in protein folding and proteostasis. *Nature* 475, 324–332. doi: 10.1038/nature10317

Herdy, J. R., Traxler, L., Agarwal, R. K., Karbacher, L., Schlachetzki, J. C. M., Boehnke, L., et al. (2022). Increased post-mitotic senescence in aged human neurons is a pathological feature of Alzheimer's disease. *Cell Stem Cell* 29, 1637–1652.e6. doi: 10.1016/j.stem.2022.11.010

Hergovich, A. (2016). The roles of NDR protein kinases in hippo signalling. *Genes* 7, 1–16. doi: 10.3390/genes7050021

Hergovich, A., Lamla, S., Nigg, E. A., and Hemmings, B. A. (2007). Centrosome-associated NDR kinase regulates centrosome duplication. *Mol. Cell* 25, 625–634. doi: 10.1016/j.molcel.2007.01.020

Hergovich, A., Schmitz, D., and Hemmings, B. A. (2006). The human tumour suppressor LATS1 is activated by human MOB1 at the membrane. *Biochem. Biophys. Res. Commun.* 345, 50–58. doi: 10.1016/j.bbrc.2006.03.244

Hu, L., Li, H., Zi, M., Li, W., Liu, J., Yang, Y., et al. (2022). Why senescent cells are resistant to apoptosis: an insight for senolytic development. *Front. Cell Dev. Biol.* 10, 822–816. doi: 10.3389/fcell.2022.822816

Humbert, N., Navaratnam, N., Augert, A., Da Costa, M., Martien, S., Wang, J., et al. (2010). Regulation of ploidy and senescence by the AMPK-related kinase NUAK1. *EMBO J.* 29, 376–386. doi: 10.1038/emboj.2009.342

Humphrey, J. D., Dufresne, E. R., and Schwartz, M. A. (2014). Mechanotransduction and extracellular matrix homeostasis. *Nat. Rev. Mol. Cell Biol.* 15, 802–812. doi: 10.1038/nrm3896

Huntoon, C. J., Nye, M. D., Geng, L., Peterson, K. L., Flatten, K. S., Haluska, P., et al. (2010). Heat shock protein 90 inhibition depletes LATS1 and LATS2, two regulators of the mammalian Hippo tumor suppressor pathway. *Cancer Res.* 70, 8642–8650. doi: 10.1158/0008-5472.CAN-10-1345

Hynes, R. O. (2009). The extracellular matrix: not just pretty fibrils. *Science (1979)* 326, 1216–1219. doi: 10.1126/science.1176009

Ji, C., Tang, M., Zeidler, C., Höhfeld, J., and Johnson, G. V. (2019). BAG3 and SYNPO (synaptopodin) facilitate phospho-MAPT/Tau degradation via autophagy in neuronal processes. *Autophagy* 15, 1199–1213. doi: 10.1080/15548627.2019.1580096

Jiang, X., Maruyama, J., Iwasa, H., Arimoto-Matsuzaki, K., Nishina, H., and Hata, Y. (2021). Heat shock induces the nuclear accumulation of YAP1 via SRC. *Exp. Cell Res.* 399:112439. doi: 10.1016/j.yexcr.2020.112439

Joffre, C., Dupont, N., Hoa, L., Gomez, V., Pardo, R., Gonçalves-Pimentel, C., et al. (2015). The Pro-apoptotic STK38 kinase is a new BECLIN1 partner positively regulating autophagy. *Curr. Biol.* 25, 2479–2492. doi: 10.1016/j.cub.2015.08.031

Kasselimi, E., Pefani, D. E., Taraviras, S., and Lygerou, Z. (2022). Ribosomal DNA and the nucleolus at the heart of aging. *Trends Biochem. Sci.* 47, 328–341. doi: 10.1016/j.tibs.2021.12.007

Kazimierczak, U., Dondajewska, E., Zajaczkowska, M., Karwacka, M., Kolenda, T., and Mackiewicz, A. (2021). Lats1 is a mediator of melanogenesis in response to oxidative stress and regulator of melanoma growth. *Int. J. Mol. Sci.* 22, 1–14. doi: 10.3390/ijms22063108

Ke, H., Pei, J., Ni, Z., Xia, H., Qi, H., Woods, T., et al. (2004). Putative tumor suppressor Lats2 induces apoptosis through downregulation of Bcl-2 and Bcl-xL. *Exp. Cell Res.* 298, 329–338. doi: 10.1016/j.yexcr.2004.04.031

Keller, M., Dubois, F., Teulier, S., Martin, A. P. J., Levallet, J., Maille, E., et al. (2019). NDR2 kinase contributes to cell invasion and cytokinesis defects induced by the inactivation of RASSF1A tumor-suppressor gene in lung cancer cells. *J. Exp. Clin. Cancer Res.* 38, 1–16. doi: 10.1186/s13046-019-1145-8

Khuong, T. M., Habets, R. L. P., Slabbaert, J. R., and Verstreken, P. (2010). WASP is activated by phosphatidylinositol-4,5-bisphosphate to restrict synapse growth in a pathway parallel to bone morphogenetic protein signaling. *Proc. Natl. Acad. Sci. U. S. A.* 107, 17379–17384. doi: 10.1073/pnas.1001794107

Kilic, U., Gok, O., Erenberk, U., Dundaroz, M. R., Torun, E., Kucukardali, Y., et al. (2015). A remarkable age-related increase in SIRT1 protein expression against oxidative stress in elderly: SIRT1 gene variants and longevity in human. *PLoS ONE* 10:e0117954. doi: 10.1371/journal.pone.0117954

Kim, M., Hwang, S., Kim, B., Shin, S., Yang, S., Gwak, J., et al. (2023). YAP governs cellular adaptation to perturbation of glutamine metabolism by regulating ATF4-mediated stress response. *Oncogene* 42, 2828–2840. doi: 10.1038/s41388-023-02811-6

Kim, N.-G., and Gumbiner, B. M. (2015). Adhesion to fibronectin regulates Hippo signaling via the FAK–Src–PI3K pathway. *J. Cell Biol.* 210, 503–515. doi: 10.1083/jcb.201501025

Kitada, M., Ogura, Y., and Koya, D. (2016). Role of Sirt1 as a regulator of autophagy. *Autophagy* 8, 89–100. doi: 10.1016/B978-0-12-802937-4.00003-X

Klimek, C., Jahnke, R., Wördehoff, J., Kathage, B., Stadel, D., Behrends, C., et al. (2019). The Hippo network kinase STK38 contributes to protein homeostasis by inhibiting BAG3-mediated autophagy. *BBA- Mol. Cell Res.* 1866, 1556–1566. doi: 10.1016/j.bbamcr.2019.07.007

Klimek, C., Kathage, B., Wördehoff, J., and Höhfeld, J. (2017). BAG3-mediated proteostasis at a glance. *J. Cell Sci.* 130, 2781–2788. doi: 10.1242/jcs.203679

Klotz, L.-O., Sánchez-Ramos, C., Prieto-Arroyo, I., Urbánek, P., Steinbrenner, H., and Monsalve, M. (2015). Redox regulation of FoxO transcription factors. *Redox Biol.* 6, 51–72. doi: 10.1016/j.redox.2015.06.019

Kodali, M., Attaluri, S., Madhu, L. N., Shuai, B., Upadhya, R., Gonzalez, J. J., et al. (2021). Metformin treatment in late middle age improves cognitive function with alleviation of microglial activation and enhancement of autophagy in the hippocampus. *Aging Cell* 20:e13277. doi: 10.1111/acel.13277

Koga, H., Kaushik, S., and Cuervo, A. M. (2011). Protein homeostasis and aging: the importance of exquisite quality control. *Ageing Res. Rev.* 10, 205–215. doi: 10.1016/j.arr.2010.02.001

Kohler, R. S., Schmitz, D., Cornils, H., Hemmings, B. A., and Hergovich, A. (2010). Differential NDR/LATS interactions with the human MOB family reveal a negative role for human MOB2 in the regulation of human NDR kinases. *Mol. Cell. Biol.* 30, 4507–4520. doi: 10.1128/MCB.00150-10

Koike-Kumagai, M., Yasunaga, K., Morikawa, R., Kanamori, T., and Emoto, K. (2009). The target of rapamycin complex 2 controls dendritic tiling of *Drosophila* sensory neurons through the Tricornered kinase signalling pathway. *EMBO J.* 28, 3879–3892. doi: 10.1038/emboj.2009.312

Kole, A. J., Annis, R. P., and Deshmukh, M. (2013). Mature neurons: equipped for survival. *Cell Death Dis.* 4:689. doi: 10.1038/cddis.2013.220

Kramer, D. A., Piper, H. K., and Chen, B. (2022). WASP family proteins: molecular mechanisms and implications in human disease. *Eur. J. Cell Biol.* 101: 151244. doi: 10.1016/j.ejcb.2022.151244

Kranenburg, O., Van Der Eb, A. J., and Zantema, A. (1996). Cyclin Dl is an essential mediator of apoptotic neuronal cell death. *EMBO J.* 15, 46–54. doi: 10.1002/j.1460-2075.1996.tb00332.x

Kular, J. K., Basu, S., and Sharma, R. I. (2014). The extracellular matrix: structure, composition, age-related differences, tools for analysis and applications for tissue engineering. *J. Tissue Eng.* 5:204173141455711. doi: 10.1177/2041731414557112

Kuninaka, S., Nomura, M., Hirota, T., Iida, S-I., Hara, T., Honda, S., et al. (2005). The tumor suppressor WARTS activates the Omi/HtrA2-dependent pathway of cell death. *Oncogene* 24, 5287–5298. doi: 10.1038/sj.onc.1208682

Kuro-o, M., Matsumura, Y., Aizawa, H., Kawaguchi, H., Suga, T., Utsugi, T., et al. (1997). Mutation of the mouse klotho gene leads to a syndrome resembling ageing. *Nature* 390, 45–51. doi: 10.1038/36285

Kurz, A. R. M., Catz, S. D., and Sperandio, M. (2018). Noncanonical Hippo signalling in the regulation of leukocyte function. *Trends Immunol.* 39, 656–669. doi: 10.1016/j.it.2018.05.003

Labbadia, J., and Morimoto, R. I. (2015). The biology of proteostasis in aging and disease. *Annu. Rev. Biochem.* 84, 435–464. doi: 10.1146/annurev-biochem-060614-033955

Lai, W. F., and Wong, W.T. (2020). Roles of the actin cytoskeleton in aging and age-associated diseases. *Ageing Res. Rev.* 58:101021. doi: 10.1016/j.arr.2020.101021

Lee, Y., Kim, N. H., Cho, E. S., Yang, J. H., Cha, Y. H., Kang, H. E., et al. (2018). Dishevelled has a YAP nuclear export function in a tumor suppressor context-dependent manner. *Nat. Commun.* 9:2301. doi: 10.1038/s41467-018-04757-w

Léger, H., Santana, E., Leu, N. A., Smith, E. T., Beltran, W. A., Aguirre, G. D., et al. (2018). Ndr kinases regulate retinal interneuron proliferation and homeostasis. *Sci. Rep.* 8, 1–21. doi: 10.1038/s41598-018-30492-9

Lima, T., Li, T. Y., Mottis, A., and Auwerx, J. (2022). Pleiotropic effects of mitochondria in aging. *Nat. Aging* 2, 199–213. doi: 10.1038/s43587-022-00191-2

Liu, B., Zheng, Y., Yin, F., Yu, J., Silverman, N., and Pan, D. (2016). Toll receptor-mediated Hippo signaling controls innate immunity in *Drosophila*. *Cell* 164, 406–419. doi: 10.1016/j.cell.2015.12.029

Liu, C.-Y., Zha, Z.-Y., Zhou, X., Zhang, H., Huang, W., Zhao, D., et al. (2010). The Hippo tumor pathway promotes TAZ degradation by phosphorylating a phosphodegron and recruiting the SCFβ-TrCP E3 ligase. *J. Biol. Chem.* 285, 37159–37169. doi: 10.1074/jbc.M110.152942

Liu, J., Li, J., Chen, H., Wang, R., Li, P., Miao, Y., et al. (2020). Metformin suppresses proliferation and invasion of drug-resistant breast cancer cells by activation of the Hippo pathway. *J. Cell. Mol. Med.* 24, 5786–5796. doi: 10.1111/jcmm.15241

López-Otín, C., Blasco, M. A., Partridge, L., Serrano, M., and Kroemer, G. (2013). The hallmarks of ageing. *Cell* 153, 1194–1217. doi: 10.1016/j.cell.2013.05.039

López-Otín, C., Blasco, M. A., Partridge, L., Serrano, M., and Kroemer, G. (2023). Hallmarks of aging: an expanding universe. *Cell* 186, 243–278. doi: 10.1016/j.cell.2022.11.001

Lu, T., Pan, Y., Kao, S. Y., Li, C., Kohane, I., Chan, J., et al. (2004). Gene regulation and DNA damage in the ageing human brain. *Nature* 429, 883–891. doi: 10.1038/nature02661

Luo, L., Guo, J., Li, Y., Liu, T., and Lai, L. (2023). Klotho promotes AMPK activity and maintains renal vascular integrity by regulating the YAP signaling pathway. *Int. J. Med. Sci.* 20, 194–205. doi: 10.7150/ijms.80220

Lupo, G., Gioia, R., Nisi, P. S., Biagioni, S., and Cacci, E. (2019). Molecular mechanisms of neurogenic aging in the adult mouse subventricular zone. *J. Exp. Neurosci.* 13:1179069519829040. doi: 10.1177/1179069519829040

Ma, C., Lin, W., Liu, Z., Tang, W., Gautam, R., Li, H., et al. (2017). NDR 1 protein kinase promotes IL-17- and TNF-α-mediated inflammation by competitively binding TRAF3. *EMBO Rep.* 18, 586–602. doi: 10.15252/embr.201642140

Ma, S., Meng, Z., Chen, R., and Guan, K-., L. (2019). The Hippo pathway: biology and pathophysiology. *Annu. Rev. Biochem.* 88, 577–604. doi: 10.1146/annurev-biochem-013118-111829

Madencioglu Kul, D. A. (2019). *Roles of the hippo pathway kinase Ndr2 in neural development and behavior* [Doctoral thesis]. Otto-Von-Guericke University, Magdeburg, Germany. doi: 10.25673/25405

Madencioglu, D. A., Çalişkan, G., Yuanxiang, P., Rehberg, K., Demiray, Y. E., Kul, E., et al. (2021). Transgenic modeling of Ndr2 gene amplification

reveals disturbance of hippocampus circuitry and function. *iScience* 24:102868. doi: 10.1016/j.isci.2021.102868

Martin, A. P., Jacquemyn, M., Lipecka, J., Chhuon, C., Aushev, V. N., Meunier, B., et al. (2019). STK38 kinase acts as XPO1 gatekeeper regulating the nuclear export of autophagy proteins and other cargoes. *EMBO Rep.* 20:e48150. doi: 10.15252/embr.201948150

Martins, R., Lithgow, G. J., and Link, W. (2016). Long live FOXO: unraveling the role of FOXO proteins in aging and longevity. *Aging Cell* 15, 196–207. doi: 10.1111/acel.12427

Mathew, R., Pal Bhadra, M., and Bhadra, U. (2017). Insulin/insulin-like growth factor-1 signalling (IIS) based regulation of lifespan across species. *Biogerontology* 18, 35–53. doi: 10.1007/s10522-016-9670-8

Matsuoka, S., Ballif, B. A., Smogorzewska, A., McDonald, E. R., III, Hurov, K. E., Luo, J., et al. (2007). ATM and ATR substrate analysis reveals extensive protein networks responsive to DNA damage. *Science (1979)* 316, 1160–1166. doi: 10.1126/science.1140321

Meltzer, S., Yadav, S., Lee, J., Soba, P., Younger, S. H., Jin, P., et al. (2016). Epidermis-derived semaphorin promotes dendrite self-avoidance by regulating dendrite-substrate adhesion in *Drosophila* sensory neurons. *Neuron* 89, 741–755. doi: 10.1016/j.neuron.2016.01.020

Menolfi, D., and Zha, S. (2002). ATM., ATR and DNA-PKcs kinases-the lessons from the mouse models: Inhibition = deletion. *Cell Biosci.* 10:8. doi: 10.1186/s13578-020-0376-x

Meriin, A. B., Narayanan, A., Meng, L., Alexandrov, I., Varelas, X., Ciss,é, I. I., et al. (2018). Hsp70–Bag3 complex is a hub for proteotoxicity-induced signaling that controls protein aggregation. *Proc. Nat. Acad. Sci. U. S. A.* 115, 7043–7052. doi: 10.1073/pnas.1803130115

Michán, S., Li, Y., Chou, M. M., Parrella, E., Ge, H., Long, J. M., et al. (2010). SIRT1 is essential for normal cognitive function and synaptic plasticity. *J. Neurosci.* 30, 9695–9707. doi: 10.1523/JNEUROSCI.0027-10.2010

Mizushima, N., Levine, B., Cuervo, A. M., and Klionsky, D. J. (2008). Autophagy fights disease through cellular self-digestion. *Nature* 451, 1069–1075. doi: 10.1038/nature06639

Mo, J., Park, H. W., and Guan, K. (2014). The Hippo signaling pathway in stem cell biology and cancer. *EMBO Rep.* 15, 642–656. doi: 10.15252/embr.201438638

Mo, J.-S., Meng, Z., Kim, Y. C., Park, H. W., Hansen, C. G., Kim, S., et al. (2015). Cellular energy stress induces AMPK-mediated regulation of YAP and the Hippo pathway. *Nat. Cell Biol.* 17, 500–510. doi: 10.1038/ncb3111

Mo, Y., Lin, R., Liu, P., Tan, M., Xiong, Y., Guan, K-L., et al. (2017). SIRT 7 deacetylates DDB 1 and suppresses the activity of the CRL4 E3 ligase complexes. *FEBS J.* 284, 3619–3636. doi: 10.1111/febs.14259

Moreno-Blas, D., Gorostieta-Salas, E., Pommer-Alba, A., Muciño-Hernández, G., Gerónimo-Olvera, C., Maciel-Barón, L. A., et al. (2019). Cortical neurons develop a senescence-like phenotype promoted by dysfunctional autophagy. *Aging* 11:6175. doi: 10.18632/aging.102181

Münz, C. (2022). Canonical and non-canonical functions of the autophagy machinery in MHC restricted antigen presentation. *Front. Immunol.* 13:868888. doi: 10.3389/fimmu.2022.868888

Musi, N, Valentine, J. M., Sickora, K. R., Baeuerle, E., Thompson, C. S., Shen, Q., et al. (2018). Tau protein aggregation is associated with cellular senescence in the brain. *Aging Cell* 17:e12840. doi: 10.1111/acel.12840

Nahm, M., Long, A. A., Paik, S. K., Kim, S., Bae, Y. C., Broadie, K., et al. (2010). The Cdc42-selective GAP rich regulates postsynaptic development and retrograde BMP transsynaptic signaling. *J. Cell Biol.* 191, 661–675. doi: 10.1083/jcb.201007086

Natarajan, R., Barber, K., Buckley, A., Cho, P., Egbejimi, A., and Wairkar, Y. P. (2015). Tricornered kinase regulates synapse development by regulating the levels of Wiskott-Aldrich Syndrome Protein. *PLoS ONE* 10:e0138188. doi: 10.1371/journal.pone.0138188

Navarro Negredo, P., Yeo, R. W., and Brunet, A. (2020). Aging and rejuvenation of neural stem cells and their niches. *Cell Stem Cell* 27, 202–223. doi: 10.1016/j.stem.2020.07.002

Ng, T. P., Feng, L., Yap, K. B., Lee, T. S., Tan, C. H., and Winblad, B. (2014). Long-term metformin usage and cognitive function among older adults with diabetes. *J. Alzheimers Dis.* 41, 61–68. doi: 10.3233/JAD-131901

Nieto-Torres, J. L. (2021). Macroautophagy and aging: the impact of cellular recycling on health and longevity. *Mol Asp Med* 82:101020. doi: 10.1016/j.mam.2021.101020

Noer, A., Lindeman, L. C., and Collas, P. (2009). Histone H3 modifications associated with differentiation and long-term culture of mesenchymal adipose stem cells. *Stem Cells Dev.* 18, 725–736. doi: 10.1089/scd.2008.0189

Nokin, M.-J., Durieux, F., Peixoto, P., Chiavarina, B., Peulen, O., Blomme, A., et al. (2016). Methylglyoxal, a glycolysis side-product, induces Hsp90 glycation and YAP-mediated tumor growth and metastasis. *Elife* 5:e19375. doi: 10.7554/eLife.19375.034

Novelle, M. G., Ali, A., Diéguez, C., Bernier, M., and de Cabo, R. (2016). Metformin: a hopeful promise in aging research. *Cold Spring Harb. Perspect. Med.* 6:a025932. doi: 10.1101/cshperspect.a025932

Nunes, V. S., da Silva Ferreira, G., and Quintão, E. C. R. (2022). Cholesterol metabolism in aging simultaneously altered in liver and nervous system. *Aging* 14, 1549–1561. doi: 10.18632/aging.203880

Oh, Y., Chang, K.-J., Orlean, P., Wloka, C., Deshaies, R., and Bi, E. (2012). Mitotic exit kinase Dbf2 directly phosphorylates chitin synthase Chs2 to regulate cytokinesis in budding yeast. *Mol. Biol. Cell* 23, 2445–2456. doi: 10.1091/mbc.e12-01-0033

Ojha, K. R., Shin, S. Y., Padgham, S., Olmedo, F. L., Guo, B., Han, G., et al. (2022). Age-associated dysregulation of integrin function in vascular smooth muscle. *Front. Physiol.* 13:913673. doi: 10.3389/fphys.2022.913673

Park, J., and Kim, C. H. (2021). Regulation of common neurological disorders by gut microbial metabolites. *Exp. Mol. Med.* 53, 1821–1833. doi: 10.1038/s12276-021-00703-x

Park, J-M., Choi, J. Y., Yi, J. M., Chung, J. W., Leem, S-H., Koh, S. S., et al. (2015). NDR1 modulates the UV-induced DNA-damage checkpoint and nucleotide excision repair. *Biochem. Biophys. Res. Commun.* 461, 543–548. doi: 10.1016/j.bbrc.2015.04.071

Pefani, D. E., Latusek, R., Pires, I., Grawenda, A. M., Yee, K. S., Hamilton, G., et al. (2014). RASSF1A-LATS1 signalling stabilizes replication forks by restricting CDK2-mediated phosphorylation of BRCA2. *Nat. Cell Biol.* 16, 962–971. doi: 10.1038/ncb3035

Peng, C., Zhu, Y., Zhang, W., Liao, Q., Chen, Y., Zhao, X., et al. (2017). Regulation of the Hippo-YAP pathway by glucose sensor O-GlcNAcylation. *Mol. Cell.* 68, 591–604.e5. doi: 10.1016/j.molcel.2017.10.010

Piletic, K., Alsaleh, G., and Simon, A. K. (2023). Autophagy orchestrates the crosstalk between cells and organs. *EMBO Rep.* 24:e57289. doi: 10.15252/embr.202357289

Porcher, L., Bruckmeier, S., Burbano, S. D., Finnell, J. E., Gorny, N., Klett, J., et al. (2021). Aging triggers an upregulation of a multitude of cytokines in the male and especially the female rodent hippocampus but more discrete changes in other brain regions. *J. Neuroinflamm.* 18, 1–19. doi: 10.1186/s12974-021-02252-6

Praskova, M., Xia, F., and Avruch, J. (2008). MOBKL1A/MOBKL1B Phosphorylation by MST1 and MST2 inhibits cell proliferation. *Curr. Biol.* 18, 311–321. doi: 10.1016/j.cub.2008.02.006

Probert, L. (2015). TNF and its receptors in the CNS: the essential, the desirable and the deleterious effects. *Neuroscience* 302, 2–22. doi: 10.1016/j.neuroscience.2015.06.038

Qian, X., He, L., Hao, M., Li, Y., Li, X., Liu, Y., et al. (2021). YAP mediates the interaction between the Hippo and PI3K/Akt pathways in mesangial cell proliferation in diabetic nephropathy. *Acta Diabetol.* 58, 47–62. doi: 10.1007/s00592-020-01582-w

Qin, B., Yu, J., Nowsheen, S., Zhao, F., Wang, L., and Lou, Z. (2020). STK38 promotes ATM activation by acting as a reader of histone H4 ufmylation. *Sci. Adv.* 6, 1–10. doi: 10.1126/sciadv.aax8214

Qu, M., Gong, Y., Jin, Y., Gao, R., He, Q., Xu, Y., et al. (2023). HSP90β chaperoning SMURF1-mediated LATS proteasomal degradation in the regulation of bone formation. *Cell. Signal.* 102:110523. doi: 10.1016/j.cellsig.2022.110523

Rajesh, K., Krishnamoorthy, J., Gupta, J., Kazimierczak, U., Papadakis, A. I., Deng, Z., et al. (2016). The eIF2α serine 51 phosphorylation-ATF4 arm promotes HIPPO signaling and cell death under oxidative stress. *Oncotarget* 7, 51044–51058. doi: 10.18632/oncotarget.10480

Ransohoff, R. M. (2016). How neuroinflammation contributes to neurodegeneration. *Science (1979)* 353, 777–783. doi: 10.1126/science.aag2590

Rawat, P., Thakur, S., Dogra, S., Jaswal, K., Dehury, B., and Mondal, P. (2023). Diet-induced induction of hepatic serine/threonine kinase STK38 triggers proinflammation and hepatic lipid accumulation. *J. Biol. Chem.* 299:104678. doi: 10.1016/j.jbc.2023.104678

Rehberg, K., Kliche, S., Madencioglu, D. A., Thiere, M., Müller, B., Meineke, B. M., et al. (2014). The serine/threonine kinase Ndr2 controls integrin trafficking and integrin-dependent neurite growth. *J. Neurosci.* 34, 5342–5354. doi: 10.1523/JNEUROSCI.2728-13.2014

Reid, D. A., Reed, P. J., Schlachetzki, J. C. M., Nitulescu, I. I., Chou, G., Tsui, E. C., et al. (2021). Incorporation of a nucleoside analog maps genome repair sites in postmitotic human neurons. *Science (1979)* 372, 91–94. doi: 10.1126/science.abb9032

Rolfe, K. J., and Grobbelaar, A. O. A. (2012). Review of fetal scarless healing. *ISRN Dermatol.* 2012:698034. doi: 10.5402/2012/698034

Roșianu, F., Mihaylov, S. R., Eder, N., Martiniuc, A., Claxton, S., Flynn, H. R., et al. (2023). Loss of NDR1/2 kinases impairs endomembrane trafficking and autophagy leading to neurodegeneration. *Life Sci. Alliance* 6:e202201712. doi: 10.26508/lsa.202201712

Rotermund, C., Machetanz, G., and Fitzgerald, J. C. (2018). The therapeutic potential of metformin in neurodegenerative diseases. *Front. Endocrinol.* 9:382563. doi: 10.3389/fendo.2018.00400

Rozo, M., Li, L., and Fan, C. M. (2016). Targeting β1-integrin signaling enhances regeneration in aged and dystrophic muscle in mice. *Nat. Med.* 22, 889–896. doi: 10.1038/nm.4116

Sack, I., Beierbach, B., Wuerfel, J., Klatt, D., Hamhaber, U., Papazoglou, S., et al. (2009). The impact of aging and gender on brain viscoelasticity. *Neuroimage* 46, 652–657. doi: 10.1016/j.neuroimage.2009.02.040

Safwan-Zaiter, H., Wagner, N., and Wagner, K. D. (2022). P16INK4A—More than a senescence marker. *Life* 12:1332. doi: 10.3390/life12091332

Salminen, A., and Kaarniranta, K. (2012). AMP-activated protein kinase (AMPK) controls the aging process via an integrated signaling network. *Ageing Res. Rev.* 11, 230–241. doi: 10.1016/j.arr.2011.12.005

Samuel, M. A., Valdez, G., Tapia, J. C., Lichtman, J. W., and Sanes, J. R. (2012). Agrin and synaptic laminin are required to maintain adult neuromuscular junctions. *PLoS ONE* 7:e46663. doi: 10.1371/journal.pone.0046663

Satoh, A., Brace, C. S., Rensing, N., Cliften, P., Wozniak, D. F., Herzog, E. D., et al. (2013). Sirt1 extends life span and delays aging in mice through the regulation of Nk2 Homeobox 1 in the DMH and LH. *Cell Metab.* 18, 416–430. doi: 10.1016/j.cmet.2013.07.013

Schmid, E. T., Schinaman, J. M., Williams, K. S., and Walker, D. W. (2023). Accumulation of F-actin drives brain aging and limits healthspan in Drosophila [Preprint]. *Res. Square.* doi: 10.21203/rs.3.rs-3158290/v1

Segel, M., Neumann, B., Hill, M. F. E., Weber, I. P., Viscomi, C., Zhao, C., et al. (2019). Niche stiffness underlies the ageing of central nervous system progenitor cells. *Nature* 573, 130–134. doi: 10.1038/s41586-019-1484-9

Seim, I., Ma, S., and Gladyshev, V. N. (2016). Gene expression signatures of human cell and tissue longevity. *NPJ Aging Mech. Dis.* 2, 1–8. doi: 10.1038/npjamd.2016.14

Seo, S. W., Gottesman, R. F., Clark, J. M., Hernaez, R., Chang, Y., Kim, C., et al. (2016). Nonalcoholic fatty liver disease is associated with cognitive function in adults. *Neurology* 86, 1136–1142. doi: 10.1212/WNL.0000000000002498

Seo, Y-H., Jung, H-J., Shin, H-T., Kim, Y-M., Yim, H., Chung, H-Y., et al. (2008). Enhanced glycogenesis is involved in cellular senescence via GSK3/GS modulation. *Aging Cell* 7, 894–907. doi: 10.1111/j.1474-9726.2008.00436.x

Shi, D.-D., Shi, H., Lu, D., Li, R., Zhang, Y., and Zhang, J. (2012). NDR1/STK38 potentiates NF-κB activation by its kinase activity. *Cell Biochem. Funct.* 30, 664–670. doi: 10.1002/cbf.2846

Shiga, S., Murata, Y., Hashimoto, T., Urushihara, Y., Fujishima, Y., Kudo, K., et al. (2020). DNA-PKcs is activated under nutrient starvation and activates Akt, MST1, FoxO3a, and NDR1. *Biochem. Biophys. Res. Commun.* 521, 668–673. doi: 10.1016/j.bbrc.2019.10.133

Shtutman, M., Chang, B. D., Schools, G. P., and Broude, E. V. (2017). Cellular model of p21-induced senescence. *Methods Mol. Biol.* 1534, 31–39. doi: 10.1007/978-1-4939-6670-7_3

Shumaker, D. K., Dechat, T., Kohlmaier, A., Adam, S. A., Bozovsky, M. R., Erdos, M. R., et al. (2006). Mutant nuclear lamin A leads to progressive alterations of epigenetic control in premature aging. *Proc. Nat. Acad. Sci. U. S. A.* 103, 8703–8708. doi: 10.1073/pnas.0602569103

Si, W., Gong, J., and Yang, X. (2023). Substrate stiffness in nerve cells. *Brain Sci. Adv.* 9, 24–34. doi: 10.26599/BSA.2023.9050002

Si, Z., Sun, L., and Wang, X. (2021). Evidence and perspectives of cell senescence in neurodegenerative diseases. *Biomed. Pharmacotherapy* 137:111327. doi: 10.1016/j.biopha.2021.111327

Singh, A., Kukreti, R., Saso, L., Kukreti, S., Singh, A., Kukreti, R., et al. (2019). Oxidative stress: a key modulator in neurodegenerative diseases. *Molecules* 24:1583. doi: 10.3390/molecules24081583

Spencer, S. J., D'Angelo, H., Soch, A., Watkins, L. R., Maier, S. F., and Barrientos, R. M. (2017). High-fat diet and aging interact to produce neuroinflammation and impair hippocampal- and amygdalar-dependent memory. *Neurobiol. Aging* 58, 88–101. doi: 10.1016/j.neurobiolaging.2017.06.014

Spitler, K. M., and Davies, B. S. J. (2020). Aging and plasma triglyceride metabolism. *J. Lipid Res.* 61, 1161–1167. doi: 10.1194/jlr.R120000922

Staley, B. K., and Irvine, K. D. (2012). Hippo signaling in *Drosophila*: recent advances and insights. *Dev. Dyn.* 241, 3–15. doi: 10.1002/dvdy.22723

Stallone, G., Infante, B., Prisciandaro, C., and Grandaliano, G. (2019). MTOR and aging: an old fashioned dress. *Int. J. Mol. Sci.* 20, 1–17. doi: 10.3390/ijms20112774

Starodubtseva, M. N. (2011). Mechanical properties of cells and ageing. *Ageing Res. Rev.* 10, 16–25. doi: 10.1016/j.arr.2009.10.005

Stein, G. H., Drullinger, L. F., Soulard, A., and Dulić, V. (1999). Differential roles for cyclin-dependent kinase inhibitors p21 and p16 in the mechanisms of senescence and differentiation in human fibroblasts. *Mol. Cell. Biol.* 19, 2109–2117. doi: 10.1128/MCB.19.3.2109

Stork, O., Zhdanov, A., Kudersky, A., Yoshikawa, T., Obata, K., and Pape, H. C. (2004). Neuronal functions of the novel serine/threonine kinase Ndr2. *J. Biol. Chem.* 279, 45773–45781. doi: 10.1074/jbc.M403552200

Stradal, T. E. B., Rottner, K., Disanza, A., Confalonieri, S., Innocenti, M., and Scita, G. (2004). Regulation of actin dynamics by WASP and WAVE family proteins. *Trends Cell Biol.* 14, 303–311. doi: 10.1016/j.tcb.2004.04.007

Su, B., Wang, X., Zheng, L., Perry, G., Smith, M. A., and Zhu, X. (2010). Abnormal mitochondrial dynamics and neurodegenerative diseases. *BBA Mol. Basis Dis.* 1802, 135–142. doi: 10.1016/j.bbadis.2009.09.013

Suzuki, A., Ogura, T., and Esumi, H. (2006). NDR2 acts as the upstream kinase of ARK5 during insulin-like growth factor-1 signaling. *J. Biol. Chem.* 281, 13915–13921. doi: 10.1074/jbc.M511354200

Swift, M. L., and Azizkhan-Clifford, J. (2022). DNA damage-induced sumoylation of Sp1 induces its interaction with RNF4 and degradation in S phase to remove 53BP1 from DSBs and permit HR. *DNA Repair.* 111:103289. doi: 10.1016/j.dnarep.2022.103289

Tacutu, R., Budovsky, A., Yanai, H., and Fraifeld, V. E. (2011). Molecular links between cellular senescence, longevity and age related diseases - A Systems biology perspective. *Aging* 3, 1178–1191. doi: 10.18632/aging.100413

Takahashi, A., Kono, S., Wada, A., Oshima, S., Abe, K., Imaizumi, H., et al. (2017). Reduced brain activity in female patients with non-alcoholic fatty liver disease as measured by near-infrared spectroscopy. *PLoS ONE* 12:e0174169. doi: 10.1371/journal.pone.0174169

Takahashi, A., Ohtani, N., Yamakoshi, K., Iida, S.-I., Tahara, H., Nakayama, K., et al. (2006). Mitogenic signalling and the p16INK4a-Rb pathway cooperate to enforce irreversible cellular senescence. *Nat. Cell Biol.* 8, 1291–1297. doi: 10.1038/ncb1491

Tamaskovic, R., Bichsel, S. J., and Hemmings, B. A. (2003). NDR family of AGC kinases - essential regulators of the cell cycle and morphogenesis. *FEBS Lett.* 546, 73–80. doi: 10.1016/S0014-5793(03)00474-5

Tang, F., Gill, J., Ficht, X., Barthlott, T., Cornils, H., Schmitz-Rohmer, D., et al. (2015). The kinases NDR1/2 act downstream of the Hippo homolog MST1 to mediate both egress of thymocytes from the thymus and lymphocyte motility. *Sci. Signal* 8:aab2425. doi: 10.1126/scisignal.aab2425

Tang, Y., and Yu, W. (2019). SIRT1 and p300/CBP regulate the reversible acetylation of serine-threonine kinase NDR2. *Biochem. Biophys. Res. Commun.* 518, 396–401. doi: 10.1016/j.bbrc.2019.08.069

Texada, M. J., Malita, A., Christensen, C. F., Dall, K. B., Faergeman, N. J., Nagy, S., et al. (2019). Autophagy-mediated cholesterol trafficking controls steroid production. *Dev. Cell* 48, 659–671.e4. doi: 10.1016/j.devcel.2019.01.007

Tonge, D. A., De Burgh, H. T., Docherty, R., Humphries, M. J., Craig, S. E., and Pizzey, J. (2012). Fibronectin supports neurite outgrowth and axonal regeneration of adult brain neurons *in vitro*. *Brain Res.* 1453, 8–16. doi: 10.1016/j.brainres.2012.03.024

Torigata, K., Daisuke, O., Mukai, S., Hatanaka, A., Ohka, F., Motooka, D., et al. (2016). LATS2 positively regulates polycomb repressive complex 2. *PLoS ONE* 11:e0158562. doi: 10.1371/journal.pone.0158562

Tsapras, P., Petridi, S., Chan, S., Geborys, M., Jacomin, A-C., Sagona, A. P., et al. (2022). Selective autophagy controls innate immune response through a TAK1/TAB2/SH3PX1 axis. *Cell Rep.* 38:110286. doi: 10.1016/j.celrep.2021.110286

Tsaridou, S., Velimezi, G., Willenbrock, F., Chatzifrangkeskou, M., Elsayed, W., Panagopoulos, A., et al. (2022). 53BP1 -mediated recruitment of RASSF1A to ribosomal DNA breaks promotes local ATM signaling. *EMBO Rep.* 23, 1–21. doi: 10.15252/embr.202154483

Tschöp, K., Conery, A. R., Litovchick, L., Decaprio, J. A., Settleman, J., Harlow, E., et al. (2011). A kinase shRNA screen links LATS2 and the pRB tumor suppressor. *Genes Dev.* 25, 814–830. doi: 10.1101/gad.2000211

Ultanir, S. K., Hertz, N. T., Li, G., Ge, W-P., Burlingame, A. L., Pleasure, S. J., et al. (2012). Chemical genetic identification of NDR1/2 kinase substrates AAK1 and Rabin8 uncovers their roles in dendrite arborization and spine development. *Neuron* 73, 1127–1142. doi: 10.1016/j.neuron.2012.01.019

Vaidya, A., Mao, Z., Tian, X., Spencer, B., Seluanov, A., and Gorbunova, V. (2014). Knock-in reporter mice demonstrate that DNA repair by non-homologous end joining declines with age. *PLoS Genet.* 10:e1004511. doi: 10.1371/journal.pgen.1004511

Verbeek, M. M., Otte-Höller, I., van den Born, J., van den Heuvel, L. P., David, G., Wesseling, P., et al. (1999). Agrin is a major heparan sulfate proteoglycan accumulating in Alzheimer's disease brain. *Am. J. Pathol.* 155, 2115–2125. doi: 10.1016/S0002-9440(10)65529-0

Vichalkovski, A., Gresko, E., Cornils, H., Hergovich, A., Schmitz, D., and Hemmings, B. A. (2008). NDR kinase is activated by RASSF1A/MST1 in response to fas receptor stimulation and promotes apoptosis. *Curr. Biol.* 18, 1889–1895. doi: 10.1016/j.cub.2008.10.060

Visser, S., and Yang, X. (2010). LATS tumor suppressor: a new governor of cellular homeostasis. *Cell Cycle* 9, 3892–3903. doi: 10.4161/cc.9.19.13386

Vyjayanti, V. N., and Rao, K. S. (2006). DNA double strand break repair in brain: reduced NHEJ activity in aging rat neurons. *Neurosci. Lett.* 393, 18–22. doi: 10.1016/j.neulet.2005.09.053

Waldt, N., Seifert, A., Demiray, Y. E., Devroe, E., Turk, B. E., Reichardt, P., et al. (2018). Filamin A phosphorylation at serine 2152 by the serine/threonine kinase Ndr2 controls TCR-induced LFA-1 activation in T cells. *Front. Immunol.* 9:2852. doi: 10.3389/fimmu.2018.02852

Wang, J., Yin, L., and Chen, Z. (2011). New insights into the altered fibronectin matrix and extrasynaptic transmission in the aging brain. *J. Clin. Gerontol. Geriatr.* 2, 35–41. doi: 10.1016/j.jcgg.2010.12.002

Wang, K., Liu, H., Hu, Q., Wang, L., Liu, J., Zheng, Z., et al. (2022). Epigenetic regulation of aging: implications for interventions of aging and diseases. *Signal Transd. Target. Therapy* 7:374. doi: 10.1038/s41392-022-01211-8

Wang, Y., Zhou, Y., and Graves, D. T. (2014). FOXO transcription factors: their clinical significance and regulation. *Biomed Res. Int.* 2014, 1–13. doi: 10.1155/2014/408514

Webb, A. E., and Brunet, A. (2014). FOXO transcription factors: key regulators of cellular quality control. *Trends Biochem. Sci.* 39, 159–169. doi: 10.1016/j.tibs.2014.02.003

Weinstein, G., Davis-Plourde, K., Himali, J. J., Zelber-Sagi, S., Beiser, A. S., and Seshadri, S. (2019). Non-alcoholic fatty liver disease, liver fibrosis score and cognitive function in middle-aged adults: the Framingham Study. *Liver In.* 39, 1713–1721. doi: 10.1111/liv.14161

Weinstein, G., Zelber-Sagi, S., Preis, S. R., Beiser, A. S., DeCarli, C., Speliotes, E. K., et al. (2018). Association of nonalcoholic fatty liver disease with lower brain volume in healthy middle-aged adults in the Framingham Study. *JAMA Neurol.* 75:97. doi: 10.1001/jamaneurol.2017.3229

Wen, M., Ma, X., Cheng, H., Jiang, W., Xu, X., Zhang, Y., et al. (2015). Stk38 protein kinase preferentially inhibits TLR9-activated inflammatory responses by promoting MEKK2 ubiquitination in macrophages. *Nat. Commun.* 6, 1–11. doi: 10.1038/ncomms8167

Wolfe, K. J., Ren, H. Y., Trepte, P., and Cyr, D. M. (2014). Polyglutamine-rich suppressors of Huntingtin toxicity act upstream of Hsp70 and Sti1 in spatial quality control of amyloid-like proteins. *PLoS ONE* 9:e95914. doi: 10.1371/journal.pone.0095914

Wrigley, S., Arafa, D., and Tropea, D. (2017). Insulin-like growth factor 1: at the crossroads of brain development and aging. *Front. Cell. Neurosci.* 11:14. doi: 10.3389/fncel.2017.00014

Wu, Z., Sawada, T., Shiba, K., Liu, S., Kanao, T., Takahashi, R., et al. (2013). Tricornered/NDR kinase signaling mediates PINK1-directed mitochondrial quality control and tissue maintenance. *Genes Dev.* 27, 157–162. doi: 10.1101/gad.203406.112

Xiang, Y-C., Peng, P., Liu, X-W., Jin, X., Shen, J., Zhang, T., et al. (2022). Paris saponin VII., a Hippo pathway activator, induces autophagy and exhibits therapeutic potential against human breast cancer cells. *Acta Pharmacol. Sin.* 43, 1568–1580. doi: 10.1038/s41401-021-00755-9

Xu, C., Wang, L., Fozouni, P., Evjen, G., Chandra, V., Jiang, J., et al. (2020). SIRT1 is downregulated by autophagy in senescence and aging. *Nat. Cell Biol.* 22, 1170–1179. doi: 10.1038/s41556-020-00579-5

Yabuta, N., Mukai, S., Okamoto, A., Okuzaki, D., Suzuki, H., Torigata, K., et al. (2013). N-terminal truncation of Lats1 causes abnormal cell growth control and chromosomal instability. *J. Cell Sci.* 126, 508–519. doi: 10.1242/jcs.113431

Yan, M., Chu, L., Qin, B., Wang, Z., Liu, X., Jin, C., et al. (2015). Regulation of NDR1 activity by PLK1 ensures proper spindle orientation in mitosis. *Sci. Rep.* 5, 1–14. doi: 10.1038/srep10449

Yang, J. H., Hayano, M., Griffin, P. T., Amorim, J. A., Bonkowski, M. S., Apostolides, J. K., et al. (2023). Loss of epigenetic information as a cause of mammalian aging. *Cell* 186, 305–326.e27. doi: 10.1016/j.cell.2022.12.027

Yang, S., Xu, W., Liu, C., Jin, J., Li, X., Jiang, Y., et al. (2022). LATS1 K751 acetylation blocks activation of Hippo signalling and switches LATS1 from a tumor suppressor to an oncoprotein. *Sci. China Life Sci.* 65, 129–141. doi: 10.1007/s11427-020-1914-3

Yang, X., Li, D.-M., Chen, W., and Xu, T. (2001). Human homologue of *Drosophila* lats, LATS1, negatively regulates growth by inducing G 2 /M arrest or apoptosis. *Oncogene* 20, 6516–6523. doi: 10.1038/sj.onc.1204817

Yang, Y., Zhu, Y., Zhou, S., Tang, P., Xu, R., Zhang, Y., et al. (2022). TRIM27 cooperates with STK38L to inhibit ULK1-mediated autophagy and promote tumorigenesis. *EMBO J.* 41:e109777. doi: 10.15252/embj.2021109777

Yuan, T., Annamalai, K., Naik, S., Lupse, B., Geravandi, S., Pal, A., et al. (2021). The Hippo kinase LATS2 impairs pancreatic β-cell survival in diabetes through the mTORC1-autophagy axis. *Nat. Commun.* 12:4928. doi: 10.1038/s41467-021-25145-x

Yue, X., Bai, C., Xie, D., Ma, T., and Zhou, P. K. (2020). DNA-PKcs: a multi-faceted player in DNA damage response. *Front. Genet.* 11:607428. doi: 10.3389/fgene.2020.607428

Zahn, J. T., Louban, I., Jungbauer, S., Bissinger, M., Kaufmann, D., Kemkemer, R., et al. (2011). Age-dependent changes in microscale stiffness and mechanoresponses of cells. *Small* 7, 1480–1487. doi: 10.1002/smll.201100146

Zallen, J. A., Peckol, E. L., Tobin, D. M., and Bargmann, C. I. (2000). Neuronal cell shape and neurite initiation are regulated by the Ndr kinase SAX-1, a member of the Orb6/COT-1/warts serine/threonine kinase family. *Mol. Biol. Cell* 11, 3177–3190. doi: 10.1091/mbc.11.9.3177

Zhang, H., Sathyamurthy, A., Liu, F., Li, L., Zhang, L., Dong, Z., et al. (2019). Agrin-Lrp4-Ror2 signaling regulates adult hippocampal neurogenesis in mice. *Elife* 8:e45303. doi: 10.7554/eLife.45303

Zhang, N., Ye, T., Lu, X., Li, Z., and Li, L. (2023). Radix scrophulariae extracts exert effect on hyperthyroidism via MST1/Hippo signaling pathway. *Chin. J. Integr. Med.* 29, 998–1006. doi: 10.1007/s11655-023-3744-7

Zhang, P., Yang, L., Li, G., Jin, Y., Wu, D., Wang, Q. M., et al. (2020). Agrin involvement in synaptogenesis induced by exercise in a rat model of experimental stroke. *Neurorehabil. Neural Repair* 34, 1124–1137. doi: 10.1177/1545968320969939

Zhao, B., Li, L., Tumaneng, K., Wang, C-., Y., and Guan, K-, L. (2010). A coordinated phosphorylation by Lats and CK1 regulates YAP stability through $SCF^{\beta-TRCP}$. *Genes Dev.* 24, 72–85. doi: 10.1101/gad.1843810

Zhao, B., Li, L., Wang, L., Wang, C.-Y., Yu, J., and Guan, K.-L. (2012). Cell detachment activates the Hippo pathway via cytoskeleton reorganization to induce anoikis. *Genes Dev.* 26, 54–68. doi: 10.1101/gad.173435.111

Zhao, B., Wei, X., Li, W., Udan, R. S., Yang, Q., Kim, J., et al. (2007). Inactivation of YAP oncoprotein by the Hippo pathway is involved in cell contact inhibition and tissue growth control. *Genes Dev.* 21, 2747–2761. doi: 10.1101/gad.1602907

Zhao, J., Zhang, L., Lu, A., Han, Y., Colangelo, D., Bukata, C., et al. (2020). ATM is a key driver of NF-κB-dependent DNA-damage-induced senescence, stem cell dysfunction and aging. *Aging* 12, 4688–4710. doi: 10.18632/aging.102863

Zheng, D., Liwinski, T., and Elinav, E. (2020). Interaction between microbiota and immunity in health and disease. *Cell Res.* 30, 492–506. doi: 10.1038/s41422-020-0332-7

Zhong, B., Zhao, Z., and Jiang, X. (2022). RP1-59D14.5 triggers autophagy and represses tumorigenesis and progression of prostate cancer via activation of the Hippo signaling pathway. *Cell Death Dis.* 13:458. doi: 10.1038/s41419-022-04865-y

Zia, A., Pourbagher-Shahri, A. M., Farkhondeh, T., and Samarghandian, S. (2021). Molecular and cellular pathways contributing to brain aging. *Behav. Brain Funct.* 17:6. doi: 10.1186/s12993-021-00179-9

Zuo, Y., He, J., Liu, S., Xu, Y., Liu, J., Qiao, C., et al. (2022). LATS1 is a central signal transmitter for achieving full type-I interferon activity. *Sci. Adv.* 8:eabj3887. doi: 10.1126/sciadv.abj3887

Glossary

AD, Alzheimer's Disease; AKT/PKB, Protein Kinases B; ALS, Amyotrophic Lateral Sclerosis; AMOT, Angiomotin; AMOTL, Angiomotin-like Protein; AMPK, Amp-activated Protein Kinase; ATF4, Activating Transcription Factor 4; ATG, Autophagy-related Protein; ATM, Ataxia-Telangiectasia Mutated; ATR, ATM-and Rad3-Related; BAG3, BCL-2-associated Athanogene 3; BC, Breast Cancer; BCL-2, B-cell Lymphoma 2; BCL-xL, B-cell Lymphoma-extra Large; CASA, Chaperone-assisted Selective Autophagy; CBK1, Cell Wall Biosynthesis Kinase; CBP, Creb-binding Protein; CDC, Cell Division Control Protein; CDK, Cyclin-dependent-kinase; CDKN1A, Cyclin-dependent-kinase-inhibitor 1a; CHEK1, Checkpoint Kinase 1; DDB1, DNA Damage-binding Protein 1; DDR, DNA Damage Response; DNA-PKcs, DNA-dependent Protein Kinase, Catalytic Subunit; DREAM, Dimerization Partner, Rb-like, E2f and Multi-vulval Class B-complex; DSBs, Double Stranded Breaks; ECM, Extracellular Matrix; ERK, Extracellular-signal Regulated Kinases; F-actin, Filamentous Actin; FAK, Focal adhesion kinase 1; FOXO, Forkhead Box O; GATA, Gata Binding Protein 4; GSK-3β, Glycogen Synthase Kinase 3 Beta; HFD, High Fat Diet; HGPS, Hutchinson-Gilford Progeria Syndrome; HSP, Heat Shock Protein; IFN1, Interferon type-I; IGF1, Insulin-like Growth Factor 1; IIS, Insulin and IGF1 Signaling; IL-6, Interleukin 6; IRS, Insulin Receptor-substrates; LATS, Large Tumor Suppressor; LC3, Microtubule-associated Proteins 1a/1b Light Chain 3; LKB-1, Liver Kinase B1; lncRNAs, Long Non-coding RNAs; MDM2, Mouse Double Minute 2 Homolog; MEKK2, Mitogen-activated Protein Kinase 2; MG, Methylglyoxal; MOB, MPS1 Binder; MQC, Mitochondrial Quality Control; MST, Mammalian Sterile 20-like; mTOR, Mechanistic Target of Rapamycin; mTORC1/2, Mechanistic Target of Rapamycin Complex 1/2; mTiRS130, Mammalian Trappii-specific Subunit 130; Mys, Myospheroid; NAFLD, Nonalcoholic Fatty Liver Diseases; NDR, Nuclear Dbf2-related; NF-κB, Nuclear Factor Kappa B; NHEJ, Non-homologous end joining; NMJ, Neuromuscular Junction; OGT, O-linked N-acetylglucosamine Transferase; OIS, Oncogene-induced Senescence; PD, Parkinson's Disease; PI3K, Phosphoinositide 3-kinase; PINK1, PTEN-induced Kinase 1; pRB, Retinoblastoma Protein; PRC2, Polycomb Repressive Complex 2; PTEN, Phosphatase and Tensin Homolog; PUMA, p53 Upregulated Modulator of Apoptosis; rDNA, Ribosomal DNA; RhoA, RAS Homolog Family Member A; ROS, Reactive Oxygen Species; SAHF, Senescence-associated Histone Foci; SASP, Senescence-associated Secretory Phenotype; SIRT, Sirtuin; SMAC, Second Mitochondria-Derived Activator of Caspases; SMURF1, Smad Ubiquitination Regulatory Factor 1; SOD1, Superoxide Dismutase 1; SP1, Specificity protein 1; TAG, Triacylglycerols; TAZ, Transcriptional Co-activator With Pdz-binding Motif; TEAD, Transcriptionally-enhanced Associate Domain; TNF-α, Tumor Necrosis Factor-alpha; Trc, Tricornered; TRIM27, Tripartite Motif Containing 27; UFM1, Ubiquitin-Fold Modifier 1; ULK1, Unc-51-like Kinase 1; VEGF, Vascular Endothelial Growth Factor; WASP, Wiskott-Aldrich Syndrome Protein; Wts/WTS, Warts; XIAP, X-linked inhibitor of Apoptosis Protein; YAP, Yes-associated Protein; Yki, Yorkie.

frontiers | Frontiers in Molecular Neuroscience

TYPE Original Research
PUBLISHED 12 June 2024
DOI 10.3389/fnmol.2024.1352782

OPEN ACCESS

EDITED BY
Miguel Diaz-Hernandez,
Complutense University of Madrid, Spain

REVIEWED BY
Paul Smolen,
University of Texas Health Science Center at Houston, United States
Pei-Lin Cheng,
Academia Sinica, Taiwan
Feng Wang,
Beijing Institute of Technology, China
Luana Fioriti,
Mario Negri Institute for Pharmacological Research (IRCCS), Italy

*CORRESPONDENCE
Nils Brose
brose@mpinat.mpg.de

†PRESENT ADDRESS
Jennifer L. Day,
Institute for Neurodegenerative Disease, University of California at San Francisco, San Francisco, CA, United States

RECEIVED 08 December 2023
ACCEPTED 14 March 2024
PUBLISHED 12 June 2024

CITATION
Day JL, Tirard M and Brose N (2024) Deletion of a core APC/C component reveals APC/C function in regulating neuronal USP1 levels and morphology.
Front. Mol. Neurosci. 17:1352782.
doi: 10.3389/fnmol.2024.1352782

Deletion of a core APC/C component reveals APC/C function in regulating neuronal USP1 levels and morphology

Jennifer L. Day†, Marilyn Tirard and Nils Brose*

Department of Molecular Neurobiology, Max Planck Institute for Multidisciplinary Sciences, Göttingen, Germany

Introduction: The Anaphase Promoting Complex (APC/C), an E3 ubiquitin ligase, plays a key role in cell cycle control, but it is also thought to operate in postmitotic neurons. Most studies linking APC/C function to neuron biology employed perturbations of the APC/C activators, cell division cycle protein 20 (Cdc20) and Cdc20 homologue 1 (Cdh1). However, multiple lines of evidence indicate that Cdh1 and Cdc20 can function in APC/C-independent contexts, so that the effects of their perturbation cannot strictly be linked to APC/C function.

Methods: We therefore deleted the gene encoding Anaphase Promoting Complex 4 (APC4), a core APC/C component, in neurons cultured from conditional knockout (cKO) mice.

Results: Our data indicate that several previously published substrates are actually not APC/C substrates, whereas ubiquitin specific peptidase 1 (USP1) protein levels are altered in APC4 knockout (KO) neurons. We propose a model where the APC/C ubiquitylates USP1 early in development, but later ubiquitylates a substrate that directly or indirectly stabilizes USP1. We further discovered a novel role of the APC/C in regulating the number of neurites exiting somata, but we were unable to confirm prior data indicating that the APC/C regulates neurite length, neurite complexity, and synaptogenesis. Finally, we show that APC4 SUMOylation does not impact the ability of the APC/C to control the number of primary neurites or USP1 protein levels.

Discussion: Our data indicate that perturbation studies aimed at dissecting APC/C biology must focus on core APC/C components rather than the APC/C activators, Cdh20 and Cdh1.

KEYWORDS

SUMO, ubiquitin, E3 ligase, protein degradation, neuron, APC/C, USP1, Anaphase Promoting Complex

1 Introduction

A complex array of post-translational modifications regulates many simultaneously active signaling pathways within cells, thereby controlling cellular physiology (Chen et al., 2017). One class of such modifications involves a cascade of E1, E2, and E3 enzymes to covalently attach ubiquitin or small ubiquitin-like modifier (SUMO) to lysine residues of substrates. Ubiquitin itself contains seven different lysine residues that each can be ubiquitylated, allowing for the formation of diverse chain types that have a variety of functions. In some cases, ubiquitylation leads to substrate degradation by the proteasome, and in this way regulates complex signaling networks by triggering spatiotemporal selective protein degradation (Oh et al., 2018).

The APC/C is an E3 ubiquitin ligase that stands out as a regulator of complex signaling networks. Upon activation by Cdc20 or Cdh1, the APC/C regulates the cell cycle via oscillating ubiquitylation of defined sets of proteins. The APC/C is a large complex of at least 11 distinct proteins (Peters, 2006), most of which are also expressed in non-dividing neurons, indicating functions of the APC/C beyond cell cycle control (Gieffers et al., 1999). Accordingly, the APC/C has been implicated in the regulation of a variety of substrates and processes in neurons, from glycolysis to synaptogenesis (Eguren et al., 2011). However, the corresponding studies involved the perturbation of the APC/C activators and not core APC/C components. Indeed, deletion of the core APC/C component, APC2, from excitatory mouse forebrain neurons does not alter levels of Ski-novel protein (SnoN) and GluA1 (Kuczera et al., 2011). While this unexpected finding might be due to the fact that the APC/C ubiquitylates substrates only transiently, in certain cells, and under specific conditions, an alternative explanation is that Cdh1 and Cdc20 have APC/C-independent "moonlighting" functions (Wan et al., 2011, 2017; Liu et al., 2016; Han et al., 2019), so that certain phenotypes caused by Cdh1 or Cdc20 depletion are unrelated to APC/C function.

In accordance with this notion, Cdh1 and Cdc20 operate independently of the APC/C to regulate protein stability and protein–protein interactions. For instance, Cdh1 regulates SMURF1 protein levels and dimerization through a mechanism that requires a D-box but is independent of the APC/C (Wan et al., 2011; Kannan et al., 2012). Similarly, APC/C-independent binding of Cdh1 to a D-box motif on c-Src inhibits its kinase activity (Han et al., 2019). Cdh1 employs an APC/C-independent mechanism to suppress dimerization and kinase activity of BRAF (Wan et al., 2017), and it suppresses the auto-ubiquitylation of WWP2, increasing its activity (Liu et al., 2016). Finally, Parkin, an E3 ubiquitin ligase involved in the development of Parkinson's disease, binds to both Cdh1 and Cdc20 independently, but not to core APC/C components, and this association regulates APC/C substrates and the cell cycle. A double knockdown of Parkin and core APC/C components are required to phenocopy a Cdh1 knockdown (Lee et al., 2015), but it is unclear if Parkin and Cdh1 also interact in neurons.

Our study was designed to directly explore the requirement for APC/C activity in nerve cell development and function. We inactivated the APC/C by genetically eliminating the core APC/C component, APC4, in cultured neurons and determined the effects on previously-proposed APC/C substrates and related phenotypes. In contrast to prior studies employing activator depletion (Eguren et al., 2011), we show that neither SnoN, NEUROD2, and FEZ1 levels, nor, synaptogenesis and neurite length and branching are affected by APC/C-inactivation. Instead, we provide evidence for a temporally-regulated pathway where the neuronal APC/C controls USP1 levels and the number of neurites exiting neuron somata. We demonstrate that these phenotypic changes are rescued by APC4 re-expression, and that APC4 SUMOylation does not alter APC/C-dependent regulation of neuron morphology and USP1 protein levels. Our data indicate that care must be taken when extrapolating APC/C function from experimental data obtained by Cdh1 or Cdc20 perturbation. Finally, we show that the APC/C has a detectable but subordinate role in early nerve cell development, and that USP1 may be an important neuronal APC/C substrate.

2 Materials and methods

2.1 Animals

All mice were in the C57/N background. Mutant lines are listed in Supplementary Table S1. For harvesting of tissue, isoflurane-anesthetized adult mice were killed by cervical dislocation, and P0 pups and E16 embryos were killed by decapitation. Mice were housed in individually ventilated cages at ambient temperature under a 12 h light/dark cycle, with free access to food and water. The sex of mice used for cell cultures was not determined. For genotyping, DNA was isolated from tail biopsies using a genomic DNA isolation kit (Nexttec, #10.924). Genotyping primers and PCR product sizes are listed in Supplementary Table S2. The genotyping PCR reaction (96°C for 3 min; 42 cycles of 94°C for 30 s, 62°C for 1 min and 72°C for 1 min; 72°C for 7 min) included 0.05 U/μL MyTaq HS DNA Polymerase (Biotool, #BIO-21113), MyTaq reaction buffer, 1 mM dNTPs, 0.2 nM primers, and 1 μL tail DNA (~15–80 ng DNA).

2.2 Plasmids

PCR was used to generate sequences encoding N-terminally HA and Myc tagged APC4. Resulting constructs were cloned into pcDNA3.1 or lentiviral vectors (kind gifts of C. Rosenmund) that drive APC4 expression with the neuron-specific Synapsin1 promoter. Cre NLS RFP and NLS RFP vectors are in the pf(syn)w-rbn lentivirus backbone. The lentiviral vector pf(syn)w-iCreRFP-P2A expresses iCre-RFP fused to a self-cleaving P2A sequence. This vector was used to generate the APC4 rescue vectors by cloning APC4 after the P2A sequence. APC4 lysines 772 and 797 were mutated to arginine using site directed mutagenesis. The EGFP pCS2+ control plasmid was cloned by replacing Cdc20 with EGFP. Supplementary Table S3 lists the remaining constructs.

2.3 Cell culture

HEK293FT cells (Invitrogen) were maintained at 37°C and 5% CO_2 in DMEM containing 10% FBS (Gibco) and 50 units/mL penicillin/streptomycin (Gibco). For overexpression experiments, cells were transfected using Lipofectamine 2000 (ThermoFisher). Primary neuron cultures were generated as described previously (Daniel et al., 2017). P0 hippocampi and E16 cortices were digested for 30–60 min at 37°C using DMEM containing papain (25 units/mL; Worthington Biochemical), 0.2 mg/mL L-cysteine (Sigma), 1 mM $CaCl_2$, and 0.5 mM EDTA (in DMEM). Dissociated neurons were plated on poly-L-lysine-coated glass coverslips (Thermo, 12 mm coverslips #1.0) or dishes (Sigma). Neurons were cultured at 37°C with 5% CO_2 in Neurobasal-A medium supplemented with 2% B27, penicillin/streptomycin, and 1% GlutaMAX-1 (Gibco). For imaging, cells were seeded on glass coverslips in a 24-well plate at 25,000–50,000 cells/well. For biochemical analysis, ~1.2 million cells were seeded per well of a 6-well plate, and the media was changed the next day to promote cell survival.

2.4 Lentivirus transduction

Lentivirus was prepared using standard methods (López-Murcia et al., 2019). HEK293 cells were plated on 15 cm dishes coated with poly-L-lysine (Sigma) and grown in standard HEK293 cell media containing 0.4 µg/µL Geneticin (Gibco). Immediately before transfection, when cells were 90% confluent, the media was changed to Opti-MEM with 10% FBS (Gibco). All vectors (expression, envelope, and packaging) were co-transfected in Opti-MEM with Lipofectamine 2000 (Invitrogen). After 6 h, the media was changed to pre-warmed media (DMEM, Gibco; 1% Penn/Strep, Gibco; 2% goat Serum, Gibco; 10 mM sodium butyrate, Merck). The virus was harvested after 44–48 h and concentrated with Amicon centrifugal filters (100 kDa; Millipore). Flash-frozen aliquots were stored at-80°C. The percentage of neurons co-expressing MAP2, RFP, and DAPI was used to determine virus titer. Infection rates were typically >90%.

2.5 Primary antibodies

Supplementary Table S4 lists the primary antibodies used.

2.6 Secondary antibodies

Supplementary Table S5 lists the secondary antibodies used.

2.7 Immunolabeling

Coverslips seeded with neurons were washed 3 times with PBS, fixed for 10 min (4% PFA; Serva), washed four times, and blocked for 30 min in imaging solution (0.1% fish skin gelatin, Sigma; 1% goat serum, Gibco; 0.3% Triton X-100, Roche; PBS; Daniel et al., 2017). Coverslips were incubated with primary antibodies in imaging solution for 16–21 h at 4°C. After washing, coverslips were incubated with secondary antibodies for 1 h in imaging solution. Coverslips were then incubated with DAPI (Thermo; 1:10,000) for 10 min, washed with PBS, and mounted onto slides with Aqua-Poly/Mount (Polyscience Inc.).

2.8 Western blotting

Neurons were lysed in lysis buffer (150 mM NaCl; 10 mM Tris pH 7.4; 1% Triton X-100) containing protease inhibitors (1 µg/mL aprotinin, Roche; 0.5 µg/mL leupeptine, Roche; 17.4 µg/mL PMSF, Roche), and fresh N-ethylmaleimide (NEM; 20 mM, Sigma) when required. Protein concentration was determined by the BCA method (Pierce). Typically, 20–25 µg of protein were loaded per lane of SDS/PAGE gel (40 µg were required for detecting Cyclin B1). After SDS-PAGE (Laemmli, 1970), samples were transferred to Nitrocellulose membranes (0.2 mm NC; Amersham Protran, #1060001; Towbin et al., 1979). To assess transfer, membranes were stained with MemCode or Ponceau S. WB was conducted using standard procedures (Daniel et al., 2017). Blocking and antibody incubation were done in PBS with 5% milk powder and 1% Tween. Signals were developed by enhanced chemiluminescence (GE Healthcare) and detected with a Chemostar Imager (INTAS Science Imaging) or, in some cases, by photographic film. For some experiments (Supplementary Figures S3A–D), WB was performed with fluorescent secondary antibodies and signals were detected by an Odyssey Infrared Imager (LI-COR Biosciences).

2.9 Immunoaffinity purification

Standard protocols (Tomomori-Sato et al., 2013) were adapted to perform IP of SUMOylated proteins. Cells were lysed in 150 mM NaCl; 10 mM Tris pH 7.4; 1% Triton X-100, protease inhibitors (1 µg/mL aprotinin, 0.5 µg/mL leupeptine, 17.4 µg/mL PMSF) and 20 mM NEM when required. The lysate was sonicated for 4 s with a sonicator probe at power level 60 (Sonopuls, Bandelin). The lysate was then ultracentrifuged at 106,000 x *g* for 30 min at 4°C. Aliquots of the supernatant were taken (Input), and the remaining sample was incubated for 4 h at 4°C with anti-HA (Sigma) or anti-c-Myc (Sigma) agarose beads. The beads were washed twice in lysis buffer and proteins were eluted in Laemmli buffer (50 mM Tris pH 6.8; 10% glycerol; 0.2 g SDS; bromophenol blue; 33 mM DTT). Eluates (1/3 of the IP eluate/lane) were analyzed by SDS-PAGE and WB. For IP of the APC/C, NEM was excluded from lysates, as it caused non-specific attachment of the APC/C to beads, two ultracentrifuge steps were performed before IP, and the lysate was transferred to a new chilled tube after each centrifugation, and after incubation of the lysate with beads, the beads were washed 4 times with lysis buffer. Anti-HA (Sigma) and anti-c-Myc (Sigma) agarose beads were used for the IP of the APC/C activators. Protein G Sepharose beads (GE Healthcare) were used with anti-APC3 antibody or an IgG isotype control (Jackson Immuno Research) for the IP of endogenous APC/C.

2.10 Subcellular fractionation

Subcellular fractions of adult mouse cortex were prepared according to a published protocol (Carlin et al., 1980), with slight modifications. All steps were performed at 4°C, and all solutions contained protease inhibitors (1 mg/mL aprotinin; 0.5 mg/mL leupeptine; 17.4 mg/mL PMSF). The Homogenate (H) was obtained by homogenizing the cortex in Solution A (0.32 M Sucrose; 1 mM HEPES pH 7.4; 1 mM $MgCl_2$; 0.5 mM $CaCl_2$) with a Dounce homogenizer (12 strokes; 900 rpm). The sample was centrifuged for 10 min at 1,400 x *g*. The supernatant was collected (synaptosomes, cytosol, mitochondria, and organelles; S1) and the pellet was resuspended in Solution A (nuclei; P1). The S1 fraction was centrifuged for 10 min at 13,800 x *g*, and the supernatant was collected (cytosol, microsomes; S2). To generate the P2 (mitochondria and crude synaptosome) fraction, the pellet from the second centrifugation was resuspended in Solution B (0.32 M Sucrose; 1 mM HEPES pH 7.4) and homogenized with a Dounce homogenizer (4 strokes; 900 rpm). Next, 2 mL of the P2 fraction were added to the top of a sucrose step gradient and centrifuged at 82,500 x *g*. The gradient was created using 4 mL 1.2 M Sucrose, 3 mL 1 M Sucrose; 3 mL 0.85 M Sucrose in layers (1 mM HEPES pH 7.4 in all layers). After centrifugation, the turbid layer between the 1 M and 1.2 M sucrose phases was collected (synaptosomes; Syn). To generate the crude post-synaptic density (PSD) fraction, Solution C (0.32 M Sucrose; 1% Triton X-100; 12 mM Tris, pH 8.1) was added to the collected interphase and incubated with mild shaking for 15 min before centrifugation at 32,000 x *g* for 20 min.

The pellet was resuspended in a 1:1 mixture of Solution B and Solution C. After 5 min, the pellet was resuspended by pipetting. One-third of the PSD fraction was loaded and 20 µg of protein from the remaining fractions were loaded per well for SDS-PAGE. Subcellular fractionation of HEK293FT cells was performed following the manufacturer's protocol, but the nuclear pellet was washed with ice-cold PBS to increase the purity (NE-PER; Thermo Scientific). All buffers contained protease inhibitors (1 mg/mL aprotinin; 0.5 mg/mL leupeptine; 17.4 mg/mL PMSF) and NEM (20 mM, Sigma #E1271-5 g). The amount of protein per fraction analyzed by SDS-PAGE was identical in mass for the Equal Protein Loading samples (E) or equal in the percent of the cell volume in the Cell Equivalent samples (P). For data analysis, the experimental average of SUMOylated protein in the nucleus was subtracted from the ratio in the cytosol and this number was compared for all three experiments to a predicted value of 0 using a paired sample *t*-test in Excel (Supplementary Figure S5C).

2.11 Estimating APC4 turnover

APC4 levels were normalized to β-Tubulin levels, and the normalized-APC4 levels upon Cre NLS RFP-infection were then normalized to the normalized-APC4 levels upon control NLS RFP-infection. The resulting values were plotted and fit by an exponential curve, which was used to calculate the half-life of APC4 using standard procedures (Belle et al., 2006).

2.12 Fluorescence microscopy and image analysis

All images were acquired using a 63x oil-immersion objective on a Leica TCS SP2 confocal microscope (1,024 × 1,024 format size; 1.2 zoom; 193.74 nm x 193.74 nm size; 12-bit; 4-lines average). Blinding was achieved for image acquisition and analysis by coverslip coding. During acquisition, all conditions were imaged each day, and the microscope settings were stored to allow for the use of the same settings over several days. Images are displayed as collected, except for MAP2 (color levels changed to 3,080 with Fiji; rescue experiment). When a neuron did not fit into a single field of view, overlapping images were acquired and stitched (Fiji, Pairwise Stitching of Images; Linear Blending Method; check peaks 5; compute overlap; Preibisch et al., 2009; Schindelin et al., 2012). Z-stacks for β III-Tubulin and MAP2 signals were taken using a 92–108 nm step-size (4–15 slices/neuron), and a single maximum intensity projection was created to analyze β III-Tubulin. Scaled images were manually traced with the Fiji SNT plugin (Tavares et al., 2017; Hessian-based analysis: σ = 0.484 and max = 3.69). All neurites shorter than 3 µm were excluded from the analysis. For rescue experiments, neurites were only traced when they might be too short for analysis or the morphology was complex. Sholl Analysis was done using a 5 µm step size (3.1.110 plugin). For synapse counting, single plane images were taken of PSD95, RFP, Synapsin1/2, and MAP2 signals. Z-stacks were taken using a 92–108 nm step size (4–15 slices/neuron) for PSD95, Synapsin1/2, and MAP2. Scaled maximum projection images were used to determine total dendritic morphology (MAP2) with the Fiji NeuronJ plug-in (Meijering et al., 2004). Synapse numbers were determined with the Fiji SynapCountJ v2 plugin (Mata et al., 2017), which determines the number of synapses by quantifying co-localized PSD95 (threshold 120) and Synapsin1/2 (threshold 255) puncta within 1.94 µm from the traced MAP2 stain.

2.13 Statistics

While one experiment was analyzed by a paired *t*-test using Excel (Supplementary Figure S5C), the statistical analyses of biochemical experiments was done in Excel using an independent sample *t*-test. Imaging data for synapse quantification and neuron morphology did not have a Gaussian distribution and had unequal variance between samples, complicating the analysis. As our data fit a heavy-tailed distribution with unequal variance, we chose to use a Welch's *t*-test instead of a non-parametric test, since the former is the most accurate test for such data (Skovlund and Fenstad, 2001; Fagerland and Sandvik, 2009; Kroeger et al., 2021). All statistical analyses of imaging data were performed using SPSS (IBM, version 27). The column graphs that include data from individual experiments were generated in Excel or in Prism 10.

3 Results

3.1 The neuronal APC/C contains APC4

Data obtained by depleting the APC/C activators, Cdh1 or Cdc20, have been the basis for implicating the APC/C in ubiquitylating a variety of neuronal substrates and in controlling neuron physiology (Eguren et al., 2011). As Cdh1 and Cdc20 can operate independently of the APC/C (Wan et al., 2011, 2017; Lee et al., 2015; Liu et al., 2016; Han et al., 2019) corresponding studies cannot unequivocally link observed effects to core APC/C dysfunction. Thus, it is not surprising that the levels of some alleged APC/C substrates are unaltered after APC2 KO (Kuczera et al., 2011). In view of these considerations, we attempted to assess APC/C function in neurons by depleting the core APC/C component APC4.

To confirm that neurons express APC4, we analyzed APC4 and APC5 protein levels in wildtype cortical cultures every 2 days *in vitro* (DIV). APC4 and APC5 levels decreased progressively from DIV3 but remained detectable until DIV17 (Figure 1A). To determine if APC4 is an APC/C component in neurons, we conducted APC3 IP and co-IP of APC4 and APC5. We found that APC4 and APC5 robustly and specifically associate with APC3 in neurons, indicating that APC4 is a component of the neuronal APC/C (Figure 1B).

3.2 Neuronal APC4 deletion affects APC5 stability

To stringently explore the function of the APC/C in neurons, we genetically deleted an essential APC/C core component, rather than an activator. We obtained an *ANAPC4* cKO mouse (IMPC, n.d.; Figure 1C-3). Cultured neurons were generated from cKO mice (*tm1c/tm1c*) and infected with a Cre-expressing lentivirus at DIV1, generating *ANAPC4* KO cells (*tm1d/tm1d*; Figure 1C). To assess the efficacy of APC4 depletion, we analyzed APC4 expression in lysates of infected cultures. We found that APC4 was depleted by DIV11

10.3389/fnmol.2024.1352782

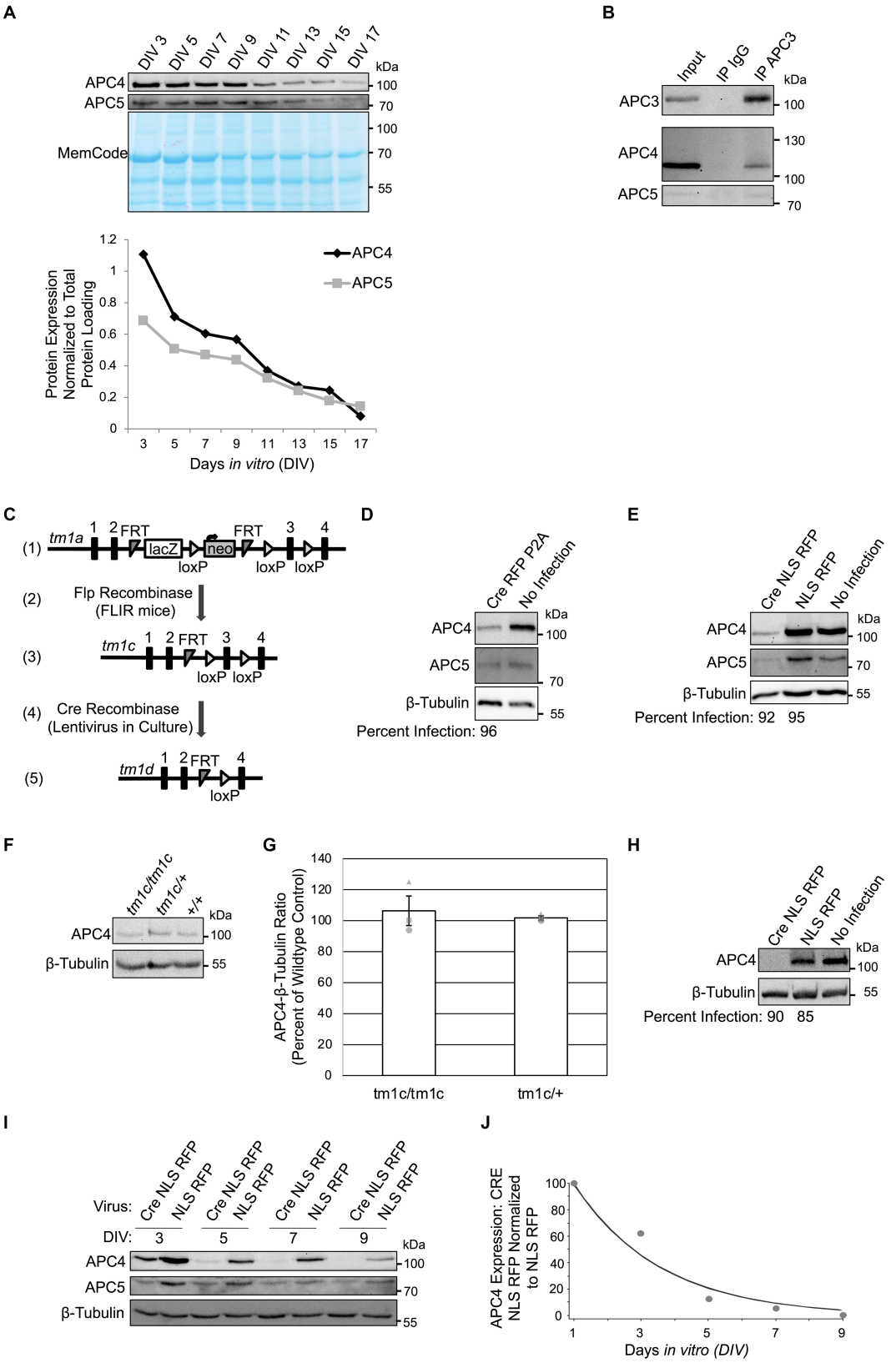

FIGURE 1
APC4 is an APC/C component in cortical neurons and APC4 is depleted from *ANAPC4* KO neurons. **(A)** The top panel shows WB analysis of APC4, APC5, and the total protein MemCode stain in wildtype primary cortical neuron cultures harvested at the indicated DIV. The bottom panel shows a graph depicting the quantification of the blots in the top panel after APC4 (black) and APC5 (gray) levels were normalized to MemCode. **(B)** WB analysis of APC3, APC4, and APC5 in wildtype DIV10 cortical cultures after lysis and IP with antibodies against APC3 or an IgG control (representative experiment). **(C)** The displayed strategy was used to generate the *ANAPC4 cKO mouse* allele. The *tm1a* allele has an insertion upstream of exon 3 of

(Continued)

FIGURE 1 (Continued)

ANAPC4 that contains *lacZ* and neomycin (neo) sequences, flanked by *FRT* and *loxP* sites (1). Mice with the *tm1a* allele were crossed to FLIR mice expressing Flp recombinase (2), generating the cKO *tm1c* allele by removing the cassette at the *FRT* sites (3). Neuron cultures generated from *ANAPC4 tm1c/tm1c* mice were infected with a lentivirus expressing Cre (4), which removes exon 3 and causes a frame shift that adds a premature stop codon. The resulting neurons express the *tm1d* allele, leading to the loss of APC4 (5). **(D)** WB shows the protein levels of APC4, APC5, and β-Tubulin in DIV11 primary hippocampal cultures prepared from *ANAPC4 cKO* neurons infected at DIV1 with Cre RFP P2A or a No Infection control. The percentage of infected cells (below WB panel) was determined by quantifying MAP2-positive cells co-expressing RFP. In Cre RFP P2A-infected cells, APC4 protein levels were reduced to ~28% and APC5 was reduced to ~62% of No Infection levels. **(E)** WB shows APC4, APC5, and β-Tubulin in DIV11 primary hippocampal cultures prepared from *ANAPC4 cKO* neurons infected at DIV1 with Cre NLS RFP, NLS RFP, or a No Infection control. The percentage of infected cells (below WB panel) was determined by quantifying MAP2-positive cells that co-express RFP. In Cre NLS RFP-infected cells, the levels of APC4 were reduced to ~16% and APC5 to ~35% of the levels in NLS RFP-infected cells. **(F)** Lysates of DIV10 cortical cultures obtained from mice with the *ANAPC4* alleles *tm1c/tm1c*, *tm1c/+*, or *+/+* were analyzed by WB with antibodies against APC4 and β-Tubulin (representative experiment). **(G)** Bar graph depicting the average APC4 levels normalized to β-Tubulin for the lysates in F. Error bars: standard error of the mean (SEM) for three experiments. Experiments 1, 2, and 3 are represented by a circle, triangle, and square, respectively. **(H–J)** Primary cortical cultures prepared from *ANAPC4 cKO* mice infected at DIV1 with Cre NLS RFP or NLS RFP were harvested in a large experiment at the indicated times. **(H)** WB shows APC4 and β-Tubulin in DIV11 cultures. The percentage of infected cells (below WB panel) was determined by quantifying MAP2-positive cells co-expressing RFP. APC4 was not detectable in Cre NLS RFP-infected cells. **(I)** WB shows APC4, APC5, and β-Tubulin levels over time. **(J)** Line graph depicting normalized APC4 levels from I. APC4 levels were first normalized to the β-Tubulin signal and then to normalized NLS RFP protein levels. The values in the line graph were fit by an exponential curve to determine APC4's half-life ($\tau = 2.6$ days, $t_{1/2} = 1.8$ days).

when hippocampal neuron cultures were infected with Cre RFP P2A- (Figure 1D) or Cre NLS RFP-lentivirus (Figure 1E).

In control experiments, we determined that the cKO allele, *tm1c,* does not affect endogenous APC4 expression. Mice were crossed to generate wild-type (+/+), heterozygous (*tm1c*/+), or homozygous (*tm1c/tm1c*) offspring. Lysates of cortical DIV11 neurons cultured from these mice exhibited comparable endogenous APC4 expression (Figures 1F,G).

We next determined the time course of APC4 loss upon Cre-infection in *ANAPC4* cKO cortical neurons. APC4 levels in KO neurons decayed rapidly to ~25% of wildtype levels by DIV5, almost completely by DIV9, and completely by DIV11. The decay was exponential, with $\tau = 2.6$ days and $t_{1/2} = 1.8$ days (Figures 1H–J).

Human cytomegalovirus viral infection targets APC4, APC5, and APC1 for degradation, resulting in loss of APC/C activity. Knockdown of any one of these components was shown to cause depletion of all three components (Wiebusch et al., 2005; Thornton et al., 2006; Tran et al., 2010; Clark and Spector, 2015). We also found that APC5 expression is drastically reduced upon APC4 depletion (Figures 1D,E,I). Interestingly, APC4 depletion was more pronounced in cortical neurons (Figure 1H) than in hippocampal neurons (Figure 1E), and APC5 expression was more strongly co-depleted in cortical neurons (Figures 1I, 3A). The parallel loss of APC5 upon APC4 depletion implies that APC/C function is compromised in *ANAPC4* KO neurons. We subsequently used cortical neurons in experiments, because APC4 depletion is more pronounced in these cells.

3.3 The neuronal APC/C regulates USP1

Since prior studies implicated Cdh1 and Cdc20 in the ubiquitylation and degradation of several neuronal substrates (Eguren et al., 2011), we tested whether these effects require the APC/C by analyzing the levels of previously-published substrates at DIV5 (Figure 2) and DIV11 (Figure 3) in *ANAPC4* KO cortical neurons.

As APC4 and APC5 are both depleted under our conditions (Figures 2A, 3A), the APC/C is likely inactive. To support this notion, we first assessed the protein levels of Cyclin B1, a canonical APC/C substrate involved in maintaining neurons in G0 (Almeida et al., 2005; Maestre et al., 2008; Malureanu et al., 2010; Ledvin et al., 2023). As expected, Cyclin B1 levels were increased upon APC4 loss at DIV5 (Figures 2B,C). Since Cyclin B1 is not detectable in neuron cultures after DIV7 (Almeida et al., 2005), we did not analyze Cyclin B1 at DIV11. Our findings indicate that the *ANAPC4* KO system is well suited to study the effects of APC/C inactivation on putative substrates and to screen for novel substrates and phenotypes.

To possibly identify novel phenotypes associated with neuronal APC/C dysfunction, we analyzed the levels of a selected subset of neuronal markers at DIV 5 (Figure 2A) and DIV11 (Figure 3D). We did not detect alterations in the levels of Synaptophysin (Figures 2A, 3D), Synapsins (Figure 3D), or PSD95 (Figure 3D) in KO neurons, indicating that the APC/C does not regulate these proteins.

The deubiquitinating enzyme, USP1, was suggested to be a substrate of Cdh1-APC/C in cycling cells (Cotto-Rios et al., 2011; Cataldo et al., 2013). Its substrate status in neurons is unknown, but it is expressed in neurons and thought to regulating neuron morphology (Anckar and Bonni, 2015). We analyzed USP1 in *ANAPC4* KO cultures and detected increased USP1 levels in DIV5 KO neurons (Figures 2D,E), indicating that USP1 may be an APC/C substrate in cortical neurons. However, USP1 protein levels were decreased in *ANAPC4* KO cells at DIV 11 (Figures 3B,C), indicating that an as yet unidentified APC/C substrate either directly or indirectly regulates USP1 in DIV11 cortical neurons.

We next analyzed previously-published candidate APC/C substrates to determine if their degradation requires the neuronal APC/C and not just Cdh1 or Cdc20. Specifically, we tested *ANAPC4* KO lysates to determine if the levels of SnoN, an axon-growth-inducing transcriptional regulator proposed to be regulated by Cdh1-APC/C (Ikeuchi et al., 2009) and the levels of FEZ1, a protein involved in neurite development and intracellular transport and is proposed to be regulated by Cdc20-APC/C (Watanabe et al., 2014), were altered. Strikingly our data are consistent with prior data from APC2 KO neurons (Kuczera et al., 2011), as we also found that the levels of SnoN and FEZ1 are unaltered in DIV5 (Figures 2F–H) and DIV11 (Figures 3E–H) *ANAPC4* KO neurons.

3.4 The APC/C does not regulate synaptogenesis

Studies employing Cdc20 knockdown in neurons led to the notion that a pathway involving APC/C-mediated NEUROD2 ubiquitylation and downstream regulation of Complexin 2 plays a key role in

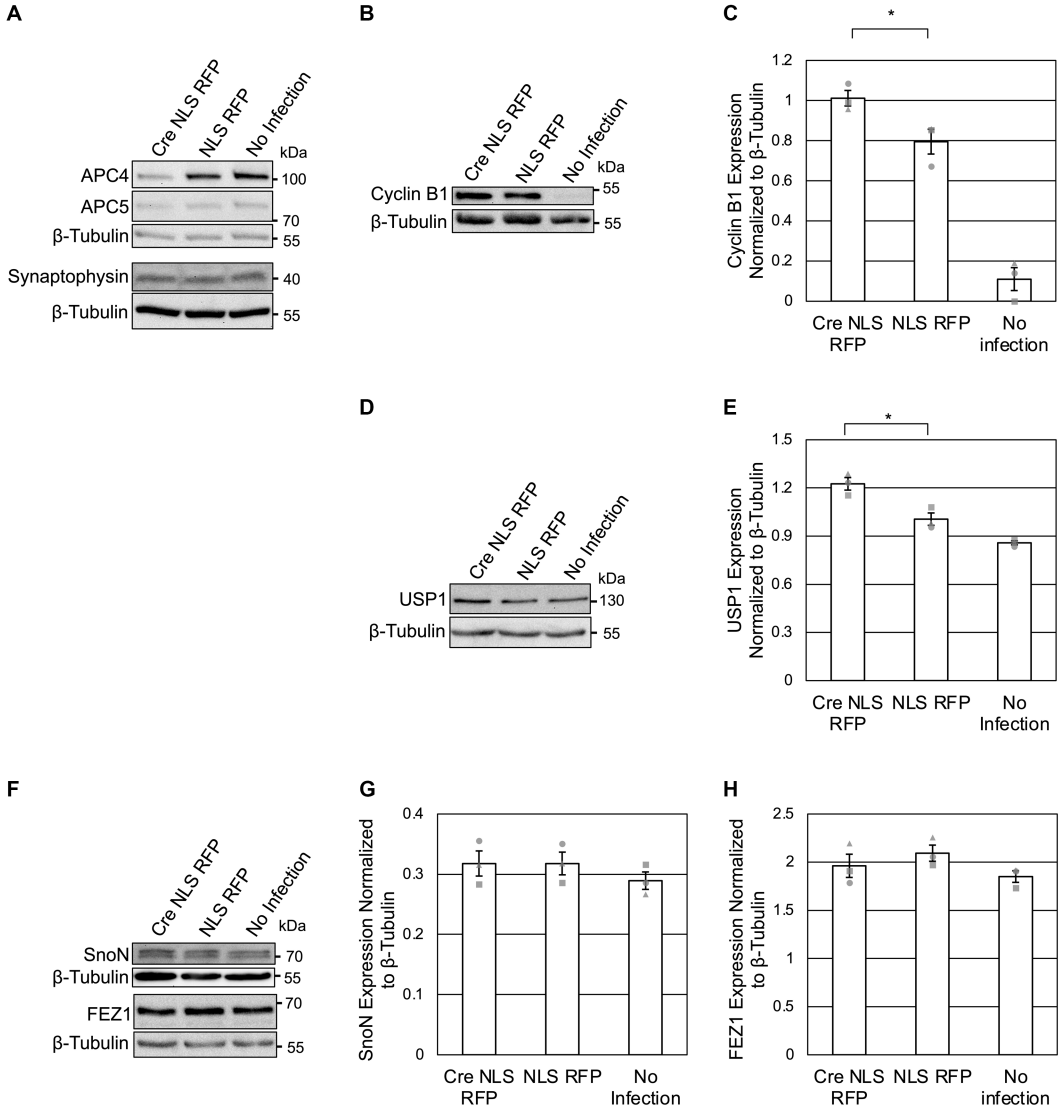

FIGURE 2
APC4 loss is accompanied by USP1 accumulation in DIV5 neurons. **(A–H)** Cortical neurons were prepared from *ANAPC4* cKO mice, and infected at DIV1 with Cre NLS RFP-or NLS RFP-expressing lentivirus. All cultures were harvested at DIV5, and lysates were analyzed by WB. Protein quantification was done by averaging values for three independent experiments (representative experiment displayed). Experiments 1, 2, and 3 are represented by a circle, triangle, and square, respectively. Error bars: SEM. **(A)** WB shows APC4, APC5, Synaptophysin, and β-Tubulin. **(B)** WB shows Cyclin B1 and β-Tubulin. **(C)** Bar graph depicting the average Cyclin B1 protein levels normalized to β-Tubulin. Cyclin B1 protein levels were increased in Cre NLS RFP-infected samples (asterisk: significance; $t(2) = 2.971$, $p = 0.041$). **(D)** WB shows USP1 and β-Tubulin. **(E)** Bar graph depicting the average levels of USP1 normalized to β-Tubulin. USP1 protein was increased in Cre NLS RFP-infected samples (asterisk: significance; $t(2) = 4.008$, $p = 0.016$). **(F)** WB shows SnoN, FEZ, and β-Tubulin. **(G)** Bar graph depicting the average levels of SnoN normalized to β-Tubulin. There was no significant difference in SnoN levels between Cre-and control-infected samples ($t(2) = -0.001$, $p = 1.000$). **(H)** Bar graph depicting FEZ1 normalized to β-Tubulin. There was no significant difference in FEZ1 levels between Cre-and control-infected samples ($t(2) = -0.894$, $p = 0.422$).

synaptogenesis (Yang et al., 2009). However, two lines of evidence challenge this notion. First, there are no changes in NEUROD2 expression or synapse numbers in mutant mice with decreased Cdc20 (Malureanu et al., 2010). Second, the complete deletion of all Complexin paralogues also has no effect on synapse numbers (Reim et al., 2001; López-Murcia et al., 2019). In view of these discrepancies, we tested whether APC4 deletion itself affects synaptogenesis or alters NEUROD2 and Complexins levels.

We first assessed Complexin levels upon *ANAPC4* KO in cortical neurons at DIV11, when Complexin expression peaks (Reim et al., 2005), and found no changes in Complexin 1, Complexin 2, or Complexin 3 levels (Supplementary Figures S1A–D). While Complexin 3 is normally not detectable in neuron cultures, it becomes detectable upon viral infection (Supplementary Figure S1D). We next analyzed the levels of NEUROD2 in KO lysates, and again did not detect alterations at DIV5 or DIV11 (Supplementary Figures S1E,F). These data show that the APC/C does not regulate NEUROD2 or Complexins in cultured cortical neurons.

While we found that the APC/C does not modulate NEUROD2 or Complexin levels in cortical neurons, it could still employ another mechanism to regulate synaptogenesis. Therefore, we counted synapse numbers in *ANAPC4* KO neurons by quantifying the number of co-localized Synapsin1/2 and

PSD95 puncta (Supplementary Figure S1G), which were the markers used in the original study (Yang et al., 2009). Synapse numbers were not altered in KO neurons (Supplementary Figure S1H), indicating that the APC/C does not regulate synaptogenesis in DIV11 cortical neurons.

3.5 The APC/C regulates primary neurite formation

Cdc20 and Cdh1 knockdown studies implicated the APC/C in ubiquitylating a variety of different substrates, which, in turn, were proposed to regulate neuron morphology, including neurite length and complexity (Bobo-Jiménez et al., 2017), axon length (Konishi et al., 2004; Lasorella et al., 2006; Stegmüller et al., 2006; Kannan et al., 2012), and dendrite length and complexity (Kim et al., 2009; Watanabe et al., 2014). However, these morphological phenotypes have usually not been formally linked to core APC/C components, which is problematic because Cdc20 and Cdh1 have APC/C-independent functions. To determine if the APC/C indeed regulates neuronal morphology, we analyzed neurite length and complexity in cortical *ANAPC4* KO neurons at DIV5, when neurite morphology can easily be assessed and APC4 expression is heavily depleted (Figures 1I,J). Similarly aged neurons (DIV3 to DIV5) were also used in earlier studies that addressed the role of the APC/C activators in neurons, with no major differences in effects between DIV3 and DIV5 neurons (Konishi et al., 2004; Lasorella et al., 2006; Stegmüller et al., 2006; Kim et al., 2009; Kannan et al., 2012; Watanabe et al., 2014). Like prior studies (Kempf et al., 1996), we could not reliably distinguish between dendrites and axons using antibodies against MAP2 and SMI-312 (Figure 4A), so we used β III-Tubulin immunolabeling to analyze all neurites longer than 3 µm (Figure 4B).

Prior studies indicated that Cdh1 knockdown increases axon length (Konishi et al., 2004; Lasorella et al., 2006; Stegmüller et al., 2006; Kannan et al., 2012) and that Cdc20 and APC2 knockdown decrease dendrite length (Kim et al., 2009; Watanabe et al., 2014). Hence, we expected to observe changes in dendrite length in *ANAPC4* KO neurons, but we did not detect any corresponding alterations (Figures 4C–E). Primary neurites were defined as neurites directly exiting the somata. Subsequent branch levels were labeled as secondary and tertiary depending on their origin. We compared the lengths of primary, secondary, and tertiary neurites individually (Figure 4C; secondary and tertiary data not shown), and the total length of all neurites (Figure 4D), but detected no KO-induced changes, indicating that the APC/C does not regulate neurite length in DIV5 cortical neurons. To assess possible changes in axon length, we measured the length of the longest neurite (Figure 4E) and detected no alterations.

While we were unable to confirm previously-proposed roles of the APC/C in regulating neurite length and complexity, we detected a novel phenotype. Cortical KO neurons had increased numbers of primary neurites exiting their somata (Figure 4F). As the average neurite length was not changed (Figure 4C), our data indicate that the APC/C regulates the initiation of neurite formation and not neurite stabilization or extension.

We next tested whether the APC/C regulates neurite complexity and branching, parameters that had been linked to Cdc20-APC/C (Kim et al., 2009). We quantified the total number of branches per cell (Figure 4G) and the total number of branches off primary neurites (Figure 4H), but did not detect effects of *ANAPC4* KO. We also analyzed the total neuron complexity with Sholl analysis by quantifying the number of times neurites intersect with equally-spaced concentric circles around the center of the neuron (Sholl, 1953; Tavares et al., 2017). We detected increased intersections at 10–25 µm distance from the center of the somata in APC4-deficient cells (Figure 4I), which can be explained by the increase in the number of primary neurites exiting the somata (Figure 4F). Finally, we did not observe alterations of the radius enclosing *ANAPC4* KO neurons (Figure 4J). These data indicate that the APC/C does not affect the size and complexity of cortical neurons at DIV5, but instead regulates the formation of neurites exiting somata.

3.6 SUMOylation of APC4 does not affect USP1 levels and neuronal morphology

Several proteomic studies (Matic et al., 2010; Schimmel et al., 2014; Cubeñas-Potts et al., 2015; Hendriks et al., 2018) as well as our own analyses of HA-His_6-SUMO1 knock-in mice (Tirard et al., 2012; data not shown) identified APC4 as a SUMOylation target, and lysines 772 and 798 were shown to be SUMOylated in human APC4 (Eifler et al., 2018; Lee et al., 2018; Yatskevich et al., 2021). We mutated the corresponding lysines 772 and 797 in mouse APC4 to generate a Myc-APC4$^{K772R/K797R}$ construct and showed that this variant cannot be SUMOylated (Supplementary Figure S2). Surprisingly, APC4 SUMOylation was very stable in the absence of NEM, an irreversible inhibitor of SENPs (Supplementary Figure S2B, arrow), indicating that these SUMOylated APC4 residues are inaccessible to SENPs.

We next tested if APC4 SUMOylation affects APC/C formation or the subcellular localization of APC4. We found that APC4 SUMOylation does not alter APC/C formation in HEK293 cells (Supplementary Figures S3A,B) or the binding of the APC/C to the APC/C activators, and that the complex primarily exists in a state where APC4 is not SUMOylated (Supplementary Figures 3A–D). We then examined whether APC4 SUMOylation affects APC4 localization. Despite major efforts to optimize fixation and immunolabeling protocols to visualize endogenous APC4 by confocal microscopy, the specific APC4 signal (absent in KO neurons) remained weak and was difficult to distinguish from background. Hence, we sought to biochemically assess the subcellular localization of SUMOylated APC4. We found that SUMOylation does not impact the gross subcellular localization of APC4, as HEK293 cells had equal fractions of Myc-APC4^{WT} and Myc-APC4$^{K772R/K797R}$ in nuclear and cytoplasmic fractions (Supplementary Figure S4).

As SUMOylation of APC4 does not affect APC4 localization (Supplementary Figure S4), APC/C formation, or activator binding (Supplementary Figures S3A–D), we tested if APC4 SUMOylation affects APC/C function, as other studies had indicated (Eifler et al., 2018; Lee et al., 2018; Yatskevich et al., 2021). We first analyzed the subcellular localization of APC4 and SUMOylated APC4. Upon

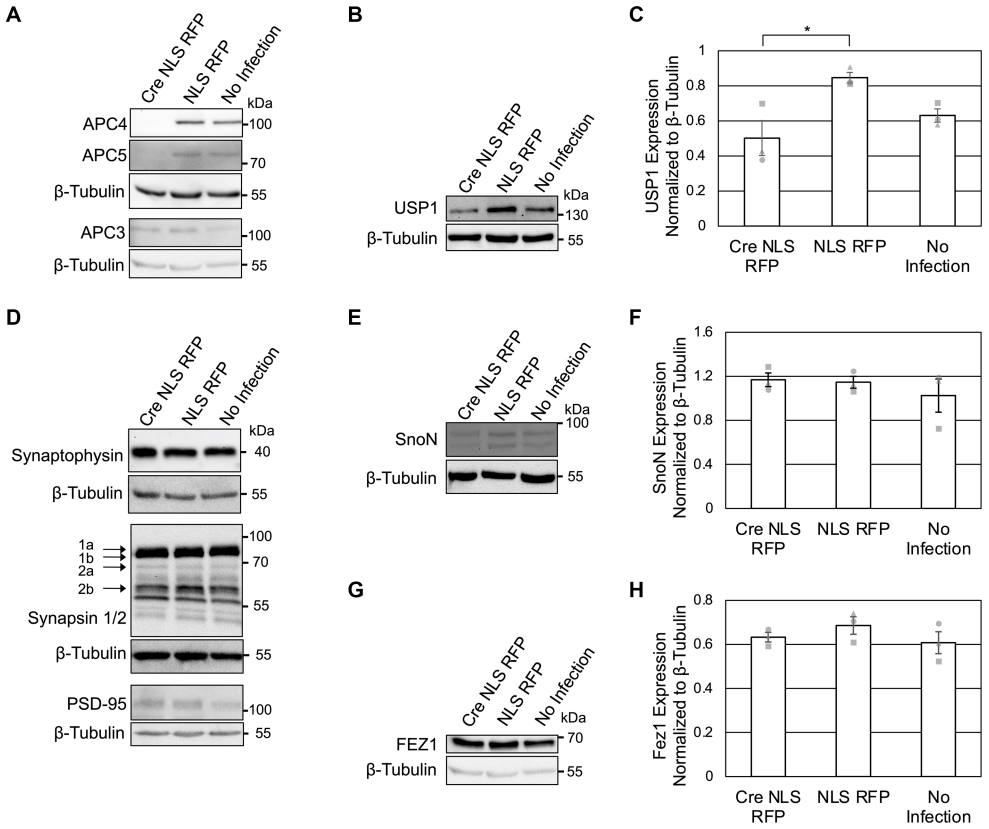

FIGURE 3
APC4 loss is accompanied by decreased USP1 protein levels in DIV11 neurons. **(A–H)** Cortical neurons were prepared from *ANAPC4* cKO mice and infected at DIV1 with Cre NLS RFP-or NLS RFP-expressing lentivirus. Cultures were harvested at DIV11, and lysates were analyzed by WB. Protein quantification was conducted by averaging values of three independent experiments (representative experiments displayed). Experiments 1, 2, and 3 are represented by a circle, triangle, and square, respectively. Error bars: SEM. **(A)** WB shows APC4, APC5, β-Tubulin, and APC3. **(B)** WB shows USP1 and β-Tubulin. **(C)** Bar graph depicting the average USP1 levels normalized to β-Tubulin. USP1 levels were increased in Cre NLS RFP-infected samples (asterisk: significance; $t(2) = -3.299$, $p = 0.030$). **(D)** WB shows Synaptophysin, β-Tubulin, Synapsin1/2, and PSD95. **(E)** WB shows SnoN and β-Tubulin. **(F)** Bar graph depicting the average levels of SnoN normalized to β-Tubulin. There was no significant difference in SnoN levels between Cre-and control-infected samples ($t(2) = 0.274$, $p = 0.798$). **(G)** WB shows FEZ1 and β-Tubulin. **(H)** Bar graph depicts the average levels of FEZ1 normalized to β-Tubulin. There was no significant difference in the FEZ1 levels between Cre-and control-infected samples ($t(2) = -1.163$, $p = 0.155$).

subcellular fractionation of mouse cortex, we detected APC4 in all fractions, including synaptosomes (Syn) and the crude PSD (PSD) fractions. APC4 was most abundant in the cytosolic fraction (S2), where it was strongly SUMOylated (Supplementary Figure S5A). In cycling HEK293 cells, APC4 was present in cytosolic and nuclear fractions, but SUMOylated APC4 was enriched in the nucleus (Supplementary Figures S5B,C).

We next examined if APC4 SUMOylation is involved in APC/C-dependent regulation of USP1 levels and the number of neurites exiting somata. We previously observed increased USP1 protein levels in DIV5 KO neurons (Figures 2D,E) and decreased USP1 protein levels in DIV11 KO neurons (Figures 3B,C). We repeated this analysis with cortical *ANAPC4* KO neurons infected with lentiviruses expressing Cre RFP, NLS RFP, or rescue viruses expressing Cre RFP APC4^{WT} (wildtype) or Cre RFP APC4$^{K772R/K797R}$ (SUMOylation-deficient). The levels of APC4 and APC5 were fully rescued in Cre RFP APC4^{WT}-and Cre RFP APC4$^{K772R/K797R}$-infected cultures, indicating that APC/C integrity was rescued (Figures 5A–D). Consistent with our prior experiments, we saw increased USP1 levels at DIV5 (Figures 5A,B) and decreased levels at DIV 11 (Figures 5C,D) in KO cultures. These changes in USP1 levels were rescued in Cre RFP APC4^{WT}-and Cre RFP APC4$^{K772R/K797R}$-infected cultures (Figures 5A–D), indicating that USP1 is indeed regulated, directly or indirectly, by the APC/C, albeit independently of APC4 SUMOylation. In a final set of experiments, we tested if APC4 SUMOylation affects the ability of the APC/C to regulate the number of primary neurites exiting somata (Figure 4F). We imaged DIV5 cortical neurons and analyzed primary neurite numbers using β III-Tubulin immunolabeling (Figures 5E–G). Similar to what we had observed previously, *ANAPC4* KO caused an increase in the number of neurites exiting somata (Figure 5G), and this KO phenotype was fully rescued in Cre RFP APC4^{WT}-and Cre RFP APC4$^{K772R/K797R}$-infected cultures (Figure 5G). This indicates that the APC/C does indeed regulate the number of primary neurites exiting somata, albeit in a manner that does not require APC4 SUMOylation.

4 Discussion

The present study was designed to examine APC/C function in developing neurons. We shut down APC/C function in cortical neurons by conditional deletion of the core APC/C component, APC4. The phenotype of APC4-deficient neurons indicates that the APC/C regulates the number of primary neurites and differentially

10.3389/fnmol.2024.1352782

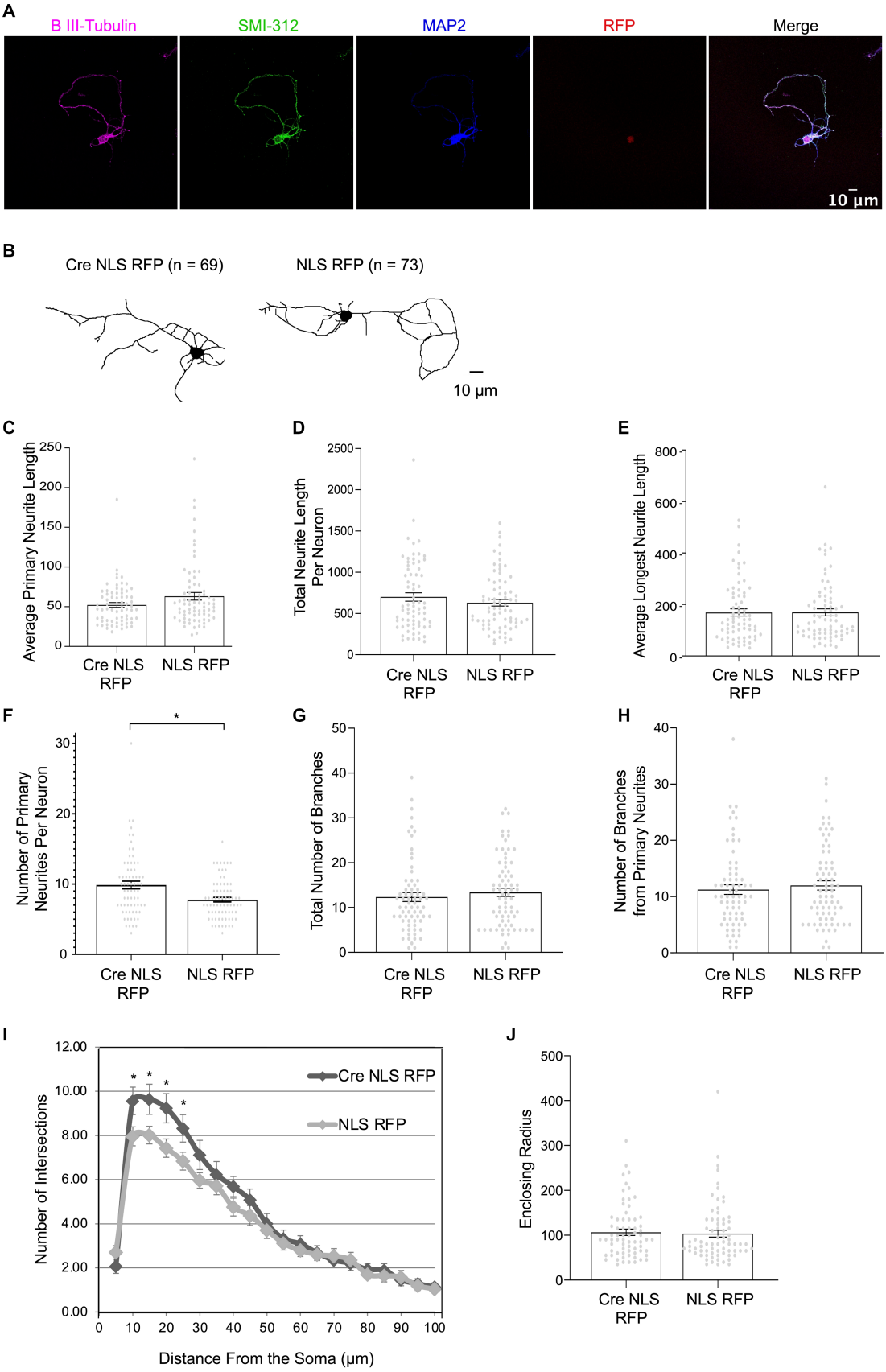

FIGURE 4
APC4-deficient cortical neurons form a greater number of primary neurites **(A–J)** Primary cortical neurons were prepared from *ANAPC4* cKO mice, and Cre-or control-infected neurons were fixed at DIV5, immunolabeled, and imaged. The β III-Tubulin label was traced and neuron morphology was

(Continued)

FIGURE 4 (Continued)

then analyzed from these traces. Statistical analysis compared the populations of Cre NLS RFP- ($n = 69$) and NLS RFP-infected neurons ($n = 73$). Asterisks: significant differences; error bars: SEM; circles: individual data points. **(A)** Representative images of a neuron infected with Cre NLS RFP shows immunolabeling of β III-Tubulin (magenta), SMI-312 (green), MAP2 (blue), RFP (red), and the merged images (black). Overlapping MAP2 and SMI-312 patterns indicate that the axon and dendrites are not specified by DIV5. Scale bar: 10 μm. **(B)** Representative skeletonized traces of β III-Tubulin in Cre NLS RFP- (left) and NLS RFP-infected neurons (right). Scale bar: 10 μm. **(C)** Bar graph depicts the average primary neurite length/cell ($t(120.829) = -1.919$, $p = 0.057$). **(D)** Bar graph depicts the average total neurite length, which is the sum of the lengths of all primary, secondary, and tertiary neurites ($t(130.812) = 1.083$, $p = 0.281$). **(E)** Bar graph depicts the average length of the longest neurite ($t(139.700) = -0.021$, $p = 0.984$). **(F)** Bar graph depicts the average number of primary neurites ≥3 μm ($t(111.91) = 3.251$, $p = 0.002$). **(G)** Bar graph depicts the average of the total number of neurite branches per cell ($t(138.785) = -0.661$, $p = 0.510$). **(H)** Bar graph depicts the average number of branches that form off a primary neurite. **(I)** Graph depicts Sholl analysis of traced neurons (10 μm: $t(122.207) = 2.119$, $p = 0.036$; 15 μm: $t(110.252) = 2.051$, $p = 0.043$; 20 μm: $t(114.993) = 2.311$, $p = 0.023$; 25 μm: $t(118.033) = 2.002$, $p = 0.048$; 30 μm: $t(103.932) = 1.546$, $p = 0.125$). **(J)** Bar graph depicts the average enclosing radius of a neuron ($t(139.496) = 0.283$, $p = 0.777$).

regulates USP1 protein levels at distinct developmental stages, and that these functions are independent of APC4 SUMOylation. Our data do not confirm prior studies employing depletion of the APC/C activators and indicating that the APC/C regulates neurite length and branching, synaptogenesis, or the levels of SnoN, NEUROD2, and FEZ1.

4.1 *ANAPC4* KO shuts down APC/C activity

After establishing that the neuronal APC/C contains APC4 (Figures 1A,B), we used a cKO mouse line to delete *ANAPC4*, the gene encoding APC4, in neuron cultures (Figure 1C). We calculated the APC4 protein half-life to be ~1.8 days in cortical cultures (Figure 1J), which is consistent with prior studies (Mathieson et al., 2018) and indicates that APC4 is rapidly depleted in cKO neurons upon Cre-mediated recombination.

Similar to studies on cycling cells (Thornton et al., 2006; Tran et al., 2010; Clark and Spector, 2015), we found that APC4 depletion causes the concomitant loss of APC5 in cortical (Figures 1I, 2A, 3A) and hippocampal (Figures 1D,E) neurons. This indicates that the loss of APC4 destabilizes the APC/C, rendering it dysfunctional. Indeed, studies on human cytomegalovirus show that the APC/C is not functional when APC4 or APC5 are depleted (Wiebusch et al., 2005; Tran et al., 2010). The fact that the canonical APC/C substrate, Cyclin B1, is increased upon *ANAPC4* KO (Figures 2B,C) supports the notion that *ANAPC4* KO leads to APC/C inactivation.

At first glance, the relatively modest increase in Cyclin B1 levels observed in KO neurons (Figures 2B,C) may appear surprising. In fact, this finding is not surprising for three reasons: (i) APC4 depletion is incomplete at DIV5 when we tested Cyclin B1 levels; (ii) the ability of the APC/C to ubiquitylate Cyclin B1 changes during the cell cycle and may vary in different cell types; (iii) other ubiquitin ligases, like Parkin, may control Cyclin B1 levels, which is also indicated by the fact that APC4 and Cyclin B1 levels decrease simultaneously during development (Lee et al., 2015).

4.2 APC/C inactivation and previously-proposed substrates

In our experiments, the levels of SnoN, FEZ1, and NEUROD2 were unaffected by *ANAPC4* KO neurons, indicating that these proteins are not APC/C substrates at DIV5 and DIV11 (Figures 2F–H, 3E–H; Supplementary Figures 1E,F). Our findings on SnoN are in accord with a previous study showing that APC2 KO in excitatory forebrain neurons does not affect SnoN levels, in spite of the fact that APC/C function requires APC2 (Wirth et al., 2004; Kuczera et al., 2011). While it is unclear why FEZ1 levels are unaffected in *ANAPC4* KO neurons, a possible explanation is that we worked with cultured neurons and the APC/C-FEZ1 link is based on an *in vivo* study (Watanabe et al., 2014).

One of the most intriguing APC/C substrates is NEUROD2, which was proposed to regulate synaptogenesis in an APC/C-modulated manner via a signaling pathway that involves Complexin 2 (Yang et al., 2009). We found NEUROD2 levels to be unaltered in *ANAPC4* KO neurons, indicating it is not an APC/C substrate in cortical neurons (Supplementary Figures S1E–F). In agreement with this, we did not detect changes in Complexin 1 and Complexin 2 levels upon APC4 loss (Supplementary Figures S1A–C). Complexin 3 levels are barely detectable in forebrain neuron cultures (Xue et al., 2008). Hence, it is intrinsically difficult to analyze Complexin 3 levels, and lentivirus infection increased Complexin 3 levels (Supplementary Figures S1A,D). Therefore, we are unable to make definitive statements regarding an interplay between the APC/C and Complexin 3. Similar, for instance, to human cytomegalovirus affecting the levels of APC/C components (Wiebusch et al., 2005; Thornton et al., 2006; Tran et al., 2010; Clark and Spector, 2015), lentiviral infection appears to affect the protein levels of Cyclin B1 (Figures 2B,C), Complexin 1 (Supplementary Figures S1A,B), and Complexin 3 (Supplementary Figures S1A,D).

Finally, we estimated the numbers of synapses per neuron in wildtype and KO cultures by counting PSD95 puncta co-localized with Synapsin1/2. While not strictly at single-synapse resolution, such an approach of combining co-labelling for pre-and postsynaptic markers and confocal imaging allows to estimate synapse numbers in neuron cultures with substantial reliability (Burgalossi et al., 2010, 2012), and a similar methodology was employed in the original study that indicated altered synapse density upon perturbation of Cdc20-APC/C function (Yang et al., 2009). Strikingly, we found no alterations in synapse numbers in KO neurons (Supplementary Figures S1G,H). Our data are in agreement with an earlier study employing a hypomorphic *Cdc20* deletion mutant mouse line, which is characterized by decreased Cdc20 expression but does not show altered NEUROD2 levels or changes in synapse numbers (Malureanu et al., 2010). Finally, a significant role of an APC/C-NEUROD2-Complexin pathway in synaptogenesis is in general implausible because

10.3389/fnmol.2024.1352782

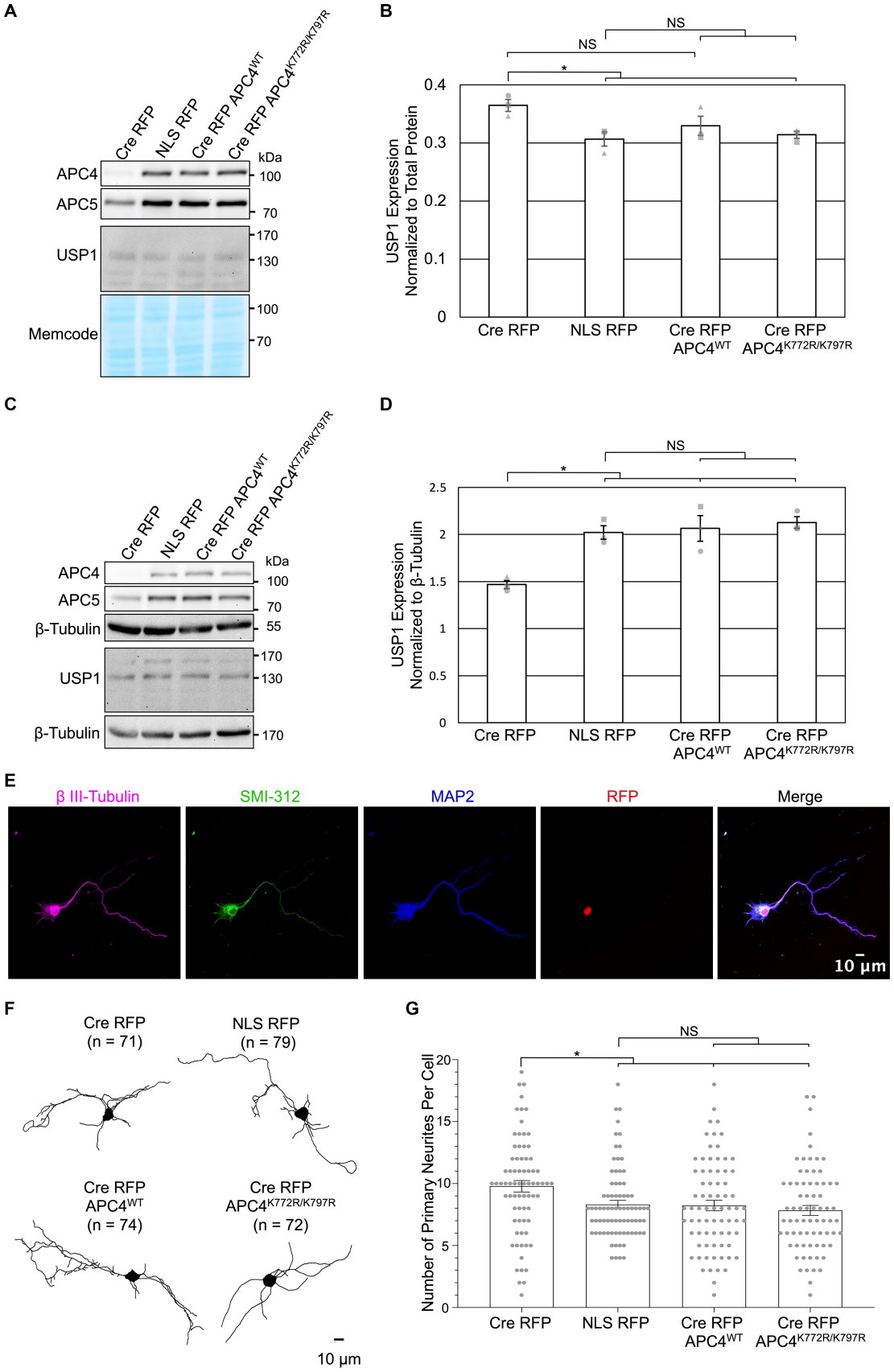

FIGURE 5
APC4 SUMOylation does not affect APC/C-dependent regulation of USP1 protein levels in DIV5 or DIV11 neurons. **(A–G)** Primary cortical neurons were prepared from *ANAPC4* cKO mice, infected at DIV1, and harvested at DIV5 or DIV11. Neurons were infected with lentivirus expressing Cre RFP, NLS RFP

(Continued)

FIGURE 5 (Continued)

control, or Cre-expressing rescue constructs in the form of Cre RFP APC4^{WT} (wildtype) or Cre RFP APC4$^{K772R/K797R}$ (SUMOylation-deficient). **(A)** WB analysis of DIV5 lysates immunoblotted for APC4, APC5, USP1, and MemCode (representative experiment). **(B)** Bar graph depicts average USP1 protein levels normalized to MemCode from three independent experiments. USP1 protein levels were elevated in Cre RFP-infected samples ($t(2) = 3.605$., $p = 0.023$), and USP1 protein levels were fully rescued to control levels by expressing APC4$^{K772R/K797R}$ (SUMOylation-deficient; $t(2) = 4.180$, $p = 0.014$) and there was a trend of rescue when APC4^{WT} (wildtype; $t(2) = 1.801$, $p = 0.146$) was expressed. Experiments 1, 2, and 3 are represented by a circle, triangle, and square, respectively. Asterisk: significant difference; NS: no significant difference; error bars: SEM. **(C)** WB analysis of DIV11 lysates immunoblotted for APC4, APC5, USP1, and β-Tubulin (representative experiment). **(D)** Bar graph depicts average USP1 levels normalized to β-Tubulin from three independent experiments. USP1 was decreased in Cre RFP-infected samples ($t(2) = -6.598$, $p = 0.003$), and the expression of Cre RFP APC4^{WT} (wildtype; $t(2) = -4.166$, $p = 0.014$) and Cre RFP APC4$^{K772R/K797R}$ (SUMOylation-deficient; $t(2) = -8.756$, $p = 0.001$) rescued this decrease. Experiments 1, 2, and 3 are represented by a circle, triangle, and square, respectively. Asterisk: significant difference; NS: no significant difference; error bars: SEM. **(E–G)** Maximum projection images of β III-tubulin was used to determine the number of neurites greater than 3 μm long that exit the somata on DIV5 cortical neurons. **(E)** Representative images of DIV5 neurons that were fixed, immunostained, and imaged. Scale bar: 10 μm. **(F)** Representative skeletonized traces of β III-Tubulin immunolabeling. Scale bar: 10 μm; (*n*), cells analyzed. **(G)** Bar graph depicts the average number of primary neurites longer than 10 μm. There was an increase in the number of primary neurites exiting the somata of neurons infected with Cre RFP ($t(127.462) = 2.602$, $p = 0.010$), and this phenotype was rescued by the expression of Cre RFP APC4^{WT} (wildtype; $t(136.883) = 3.201$, $p = 0.002$) and Cre RFP APC4$^{K772R/K797R}$ (SUMOylation-deficient; $t(117.113) = 6.964$, $p < 0.001$). Asterisk: significant difference; NS: no significant difference; error bars: SEM; circles: individual data points.

Complexin-deficient neurons show no changes in synaptogenesis (Reim et al., 2001; López-Murcia et al., 2019).

4.3 APC/C inactivation and neuronal morphology

Multiple studies involving the perturbation of the APC/C activators, Cdc20 or Cdh1, implicated the APC/C in regulating neurite length and complexity (Bobo-Jiménez et al., 2017), dendrite length and complexity (Kim et al., 2009; Watanabe et al., 2014), and axon length (Lasorella et al., 2006; Stegmüller et al., 2006, 2008; Li et al., 2019). FEZ1 (Watanabe et al., 2014) and SnoN (Stegmüller et al., 2006, 2008; Li et al., 2019) were suggested to be APC/C substrates involved in this context. Our data do not support these findings. First, our data indicate that FEZ1 and SnoN are not APC/C substrates in cultured mouse forebrain neurons (Figures 2F–H, 3E–H). Further, we did not detect effects of *ANAPC4* KO on neurite length (Figures 4C–E) and branching (Figures 4G,H), or overall neurite complexity (Figures 4I,J). Likewise, axon morphology does not appear to be affected by *ANAPC4* KO, as the enclosing radii of neurons (Figure 4J) and the length of the longest neurite were unaltered (Figure 4E). In agreement with our data, a hypomorphic *Cdc20* deletion mutant mouse neurons also showed normal dendrite lengths (Malureanu et al., 2010).

4.4 APC/C regulation of USP1 and the number of primary neurites

USP1 removes ubiquitin from substrate proteins, thereby stabilizing the substrate. Similar to prior studies indicating that USP1 is a Cdh1-APC/C substrate in cycling cells (Cotto-Rios et al., 2011; Cataldo et al., 2013), we found that USP1 protein levels are upregulated in *ANAPC4* KO cortical cultures at DIV5 (Figures 2D,E). A prior study showed that the APC/C ubiquitylates USP1 *in vitro* (Cotto-Rios et al., 2011), but corresponding *in vitro* assays often lead to false positives, which is evident when one compares prior data on SnoN (Stegmüller et al., 2006, 2008; Li et al., 2019) with our data (Figures 2F,G, 3E,F). Hence, it is unclear whether the APC/C directly ubiquitylates USP1 in neurons, and methods to address this question are currently lacking.

Strikingly, elevated USP1 protein levels observed in KO cultures at DIV5 (Figures 2D,E) reverted to decreased levels at DIV11 (Figures 3B,C). This observation is compatible with the notion that the APC/C ubiquitylates an unknown substrate in DIV11 cortical neurons that either directly or indirectly regulates USP1 levels. The physiological relevance of this differential regulation of USP1 by the APC/C is unclear. While it might simply reflect a transient requirement for a certain functionality during neuronal differentiation or development, the phenomenon may also represent a feedback mechanism in neurons, where the cell senses elevated USP1 levels or altered USP1 substrate levels and responds by decreasing USP1 protein levels. Such a feedback mechanism would be important for cells with chronic USP1 overexpression, as USP1 regulates genomic stability, thereby affecting the ability of neurons to correct DNA damage. USP1 is currently a major target for the development of cancer therapeutics, as USP1 inhibitors are effective in treating cancers with a BRCA1 mutation (García-Santisteban et al., 2013; Simoneau et al., 2023). Neurodegeneration is also associated with a dysregulation of genomic stability and changes in APC/C substrates (Fuchsberger et al., 2016), so USP1 may also be dysregulated during neurodegeneration. Recent studies indicate that USP1 may also regulate the circadian clock (Hu et al., 2024). In view of these considerations, a detailed understanding of how the neuronal APC/C differentially regulates USP1 protein levels may be important for developing cancer and neurodegeneration treatments.

While we did not observe changes in neurite length (Figures 4C,E) or branching (Figures 4G,H) upon APC4 loss, we discovered a phenotype that had previously not been attributed to APC/C function, namely an increase in the number of neurites exiting the somata of cortical neurons (Figure 4F). Given that neurite lengths were not altered, our data indicate that the APC/C affects a very early step in neurite formation, likely the step where actin is rearranged to form new neurites (Flynn, 2013). Interestingly, USP1 depletion in cultured neurons was previously reported to induce a decrease in the number of primary neurites exiting the somata (Anckar and Bonni, 2015). We observed the opposite effect in *ANAPC4* KO neurons, where increased USP1 levels were correlated with more primary neurites (Figure 4F), so the APC/C may in fact regulate neuron morphology through a pathway that involves USP1. Unfortunately, elucidating this pathway and its involvement in regulating the number of primary neurites is complicated by a

feedback mechanism connecting ID1, which is an USP1 substrate, to APC/C inhibition (Man et al., 2008; Chow et al., 2012).

4.5 APC4 SUMOylation does not impact APC/C activity

Our data confirm prior studies (Eifler et al., 2018; Lee et al., 2018) indicating that APC4 SUMOylation does not affect APC/C formation (Supplementary Figure S3) or APC4 localization (Supplementary Figure S4). Furthermore, we found that APC4 SUMOylation does not affect activator binding to the APC/C (Supplementary Figures 3C,D). Interestingly, the APC/C appeared to normally reside in a state where APC4 is non-SUMOylated, even when it was bound to an activator (Supplementary Figures 3C,D), which indicates that APC4 is only transiently SUMOylated. In view of this, we explored whether APC4 SUMOylation affects APC/C function.

We tested if APC4 SUMOylation affects the ability of the APC/C to regulate USP1 levels and neurite formation (Figures 2D,E, 3B,C, 4F). We found that wild-type and SUMOylation-deficient APC4 fully rescue the key *ANAPC4* KO phenotypes observed, including the concomitant loss of APC5, altered USP1 levels, and increased numbers of primary neurites. Our data indicate that these phenotypes are indeed due to *ANAPC4* KO and APC/C dysfunction, and that APC4 SUMOylation does not affect the corresponding APC/C functions (Figure 5).

Evidence from cycling cells indicates that APC4 SUMOylation affects the ability of APC/C to ubiquitylate a subset of substrates (Eifler et al., 2018; Lee et al., 2018; Yatskevich et al., 2021). For example, Hsl1 is ubiquitylated by the Cdh1-and the Cdc20-APC/C, but APC4 SUMOylation only affects the ability of the Cdh1-APC/C to ubiquitylate Hsl1 (Eifler et al., 2018; Yatskevich et al., 2021). The SUMOylated APC4 residues are located in the interior of the APC/C and thought to alter the conformation of the APC/C when it is bound to the MCC, which affects the ability of the Cdc20-APC/C to ubiquitylate Cyclin B1 and Securin (Yatskevich et al., 2021). Consistent with this notion, we show that APC4 SUMOylation is remarkably stable in buffers lacking NEM (Supplementary Figure S2B), indicating that the SUMOylated residues are not accessible to SENPs. While APC4 SUMOylation did not affect the ability of the APC/C to alter USP1 levels (Figures 5A–D), identification of novel neuronal APC/C substrates in the cytosol may enable the discovery of substrates that are likely differentially ubiquitylated by the SUMOylated complex.

4.6 Discrepancies between present and prior studies

Overall, our study indicates that many previously-proposed APC/C-linked substrates and phenotypes are not regulated by the APC/C in cortical neuron cultures. Several explanations can account for these discrepancies. First, species and cell-type differences may be the basis for the discrepant datasets, as we used mouse cortical neurons and other studies primarily employed rat cerebellar granule neurons. Second, knockdown approaches in neuron cultures are notorious for off-target effects that alter synaptic marker localization and neuronal morphology (Alvarez et al., 2006). Hence, some of the previously-published phenotypes may be due to off-target effects of corresponding knockdown approaches. Finally, most studies involved the depletion of Cdh1 or Cdc20 as a means to inactivate the APC/C, which is problematic because Cdh1 and Cdc20 can also function in an APC/C-independent manner (Wan et al., 2011, 2017; Kannan et al., 2012; Lee et al., 2015; Han et al., 2019). Hence, some of the substrates and phenotypes that were previously linked to the APC/C may be related to such "moonlighting" functions of Cdh1 and Cdc20. In any case, our data demonstrate that care must be taken when extrapolating APC/C function from experimental data obtained by perturbing APC/C activators, and that more stringent approaches are required to tie substrates and phenotypes to APC/C function.

Data availability statement

The original contributions presented in the study are included in the article/Supplementary material, further inquiries can be directed to the corresponding author.

Ethics statement

Ethical approval was not required for studies on humans in accordance with the local legislation and institutional requirements because only commercially available established cell lines were used. The animal study was approved by Niedersächsisches Landesamt für Verbraucherschutz und Lebensmittelsicherheit. The study was conducted in accordance with the local legislation and institutional requirements.

Author contributions

JD: Conceptualization, Data curation, Formal analysis, Investigation, Methodology, Project administration, Resources, Validation, Visualization, Writing – original draft, Writing – review & editing. MT: Conceptualization, Funding acquisition, Supervision, Visualization, Writing – original draft, Writing – review & editing. NB: Conceptualization, Funding acquisition, Supervision, Visualization, Writing – original draft, Writing – review & editing.

Funding

The author(s) declare financial support was received for the research, authorship, and/or publication of this article. This work was supported by the Deutsche Forschungsgemeinschaft (SFB1286-A09, MT and NB).

Acknowledgments

The *ANAPC4* cKO mouse line was obtained from EUCOMM. We thank the MPI-NAT AGTC Lab for genotyping,

primer synthesis, and sequencing, U. Fuenfschilling and the MPI-NAT Animal Facility for establishing and maintaining our mouse line, and J. Chua, J. Stegmüller, K.A. Nave, F. Melchior, M. Kirschner, A. Zeuch, and C. Rosenmund for reagents. We are indebted to H. Bastians, J. Daniel, H. Kawabe, E. Gideons, H. Taschenberger, A. Günther, D. Krüger-Burg, M. Mitkovski, H. Roehse, and C. Thomas for thoughtful discussions. A substantial dataset of this paper is part of the PhD thesis of JD.

Conflict of interest

The authors declare that the research was conducted in the absence of any commercial or financial relationships that could be construed as a potential conflict of interest.

Publisher's note

Supplementary material

The Supplementary material for this article can be found online at: https://www.frontiersin.org/articles/10.3389/fnmol.2024.1352782/full#supplementary-material

References

Almeida, A., Bolaños, J. P., and Moreno, S. (2005). Cdh1/Hct1-APC is essential for the survival of postmitotic neurons. *J. Neurosci.* 25, 8115–8121. doi: 10.1523/jneurosci.1143-05.2005

Alvarez, V. A., Ridenour, D. A., and Sabatini, B. L. (2006). Retraction of synapses and dendritic spines induced by off-target effects of RNA interference. *J. Neurosci.* 26, 7820–7825. doi: 10.1523/jneurosci.1957-06.2006

Anckar, J., and Bonni, A. (2015). Regulation of neuronal morphogenesis and positioning by ubiquitin-specific proteases in the cerebellum. *PLoS One* 10:e0117076. doi: 10.1371/journal.pone.0117076

Belle, A., Tanay, A., Bitincka, L., Shamir, R., and O'Shea, E. K. (2006). Quantification of protein half-lives in the budding yeast proteome. *Proc. Natl. Acad. Sci. USA* 103, 13004–13009. doi: 10.1073/pnas.0605420103

Bobo-Jiménez, V., Delgado-Esteban, M., Angibaud, J., Sánchez-Morán, I., de la Fuente, A., Yajeya, J., et al. (2017). APC/CCdh1-Rock2 pathway controls dendritic integrity and memory. *Proc. Natl. Acad. Sci. USA* 114, 4513–4518. doi: 10.1073/pnas.1616024114

Burgalossi, A., Jung, S., Man, K. N., Nair, R., Jockusch, W. J., Wojcik, S. M., et al. (2012). Analysis of neurotransmitter release mechanisms by photolysis of caged Ca^{2+} in an autaptic neuron culture system. *Nat. Protoc.* 7, 1351–1365. doi: 10.1038/nprot.2012.074

Burgalossi, A., Jung, S., Meyer, G., Jockusch, W. J., Jahn, O., Taschenberger, H., et al. (2010). SNARE protein recycling by αSNAP and βSNAP supports synaptic vesicle priming. *Neuron* 68, 473–487. doi: 10.1016/j.neuron.2010.09.019

Carlin, R. K., Grab, D. J., Cohen, R. S., and Siekevitz, P. (1980). Isolation and characterization of postsynaptic densities from various brain regions: enrichment of different types of postsynaptic densities. *J. Cell Biol.* 86, 831–845. doi: 10.1083/jcb.86.3.831

Cataldo, F., Peche, L. Y., Klaric, E., Brancolini, C., Myers, M. P., Demarchi, F., et al. (2013). CAPNS1 regulates USP1 stability and maintenance of genome integrity. *Mol. Cell. Biol.* 33, 2485–2496. doi: 10.1128/mcb.01406-12

Chen, B.-J., Lam, T. C., and Liu, L.-Q.To, C.-H (2017). Post-translational modifications and their applications in eye research. *Mol. Med. Rep.* 15, 3923–3935. doi: 10.3892/mmr.2017.6529

Chow, C., Wong, N., Pagano, M., Lun, S., Nakayama, K., Nakayama, K., et al. (2012). Regulation of APC/C Cdc20 activity by RASSF1A–APC/C Cdc20 circuitry. *Oncogene* 31, 1975–1987. doi: 10.1038/onc.2011.372

Clark, E., and Spector, D. H. (2015). Studies on the contribution of human cytomegalovirus UL21a and UL97 to viral growth and inactivation of the anaphase-promoting complex/Cyclosome (APC/C) E3 ubiquitin ligase reveal a unique cellular mechanism for downmodulation of the APC/C subunits APC1, APC4, and APC5. *J. Virol.* 89, 6928–6939. doi: 10.1128/jvi.00403-15

Cotto-Rios, X. M., Jones, M. J. K., Busino, L., Pagano, M., and Huang, T. T. (2011). APC/CCdh1-dependent proteolysis of USP1 regulates the response to UV-mediated DNA damage. *J. Cell Biol.* 194, 177–186. doi: 10.1083/jcb.201101062

Cubeñas-Potts, C., Srikumar, T., Lee, C., Osula, O., Subramonian, D., Zhang, X., et al. (2015). Identification of SUMO-2/3-modified proteins associated with mitotic chromosomes. *Proteomics* 15, 763–772. doi: 10.1002/pmic.201400400

Daniel, J. A., Cooper, B. H., Palvimo, J. J., Zhang, F.-P., Brose, N., and Tirard, M. (2017). Analysis of SUMO1-conjugation at synapses. *eLife* 6:e26338. doi: 10.7554/elife.26338

Eguren, M., Manchado, E., and Malumbres, M. (2011). Non-mitotic functions of the anaphase-promoting complex. *Semin. Cell Dev. Biol.* 22, 572–578. doi: 10.1016/j.semcdb.2011.03.010

Eifler, K., Cuijpers, S. A. G., Willemstein, E., Raaijmakers, J. A., Atmioui, D. E., Ovaa, H., et al. (2018). SUMO targets the APC/C to regulate transition from metaphase to anaphase. *Nat. Commun.* 9:1119. doi: 10.1038/s41467-018-03486-4

Fagerland, M. W., and Sandvik, L. (2009). Performance of five two-sample location tests for skewed distributions with unequal variances. *Contemp. Clin. Trials* 30, 490–496. doi: 10.1016/j.cct.2009.06.007

Flynn, K. C. (2013). The cytoskeleton and neurite initiation. *BioArchitecture* 3, 86–109. doi: 10.4161/bioa.26259

Fuchsberger, T., Martínez-Bellver, S., Giraldo, E., Teruel-Martí, V., Lloret, A., and Viña, J. (2016). Aβ induces excitotoxicity mediated by APC/C-Cdh1 depletion that can be prevented by glutaminase inhibition promoting neuronal survival. *Sci. Rep.* 6:31158. doi: 10.1038/srep31158

García-Santisteban, I., Peters, G. J., Giovannetti, E., and Rodríguez, J. A. (2013). USP1 deubiquitinase: cellular functions, regulatory mechanisms and emerging potential as target in cancer therapy. *Mol. Cancer* 12:91. doi: 10.1186/1476-4598-12-91

Gieffers, C., Peters, B. H., Kramer, E. R., Dotti, C. G., and Peters, J.-M. (1999). Expression of the CDH1-associated form of the anaphase-promoting complex in postmitotic neurons. *Proc. Natl. Acad. Sci. USA* 96, 11317–11322. doi: 10.1073/pnas.96.20.11317

Han, T., Jiang, S., Zheng, H., Yin, Q., Xie, M., Little, M. R., et al. (2019). Interplay between c-Src and the APC/C co-activator Cdh1 regulates mammary tumorigenesis. *Nat. Commun.* 10:3716. doi: 10.1038/s41467-019-11618-7

Hendriks, I. A., Lyon, D., Su, D., Skotte, N. H., Daniel, J. A., Jensen, L. J., et al. (2018). Site-specific characterization of endogenous SUMOylation across species and organs. *Nat. Commun.* 9:2456. doi: 10.1038/s41467-018-04957-4

Hu, Y., Li, X., Zhang, J., Liu, D., Lu, R., and Li, J. D. (2024). A genome-wide CRISPR screen identifies USP1 as a novel regulator of the mammalian circadian clock. *FEBS J.* 291, 445–457. doi: 10.1111/febs.16990

Ikeuchi, Y., Stegmüller, J., Netherton, S., Huynh, M. A., Masu, M., Frank, D., et al. (2009). A SnoN–Ccd1 pathway promotes axonal morphogenesis in the mammalian brain. *J. Neurosci.* 29, 4312–4321. doi: 10.1523/jneurosci.0126-09.2009

IMPC. (n.d.) Gene ANAPC4. International Mouse Phenotyping Consortium. Available at: https://www.mousephenotype.org/data/genes/MGI%3A1098673.

Kannan, M., Lee, S.-J., Schwedhelm-Domeyer, N., Nakazawa, T., and Stegmüller, J. (2012). p250GAP is a novel player in the Cdh1-APC/Smurf1 pathway of axon growth regulation. *PLoS One* 7:e50735. doi: 10.1371/journal.pone.0050735

Kempf, M., Clement, A., Faissner, A., Lee, G., and Brandt, R. (1996). Tau binds to the distal axon early in development of polarity in a microtubule-and microfilament-dependent manner. *J. Neurosci.* 16, 5583–5592. doi: 10.1523/jneurosci.16-18-05583.1996

Kim, A. H., Puram, S. V., Bilimoria, P. M., Ikeuchi, Y., Keough, S., Wong, M., et al. (2009). A centrosomal Cdc20-APC pathway controls dendrite morphogenesis in postmitotic neurons. *Cell* 136, 322–336. doi: 10.1016/j.cell.2008.11.050

Konishi, Y., Stegmüller, J., Matsuda, T., Bonni, S., and Bonni, A. (2004). Cdh1-APC controls axonal growth and patterning in the mammalian brain. *Science* 303, 1026–1030. doi: 10.1126/science.1093712

Kroeger, C. M., Ejima, K., Hannon, B. A., Halliday, T. M., McComb, B., Teran-Garcia, M., et al. (2021). Persistent confusion in nutrition and obesity research about the validity of classic nonparametric tests in the presence of heteroscedasticity:

evidence of the problem and valid alternatives. *Am. J. Clin. Nutr.* 113, 517–524. doi: 10.1093/ajcn/nqaa357

Kuczera, T., Stilling, R. M., Hsia, H.-E., Bahari-Javan, S., Irniger, S., Nasmyth, K., et al. (2011). The anaphase promoting complex is required for memory function in mice. *Learn. Mem.* 18, 49–57. doi: 10.1101/lm.1998411

Laemmli, U. K. (1970). Cleavage of structural proteins during the assembly of the head of bacteriophage T4. *Nature* 227, 680–685. doi: 10.1038/227680a0

Lasorella, A., Stegmüller, J., Guardavaccaro, D., Liu, G., Carro, M. S., Rothschild, G., et al. (2006). Degradation of Id2 by the anaphase-promoting complex couples cell cycle exit and axonal growth. *Nature* 442, 471–474. doi: 10.1038/nature04895

Ledvin, L., Gassaway, B. M., Tawil, J., Urso, O., Pizzo, D., Welsh, K. A., et al. (2023). The anaphase-promoting complex controls a ubiquitination-phosphoprotein axis in chromatin during neurodevelopment. *Dev. Cell* 58, 2666–2683.e9. doi: 10.1016/j.devcel.2023.10.002

Lee, S. B., Kim, J. J., Nam, H.-J., Gao, B., Yin, P., Qin, B., et al. (2015). Parkin regulates mitosis and genomic stability through Cdc20/Cdh1. *Mol. Cell* 60, 21–34. doi: 10.1016/j.molcel.2015.08.011

Lee, C. C., Li, B., Yu, H., and Matunis, M. J. (2018). Sumoylation promotes optimal APC/C activation and timely anaphase. *eLife* 7:e29539. doi: 10.7554/elife.29539

Li, Z., Zhang, B., Yao, W., Zhang, C., Wan, L., and Zhang, Y. (2019). APC-Cdh1 regulates neuronal apoptosis through modulating glycolysis and pentose-phosphate pathway after oxygen-glucose deprivation and reperfusion. *Cell. Mol. Neurobiol.* 39, 123–135. doi: 10.1007/s10571-018-0638-x

Liu, J., Wan, L., Liu, J., Yuan, Z., Zhang, J., Guo, J., et al. (2016). Cdh1 inhibits WWP2-mediated ubiquitination of PTEN to suppress tumorigenesis in an APC-independent manner. *Cell Discov.* 2:15044. doi: 10.1038/celldisc.2015.44

López-Murcia, F. J., Reim, K., Jahn, O., Taschenberger, H., and Brose, N. (2019). Acute Complexin knockout abates spontaneous and evoked transmitter release. *Cell Rep.* 26, 2521–2530.e5. doi: 10.1016/j.celrep.2019.02.030

Maestre, C., Delgado-Esteban, M., Gomez-Sanchez, J. C., Bolaños, J. P., and Almeida, A. (2008). Cdk5 phosphorylates Cdh1 and modulates cyclin B1 stability in excitotoxicity. *EMBO J.* 27, 2736–2745. doi: 10.1038/emboj.2008.195

Malureanu, L., Jeganathan, K. B., Jin, F., Baker, D. J., van Ree, J. H., Gullon, O., et al. (2010). Cdc20 hypomorphic mice fail to counteract de novo synthesis of cyclin B1 in mitosis. *J. Cell Biol.* 191, 313–329. doi: 10.1083/jcb.201003090

Man, C., Rosa, J., Yip, Y. L., Cheung, A. L.-M., Kwong, Y. L., Doxsey, S. J., et al. (2008). Id1 overexpression induces tetraploidization and multiple abnormal mitotic phenotypes by modulating Aurora a. *Mol. Biol. Cell* 19, 2389–2401. doi: 10.1091/mbc.e07-09-0875

Mata, G., Cuesto, G., Heras, J., Morales, M., Romero, A., and Rubio, J. (2017). Biomedical engineering systems and technologies, 9th international joint conference, BIOSTEC 2016, Rome, Italy, February 21–23, 2016, revised selected papers. Commun. Comput. Inf. Sci., 41–55.

Mathieson, T., Franken, H., Kosinski, J., Kurzawa, N., Zinn, N., Sweetman, G., et al. (2018). Systematic analysis of protein turnover in primary cells. *Nat. Commun.* 9:689. doi: 10.1038/s41467-018-03106-1

Matic, I., Schimmel, J., Hendriks, I. A., van de Rijke, F., van Dam, H., Gnad, F., et al. (2010). Site-specific identification of SUMO-2 targets in cells reveals an inverted SUMOylation motif and a hydrophobic cluster SUMOylation motif. *Mol. Cell* 39, 641–652. doi: 10.1016/j.molcel.2010.07.026

Meijering, E., Jacob, M., Sarria, J. -C. F., Steiner, P., Hirling, H., and Unser, M. (2004). Design and validation of a tool for neurite tracing and analysis in fluorescence microscopy images. *Cytometry A* 58A, 167–176. doi: 10.1002/cyto.a.20022

Oh, E., Akopian, D., and Rape, M. (2018). Principles of ubiquitin-dependent signaling. *Annu. Rev. Cell Dev. Biol.* 34, 137–162. doi: 10.1146/annurev-cellbio-100617-062802

Peters, J.-M. (2006). The anaphase promoting complex/cyclosome: a machine designed to destroy. *Nat. Rev. Mol. Cell Biol.* 7, 644–656. doi: 10.1038/nrm1988

Preibisch, S., Saalfeld, S., and Tomancak, P. (2009). Globally optimal stitching of tiled 3D microscopic image acquisitions. *Bioinformatics* 25, 1463–1465. doi: 10.1093/bioinformatics/btp184

Reim, K., Mansour, M., Varoqueaux, F., McMahon, H. T., Südhof, T. C., Brose, N., et al. (2001). Complexins regulate a late step in Ca2+−dependent neurotransmitter release. *Cell* 104, 71–81. doi: 10.1016/s0092-8674(01)00192-1

Reim, K., Wegmeyer, H., Brandstätter, J. H., Xue, M., Rosenmund, C., Dresbach, T., et al. (2005). Structurally and functionally unique complexins at retinal ribbon synapses. *J. Cell Biol.* 169, 669–680. doi: 10.1083/jcb.200502115

Schimmel, J., Eifler, K., Sigurðsson, J. O., Cuijpers, S. A. G., Hendriks, I. A., Verlaan-de Vries, M., et al. (2014). Uncovering SUMOylation dynamics during cell-cycle progression reveals FoxM1 as a key mitotic SUMO target protein. *Mol. Cell* 53, 1053–1066. doi: 10.1016/j.molcel.2014.02.001

Schindelin, J., Arganda-Carreras, I., Frise, E., Kaynig, V., Longair, M., Pietzsch, T., et al. (2012). Fiji: an open-source platform for biological-image analysis. *Nat. Methods* 9, 676–682. doi: 10.1038/nmeth.2019

Sholl, D. A. (1953). Dendritic organization in the neurons of the visual and motor cortices of the cat. *J. Anat.* 87, 387–406.

Simoneau, A., Engel, J. L., Bandi, M., Lazarides, K., Liu, S., Meier, S. R., et al. (2023). Ubiquitinated PCNA drives USP1 synthetic lethality in cancer. *Mol. Cancer Ther.* 22, 215–226. doi: 10.1158/1535-7163.MCT-22-0409

Skovlund, E., and Fenstad, G. U. (2001). Should we always choose a nonparametric test when comparing two apparently nonnormal distributions? *J. Clin. Epidemiol.* 54, 86–92. doi: 10.1016/s0895-4356(00)00264-x

Stegmüller, J., Huynh, M. A., Yuan, Z., Konishi, Y., and Bonni, A. (2008). TGFβ-Smad2 signaling regulates the Cdh1-APC/SnoN pathway of axonal morphogenesis. *J. Neurosci.* 28, 1961–1969. doi: 10.1523/jneurosci.3061-07.2008

Stegmüller, J., Konishi, Y., Huynh, M. A., Yuan, Z., DiBacco, S., and Bonni, A. (2006). Cell-intrinsic regulation of axonal morphogenesis by the Cdh1-APC target SnoN. *Neuron* 50, 389–400. doi: 10.1016/j.neuron.2006.03.034

Tavares, G., Martins, M., Correia, J. S., Sardinha, V. M., Guerra-Gomes, S., das Neves, S. P., et al. (2017). Employing an open-source tool to assess astrocyte tridimensional structure. *Brain Struct. Funct.* 222, 1989–1999. doi: 10.1007/s00429-016-1316-8

Tirard, M., Hsiao, H.-H., Nikolov, M., Urlaub, H., Melchior, F., Brose, N.. (2012). In vivo localization and identification of SUMOylated proteins in the brain of His6-HA-SUMO1 knock-in mice. *Proc. Natl. Acad. Sci.* 109, 21122–21127. doi: 10.1073/pnas.1215366110

Thornton, B. R., Ng, T. M., Matyskiela, M. E., Carroll, C. W., Morgan, D. O., and Toczyski, D. P. (2006). An architectural map of the anaphase-promoting complex. *Genes Dev.* 20, 449–460. doi: 10.1101/gad.1396906

Tomomori-Sato, C., Sato, S., Conaway, R. C., and Conaway, J. W. (2013). Gene regulation, methods and protocols. *Methods Mol. Biol.* 977, 273–287. doi: 10.1007/978-1-62703-284-1_22

Towbin, H., Staehelin, T., and Gordon, J. (1979). Electrophoretic transfer of proteins from polyacrylamide gels to nitrocellulose sheets: procedure and some applications. *Proc. Natl. Acad. Sci. USA* 76, 4350–4354. doi: 10.1073/pnas.76.9.4350

Tran, K., Kamil, J. P., Coen, D. M., and Spector, D. H. (2010). Inactivation and disassembly of the anaphase-promoting complex during human cytomegalovirus infection is associated with degradation of the APC5 and APC4 subunits and does not require UL97-mediated phosphorylation of Cdh1. *J. Virol.* 84, 10832–10843. doi: 10.1128/jvi.01260-10

Wan, L., Chen, M., Cao, J., Dai, X., Yin, Q., Zhang, J., et al. (2017). The APC/C E3 ligase complex activator FZR1 restricts BRAF oncogenic function. *Cancer Discov.* 7, 424–441. doi: 10.1158/2159-8290.cd-16-0647

Wan, L., Zou, W., Gao, D., Inuzuka, H., Fukushima, H., Berg, A. H., et al. (2011). Cdh1 regulates osteoblast function through an APC/C-independent modulation of Smurf1. *Mol. Cell* 44, 721–733. doi: 10.1016/j.molcel.2011.09.024

Watanabe, Y., Khodosevich, K., and Monyer, H. (2014). Dendrite development regulated by the schizophrenia-associated gene FEZ1 involves the ubiquitin proteasome system. *Cell Rep.* 7, 552–564. doi: 10.1016/j.celrep.2014.03.022

Wiebusch, L., Bach, M., Uecker, R., and Hagemeier, C. (2005). Human cytomegalovirus inactivates the G0/G1-APC/C ubiquitin ligase by Cdh1 dissociation. *Cell Cycle* 4, 1435–1439. doi: 10.4161/cc.4.10.2077

Wirth, K. G., Ricci, R., Giménez-Abián, J. F., Taghybeeglu, S., Kudo, N. R., Jochum, W., et al. (2004). Loss of the anaphase-promoting complex in quiescent cells causes unscheduled hepatocyte proliferation. *Genes Dev.* 18, 88–98. doi: 10.1101/gad.285404

Xue, M., Stradomska, A., Chen, H., Brose, N., Zhang, W., Rosenmund, C., et al. (2008). Complexins facilitate neurotransmitter release at excitatory and inhibitory synapses in mammalian central nervous system. *Proc. Natl. Acad. Sci. USA* 105, 7875–7880. doi: 10.1073/pnas.0803012105

Yang, Y., Kim, A. H., Yamada, T., Wu, B., Bilimoria, P. M., Ikeuchi, Y., et al. (2009). A Cdc20-APC ubiquitin signaling pathway regulates presynaptic differentiation. *Science* 326, 575–578. doi: 10.1126/science.1177087

Yatskevich, S., Kroonen, J. S., Alfieri, C., Tischer, T., Howes, A. C., Clijsters, L., et al. (2021). Molecular mechanisms of APC/C release from spindle assembly checkpoint inhibition by APC/C SUMOylation. *Cell Rep.* 34:108929. doi: 10.1016/j.celrep.2021.108929

frontiers | Frontiers in Molecular Neuroscience

TYPE Original Research
PUBLISHED 24 June 2024
DOI 10.3389/fnmol.2024.1375297

OPEN ACCESS

EDITED BY
Jiusheng Yan,
University of Texas MD Anderson Cancer Center, United States

REVIEWED BY
Maria Joana Guimarães Pinto,
Universidade do Porto, Portugal
Tao Wang,
National Institute of Biological Sciences (NIBS), China

*CORRESPONDENCE
Patricia Franzka
✉ Patricia.Franzka@med.uni-jena.de
Christian A. Hübner
✉ Christian.Huebner@med.uni-jena.de

RECEIVED 23 January 2024
ACCEPTED 31 May 2024
PUBLISHED 24 June 2024

CITATION
Franzka P, Mittag S, Chakraborty A, Huber O and Hübner CA (2024) Ubiquitination contributes to the regulation of GDP-mannose pyrophosphorylase B activity. *Front. Mol. Neurosci.* 17:1375297. doi: 10.3389/fnmol.2024.1375297

Ubiquitination contributes to the regulation of GDP-mannose pyrophosphorylase B activity

Patricia Franzka[1]*, Sonnhild Mittag[2], Abhijnan Chakraborty[1], Otmar Huber[2] and Christian A. Hübner[1]*

[1]Institute of Human Genetics, Jena University Hospital, Friedrich Schiller University, Jena, Germany, [2]Department of Biochemistry II, Jena University Hospital, Friedrich Schiller University, Jena, Germany

GDP-mannose pyrophosphorylase B (GMPPB) loss-of-function is associated with muscular dystrophy and variable additional neurological symptoms. GMPPB facilitates the catalytic conversion of mannose-1-phosphate and GTP to GDP-mannose, which serves as a mannose donor for glycosylation. The activity of GMPPB is regulated by its non-catalytic paralogue GMPPA, which can bind GDP-mannose and interact with GMPPB, thereby acting as an allosteric feedback inhibitor of GMPPB. Using pulldown, immunoprecipitation, turnover experiments as well as immunolabeling and enzyme activity assays, we provide first direct evidence that GMPPB activity is regulated by ubiquitination. We further show that the E3 ubiquitin ligase TRIM67 interacts with GMPPB and that knockdown of TRM67 reduces ubiquitination of GMPPB, thus reflecting a candidate E3 ligase for the ubiquitination of GMPPB. While the inhibition of GMPPB ubiquitination decreases its enzymatic activity, its ubiquitination neither affects its interaction with GMPPA nor its turnover. Taken together, we show that the ubiquitination of GMPPB represents another level of regulation of GDP-mannose supply.

KEYWORDS

GMPPB, ubiquitination, activity, Neuro-2a, glycosylation, TRIM67

Introduction

GDP-mannose pyrophosphorylase B (GMPPB) catalyzes the conversion of guanosine triphosphate and mannose-1-phosphate to GDP-mannose, which serves as the activated form of mannose required for glycosylation. This complex process is initiated in the endoplasmic reticulum (ER) and proceeds in the Golgi apparatus. Glycosylation can have important consequences for protein folding, stability, localization, turnover, and protein-protein interactions (Varki et al., 2009). For example, hypoglycosylation due to decreased GMPPB activity decreases the stability and abundance of α-dystroglycan (Franzka et al., 2021a). α-dystroglycan is a peripheral membrane component of the dystrophin-glycoprotein complex (DGC), which can be found in the muscle, nerve, heart, and brain (Ervasti and Campbell, 1991; Carss et al., 2013; Belaya et al., 2015; Jensen et al., 2015; Astrea et al., 2018). Mutations in GMPPB lead to variable neurological diseases ranging from severe congenital muscular dystrophy to myasthenic syndromes with eye and brain symptoms (Carss et al., 2013; Belaya et al., 2015). Notably, disease severity correlates with residual GMPPB activity (Liu et al., 2021).

GDP-mannose pyrophosphorylase A (GMPPA) is a catalytically inactive paralogue of GMPPB, which can still bind GDP-mannose. We have previously shown that GMPPA directly interacts with GMPPB and inhibits the activity of GMPPB in a GDP-mannose-dependent manner (Franzka et al., 2021a). Thus, the absence of GMPPA in men (Koehler et al., 2013) or mice (Franzka et al., 2021a) results in increased GDP-mannose levels, hypermannosylation of

different proteins, including α-dystroglycan, and characteristic neurological symptoms (Franzka et al., 2021a).

Notably, GMPPB itself is also a substrate for post-translational modifications, including glycosylation, phosphorylation, and ubiquitination (Hornbeck et al., 2015). Ubiquitination refers to the covalent binding of ubiquitin at lysine residues of the target protein, which involves the concerted action of E1 ubiquitin-activating enzymes, E2 ubiquitin-conjugating enzymes, and E3 ubiquitin-protein ligases (Hershko and Ciechanover, 1998; Dikic and Schulman, 2023). The latter constitutes a large superfamily with three main subclasses: Homologous to E6AP C-Terminus (HECT) E3 ubiquitin ligases, Really Interesting New Gene/U-box (RING) E3 ubiquitin ligases, and RING between RING (RBR) E3 ubiquitin ligases (Uchida and Kitagawa, 2016; Yang et al., 2021). Ubiquitination occurs in various forms, ranging from simple mono-ubiquitination to polymeric ubiquitin chains with complex topologies (Kwon and Ciechanover, 2017).

One of the best-understood functions of ubiquitination is protein degradation, which is achieved by targeting proteins to the proteasome (Kaiser and Huang, 2005; Kirkpatrick et al., 2006). Ubiquitin tagging can also provide a signal to target proteins for lysosomal degradation (Komander and Rape, 2012). However, ubiquitination can also act as a regulatory signal that alters the activity, localization, and ultimate fate of the respective protein. For example, we recently showed that ubiquitination promotes the clustering of ER membrane-shaping proteins and its binding to LC3, thus regulating the degradation of ER-fragments by ER-phagy (Khaminets et al., 2015; Foronda et al., 2023; González et al., 2023). Ubiquitination can also promote the interaction between proteins and even regulate enzyme activities (Walczak et al., 2012; Swatek and Komander, 2016; Wang et al., 2022).

In this study, we provide the first evidence that the enzymatic activity of GMPPB is modulated by ubiquitination, revealing an additional level of regulation in addition to allosteric feedback inhibition via GMPPA.

Methods

Cell culture

All cell lines used in this study were obtained from ATCC, Wesel (Germany). HEK-293 T, HEK-293, and Neuro-2a (N2A) cells were cultured in DMEM Glutamax (Sigma-Aldrich, Sant Gallen, Switzerland) supplemented with 10% (v/v) of FBS (Gibco, Dreieich, Germany) and 1% (v/v) of penicillin/streptomycin (Gibco, Dreieich, Germany) at 37°C.

MG132, bafilomycin A1, and cycloheximide treatment

HEK-293 T cells were seeded and treated with either 10 µM of MG132 (Merck, Darmstadt, Germany) or 100 nM of bafilomycin A1 (Merck, Darmstadt, Germany) for different time points. Then, cells were lysed in lysis buffer (50 mM of Tris–HCl pH 7.4, 150 mM of NaCl, 1% (v/v) of NP-40, 1% (w/v) of sodium deoxycholate, 0.1% (w/v) of SDS, and 1 mM of EDTA) and complete protease inhibitor (Roche, Mannheim, Germany). Homogenates were centrifuged at 16,900 *g* to remove nuclei and insoluble debris. Protein concentration was determined using the Pierce BCA assay kit (Thermo Fischer, Dreieich, Germany). The supernatant was stored at −80°C until further use. For degradation analysis of overexpressed GMPPB WT and mutant constructs, HEK-293 T cells were transfected with vectors encoding 3xFLAG-GMPPB, 3xFLAG-GMPPB D334N, and 3xFLAG-GMPPB K143/162/195R with lipofectamine 200 reagent (Invitrogen, Dreieich, Germany). The next day, cells were treated with 100 nM of bafilomycin (Merck, Darmstadt, Germany) for 15 h. Then, the cells were lysed and processed as described above. For turnover experiments, HEK-293 T cells were either transfected with vectors encoding 3xFLAG-GMPPB, 3xFLAG-GMPPB D334N, or 3xFLAG-GMPPB K143/162/195R with lipofectamine 200 reagent (Invitrogen, Dreieich, Germany). The next day, cells were treated with 10 µM of cycloheximide (Sigma-Aldrich, Sant Gallen, Switzerland) at different time points. Then, cells were lysed and processed as described above.

Co-localization and immunofluorescence microscopy

N2A cells were seeded, either not transfected or transfected with the vector encoding 3xFLAG-GMPPB WT using the lipofectamine 2000 reagent (Invitrogen, Dreieich, Germany), and treated with Earle's Balanced Salt Solution (EBSS, Thermo Fischer, Dreieich, Germany) containing 1% (v/v) of penicillin/streptomycin and/or 100 nM of bafilomycin (Merck, Darmstadt, Germany) for 6 h. Cells were fixed with 4% of paraformaldehyde (PFA), blocked with 5% (v/v) with normal goat serum, and incubated with primary antibodies overnight at 4°C. For immunofluorescence detection, the following primary antibodies were used: rabbit anti-GMPPB (Proteintech, 15,094-1-AP, Planegg-Martinsried, Germany) 1:100, mouse anti-p62 (Abcam, ab56416, Cambridge, United Kingdom) 1:500, rat anti-LAMP1 (BD Pharmingen, 553,792, Heidelberg, Germany) 1:500, and rabbit anti-FLAG (Sigma-Aldrich, F7425) 1:1000. Corresponding secondary antibodies were obtained from Invitrogen. Nuclei were stained with DAPI 1:10,000 (Thermo Fischer, H3569, Dreieich, Germany). Samples were mounted with Fluoromount-G (Southern Biotech, Eching, Germany). Images were taken using a Zeiss LSM880, Jena (Germany) Airyscan confocal microscope. Z-projections with average intensities processed with ImageJ are shown. Co-localization was analyzed with the Comdet v05 plugin from ImageJ.

For localization analysis of overexpressed WT and mutant GMPPB protein, HEK-293 T cells were either transfected with 3xFLAG-GMPPB WT, 3xFLAG-GMPPB D334N, or 3xFLAG-GMPPB K143/162/195R with lipofectamine 2000 (Invitrogen, Dreieich, Germany). The next day, cells were fixed with 4% of PFA, blocked with 5% (v/v) of normal goat serum, and incubated with rabbit anti-FLAG M2 antibody (Sigma-Aldrich, F3165, Sant Gallen, Switzerland) 1:1,000 overnight at 4°C. After washing with phosphate-buffered saline (PBS) buffer, specimens were incubated with the respective secondary antibodies (Invitrogen, Dreieich, Germany) for 2 h and subsequently treated with a mounting medium. Imaging was performed using a Keyence BZ-X800E, Erfurt (Germany) microscope.

Co-immunoprecipitation and Ni-NTA pulldown

HEK-293 T or HEK-293 cells were either transfected with vectors encoding GMPPA-Myc$_6$, 3xFLAG-GMPPB, 3xFLAG-GMPPB D27H,

3xFLAG-GMPPB P103L, 3xFLAG-GMPPB R287Q, 3xFLAG-GMPPB D334N, 3xFLAG-GMPPB K143/162/195R, His_6-ubiquitin or HA-ubiquitin, or HA-TRIM67 (the TRIM67 cDNA was a gift from Sevin Turcan (DKFZ Heidelberg, Germany)), using lipofectamine 2000 reagent (Invitrogen, Dreieich, Germany) or polyethylenimine. For the knockdown of TRIM67, cells were transfected with 600 pmol of siRNA either directed against TRIM67 (Thermo Fischer, Dreieich, Germany) or scrambled control (Dharmacon, Colorado, Unites States) using the lipofectamine 2000 reagent (Invitrogen, Dreieich, Germany) a day before transfection with the respective vectors. Two days after transfection, cells were lysed using imidazole lysis buffer (20 mM of imidazole pH 8.0, 150 mM of NaCl, 2 mM of $MgCl_2$, 300 mM of sucrose, and 0.25% (v/v) of Triton X-100) and centrifuged at 16,900 *g*. The supernatant was incubated with either anti-Myc- and anti-FLAG-antibodies coupled to Protein A Sepharose™ CL-4B (Cytiva, Glattbrugg, Switzerland) or Ni-NTA agarose (Qiagen, Hilden, Germany) at 4°C for 2 h. After 3–6 washing cycles with lysis buffer, samples were boiled at 95°C for 10 min in Laemmli sample buffer.

Western blot analysis

Proteins were denatured at 95°C for 5 min in Laemmli buffer. After separation by SDS-PAGE (10% of polyacrylamide gels), proteins were transferred onto PVDF membranes (Whatman, Hilden, Germany, Roth, Dautphetal, Germany). Membranes were blocked in 2% (w/v) of bovine serum albumin (BSA) and incubated with primary antibodies at appropriate dilutions overnight at 4°C. The following primary antibodies were used: rabbit anti-GMPPA (Proteintech, 15,517-1-AP, Planegg-Martinsried, Germany) 1:500, rabbit anti-GMPPB (Proteintech, 15,094-1-AP, Planegg-Martinsried, Germany) 1:500, rabbit anti-GAPDH (Proteintech, 10,494-1-AP, Planegg-Martinsried, Germany) 1:1,000, rabbit anti-Myc (Merck, 06–340, Darmstadt, Germany) 1:1,000, rabbit anti-FLAG M2 (Sigma-Aldrich, F3165, Sant Gallen, Switzerland) 1:1,000, rabbit anti-ubiquitin (Proteintech, 10,201-2-AP, Planegg-Martinsried, Germany) 1:1,000, and rat anti-HA (Roche, 11,867,423,001, Mannheim, Germany) 1:1,000. Primary antibodies were detected with HRP-conjugated secondary antibodies. The detection was performed using the Clarity Western ECL Substrate Kit (BioRad). The quantification of bands was performed with ImageJ.

Coomassie blue staining of PVDF membranes was performed as described before (Franzka et al., 2021b) after protein detection. For Coomassie blue staining of transferred proteins, PVDF membranes were fixed for 3 min (10% (v/v) of acetic acid and 40% (v/v) of EtOH), stained in Coomassie blue solution (0.1% (w/v) of Brilliant Blue R (Serva), 45% (v/v) of EtOH, and 10% (v/v) of acetic acid) for 5 min, destained (10% (v/v) of acetic acid, 20% (v/v) of EtOH), rinsed in H_2O, and then imaged.

Enzyme activity assays

HEK-293 T cells were transfected with vectors either encoding 3xFLAG-GMPPB WT, 3xFLAG-GMPPB D334N, 3xFLAG-GMPPB K143/162/195R, or 3xFLAG-GMPPB K143/162/195R D334N with lipofectamine 2000 (Invitrogen, Dreieich, Germany). After 24 h, cells were treated with or without PYR-41 (Merck, Darmstadt, Germany) to inhibit ubiquitination. After another 24 h, proteins were isolated and enriched via methanol/chloroform precipitation for protein quantification. Protein pellets were homogenized in assay buffer (25 mM of Tris–HCl pH 7.5, 150 mM of NaCl, 4 mM of $MgCl_2$, 0.01% (v/v) of Tween 20, 1 mM of dithiothreitol in ultrapure water supplemented with complete protein inhibitor cocktail (Roche, Mannheim, Germany)), and protein concentration was measured using the BCA assay kit (Thermo Fischer, Dreieich, Germany).

Recombinant human MBP-GMPPB and MBP-GMPPB K143/162/195R were expressed in *E. coli* (Merck, Darmstadt, Germany) using the pMal-c2X plasmids and purified on amylose-resin (New England Biolabs, Frankfurt, Germany).

The GDP-mannose-pyrophosphorylase activity was measured as described before (Franzka et al., 2021a) by determining the quantity of inorganic phosphate generated from pyrophosphate in the presence of mannose-1-phosphate (150 µM), GTP (300 µM), and excess pyrophosphatase (1 U/mL, Merck, Darmstadt, Germany) in assay buffer at 37°C for 60 min. Biochemical reactions were terminated by adding equal volumes of revelation buffer (0.03% (w/v) of malachite green (Sigma-Aldrich, Sant Gallen, Switzerland), 0.2% (w/v) of ammonium molybdate, 0.05% (v/v) of Triton X-100 in 0.7 M HCl) at 30°C for 5 min, and the absorbance was measured at 650 nm.

Statistical analyses

For statistical analysis, raw data were analyzed for normal distribution with the Kolmogorov–Smirnov goodness-of-fit test or with graphical analysis using the Box-Plot and QQ-Plot. If appropriate, we either used one-way ANOVA, two-way ANOVA, or Student's t-test. * indicates $p < 0.01$, *** $p < 0.001$ and **** $p < 0.0001$. For statistical analysis, we used GraphPad Prism 5. For all data, means with the standard error of the mean (SEM) or individual data points with SEM were shown.

Results

GMPPB is ubiquitinated

According to the PhosphoSitePlus database, lysines 143, 162, and 195 of GMPPB are reported to be ubiquitinated (Hornbeck et al., 2015; Akimov et al., 2018). To confirm that GMPPB is indeed a target for ubiquitination, we co-transfected HEK-293 T cells with FLAG-GMPPB and His_6-ubiquitin constructs. Subsequently, ubiquitin and ubiquitinated proteins were pulled down from cell lysates with Ni-NTA beads and analyzed by Western blotting. Indeed, bands for ubiquitinated FLAG-tagged GMPPB were detectable in the pulldown (Figure 1A). Notably, upon co-precipitation of GMPPB with ubiquitin, a second higher molecular weight band of around 60 kDa was present, which was not visible in input samples that contained 5% of the input used for precipitation (Figure 1A). This higher molecular weight band potentially represents mono- and poly/multi-ubiquitinated GMPPB. To further confirm this assumption, we co-transfected HEK-293 T cells with FLAG-GMPPB and HA-ubiquitin constructs and immunoprecipitated GMPPB with anti-FLAG antibodies. Subsequent SDS-PAGE and Western blotting with an anti-HA-tag antibody revealed a ladder of ubiquitinated bands in co-transfected cells but not in cells transfected with HA-ubiquitin or FLAG-GMPPB alone (Figure 1B).

Next, we co-transfected HEK-293 T cells with FLAG-GMPPB and different ubiquitin variants (K0, K63R, K48R, and K29R).

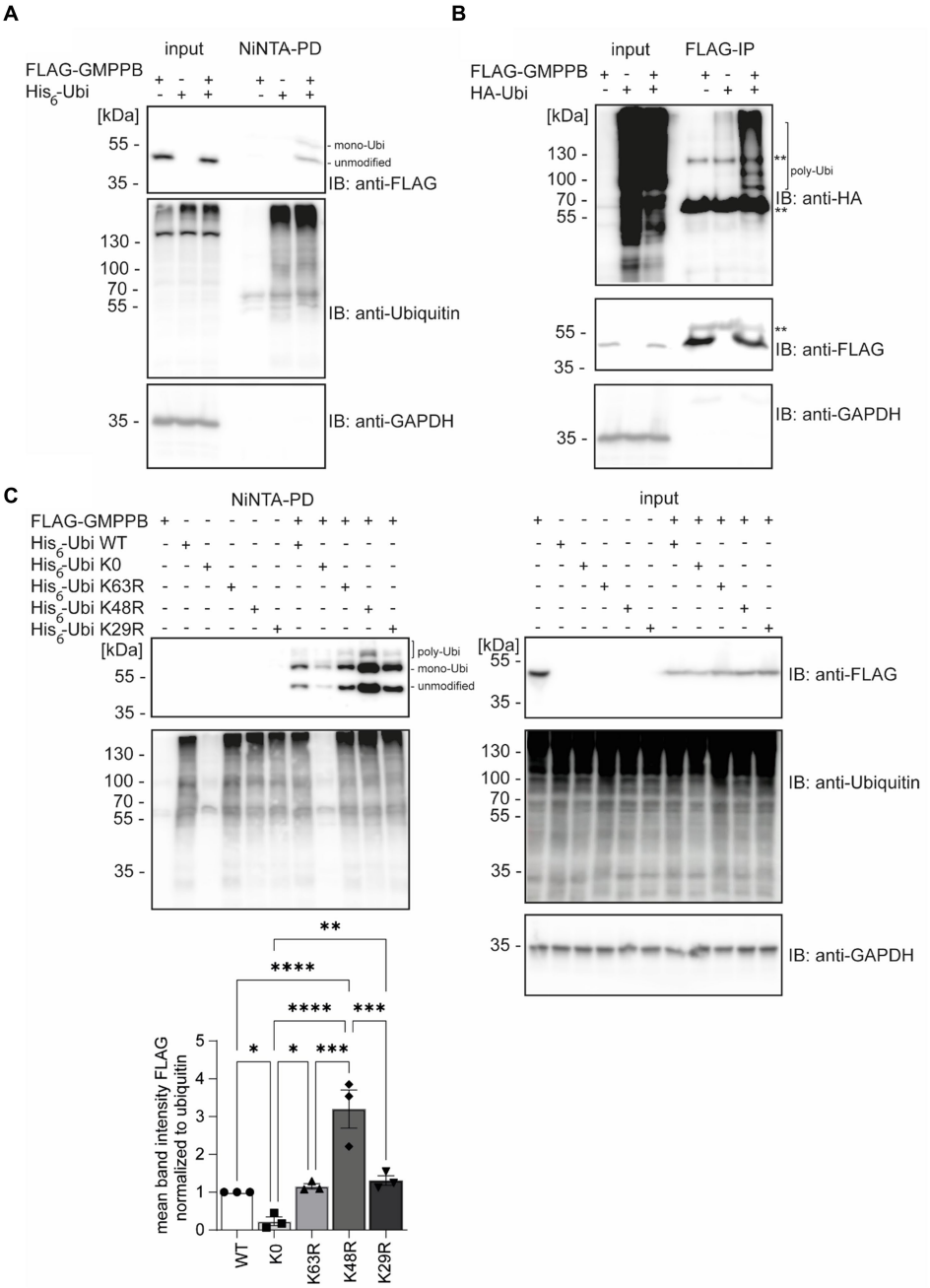

FIGURE 1
GMPPB is ubiquitinated. **(A)** Ubiquitinated GMPPB is pulled down with Ni-NTA beads from lysates of HEK-293 T cells, transiently overexpressing His_6-ubiquitin and $FLAG_3$-GMPPB. Input boxes represent 5% of the input used for pulldown. Unmodified and mono-ubiquitinated GMPPB bands (mono-Ubi) are indicated. **(B)** Ubiquitination is also evident upon overexpression of HA-ubiquitin and $FLAG_3$-GMPPB and subsequent immunoprecipitation with anti-FLAG M2 antibodies. **heavy chain of the precipitating antibody. Poly-Ubiquitin bands (poly-Ubi) are indicated. Input boxes represent 5% of the input used for immunoprecipitation. **(C)** Ni-NTA pulldown experiments from cell lysates overexpressing $FLAG_3$-GMPPB and His_6-ubiquitin WT or His_6-ubiquitin mutant constructs (K0, K29R, K48R, and K63R) show significantly reduced ubiquitination of GMPPB with the ubiquitin mutant K0, while GMPPB ubiquitination is increased with the ubiquitin mutant K48R compared to ubiquitin WT ($n = 3$ experiments, 1-way-ANOVA with Fischer's LSD test). Unmodified, mono-ubiquitinated (mono-Ubi), and poly-ubiquitinated (poly-Ubi) GMPPB bands are indicated. Input boxes represent 5% of the input used for NiNTA-pulldown. Quantitative data are presented as mean ± SEM with individual data points. *$p < 0.05$; **$p < 0.01$; ***$p < 0.001$; ****$p < 0.0001$.

Again, we detected bands for FLAG-GMPPB at 50, 60, and 70 kDa, confirming the previous results (Figure 1C). In the ubiquitin K0 variant, all seven lysines were replaced by arginine, thus only allowing the ligation to the substrate as mono-ubiquitin. When we co-transfected the FLAG-GMPPB with the K0 construct, only weak signals for ubiquitinated GMPPB were detectable after pulldown with Ni-NTA agarose (Figure 1C, lane 8). The presence of two bands for ubiquitin K0-modified GMPPB suggests that GMPPB is ubiquitinated at more than one site. However, for unknown reasons, the enrichment of ubiquitin K0 was not as

efficient as compared to WT ubiquitin variants (Figure 1C). We also assessed constructs, in which K29, K48, or K63 of ubiquitin were substituted by arginine, thus precluding the formation of the respective poly-ubiquitin chains. Although we did not observe a major difference upon co-transfection with either the ubiquitin K29R or K63R construct compared to ubiquitin WT (Figure 1C), the ubiquitination of GMPPB was significantly increased upon co-transfection of FLAG-GMPPB with the ubiquitin K48R variant. This suggests that either K48 is obstructive for poly-ubiquitination of GMPPB or that mono- or multi-ubiquitination of GMPPB via ubiquitin K48 leads to either stabilization or destabilization of the protein. Alternatively, the increase in ubiquitinated GMPPB upon co-transfection of FLAG-GMPPB with the WT ubiquitin may trigger proteasomal degradation, which is impaired when K48-poly-ubiquitination is prevented, thus leading to the accumulation of the protein.

Overall, our findings suggest that GMPPB is indeed ubiquitinated.

Patient's mutations can alter GMPPB ubiquitination

Disease-associated GMPPB variants include missense, nonsense, and frameshift mutations, which are assumed to result in GMPPB loss-of-function (Astrea et al., 2018; Tian et al., 2019). GMPPB activity is more severely compromised by missense mutations located in its N-terminal nucleotidyl-transferase domain compared to its C-terminal β-helix domain (Liu et al., 2021). The latter, however, often alters the subcellular localization of GMPPB (Carss et al., 2013; Belaya et al., 2015; Tian et al., 2019) or decreases the overall abundance of GMPPB (Belaya et al., 2015; Tian et al., 2019). We speculated whether the position of the respective patient variant might affect the ubiquitination of GMPPB. To this end, we analyzed the ubiquitination of the disease-associated variants D27H and P103L, which are located in the N-terminal part of GMPPB, as well as R287Q and D334N, which are located in the C-terminal part of GMPPB, in HEK-293 T cells (Figure 2). In addition, we cloned a construct in which the three

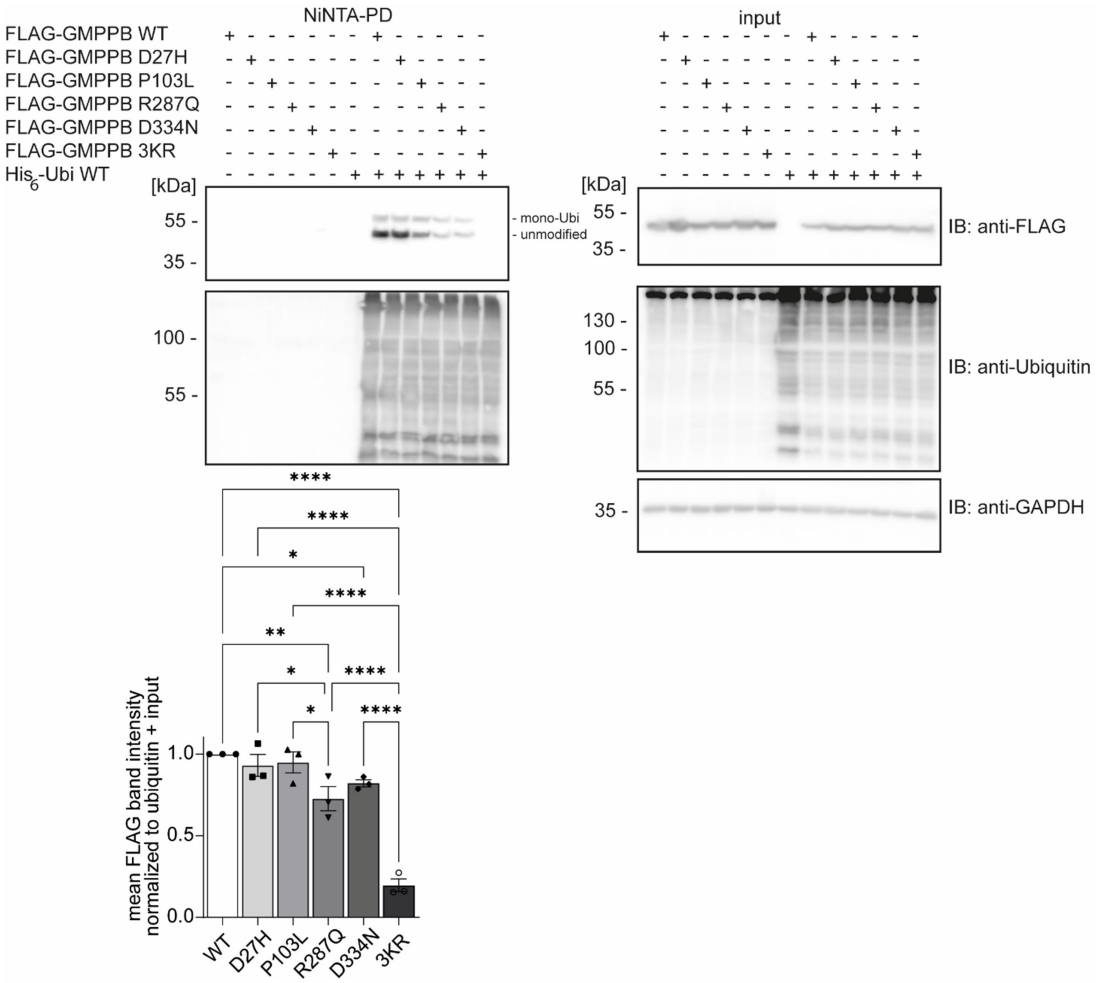

FIGURE 2
Patient mutations can alter the ubiquitination of GMPPB. Representative blots of Ni-NTA pulldown of overexpressed His_6-ubiquitin and $FLAG_3$-GMPPB WT and mutant constructs (D27H, P103L, R287Q, D334N, and K143/162/195R) and quantification ($n = 3$ experiments, 1-way-ANOVA with Fischer's LSD test). GAPDH is the loading control for input samples. Intensities of pulled-down FLAG-GMPPB bands are normalized to the intensities of pulled-down ubiquitin bands and $FLAG_3$-GMPPB bands detected in the input control (normalized to GAPDH). Unmodified and mono-ubiquitinated GMPPB bands (mono-Ubi) are indicated. Input boxes represent 5% of the input used for pulldown. Quantitative data are presented as mean ± SEM with individual data points. *$p < 0.05$; **$p < 0.01$; ***$p < 0.001$; ****$p < 0.0001$.

ubiquitination sites K143, K162, and K195 were replaced by arginine (GMPPB 3KR) (Figure 2). Notably, we could not detect FLAG-GMPPB 3KR upon Ni-NTA pulldown of His_6-ubiquitin (Figure 2). GMPPB mutants R287Q and D334N harboring patient mutations in the C-terminal part of the protein showed reduced ubiquitination (Figure 2), while GMPPB mutants with patient mutations in its N-terminal part were not affected (Figure 2).

Overall, these data suggest that patient mutations located in the C-terminal part of GMPPB may influence the ubiquitination status of GMPPB.

GMPPB interacts with the E3 ubiquitin ligase TRIM67

In the biogrid database, we found that the RING E3 ligase TRIM67 is predicted to interact with GMPPB (Oughtred et al., 2021; Demirdizen et al., 2023). To verify the GMPPB interaction with TRIM67, we transfected HEK-293 T cells with $FLAG_3$-GMPPB and HA-TRIM67 constructs, respectively. Indeed, upon immunoprecipitation of HA-TRIM67, a band for FLAG-tagged GMPPB was clearly visible (Figure 3A). To further confirm this result, we co-transfected HEK-293 T cells with the constructs for HA-TRIM67 and $FLAG_3$-GMPPB WT and the mutant devoid of all three reported ubiquitination sites (K143/162/195R: GMPPB 3KR) and immunoprecipitated GMPPB WT and variant protein with anti-FLAG M2 antibodies. On Western blots, bands for HA-TRIM67 were visible when GMPPB WT and mutated constructs were present (Figure 3B). To further validate this finding, we knocked down TRIM67 in HEK-293 T cells before co-transfection of $FLAG_3$-GMPPB and His_6-ubiquitin. Upon Ni-NTA pulldown of His_6-ubiquitin, approximately 50% less ubiquitination of GMPPB was visible upon TRIM67 knockdown (Figure 3C).

In summary, these data show that the ubiquitination of GMPPB is at least in part mediated by TRIM67.

GMPPB abundance is controlled by autophagy

Ubiquitination can target proteins for proteasomal (Kaiser and Huang, 2005; Kirkpatrick et al., 2006) or lysosomal degradations (Marques et al., 2004; Clague and Urbé, 2010). To test whether ubiquitination controls the turnover of GMPPB, we treated HEK-293 T cells with either MG132 to block proteasomal function or bafilomycin A1 to block lysosomal degradation. Increasing ubiquitin levels confirmed that MG132 treatment was effective (Figure 4A). The inhibition of lysosomal degradation by bafilomycin A1 was confirmed by the increase in the abundance of SQSTM1/p62 (Figure 4B). Because SQSTM1/p62 targets proteins in autophagosomes for degradation and is degraded itself during autophagy, increasing SQSTM1/p62 levels reflect efficient inhibition of lysosomal degradation by bafilomycin A1. While the abundance of GMPPB did not change by inhibiting proteasomal degradation (Figure 4A), the accumulation of GMPPB upon bafilomycin A1 treatment suggested that GMPPB is degraded by the lysosomal pathway (Figure 4B).

There are two major lysosomal-based degradation pathways: the degradation of endocytosed proteins by the endosomal pathway and the degradation of proteins and damaged organelles by autophagy. To further study the role of autophagy for GMPPB turnover, we starved neuroblastoma-derived N2A cells (Evangelopoulos et al., 2005) for 6 h with Earle's Balanced Salt Solution (EBSS) to induce autophagy by cell starvation (Figure 4C; Supplementary Figure S1B): Bafilomycin A1 treatment served as positive control for inhibition of autophagy. Immunofluorescence microscopic analysis for GMPPB, SQSTM1/p62, a marker for autophagosomes, and the lysosomal marker protein, LAMP1, allowed us to assess the co-localization of GMPPB with autolysosomes (p62- and LAMP1-positive structures) under normal conditions and upon induction of autophagy and upon inhibition of autophagy. Notably, EBSS treatment increased the co-localization of GMPPB with autolysosomes (p62- and LAMP1-positive), which drastically increased upon simultaneous inhibition of lysosomal degradation with bafilomycin A1 (Figure 4C; Supplementary Figure S1B). To further validate this finding, we overexpressed FLAG-tagged GMPPB in N2A cells and either induced autophagy by EBSS treatment for 6 h or blocked autophagy simultaneously with bafilomycin A1. Co-labeling of LAMP1, p62, and FLAG-tagged of GMPPB allowed us to quantify the co-localization of GMPPB with LAMP1 and p62. In agreement with Figure 4C, EBSS treatment increased the co-localization of GMPPB with autolysosomes, which was further triggered with bafilomycin A1 treatment (Supplementary Figures S1A,B). These data suggest that GMPPB is predominantly degraded via autophagy.

To assess whether the ubiquitination of GMPPB is necessary for its lysosomal degradation, we transfected HEK-293 T cells with a construct either encoding GMPPB WT, the disease-associated point-mutation GMPPB D334N, or GMPPB 3KR and blocked autophagy with bafilomycin A1 (Supplementary Figure S2A). Notably, the abundance of overexpressed WT and mutant GMPPB increased upon bafilomycin A1 treatment (Supplementary Figure S2A).

To assess whether the ubiquitination of GMPPB is important for its protein stability and turnover, we overexpressed GMPPB WT, the disease-associated variant GMPPB D334N or GMPPB 3KR in HEK-293 T cells, and blocked protein translation by cycloheximide (CHX). Decreasing ubiquitin levels confirmed an efficient inhibition of protein translation (Supplementary Figure S2B). GMPPB WT, D334N, and 3KR protein levels decreased over time in a similar ratio (Supplementary Figure S2B).

To assess if overexpression of GMPPB results in an accumulation within vesicular structures, such as lysosomes, we overexpressed GMPPB WT as well as mutant constructs in HEK-293T cells in the absence of bafilomycin A1 or EBSS. Cells transfected with GMPPB WT and GMPPB 3KR mutant showed a diffuse cytoplasmic staining pattern for GMPPB, whereas cells transfected with the GMPPB D334N mutant showed a more aggregated staining pattern (Supplementary Figure S2C). Overall, ubiquitination does not seem to regulate the degradation of GMPPB.

The interaction of GMPPB and GMPPA is independent of the ubiquitination of GMPPB

Since ubiquitination can influence protein interactions (Foronda et al., 2023), we speculated whether the ubiquitination of GMPPB affects its interaction with GMPPA. To this end, we overexpressed $FLAG_3$-GMPPB WT and the disease-associated variant D334N, which is less ubiquitinated (Figure 2), and the ubiquitination-deficient mutant

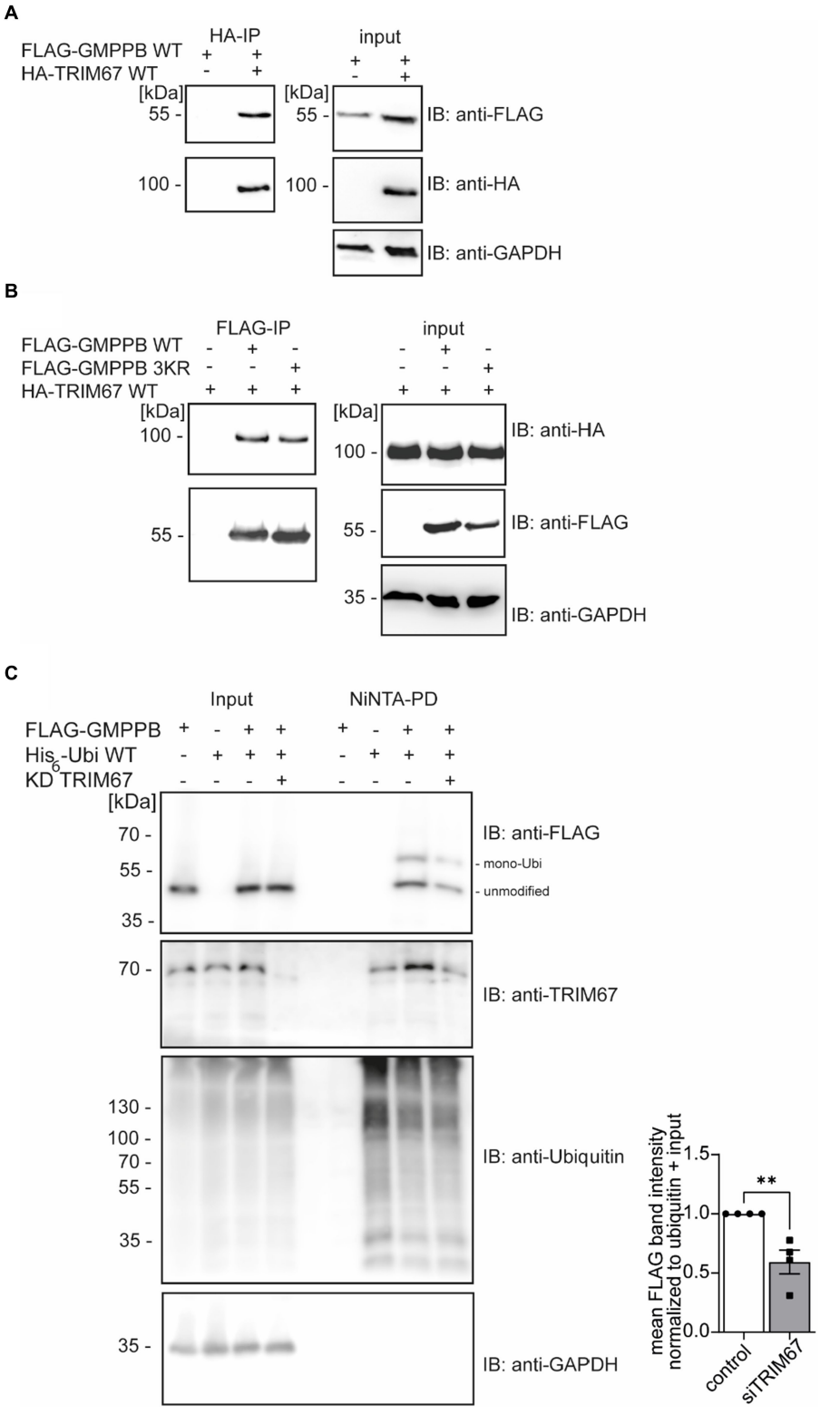

FIGURE 3
GMPPB interacts with the E3 ubiquitin ligase TRIM67. **(A)** Overexpressed $FLAG_3$-GMPPB co-precipitates with HA-TRIM67. GAPDH is the loading control for the input. Input boxes represent 5% of the input used for precipitation. **(B)** Overexpressed HA-TRIM67 co-precipitates with $FLAG_3$-GMPPB WT and $FLAG_3$-GMPPB 3KR (K143R, K162R, and K195R) upon IP with anti-FLAG M2 antibodies. GAPDH is the loading control for input samples. Input boxes represent 5% of the input used for precipitation. **(C)** Representative immunoblots of Ni-NTA pulldown of overexpressed His_6-ubiquitin and $FLAG_3$-GMPPB WT at control condition (scrambled siRNA) or upon siRNA mediated knockdown and quantification ($n = 4$ experiments, Student's t-Test). GAPDH is the loading control for input samples. The Intensities of pulled-down $FLAG_3$-GMPPB bands are normalized to the intensity of pulled-down ubiquitin bands and $FLAG_3$-GMPPB bands detected in the input control (normalized to GAPDH). Unmodified and mono-ubiquitinated GMPPB bands (mono-Ubi) are indicated. Input boxes represent 5% of the input used for precipitation. Quantitative data are presented as mean ± SEM with individual data points. $^{**}p < 0.01$.

10.3389/fnmol.2024.1375297

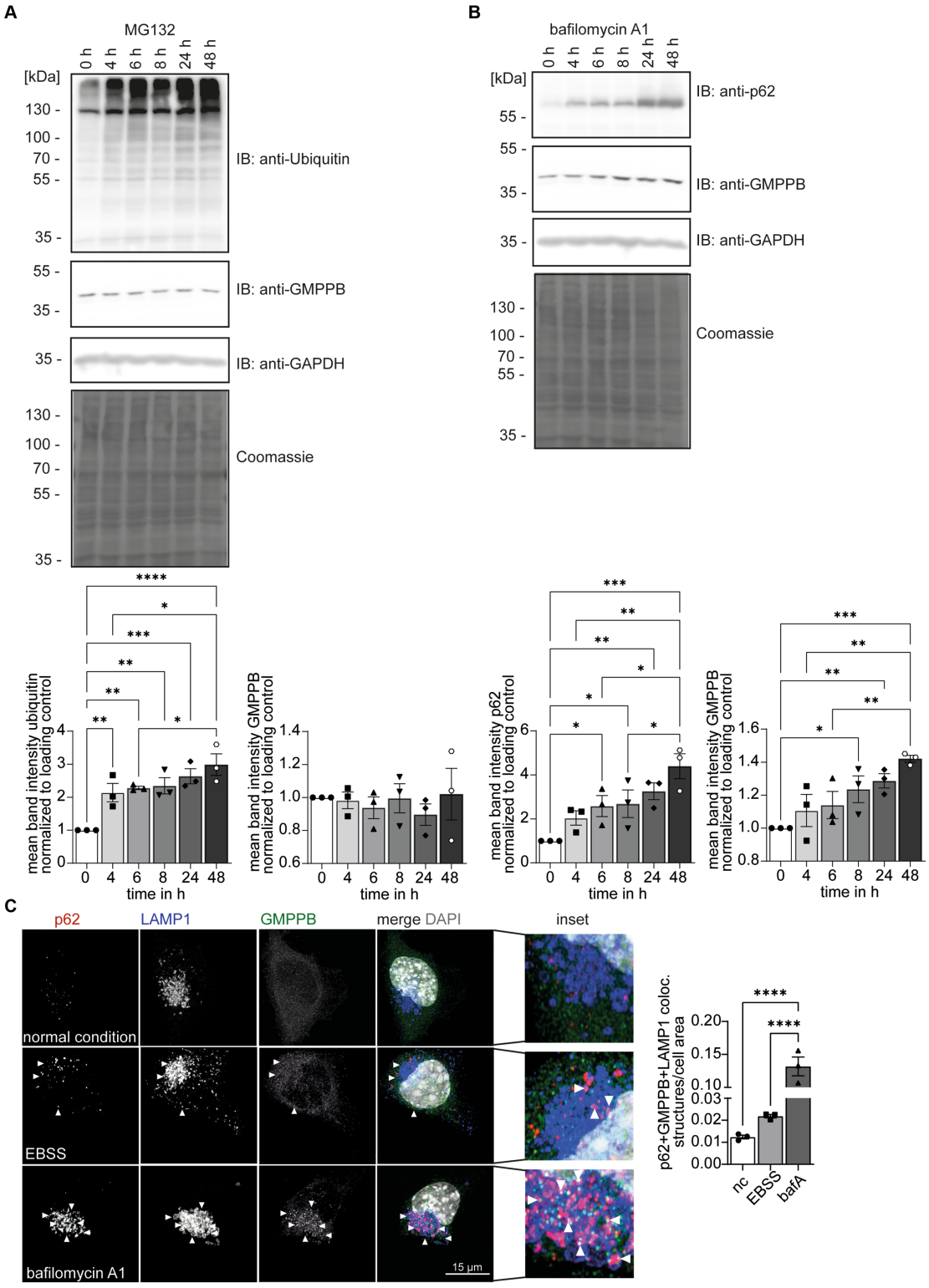

FIGURE 4
GMPPB protein levels are controlled via autophagy. **(A)** The inhibition of proteasomal protein degradation with MG132 does not affect the abundance of endogenous GMPPB in HEK-293 T cells. Detection of ubiquitin served as a control for efficient MG132 treatment. GAPDH and Coomassie staining are the loading control. Mean band intensities are normalized to GAPDH ($n = 3$ experiments, 1-way-ANOVA with Fischer's LSD test). **(B)** The inhibition of lysosomal degradation with bafilomycin A1 in HEK-293 T cells leads to an increase in the abundance of GMPPB. The accumulation of SQSTM1/p62 in the presence of bafilomycin A1 confirms the inhibition of lysosomal degradation. GAPDH and Coomassie staining served as loading control. Mean band intensities are normalized to GAPDH ($n = 3$ experiments, 1-way-ANOVA with Fischer's LSD test). **(C)** EBSS starvation for 6 h or the inhibition of lysosomal degradation with bafilomycin A1 increases the co-localization of GMPPB with autolysosomes (LAMP1- and p62-positive puncta) in N2A cells. Co-localization is analyzed with the Comdet v05 plugin from ImageJ. $N = 3$ experiments with 10–15 cells/genotype per condition and experiment, scale bar: 15 µm. White arrowheads indicate exemplary co-localization. Quantitative data are presented as mean ± SEM with individual data points. *$p < 0.05$; **$p < 0.01$; ***$p < 0.001$; ****$p < 0.0001$.

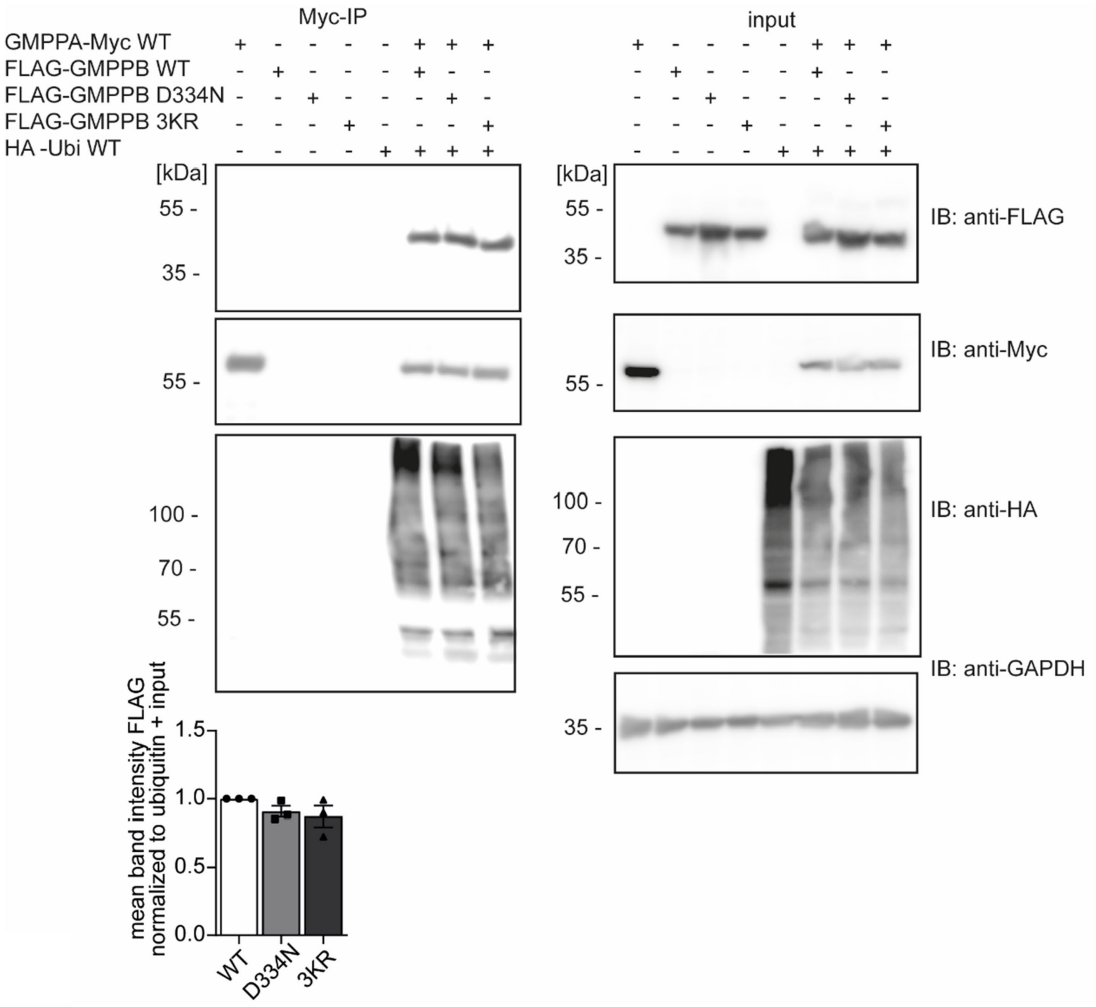

FIGURE 5
The ubiquitination of GMPPB does not affect its interaction with GMPPA. HEK-293 T are co-transfected with constructs for GMPPA-Myc$_6$ together with or without HA-ubiquitin and either FLAG$_3$-GMPPB WT, D334N, or GMPPB 3KR, immunoprecipitated via anti-Myc antibodies coupled to beads and analyzed by immunoblot (n = 3 experiments, one-way-ANOVA with Fischer's LSD test). GAPDH is the loading control for input samples. Intensities of pulled-down FLAG-tagged proteins are normalized to the intensity of pulled-down ubiquitinated proteins and FLAG-tagged proteins detected in the input control (normalized to GAPDH). Input boxes represent 5% of the input used for precipitation. Quantitative data are presented as mean ± SEM with individual data points.

FLAG$_3$-GMPPB 3KR together with HA-ubiquitin and GMPPA-Myc$_6$ in HEK-293 T cells. We did not observe any difference in the interaction between GMPPA and GMPPB WT or mutated GMPPB variants, and co-expression of HA-ubiquitin also did not influence their interaction (Figure 5; Supplementary Figure S2A). Overall, these data suggest that ubiquitination does not affect the interaction between GMPPB and GMPPA.

The ubiquitination of GMPPB regulates its enzymatic activity

In addition to protein turnover and degradation, localization, protein interaction, trafficking, and secretion, ubiquitination can also affect the activity of enzymes (Pickart and Eddins, 2004; Yang et al., 2021). Therefore, we speculated whether this also applies to GMPPB. To this end, we either overexpressed FLAG3-GMPPB WT or the disease-associated D334N variant, the ubiquitination-deficient variant GMPPB 3KR or the 3KR D334N double mutant in HEK-293T cells. After protein enrichment by methanol–chloroform precipitation, we measured the enzymatic activity by colorimetric read-out of generated phosphate in the presence of mannose-1-phosphate, GDP-mannose, GTP, and pyrophosphatase (Figure 6A). Of note, lysine 162 has been reported to be a part of the catalytic center of GMPPB (Zheng et al., 2021). As a control, we also incubated cells expressing FLAG$_3$-GMPPB WT with PYR-41, which irreversibly blocks E1 ligases and thus ubiquitination (Yang et al., 2007). Notably, GMPPB activity was significantly reduced for GMPPB D334N, for GMPPB 3KR, and GMPPB 3KR D334N compared to WT (Figure 6B; Supplementary Figures S2B,C). The GMPPB 3KR D334N variant showed a slightly more decreased GMPPB activity compared to the single mutants (Figure 6B; Supplementary Figure S3B). The incubation of the WT control with the ubiquitination blocking agent PYR-41 significantly decreased the enzymatic activity of GMPPB WT

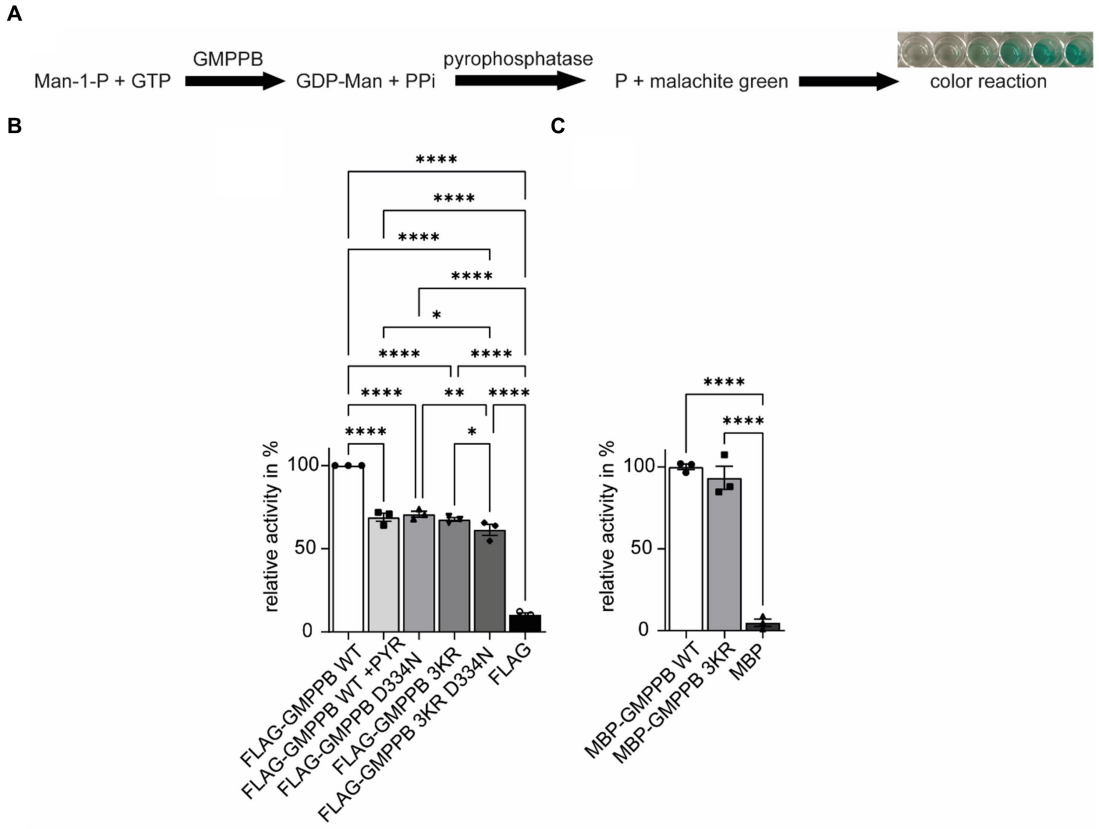

FIGURE 6
The ubiquitination of GMPPB is important for its enzymatic activity. **(A)** Rationale to monitor the activity of GMPPB. **(B)** Activity measurements were performed in a cuvette format. While $FLAG_3$-GMPPB WT displayed enzymatic activity, the activity is significantly reduced for $FLAG_3$-GMPPB D334N, $FLAG_3$-GMPPB 3KR, and $FLAG_3$-GMPPB 3KR D334N. As a control, the ubiquitination of $FLAG_3$-GMPPB WT is inhibited with PYR-41 before measuring enzymatic activity. Purified proteins from cells transfected with the empty $FLAG_3$-vector alone served as a negative control. Lysate of empty vector-transfected cells served as a negative control ($n = 3$ experiments, one-way-ANOVA with Fischer's LSD test). **(C)** Activity measurements using recombinant unubiquitinated MBP-GMPPB WT and MBP-GMPPB 3KR. Quantitative data are presented as mean ± SEM with individual data points. $*p < 0.05$; $**p < 0.01$; $***p < 0.001$; $****p < 0.0001$.

(Figure 6B; Supplementary Figure S3B). To exclude that the amino acid substitutions in the GMPPB 3KR mutant might affect the overall structure or arrangement of its active center without ubiquitination being involved, we generated a recombinant GMPPB WT and GMPPB 3KR mutant and measured their enzymatic activity. Notably, we did not detect differences between WT and mutant, suggesting that the amino acid substitutions did not change the arrangement of the catalytic center (Figure 6C; Supplementary Figure S3C).

In summary, the ubiquitination of GMPPB affects its enzymatic activity.

Discussion

We and others have previously shown that GMPPB, which facilitates the conversion of mannose-1-phosphate and GTP to GDP-mannose (Ning and Elbein, 2000), interacts with its paralogue GMPPA (Zheng et al., 2021; Franzka et al., 2021a). GMPPA lacks enzymatic activity but can still bind GDP-mannose and thus provides a feedback mechanism to limit GMPPB activity as an allosteric feedback inhibitor. Mutations in GMPPB are associated with variable disorders such as muscular dystrophy and other neurological symptoms, including intellectual disability, epilepsy, and cerebellar hypoplasia (Carss et al., 2013; Belaya et al., 2015; Liu et al., 2021).

According to the PhosphoSitePlus database (Hornbeck et al., 2015; Akimov et al., 2018), GMPPB is predicted to be ubiquitinated. In agreement with this prediction, we here show that GMPPB can be precipitated with Ni-NTA beads, which bind to His_6-ubiquitin. Notably, we observed a second and a faint third band of higher molecular weight, likely representing mono- and poly/multi-ubiquitinated GMPPB proteins. Because these bands were absent from input samples, we hypothesize that they are only detected upon enrichment for ubiquitinated proteins. This suggests that only a fraction of GMPPB is modified by ubiquitination. The lower molecular weight band showed a more prominent intensity compared to the higher molecular weight bands. Possibly, GMPPB forms oligomeric complexes (Zheng et al., 2021) with GMPPA, and thus, potential ubiquitination sites might be covered by this interaction. Upon $FLAG_3$-GMPPB co-immunoprecipitation with HA-ubiquitin, we detected several bands at different molecular heights for HA-ubiquitin. These bands might represent mono- and poly/multi-ubiquitinated GMPPB or ubiquitinated interaction partners of GMPPB.

Protein ubiquitination plays a crucial role in various biological processes, including development, cancer (Shi and Grossman, 2010), aging (Hughes et al., 2022), neuronal differentiation and survival (Bax et al., 2019), and synaptic function (Hegde, 2010; Mabb and Ehlers, 2010), as well as axonal guidance and cognitive function (Pinto et al., 2021). Interestingly, ubiquitination is in crosstalk with various other post-translational modifications, including SUMOylation, phosphorylation, acetylation, methylation, hydroxylation, prolyl isomerization, PARylation, neddylation, and *O*-GlcNAcylation (Guan et al., 2018; Barbour et al., 2023). Moreover, ubiquitination can be modulated by *O*-GlcNAcylation (Guinez et al., 2008). In addition to ubiquitination, GMPPB has been predicted to be phosphorylated, methylated, and *O*-GlcNAcylated (Hornbeck et al., 2015), but the functional consequences of the PTMs have not been addressed so far.

Substrate specificity of ubiquitination is brought about by different E3 ligases. Because the E3 ligase TRIM67 was found in the interactome of GMPPB (Oughtred et al., 2021; Demirdizen et al., 2023), we assessed whether TRIM67 and GMPPB indeed interact. Our co-immunoprecipitation studies confirm the interaction, suggesting that TRIM67 might serve as an E3 ligase for GMPPB. Indeed, ubiquitinated GMPPB was almost halved upon knockdown of TRIM67, confirming that TRIM67 acts as an E3 ligase for GMPPB. However, this also indicates that TRIM67 is not the only ligase responsible for GMPPB ubiquitination. Notably, GMPPA was also predicted to be ubiquitinated (Hornbeck et al., 2015) and also interacts with TRIM67 (Oughtred et al., 2021; Demirdizen et al., 2023). TRIM67 is involved in cancer progression (Jiang et al., 2020; Demirdizen et al., 2023), neuritogenesis (Yaguchi et al., 2012), and axonal guidance (Boyer et al., 2020), as well as brain development and cognitive function (Boyer et al., 2018). Remarkably, some disease-associated mutations with reduced enzymatic activity compromised the ubiquitination of GMPPB. Possibly, these mutations impair the binding of the E3 ligase to GMPPB. Since the E3 ligaseTRIM28 and the E2 enzyme UBE2V1 have been found to interact with GMPPB (Jang et al., 2018; Oughtred et al., 2021), and TRIM28 and PARK2 have been found in the interactome of GMPPA (Wan et al., 2015; Jang et al., 2018; Oughtred et al., 2021; Sun et al., 2022), both proteins represent further potential E3 ligase candidates contributing to GMPPB ubiquitination, which should be assessed in future studies.

Ubiquitin itself contains seven different lysine residues (K6, K11, K27, K29, K33, K48, and K63) that potentially can be used for ubiquitin modifications (Mallette and Richard, 2012; Callis, 2014). Depending upon the amount of ubiquitin molecules attached to a protein and the lysine linkage, proteins are targeted to different outcomes. Mono-ubiquitination, for example, is involved in DNA repair and gene expression (Passmore and Barford, 2004), while poly-ubiquitination is involved in protein degradation, signal transduction, or kinase activation (Passmore and Barford, 2004). Notably, GMPPB ubiquitination was increased for a modified ubiquitin, with lysine 48 being replaced by arginine. This suggests that ubiquitination of GMPPB stabilizes the protein at conditions where GMPPB is not predominantly poly-ubiquitinated at K48.

Ubiquitination often targets proteins for proteasomal degradation via K48-linked poly-ubiquitination (Kaiser and Huang, 2005; Kirkpatrick et al., 2006). Because the abundance of GMPPB did not increase upon the inhibition of proteasomal degradation, we also considered that the ubiquitination may target GMPPB for lysosomal degradation (Marques et al., 2004; Clague and Urbé, 2010). This assumption was confirmed by increased GMPPB levels upon the inhibition of lysosomal degradation with bafilomycin A1 and was further verified by the co-localization of GMPPB with autophagic vesicles, which strongly increased upon the inhibition of autophagy as seen in immunofluorescence and immunoblot analysis. In agreement, a previous study showed that disease-associated GMPPB variants were degraded via autophagy (Tian et al., 2019). Notably, the protein abundance of a GMPPB mutant devoid of all three reported ubiquitin sites still increased upon inhibition of lysosomal degradation. This finding suggests that GMPPB degradation is independent of its ubiquitination. Of note, other proteins necessary for protein mannosylation, such as mannose-phosphate isomerase (MPI) or phospho-mannomutase (PMM), are predicted to be ubiquitinated as well in the PhosphoSitePlus database (Hornbeck et al., 2015). In contrast to GMPPB, however, PMM is degraded by the proteasomal pathway (Vilas et al., 2020). Whether other mannosylation-associated enzymes, such as MPI, are degraded via the proteasomal or lysosomal pathway is still elusive.

Ubiquitin can act as a reversible and dynamic platform for protein–protein interactions. Proteins that contain ubiquitin-binding domains can interact with each other by using ubiquitin as a linker molecule (Magits and Sablina, 2022). Since both GMPPB and GMPPA have been reported to be ubiquitinated (Hornbeck et al., 2015), we speculated whether the ubiquitination of GMPPB is important for its interaction with GMPPA. However, disruption of the three reported ubiquitination sites in GMPPB did not compromise the interaction between GMPPB and GMPPA. Upon HA-ubiquitin and $FLAG_3$-GMPPB co-immunoprecipitation with GMPPA-Myc_6, we detected several bands at different molecular heights for HA-ubiquitin. These bands might represent mono- and poly/multi-ubiquitinated GMPPA or ubiquitinated interaction partners of GMPPA. To date, no other ubiquitinated interaction partners are known for GMPPA besides GMPPB, and it remains elusive whether the ubiquitination of GMPPA might be important for its interaction with GMPPB.

It has been shown that ubiquitination may also affect the activity of transcription factors and signaling proteins (Kim et al., 2003; Zhu et al., 2021). Thus, we considered whether the loss of GMPPB ubiquitination may affect its enzymatic activity. Indeed, blocking protein ubiquitination by irreversible inhibition of E1 ligases with PYR-41 or replacing the three potential ubiquitinated lysines of GMPPB with arginine decreased its catalytic activity. The disease-associated patient variant GMPPB D334N, which is less ubiquitinated, also displayed reduced enzymatic activity, which is in agreement with a recent study (Liu et al., 2021), but it was assumed that this may also be related to a different subcellular localization of the mutant protein (Carss et al., 2013). Interestingly, several enzymes important for protein mannosylation, such as phospho-mannomutase (PMM), mannose-6-phosphate-isomerase (MPI), or protein O-linked mannose *N*-acetylglucosaminyltransferase 1 (POMGNT1), are predicted to be ubiquitinated as well (Hornbeck et al., 2015) and also interact with the E3 ligase TRIM67 (Oughtred et al., 2021; Demirdizen et al., 2023), suggesting that ubiquitination might be common feature of enzymes in the mannosylation pathway. However, this has not been addressed experimentally so far.

In summary, our study shows that ubiquitination of GMPPB does affect neither its stability nor its interaction with GMPPA but modulates its enzymatic activity. Thus, ubiquitination provides another level to regulate GMPPB activity and mannosylation.

Data availability statement

The original contributions presented in the study are included in the article/Supplementary material, further inquiries can be directed to the corresponding authors.

Author contributions

PF: Conceptualization, Funding acquisition, Investigation, Methodology, Project administration, Software, Writing – original draft, Writing – review & editing. SM: Conceptualization, Investigation, Methodology, Writing – original draft, Writing – review & editing. AC: Formal analysis, Visualization, Writing – review & editing. OH: Conceptualization, Supervision, Writing – original draft, Writing – review & editing. CH: Conceptualization, Funding acquisition, Project administration, Supervision, Writing – original draft, Writing – review & editing.

Funding

The author(s) declare that financial support was received for the research, authorship, and/or publication of this article. This study was funded by the DFG GRK 2155 ProMoAge and the DFG grant HU 800/15–1 to CH. This study was supported by a Medical Scientist Award from the Interdisciplinary Center for Clinical Research (IZKF) at the Jena University Hospital (MSP13) and by IMPULSE funding (FKZ IP 2021–04) from the Friedrich-Schiller-University Jena to PF.

Acknowledgments

The authors gratefully acknowledge support from Johanna Fischer and Manuela Neumann.

Conflict of interest

The authors declare that the research was conducted in the absence of any commercial or financial relationships that could be construed as a potential conflict of interest.

Publisher's note

Supplementary material

The Supplementary material for this article can be found online at: https://www.frontiersin.org/articles/10.3389/fnmol.2024.1375297/full#supplementary-material

References

Akimov, V., Barrio-Hernandez, I., Hansen, S. V. F., Hallenborg, P., Pedersen, A. K., Bekker-Jensen, D. B., et al. (2018). UbiSite approach for comprehensive mapping of lysine and N-terminal ubiquitination sites. *Nat. Struct. Mol. Biol.* 25, 631–640. doi: 10.1038/s41594-018-0084-y

Astrea, G., Romano, A., Angelini, C., Antozzi, C. G., Barresi, R., Battini, R., et al. (2018). Broad phenotypic spectrum and genotype-phenotype correlations in GMPPB-related dystroglycanopathies: an Italian cross-sectional study. *Orphanet J. Rare Dis.* 13:170. doi: 10.1186/s13023-018-0863-x

Barbour, H., Nkwe, N. S., Estavoyer, B., Messmer, C., Gushul-Leclaire, M., Villot, R., et al. (2023). An inventory of crosstalk between ubiquitination and other post-translational modifications in orchestrating cellular processes. *iScience* 26:106276. doi: 10.1016/j.isci.2023.106276

Bax, M., McKenna, J., Do-Ha, D., Stevens, C. H., Higginbottom, S., Balez, R., et al. (2019). The ubiquitin proteasome system is a key regulator of pluripotent stem cell survival and motor neuron differentiation. *Cells* 8:581. doi: 10.3390/cells8060581

Belaya, K., Rodriguez Cruz, P. M., Liu, W. W., Maxwell, S., McGowan, S., Farrugia, M. E., et al. (2015). Mutations in GMPPB cause congenital myasthenic syndrome and bridge myasthenic disorders with dystroglycanopathies. *Brain* 138, 2493–2504. doi: 10.1093/brain/awv185

Boyer, N. P., McCormick, L. E., Menon, S., Urbina, F. L., and Gupton, S. L. (2020). A pair of E3 ubiquitin ligases compete to regulate filopodial dynamics and axon guidance. *J. Cell Biol.* 219:e201902088. doi: 10.1083/jcb.201902088

Boyer, N. P., Monkiewicz, C., Menon, S., Moy, S. S., and Gupton, S. L. (2018). Mammalian TRIM67 functions in brain development and behavior. *eNeuro* 5, ENEURO.0186–ENEU18.2018. doi: 10.1523/ENEURO.0186-18.2018

Callis, J. (2014). The ubiquitination machinery of the ubiquitin system. *Arabidopsis Book* 12:e0174. doi: 10.1199/tab.0174

Carss, K. J., Stevens, E., Foley, A. R., Cirak, S., Riemersma, M., Torelli, S., et al. (2013). Mutations in GDP-mannose pyrophosphorylase B cause congenital and limb-girdle muscular dystrophies associated with hypoglycosylation of α-dystroglycan. *Am. J. Hum. Genet.* 93, 29–41. doi: 10.1016/j.ajhg.2013.05.009

Clague, M. J., and Urbé, S. (2010). Ubiquitin: same molecule, different degradation pathways. *Cell* 143, 682–685. doi: 10.1016/j.cell.2010.11.012

Demirdizen, E., Al-Ali, R., Narayanan, A., Sun, X., Varga, J. P., Steffl, B., et al. (2023). TRIM67 drives tumorigenesis in oligodendrogliomas through rho GTPase-dependent membrane blebbing. *Neuro-Oncology* 25, 1031–1043. doi: 10.1093/neuonc/noac233

Dikic, I., and Schulman, B. A. (2023). An expanded lexicon for the ubiquitin code. *Nat. Rev. Mol. Cell Biol.* 24, 273–287. doi: 10.1038/s41580-022-00543-1

Ervasti, J. M., and Campbell, K. P. (1991). Membrane organization of the dystrophin-glycoprotein complex. *Cell* 66, 1121–1131. doi: 10.1016/0092-8674(91)90035-w

Evangelopoulos, M. E., Weis, J., and Krüttgen, A. (2005). Signalling pathways leading to neuroblastoma differentiation after serum withdrawal: HDL blocks neuroblastoma differentiation by inhibition of EGFR. *Oncogene* 24, 3309–3318. doi: 10.1038/sj.onc.1208494

Foronda, H., Fu, Y., Covarrubias-Pinto, A., Bocker, H. T., González, A., Seemann, E., et al. (2023). Heteromeric clusters of ubiquitinated ER-shaping proteins drive ER-phagy. *Nature* 618, 402–410. doi: 10.1038/s41586-023-06090-9

Franzka, P., Henze, H., Jung, M. J., Schüler, S. C., Mittag, S., Biskup, K., et al. (2021a). GMPPA defects cause a neuromuscular disorder with α-dystroglycan hyperglycosylation. *J. Clin. Invest.* 131:e139076. doi: 10.1172/JCI139076

Franzka, P., Krüger, L., Schurig, M. K., Olecka, M., Hoffmann, S., Blanchard, V., et al. (2021b). Altered glycosylation in the aging heart. *Front. Mol. Biosci.* 8:673044. doi: 10.3389/fmolb.2021.673044

González, A., Covarrubias-Pinto, A., Bhaskara, R. M., Glogger, M., Kuncha, S. K., Xavier, A., et al. (2023). Ubiquitination regulates ER-phagy and remodelling of endoplasmic reticulum. *Nature* 618, 394–401. doi: 10.1038/s41586-023-06089-2

Guan, J., Yu, S., and Zheng, X. (2018). NEDDylation antagonizes ubiquitination of proliferating cell nuclear antigen and regulates the recruitment of polymerase η in response to oxidative DNA damage. *Protein Cell* 9, 365–379. doi: 10.1007/s13238-017-0455-x

Guinez, C., Mir, A. M., Dehennaut, V., Cacan, R., Harduin-Lepers, A., Michalski, J. C., et al. (2008). Protein ubiquitination is modulated by O-GlcNAc glycosylation. *FASEB J.* 22, 2901–2911. doi: 10.1096/fj.07-102509

Hegde, A. N. (2010). The ubiquitin-proteasome pathway and synaptic plasticity. *Learn. Mem.* 17, 314–327. doi: 10.1101/lm.1504010

Hershko, A., and Ciechanover, A. (1998). The ubiquitin system. *Annu. Rev. Biochem.* 67, 425–479. doi: 10.1146/annurev.biochem.67.1.425

Hornbeck, P. V., Zhang, B., Murray, B., Kornhauser, J. M., Latham, V., and Skrzypek, E. (2015). PhosphoSitePlus, 2014: mutations, PTMs and recalibrations. *Nucleic Acids Res.* 43, D512–D520. doi: 10.1093/nar/gku1267

Hughes, D. C., Baehr, L. M., Waddell, D. S., Sharples, A. P., and Bodine, S. C. (2022). Ubiquitin ligases in longevity and aging skeletal muscle. *Int. J. Mol. Sci.* 23:7602. doi: 10.3390/ijms23147602

Jang, S. M., Kauzlaric, A., Quivy, J. P., Pontis, J., Rauwel, B., Coluccio, A., et al. (2018). KAP1 facilitates reinstatement of heterochromatin after DNA replication. *Nucleic Acids Res.* 46, 8788–8802. doi: 10.1093/nar/gky580

Jensen, B. S., Willer, T., Saade, D. N., Cox, M. O., Mozaffar, T., Scavina, M., et al. (2015). GMPPB-associated Dystroglycanopathy: emerging common variants with phenotype correlation. *Hum. Mutat.* 36, 1159–1163. doi: 10.1002/humu.22898

Jiang, J., Ren, H., Xu, Y., Wudu, M., Wang, Q., Liu, Z., et al. (2020). TRIM67 promotes the proliferation, migration, and invasion of non-small-cell lung Cancer by positively regulating the notch pathway. *J. Cancer* 11, 1240–1249. doi: 10.7150/jca.38286

Kaiser, P., and Huang, L. (2005). Global approaches to understanding ubiquitination. *Genome Biol.* 6:233. doi: 10.1186/gb-2005-6-10-233

Khaminets, A., Heinrich, T., Mari, M., Grumati, P., Huebner, A. K., Akutsu, M., et al. (2015). Regulation of endoplasmic reticulum turnover by selective autophagy. *Nature* 522, 354–358. doi: 10.1038/nature14498

Kim, S. Y., Herbst, A., Tworkowski, K. A., Salghetti, S. E., and Tansey, W. P. (2003). Skp2 regulates Myc protein stability and activity. *Mol. Cell* 11, 1177–1188. doi: 10.1016/s1097-2765(03)00173-4

Kirkpatrick, D. S., Hathaway, N. A., Hanna, J., Elsasser, S., Rush, J., Finley, D., et al. (2006). Quantitative analysis of in vitro Ubiquitinated cyclin B1 reveals complex chain topology. *Nat. Cell Biol.* 8, 700–710. doi: 10.1038/ncb1436

Koehler, K., Malik, M., Mahmood, S., Gießelmann, S., Beetz, C., Hennings, J. C., et al. (2013). Mutations in GMPPA cause a glycosylation disorder characterized by intellectual disability and autonomic dysfunction. *Am. J. Hum. Genet.* 93, 727–734. doi: 10.1016/j.ajhg.2013.08.002

Komander, D., and Rape, M. (2012). The ubiquitin code. *Annu. Rev. Biochem.* 81, 203–229. doi: 10.1146/annurev-biochem-060310-170328

Kwon, Y. T., and Ciechanover, A. (2017). The ubiquitin code in the ubiquitin-proteasome system and autophagy. *Trends Biochem. Sci.* 42, 873–886. doi: 10.1016/j.tibs.2017.09.002

Liu, Z., Wang, Y., Yang, F., Yang, Q., Mo, X., Burstein, E., et al. (2021). GMPPB-congenital disorders of glycosylation associate with decreased enzymatic activity of GMPPB. *Mol Biomed* 2:13. doi: 10.1186/s43556-021-00027-2

Mabb, A. M., and Ehlers, M. D. (2010). Ubiquitination in postsynaptic function and plasticity. *Annu. Rev. Cell Dev. Biol.* 26, 179–210. doi: 10.1146/annurev-cellbio-100109-104129

Magits, W., and Sablina, A. A. (2022). The regulation of the protein interaction network by monoubiquitination. *Curr. Opin. Struct. Biol.* 73:102333. doi: 10.1016/j.sbi.2022.102333

Mallette, F. A., and Richard, S. (2012). K48-linked ubiquitination and protein degradation regulate 53BP1 recruitment at DNA damage sites. *Cell Res.* 22, 1221–1223. doi: 10.1038/cr.2012.58

Marques, C., Pereira, P., Taylor, A., Liang, J. N., Reddy, V. N., Szweda, L. I., et al. (2004). Ubiquitin-dependent lysosomal degradation of the HNE-modified proteins in lens epithelial cells. *FASEB J.* 18, 1424–1426. doi: 10.1096/fj.04-1743fje

Ning, B., and Elbein, A. D. (2000). Cloning, expression and characterization of the pig liver GDP-mannose pyrophosphorylase. Evidence that GDP-mannose and GDP-Glc pyrophosphorylases are different proteins. *Eur. J. Biochem.* 267, 6866–6874. doi: 10.1046/j.1432-1033.2000.01781.x

Oughtred, R., Rust, J., Chang, C., Breitkreutz, B. J., Stark, C., Willems, A., et al. (2021). The BioGRID database: a comprehensive biomedical resource of curated protein, genetic, and chemical interactions. *Protein Sci.* 30, 187–200. doi: 10.1002/pro.3978

Passmore, L. A., and Barford, D. (2004). Getting into position: the catalytic mechanisms of protein ubiquitylation. *Biochem. J.* 379, 513–25. doi: 10.1042/BJ20040198

Pickart, C. M., and Eddins, M. J. (2004). Ubiquitin: structures, functions, mechanisms. *Biochim. Biophys. Acta* 1695, 55–72. doi: 10.1016/j.bbamcr.2004.09.019

Pinto, M. J., Tomé, D., and Almeida, R. D. (2021). The Ubiquitinated axon: local control of axon development and function by ubiquitin. *J. Neurosci.* 41, 2796–2813. doi: 10.1523/JNEUROSCI.2251-20.2021

Shi, D., and Grossman, S. R. (2010). Ubiquitin becomes ubiquitous in cancer: emerging roles of ubiquitin ligases and deubiquitinases in tumorigenesis and as therapeutic targets. *Cancer Biol. Ther.* 10, 737–747. doi: 10.4161/cbt.10.8.13417

Sun, X., Shu, Y., Ye, G., Wu, C., Xu, M., Gao, R., et al. (2022). Histone deacetylase inhibitors inhibit cervical cancer growth through Parkin acetylation-mediated mitophagy. *Acta Pharm. Sin. B* 12, 838–852. doi: 10.1016/j.apsb.2021.07.003

Swatek, K. N., and Komander, D. (2016). Ubiquitin modifications. *Cell Res.* 26, 399–422. doi: 10.1038/cr.2016.39

Tian, W. T., Zhou, H. Y., Zhan, F. X., Zhu, Z. Y., Yang, J., Chen, S. D., et al. (2019). Lysosomal degradation of GMPPB is associated with limb-girdle muscular dystrophy type 2T. *Ann. Clin. Transl. Neurol.* 6, 1062–1071. doi: 10.1002/acn3.787

Uchida, C., and Kitagawa, M. (2016). RING-, HECT-, and RBR-type E3 ubiquitin ligases: involvement in human Cancer. *Curr. Cancer Drug Targets* 16, 157–174. doi: 10.2174/1568009616666151112122801

Varki, A., Cummings, R. D., Esko, J. D., Freeze, H. H., Stanley, P., Bertozzi, C. R., et al. (2009). "Essentials of Glycobiology" in *Essentials of Glycobiology*. eds. A. Varki, R. D. Cummings, J. D. Esko, H. H. Freeze, P. Stanley and C. R. Bertozzi (Cold Spring Harbor, NY: Cold Spring Harbor Laboratory Press).

Vilas, A., Yuste-Checa, P., Gallego, D., Desviat, L. R., Ugarte, M., Pérez-Cerdá, C., et al. (2020). Proteostasis regulators as potential rescuers of PMM2 activity. *Biochim. Biophys. Act.a Mol. Basis Dis.* 1866:165777. doi: 10.1016/j.bbadis.2020.165777

Walczak, H., Iwai, K., and Dikic, I. (2012). Generation and physiological roles of linear ubiquitin chains. *BMC Biol.* 10:23. doi: 10.1186/1741-7007-10-23

Wan, C., Borgeson, B., Phanse, S., Tu, F., Drew, K., Clark, G., et al. (2015). Panorama of ancient metazoan macromolecular complexes. *Nature* 525, 339–344. doi: 10.1038/nature14877

Wang, J., Zhou, Q., Ding, J., Yin, T., Ye, P., and Zhang, Y. (2022). The conceivable functions of protein ubiquitination and Deubiquitination in reproduction. *Front. Physiol.* 13:886261. doi: 10.3389/fphys.2022.886261

Yaguchi, H., Okumura, F., Takahashi, H., Kano, T., Kameda, H., Uchigashima, M., et al. (2012). TRIM67 protein negatively regulates Ras activity through degradation of 80K-H and induces neuritogenesis. *J. Biol. Chem.* 287, 12050–12059. doi: 10.1074/jbc.M111.307678

Yang, Y., Kitagaki, J., Dai, R. M., Tsai, Y. C., Lorick, K. L., Ludwig, R. L., et al. (2007). Inhibitors of ubiquitin-activating enzyme (E1), a new class of potential cancer therapeutics. *Cancer Res.* 67, 9472–9481. doi: 10.1158/0008-5472.CAN-07-0568

Yang, Q., Zhao, J., Chen, D., and Wang, Y. (2021). E3 ubiquitin ligases: styles, structures and functions. *Mol. Biomed.* 2:23. doi: 10.1186/s43556-021-00043-2

Zheng, L., Liu, Z., Wang, Y., Yang, F., Wang, J., Huang, W., et al. (2021). Cryo-EM structures of human GMPPA-GMPPB complex reveal how cells maintain GDP-mannose homeostasis. *Nat. Struct. Mol. Biol.* 28, 1–12. doi: 10.1038/s41594-021-00591-9

Zhu, G., Herlyn, M., and Yang, X. (2021). TRIM15 and CYLD regulate ERK activation via lysine-63-linked polyubiquitination. *Nat. Cell Biol.* 23, 978–991. doi: 10.1038/s41556-021-00732-8

frontiers | Frontiers in Molecular Neuroscience

TYPE Review
PUBLISHED 01 July 2024
DOI 10.3389/fnmol.2024.1405415

OPEN ACCESS

EDITED BY
Jean-Marc Taymans,
Institut National de la Santé et de la Recherche Médicale (INSERM), France

REVIEWED BY
Jana Alonso,
Spanish National Research Council (CSIC), Spain
Xiang Zhao,
Chan Zuckerberg Biohub, United States

*CORRESPONDENCE
Benoit Schneider
✉ Benoit.schneider@polytechnique.edu

†These authors have contributed equally to this work and share first authorship

RECEIVED 22 March 2024
ACCEPTED 14 June 2024
PUBLISHED 01 July 2024

CITATION
Bizingre C, Bianchi C, Baudry A, Alleaume-Butaux A, Schneider B and Pietri M (2024) Post-translational modifications in prion diseases. *Front. Mol. Neurosci.* 17:1405415. doi: 10.3389/fnmol.2024.1405415

Post-translational modifications in prion diseases

Chloé Bizingre[1,2†], Clara Bianchi[1,2†], Anne Baudry[1,2], Aurélie Alleaume-Butaux[1,2], Benoit Schneider[1,2,3*] and Mathéa Pietri[1,2]

[1]INSERM UMR-S 1124, Paris, France, [2]Université Paris Cité, UMR-S 1124, Paris, France, [3]Ecole polytechnique, Institut Polytechnique de Paris, CNRS UMR7654, Palaiseau, France

More than 650 reversible and irreversible post-translational modifications (PTMs) of proteins have been listed so far. Canonical PTMs of proteins consist of the covalent addition of functional or chemical groups on target backbone amino-acids or the cleavage of the protein itself, giving rise to modified proteins with specific properties in terms of stability, solubility, cell distribution, activity, or interactions with other biomolecules. PTMs of protein contribute to cell homeostatic processes, enabling basal cell functions, allowing the cell to respond and adapt to variations of its environment, and globally maintaining the constancy of the *milieu interieur* (the body's inner environment) to sustain human health. Abnormal protein PTMs are, however, associated with several disease states, such as cancers, metabolic disorders, or neurodegenerative diseases. Abnormal PTMs alter the functional properties of the protein or even cause a loss of protein function. One example of dramatic PTMs concerns the cellular prion protein (PrP^C), a GPI-anchored signaling molecule at the plasma membrane, whose irreversible post-translational conformational conversion (PTCC) into pathogenic prions (PrP^{Sc}) provokes neurodegeneration. PrP^C PTCC into PrP^{Sc} is an additional type of PTM that affects the tridimensional structure and physiological function of PrP^C and generates a protein conformer with neurotoxic properties. PrP^C PTCC into PrP^{Sc} in neurons is the first step of a deleterious sequence of events at the root of a group of neurodegenerative disorders affecting both humans (Creutzfeldt–Jakob diseases for the most representative diseases) and animals (scrapie in sheep, bovine spongiform encephalopathy in cow, and chronic wasting disease in elk and deer). There are currently no therapies to block PrP^C PTCC into PrP^{Sc} and stop neurodegeneration in prion diseases. Here, we review known PrP^C PTMs that influence PrP^C conversion into PrP^{Sc}. We summarized how PrP^C PTCC into PrP^{Sc} impacts the PrP^C interactome at the plasma membrane and the downstream intracellular controlled protein effectors, whose abnormal activation or trafficking caused by altered PTMs promotes neurodegeneration. We discussed these effectors as candidate drug targets for prion diseases and possibly other neurodegenerative diseases.

KEYWORDS

neurodegenerative diseases, signaling, sialylation, phosphorylation, α-Secretases, ROCK, PDK1 (PDPK1), PDK4

1 Introduction

The structure, dynamics, and functionalities of proteins depend on or are influenced by post-translational modifications (PTMs), i.e., chemical reactions that occur after the synthesis of proteins. Protein PTMs can be reversible or irreversible and are, most often, driven by enzymes. Reversible PTMs of proteins are associated with the covalent addition of functional

or chemical groups, such as the acetyl, phosphate, methyl, glycan, short- and long-chain acyl, or ubiquitin groups, among others, on the side-chain of key amino acids of the targeted protein (Ramazi and Zahiri, 2021). The addition of those chemical functions relies on the activity of specific enzymes (acetylases, kinases, methylases, glycanases, ubiquitinases, etc) that catalyze the transfer of the group from a specific donor to the protein. Those PTMs are reversible as they are removed by hydrolytic enzymes (deacetylases, phosphatases, demethylases, deubiquitinases, etc.) that regenerate a naked protein with functional properties distinct from those of the post-translational modified counterpart. Reversible PTMs contribute to the spatio-temporal regulation of biological processes that notably relate to cell signaling events, genome plasticity, the regulation of gene expression, or energy metabolism (Humphrey et al., 2015; Millán-Zambrano et al., 2022). By contrast, irreversible PTMs of proteins sometimes refer to glycation and deamidation but mostly relate to the proteolytic modifications of proteins. Several proteases achieve the cleavage of the concerned protein, giving rise to protein fragments with distinct biological functions (Walsh et al., 2005). For example, some enzymes (e.g., digestive enzymes) and hormones (e.g., insulin) are synthesized in an immature form, called the pro-form, and turn activated after the proteolytic removal of one or several fragments (Triebel et al., 2022). Those PTMs are irreversible, so the degradation of the modified protein is necessary to regulate the biological process in which the protein is involved. Another type of irreversible, non-classical PTMs relates to the transconformational conversion of proteins, which differs from the subtle protein structural changes associated with protein activity and regulation. The transconformational conversion of proteins consists of deep modifications of the protein folding, i.e., the rearrangement of the protein with changes in the ratio between α-helix and β-sheet elementary folding motifs (Louros et al., 2023). These PTMs that affect the global architecture of the protein cause changes in the physicochemical properties of the protein, such as the surface charges and solubility, thereby leading to protein conformers that often display biological activity distinct from the conformer they derive (Louros et al., 2023). One unfortunate famous example of such post-translational conformational conversion (PTCC) of proteins relates to prions. Prions were highly publicized in the late 20th century with the mad cow disease crisis and the emergence of the variant Creutzfeldt–Jakob disease in humans caused by the transmission of prion pathology from cows to humans through food contaminated with prions (Knight, 2017). Even if the mad cow crisis is behind us, the emergence of chronic wasting disease (CWD) that concerns elk and deer and, for the moment, is confined to North America, Japan, and Scandinavia (Tranulis and Tryland, 2023), combined with the risk of CWD transmission to humans (Hannaoui et al., 2022), necessitates improving our knowledge of the mechanisms underlying prion diseases to rationalize therapeutic strategies to combat these devastating neurodegenerative disorders.

Prion diseases are caused by an infectious and neurotoxic protein, the scrapie protein (PrP^{Sc}), which results from the post-translational conformational conversion of the normal cellular prion protein PrP^{C} (Prusiner, 1998). While the 3D structure of PrP^{C} contains three α-helices in the ordered globular domain of the protein, the α-helices are remodeled in favor of the formation of β-sheets in the 3D structure of PrP^{Sc}. Such changes in PrP structure confer PrP^{Sc} insoluble properties in detergents and partial resistance to proteolysis. Moreover, PrP^{Sc} β-sheets are responsible for the aggregation of PrP^{Sc} molecules and the formation of fibrillar amyloid assemblies (Cobb et al., 2007; Kraus et al., 2021). As PrP^{Sc} promotes the conversion of PrP^{C} through direct interaction of PrP^{Sc} with PrP^{C}, post-translational conformational changes of PrP^{C} into PrP^{Sc} are autocatalytic, which sustains the prion concept formulated in the 80s (Prusiner, 1986). It is established that PrP^{C} conversion into PrP^{Sc} in neurons is at the root of prion diseases (Mallucci et al., 2003). PrP^{C} is a ubiquitous protein that is more expressed in neurons and is present at the cell surface. Acting at the plasma membrane as a neuronal receptor or co-receptor (Mouillet-Richard et al., 2000) or a scaffolding protein that governs the dynamic assembly of signaling modules (Linden et al., 2008), PrP^{C} controls signaling effectors that all contribute to the regulation of neuronal functions (Schneider, 2011). As PrP^{C} is subjected to several PTMs, we here review how those PTMs of PrP^{C} impact the transconformational conversion of PrP^{C} into PrP^{Sc}. We also summarize how PrP^{C} PTCC into PrP^{Sc} (i) affects PrP^{C} interactome at the plasma membrane and (ii) impacts PrP^{C} downstream signaling effectors, whose activity or trafficking disturbed by imbalanced PTMs contribute to the progression of prion diseases.

2 Post-translational modifications of PrP^{C}: friends or foes in prion diseases?

2.1 Several PrP^{C} PTMs generate heterogeneity in the PrP^{C} landscape

PrP^{C} is coded by the PRNP gene located in chromosome 20 in the human genome (chromosome 2 in mice). The translation of the protein generates a single polypeptide chain of 253 amino-acids that folds as three α-helices and two short anti-parallel β-sheets in the C-terminal PrP^{C} domain, while the N-terminal domain remains flexible (Zahn et al., 2000) and its conformation varies depending on the ligand interacting with this region (Zahn, 2003). Several PTMs occur on PrP^{C} consisting of the removal of the N-terminus signal sequence when the protein enters the endoplasmic reticulum, the attachment of a GlycosylPhosphatidylInositol (GPI) moiety at residue 230 of PrP^{C} C-terminus, two N-glycosylations at Asn181 and Asn197, the formation of a disulfide bridge between Cys179 and Cys214 that ensures the stability of the C-terminal domain of PrP^{C}, and the cleavage of the protein between amino-acids 111 and 112 by ADAM10 and TACE (aka ADAM17) α-secretases (Figure 1) (Vincent et al., 2001; Rudd et al., 2002). Such PTMs of PrP^{C} give rise to a heterogeneous population of GPI-anchored PrP^{C} molecules at the plasma membrane, i.e., full-length and truncated PrP^{C} carrying no, one, or two N-glycans (Figure 1). Nevertheless, unglycosylated PrP^{C} represents a minor proportion of PrP^{C} molecules present in the plasma membrane. The nature of the sugars composing the glycans (Ermonval et al., 2009b), which are more or less decorated with sialic acid (Baskakov and Katorcha, 2016), expands the diversity of cell surface PrP^{C} molecules with an apparent molecular mass ranging from 17 to 35 kDa. In cells, sialoglycosylated PrP^{C} resides in lipid rafts of the plasma membrane (Taylor and Hooper, 2006). Sialylation of PrP^{C} GPI anchor acts as a signal that targets the protein to the synapse in neurons (Figure 1) (Bate et al., 2016).

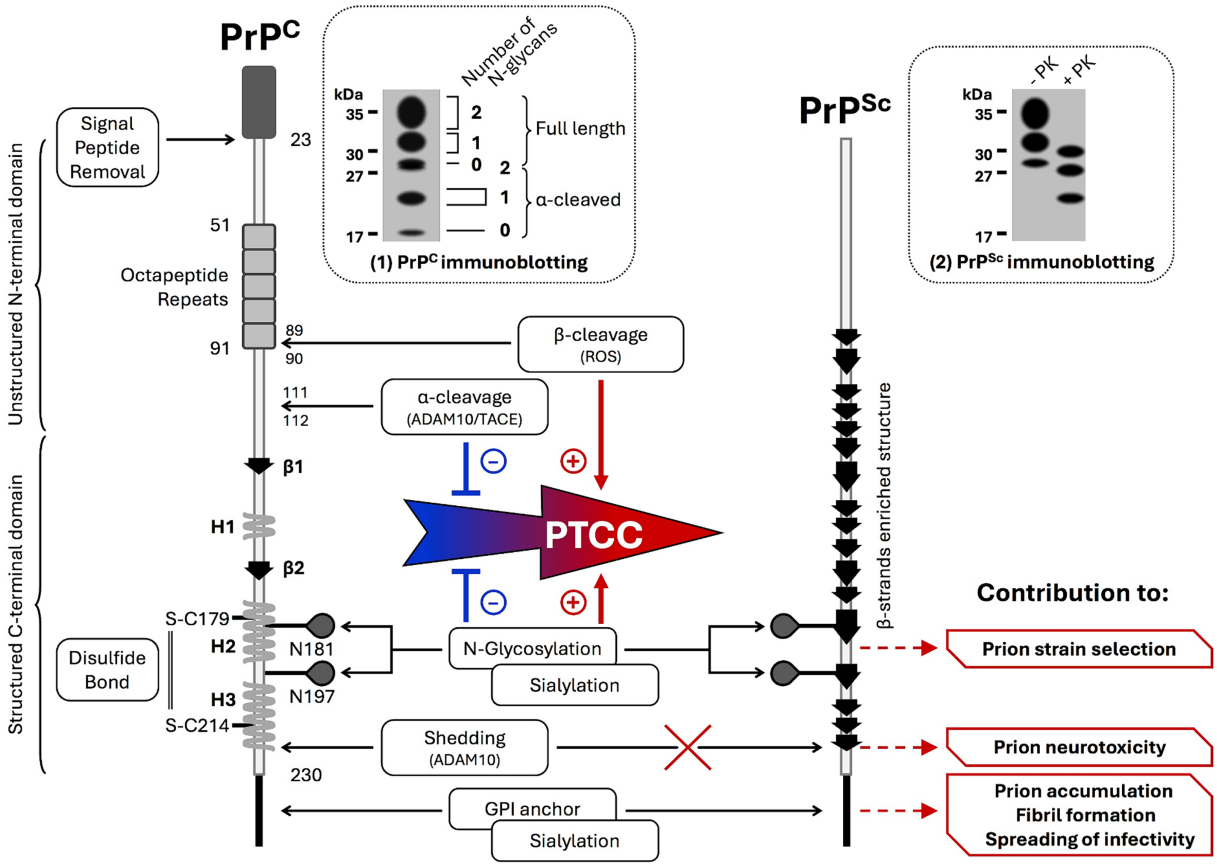

FIGURE 1
PrP^{C} PTMs influence the post-translational conformational conversion of PrP^{C} into PrP^{Sc} and determine features of prion diseases. Schematic representations of (i) PrP^{C} structure showing PrP^{C} PTMs (glycosylation, sialylation, disulfide bond, GPI anchoring, and α-cleavage) and (ii) PrP^{C} isoforms (non, mono, or biglycosylated full-length and truncated PrP^{C}) ranging from 17 to 35 kDa revealed by PrP immunoblotting (insert 1). The post-translational conformational conversion (PTCC) of PrP^{C} into pathogenic prions (PrP^{Sc}) changes the 3D structure of PrP^{C} with the suppression of the three α-helices (H1, H2, and H3) and modification of the two β-sheets (β1 and β2) in favor of a global β-sheet enrichment in PrP^{Sc}. PrP^{Sc} displays physicochemical properties distinct from PrP^{C}, including partial resistance to proteolysis of PrP^{Sc} submitted to proteinase K (PK) digestion (insert 2). Depending on the nature of PrP^{C} PTMs, PrP^{C} PTMs influence, positively or negatively, PrP^{C} PTCC into PrP^{Sc} and take part in prion strain selection, prion accumulation, fibril formation, prion neurotoxicity, and spreading of prion infectivity.

2.2 The GPI anchor of PrP^{C} favors the amplification and spread of prion infectivity

As the GPI anchor is found attached to the C-terminus of both PrP^{C} and PrP^{Sc} (Stahl et al., 1990), the GPI anchor has been initially proposed to play an active role in the replication of PrP^{Sc}. However, PrP^{Sc} replication occurs when using recombinant PrP^{C} purified from bacteria, i.e., devoid of GPI anchor (Colby et al., 2007). PrP^{C} PTCC into PrP^{Sc} also occurs in mice expressing GPI anchorless-PrP^{C} (Chesebro et al., 2005; Aguilar-Calvo et al., 2017) and in patients with Gerstmann–Sträussler–Scheinker (GSS) Syndrome who express anchorless PrP^{C} due to Q227X stop codon mutation in PRNP gene, i.e., before the site of insertion of the GPI anchor (Shen et al., 2021). Thus, the GPI moiety does not appear to be fundamental to PrP^{C} PTCC into PrP^{Sc}. Nevertheless, based on the observation that mice expressing GPI anchorless-PrP^{C} and infected with prions display fibril-containing plaques larger than those in prion-infected wild-type mice, the GPI anchor is suspected to obstruct fibril assembly (Aguilar-Calvo et al., 2017).

Additional experiments combining cell-based assays and *in vivo* approaches also revealed that the GPI anchor is needed for the establishment and maintenance of chronic prion infection within a cell (McNally et al., 2009). Such a role of the GPI anchor in the persistence of prion infection is presumably not attributed to the targeting of PrP^{C} to specific membrane environments compatible with prion formation. GPI-anchored PrP^{C} would rather serve to amplify PrP^{Sc} production, thus enabling the spreading of infectivity between cells (Figure 1) according to different cell modalities (Vilette et al., 2018).

2.3 Sialylation of N-glycans of PrP^{C} acts as a filter for prion strain selection

Mutagenesis experiments designed to suppress the two N-linked glycosylation sites in the C-terminal PrP^{C} domain indicated that glycans limit the formation of fibrils and spongiosis in the brains of prion-infected mice (Sevillano et al., 2020). By stabilizing

intramolecular interactions with the N-terminal domain of PrP^C, the N-glycans maintain a PrP^C physiological fold that resists the acquisition of a toxic conformation (Schilling et al., 2023). In addition, the sialylation of the N-linked carbohydrates, but not of the GPI anchor, was shown to create a prion replication barrier due to electrostatic repulsion forces between sialic residues that constraint PrP^C structure (Katorcha et al., 2015, 2016). Thus, PrP^C molecules that are poorly glycosylated with hyposialylated N-linked glycans would be more prone to convert into PrP^{Sc} (Bosques and Imperiali, 2003). Baskakov's laboratory further showed that the sialoglycan profile of cell surface PrP^C dictates the selective recruitment of PrP^C molecules by pathogenic prions, leading to the emergence of a prion strain with a unique sialoglycoform signature and prion disease phenotype (Figure 1) (Makarava et al., 2020). Of note, the sialylation state of PrP^{Sc} evolves with PrP^{Sc} invasion of secondary lymphoid organs, such as the spleen, in which PrP^{Sc} is more sialylated than in the brain. The hypersialylation of N-glycans of PrP^{Sc} in secondary lymphoid organs vs. the brain reflects different equipment of sialyltransferases between organs and is proposed as a mechanism that dissimulates PrP^{Sc} from the immune survey (Srivastava et al., 2015). The selection of PrP^C molecules with a definite level of sialic acid on N-glycans enters the complex process of prion strain evolution that balances the rapid conversion of PrP^C into PrP^{Sc} and PrP^{Sc} protection against the immune system (Makarava and Baskakov, 2023).

2.4 The α-cleavage and shedding of PrP^C brake PrP^C conversion into PrP^{Sc}

ADAM10/17-mediated α-cleavage of PrP^C between the amino acids 111 and 112 exerts protection against prion infection. Truncated PrP^C (also called PrP C1 fragment) resists the post-translational conformational conversion induced by PrP^{Sc} and exerts a dominant negative effect on the conversion of full-length PrP^C into PrP^{Sc} (Westergard et al., 2011). However, prion infection cancels PrP^C α-cleavage in favor of a redox-induced β-cleavage of PrP^C between residues 89/90, generating PrP C2 fragment (Chen et al., 1995). As the C2 fragment converts into PrP^{Sc} and does not inhibit the conversion of full-length PrP^C into PrP^{Sc}, the PTM switch between the α- and β-cleavage of PrP^C contributes to the exponential accumulation of PrP^{Sc}. ADAM10 α-secretase also displays the capacity to execute PrP^C cleavage upstream of the GPI anchor, which generates a GPI-anchorless PrP called shed PrP (Kovač and Čurin Šerbec, 2018). Shed PrP floats in bodily fluids, binds PrP^{Sc} oligomers, prevents their replication, or acts as nucleation seeds that promote the deposition and neutralization of PrP^{Sc} (Mohammadi et al., 2023). Deficit in ADAM10-mediated shedding of PrP^C within a prion infectious context contributes to PrP^{Sc} accumulation and progression of prion diseases (Figure 1) (Chen et al., 2014; Altmeppen et al., 2015).

2.5 PTMs of PrP^C, prion strains, and prion diseases

While PrP^C PTCC into PrP^{Sc} is at the root of all prion diseases, these neurodegenerative diseases constitute a heterogeneous group. Considering the same host, prion diseases can exhibit different phenotypes characterized by distinct clinical signs, magnetic resonance imaging (MRI) signals, disease incubation times, brain lesion profiles, and PrP^{Sc} deposit types. These phenotypes are associated with specific PrP^{Sc} biochemical properties in terms of electrophoretic profiles, degree of N-glycosylation, and resistance to proteinase K digestion (Silva et al., 2015). The biochemical and pathological characteristics of PrP^{Sc} are stable and conserved when PrP^{Sc} is successively transmitted to the same host species, leading to the concept of prion strains and their classification into several disease-associated PrP^{Sc} types (Parchi et al., 1999; Collinge and Clarke, 2007; Carta and Aguzzi, 2022). The structure analysis of *ex vivo* pathogenic prions at high resolution by cryogenic electron microscopy (Cryo-Em) revealed that prion strains display analogous β-arch topologies but differ in their conformation details (Kraus et al., 2021; Hoyt et al., 2022; Manka et al., 2022; Cracco et al., 2023). Conformational differences between strains would relate to constraints exerted by PrP^C PTMs at the level of N-glycans and the GPI anchor (Vázquez-Fernández et al., 2016).

As mentioned above, the post-translational modifications of PrP^C by N-glycosylation, sialylation, and cleavage give rise to a great diversity of PrP^C molecules at the cell surface. The PTM profile of PrP^C varies according to the cell context due to cell-type specific equipment in sialyltransferases, glycosidases, α-secretases, etc. Specific PTM combinations at the proximal level of PrP^C in defined brain areas and peripheral tissues would thus sustain the regio-selective emergence of peculiar prion strains, their accumulation, tropism toward definite neuronal cell types, and the susceptibility of specific neuronal populations to respond to prion strain infection, ultimately leading to neurodegeneration. Supporting the idea of an intricate link between PrP^C PTM profiles, regionalized PTCC of PrP^C into PrP^{Sc}, and prion strain-associated neuropathological lesions, post-mortem detection of spongiform degeneration in sporadic Creutzfeldt–Jakob disease (CJD) brain using diffusion MRI showed that the location of the epicenter and the propagation profile of lesions depend on the prion strain (Pascuzzo et al., 2020). In the near future, single-cell approaches, transcriptomic and proteomic analyses, and the profiling of PrP^C PTMs should permit the categorization of brain cell populations that select, replicate, and propagate specific prion strains.

In prion diseases, PrP^C PTCC into PrP^{Sc} represents the first critical step in neuropathogenesis, which is, positively or negatively, influenced by a set of limited PTMs that concern the N-glycans, GPI-anchor, and cleavages of PrP^C (Figure 1). In the PrP^{Sc}-induced neurodegenerative domino game, PrP^C PTCC into PrP^{Sc} impacts PrP^C signaling partners in the plasma membrane (i.e., PrP^C interactome) and downstream PrP^C-coupled neuronal signaling effectors, whose deregulation causes the death of prion-infected neurons.

3 Post-translational modifications of PrP^C interactome and prion diseases

3.1 PrP^C interactome: PrP^C orchestrates the organization and activity of membrane signalosomes

Many studies have been conducted to define the interactome of PrP^C, which currently includes more than 30 protein and non-protein partners. These interactors of PrP^C include soluble factors (copper, STI-1, etc.), components of the extracellular matrix (laminin,

vitronectin, etc.), or membrane proteins (caveolin 1, NCAM, MARCKS, neuronal receptors, β-integrins, laminin receptor, etc.) (Miranzadeh Mahabadi and Taghibiglou, 2020). The interaction of PrP^{C} with all those partners underlies the complex role of PrP^{C} in membrane signalosomes, i.e., signaling platforms in lipid rafts of the plasma membrane in which PrP^{C} modulates the interactions of cell adhesion molecules with the extracellular matrix or the signaling activity of receptors (Linden et al., 2008; Schneider, 2011). This regulatory role of PrP^{C} in the assembly, dynamics, and activity of membrane signalosomes depends on PrP^{C}-induced reversible PTMs of PrP^{C} interactors. Within a prion infectious context, the conversion of PrP^{C} into PrP^{Sc} impacts the PrP^{C} interactome and the PTMs physiologically involved in the regulation of PrP^{C} signalosomes.

3.2 PrP^{Sc}-induced alteration of PTMs linked to the PrP^{C}-caveolin-1 signaling hub disrupts caveolae dynamics and promotes PrP^{C} oversignaling in prion diseases

Our laboratory identified the first PrP^{C}-associated signaling platform in neurite extensions of 1C11-derived serotonergic and noradrenergic neuronal cells (Mouillet-Richard et al., 2000). This platform results from the assembly of GPI-anchored PrP^{C} with caveolin-1 (Cav1), a scaffolding protein partially inserted into the inner leaflet of the plasma membrane. Cav1 would interact with the GPI anchor of PrP^{C} via palmitoyl groups present at cysteine residues in the carboxy-terminal domain of Cav1 (Dietzen et al., 1995; Arbuzova et al., 2000). The PrP^{C}-Cav1 complex activates the Src tyrosine kinase Fyn on the cytosolic face of the plasma membrane by dephosphorylating the Fyn inhibitory site at Tyr528 (Mouillet-Richard et al., 2000), possibly via the protein tyrosine phosphatase α (PTPα) (Wang et al., 2009). Subsequent phosphorylation of Cav1 at Tyr14 by activated Fyn stabilizes the PrP^{C}-Cav1-Fyn platform (Pantera et al., 2009; Gottlieb-Abraham et al., 2013) and initiates downstream intracellular signaling events (Schneider et al., 2003). Depending on the cell type and cell compartment, the PrP^{C}-Cav1 complex recruits and activates Fyn but also other tyrosine kinases of the Src family, such as Lyn or Src, in neurons (Lopes et al., 2005; Toni et al., 2006; Caetano et al., 2008), astrocytes (Dias et al., 2016), or immune cells (Stuermer et al., 2004; Krebs et al., 2006).

In addition to its role in the formation and regulation of signalosomes, Cav1 is the major scaffolding protein involved in caveolae formation. Cav1 oligomerization enables the formation of the caveolar coat. The Cav1 phosphorylation or dephosphorylation at Tyr14 destabilizes or stabilizes Cav1 oligomers, respectively, sustaining the bidirectional "kiss-and-run" movement of caveolae between the plasma membrane and the cytosol (Parton et al., 1994; Parton and Simons, 2007; Zimnicka et al., 2016). The Cav1 phosphorylation also drives caveolae anchorage to actin filaments thanks to the interaction between phosphorylated Cav1 and phosphorylated filamin A (Sverdlov et al., 2009). By promoting Cav1 phosphorylation and influencing caveolae movement, PrP^{C} would thus modulate the signaling activity of receptors present in caveolae (Luo et al., 2021).

Within a prion infectious context, co-immunoprecipitation experiments showed that PrP^{Sc} also interacts with Cav1 in brain homogenates of prion-infected hamsters (Shi et al., 2013). Our laboratory provided evidence in 1C11 neuronal cells and mouse brains infected by prions that PrP^{Sc} chronically activates Fyn kinase (Pietri et al., 2006; Pradines et al., 2013) and disrupts the "kiss-and-run" dynamics of caveolae, leading to the accumulation and freezing of Cav1-enriched vesicles underneath the plasma membrane (Figure 2) (Pietri et al., 2013). The freezing of Cav1-enriched vesicles within prion-infected neurons likely reduces the stock of Cav1 available at the plasma membrane and dampens Cav1 regulatory functions in signal transduction, lipid raft-dependent endocytosis, etc. (Cha et al., 2015). We anticipate that, in prion-infected neurons, the sequestration of signalosomes in intracellular freeze caveolae alters the physiological homeostatic activity of signalosomes at the plasma membrane.

Interestingly, the fluidity of the plasma membrane also depends on caveolae fusion with the plasma membrane (Sohn et al., 2018; Yang et al., 2020). Whether, in prion-infected neurons, the freezing of caveolae in the cytosol caused by the excessive phosphorylation of Cav1 at Tyr14 affects the elastic properties of the plasma membrane and thus contributes to neurodegeneration deserves further investigation.

3.3 PrP^{Sc}-induced alteration of PTMs linked to PrP^{C} interaction with adhesion molecules impacts cell adhesion and neuronal polarity in prion diseases

Although varying with the cell type, the molecular composition of the PrP^{C} interactome always includes several proteins involved in cell adhesion, e.g., extracellular matrix proteins, such as laminin, vitronectin, and fibronectin, and membrane proteins, including integrins, neural cell adhesion molecule (NCAM), and myristoylated alanine-rich C-kinase substrate (MARCKS) proteins (Ghodrati et al., 2018). MARCKS are proteins inserted into the inner leaflet of the plasma membrane via a positively charged domain and a myristoyl group added to Gly2 (Arbuzova et al., 2000). These proteins likely interact with the GPI anchor of PrP^{C}.

A global proteomic study comparing PrP^{C} interactomes of four mouse cell lines and the mouse brain revealed a highly conserved functional relationship between PrP^{C}, MARCKS, and NCAM1 (Mehrabian et al., 2016). PrP^{C} directly interacts with NCAM1, promoting NCAM1 recruitment to lipid rafts and NCAM1-dependent Fyn kinase activation (Santuccione et al., 2005; Lehembre et al., 2008). Through its coupling to MARCKS, PrP^{C} indirectly controls NCAM1 sialylation by regulating the expression of the polysialyltransferase ST8SIA2 (Boutin et al., 2009; Mehrabian et al., 2015). The PrP^{C}-induced increase in NCAM1 polysialylation limits homophilic and heterophilic NCAM1 interactions and thereby modulates cell adhesion, a critical event for the onset and maintenance of neuronal polarity (Mehrabian et al., 2016). Any PrP^{Sc}-induced disturbance of the PrP^{C}-NCAM1-MARCKS signalosome would affect neuronal polarity in prion diseases.

Beyond NCAM1, PrP^{C} is also functionally involved in the regulation of other adhesion proteins, such as β1 integrins, which orchestrate the assembly and the turnover of focal adhesions (FAs). PrP^{C} prevents β1 integrin microclustering and attenuates β1 integrin signaling in 1C11 and PC12 cells (Loubet et al., 2012). By interacting with β1 integrins, PrP^{C} would block the structural modifications required for β1 integrin activation. Alternatively, PrP^{C} would limit β1 integrin signaling by neutralizing some β1 integrin activators such as CD98 or thrombospondin-1 (Ghodrati et al., 2018). In prion-infected neuronal

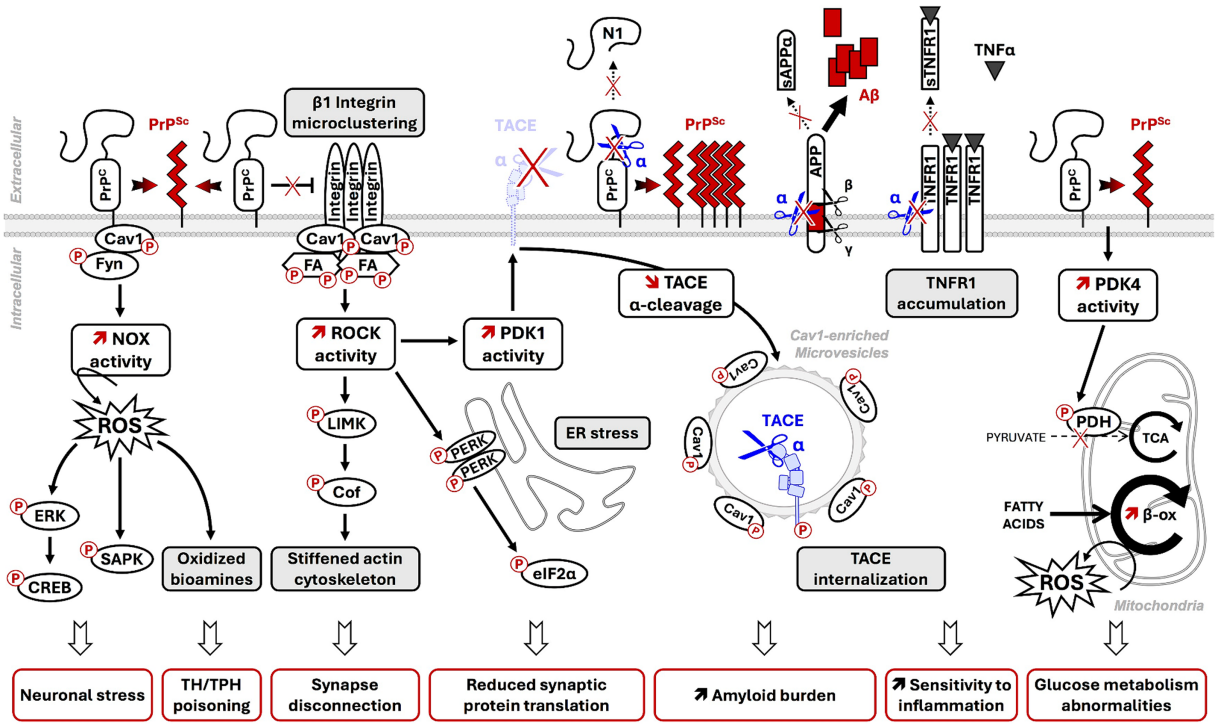

FIGURE 2
Contribution of PrP^{Sc}-induced PTMs dysregulation of PrP^{C} membrane partners and coupled signaling effectors to prion neuropathogenesis. In prion diseases, post-translational conformational conversion (PTCC) of PrP^{C} into PrP^{Sc} alters PTMs of PrP^{C} membrane partners in PrP^{C} signalosomes [Cav1, Fyn, components of focal adhesions (FA)] and deregulates downstream intracellular signaling effectors (NADPH oxidase-NOX, ROCK, PDK1, PDK4). The deregulation of PrP^{C}-coupled signaling pathways on PrP^{C} PTCC into PrP^{Sc} contributes to neurodegeneration through multiple deleterious events: onset of oxidative stress conditions, MAPK/SAPK-dependent neuronal stress, alteration of neuronal polarity and functions, amplification of PrP^{Sc} and Aβ production, increased vulnerability to TNFα inflammation by reduced shedding of plasma membrane TNFR into sTNFR, and energy metabolism abnormalities. NOX: NADPH oxidase; ROS: reactive oxygen species; ERK: extracellular-regulated kinases; SAPK: stress-associated protein kinases (p38 and JNK); ROCK: RhoA-associated coiled-coil containing kinases; PERK: PKR-related endoplasmic reticulum kinase; PDK1: 3-phosphoinositide-dependent kinase 1; TACE: TNFα converting enzyme; (s)TNFR: (soluble) TNFα receptor; N1: N-terminal fragment of α-cleaved PrP^{C}; α/β/γ: α-, β-, and γ-secretases; sAPPα: neuroprotective α-cleaved APP fragment; Aβ: neurotoxic amyloid β-peptides; PDK4: Pyruvate Dehydrogenase Kinase 4; PDH: Pyruvate Dehydrogenase. TCA: tricyclic acid cycle or Krebs cycle; β-ox: fatty acid β-oxidation.

cells (Alleaume-Butaux et al., 2015), as well as in the brains of mice infected with the Chandler or Rocky Mountain Laboratory (RML) prion strains (Albert-Gasco et al., 2024), PrP^{Sc}-induced depletion of plasma membrane PrP^{C} causes a loss of PrP^{C}'s regulatory role toward β1 integrins. This depletion leads to β1 integrin microclustering and oversignaling (Alleaume-Butaux et al., 2015). β1 integrin oversignaling induced by PrP^{Sc} likely promotes chronic Src kinase phosphorylation at Tyr418 and activation, the subsequent phosphorylation of focal adhesion kinase (FAK) at Tyr861 by Src kinases, and the phosphorylation of paxillin at Tyr31 and Tyr118 by both Src kinases and FAK, as observed in cells depleted for PrP^{C} (Loubet et al., 2012; Alleaume-Butaux et al., 2015; Ezpeleta et al., 2017). Such an overphosphorylated state of FA components enhances FA stability and reduces FA dynamics that disturb the adhesion properties of prion-infected neurons. This mechanism would contribute, at least in part, to the loss of neuronal polarity on prion infection (Figure 2) (Alleaume-Butaux et al., 2015).

Finally, PrP^{C} modulates the laminin-mediated attachment of neurons to the extracellular matrix. PrP^{C} interacts with laminin and laminin receptors (LRs) and limits laminin binding to its membrane receptor (Baloui et al., 2004). Our laboratory further showed in 1C11 neuronal cells that PrP^{C}, through its coupling to Cav1 and Fyn, regulates the activity of tissue non-specific alkaline phosphatase (TNAP), which phosphorylates laminin and reduces laminin-dependent adhesion of cells (Ermonval et al., 2009a). As PrP^{Sc} interacts with LR in neuronal cells (Morel et al., 2005) and overactivates the PrP^{C}-Cav1-Fyn platform, the excessive phosphorylation of laminin induced by PrP^{Sc} would also destabilize the neuronal cell-matrix interaction and neuronal polarity in prion-infected neurons.

Thus, by affecting several homeostatic PTMs in the PrP^{C} adhesion interactome, PrP^{Sc} alters cell–cell and cell-extracellular matrix contacts required for the onset and stability of the neuronal polarity and the neuronal plasticity.

3.4 PrP^{Sc}-induced alteration of PTMs linked to PrP^{C} interaction with synaptic protagonists disturbs neurotransmission in prion diseases

At the presynaptic and post-synaptic membrane of neurons, PrP^{C} interacts with several ionotropic (NMDAR, AMPAR GluA1/2, KAR GluR6/7, and α7nAChR) and metabotropic (mGluR1/5) receptors (Kleene et al., 2007; Beraldo et al., 2010, 2011; Carulla et al., 2011; Watt et al., 2012; Um et al., 2013).

Several studies have highlighted that group I metabotropic glutamate receptors (mGluR1/5) act as co-receptors of PrP^C. The binding of laminin or STI1 to PrP^C activates PrP^C, which in turn recruits and activates mGluR1/5 (Coitinho et al., 2006; Beraldo et al., 2011). mGluR1/5 are G protein-coupled receptors (GPCR) coupled to heterotrimeric Gαq/11 proteins involved in glutamate-dependent memory consolidation through neuritogenesis and neuronal plasticity events. The molecular mechanisms underlying PrP^C modulation of mGluR1/5 activity remain, however, elusive. Nevertheless, the beneficial effect of mGluR1/5 inhibition in scrapie-infected mice suggests that PrP^{Sc} impacts the PrP^C-mediated regulation of mGluR1/5 activity (Goniotaki et al., 2017). Since activation of mGluR1/5 involves binding of Fyn kinase to the C-terminal domain of mGluR1/5 and Fyn-dependent phosphorylation of mGluR1/5 at Tyr937 (Jin et al., 2017), chronic activation of Fyn by PrP^{Sc} may corrupt mGluR1/5 activity by imbalanced phosphorylation of mGluR1/5.

NMDAR is a calcium-permeable channel composed of two GluN1 and two GluN2 or GluN3 subunits involved in glutamate-mediated neuronal plasticity and excitotoxicity. PrP^C interacts with GluN2D and GluN2B subunits (Khosravani et al., 2008; Barnes et al., 2020) and controls NMDA receptor activity through nitrosylation of GluN1 and GluN2A subunits (Gasperini et al., 2015). PrP^C-bound Cu^{2+} acts as an electron acceptor that induces NO oxidation and subsequent S-nitrosylation of two cysteines on GluN1 and three cysteines on GluN2A, including Cys399, which mediates the predominant inhibitory effect on NMDAR activity. The reduction of NMDAR S-nitrosylation in prion-infected mice before the onset of clinical signs increases NMDAR-dependent excitation (Ratté et al., 2008). PrP^{Sc} also induces phosphorylation of the NMDAR GluN2B subunit at Tyr1472, probably via sustained activation of Fyn, and potentiates NMDAR activity in the hippocampus of a mouse model of CJD (Bertani et al., 2017). By decreasing S-nitrosylation and increasing phosphorylation of NMDAR, PrP^{Sc} enhances NMDAR activity and renders prion-infected neurons hypersensitive to NMDA-induced excitotoxicity (Meneghetti et al., 2019). Disturbance of PrP^C-governed PTMs of neuronal receptors by PrP^{Sc} thus alters neurotransmission in prion diseases.

Of note, the synapse interactome of PrP^C also includes synapse-associated proteins (synaptophysin and PSD-95), vesicle-associated proteins (synapsin), and ion pumps (Kv4.2 DPP6 and VGCC). Through these interactions, PrP^C contributes to the assembly of functional complexes involved in neurotransmission at the pre- and post-synaptic membranes. Further investigations are needed to assess whether PrP^{Sc}-mediated disruption of those complexes or imbalanced PTMs of the above-mentioned synapse effectors would also contribute to the alteration of neurotransmission in prion diseases (Russelakis-Carneiro et al., 2004).

4 PTMs of signaling effectors downstream of PrP^C in prion diseases

4.1 PrP^C contribution to neuronal homeostasis depends on PrP^C coupling to several signaling effectors

The use of diverse neuronal cell lines (N2a neuroblastoma cells, 1C11 neuronal stem cells and their serotonergic or noradrenergic neuronal progenies, PC12 pheochromocytoma cells, etc.) and primary cultures of neurons (cerebellar granule neurons, cortical or hippocampal neurons) showed that PrP^C is involved in the regulation of a wide range of cellular functions, including cell adhesion (see Section 3.3), neuronal differentiation, synaptic plasticity, cell survival, redox equilibrium, stress protection, or energy metabolism (Schneider, 2011; Castle and Gill, 2017; Wulf et al., 2017; Schneider et al., 2021). This multifaceted role of PrP^C involves its capacity to act as a receptor/co-receptor, governing a complex signaling network, and as a scaffolding protein that regulates the lipid rafts of the plasma membrane. This regulation affects the assembly and stoichiometry of interaction between partners such as integrins, laminin receptors, and mGluR, thereby controlling the activity of diverse signaling modules. Regardless of the context, PrP^C is coupled to several intracellular signaling effectors, including Src kinase Fyn, NADPH oxidase, ERK1/2 MAP kinases, glycogen synthase kinase 3β (GSK3β), Protein kinase A (PKA), RhoA-associated coiled-coil containing kinases (ROCKs), 3-phosphoinositide-dependent kinase 1 (PDK1), Pyruvate Dehydrogenase Kinase 4 (PDK4), TACE α-secretase (aka ADAM17), and CREB transcription factor. These effectors all play a part in maintaining the homeostasis of neuronal functions (Chiarini et al., 2002; Hernandez-Rapp et al., 2014; Arnould et al., 2021; Schneider et al., 2021). For most of the signaling intermediates downstream of PrP^C, their regulation depends on reversible and transient PTMs by phosphorylation, which sustains the fine-tuning of neuronal functions. Within a prion infectious context, the corruption of PrP^C signaling in response to PrP^C PTCC into PrP^{Sc} leads to imbalance PTMs of PrP^C-coupled signaling effectors, thus generating aberrant and deleterious signals for prion-infected neurons (Figure 2). A global comparative phospho-proteome analysis between PrP^{Sc}-infected N2a cells and non-infected cells identified 105 proteins differentially phosphorylated with chronic and excessive phosphorylation of some effectors (e.g., cofilin) or loss of phosphorylation for some others (e.g., stathmin) (Wagner et al., 2010). We here review PTMs of some PrP^C-coupled signaling effectors affected by prion infection and the consequences thereof for neurons.

4.2 PrP^{Sc}-induced corruption of PrP^C/Fyn/NADPH oxidase signaling causes the recruitment of stress-sensitive SAPK and the accumulation of bioamine-derived neurotoxins

One signaling pathway impacted by PrP^{Sc} in prion-infected neurons is the PrP^C/Fyn/NADPH oxidase cascade. The chronic stimulation of this pathway triggers excessive production of reactive oxygen species (ROS) by NADPH oxidase (NOX) at the root of oxidative stress conditions. Overproduced ROS promote robust phosphorylation of MAPKs ERK1/2 (at Thr185/Tyr187) and additionally recruit stress-associated protein kinases (SAPKs) p38 and JNK1/2, which are activated by phosphorylations at Thr180/Tyr182 and Thr183/Tyr185, respectively. The subsequent sustained activation of MAPKs and SAPKs contributes to the death of prion-infected neurons by apoptosis (Figure 2) (Pietri et al., 2006; Pradines et al., 2013). The local rise of p38 phosphorylation at Thr180 and Tyr182 in dendritic spines of prion-infected hippocampal neurons was also shown to promote synaptic degeneration and decrement in synaptic transmission (Fang et al., 2018). Augmented phosphorylation of ERK1/2, p38, and JNK was confirmed *in vivo* in the brains of hamsters

infected with the 263 K prion strain (Lee et al., 2005; Pamplona et al., 2008). Of note, downregulating this pathway through the use of siRNAs against Fyn or the p22phox subunit of NADPH oxidase reverts those PTMs on ERK1/2, p38, and JNK induced by prion infection, supporting the therapeutic potential of targeting Fyn or NADPH oxidase to protect neurons in prion diseases (Pradines et al., 2013).

In addition, ROS overproduced by NADPH oxidase in prion-infected serotonergic or noradrenergic neurons promote the generation of oxidized derivatives of serotonin (5-HT), such as tryptamine 4,5-dione (T-4,5-D) and 5,6-dihydroxytryptamine (5,6-DHT), or catecholamines, such as 6-hydroxydopamine and tetrahydroisoquinolines. These derivatives are considered neurotoxins (Mouillet-Richard et al., 2008). Their neurotoxic action relies on the poisoning of metabolic enzymes involved in the synthesis of 5-HT or noradrenalin (NE), that is, a set of "toxic and accidental PTMs" affecting the tryptophan hydroxylase TPH (the rate-limiting enzyme for 5-HT synthesis) and possibly the tyrosine hydroxylase TH (the rate-limiting enzyme for NE synthesis) through the covalent grafting of 5-HT/catecholamine-derived neurotoxins at catalytic Cys residues of those biosynthetic enzymes (Figure 2).

Another consequence of ERK1/2 activation is the downstream activation of the transcription factor CREB by phosphorylation at Ser133 (Figure 2) (Lee et al., 2005; Pradines et al., 2013). In prion-infected neurons, sustained CREB phosphorylation stimulates the expression of the immediate-early genes Egr-1 implicated in cell survival but lockdowns the transcription of the MMP9 encoding gene, which attenuates the metalloproteinase activity of MMP9. The decrease in MMP9 enzymatic activity leads to a reduction of β-dystroglycan cleavage at the neuronal cell surface that alters the interactions between neurons and the extracellular matrix (Pradines et al., 2013). Such CREB PTMs and subsequent modifications of gene expression in prion-infected neurons would contribute to the alterations of neuronal plasticity associated with prion diseases.

4.3 Rock oversignaling upon prion infection alters neuronal polarity and takes part in the unfolded protein response

Our study documented that PrP^{Sc} abrogates the negative regulatory role exerted by PrP^{C} on ROCK signaling due to a loss of PrP^{C} control of β1 integrin microclustering and signaling activity (Alleaume-Butaux et al., 2015). In prion-infected 1C11 neuronal cells, N2a58 neuroblastoma cells, mouse cerebellar granule neurons, hippocampal neurons, and the brains of prion-infected mice, ROCK overactivity leads to excessive phosphorylation of LIMK1/2 at Thr505 and Thr508 and cofilin at Ser3. Stable phosphorylation of cofilin in prion-infected neurons cancels the severing activity of cofilin on the actin cytoskeleton (Figure 2) (Wagner et al., 2010; Alleaume-Butaux et al., 2015; Kim et al., 2020). The resulting PrP^{Sc}-induced stiffening of the actin cytoskeleton associated with fewer dynamics of focal adhesions (see section 3.3) disrupts neuronal polarity and provokes synaptic disconnection and dendrite/axon degeneration (Alleaume-Butaux et al., 2015; Kim et al., 2020). Such neuronal damages are counteracted by ROCK inhibition with pharmacological compounds (Alleaume-Butaux et al., 2015). Alterations in ROCK, LIMK1, and cofilin were also evidenced in the post-mortem cortex and cerebellum samples of sporadic Creutzfeldt–Jakob disease (sCJD) patients at clinical and pre-clinical stages (Zafar et al., 2018), paving the road for developing therapeutic strategies targeting ROCK to limit neurodegeneration in prion diseases.

Apart from the action of ROCK on the actin cytoskeleton, our laboratory showed that overactivated ROCK plays a role in the unfolded protein response (UPR). In 1C11-derived serotonergic neurons infected by mouse-adapted human GSS prions (Fukuoka strain), overactivated ROCK enhances the phosphorylation of PERK at Thr980 in the endoplasmic reticulum. Phosphorylated PERK, in turn, promotes the hyperphosphorylation of the translational initiation factor eiF2α at Ser51 (Schneider et al., 2021), which halts the translation of some proteins involved in the maintenance of synaptic connections (Moreno et al., 2012), likely contributing to synapse failure in prion-infected neurons (Figure 2). It remains unknown whether PERK is a direct substrate of ROCK. In any case, ROCK inhibition decreases the phosphorylation of PERK and eiF2α (Schneider et al., 2021), allowing restarting the expression of synaptic proteins and preserving neuronal transmission within a prion-infectious context.

4.4 PrP^{Sc}-Induced deregulation of the PrP^{C}/PDK1/TACE signaling axis renders prion-infected neurons highly vulnerable to inflammation and amplifies the production of PrP^{Sc} and Aβ

In 2013, our laboratory provided prime evidence that the corruption of PrP^{C} coupling to 3-phosphoinositide-dependent kinase 1 (PDK1) and downstream TACE α-secretase plays a critical role in the neuropathogenesis of prion diseases (Pietri et al., 2013). In prion-infected neurons, overactivated PDK1 promotes TACE phosphorylation at Thr735 and TACE displacement from the plasma membrane to caveolin-1-enriched microvesicles, which neutralizes TACE neuroprotective shedding activity (Figure 2). As PDK1 only admits AGC kinases as substrates (Leroux and Biondi, 2023), it is unlikely that TACE phosphorylation results from a direct action of PDK1 on TACE. The phosphorylation of TACE at Thr735 would be part of signals that impact the subcellular localization of TACE and modulate its shedding activity. Internalized, phosphorylated TACE in prion-infected neurons becomes uncoupled from three major substrates: (i) TNFα receptors (TNFR), which accumulate at the cell surface, rendering neurons hypersensitive to TNFα, (ii) PrP^{C}, where the loss of PrP^{C} PTM by α-cleavage between amino-acids 111/112 strongly reduces the C1 fragment of PrP^{C} in favor of full-length PrP^{C} (and C2 fragment), which is highly prone to converting into PrP^{Sc}, and (iii) the amyloid precursor protein (APP), where the loss of APP PTM by α-cleavage in favor of APP PTM by β- and γ-secretases leads to the accumulation of neurotoxic Aβ peptides (Figure 2) (Pietri et al., 2013; Ezpeleta et al., 2019). Importantly, inhibiting PDK1 suppresses TACE phosphorylation at Thr735. The subsequent redirection of TACE at the plasma membrane allows TACE to reintegrate cell surface signalosomes and recover its protective shedding activity. This activity includes the cleavages of TNFR, PrP^{C}, and APP. Such restored irreversible PTMs of TNFR, PrP^{C}, and APP protect prion-infected neurons from TNFα toxicity and limit the production of toxic amyloids (Pietri et al., 2013; Ezpeleta et al., 2019).

PDK1 activity is known to be governed by several events: (i) translocation to the plasma membrane, (ii) post-translational modifications by phosphorylation, (iii) conformational changes, and (iv) interaction with different effectors (Sacerdoti et al., 2023). We demonstrated that the overactivation of PDK1 in prion-infected neurons depends on the upstream kinase ROCK (Alleaume-Butaux et al., 2015). ROCK interacts with PDK1 and promotes phosphorylation of PDK1, a PTM that accounts for the increase in PDK1 enzymatic activity within a prion infectious context. Of note, ROCK-dependent phosphorylation of PDK1 occurs only after autophosphorylation of PDK1 at Ser241. The additional phosphorylation of PDK1 by ROCK leads to sustained PDK1 activity in prion-infected neurons. Importantly, as the pharmacological inhibition of PDK1 or ROCK reduces motor impairment, lowers brain PrP^{Sc} and Aβ levels, and prolongs the lifespan of prion-infected mice, PDK1 and ROCK are currently considered as potential therapeutic targets to combat prion diseases (Pietri et al., 2013; Alleaume-Butaux et al., 2015; Ezpeleta et al., 2019). Therefore, any strategies aiming at rescuing the α-cleavage or shedding of PrP^{C} and APP should help to limit the production of PrP^{Sc} and Aβ and thereby mitigate prion diseases (Linsenmeier et al., 2021).

4.5 PrP^{Sc} Deviates the energy metabolism by altering the PrP^{C}/PDK4 coupling

We evidenced that prion infection also cancels the regulatory role of PrP^{C} on glucose metabolism, leading to a metabolic reprogramming of infected neurons, i.e., a conversion from glucose oxidative degradation to β-oxidation of fatty acids (Arnould et al., 2021). From a mechanistic point of view, PrP^{Sc} abrogates the negative control exerted by PrP^{C} on the expression of Pyruvate Deshydrogenase Kinase 4 (PDK4) encoding gene, causing a high rise in PDK4 enzymatic activity. By phosphorylating the mitochondrial Pyruvate Dehydrogenase (PDH) complex, overactivated PDK4 decreases the activity of PDH that normally ensures the transfer of cytosolic pyruvate in the mitochondria and its conversion into acetylCoA for the production of energy. The consequences of such PTM of PDH and subsequently reduced activity of PDH are a slowdown of the glycolytic flux and limited oxidative degradation of glucose. To compensate for energy restriction, prion-infected neurons divert their metabolism toward fatty acids β-oxidation. Since fatty acids can act as pro-oxidant molecules, the oxidative stress resulting from the degradation of fatty acids by the β-oxidation pathway has been shown to contribute to neurodegeneration in prion diseases (Figure 2). Interestingly, pharmacological inhibition of PDK4 with dichloroacetate (DCA), a medicine approved for treating congenital lactic acidosis, restores, at least partly, PDH activity in the brains of prion-infected mice, which favors the recovery of glucose metabolism over fatty acids β-oxidation and extends the lifespan of DCA-treated prion-infected mice (Arnould et al., 2021).

4.6 PrP^{Sc} alters Ca^{2+} signaling downstream of PrP^{C} interacting neuronal receptors

PrP^{Sc}-induced dysregulation of ionotropic (NMDAR) and metabotropic receptors (mGluR) increases the intracellular Ca^{2+} level (Hu et al., 2022). Exposure of mouse cerebellar granule neurons to the neurotoxic PrP amyloidogenic polypeptide (PrP90-231) increases NMDAR-dependent uptake of Ca^{2+} (Thellung et al., 2017). In prion-infected SMB-S15 cells, mGluR oversignaling enhances the release of Ca^{2+} from ER in response to PLC-mediated hydrolysis of 4.5-biphosphate phosphatidylinositol and subsequent IP3 increase, combined with an increased level of IP3 receptor in the ER (Hu et al., 2022). Calmodulin (CaM), a transducer of Ca^{2+} signals that activates different kinases, is upregulated in the cortex of sporadic CJD (sCJD) patients and in the brains of prion-infected hamsters (Shi et al., 2015; Zhang et al., 2017). On prion infection, the upregulation of the Ca^{2+}/calmodulin complex increases the Ca^{2+}/calmodulin-dependent calcineurin (CaN) phosphatase activity. CaN is a type 2 phosphatase highly expressed in neurons, physiologically involved in synaptic plasticity, memory, and neuronal death. In prion-infected neurons, CaN dephosphorylates the pro-apoptotic protein Bad at Ser112, causing Bad translocation in mitochondria and the subsequent release of cytochrome c from mitochondria to the cytoplasm where it activates caspase-dependent apoptosis pathways (Agostinho et al., 2008). PrP^{Sc}-induced CaN overactivity would also alter synaptic plasticity and trigger neurodegeneration by dephosphorylating the substrate slingshot 1 (SHH1) in prion diseases. SHH1 activates cofilin and triggers the formation of cofilin-actin rods, which are involved in glutamate-mediated excitotoxicity (Bamburg et al., 2021). Pharmacological inhibition of CaN with the immunosuppressive drug FK506 limits neurodegeneration, reduces motor deficits, and increases the survival of mice infected with RML or Fukuoka-1 strains (Mukherjee et al., 2010; Nakagaki et al., 2013), introducing an additional way of therapeutic intervention for prion diseases.

The Calpain non-lysosomal cysteine proteases are other enzymes dysregulated by Ca^{2+} overload in prion-infected neurons (Baudry and Bi, 2024). In a sCJD mouse model, prion infection downregulates the neuroprotective Calpain-1 and upregulates the neurodegenerative Calpain-2, leading to global Calpain overactivity in the brain. Overactivated pathological Calpain- 2 enhances the cleavage of Calpain substrates such as Neurofilament Light Chain and γ-tubulin, additionally contributing to the loss of neuronal polarity (Llorens et al., 2017).

5 Conclusion

In prion diseases, the initial aberrant PTM concerns normal cellular prion protein PrP^{C} with the post-translational conformational conversion (PTCC) of PrP^{C} into pathogenic prions PrP^{Sc}. This dramatic change in PrP^{C} folding is influenced by several PrP^{C} PTMs (glycosylation, sialylation, cleavages, etc.) that oppose or favor the production of PrP^{Sc}. One consequence of the conversion of PrP^{C} PTCC into PrP^{Sc} is the deregulation of PTMs at the proximal level of PrP^{C} partners in PrP^{C} signalosomes. Altered PTMs of PrP^{C} partners in prion-infected neurons affect the homeostatic activity of plasma membrane adhesion proteins, neuronal receptors, or ion channels, likely contributing to neuronal polarity and neurotransmission defects in prion diseases. Altered PTMs in PrP^{C} signalosomes impact downstream intracellular effectors such as Src kinases, ROCK, PDK1, PDK4, α-secretases, CREB transcription factor, and others. The imbalanced PTMs modify the biological activity or subcellular localization of these signaling effectors, thus hampering the signaling pathways they are involved in. It manifests by changes in redox equilibrium, metabolic reprogramming toward pro-oxidant fatty acids

metabolism, high sensitivity to several stresses such as inflammation, and possibly autophagy derangement (López-Pérez et al., 2019), which compromise neuronal homeostasis and contribute to neurodegeneration in prion diseases. Most of the signaling effectors with disturbed PTMs listed in this review were identified with the help of prion-infected cell lines and primary neuronal cultures and confirmed *in vivo* in the brains of mouse models with prion-like diseases or even in the post-mortem brains of Creutzfeldt–Jakob disease patients. These signaling effectors currently represent attractive therapeutic targets to combat prion diseases and possibly other neurodegenerative diseases, such as Alzheimer's and Parkinson's diseases. Several studies have reported on the mechanistic convergence of these amyloid-based neurodegenerative diseases to PrP^{C}. PrP^{C} displays the capacity to interact with several unrelated amyloid proteins, including PrP^{Sc}, Alzheimer-linked Aβ oligomers, and Parkinson-linked pre-formed fibrils of pathological α-synuclein, and to relay their neurotoxicity (Laurén et al., 2009; Um et al., 2012; Aulić et al., 2017). Oligomers of Aβ or α-synuclein bind with a nanomolar affinity PrP^{C} at the same epitopes, including one epitope in the hinge region of PrP^{C} involved in PrP^{C} PTCC into PrP^{Sc} (Chen et al., 2010; Smith et al., 2019; Corbett et al., 2020; Scialò and Legname, 2020). It would be tempting to genetically modify those PrP^{C} epitopes with gene-editing technologies to generate PrP^{C} molecules that are unable to bind amyloids or to be converted into PrP^{Sc} with the perspective of limiting or canceling amyloid neurotoxicity. Because PrP^{C} is essential for the homeostasis of neurons and other cell types, such a genetic protective approach will be successful only if we are able to keep the PrP^{C} cell functions intact, including PrP^{C} signaling activity.

Of note, the binding to PrP^{C} of Aβ or α-synuclein does not promote the conversion of PrP^{C} into PrP^{Sc}, as PrP^{C} PTCC into PrP^{Sc} is restricted to prion diseases. The binding to PrP^{C} of Aβ/α-synuclein oligomers would deregulate PrP^{C} signalosomes and downstream coupled signaling effectors on the removal of PrP^{C} from signalosomes (loss-of-PrP^{C} function). Alternatively, the binding to PrP^{C} of Aβ/α-synuclein oligomers would freeze PrP^{C} in signalosomes, maintaining PrP^{C} signalosomes in an active state (gain-of-PrP^{C} function). Whatever the scenario, the corruption of PrP^{C} signalosomes by PrP^{Sc}, Aβ, or α-synuclein leads to post-translation modifications and deregulation of the same signaling effectors, such as ROCK, PDK1, and others (Pietri et al., 2013; Ferreira et al., 2017; Koch et al., 2018; Abd-Elrahman et al., 2020). In conclusion, common PTM patterns appear to contribute to neurodegeneration in prion diseases, Alzheimer's diseases, and Parkinson's diseases. However, the pending question remains as to which other specific PTM patterns can be specifically associated with each of these amyloid-based neurodegenerative diseases, as these diseases display different clinical manifestations.

Author contributions

ChB: Writing – original draft, Writing – review & editing. ClB: Writing – original draft, Writing – review & editing. AB: Writing – original draft, Writing – review & editing. AA-B: Writing – original draft, Writing – review & editing. BS: Writing – original draft, Writing – review & editing. MP: Writing – original draft, Writing – review & editing.

Funding

The author(s) declare financial support was received for the research, authorship, and/or publication of this article. This study was supported by the INSERM. ChB was supported by the Fondation pour la Recherche Medicale (FRM).

Conflict of interest

The authors declare that the research was conducted in the absence of any commercial or financial relationships that could be construed as a potential conflict of interest.

The author(s) declared that they were an editorial board member of Frontiers, at the time of submission. This had no impact on the peer review process and the final decision.

Publisher's note

References

Abd-Elrahman, K. S., Albaker, A., de Souza, J. M., Ribeiro, F. M., Schlossmacher, M. G., Tiberi, M., et al. (2020). Aβ oligomers induce pathophysiological mGluR5 signaling in Alzheimer's disease model mice in a sex-selective manner. *Sci. Signal.* 13:eabd2494. doi: 10.1126/scisignal.abd2494

Agostinho, P., Lopes, J. P., Velez, Z., and Oliveira, C. R. (2008). Overactivation of calcineurin induced by amyloid-beta and prion proteins. *Neurochem. Int.* 52, 1226–1233. doi: 10.1016/j.neuint.2008.01.005

Aguilar-Calvo, P., Xiao, X., Bett, C., Eraña, H., Soldau, K., Castilla, J., et al. (2017). Post-translational modifications in PrP expand the conformational diversity of prions in vivo. *Sci. Rep.* 7:43295. doi: 10.1038/srep43295

Albert-Gasco, H., Smith, H. L., Alvarez-Castelao, B., Swinden, D., Halliday, M., Janaki-Raman, S., et al. (2024). Trazodone rescues dysregulated synaptic and mitochondrial nascent proteomes in prion neurodegeneration. *Brain* 147, 649–664. doi: 10.1093/brain/awad313

Alleaume-Butaux, A., Nicot, S., Pietri, M., Baudry, A., Dakowski, C., Tixador, P., et al. (2015). Double-edge sword of sustained ROCK activation in prion diseases through Neuritogenesis defects and prion accumulation. *PLoS Pathog.* 11:e1005073. doi: 10.1371/journal.ppat.1005073

Altmeppen, H. C., Prox, J., Krasemann, S., Puig, B., Kruszewski, K., Dohler, F., et al. (2015). The sheddase ADAM10 is a potent modulator of prion disease. *eLife* 4:e04260. doi: 10.7554/eLife.04260

Arbuzova, A., Wang, L., Wang, J., Hangyás-Mihályné, G., Murray, D., Honig, B., et al. (2000). Membrane binding of peptides containing both basic and aromatic residues. Experimental studies with peptides corresponding to the scaffolding region of Caveolin and the effector region of MARCKS. *Biochemistry* 39, 10330–10339. doi: 10.1021/bi001039j

Arnould, H., Baudouin, V., Baudry, A., Ribeiro, L. W., Ardila-Osorio, H., Pietri, M., et al. (2021). Loss of prion protein control of glucose metabolism promotes neurodegeneration in model of prion diseases. *PLoS Pathog.* 17:e1009991. doi: 10.1371/journal.ppat.1009991

Aulić, S., Masperone, L., Narkiewicz, J., Isopi, E., Bistaffa, E., Ambrosetti, E., et al. (2017). α-Synuclein amyloids hijack prion protein to gain cell entry, facilitate cell-to-cell

spreading and block prion replication. *Sci. Rep.* 7:10050. doi: 10.1038/s41598-017-10236-x

Baloui, H., Von Boxberg, Y., Vinh, J., Weiss, S., Rossier, J., Nothias, F., et al. (2004). Cellular prion protein/laminin receptor: distribution in adult central nervous system and characterization of an isoform associated with a subtype of cortical neurons. *Eur. J. Neurosci.* 20, 2605–2616. doi: 10.1111/j.1460-9568.2004.03728.x

Bamburg, J. R., Minamide, L. S., Wiggan, O., Tahtamouni, L. H., and Kuhn, T. B. (2021). Cofilin and actin dynamics: multiple modes of regulation and their impacts in neuronal development and degeneration. *Cells* 10:2726. doi: 10.3390/cells10102726

Barnes, J. R., Mukherjee, B., Rogers, B. C., Nafar, F., Gosse, M., and Parsons, M. P. (2020). The relationship between glutamate dynamics and activity-dependent synaptic plasticity. *J. Neurosci.* 40, 2793–2807. doi: 10.1523/JNEUROSCI.1655-19.2020

Baskakov, I. V., and Katorcha, E. (2016). Multifaceted role of sialylation in prion diseases. *Front. Neurosci.* 10:358. doi: 10.3389/fnins.2016.00358

Bate, C., Nolan, W., McHale-Owen, H., and Williams, A. (2016). Sialic acid within the Glycosylphosphatidylinositol anchor targets the cellular prion protein to synapses *. *J. Biol. Chem.* 291, 17093–17101. doi: 10.1074/jbc.M116.731117

Baudry, M., and Bi, X. (2024). Revisiting the calpain hypothesis of learning and memory 40 years later. *Front. Mol. Neurosci.* 17:1337850. doi: 10.3389/fnmol.2024.1337850

Beraldo, F. H., Arantes, C. P., Santos, T. G., Machado, C. F., Roffe, M., Hajj, G. N., et al. (2011). Metabotropic glutamate receptors transduce signals for neurite outgrowth after binding of the prion protein to laminin γ1 chain. FASEB. *J. Off. Publ. Fed. Am. Soc. Exp. Biol.* 25, 265–279. doi: 10.1096/fj.10-161653

Beraldo, F. H., Arantes, C. P., Santos, T. G., Queiroz, N. G. T., Young, K., Rylett, R. J., et al. (2010). Role of α7 nicotinic acetylcholine receptor in calcium signaling induced by prion protein interaction with stress-inducible protein 1. *J. Biol. Chem.* 285, 36542–36550. doi: 10.1074/jbc.M110.157263

Bertani, I., Iori, V., Trusel, M., Maroso, M., Foray, C., Mantovani, S., et al. (2017). Inhibition of IL-1β signaling normalizes NMDA-dependent neurotransmission and reduces seizure susceptibility in a mouse model of Creutzfeldt–Jakob disease. *J. Neurosci.* 37, 10278–10289. doi: 10.1523/JNEUROSCI.1301-17.2017

Bosques, C. J., and Imperiali, B. (2003). The interplay of glycosylation and disulfide formation influences fibrillization in a prion protein fragment. *Proc. Natl. Acad. Sci. USA* 100, 7593–7598. doi: 10.1073/pnas.1232504100

Boutin, C., Schmitz, B., Cremer, H., and Diestel, S. (2009). NCAM expression induces neurogenesis in vivo. *Eur. J. Neurosci.* 30, 1209–1218. doi: 10.1111/j.1460-9568.2009.06928.x

Caetano, F. A., Lopes, M. H., Hajj, G. N. M., Machado, C. F., Arantes, C. P., Magalhães, A. C., et al. (2008). Endocytosis of prion protein is required for ERK1/2 signaling induced by stress-inducible protein 1. *J. Neurosci.* 28, 6691–6702. doi: 10.1523/JNEUROSCI.1701-08.2008

Carta, M., and Aguzzi, A. (2022). Molecular foundations of prion strain diversity. *Curr. Opin. Neurobiol.* 72, 22–31. doi: 10.1016/j.conb.2021.07.010

Carulla, P., Bribián, A., Rangel, A., Gavín, R., Ferrer, I., Caelles, C., et al. (2011). Neuroprotective role of PrPC against kainate-induced epileptic seizures and cell death depends on the modulation of JNK3 activation by GluR6/7-PSD-95 binding. *Mol. Biol. Cell* 22, 3041–3054. doi: 10.1091/mbc.E11-04-0321

Castle, A. R., and Gill, A. C. (2017). Physiological functions of the cellular prion protein. *Front. Mol. Biosci.* 4:19. doi: 10.3389/fmolb.2017.00019

Cha, S.-H., Choi, Y. R., Heo, C.-H., Kang, S.-J., Joe, E.-H., Jou, I., et al. (2015). Loss of parkin promotes lipid rafts-dependent endocytosis through accumulating caveolin-1: implications for Parkinson's disease. *Mol. Neurodegener.* 10:63. doi: 10.1186/s13024-015-0060-5

Chen, C., Lv, Y., Zhang, B.-Y., Zhang, J., Shi, Q., Wang, J., et al. (2014). Apparent reduction of ADAM10 in scrapie-infected cultured cells and in the brains of scrapie-infected rodents. *Mol. Neurobiol.* 50, 875–887. doi: 10.1007/s12035-014-8708-7

Chen, S. G., Teplow, D. B., Parchi, P., Teller, J. K., Gambetti, P., and Autilio-Gambetti, L. (1995). Truncated forms of the human prion protein in Normal brain and in prion diseases. *J. Biol. Chem.* 270, 19173–19180. doi: 10.1074/jbc.270.32.19173

Chen, S., Yadav, S. P., and Surewicz, W. K. (2010). Interaction between human prion protein and amyloid-β (Aβ) oligomers role of n-terminal residues. *J. Biol. Chem.* 285, 26377–26383. doi: 10.1074/jbc.M110.145516

Chesebro, B., Trifilo, M., Race, R., Meade-White, K., Teng, C., LaCasse, R., et al. (2005). Anchorless prion protein results in infectious amyloid disease without clinical scrapie. *Science* 308, 1435–1439. doi: 10.1126/science.1110837

Chiarini, L. B., Freitas, A. R. O., Zanata, S. M., Brentani, R. R., Martins, V. R., and Linden, R. (2002). Cellular prion protein transduces neuroprotective signals. *EMBO J.* 21, 3317–3326. doi: 10.1093/emboj/cdf324

Cobb, N. J., Sönnichsen, F. D., McHaourab, H., and Surewicz, W. K. (2007). Molecular architecture of human prion protein amyloid: a parallel, in-register beta-structure. *Proc. Natl. Acad. Sci. USA* 104, 18946–18951. doi: 10.1073/pnas.0706522104

Coitinho, A. S., Freitas, A. R. O., Lopes, M. H., Hajj, G. N. M., Roesler, R., Walz, R., et al. (2006). The interaction between prion protein and laminin modulates memory consolidation. *Eur. J. Neurosci.* 24, 3255–3264. doi: 10.1111/j.1460-9568.2006.05156.x

Colby, D. W., Zhang, Q., Wang, S., Groth, D., Legname, G., Riesner, D., et al. (2007). Prion detection by an amyloid seeding assay. *Proc. Natl. Acad. Sci. USA* 104, 20914–20919. doi: 10.1073/pnas.0710152105

Collinge, J., and Clarke, A. R. (2007). A general model of prion strains and their pathogenicity. *Science* 318, 930–936. doi: 10.1126/science.1138718

Corbett, G. T., Wang, Z., Hong, W., Colom-Cadena, M., Rose, J., Liao, M., et al. (2020). PrP is a central player in toxicity mediated by soluble aggregates of neurodegeneration-causing proteins. *Acta Neuropathol. (Berl.)* 139, 503–526. doi: 10.1007/s00401-019-02114-9

Cracco, L., Puoti, G., Cornacchia, A., Glisic, K., Lee, S.-K., Wang, Z., et al. (2023). Novel histotypes of sporadic Creutzfeldt-Jakob disease linked to 129MV genotype. *Acta Neuropathol. Commun.* 11:141. doi: 10.1186/s40478-023-01631-9

Dias, M. V. S., Teixeira, B. L., Rodrigues, B. R., Sinigaglia-Coimbra, R., Porto-Carreiro, I., Roffé, M., et al. (2016). PRNP/prion protein regulates the secretion of exosomes modulating CAV1/caveolin-1-suppressed autophagy. *Autophagy* 12, 2113–2128. doi: 10.1080/15548627.2016.1226735

Dietzen, D. J., Hastings, W. R., and Lublin, D. M. (1995). Caveolin is Palmitoylated on multiple cysteine residues: palmitoylation is not necessary for localization of caveolin to caveolae (∗). *J. Biol. Chem.* 270, 6838–6842. doi: 10.1074/jbc.270.12.6838

Ermonval, M., Baudry, A., Baychelier, F., Pradines, E., Pietri, M., Oda, K., et al. (2009a). The cellular prion protein interacts with the tissue non-specific alkaline phosphatase in membrane microdomains of Bioaminergic neuronal cells. *PLoS One* 4:e6497. doi: 10.1371/journal.pone.0006497

Ermonval, M., Petit, D., Le Duc, A., Kellermann, O., and Gallet, P.-F. (2009b). Glycosylation-related genes are variably expressed depending on the differentiation state of a bioaminergic neuronal cell line: implication for the cellular prion protein. *Glycoconj. J.* 26, 477–493. doi: 10.1007/s10719-008-9198-5

Ezpeleta, J., Baudouin, V., Arellano-Anaya, Z. E., Boudet-Devaud, F., Pietri, M., Baudry, A., et al. (2019). Production of seedable amyloid-β peptides in model of prion diseases upon PrPSc-induced PDK1 overactivation. *Nat. Commun.* 10:3442. doi: 10.1038/s41467-019-11333-3

Ezpeleta, J., Boudet-Devaud, F., Pietri, M., Baudry, A., Baudouin, V., Alleaume-Butaux, A., et al. (2017). Protective role of cellular prion protein against TNFα-mediated inflammation through TACE α-secretase. *Sci. Rep.* 7:7671. doi: 10.1038/s41598-017-08110-x

Fang, C., Wu, B., Le, N. T. T., Imberdis, T., Mercer, R. C. C., and Harris, D. A. (2018). Prions activate a p38 MAPK synaptotoxic signaling pathway. *PLoS Pathog.* 14:e1007283. doi: 10.1371/journal.ppat.1007283

Ferreira, D. G., Temido-Ferreira, M., Vicente Miranda, H., Batalha, V. L., Coelho, J. E., Szegö, É. M., et al. (2017). α-Synuclein interacts with PrPC to induce cognitive impairment through mGluR5 and NMDAR2B. *Nat. Neurosci.* 20, 1569–1579. doi: 10.1038/nn.4648

Gasperini, L., Meneghetti, E., Pastore, B., Benetti, F., and Legname, G. (2015). Prion protein and copper cooperatively protect neurons by modulating NMDA receptor through S-nitrosylation. *Antioxid. Redox Signal.* 22, 772–784. doi: 10.1089/ars.2014.6032

Ghodrati, F., Mehrabian, M., Williams, D., Halgas, O., Bourkas, M. E. C., Watts, J. C., et al. (2018). The prion protein is embedded in a molecular environment that modulates transforming growth factor β and integrin signaling. *Sci. Rep.* 8:8654. doi: 10.1038/s41598-018-26685-x

Goniotaki, D., Lakkaraju, A. K. K., Shrivastava, A. N., Bakirci, P., Sorce, S., Senatore, A., et al. (2017). Inhibition of group-I metabotropic glutamate receptors protects against prion toxicity. *PLoS Pathog.* 13:e1006733. doi: 10.1371/journal.ppat.1006733

Gottlieb-Abraham, E., Shvartsman, D. E., Donaldson, J. C., Ehrlich, M., Gutman, O., Martin, G. S., et al. (2013). Src-mediated caveolin-1 phosphorylation affects the targeting of active Src to specific membrane sites. *Mol. Biol. Cell* 24, 3881–3895. doi: 10.1091/mbc.e13-03-0163

Hannaoui, S., Zemlyankina, I., Chang, S. C., Arifin, M. I., Béringue, V., McKenzie, D., et al. (2022). Transmission of cervid prions to humanized mice demonstrates the zoonotic potential of CWD. *Acta Neuropathol. (Berl.)* 144, 767–784. doi: 10.1007/s00401-022-02482-9

Hernandez-Rapp, J., Martin-Lannerée, S., Hirsch, T. Z., Pradines, E., Alleaume-Butaux, A., Schneider, B., et al. (2014). A PrPC-caveolin-Lyn complex negatively controls neuronal GSK3β and serotonin 1B receptor. *Sci. Rep.* 4:4881. doi: 10.1038/srep04881

Hoyt, F., Standke, H. G., Artikis, E., Schwartz, C. L., Hansen, B., Li, K., et al. (2022). Cryo-EM structure of anchorless RML prion reveals variations in shared motifs between distinct strains. *Nat. Commun.* 13:4005. doi: 10.1038/s41467-022-30458-6

Hu, C., Chen, C., Xia, Y., Chen, J., Yang, W., Wang, L., et al. (2022). Different aberrant changes of mGluR5 and its downstream signaling pathways in the scrapie-infected cell line and the brains of scrapie-infected experimental rodents. *Front. Cell Dev. Biol.* 10:844378. doi: 10.3389/fcell.2022.844378

Humphrey, S. J., James, D. E., and Mann, M. (2015). Protein phosphorylation: a major switch mechanism for metabolic regulation. *Trends Endocrinol. Metab.* 26, 676–687. doi: 10.1016/j.tem.2015.09.013

Jin, D.-Z., Mao, L.-M., and Wang, J. Q. (2017). An essential role of Fyn in the modulation of metabotropic glutamate receptor 1 in neurons. *eNeuro* 4, ENEURO.0096–ENEU17.2017. doi: 10.1523/ENEURO.0096-17.2017

Katorcha, E., Makarava, N., Savtchenko, R., and Baskakov, I. V. (2015). Sialylation of the prion protein glycans controls prion replication rate and glycoform ratio. *Sci. Rep.* 5:16912. doi: 10.1038/srep16912

Katorcha, E., Srivastava, S., Klimova, N., and Baskakov, I. V. (2016). Sialylation of Glycosylphosphatidylinositol (GPI) anchors of mammalian prions is regulated in a host-, tissue-, and cell-specific manner *. *J. Biol. Chem.* 291, 17009–17019. doi: 10.1074/jbc.M116.732040

Khosravani, H., Zhang, Y., Tsutsui, S., Hameed, S., Altier, C., Hamid, J., et al. (2008). Prion protein attenuates excitotoxicity by inhibiting NMDA receptors. *J. Cell Biol.* 181, 551–565. doi: 10.1083/jcb.200711002

Kim, H.-J., Kim, M.-J., Mostafa, M. N., Park, J.-H., Choi, H.-S., Kim, Y.-S., et al. (2020). RhoA/ROCK regulates prion pathogenesis by controlling Connexin 43 activity. *Int. J. Mol. Sci.* 21:1255. doi: 10.3390/ijms21041255

Kleene, R., Loers, G., Langer, J., Frobert, Y., Buck, F., and Schachner, M. (2007). Prion protein regulates glutamate-dependent lactate transport of astrocytes. *J. Neurosci.* 27, 12331–12340. doi: 10.1523/JNEUROSCI.1358-07.2007

Knight, R. (2017). "Chapter thirteen - infectious and sporadic prion diseases," in Progress in Molecular Biology and Translational Science, eds. G. Legname and S. Vanni (Academic Press), 293–318.

Koch, J. C., Tatenhorst, L., Roser, A.-E., Saal, K.-A., Tönges, L., and Lingor, P. (2018). ROCK inhibition in models of neurodegeneration and its potential for clinical translation. *Pharmacol. Ther.* 189, 1–21. doi: 10.1016/j.pharmthera.2018.03.008

Kovač, V., and Čurin Šerbec, V. (2018). Prion proteins without the glycophosphatidylinositol anchor: potential biomarkers in neurodegenerative diseases. *Biomark. Insights* 13:1177271918756648. doi: 10.1177/1177271918756648

Kraus, A., Hoyt, F., Schwartz, C. L., Hansen, B., Artikis, E., Hughson, A. G., et al. (2021). High-resolution structure and strain comparison of infectious mammalian prions. *Mol. Cell* 81, 4540–4551.e6. doi: 10.1016/j.molcel.2021.08.011

Krebs, B., Dorner-Ciossek, C., Schmalzbauer, R., Vassallo, N., Herms, J., and Kretzschmar, H. A. (2006). Prion protein induced signaling cascades in monocytes. *Biochem. Biophys. Res. Commun.* 340, 13–22. doi: 10.1016/j.bbrc.2005.11.158

Laurén, J., Gimbel, D. A., Nygaard, H. B., Gilbert, J. W., and Strittmatter, S. M. (2009). Cellular prion protein mediates impairment of synaptic plasticity by amyloid-β oligomers. *Nature* 457, 1128–1132. doi: 10.1038/nature07761

Lee, H.-P., Jun, Y.-C., Choi, J.-K., Kim, J.-I., Carp, R. I., and Kim, Y.-S. (2005). Activation of mitogen-activated protein kinases in hamster brains infected with 263K scrapie agent. *J. Neurochem.* 95, 584–593. doi: 10.1111/j.1471-4159.2005.03429.x

Lehembre, F., Yilmaz, M., Wicki, A., Schomber, T., Strittmatter, K., Ziegler, D., et al. (2008). NCAM-induced focal adhesion assembly: a functional switch upon loss of E-cadherin. *EMBO J.* 27, 2603–2615. doi: 10.1038/emboj.2008.178

Leroux, A. E., and Biondi, R. M. (2023). The choreography of protein kinase PDK1 and its diverse substrate dance partners. *Biochem. J.* 480, 1503–1532. doi: 10.1042/BCJ20220396

Linden, R., Martins, V. R., Prado, M. A. M., Cammarota, M., Izquierdo, I., and Brentani, R. R. (2008). Physiology of the prion protein. *Physiol. Rev.* 88, 673–728. doi: 10.1152/physrev.00007.2007

Linsenmeier, L., Mohammadi, B., Shafiq, M., Frontzek, K., Bär, J., Shrivastava, A. N., et al. (2021). Ligands binding to the prion protein induce its proteolytic release with therapeutic potential in neurodegenerative proteinopathies. *Sci. Adv.* 7:eabj1826. doi: 10.1126/sciadv.abj1826

Llorens, F., Thüne, K., Sikorska, B., Schmitz, M., Tahir, W., Fernández-Borges, N., et al. (2017). Altered Ca2+ homeostasis induces Calpain-Cathepsin axis activation in sporadic Creutzfeldt-Jakob disease. *Acta Neuropathol. Commun.* 5:35. doi: 10.1186/s40478-017-0431-y

Lopes, M. H., Hajj, G. N. M., Muras, A. G., Mancini, G. L., Castro, R. M. P. S., Ribeiro, K. C. B., et al. (2005). Interaction of cellular prion and stress-inducible protein 1 promotes Neuritogenesis and neuroprotection by distinct signaling pathways. *J. Neurosci.* 25, 11330–11339. doi: 10.1523/JNEUROSCI.2313-05.2005

López-Pérez, Ó., Otero, A., Filali, H., Sanz-Rubio, D., Toivonen, J. M., Zaragoza, P., et al. (2019). Dysregulation of autophagy in the central nervous system of sheep naturally infected with classical scrapie. *Sci. Rep.* 9:1911. doi: 10.1038/s41598-019-38500-2

Loubet, D., Dakowski, C., Pietri, M., Pradines, E., Bernard, S., Callebert, J., et al. (2012). Neuritogenesis: the prion protein controls β1 integrin signaling activity. *FASEB J.* 26, 678–690. doi: 10.1096/fj.11-185579

Louros, N., Schymkowitz, J., and Rousseau, F. (2023). Mechanisms and pathology of protein misfolding and aggregation. *Nat. Rev. Mol. Cell Biol.* 24, 912–933. doi: 10.1038/s41580-023-00647-2

Luo, S., Yang, M., Zhao, H., Han, Y., Jiang, N., Yang, J., et al. (2021). Caveolin-1 regulates cellular metabolism: a potential therapeutic target in kidney disease. *Front. Pharmacol.* 12:768100. doi: 10.3389/fphar.2021.768100

Makarava, N., and Baskakov, I. V. (2023). Role of sialylation of N-linked glycans in prion pathogenesis. *Cell Tissue Res.* 392, 201–214. doi: 10.1007/s00441-022-03584-2

Makarava, N., Chang, J. C.-Y., Molesworth, K., and Baskakov, I. V. (2020). Posttranslational modifications define course of prion strain adaptation and disease phenotype. *J. Clin. Invest.* 130, 4382–4395. doi: 10.1172/JCI138677

Mallucci, G., Dickinson, A., Linehan, J., Klöhn, P.-C., Brandner, S., and Collinge, J. (2003). Depleting neuronal PrP in prion infection prevents disease and reverses Spongiosis. *Science* 302, 871–874. doi: 10.1126/science.1090187

Manka, S. W., Zhang, W., Wenborn, A., Betts, J., Joiner, S., Saibil, H. R., et al. (2022). 2.7 Å cryo-EM structure of ex vivo RML prion fibrils. *Nat. Commun.* 13:4004. doi: 10.1038/s41467-022-30457-7

McNally, K. L., Ward, A. E., and Priola, S. A. (2009). Cells expressing anchorless prion protein are resistant to scrapie infection. *J. Virol.* 83, 4469–4475. doi: 10.1128/jvi.02412-08

Mehrabian, M., Brethour, D., Wang, H., Xi, Z., Rogaeva, E., and Schmitt-Ulms, G. (2015). The prion protein controls Polysialylation of neural cell adhesion molecule 1 during cellular morphogenesis. *PLoS One* 10:e0133741. doi: 10.1371/journal.pone.0133741

Mehrabian, M., Hildebrandt, H., and Schmitt-Ulms, G. (2016). NCAM1 Polysialylation: the prion Protein's elusive reason for being? *ASN Neuro* 8:175909141667907. doi: 10.1177/1759091416679074

Meneghetti, E., Gasperini, L., Virgilio, T., Moda, F., Tagliavini, F., Benetti, F., et al. (2019). Prions strongly reduce NMDA receptor S-Nitrosylation levels at pre-symptomatic and terminal stages of prion diseases. *Mol. Neurobiol.* 56, 6035–6045. doi: 10.1007/s12035-019-1505-6

Millán-Zambrano, G., Burton, A., Bannister, A. J., and Schneider, R. (2022). Histone post-translational modifications — cause and consequence of genome function. *Nat. Rev. Genet.* 23, 563–580. doi: 10.1038/s41576-022-00468-7

Miranzadeh Mahabadi, H., and Taghibiglou, C. (2020). Cellular prion protein (PrPc): putative interacting partners and consequences of the interaction. *Int. J. Mol. Sci.* 21:7058. doi: 10.3390/ijms21197058

Mohammadi, B., Song, F., Matamoros-Angles, A., Shafiq, M., Damme, M., Puig, B., et al. (2023). Anchorless risk or released benefit? An updated view on the ADAM10-mediated shedding of the prion protein. *Cell Tissue Res.* 392, 215–234. doi: 10.1007/s00441-022-03582-4

Morel, E., Andrieu, T., Casagrande, F., Gauczynski, S., Weiss, S., Grassi, J., et al. (2005). Bovine prion is endocytosed by human enterocytes via the 37 kDa/67 kDa laminin receptor. *Am. J. Pathol.* 167, 1033–1042. doi: 10.1016/S0002-9440(10)61192-3

Moreno, J. A., Radford, H., Peretti, D., Steinert, J. R., Verity, N., Martin, M. G., et al. (2012). Sustained translational repression by eIF2α-P mediates prion neurodegeneration. *Nature* 485, 507–511. doi: 10.1038/nature11058

Mouillet-Richard, S., Ermonval, M., Chebassier, C., Laplanche, J. L., Lehmann, S., Launay, J. M., et al. (2000). Signal transduction through prion protein. *Science* 289, 1925–1928. doi: 10.1126/science.289.5486.1925

Mouillet-Richard, S., Nishida, N., Pradines, E., Laude, H., Schneider, B., Féraudet, C., et al. (2008). Prions impair bioaminergic functions through serotonin- or catecholamine-derived neurotoxins in neuronal cells. *J. Biol. Chem.* 283, 23782–23790. doi: 10.1074/jbc.M802433200

Mukherjee, A., Morales-Scheihing, D., Gonzalez-Romero, D., Green, K., Taglialatela, G., and Soto, C. (2010). Calcineurin inhibition at the clinical phase of prion disease reduces neurodegeneration, improves behavioral alterations and increases animal survival. *PLoS Pathog.* 6:e1001138. doi: 10.1371/journal.ppat.1001138

Nakagaki, T., Satoh, K., Ishibashi, D., Fuse, T., Sano, K., Kamatari, Y. O., et al. (2013). FK506 reduces abnormal prion protein through the activation of autolysosomal degradation and prolongs survival in prion-infected mice. *Autophagy* 9, 1386–1394. doi: 10.4161/auto.25381

Pamplona, R., Naudí, A., Gavín, R., Pastrana, M. A., Sajnani, G., Ilieva, E. V., et al. (2008). Increased oxidation, glycoxidation, and lipoxidation of brain proteins in prion disease. *Free Radic. Biol. Med.* 45, 1159–1166. doi: 10.1016/j.freeradbiomed.2008.07.009

Pantera, B., Bini, C., Cirri, P., Paoli, P., Camici, G., Manao, G., et al. (2009). PrPc activation induces neurite outgrowth and differentiation in PC12 cells: role for caveolin-1 in the signal transduction pathway. *J. Neurochem.* 110, 194–207. doi: 10.1111/j.1471-4159.2009.06123.x

Parchi, P., Giese, A., Capellari, S., Brown, P., Schulz-Schaeffer, W., Windl, O., et al. (1999). Classification of sporadic Creutzfeldt-Jakob disease based on molecular and phenotypic analysis of 300 subjects. *Ann. Neurol.* 46, 224–233. doi: 10.1002/1531-8249(199908)46:2<224::AID-ANA12>3.0.CO;2-W

Parton, R. G., Joggerst, B., and Simons, K. (1994). Regulated internalization of caveolae. *J. Cell Biol.* 127, 1199–1215. doi: 10.1083/jcb.127.5.1199

Parton, R. G., and Simons, K. (2007). The multiple faces of caveolae. *Nat. Rev. Mol. Cell Biol.* 8, 185–194. doi: 10.1038/nrm2122

Pascuzzo, R., Oxtoby, N. P., Young, A. L., Blevins, J., Castelli, G., Garbarino, S., et al. (2020). Prion propagation estimated from brain diffusion MRI is subtype dependent in sporadic Creutzfeldt-Jakob disease. *Acta Neuropathol. (Berl.)* 140, 169–181. doi: 10.1007/s00401-020-02168-0

Pietri, M., Caprini, A., Mouillet-Richard, S., Pradines, E., Ermonval, M., Grassi, J., et al. (2006). Overstimulation of PrPC signaling pathways by prion peptide 106-126 causes oxidative injury of Bioaminergic neuronal cells *. *J. Biol. Chem.* 281, 28470–28479. doi: 10.1074/jbc.M602774200

Pietri, M., Dakowski, C., Hannaoui, S., Alleaume-Butaux, A., Hernandez-Rapp, J., Ragagnin, A., et al. (2013). PDK1 decreases TACE-mediated α-secretase activity and promotes disease progression in prion and Alzheimer's diseases. *Nat. Med.* 19, 1124–1131. doi: 10.1038/nm.3302

Pradines, E., Hernandez-Rapp, J., Villa-Diaz, A., Dakowski, C., Ardila-Osorio, H., Haik, S., et al. (2013). Pathogenic prions deviate PrPC signaling in neuronal cells and impair A-beta clearance. *Cell Death Dis.* 4:e456. doi: 10.1038/cddis.2012.195

Prusiner, S. B. (1986). Prions are novel infectious pathogens causing scrapie and Creutzfeldt-Jakob disease. BioEssays news rev. *Mol. Cell. Dev. Biol.* 5, 281–286. doi: 10.1002/bies.950050612

Prusiner, S. B. (1998). Prions. *Proc. Natl. Acad. Sci. USA* 95, 13363–13383. doi: 10.1073/pnas.95.23.13363

Ramazi, S., and Zahiri, J. (2021). Post-translational modifications in proteins: resources, tools and prediction methods. *Database* 2021:baab012. doi: 10.1093/database/baab012

Ratté, S., Prescott, S. A., Collinge, J., and Jefferys, J. G. R. (2008). Hippocampal bursts caused by changes in NMDA receptor-dependent excitation in a mouse model of variant CJD. *Neurobiol. Dis.* 32, 96–104. doi: 10.1016/j.nbd.2008.06.007

Rudd, P. M., Merry, A. H., Wormald, M. R., and Dwek, R. A. (2002). Glycosylation and prion protein. *Curr. Opin. Struct. Biol.* 12, 578–586. doi: 10.1016/s0959-440x(02)00377-9

Russelakis-Carneiro, M., Hetz, C., Maundrell, K., and Soto, C. (2004). Prion replication alters the distribution of Synaptophysin and Caveolin 1 in neuronal lipid rafts. *Am. J. Pathol.* 165, 1839–1848. doi: 10.1016/S0002-9440(10)63439-6

Sacerdoti, M., Gross, L. Z. F., Riley, A. M., Zehnder, K., Ghode, A., Klinke, S., et al. (2023). Modulation of the substrate specificity of the kinase PDK1 by distinct conformations of the full-length protein. *Sci. Signal.* 16:eadd3184. doi: 10.1126/scisignal.add3184

Santuccione, A., Sytnyk, V., Leshchyns'ka, I., and Schachner, M. (2005). Prion protein recruits its neuronal receptor NCAM to lipid rafts to activate p59fyn and to enhance neurite outgrowth. *J. Cell Biol.* 169, 341–354. doi: 10.1083/jcb.200409127

Schilling, K. M., Jorwal, P., Ubilla-Rodriguez, N. C., Assafa, T. E., Gatdula, J. R. P., Vultaggio, J. S., et al. (2023). N-glycosylation is a potent regulator of prion protein neurotoxicity. *J. Biol. Chem.* 299:105101. doi: 10.1016/j.jbc.2023.105101

Schneider, B. (2011). Understanding the neurospecificity of prion protein signaling. *Front. Biosci.* 16, 169–186. doi: 10.2741/3682

Schneider, B., Baudry, A., Pietri, M., Alleaume-Butaux, A., Bizingre, C., Nioche, P., et al. (2021). The cellular prion protein-ROCK connection: contribution to neuronal homeostasis and neurodegenerative diseases. *Front. Cell. Neurosci.* 15:660683. doi: 10.3389/fncel.2021.660683

Schneider, B., Mutel, V., Pietri, M., Ermonval, M., Mouillet-Richard, S., and Kellermann, O. (2003). NADPH oxidase and extracellular regulated kinases 1/2 are targets of prion protein signaling in neuronal and nonneuronal cells. *Proc. Natl. Acad. Sci. USA* 100, 13326–13331. doi: 10.1073/pnas.2235648100

Scialò, C., and Legname, G. (2020). The role of the cellular prion protein in the uptake and toxic signaling of pathological neurodegenerative aggregates. *Prog. Mol. Biol. Transl. Sci.* 175, 297–323. doi: 10.1016/bs.pmbts.2020.08.008

Sevillano, A. M., Aguilar-Calvo, P., Kurt, T. D., Lawrence, J. A., Soldau, K., Nam, T. H., et al. (2020). Prion protein glycans reduce intracerebral fibril formation and spongiosis in prion disease. *J. Clin. Invest.* 130, 1350–1362. doi: 10.1172/JCI131564

Shen, P., Dang, J., Wang, Z., Zhang, W., Yuan, J., Lang, Y., et al. (2021). Characterization of anchorless human PrP with Q227X stop mutation linked to Gerstmann-Sträussler-Scheinker syndrome in vivo and in vitro. *Mol. Neurobiol.* 58, 21–33. doi: 10.1007/s12035-020-02098-8

Shi, Q., Chen, L.-N., Zhang, B.-Y., Xiao, K., Zhou, W., Chen, C., et al. (2015). Proteomics analyses for the global proteins in the brain tissues of different human prion diseases. *Mol. Cell. Proteomics MCP* 14, 854–869. doi: 10.1074/mcp.M114.038018

Shi, Q., Jing, Y.-Y., Wang, S.-B., Chen, C., Sun, H., Xu, Y., et al. (2013). PrP octarepeats region determined the interaction with caveolin-1 and phosphorylation of caveolin-1 and Fyn. *Med. Microbiol. Immunol.* 202, 215–227. doi: 10.1007/s00430-012-0284-8

Silva, C. J., Vázquez-Fernández, E., Onisko, B., and Requena, J. R. (2015). Proteinase K and the structure of PrPSc: the good, the bad and the ugly. *Virus Res.* 207, 120–126. doi: 10.1016/j.virusres.2015.03.008

Smith, L. M., Kostylev, M. A., Lee, S., and Strittmatter, S. M. (2019). Systematic and standardized comparison of reported amyloid-β receptors for sufficiency, affinity, and Alzheimer's disease relevance. *J. Biol. Chem.* 294, 6042–6053. doi: 10.1074/jbc.RA118.006252

Sohn, J., Lin, H., Fritch, M. R., and Tuan, R. S. (2018). Influence of cholesterol/caveolin-1/caveolae homeostasis on membrane properties and substrate adhesion characteristics of adult human mesenchymal stem cells. *Stem Cell Res Ther* 9:86. doi: 10.1186/s13287-018-0830-4

Srivastava, S., Makarava, N., Katorcha, E., Savtchenko, R., Brossmer, R., and Baskakov, I. V. (2015). Post-conversion sialylation of prions in lymphoid tissues. *Proc. Natl. Acad. Sci.* 112, E6654–E6662. doi: 10.1073/pnas.1517993112

Stahl, N., Borchelt, D. R., and Prusiner, S. B. (1990). Differential release of cellular and scrapie prion proteins from cellular membranes by phosphatidylinositol-specific phospholipase C. *Biochemistry* 29, 5405–5412. doi: 10.1021/bi00474a028

Stuermer, C. A. O., Langhorst, M. F., Wiechers, M. F., Legler, D. F., Hanwehr, S. H.Von, Guse, A. H., et al. (2004). PrPc capping in T cells promotes its association with the lipid raft proteins reggie-1 and reggie-2 and leads to signal transduction. *FASEB J.* 18, 1731–1733. doi: 10.1096/fj.04-2150fje

Sverdlov, M., Shinin, V., Place, A. T., Castellon, M., and Minshall, R. D. (2009). Filamin a regulates Caveolae internalization and trafficking in endothelial cells. *Mol. Biol. Cell* 20, 4531–4540. doi: 10.1091/mbc.e08-10-0997

Taylor, D. R., and Hooper, N. M. (2006). The prion protein and lipid rafts (review). *Mol. Membr. Biol.* 23, 89–99. doi: 10.1080/09687860500449994

Thellung, S., Gatta, E., Pellistri, F., Villa, V., Corsaro, A., Nizzari, M., et al. (2017). Different molecular mechanisms mediate direct or glia-dependent prion protein fragment 90–231 neurotoxic effects in cerebellar granule neurons. *Neurotox. Res.* 32, 381–397. doi: 10.1007/s12640-017-9749-2

Toni, M., Spisni, E., Griffoni, C., Santi, S., Riccio, M., Lenaz, P., et al. (2006). Cellular prion protein and Caveolin-1 interaction in a neuronal cell line precedes Fyn/Erk 1/2 signal transduction. *Biomed. Res. Int.* 2006:e69469. doi: 10.1155/JBB/2006/69469

Tranulis, M. A., and Tryland, M. (2023). The zoonotic potential of chronic wasting disease—a review. *Food Secur.* 12:824. doi: 10.3390/foods12040824

Triebel, J., Robles, J. P., Zamora, M., Clapp, C., and Bertsch, T. (2022). New horizons in specific hormone proteolysis. *Trends Endocrinol. Metab. TEM* 33, 371–377. doi: 10.1016/j.tem.2022.03.004

Um, J. W., Kaufman, A. C., Kostylev, M., Heiss, J. K., Stagi, M., Takahashi, H., et al. (2013). Metabotropic glutamate receptor 5 is a coreceptor for Alzheimer aβ oligomer bound to cellular prion protein. *Neuron* 79, 887–902. doi: 10.1016/j.neuron.2013.06.036

Um, J. W., Nygaard, H. B., Heiss, J. K., Kostylev, M. A., Stagi, M., Vortmeyer, A., et al. (2012). Alzheimer amyloid-β oligomer bound to postsynaptic prion protein activates Fyn to impair neurons. *Nat. Neurosci.* 15, 1227–1235. doi: 10.1038/nn.3178

Vázquez-Fernández, E., Vos, M. R., Afanasyev, P., Cebey, L., Sevillano, A. M., Vidal, E., et al. (2016). The structural architecture of an infectious mammalian prion using Electron Cryomicroscopy. *PLoS Pathog.* 12:e1005835. doi: 10.1371/journal.ppat.1005835

Vilette, D., Courte, J., Peyrin, J. M., Coudert, L., Schaeffer, L., Andréoletti, O., et al. (2018). Cellular mechanisms responsible for cell-to-cell spreading of prions. *Cell. Mol. Life Sci.* 75, 2557–2574. doi: 10.1007/s00018-018-2823-y

Vincent, B., Paitel, E., Saftig, P., Frobert, Y., Hartmann, D., Strooper, B. D., et al. (2001). The Disintegrins ADAM10 and TACE contribute to the constitutive and Phorbol Ester-regulated Normal cleavage of the cellular prion protein *. *J. Biol. Chem.* 276, 37743–37746. doi: 10.1074/jbc.M105677200

Wagner, W., Ajuh, P., Löwer, J., and Wessler, S. (2010). Quantitative phosphoproteomic analysis of prion-infected neuronal cells. *Cell Commun. Signal* 8:28. doi: 10.1186/1478-811X-8-28

Walsh, C. T., Garneau-Tsodikova, S., and Gatto, G. J. (2005). Protein posttranslational modifications: the chemistry of proteome diversifications. *Angew. Chem. Int. Ed. Engl.* 44, 7342–7372. doi: 10.1002/anie.200501023

Wang, P.-S., Wang, J., Xiao, Z.-C., and Pallen, C. J. (2009). Protein-tyrosine phosphatase α acts as an upstream regulator of Fyn signaling to promote oligodendrocyte differentiation and myelination. *J. Biol. Chem.* 284, 33692–33702. doi: 10.1074/jbc.M109.061770

Watt, N. T., Taylor, D. R., Kerrigan, T. L., Griffiths, H. H., Rushworth, J. V., Whitehouse, I. J., et al. (2012). Prion protein facilitates uptake of zinc into neuronal cells. *Nat. Commun.* 3:1134. doi: 10.1038/ncomms2135

Westergard, L., Turnbaugh, J. A., and Harris, D. A. (2011). A naturally occurring C-terminal fragment of the prion protein (PrP) delays disease and acts as a dominant-negative inhibitor of PrPSc formation. *J. Biol. Chem.* 286, 44234–44242. doi: 10.1074/jbc.M111.286195

Wulf, M.-A., Senatore, A., and Aguzzi, A. (2017). The biological function of the cellular prion protein: an update. *BMC Biol.* 15:34. doi: 10.1186/s12915-017-0375-5

Yang, W., Geng, C., Yang, Z., Xu, B., Shi, W., Yang, Y., et al. (2020). Deciphering the roles of caveolin in neurodegenerative diseases: the good, the bad and the importance of context. *Ageing Res. Rev.* 62:101116. doi: 10.1016/j.arr.2020.101116

Zafar, S., Younas, N., Sheikh, N., Tahir, W., Shafiq, M., Schmitz, M., et al. (2018). Cytoskeleton-associated risk modifiers involved in early and rapid progression of sporadic Creutzfeldt-Jakob disease. *Mol. Neurobiol.* 55, 4009–4029. doi: 10.1007/s12035-017-0589-0

Zahn, R. (2003). The Octapeptide repeats in mammalian prion protein constitute a pH-dependent folding and aggregation site. *J. Mol. Biol.* 334, 477–488. doi: 10.1016/j.jmb.2003.09.048

Zahn, R., Liu, A., Lührs, T., Riek, R., von Schroetter, C., López García, F., et al. (2000). NMR solution structure of the human prion protein. *Proc. Natl. Acad. Sci. USA* 97, 145–150. doi: 10.1073/pnas.97.1.145

Zhang, R.-Q., Chen, C., Xiao, L.-J., Sun, J., Ma, Y., Yang, X.-D., et al. (2017). Aberrant alterations of the expressions and S-nitrosylation of calmodulin and the downstream factors in the brains of the rodents during scrapie infection. *Prion* 11, 352–367. doi: 10.1080/19336896.2017.1367082

Zimnicka, A. M., Husain, Y. S., Shajahan, A. N., Sverdlov, M., Chaga, O., Chen, Z., et al. (2016). Src-dependent phosphorylation of caveolin-1 Tyr-14 promotes swelling and release of caveolae. *Mol. Biol. Cell* 27, 2090–2106. doi: 10.1091/mbc.E15-11-0756

frontiers | Frontiers in Cell and Developmental Biology

TYPE Review
PUBLISHED 10 July 2024
DOI 10.3389/fcell.2024.1378548

OPEN ACCESS

EDITED BY
Beatriz Alvarez,
Complutense University of Madrid, Spain

REVIEWED BY
Fumihito Ono,
Osaka Medical and Pharmaceutical University, Japan
Luis R. Hernandez-Miranda,
Charité University Medicine Berlin, Germany

*CORRESPONDENCE
Julia von Maltzahn,
julia.vonmaltzahn@b-tu.de

†These authors have contributed equally to this work

RECEIVED 29 January 2024
ACCEPTED 18 June 2024
PUBLISHED 10 July 2024

CITATION
Majchrzak K, Hentschel E, Hönzke K, Geithe C and von Maltzahn J (2024), We need to talk—how muscle stem cells communicate. *Front. Cell Dev. Biol.* 12:1378548. doi: 10.3389/fcell.2024.1378548

We need to talk—how muscle stem cells communicate

Karolina Majchrzak[1†], Erik Hentschel[1†], Katja Hönzke[1,2], Christiane Geithe[1] and Julia von Maltzahn[1,3,4*]

[1]Faculty of Health Sciences Brandenburg, Brandenburg University of Technology Cottbus–Senftenberg, Senftenberg, Germany, [2]Department of Infectious Diseases and Respiratory Medicine, Charité-Universitätsmedizin Berlin, Corporate Member of Freie Universität Berlin and Humboldt Universität zu Berlin, Berlin, Germany, [3]Leibniz Institute on Aging, Fritz Lipmann Institute, Jena, Germany, [4]Faculty for Environment and Natural Sciences, Brandenburg University of Technology Cottbus—Senftenberg, Senftenberg, Germany

Skeletal muscle is one of the tissues with the highest ability to regenerate, a finely controlled process which is critically depending on muscle stem cells. Muscle stem cell functionality depends on intrinsic signaling pathways and interaction with their immediate niche. Upon injury quiescent muscle stem cells get activated, proliferate and fuse to form new myofibers, a process involving the interaction of multiple cell types in regenerating skeletal muscle. Receptors in muscle stem cells receive the respective signals through direct cell-cell interaction, signaling via secreted factors or cell-matrix interactions thereby regulating responses of muscle stem cells to external stimuli. Here, we discuss how muscle stem cells interact with their immediate niche focusing on how this controls their quiescence, activation and self-renewal and how these processes are altered in age and disease.

KEYWORDS

muscle stem cell, satellite cell, skeletal muscle, regeneration, niche, receptor, aging, rhabdomyosarcoma

Introduction

Skeletal muscle fulfills a variety of functions in the body and makes up over 40% of the human body weight (Frontera and Ochala, 2015). The essential functions of skeletal muscle include respiration, locomotion, body posture, thermogenesis, carbohydrate and amino acid storage as well as glucose and energy metabolism of the body (Jensen et al., 2011; Rowland et al., 2015; Sharma et al., 2019). Moreover, skeletal muscle tissue is also responsible for the secretion of messenger molecules to facilitate communication with other tissues (Pedersen and Febbraio, 2012). Loss of muscle mass and functionality, e.g., due to hormonal changes, malnutrition, aging or disease, can have a prominent impact on the quality of life and general health (Larsson et al., 2019).

The components of skeletal muscle

For fulfilling its essential functions skeletal muscle consists of a multitude of cell types including myofibers, blood vessels, muscle stem cells as well as different support cells such as fibrogenic adipogenic progenitor cells (FAPs) (Figure 1A). Furthermore, the multinucleated myofibers are innervated by motor neurons, which facilitate coordinated movements (Heckman and Enoka, 2012). However, postmitotic myofibers make up the largest portion of cells in skeletal muscle (Figure 1A) containing several

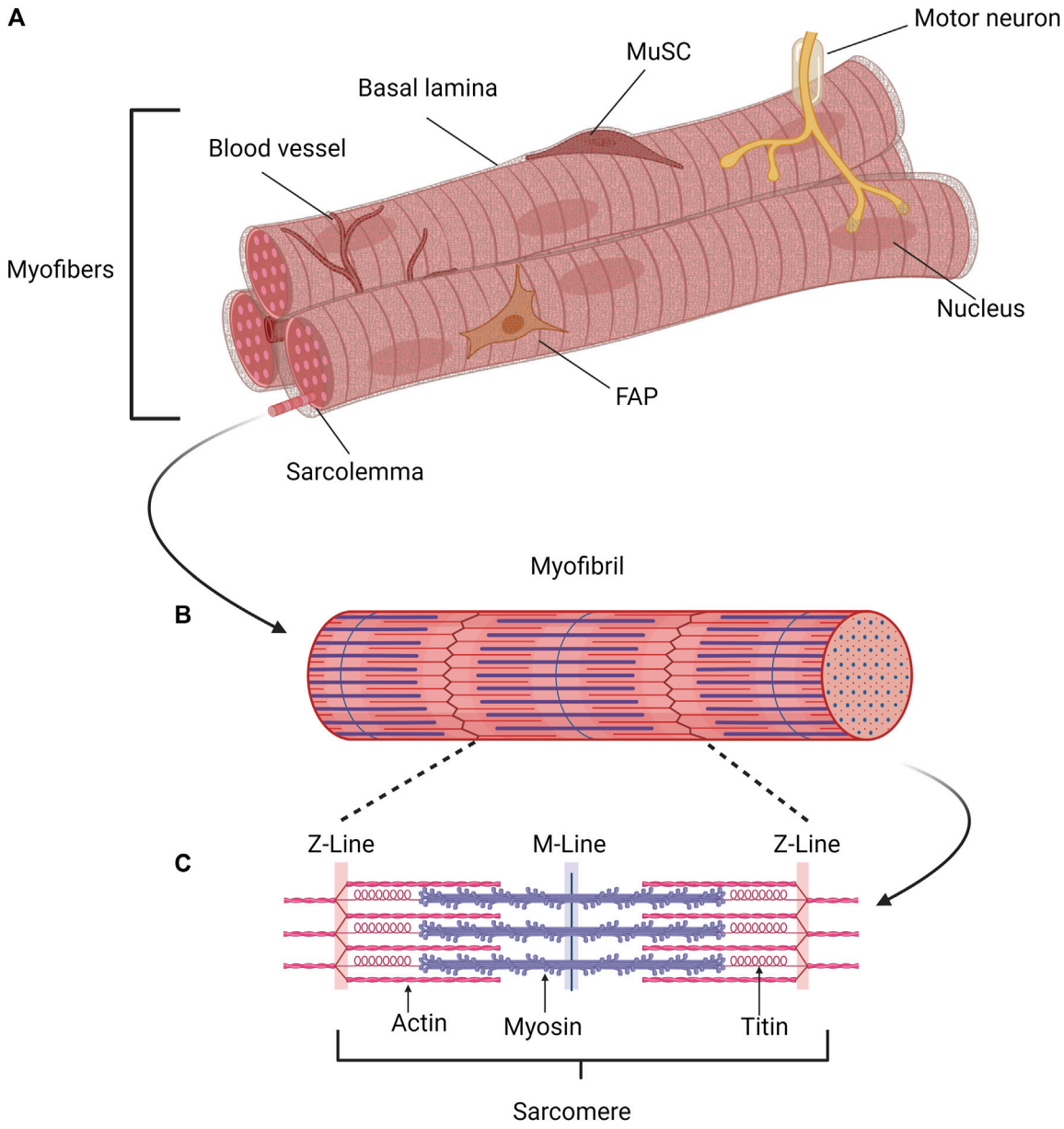

FIGURE 1
Schematic of the structure of skeletal muscle. **(A)** Myofibers, connective tissue, blood vessels, muscle stem cells (MuSCs), and various support cell types, such as fibrogenic adipogenic progenitor cells (FAPs), are found in skeletal muscle. Motor neurons innervate the multinucleated myofibers, enabling coordinated movement. The postmitotic myofiber is the primary cell type in skeletal muscle, responsible for force production and muscular contraction. **(B)** Each myofiber contains several parallel myofibrils, composed of repeating contractile units, the sarcomeres. **(C)** Muscle contraction is mediated by the sarcomere, the smallest contractile unit formed by overlapping elastic, thick, and thin filaments. Created with BioRender.com.

myofibrils (Figure 1B) and are allowing muscle contraction and force generation (Dave et al., 2024). Contraction of skeletal muscle depends on its smallest contractile unit, the sarcomere (Figure 1C), consisting of thin and thick myofilaments. The thin myofilaments are composed of two filamentous actin chains (α-actin) which are anchored at the Z-discs (Cooper and September, 2008; Frontera and Ochala, 2015; Wang et al., 2021), while the thick myofilaments are formed by several hundred myosin motor proteins, which slide on top of the thin myofilaments and thereby accomplish contraction of skeletal muscle. A third myofilament, titin, is required for regulating force generation, sarcomere organization and mechanosensing (Linke and Kruger, 2010; Nishikawa et al., 2020).

Different cell types in adult skeletal muscle

Skeletal muscle requires a multitude of cell types for full functionality and to allow proper regeneration. While contraction is carried out by myofibers, muscle stem cells (MuSCs) and different kind of support cells such as FAPs (fibrogenic adipogenic progenitor cells) are required for its regeneration. A fine network of blood

vessels provide myofibers with oxygen and nutrients, while motor neurons are required for coordinated contraction of myofibers and thereby coordinated movements. Blood vessels provide oxygen and nutrients and motor neurons are required for coordinated movement of skeletal muscle. Interaction of the different cell types in skeletal muscle–either through direct cell-cell contact or via paracrine signaling–is required for homeostasis and full functionality of skeletal muscle and is a prerequisite for regeneration of skeletal muscle.

Myofibers make up the largest proportion of skeletal muscle, they contain the sarcoplasmic reticulum and the mitochondrial network within the inter-myofilament space which is providing storage, release and reuptake of calcium after activation as well as ATP for muscle activity (Hargreaves and Spriet, 2020; Rossi et al., 2022). Of note, the myonuclei are evenly distributed in myofibers resulting in the control of transcriptional activity in the surrounding area of the cytoplasm which is termed the myonuclear domain (Qaisar and Larsson, 2014). However, at neuromuscular junctions (NMJ) an accumulation of nuclei occurs (Bruusgaard et al., 2003).

Each myofiber is surrounded by a basal lamina consisting of different collagens and laminins among other proteins. The endomysium, a fibrillar connective tissue surrounding each myofiber, forms a continuous three-dimensional network and provides a connection between adjacent myofibers (Sanes, 2003; Purslow, 2020). MuSCs are located underneath the basal lamina next to the myofibers (Figure 1A). Regeneration of skeletal muscle is crucially dependent on those adult stem cells which are also termed satellite cells (Lepper et al., 2011; Murphy et al., 2011; Sambasivan et al., 2011). In addition to their role in regeneration of skeletal muscle, MuSCs are contributing to adaptation of skeletal muscle to physiological demands such as training and growth. Under resting conditions, MuSCs are mitotically quiescent and are characterized by the expression of paired box protein 7 (Pax7), sprouty-1, and calcitonin receptor (CalcR) among others (Fuchs and Blau, 2020; von Maltzahn, 2021; Yamaguchi et al., 2015; Yin et al., 2013). Several myofibers with their adjacent MuSCs are grouped into muscle fascicles or myofiber bundles, which are surrounded by a second connective tissue termed the perimysium. The complete muscle is composed of a multitude of muscle fascicles, surrounded by a thick layer of connective tissue, the epimysium, which is extending from the tendons (Zhang W. et al., 2021). This connective tissue is maintained by residual fibroblasts in skeletal muscle (Purslow, 2020). It provides the connection of the myofiber bundles to the tendons while the vasculature supplies the individual myofibers with nutrients, oxygen or signal molecules and removes waste products. The vasculature consists of endothelial cells, smooth muscle cells and connective tissue which are embedded as small capillaries in the endomysium (Pittman, 2000; Korthuis, 2011). However, during regeneration of skeletal muscle new myofibers are formed along with the different layers of connective tissue. Especially during regeneration tissue monocytes and differentiated macrophages play fundamental roles including the removal of cell debris. Differentiated macrophages arise either from residential monocytes within the muscle tissue or are entering skeletal muscle via the bloodstream (Pillon et al., 2013).

To allow proper control of muscle contraction, motor neurons are in close contact with individual myofibers at the NMJs (Figure 1A). Typically, only one NMJ is connected to one myofiber (Rodriguez Cruz et al., 2020). These chemical synapses are located between a myofiber and a motor neuron, allow the signal transmission from the neuron to the myofiber and control the induction of contraction of individual myofibers (Ang et al., 2022). The neurotransmitter acetylcholine (ACh) binds to acetylcholine receptors (AChRs) in myofibers after release by the motor neuron. AChR subunits undergo a conformational change resulting in the influx of positively charged ions changing the membrane potential thereby triggering an endplate potential resulting in local depolarization. The generated action potential is spreading from the endplate finally resulting in muscle contraction (Sanes and Lichtman, 1999; Rodriguez Cruz et al., 2020). Performance of skeletal muscle declines if innervation and signal transmission via NMJs are impaired, a condition occurring for instance during aging and in neuromuscular pathologies such as spinal muscular atrophy. This emphasizes the need for proper innervation of skeletal muscle (Tintignac et al., 2015). However, loss of innervation also affects regeneration of skeletal muscle (Jejurikar et al., 2002; Wong et al., 2021; Henze et al., 2024). Of note, also MuSCs actively participate in regeneration of the NMJ underscoring the importance of proper crosstalk between NMJs and MuSCs (Liu et al., 2015; Liu et al., 2017).

The myotendinous junction (MTJ) regulates force transmission between myofibers and tendons (Charvet et al., 2012). MTJs are responsible for transmitting the force which is generated by the muscle to the collagen fibers of the adjacent tendon (Ciena et al., 2010). Recent studies have provided insights into the development and regeneration of muscles and MTJs. These findings indicate that even in case of severely damaged MTJs they can still undergo regeneration, a process which occurs simultaneously with regeneration of muscle tissue and allows full functionality of skeletal muscle after completion of the regeneration process (Yamamoto et al., 2022).

Regeneration of skeletal muscle

Skeletal muscle is one of the tissues with the highest ability to regenerate after injury, a process which involves different cell types residing in skeletal muscle and requires a proper cross talk among them (Bentzinger et al., 2013a) (Figure 2). The fine balance between different signaling pathways and proper timing of cellular processes are a prerequisite for effective regeneration of skeletal muscle. Regeneration of skeletal muscle can be divided in the following phases: the phase of degeneration, the inflammatory phase, the regeneration phase and the maturation/remodeling phase followed by functional recovery (Schmidt et al., 2019; Forcina et al., 2020).

Injury of skeletal muscle triggers a precisely orchestrated inflammatory process (Figure 2). Damage-activated mast cells secrete Tumor Necrosis Factor α (TNF-α), histamine and Tryptase and then initiate the synthesis of cytokines like IL-6 (Gibbs et al., 2001). This leads to the rapid attraction of circulating granulocytes mainly consisting of neutrophils which promote the proinflammatory environment required for the clearance of cellular debris (Tidball, 1995). Neutrophils then secrete the chemokines Mip-12, Mcp-1 among others leading to the recruitment of monocytes (Kasama et al., 1993). Monocytes then

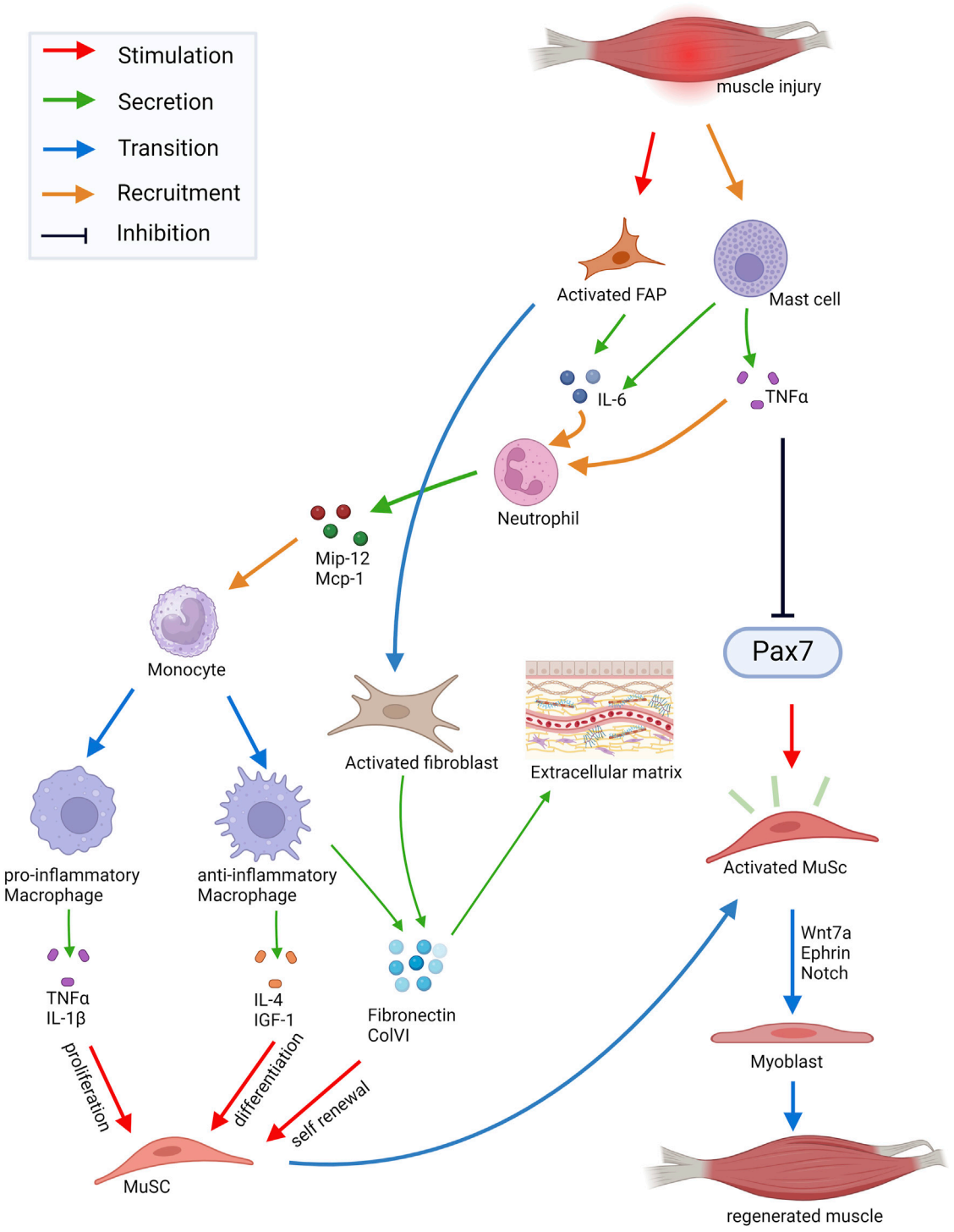

FIGURE 2
Schematic of cell-cell interactions in skeletal muscle during regeneration. Injury of skeletal muscle triggers mast cells secreting TNF-α and IL-6. This leads to the rapid attraction of granulocytes mainly consisting of neutrophils. Secreted chemokines (Mip-1α, Mcp-1) recruit monocytes which then start to differentiate into pro- and anti-inflammatory macrophages. The pro-inflammatory macrophages secrete TNF-α and IL-1β inducing proliferation of MuSC (muscle stem cells), whereas factors secreted by anti-inflammatory macrophages, such as IL-4 or IGF-1, stimulate myogenic differentiation. Moreover, ECM proteins secreted by anti-inflammatory macrophages, such as Fibronectin and ColVI, promote self-renewal of MuSCs. Upon injury, MuSCs leave the quiescent state and enter the cell cycle. Activated MuSCs can migrate to the site of injury and fuse with the damaged myofibers, which is controlled by Ephrins and Wnt7a signaling. Abbreviations: FAP, fibrogenic adipogenic progenitor cells; IL, Interleukin; TNFα, Tumor necrosis factor α; Mip-12, Macrophage Inflammatory Protein 12; Mcp-1, Monocyte Chemotactic Protein 1; IGF-1, Insulin Growth-Like Factor 1; ColVI, Collagen type VI. Created with BioRender.com.

start to differentiate into two subtypes of macrophages (Figure 2). The pro-inflammatory macrophages, formerly termed M1 macrophages, secrete IL-1β, IL-6 and TNF-α inducing proliferation of myogenic cells. The anti-inflammatory macrophages, formerly termed M2 macrophages, release IL-4 and IGF-1 thereby promoting myogenic differentiation (Horsley et al., 2003; Dumont and Frenette, 2010; Saclier et al., 2013). Moreover, anti-inflammatory macrophages secrete different extracellular matrix (ECM) proteins which are important components of the MuSC niche and promote their self-renewal, among them Fibronectin and Collagen type VI (ColVI) (Gratchev et al., 2001; Schnoor et al., 2008; Bentzinger et al., 2013b; Urciuolo et al., 2013). Upon injury MuSCs get activated and enter the cell cycle (Bentzinger et al., 2010). They then become myogenic progenitor cells or fuse with the damaged myofibers after migration to the site of injury, a process which is controlled by signaling through Ephrins and Wnt7a (Stark et al., 2011; Bentzinger et al., 2014). Wnt signaling is one of the important signaling pathways in muscle regeneration. Wnt5a, Wnt5b, and Wnt7a are upregulated at early phases of regeneration while Wnt3a and Wnt7b expression increase at later phases (Polesskaya et al., 2003; Brack et al., 2008). While Wnt3a drives differentiation of MuSCs through activation of the canonical Wnt signaling pathway, Wnt7a promotes asymmetric MuSC division together with the ECM protein Fibronectin. Furthermore, Wnt7a induces migration of MuSCs and growth of myofibers through activation of different non-canonical Wnt pathways (Polesskaya et al., 2003; Brack et al., 2008; Otto et al., 2008; Le Grand et al., 2009; Bentzinger et al., 2014). Interestingly, Wnt7a always signals through Fzd7 in skeletal muscle activating different signaling pathways in the respective cell types, among them the planar cell polarity pathway and the AKT/mTOR pathway (von Maltzahn et al., 2012). A fine regulation of Wnt signaling is required for proper regeneration of skeletal muscle. For instance, increased canonical Wnt signaling during aging causes impaired regeneration of skeletal muscle and increased fibrosis (Brack et al., 2007). However, the anti-aging hormone soluble Klotho (sKlotho) is an antagonist of canonical Wnt signaling and important for maintaining MuSC functionality. This suggests that Klotho may be a naturally occurring inhibitor of increased canonical Wnt signaling in aged skeletal muscle and its availability could overcome over live time acquired changes in aged MuSCs (Ahrens et al., 2018). Furthermore, R-spondin plays a role in differentiation of myogenic progenitor cells during regeneration by positively regulating canonical Wnt signaling (Lacour et al., 2017). In addition to regulating Wnt activity, a temporal switch from Notch to canonical Wnt signaling is required for proper myogenic differentiation during regeneration (Brack et al., 2008). Here, Notch ligands control MuSC proliferation and differentiation (Conboy and Rando, 2002; Conboy et al., 2007; Brack et al., 2008; Mourikis et al., 2012). Especially the interplay between Notch and the transmembrane receptor Syndecan-3 (Sdc3) controls the maintenance of the MuSC pool and myofiber size after regeneration (Pisconti et al., 2010). Myogenic Regulatory Factors (MRFs) like Myf5, MyoD, Myogenin and Mrf4 facilitate myogenic differentiation of MuSCs allowing myogenic lineage progression required for regeneration of skeletal muscle (Braun et al., 1992; Rudnicki et al., 1992; Rudnicki et al., 1993; Singh and Dilworth, 2013). Myogenic progenitor cells become elongated and then fuse to form multinucleated myotubes expressing developmental myosin heavy chains (MHCs) (Bentzinger et al., 2010; Yin et al., 2013). In addition to the formation of new myofibers during regeneration reinnervation takes place, important for controlling MuSC behavior and maturation of myofibers (Vignaud et al., 2007; Forcina et al., 2020; Henze et al., 2024).

Muscle stem cells and myogenic lineage progression in the adult

Regeneration of skeletal muscle is critically depending on MuSCs, a stem cell population residing underneath the basal lamina of myofibers first described by Alexander Mauro in 1961 (Mauro, 1961; Lepper et al., 2011; Murphy et al., 2011; Sambasivan et al., 2011; Schmidt et al., 2019) (Figure 1A). In adult skeletal muscle all MuSCs express the paired box transcription factor Pax7, which is essential for MuSC functionality, while subsets of them also express Pax3 or myogenic regulatory factor 5 (Myf5) (Relaix et al., 2005; Kuang et al., 2007; Lepper et al., 2011; Relaix and Zammit, 2012; Relaix et al., 2021). Although all MuSCs are expressing the canonical marker Pax7, the MuSC population is heterogeneous (Kuang et al., 2007; Mourikis et al., 2012; Chakkalakal et al., 2014). Under resting conditions MuSCs are quiescent but can be readily activated due to injury or other stimuli such as exercise (Fry et al., 2015; Schmidt et al., 2019).

After injury of skeletal muscle quiescent MuSCs become activated and then undergo myogenic lineage progression resulting in the expression of MyoD and Myf5. This causes their transformation into myogenic precursor cells (Chang and Rudnicki, 2014; Henze et al., 2020; von Maltzahn, 2021). However, MuSCs are capable of self-renewal thereby maintaining the MuSC pool and giving rise to myogenic progenitor cells required for regeneration of skeletal muscle (Blau et al., 2015). Myogenic differentiation is driven by the MRFs which comprise Myf5, MyoD, Myogenin and Mrf4, which control the process of elongation of myogenic progenitor cells into myocytes (Soleimani et al., 2012; Singh and Dilworth, 2013; Hernandez-Hernandez et al., 2017). Of note, fusion of myocytes into multinucleated myotubes depends on the expression of myomaker and myomerger (Millay et al., 2013; Leikina et al., 2018). The final step in regeneration of skeletal muscle is the maturation of myofibers which is coinciding with the migration of the centrally located nuclei into the periphery of myofibers (Forcina et al., 2020).

Receptors in muscle stem cells

Proper regeneration of skeletal muscle requires an effective communication between the different cell types in skeletal muscle and MuSCs (Figure 2). MuSCs receive signals from the immediate niche and surrounding cells through a variety of transmembrane receptors. The interactions of signaling molecules with the transmembrane receptors in MuSCs activate signaling pathways which regulate their quiescence, activation and differentiation (Figure 3). Interactions of MuSCs with their surroundings can be

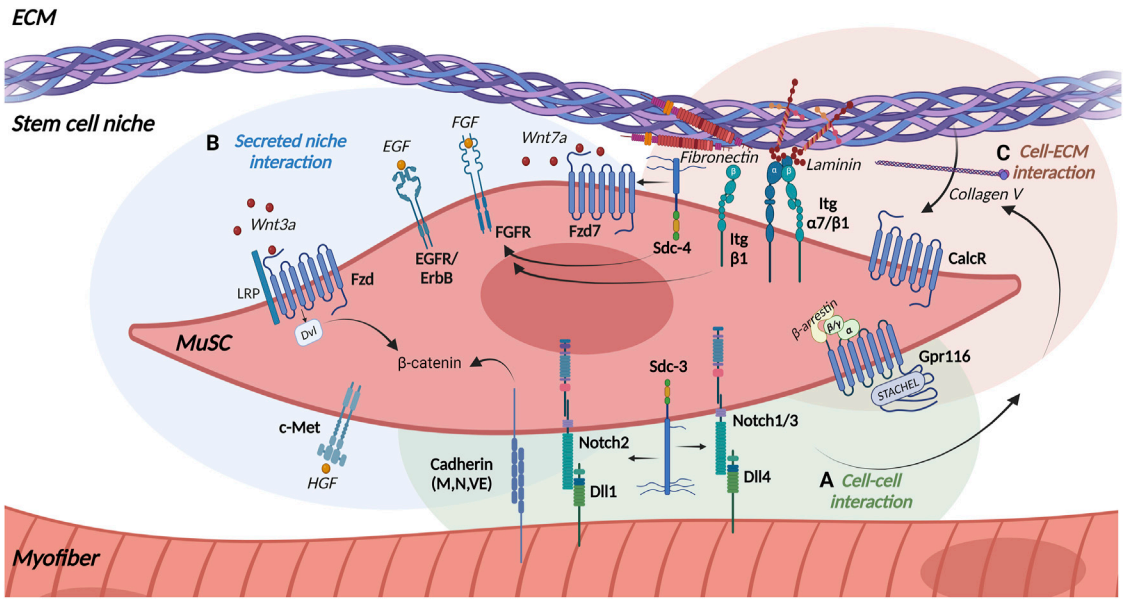

FIGURE 3
Receptors in MuSCs. MuSCs expresses various transmembrane receptors to interact with their local niche including **(A)** the myofiber (green background), **(B)** the stem cell niche (blue background), and **(C)** the extracellular matrix (ECM) (light brown background). Arrows indicate interaction partners. Abbreviations: Dvl, Dishevelled; LRP, Low density lipoprotein Receptor-related Protein; Wnt, Wingless-related integration site; Fzd, Frizzled receptor; Sdc, Syndecan; Itg, Integrin; Dll, Delta-like protein; Notch, Neurogenic locus notch homolog protein; EGF, Epidermal Growth Factor; EGFR, Epidermal Growth Factor Receptor; ErbB, Anti-apoptotic ErbB receptor; FGF, Fibroblast growth factor; FGFR, Fibroblast Growth Factor Receptor; HGF, Hepatocyte growth factor; c-Met, Mesenchymal epithelial transition factor; CalcR, Calcitonin receptor; Gpr116, adhesion G-protein-coupled receptor 116. Created with BioRender.com.

divided into the following categories: direct cell-cell interactions (Figure 3A), signaling via secreted factors (Figure 3B) or cell-matrix interactions (Figure 3C) which we will discuss in detail in the following paragraphs.

Direct cell-cell interactions

Notch signaling

One of the main receptors in MuSCs controlling quiescence and differentiation are the Notch receptors. They are highly conserved single-pass transmembrane proteins with a large extracellular portion (Figure 3A). Mammals comprise four different Notch receptors (Notch 1–4) which are expressed on the cell surface of the signal-receiving cell. The Notch ligands Delta-like (Dll) −1, −4 and Jagged (Jag) −1, −2 are also transmembrane proteins located on the opposing signal-sending cell making a direct cell-cell communication a prerequisite for activation of the Notch signaling pathway. Activation of the Notch receptor by its ligands then leads to proteolytic cleavage of the receptor into a Notch extracellular domain (NECD) by Adam10 and into a Notch intracellular domain (NICD) by γ-secretases. The ligand remains bound to the extracellular part and is endocytosed by the signal-sending cell, while the cytosolic part migrates to the nucleus and binds to the transcription factor Recombination Signal Binding Protein for Immunoglobulin Kappa J Region (RBPJ) regulating the expression of Notch target genes (Vasyutina et al., 2007a; Kopan and Ilagan, 2009; Gioftsidi et al., 2022).

Notch signaling controls asymmetric division and quiescence of MuSCs. Importantly, high levels of Notch keep MuSCs in a quiescent state (Bjornson et al., 2012; Wen et al., 2012). The essential role of Notch signaling in maintaining MuSC quiescence was further supported by the finding that loss of Notch 1 and Notch 2 receptor in murine MuSCs results in break of quiescence (Fujimaki et al., 2018). Of note, expression of RBPJ, a downstream factor of Notch signaling, is a prerequisite for maintenance of MuSC quiescence (Bjornson et al., 2012; Mourikis et al., 2012). The genetic loss of RPBJ induces a break of quiescence and leads to spontaneous activation and premature differentiation of MuSCs (Bjornson et al., 2012; Bentzinger et al., 2013a). RBPJ and the Notch ligand Dll1 play an essential role in the maintenance of muscle progenitor cells (Vasyutina et al., 2007a), e.g. mutations in RBPJ and Dll1 lead to extensive and uncontrolled differentiation of progenitor cells resulting in an increased population of differentiated myogenic cells expressing MyoD and Myogenin and a reduced number of progenitors expressing Lbx1 and Pax3 (Vasyutina et al., 2007b; Schuster-Gossler et al., 2007). This uncontrolled myogenic differentiation leads to the depletion of the progenitor cell pool, resulting in insufficient muscle growth during development and severe muscle hypotrophy (Vasyutina et al., 2007a; Vasyutina et al., 2007b; Brohl et al., 2012).

While the Notch 2/Dll1 signaling pair was identified as the mediator of MuSC self-renewal (Yartseva et al., 2020), Dll1 also controls the differentiation of early myoblasts and the maintenance of myogenic progenitor cells in mouse embryos (Schuster-Gossler et al., 2007). In addition to its role in regulating MuSC functionality in the adult, Notch signaling plays an important role in embryonic

and postnatal myogenesis controlling processes such as maintenance of the quiescent state, regulation of self-renewal and differentiation (Bjornson et al., 2012).

Furthermore, Notch signaling controls the interaction of MuSCs with their immediate niche, e.g., Notch1/RBPJ regulates the expression of the ECM molecule ColV, which promotes quiescence of MuSCs by binding to the Calcitonin receptor (CalcR) in an autocrine manner (Baghdadi et al., 2018) (Figures 3A, B). Notch also interacts with the single-pass transmembrane proteoglycan Sdc3 to regulate maintenance of the MuSC pool as well as self-renewal and reversible quiescence of MuSCs (Pisconti et al., 2010) (Figure 3). Syndecans interact with ECM proteins (e.g., Collagens, Laminins, Fibronectin) and growth factors (e.g., FGF-2, HGF, EGF, VEGF) via their ectodomain and with intracellular signaling molecules and cytoskeletal proteins through their intracellular domain (Leonova and Galzitskaya, 2013; Gondelaud and Ricard-Blum, 2019). Sdc3, along with Notch, is expressed in MuSCs and regulates their maintenance, proliferation and differentiation emphasizing the connection of the different signaling pathways (Fuentealba et al., 1999). Furthermore, Sdc3 controls myofiber size after regeneration and can be used as a membranous molecular marker to identify MuSCs next to Sdc4 (Pisconti et al., 2010; Wang et al., 2014).

Cadherins

Quiescence of MuSCs is controlled by Notch signaling as well as through signaling via cadherins. Cadherins are single pass transmembrane glycoproteins, which mediate calcium-dependent cell-cell adhesion (Ivanov et al., 2001). Cadherins facilitate the direct binding of MuSCs to myofibers (Figure 3A). Three different cadherins are expressed by MuSCs and adult myofibers: M-, N- and VE-Cadherin. However, not all Cadherins appear to play similar roles in skeletal muscle (Kann et al., 2021). M-cadherin was found in quiescent and activated MuSCs and is one of the molecular markers of MuSCs (Wang et al., 2014). M- and N-cadherin regulate MuSC quiescence through the canonical Wnt/β-catenin signaling (Goel et al., 2017). In the absence of injury, removal of N-cadherin from adult MuSCs induces a break in quiescence, which can be enhanced by additional removal of M-cadherin. Removal of N-cadherin alone from MuSCs does not lead to an exit from the niche or loss of cell polarity, suggesting that the function of N-cadherin is rather related to maintenance of MuSC quiescence (Goel et al., 2017). Under homeostatic conditions, expression of M-cadherin in MuSCs mediates their adhesion to myofibers (Marti et al., 2013). Furthermore, M-cadherin is crucial for activation of cell division, e.g., *in vitro* treatment of MuSCs with M-cadherin stimulates cell division, whereas incubation with M-cadherin blocking antibodies reduces cell divisions (Marti et al., 2013).

Gpr116

Another important regulator of MuSC quiescence is the adhesion G-protein-coupled receptor Gpr116, which belongs to the G-protein-coupled receptor (GPCR) superfamily. GPCRs are seven-pass-transmembrane receptors which are stimulated by extracellular ligands leading to the dissociation of the heterotrimeric G-protein (Gα, Gβ, Gγ) resulting in the activation of the respective intrinsic signaling cascades. Nevertheless, adhesion GPCRs have several atypical characteristics, including an exceptionally long extracellular N-terminus, which contains adhesion domains and a highly conserved region for autoproteolytic cleavage (Bassilana et al., 2019). Adhesion GPCRs like Gpr116 carry an agonistic sequence within the autoproteolysis-inducing (GAIN) domain. Short peptides derived from this region, called Stachel sequence, serve as a tethered agonist and can activate the respective receptor and initiate the respective signaling cascade (Stoveken et al., 2015; Demberg et al., 2017). Sénéchal and colleagues recently showed that adhesion GPCR Gpr116 is present at high levels in quiescent MuSCs being essential for long-term maintenance of the MuSC pool regarding quiescence and self-renewal capacity (Figure 3C). Of note, stimulation of MuSCs with the Gpr116 *Stachel* peptide prevents activation and differentiation of MuSCs. This stimulation also leads to a strong association with β-arrestins and increases the nuclear localization of β-arrestin 1, where it interacts with the cAMP response element binding protein (CREB) to regulate gene expression (Senechal et al., 2022). Furthermore, expression of Gpr116 is rapidly downregulated in activated MuSCs. MuSCs lacking Gpr116 are incapable of maintaining quiescence by showing progressive depletion over time and impaired self-renewal underscoring the importance of Gpr116 for maintenance of MuSC quiescence (Senechal et al., 2022).

Interaction with secreted niche factors

Wnt signaling

In addition to direct cell-cell-interactions controlling mainly MuSC quiescence, MuSC functionality is regulated by secreted niche factors, e. g., Wnt signaling regulating divisions of MuSCs. Wnt signaling through Frizzled (Fzd) receptors plays an important role in asymmetric division and migration of MuSCs. Fzd receptors are seven-pass transmembrane proteins with a large extracellular cysteine-rich domain (CRD), which is involved in ligand binding (Nusse, 2008; Sethi and Vidal-Puig, 2010; Clevers and Nusse, 2012). Fzd receptors are activated by different Wnt proteins, a large family of secreted glycoproteins, related to the wingless gene in *Drosophila* (Sethi and Vidal-Puig, 2010; Willert and Nusse, 2012). In mammals, the Wnt family comprises 19 members, with high amino acid sequence identities but distinct signaling properties resulting in multiple intracellular responses (Nusse, 2008).

The canonical Wnt signaling pathway, also known as Wnt/β-catenin pathway, requires the transmembrane low density lipoprotein receptor-related protein (LRP) as a co-receptor as well as the transcriptional activity of β-catenin (Nusse, 2012). β-catenin forms a degradation complex with axin, adenomatous polyposis coli (APC) and glycogen synthase kinase-3 beta (GSK-3β). In the absence of Wnt, β-catenin is phosphorylated within the degradation complex, leading to its own degradation (Katoh and Katoh, 2007). Binding of Wnt ligands to their respective Fzd receptors causes the activation of heterotrimeric G-proteins and the cytoplasmic phosphoprotein Dishevelled (Dvl). This results in a phosphorylation-dependent recruitment of axin to the Fzd co-

receptor LRP and inactivation of the β-catenin degradation complex, followed by the accumulation and stabilization of β-catenin in the cytoplasm and its translocation into the nucleus. Here, β-catenin binds to the transcription factors T-cell factor (TCF) and lymphoid enhancer factor (LEF) and acts as a transcriptional coactivator inducing Wnt/β-catenin target genes (Abu-Elmagd et al., 2010; Grumolato et al., 2010). In adult skeletal muscle canonical Wnt signaling is mainly mediated through the Fzd ligand Wnt3a which drives differentiation of MuSCs (Otto et al., 2008; von Maltzahn et al., 2012) (Figure 3B). Upon activation of MuSCs canonical Wnt signaling increases and antagonizes the effects of Notch signaling. The temporal switch from Notch to Wnt signaling is essential for normal myogenesis regarding differentiation and progression of myogenic commitment (Brack et al., 2008). Additionally, maintaining a balanced and proper canonical Wnt signaling is crucial for successful regeneration. It has been demonstrated that R-spondin, a modulator of canonical Wnt signaling, plays an important role in differentiation of myogenic progenitor cells during regeneration (Lacour et al., 2017). Furthermore, it was shown that conditional activation or disruption of β-catenin in adult MuSCs also impairs regeneration of skeletal muscle (Rudolf et al., 2016).

In contrast to the canonical pathway, non-canonical Wnt ligands activate several non-canonical pathways in MuSCs and myofibers, such as the planar cell polarity, the PI3K/AKT/mTOR and the Wnt/Calcium pathway (von Maltzahn et al., 2011; von Maltzahn et al., 2013a; von Maltzahn et al., 2013b). Of note, all ligands signal through Fzd receptors independently of β-catenin and LRP (Nusse, 2012; von Maltzahn et al., 2012). In skeletal muscle, Wnt7a and its receptor Fzd7 mediate non-canonical Wnt signaling thereby regulating regeneration and growth of skeletal muscle (Bentzinger et al., 2014; Bentzinger et al., 2013b; Le Grand et al., 2009; Schmidt et al., 2022; von Maltzahn et al., 2011; von Maltzahn et al., 2013b) (Figure 3B). Wnt7a signaling specifically promotes symmetric satellite stem cell divisions, a subpopulation of MuSCs, via the formation of a coreceptor complex with the ECM glycoprotein Fibronectin and the receptor Sdc4 (Le Grand et al., 2009; Bentzinger et al., 2013b) (Figure 3B). Another Wnt family protein, Wnt4, is released by myofibers and controls MuSC quiescence by activating the Rho GTPase and repressing the Yes-associated protein (YAP) via a non-canonical Wnt pathway (Eliazer et al., 2019).

FGF, EGF, and HGF signaling

While Wnt signaling mainly regulates MuSC divisions, FGF signaling preferentially controls proliferation of MuSCs. Fibroblast growth factor receptors (FGFRs) are receptor tyrosine kinases (RTKs) comprising the four homologous members FGFR1-4. Like all common RTKs, they contain an intracellular tyrosine kinase domain and a large extracellular ligand-binding domain, which binds fibroblast growth factors (FGFs) as their native ligands. FGFR signaling is involved in various physiological processes like proliferation, differentiation, cell migration and survival (Dai et al., 2019).

The expression of all four FGF receptors was shown in myofiber cultures and in MuSCs (Kastner et al., 2000). The fibroblast growth factors FGF-2 and FGF-6 regulate MuSC function via various signaling pathways including ERK MAPK, p38α/β-MAPK, PI3 kinase, PLCγ or STAT signaling (Pawlikowski et al., 2017). FGF-2 and FGF-6 promote proliferation of MuSCs and inhibit their differentiation in mice (Bentzinger et al., 2010; Pawlikowski et al., 2017). In rat myofiber cultures, FGF-1, FGF-4 and FGF-6 enhance proliferation of MuSCs similar to FGF-2 in mice (Kastner et al., 2000). FGF-6 is present at high concentrations in isolated myofibers, suggesting that the myofiber is the main source of FGF-6 *in vivo* (Kastner et al., 2000). The unique localization of FGF-6 and FGFR4 may have a specific function during myogenesis (Kastner et al., 2000). However, presumably FGF-6 has a dual role during myoblast proliferation, migration and muscle differentiation, hypertrophy and regeneration which is depending on the activation of distinct signaling pathways that recruit either FGFR1 or FGFR4 receptors in a dose-dependent manner (Armand et al., 2006). Proper FGF signaling in MuSCs requires the interaction with Sdc4, β1-Integrin and Fibronectin (Pawlikowski et al., 2017) (Figure 3B). Alteration or reduction of levels of either β1-Integrin, Fibronectin or Sdc4 modulates FGF signaling in MuSCs and affects their behavior (Pawlikowski et al., 2017). For example, an abnormal localization of β1-Integrin during aging leads to a diminished FGF-2 response, resulting in aberrant ERK signaling controlling activation of MuSCs (Rozo et al., 2016).

In addition to FGF receptors, MuSCs express another class of RTK receptors, the anti-apoptotic ErbB receptors which comprise four members: the epidermal growth factor (EGF) receptor (also known as ErbB1), ErbB2, ErbB3 and ErbB4. They are single-pass transmembrane proteins with an extracellular ligand-binding domain for EGF-related growth factors, and a cytoplasmic protein tyrosine kinase domain being able to form homo- and heterodimers (Olayioye et al., 2000) (Figure 3B). Golding et al. demonstrated in 2007 that MuSCs do not express any ErbB receptors in the quiescent state. However, within 6 h of activation ErbB1, ErbB2 and ErbB3 are expressed, while ErbB4 is activated in the first 24 h of activation. Furthermore, Golding and colleagues show that ErbB2 signaling plays a role in preventing apoptosis thereby preserving MuSCs during the critical phase of stem cell activation (Golding et al., 2007).

Receptors can be also used as molecular surface markers to identify MuSCs, among them c-Met and CXCR4 (Figure 3B). Mesenchymal epithelial transition factor (c-Met) is a single-pass, disulfide-linked α/β-heterodimer of the RTK family with high affinity to hepatocyte growth factors (HGF). Ligand/receptor interaction activates different signaling pathways, which are involved in proliferation, motility, migration, invasion and evasion of apoptosis (Organ and Tsao, 2011). c-Met is one of the molecular markers of MuSCs and required for regeneration of skeletal muscle (Webster and Fan, 2013; Wang et al., 2014; Lahmann et al., 2021). The study by Lahmann et al. (2021) showed that c-Met and *C-X-C* chemokine receptor type 4 (CXCR4) signaling cooperate during muscle regeneration. CXCR4 is a GPCR of the chemokine family, which is activated by the chemokine CXCL12 (Sdf-1α) and stimulates proliferation and migration of MuSCs (Vasyutina et al., 2005; Griffin et al., 2010). Consequently, MuSCs deficient of c-Met and CXCR4 are susceptible to apoptosis, while c-Met and CXCR4 signaling protects MuSCs from TNF-α-induced apoptosis (Lahmann et al., 2021).

Cell-matrix interactions

Integrin signaling

MuSCs are embedded in their niche. ECM molecules make up a large portion of the MuSC niche and regulate MuSC functionality. Here, Integrin receptors (Itg) are responsible for cell-matrix and cell-cell interactions. They function as extracellular receptors for ECM ligands such as Fibronectin, Laminin, Collagens or Vitronectin and thus form the structural and functional link between the ECM and intracellular cytoskeletal proteins (Figure 3C). Integrins consist of non-covalently bound α- and β-subunits. In the resting state they present in an inactive conformation, while binding of chemokines and growth factors results in their activation and binding of intracellular molecules such as Paxillin, Talin and Kindlin to the β-subunit thereby allowing binding to ECM components. This binding promotes the recruitment of signaling molecules such as Integrin Linked Tyrosine (ILK), Focal Adhesion Kinases (FAK) and modulation of signaling pathways such as AKT, ERK, Rho-GTPases and mTOR (Hynes, 2002; Takada et al., 2007; Campbell and Humphries, 2011; Taylor et al., 2022).

The heterodimer α7/β1-Integrin can be mainly found in skeletal muscle and has a high affinity for Laminin (Kramer et al., 1991; Loreti and Sacco, 2022) (Figure 3C). Quiescent MuSCs express high levels of α7- and β1-Integrin, which makes them good molecular markers of MuSCs (Blanco-Bose et al., 2001; Wang et al., 2014). Of note, β1-Integrin is involved in the maintenance of MuSC homeostasis as well as the expansion and self-renewal of MuSCs during regeneration. Moreover, β1-Integrin interacts with FGF-2 thereby controlling MuSC proliferation and self-renewal while β3-Integrin regulates differentiation of MuSCs in regenerating muscle (Liu et al., 2011; Rozo et al., 2016). Integrins also play an important role in the interaction of MuSCs with their immediate niche, MuSCs adhere to the ECM molecule Fibronectin via α4/β1-, α4/β7-and α5/β1-Integrins or to Laminin via α6/β1-Integrin (Figure 3C), interactions which are especially important during myogenesis (Taylor et al., 2022). Here, Fibronectin mediates the peripheral nuclear positioning through binding to α5-Integrin, a process depending on activation of FAK and the tyrosine kinase Src (Roman et al., 2018).

Signaling through the calcitonin receptor

While the ECM molecules Fibronectin and Laminin mainly interact with Integrins, ColIV binding to the Calcitonin receptor (CalcR) regulates quiescence of MuSCs (Baghdadi et al., 2018) (Figure 3C). The CalcR is another member of the GPCRs which regulates quiescence of MuSCs, similar to Gpr116. Binding of the peptide hormone Calcitonin to the CalcR causes its activation resulting in the activation of multiple signaling pathways through its interaction with different G-protein family members (Gs and Gq) involved in maintaining calcium homeostasis (Masi and Brandi, 2007). In addition to regulating quiescence by signaling via the CalcR-protein kinase A (PKA)-Yes-associated protein 1 (Yap1) axis, CalcR is a molecular marker of MuSCs (Wang et al., 2014; Yamaguchi et al., 2015; Zhang et al., 2019; Zhang L. et al., 2021). MuSCs are retained in a quiescent state by the Notch-ColV-CalcR signaling pathway (Baghdadi et al., 2018). Here, ColV is produced as a result of Notch signaling and acts as a ligand for the CalcR. ColV production is reduced upon MuSC activation and inhibition of ColV synthesis leads to their activation and differentiation (Baghdadi et al., 2018).

The MuSC niche and its remodeling after injury

Receptors in MuSCs are connecting MuSCs to the local environment, also known as the MuSC niche. The niche plays a prominent role in regulating quiescence and activation of MuSCs, myogenic differentiation and thereby regeneration of skeletal muscle. For instance, quiescence of MuSCs is regulated through the tight expression of multiple transcription factors in MuSCs. Binding of ECM components from the MuSC niche by receptors in MuSCs controls their expression and thereby the state of quiescence (Chang and Rudnicki, 2014). The ECM, a complex network of proteins and carbohydrates, provides structural support to MuSCs. Its composition is tightly connected to the age of an individual and state of regeneration regulating MuSC functionality. The most prominent components of the ECM in the MuSC niche include Collagens, Laminins, Vitronectin, Fibronectin and other glycoproteins as well as adhesion molecules such as M-Cadherin and CD34 (Casaroli Marano and Vilaro, 1994; Beauchamp et al., 2000). Post-translational modifications (PTMs) are essential for the proper functionality of ECM molecules and play an important role in regulating cellular behavior (Hu et al., 2022). These PTMs can occur at various stages of ECM protein synthesis, secretion or degradation and include mostly phosphorylation, glycosylation, acetylation and ubiquitination (Yuan and Ye, 2021).

The MuSC niche is severely remodeled during regeneration of skeletal muscle including a change in the composition of cell types in the immediate MuSC niche. Here, the interplay between MuSCs and various muscle resident cell types such as fibroblasts, immune cells (including macrophages, eosinophils and neutrophils) and FAPs affects and controls proper regeneration of skeletal muscle (Abou-Khalil et al., 2010; Lander et al., 2012). During regeneration dynamic remodeling of the ECM takes place, which is driven by changes in expression and thereby secretion of ECM molecules by MuSCs and other cell types in regenerating muscle. This remodeling causes alterations in MuSC behavior required for regeneration. For instance, MuSCs become activated through upregulation of Fibronectin expression and consequently activation of the respective receptors (Bentzinger et al., 2010; Shirakawa et al., 2022). Of note, activated mast cells create a pro-inflammatory environment after injury through secretion of cytokines, tryptase and TNF-α, which in turn is responsible for the downregulation of the expression of Pax7 (Palacios et al., 2010). Afterwards, monocytes differentiate into macrophages (pro-inflammatory and anti-inflammatory) which stimulate the early and late phases of myogenic processes by secretion of ECM components including Fibronectin and ColVI, respectively (Bentzinger et al., 2014; Mashinchian et al., 2018). In addition to MuSCs and immune cells, FAPs get activated after injury and rapidly increase in number (Sastourne-Arrey et al., 2023). They contribute to myogenic differentiation by secretion of the cytokine interleukin

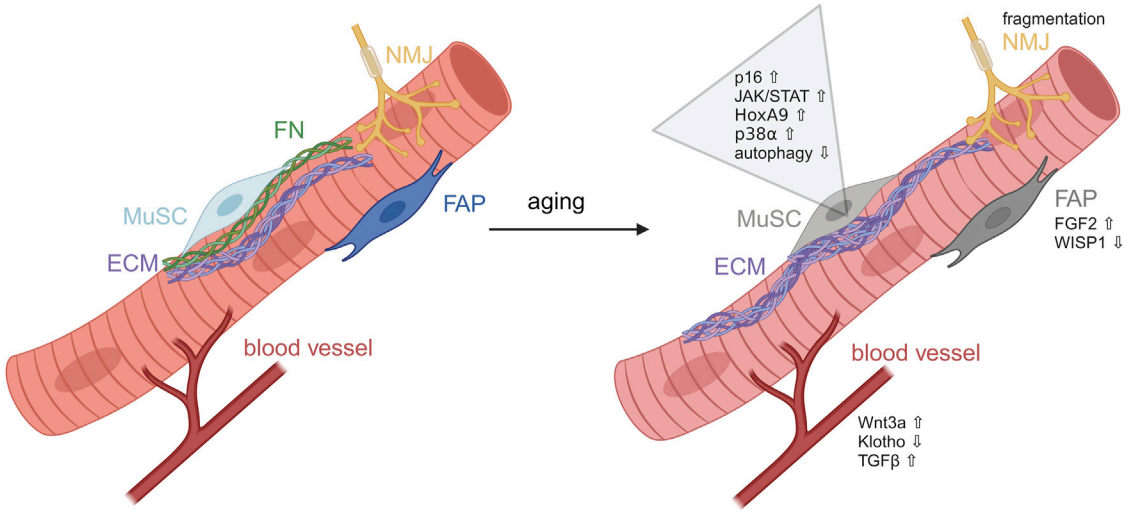

FIGURE 4
Alterations in MuSCs during aging. Induction of developmental pathways during aging impairing MuSCs functionality. MuSC, muscle stem cell; ECM, extracellular matrix; FN, fibronectin; FAP, fibro-adipogenic progenitor; NMJ, neuromuscular junction. Figure was modified from Henze et al. (2020).

(IL)-6. However, eosinophils secrete additional cytokines such as IL-4 or IL-3, which are responsible for blocking the adipogenic differentiation of FAPs (Bentzinger et al., 2013a). Moreover, endothelial cells secrete a variety of antiapoptotic factors (e.g., VEGF) which stimulate the proliferation of MuSCs during regeneration (Frey et al., 2012).

Alterations in regeneration of skeletal muscle in age and disease

As outlined above, regeneration of skeletal muscle is a highly orchestrated process in which each step is tightly controlled. During aging as well as in different disease states this precise control is out of balance resulting in impairments or delays of regeneration.

Aging is characterized by a decline of organ function and integrity, accompanied by a decrease of regenerative capacity and an increase in vulnerability. The reduced ability of tissues to regenerate is mainly caused by stem cell exhaustion and deterioration (Kirkwood, 2005; Sousa-Victor et al., 2014; Lopez-Otin et al., 2023). Aging of skeletal muscle is marked by the gradual loss of muscle mass, strength and overall impaired physical performance, also called sarcopenia (Cruz-Jentoft et al., 2019). Additionally, muscle tissue is often replaced by adipose tissue (Rahemi et al., 2015; Yoshiko et al., 2017). During aging MuSCs switch to an irreversible cell cycle arrest and show increased levels of H3K27me3, which is associated with transcriptional repression (Liu et al., 2013; Sousa-Victor et al., 2014; Sousa-Victor et al., 2018) (Figure 4). Furthermore, functionality of MuSCs is impaired through the aberrant induction of developmental pathways caused by permissive chromatin states (Figure 4). For example, expression of Hoxa9 is induced and activates pathways such as JAK/STAT signaling limiting MuSC function (Schworer et al., 2016). Also, p38α/β-MAPK signaling displays aberrant upregulation in aged MuSCs inhibiting their self-renewal and thus regenerative potential (Cosgrove et al., 2014). Upregulation of developmentally important signaling pathways such as canonical Wnt signaling, JAK/STAT signaling and downregulation of Notch signaling further diminishes MuSCs functionality and drives them into a fibrogenic fate (Brack et al., 2007; Carlson et al., 2009; Price et al., 2014; Tierney et al., 2014) (Figure 4). In MuSCs from geriatric mice epigenetic p16INK4a depression is lost driving MuSCs into an irreversible pre-senescent state (Sousa-Victor et al., 2014; Schworer et al., 2016). An additional driver for loss of stem cell functionality with increasing age is their reduced autophagic activity leading to an accumulation of damaged mitochondria and increased ROS levels (Garcia-Prat et al., 2016). In addition to intrinsic changes in MuSCs, systemic factors show alterations during aging, e.g., serum levels of TGF-β1 are increased in elderly humans and mice which stimulates the expansion of tissue-resident fibroblasts and inhibits the myogenic differentiation of MuSCs, leading to a diminished regenerative capacity of aged muscle (Carlson et al., 2009). Furthermore, reduced levels of the well-known anti-aging hormone Klotho lead to a perturbed number and functionality of MuSCs resulting in a reduction of the regenerative capacity of skeletal muscle (Ahrens et al., 2018).

As outlined above, MuSCs are also directly affected by their local environment. Here, the ECM shows the biggest alterations during aging (Birch, 2018). With increasing age, systemic cytokine levels are altered and shift towards a low-grade chronic inflammation, a process also known as “inflammaging” (Franceschi et al., 2018). In skeletal muscle, this leads to the deregulation of ECM remodeling enzymes and their inhibitors, thereby increasing the amount of fibrotic tissue and impairing differentiation of myoblasts into myofibers (Blau et al., 2015). Additionally, the altered elasticity of fibrotic muscle tissue is likely to impair self-renewal of MuSCs (Urciuolo et al., 2013). Furthermore, it was shown that the direct interactions between MuSCs and the myofiber are controlling MuSC behavior (Bischoff, 1990). The exact mechanism for this interaction is not known but FGF-2 is increasingly secreted by aged myofibers

and, at least in part, responsible for the age-related depletion of the MuSC pool (Chakkalakal et al., 2012). Increased FGF-2 levels hinder MuSCs to return to quiescence via constant activation of ERK signaling (Chakkalakal et al., 2012). In addition to alterations in the secretome of myofibers, the myofiber size seems to directly affect number and function of MuSCs, both of which are reduced during aging (Verdijk et al., 2007). Moreover, other muscle resident cell types change their functionality during aging, e.g., FAPs, which contribute to muscle homeostasis and regeneration, are displaying alterations during aging. For instance, it was shown that the matricellular protein Wisp1 is important to promote the expansion of MuSCs during regeneration. However, with increasing age Wisp1 secretion by FAPs is reduced, contributing to impaired MuSC functionality which then causes a reduced regenerative capacity. This is reminiscent of the observation that loss of Fibronectin expression in aged skeletal muscle impairs its regeneration (Lukjanenko et al., 2016; Lukjanenko et al., 2019).

With increasing age regeneration of skeletal muscle is reduced. However, other physiological states or diseases can also lead to an insufficient tissue restoration and/or maintenance of skeletal muscle. Among those are cancer cachexia, congestive heart failure, chronic obstructive pulmonary disease, chronic infectious diseases, neuromuscular diseases, chronic inflammatory diseases and acute critical illness. In those diseases functionality of MuSCs is affected through increased inflammation, oxidative stress, metabolic changes or unbalanced nutrition (Sharifi-Rad et al., 2020). Duchenne Muscular Dystrophy (DMD) pathology is one of the degenerative diseases affecting regeneration and maintenance of skeletal muscle. Here, the absence of the Dystrophin protein leads to sarcolemma instability and fragility. DMD is associated with extensive damage of myofibers upon contraction which cannot be rescued by newly regenerated myotubes (Ohlendieck et al., 1993; Grounds et al., 2008). Furthermore, divisions of MuSCs are affected in mdx mice, the mouse model of DMD (Dumont et al., 2015). Another example for muscle wasting diseases is myositis which affects proximal skeletal muscles and is clinically characterized by muscle weakness and a low level of muscle endurance (Lundberg et al., 2016). Here, an inflammatory cell infiltration, mainly composed of T-cells, macrophages and dendritic cells, occurs in skeletal muscle although the molecular mechanisms causing muscle wasting is not fully understood yet (Engel and Arahata, 1984; Greenberg et al., 2005). However, it was suggested that muscle weakness is caused by a loss of capillaries leading to tissue hypoxia and a loss of myofibers due to degeneration and necrosis of myofibers as a result of direct cytotoxic effects of T-cells (Emslie-Smith and Engel, 1990; Hohlfeld and Engel, 1991). Severe muscle wasting and loss of MuSC functionality is also occurring in cancer cachexia, the loss of muscle mass and functionality due to cancer. Here, Wnt7a was shown to effectively counteract muscle wasting through activation of the anabolic AKT/mTOR pathway as well as improve MuSC functionality (Schmidt et al., 2020). In addition to loss of muscle mass, cancer cachexia is associated with muscle damage which results in activation of MuSCs. Although MuSCs are activated, they fail to properly differentiate due to aberrant expression of Pax7 (He et al., 2013), a situation which shows similarities to rhabdomyosarcoma cells, a type of cancer cells thought to arise from myogenic precursor cells and which are also characterized by impaired myogenic differentiation.

Rhabdomyosarcomas

Although skeletal muscle is a tissue which does not undergo extensive tissue replacement and proliferation in the adult–except after injury - myogenic cells undergo proliferation during development, the time when rhabdomyosarcomas (RMS) arise. Rhabdomyosarcomas are the most common soft-tissue sarcoma in children and resemble cells committed to the skeletal muscle lineage in embryonic and fetal stages of development (Wei et al., 2022). However, the cell of origin is not well characterized so far. Literature suggests that RMS tumors could be initiated by cells of myogenic origin or by cells of non-myogenic origin (Keller et al., 2004; Hatley et al., 2012; Blum et al., 2013; Drummond et al., 2018).

RMS can be divided in two main subtypes, the most common embryonal rhabdomyosarcoma [ERMS, (~70%)] and the more aggressive alveolar rhabdomyosarcoma [ARMS, (~20%)]. The remaining RMS cases are caused by pleomorphic and spindle cell/sclerosing RMS (Ognjanovic et al., 2009). Classification in the clinics is mainly done by morphological and cytological assessment of hematoxylin and eosin-stained histology sections (Asmar et al., 1994; Davicioni et al., 2009). RMS tumors tend to occur at three main anatomical regions of the human body including the head and neck regions, the genitourinary system and the extremities (Arndt and Crist, 1999; Ma et al., 2015). However, RMS tumors can arise also at other locations in the human body. Of note, in all types of RMS a deregulated myogenic differentiation program leads to continuous proliferation and impaired terminal myogenic differentiation (Skapek et al., 2019).

The genetic alterations in most ARMS cases (approximately 80%) are well understood, here a chromosomal translocation between the *PAX3* [t (2; 13) (q35; q14)] or *PAX7* [t (1; 13) (q36; q14)] and Forkhead box protein O1 (*FOXO1*) occurs. This results in fusion genes thereby generating oncogenic transcription factors consisting of the DNA binding domain of the PAX and the transactivation domain of FOXO1, PAX-FOXO1. A minority of ARMS cases (~20%) lacks these translocations and shares clinical and biological features of ERMS (Parham and Barr, 2013). The presence of a PAX-FOXO1 fusion (fusion-positive/FP RMS cases) drives unfavorable outcomes in children and is recognized as an important prognostic factor (Hibbitts et al., 2019). Both PAX-FOXO1 fusion proteins show more transcriptional activity, are expressed at a higher level and are proteolytically more stable than their wild-type PAX counterparts (Davis and Barr, 1997; Bennicelli et al., 1999; Miller and Hollenbach, 2007). Thereby, they contribute to tumorigenicity through affecting growth, apoptosis, differentiation and cell migration. The enhanced expression of PAX3 or PAX7 in ARMS–here as a fusion protein–is reminiscent of MuSCs in cancer cachexia which are also displaying aberrant high levels of Pax7 expression (He et al., 2013). The aberrant expression of Pax7 or Pax3 might be one of the main drivers of impaired myogenic differentiation in ARMS as observed in MuSCs in cancer cachexia.

While ARMS tumors are classified as fusion-positive tumors ERMS tumors are fusion-negative and show a high variability in the genetic alterations causing cancer. Among those alterations are a loss of heterozygosity at chromosome 11p15.5, an increase in aneuploidy, mutations of *TP53*, *RAS* genes, *PIK3CA*, β-catenin and *FGFR4*, as well as *NF1*, *FBXW7* and *BCOR* affecting RTK-

RAS-RAF-MAPK, PI3K-AKT-mTOR signaling, cell cycle progression, apoptosis and developmental pathways such as Wnt, Notch, SHH and Hippo among others (Scrable et al., 1989; Stratton et al., 1989; Taylor et al., 2009; Zibat et al., 2010; Annavarapu et al., 2013; Shern et al., 2014; Mohamed et al., 2015; Conti et al., 2016; Skapek et al., 2019). Interestingly, mutations in ERMS often affect signaling pathways and receptors which also control MuSC functionality (Figure 3). However, in the vast majority of ERMS tumors the transcriptional repressor TRPS1 displays an increased expression causing impaired myogenic differentiation (Huttner et al., 2023). Of note, reduction of aberrant TRPS1 levels in ERMS tumor cells permits myogenic differentiation (Huttner et al., 2023).

All RMS tumors are diagnosed by the expression of myogenic markers such as the myogenic regulatory proteins MYOD and MYOGENIN, MHCs, skeletal α-ACTIN, Creatine Kinase and DESMIN (Tonin et al., 1991; Dias et al., 2000; Sebire and Malone, 2003). Histologically ERMS resembles an undifferentiated and embryonal state, while ARMS tumors are characterized by a more widely expression of key myogenic regulatory factors responsible for terminal differentiation such as MYOD and MYOGENIN (DeMartino et al., 2023). RMS treatment involves a multimodal approach including surgical excision, chemotherapy and radiation therapy. The outcome of metastatic or recurrent RMS patients remains poor, but localized instances are curable (Malempati and Hawkins, 2012; Dantonello et al., 2013). In recent decades, chemotherapy regimens have steadily improved, but remain non-specific to the tumor and include the application of vincristine, actinomycin D combined with cyclophosphamide or ifosfamide. However, recent modifications of these standard regimens have shown improvements in the outcomes of patients with rhabdomyosarcoma (Chen et al., 2019; Miwa et al., 2020). Nevertheless, additional treatment options for RMS would be desirable, potentially through inducing myogenic differentiation in tumor cells.

Conclusion

Skeletal muscle is the most abundant tissue of the human body, it is characterized by a high plasticity and ability to self-renew. Skeletal muscle supports mobility and body posture. Any kind of muscle impairments, such as disease, aging, injury, etc. has an impact on the general health and therefore quality of life. Regeneration of skeletal muscle is a highly orchestrated process involving the reception of signals from the niche through a variety of receptors located in the plasma membrane of MuSCs. A better understanding of the interplay of the different cell types and signaling pathways during regeneration of skeletal muscle is required, especially in age and disease. A focus on the secretome of the different cell types in skeletal muscle and how the secreted factors are affecting MuSC functionality might be a promising approach to the development of new therapies for improving regeneration of skeletal muscle.

Author contributions

KM: Writing–original draft, Writing–review and editing. EH: Writing–original draft, Writing–review and editing. KH: Writing–original draft, Writing–review and editing. CG: Writing–original draft, Writing–review and editing. JM: Supervision, Writing–original draft, Writing–review and editing.

Funding

The author(s) declare that financial support was received for the research, authorship, and/or publication of this article. This work was supported by a grant to JM by the Wilhelm-Sander-Stiftung (2021.101.1).

Conflict of interest

The authors declare that the research was conducted in the absence of any commercial or financial relationships that could be construed as a potential conflict of interest.

The author(s) declared that they were an editorial board member of Frontiers, at the time of submission. This had no impact on the peer review process and the final decision.

Publisher's note

References

Abou-Khalil, R., Mounier, R., and Chazaud, B. (2010). Regulation of myogenic stem cell behavior by vessel cells: the "menage a trois" of satellite cells, periendothelial cells and endothelial cells. *Cell Cycle* 9, 892–896. doi:10.4161/cc.9.5.10851

Abu-Elmagd, M., Robson, L., Sweetman, D., Hadley, J., Francis-West, P., and Munsterberg, A. (2010). Wnt/Lef1 signaling acts via Pitx2 to regulate somite myogenesis. *Dev. Biol.* 337, 211–219. doi:10.1016/j.ydbio.2009.10.023

Ahrens, H. E., Huettemeister, J., Schmidt, M., Kaether, C., and von Maltzahn, J. (2018). Klotho expression is a prerequisite for proper muscle stem cell function and regeneration of skeletal muscle. *Skelet. Muscle* 8, 20. doi:10.1186/s13395-018-0166-x

Ang, S. J., Crombie, E. M., Dong, H., Tan, K. T., Hernando, A., Yu, D., et al. (2022). Muscle 4EBP1 activation modifies the structure and function of the neuromuscular junction in mice. *Nat. Commun.* 13, 7792. doi:10.1038/s41467-022-35547-0

Annavarapu, S. R., Cialfi, S., Dominici, C., Kokai, G. K., Uccini, S., Ceccarelli, S., et al. (2013). Characterization of Wnt/β-catenin signaling in rhabdomyosarcoma. *Lab. Invest.* 93, 1090–1099. doi:10.1038/labinvest.2013.97

Armand, A. S., Laziz, I., and Chanoine, C. (2006). FGF6 in myogenesis. *Biochim. Biophys. Acta* 1763, 773–778. doi:10.1016/j.bbamcr.2006.06.005

Arndt, C. A., and Crist, W. M. (1999). Common musculoskeletal tumors of childhood and adolescence. *N. Engl. J. Med.* 341, 342–352. doi:10.1056/NEJM199907293410507

Asmar, L., Gehan, E. A., Newton, W. A., Webber, B. L., Marsden, H. B., van Unnik, A. J., et al. (1994). Agreement among and within groups of pathologists in the classification of rhabdomyosarcoma and related childhood sarcomas. Report of an international study of four pathology classifications. *Cancer.* 74, 2579–2588. doi:10.1002/1097-0142(19941101)74:9<2579::aid-cncr2820740928>3.0.co;2-a

Baghdadi, M. B., Castel, D., Machado, L., Fukada, S. I., Birk, D. E., Relaix, F., et al. (2018). Reciprocal signalling by Notch-Collagen V-CALCR retains muscle stem cells in their niche. *Nature* 557, 714–718. doi:10.1038/s41586-018-0144-9

Bassilana, F., Nash, M., and Ludwig, M. G. (2019). Adhesion G protein-coupled receptors: opportunities for drug discovery. *Nat. Rev. Drug Discov.* 18, 869–884. doi:10.1038/s41573-019-0039-y

Beauchamp, J. R., Heslop, L., Yu, D. S., Tajbakhsh, S., Kelly, R. G., Wernig, A., et al. (2000). Expression of CD34 and Myf5 defines the majority of quiescent adult skeletal muscle satellite cells. *J. Cell Biol.* 151, 1221–1234. doi:10.1083/jcb.151.6.1221

Bennicelli, J. L., Advani, S., Schafer, B. W., and Barr, F. G. (1999). PAX3 and PAX7 exhibit conserved cis-acting transcription repression domains and utilize a common gain of function mechanism in alveolar rhabdomyosarcoma. *Oncogene* 18, 4348–4356. doi:10.1038/sj.onc.1202812

Bentzinger, C. F., von Maltzahn, J., Dumont, N. A., Stark, D. A., Wang, Y. X., Nhan, K., et al. (2014). Wnt7a stimulates myogenic stem cell motility and engraftment resulting in improved muscle strength. *J. Cell Biol.* 205, 97–111. doi:10.1083/jcb.201310035

Bentzinger, C. F., von Maltzahn, J., and Rudnicki, M. A. (2010). Extrinsic regulation of satellite cell specification. *Stem Cell Res. Ther.* 1, 27. doi:10.1186/scrt27

Bentzinger, C. F., Wang, Y. X., Dumont, N. A., and Rudnicki, M. A. (2013a). Cellular dynamics in the muscle satellite cell niche. *EMBO Rep.* 14, 1062–1072. doi:10.1038/embor.2013.182

Bentzinger, C. F., Wang, Y. X., von Maltzahn, J., Soleimani, V. D., Yin, H., and Rudnicki, M. A. (2013b). Fibronectin regulates Wnt7a signaling and satellite cell expansion. *Cell Stem Cell* 12, 75–87. doi:10.1016/j.stem.2012.09.015

Birch, H. L. (2018). Extracellular matrix and ageing. *Subcell. Biochem.* 90, 169–190. doi:10.1007/978-981-13-2835-0_7

Bischoff, R. (1990). Interaction between satellite cells and skeletal muscle fibers. *Development* 109, 943–952. doi:10.1242/dev.109.4.943

Bjornson, C. R., Cheung, T. H., Liu, L., Tripathi, P. V., Steeper, K. M., and Rando, T. A. (2012). Notch signaling is necessary to maintain quiescence in adult muscle stem cells. *Stem Cells* 30, 232–242. doi:10.1002/stem.773

Blanco-Bose, W. E., Yao, C. C., Kramer, R. H., and Blau, H. M. (2001). Purification of mouse primary myoblasts based on alpha 7 integrin expression. *Exp. Cell Res.* 265, 212–220. doi:10.1006/excr.2001.5191

Blau, H. M., Cosgrove, B. D., and Ho, A. T. (2015). The central role of muscle stem cells in regenerative failure with aging. *Nat. Med.* 21, 854–862. doi:10.1038/nm.3918

Blum, J. M., Ano, L., Li, Z., Van Mater, D., Bennett, B. D., Sachdeva, M., et al. (2013). Distinct and overlapping sarcoma subtypes initiated from muscle stem and progenitor cells. *Cell Rep.* 5, 933–940. doi:10.1016/j.celrep.2013.10.020

Brack, A. S., Conboy, I. M., Conboy, M. J., Shen, J., and Rando, T. A. (2008). A temporal switch from notch to Wnt signaling in muscle stem cells is necessary for normal adult myogenesis. *Cell Stem Cell* 2, 50–59. doi:10.1016/j.stem.2007.10.006

Brack, A. S., Conboy, M. J., Roy, S., Lee, M., Kuo, C. J., Keller, C., et al. (2007). Increased Wnt signaling during aging alters muscle stem cell fate and increases fibrosis. *Science.* 317, 807–810. doi:10.1126/science.1144090

Braun, T., Rudnicki, M. A., Arnold, H. H., and Jaenisch, R. (1992). Targeted inactivation of the muscle regulatory gene Myf-5 results in abnormal rib development and perinatal death. *Cell* 71, 369–382. doi:10.1016/0092-8674(92)90507-9

Brohl, D., Vasyutina, E., Czajkowski, M. T., Griger, J., Rassek, C., Rahn, H. P., et al. (2012). Colonization of the satellite cell niche by skeletal muscle progenitor cells depends on Notch signals. *Dev. Cell* 23, 469–481. doi:10.1016/j.devcel.2012.07.014

Bruusgaard, J. C., Liestol, K., Ekmark, M., Kollstad, K., and Gundersen, K. (2003). Number and spatial distribution of nuclei in the muscle fibres of normal mice studied *in vivo*. *J. Physiol.* 551, 467–478. doi:10.1113/jphysiol.2003.045328

Campbell, I. D., and Humphries, M. J. (2011). Integrin structure, activation, and interactions. *Cold Spring Harb. Perspect. Biol.* 3, a004994. doi:10.1101/cshperspect.a004994

Carlson, M. E., Conboy, M. J., Hsu, M., Barchas, L., Jeong, J., Agrawal, A., et al. (2009). Relative roles of TGF-beta1 and Wnt in the systemic regulation and aging of satellite cell responses. *Aging Cell* 8, 676–689. doi:10.1111/j.1474-9726.2009.00517.x

Casaroli Marano, R. P., and Vilaro, S. (1994). The role of fibronectin, laminin, vitronectin and their receptors on cellular adhesion in proliferative vitreoretinopathy. *Invest. Ophthalmol. Vis. Sci.* 35, 2791–2803.

Chakkalakal, J. V., Christensen, J., Xiang, W., Tierney, M. T., Boscolo, F. S., Sacco, A., et al. (2014). Early forming label-retaining muscle stem cells require p27kip1 for maintenance of the primitive state. *Development* 141, 1649–1659. doi:10.1242/dev.100842

Chakkalakal, J. V., Jones, K. M., Basson, M. A., and Brack, A. S. (2012). The aged niche disrupts muscle stem cell quiescence. *Nature* 490, 355–360. doi:10.1038/nature11438

Chang, N. C., and Rudnicki, M. A. (2014). Satellite cells: the architects of skeletal muscle. *Curr. Top. Dev. Biol.* 107, 161–181. doi:10.1016/B978-0-12-416022-4.00006-8

Charvet, B., Ruggiero, F., and Le Guellec, D. (2012). The development of the myotendinous junction. A review. *Muscles Ligaments Tendons J.* 2(2), 53–63.

Chen, C., Dorado Garcia, H., Scheer, M., and Henssen, A. G. (2019). Current and future treatment strategies for rhabdomyosarcoma. *Front. Oncol.* 9, 1458. doi:10.3389/fonc.2019.01458

Ciena, A. P., Luques, I. U., Dias, F. J., Yokomizo de Almeida, S. R., Iyomasa, M. M., and Watanabe, I. S. (2010). Ultrastructure of the myotendinous junction of the medial pterygoid muscle of adult and aged Wistar rats. *Micron* 41, 1011–1014. doi:10.1016/j.micron.2010.04.006

Clevers, H., and Nusse, R. (2012). Wnt/β-catenin signaling and disease. *Cell* 149, 1192–1205. doi:10.1016/j.cell.2012.05.012

Conboy, I. M., and Rando, T. A. (2002). The regulation of Notch signaling controls satellite cell activation and cell fate determination in postnatal myogenesis. *Dev. Cell* 3, 397–409. doi:10.1016/s1534-5807(02)00254-x

Conboy, L., Seymour, C. M., Monopoli, M. P., O'Sullivan, N. C., Murphy, K. J., and Regan, C. M. (2007). Notch signalling becomes transiently attenuated during long-term memory consolidation in adult Wistar rats. *Neurobiol. Learn Mem.* 88, 342–351. doi:10.1016/j.nlm.2007.04.006

Conti, B., Slemmons, K. K., Rota, R., and Linardic, C. M. (2016). Recent insights into notch signaling in embryonal rhabdomyosarcoma. *Curr. Drug Targets* 17, 1235–1244. doi:10.2174/1389450116666150907105756

Cooper, J. A., and Sept, D. (2008). New insights into mechanism and regulation of actin capping protein. *Int. Rev. Cell Mol. Biol.* 267, 183–206. doi:10.1016/S1937-6448(08)00604-7

Cosgrove, B. D., Gilbert, P. M., Porpiglia, E., Mourkioti, F., Lee, S. P., Corbel, S. Y., et al. (2014). Rejuvenation of the muscle stem cell population restores strength to injured aged muscles. *Nat. Med.* 20, 255–264. doi:10.1038/nm.3464

Cruz-Jentoft, A. J., Bahat, G., Bauer, J., Boirie, Y., Bruyere, O., Cederholm, T., et al. (2019). Sarcopenia: revised European consensus on definition and diagnosis. *Age Ageing* 48, 601. doi:10.1093/ageing/afz046

Dai, S., Zhou, Z., Chen, Z., Xu, G., and Chen, Y. (2019). Fibroblast growth factor receptors (FGFRs): structures and small molecule inhibitors. *Cells* 8, 614. doi:10.3390/cells8060614

Dantonello, T. M., Int-Veen, C., Schuck, A., Seitz, G., Leuschner, I., Nathrath, M., et al. (2013). Survival following disease recurrence of primary localized alveolar rhabdomyosarcoma. *Pediatr. Blood Cancer* 60, 1267–1273. doi:10.1002/pbc.24488

Dave, H. D., Shook, M., and Varacallo, M. (2024). *Anatomy, skeletal muscle*. Treasure Isl. (FL): StatPearls.

Davicioni, E., Anderson, M. J., Finckenstein, F. G., Lynch, J. C., Qualman, S. J., Shimada, H., et al. (2009). Molecular classification of rhabdomyosarcoma--genotypic and phenotypic determinants of diagnosis: a report from the Children's Oncology Group. *Am. J. Pathol.* 174, 550–564. doi:10.2353/ajpath.2009.080631

Davis, R. J., and Barr, F. G. (1997). Fusion genes resulting from alternative chromosomal translocations are overexpressed by gene-specific mechanisms in alveolar rhabdomyosarcoma. *Proc. Natl. Acad. Sci. U. S. A.* 94, 8047–8051. doi:10.1073/pnas.94.15.8047

DeMartino, J., Meister, M. T., Visser, L. L., Brok, M., Groot Koerkamp, M. J. A., Wezenaar, A. K. L., et al. (2023). Single-cell transcriptomics reveals immune suppression and cell states predictive of patient outcomes in rhabdomyosarcoma. *Nat. Commun.* 14, 3074. doi:10.1038/s41467-023-38886-8

Demberg, L. M., Winkler, J., Wilde, C., Simon, K. U., Schon, J., Rothemund, S., et al. (2017). Activation of adhesion G protein-coupled receptors: AGONIST specificity of stachel SEQUENCE-DERIVED peptides. *J. Biol. Chem.* 292, 4383–4394. doi:10.1074/jbc.M116.763656

Dias, P., Chen, B., Dilday, B., Palmer, H., Hosoi, H., Singh, S., et al. (2000). Strong immunostaining for myogenin in rhabdomyosarcoma is significantly associated with tumors of the alveolar subclass. *Am. J. Pathol.* 156, 399–408. doi:10.1016/S0002-9440(10)64743-8

Drummond, C. J., Hanna, J. A., Garcia, M. R., Devine, D. J., Heyrana, A. J., Finkelstein, D., et al. (2018). Hedgehog pathway drives fusion-negative rhabdomyosarcoma initiated from non-myogenic endothelial progenitors. *Cancer Cell* 33, 108–124. doi:10.1016/j.ccell.2017.12.001

Dumont, N., and Frenette, J. (2010). Macrophages protect against muscle atrophy and promote muscle recovery *in vivo* and *in vitro*: a mechanism partly dependent on the insulin-like growth factor-1 signaling molecule. *Am. J. Pathol.* 176, 2228–2235. doi:10.2353/ajpath.2010.090884

Dumont, N. A., Wang, Y. X., von Maltzahn, J., Pasut, A., Bentzinger, C. F., Brun, C. E., et al. (2015). Dystrophin expression in muscle stem cells regulates their polarity and asymmetric division. *Nat. Med.* 21, 1455–1463. doi:10.1038/nm.3990

Eliazer, S., Muncie, J. M., Christensen, J., Sun, X., D'Urso, R. S., Weaver, V. M., et al. (2019). Wnt4 from the niche controls the mechano-properties and quiescent state of muscle stem cells. *Cell Stem Cell* 25, 654–665. doi:10.1016/j.stem.2019.08.007

Emslie-Smith, A. M., and Engel, A. G. (1990). Microvascular changes in early and advanced dermatomyositis: a quantitative study. *Ann. Neurol.* 27, 343–356. doi:10.1002/ana.410270402

Engel, A. G., and Arahata, K. (1984). Monoclonal antibody analysis of mononuclear cells in myopathies. II: phenotypes of autoinvasive cells in polymyositis and inclusion body myositis. *Ann. Neurol.* 16, 209–215. doi:10.1002/ana.410160207

Forcina, L., Cosentino, M., and Musaro, A. (2020). Mechanisms regulating muscle regeneration: insights into the interrelated and time-dependent phases of tissue healing. *Cells* 9, 1297. doi:10.3390/cells9051297

Franceschi, C., Garagnani, P., Parini, P., Giuliani, C., and Santoro, A. (2018). Inflammaging: a new immune-metabolic viewpoint for age-related diseases. *Nat. Rev. Endocrinol.* 14, 576–590. doi:10.1038/s41574-018-0059-4

Frey, S. P., Jansen, H., Raschke, M. J., Meffert, R. H., and Ochman, S. (2012). VEGF improves skeletal muscle regeneration after acute trauma and reconstruction of the limb in a rabbit model. *Clin. Orthop. Relat. Res.* 470, 3607–3614. doi:10.1007/s11999-012-2456-7

Frontera, W. R., and Ochala, J. (2015). Skeletal muscle: a brief review of structure and function. *Calcif. Tissue Int.* 96, 183–195. doi:10.1007/s00223-014-9915-y

Fry, C. S., Lee, J. D., Mula, J., Kirby, T. J., Jackson, J. R., Liu, F., et al. (2015). Inducible depletion of satellite cells in adult, sedentary mice impairs muscle regenerative capacity without affecting sarcopenia. *Nat. Med.* 21, 76–80. doi:10.1038/nm.3710

Fuchs, E., and Blau, H. M. (2020). Tissue stem cells: architects of their niches. *Cell Stem Cell* 27, 532–556. doi:10.1016/j.stem.2020.09.011

Fuentealba, L., Carey, D. J., and Brandan, E. (1999). Antisense inhibition of syndecan-3 expression during skeletal muscle differentiation accelerates myogenesis through a basic fibroblast growth factor-dependent mechanism. *J. Biol. Chem.* 274, 37876–37884. doi:10.1074/jbc.274.53.37876

Fujimaki, S., Seko, D., Kitajima, Y., Yoshioka, K., Tsuchiya, Y., Masuda, S., et al. (2018). Notch1 and Notch2 coordinately regulate stem cell function in the quiescent and activated states of muscle satellite cells. *Stem Cells* 36, 278–285. doi:10.1002/stem.2743

Garcia-Prat, L., Martinez-Vicente, M., Perdiguero, E., Ortet, L., Rodriguez-Ubreva, J., Rebollo, E., et al. (2016). Autophagy maintains stemness by preventing senescence. *Nature* 529, 37–42. doi:10.1038/nature16187

Gibbs, B. F., Wierecky, J., Welker, P., Henz, B. M., Wolff, H. H., and Grabbe, J. (2001). Human skin mast cells rapidly release preformed and newly generated TNF-alpha and IL-8 following stimulation with anti-IgE and other secretagogues. *Exp. Dermatol* 10, 312–320. doi:10.1034/j.1600-0625.2001.100503.x

Gioftsidi, S., Relaix, F., and Mourikis, P. (2022). The Notch signaling network in muscle stem cells during development, homeostasis, and disease. *Skelet. Muscle* 12, 9. doi:10.1186/s13395-022-00293-w

Goel, A. J., Rieder, M. K., Arnold, H. H., Radice, G. L., and Krauss, R. S. (2017). Niche cadherins control the quiescence-to-activation transition in muscle stem cells. *Cell Rep.* 21, 2236–2250. doi:10.1016/j.celrep.2017.10.102

Golding, J. P., Calderbank, E., Partridge, T. A., and Beauchamp, J. R. (2007). Skeletal muscle stem cells express anti-apoptotic ErbB receptors during activation from quiescence. *Exp. Cell Res.* 313, 341–356. doi:10.1016/j.yexcr.2006.10.019

Gondelaud, F., and Ricard-Blum, S. (2019). Structures and interactions of syndecans. *FEBS J.* 286, 2994–3007. doi:10.1111/febs.14828

Gratchev, A., Guillot, P., Hakiy, N., Politz, O., Orfanos, C. E., Schledzewski, K., et al. (2001). Alternatively activated macrophages differentially express fibronectin and its splice variants and the extracellular matrix protein betaIG-H3. *Scand. J. Immunol.* 53, 386–392. doi:10.1046/j.1365-3083.2001.00885.x

Greenberg, S. A., Bradshaw, E. M., Pinkus, J. L., Pinkus, G. S., Burleson, T., Due, B., et al. (2005). Plasma cells in muscle in inclusion body myositis and polymyositis. *Neurology* 65, 1782–1787. doi:10.1212/01.wnl.0000187124.92826.20

Griffin, C. A., Apponi, L. H., Long, K. K., and Pavlath, G. K. (2010). Chemokine expression and control of muscle cell migration during myogenesis. *J. Cell Sci.* 123, 3052–3060. doi:10.1242/jcs.066241

Grounds, M. D., Radley, H. G., Lynch, G. S., Nagaraju, K., and De Luca, A. (2008). Towards developing standard operating procedures for pre-clinical testing in the mdx mouse model of Duchenne muscular dystrophy. *Neurobiol. Dis.* 31, 1–19. doi:10.1016/j.nbd.2008.03.008

Grumolato, L., Liu, G., Mong, P., Mudbhary, R., Biswas, R., Arroyave, R., et al. (2010). Canonical and noncanonical Wnts use a common mechanism to activate completely unrelated coreceptors. *Genes Dev.* 24, 2517–2530. doi:10.1101/gad.1957710

Hargreaves, M., and Spriet, L. L. (2020). Skeletal muscle energy metabolism during exercise. *Nat. Metab.* 2, 817–828. doi:10.1038/s42255-020-0251-4

Hatley, M. E., Tang, W., Garcia, M. R., Finkelstein, D., Millay, D. P., Liu, N., et al. (2012). A mouse model of rhabdomyosarcoma originating from the adipocyte lineage. *Cancer Cell* 22, 536–546. doi:10.1016/j.ccr.2012.09.004

He, W. A., Berardi, E., Cardillo, V. M., Acharyya, S., Aulino, P., Thomas-Ahner, J., et al. (2013). NF-κB-mediated Pax7 dysregulation in the muscle microenvironment promotes cancer cachexia. *J. Clin. Invest.* 123, 4821–4835. doi:10.1172/JCI68523

Heckman, C. J., and Enoka, R. M. (2012). Motor unit. *Compr. Physiol.* 2, 2629–2682. doi:10.1002/cphy.c100087

Henze, H., Huttner, S. S., Koch, P., Schuler, S. C., Groth, M., von Eyss, B., et al. (2024). Denervation alters the secretome of myofibers and thereby affects muscle stem cell lineage progression and functionality. *NPJ Regen. Med.* 9, 10. doi:10.1038/s41536-024-00353-3

Henze, H., Jung, M. J., Ahrens, H. E., Steiner, S., and von Maltzahn, J. (2020). Skeletal muscle aging - stem cells in the spotlight. *Mech. Ageing Dev.* 189, 111283. doi:10.1016/j.mad.2020.111283

Hernandez-Hernandez, J. M., Garcia-Gonzalez, E. G., Brun, C. E., and Rudnicki, M. A. (2017). The myogenic regulatory factors, determinants of muscle development, cell identity and regeneration. *Semin. Cell Dev. Biol.* 72, 10–18. doi:10.1016/j.semcdb.2017.11.010

Hibbitts, E., Chi, Y. Y., Hawkins, D. S., Barr, F. G., Bradley, J. A., Dasgupta, R., et al. (2019). Refinement of risk stratification for childhood rhabdomyosarcoma using FOXO1 fusion status in addition to established clinical outcome predictors: a report from the Children's Oncology Group. *Cancer Med.* 8, 6437–6448. doi:10.1002/cam4.2504

Hohlfeld, R., and Engel, A. G. (1991). Coculture with autologous myotubes of cytotoxic T cells isolated from muscle in inflammatory myopathies. *Ann. Neurol.* 29, 498–507. doi:10.1002/ana.410290509

Horsley, V., Jansen, K. M., Mills, S. T., and Pavlath, G. K. (2003). IL-4 acts as a myoblast recruitment factor during mammalian muscle growth. *Cell* 113, 483–494. doi:10.1016/s0092-8674(03)00319-2

Hu, M., Ling, Z., and Ren, X. (2022). Extracellular matrix dynamics: tracking in biological systems and their implications. *J. Biol. Eng.* 16, 13. doi:10.1186/s13036-022-00292-x

Huttner, S. S., Henze, H., Elster, D., Koch, P., Anderer, U., von Eyss, B., et al. (2023). A dysfunctional miR-1-TRPS1-MYOG axis drives ERMS by suppressing terminal myogenic differentiation. *Mol. Ther.* 31, 2612–2632. doi:10.1016/j.ymthe.2023.07.003

Hynes, R. O. (2002). Integrins: bidirectional, allosteric signaling machines. *Cell* 110, 673–687. doi:10.1016/s0092-8674(02)00971-6

Ivanov, D. B., Philippova, M. P., and Tkachuk, V. A. (2001). Structure and functions of classical cadherins. *Biochem. (Mosc).* 66, 1174–1186. doi:10.1023/a:1012445316415

Jejurikar, S. S., Marcelo, C. L., and Kuzon, W. M., Jr. (2002). Skeletal muscle denervation increases satellite cell susceptibility to apoptosis. *Plast. Reconstr. Surg.* 110, 160–168. doi:10.1097/00006534-200207000-00027

Jensen, J., Rustad, P. I., Kolnes, A. J., and Lai, Y. C. (2011). The role of skeletal muscle glycogen breakdown for regulation of insulin sensitivity by exercise. *Front. Physiol.* 2, 112. doi:10.3389/fphys.2011.00112

Kann, A. P., Hung, M., and Krauss, R. S. (2021). Cell-cell contact and signaling in the muscle stem cell niche. *Curr. Opin. Cell Biol.* 73, 78–83. doi:10.1016/j.ceb.2021.06.003

Kasama, T., Strieter, R. M., Standiford, T. J., Burdick, M. D., and Kunkel, S. L. (1993). Expression and regulation of human neutrophil-derived macrophage inflammatory protein 1 alpha. *J. Exp. Med.* 178, 63–72. doi:10.1084/jem.178.1.63

Kastner, S., Elias, M. C., Rivera, A. J., and Yablonka-Reuveni, Z. (2000). Gene expression patterns of the fibroblast growth factors and their receptors during myogenesis of rat satellite cells. *J. Histochem Cytochem* 48, 1079–1096. doi:10.1177/002215540004800805

Katoh, M., and Katoh, M. (2007). WNT signaling pathway and stem cell signaling network. *Clin. Cancer Res.* 13, 4042–4045. doi:10.1158/1078-0432.CCR-06-2316

Keller, C., Arenkiel, B. R., Coffin, C. M., El-Bardeesy, N., DePinho, R. A., and Capecchi, M. R. (2004). Alveolar rhabdomyosarcomas in conditional Pax3:Fkhr mice: cooperativity of Ink4a/ARF and Trp53 loss of function. *Genes Dev.* 18, 2614–2626. doi:10.1101/gad.1244004

Kirkwood, T. B. (2005). Understanding the odd science of aging. *Cell* 120, 437–447. doi:10.1016/j.cell.2005.01.027

Kopan, R., and Ilagan, M. X. (2009). The canonical Notch signaling pathway: unfolding the activation mechanism. *Cell* 137, 216–233. doi:10.1016/j.cell.2009.03.045

Korthuis, R. J. (2011). *Skeletal Muscle Circulation*. San Rafael (CA): Morgan and Claypool Life Sciences.

Kramer, R. H., Vu, M. P., Cheng, Y. F., Ramos, D. M., Timpl, R., and Waleh, N. (1991). Laminin-binding integrin alpha 7 beta 1: functional characterization and expression in normal and malignant melanocytes. *Cell Regul.* 2, 805–817. doi:10.1091/mbc.2.10.805

Kuang, S., Kuroda, K., Le Grand, F., and Rudnicki, M. A. (2007). Asymmetric self-renewal and commitment of satellite stem cells in muscle. *Cell* 129, 999–1010. doi:10.1016/j.cell.2007.03.044

Lacour, F., Vezin, E., Bentzinger, C. F., Sincennes, M. C., Giordani, L., Ferry, A., et al. (2017). R-spondin1 controls muscle cell fusion through dual regulation of antagonistic Wnt signaling pathways. *Cell Rep.* 18, 2320–2330. doi:10.1016/j.celrep.2017.02.036

Lahmann, I., Griger, J., Chen, J. S., Zhang, Y., Schuelke, M., and Birchmeier, C. (2021). Met and Cxcr4 cooperate to protect skeletal muscle stem cells against inflammation-induced damage during regeneration. *Elife* 10, e57356. doi:10.7554/eLife.57356

Lander, A. D., Kimble, J., Clevers, H., Fuchs, E., Montarras, D., Buckingham, M., et al. (2012). What does the concept of the stem cell niche really mean today? *BMC Biol.* 10, 19. doi:10.1186/1741-7007-10-19

Larsson, L., Degens, H., Li, M., Salviati, L., Lee, Y. I., Thompson, W., et al. (2019). Sarcopenia: aging-related loss of muscle mass and function. *Physiol. Rev.* 99, 427–511. doi:10.1152/physrev.00061.2017

Le Grand, F., Jones, A. E., Seale, V., Scime, A., and Rudnicki, M. A. (2009). Wnt7a activates the planar cell polarity pathway to drive the symmetric expansion of satellite stem cells. *Cell Stem Cell* 4, 535–547. doi:10.1016/j.stem.2009.03.013

Leikina, E., Gamage, D. G., Prasad, V., Goykhberg, J., Crowe, M., Diao, J., et al. (2018). Myomaker and myomerger work independently to control distinct steps of membrane remodeling during myoblast fusion. *Dev. Cell* 46, 767–780. doi:10.1016/j.devcel.2018.08.006

Leonova, E. I., and Galzitskaya, O. V. (2013). Structure and functions of syndecans in vertebrates. *Biochem. (Mosc).* 78, 1071–1085. doi:10.1134/S0006297913100015

Lepper, C., Partridge, T. A., and Fan, C. M. (2011). An absolute requirement for Pax7-positive satellite cells in acute injury-induced skeletal muscle regeneration. *Development* 138, 3639–3646. doi:10.1242/dev.067595

Linke, W. A., and Kruger, M. (2010). The giant protein titin as an integrator of myocyte signaling pathways. *Physiol. (Bethesda)* 25, 186–198. doi:10.1152/physiol.00005.2010

Liu, H., Niu, A., Chen, S. E., and Li, Y. P. (2011). Beta3-integrin mediates satellite cell differentiation in regenerating mouse muscle. *FASEB J.* 25, 1914–1921. doi:10.1096/fj.10-170449

Liu, L., Cheung, T. H., Charville, G. W., Hurgo, B. M., Leavitt, T., Shih, J., et al. (2013). Chromatin modifications as determinants of muscle stem cell quiescence and chronological aging. *Cell Rep.* 4, 189–204. doi:10.1016/j.celrep.2013.05.043

Liu, W., Klose, A., Forman, S., Paris, N. D., Wei-LaPierre, L., Cortes-Lopez, M., et al. (2017). Loss of adult skeletal muscle stem cells drives age-related neuromuscular junction degeneration. *Elife* 6, e26464. doi:10.7554/eLife.26464

Liu, W., Wei-LaPierre, L., Klose, A., Dirksen, R. T., and Chakkalakal, J. V. (2015). Inducible depletion of adult skeletal muscle stem cells impairs the regeneration of neuromuscular junctions. *Elife* 4, e09221. doi:10.7554/eLife.09221

Lopez-Otin, C., Blasco, M. A., Partridge, L., Serrano, M., and Kroemer, G. (2023). Hallmarks of aging: an expanding universe. *Cell* 186, 243–278. doi:10.1016/j.cell.2022.11.001

Loreti, M., and Sacco, A. (2022). The jam session between muscle stem cells and the extracellular matrix in the tissue microenvironment. *NPJ Regen. Med.* 7, 16. doi:10.1038/s41536-022-00204-z

Lukjanenko, L., Jung, M. J., Hegde, N., Perruisseau-Carrier, C., Migliavacca, E., Rozo, M., et al. (2016). Loss of fibronectin from the aged stem cell niche affects the regenerative capacity of skeletal muscle in mice. *Nat. Med.* 22, 897–905. doi:10.1038/nm.4126

Lukjanenko, L., Karaz, S., Stuelsatz, P., Gurriaran-Rodriguez, U., Michaud, J., Dammone, G., et al. (2019). Aging disrupts muscle stem cell function by impairing matricellular WISP1 secretion from fibro-adipogenic progenitors. *Cell Stem Cell* 24, 433–446. doi:10.1016/j.stem.2018.12.014

Lundberg, I. E., Miller, F. W., Tjarnlund, A., and Bottai, M. (2016). Diagnosis and classification of idiopathic inflammatory myopathies. *J. Intern Med.* 280, 39–51. doi:10.1111/joim.12524

Ma, X., Huang, D., Zhao, W., Sun, L., Xiong, H., Zhang, Y., et al. (2015). Clinical characteristics and prognosis of childhood rhabdomyosarcoma: a ten-year retrospective multicenter study. *Int. J. Clin. Exp. Med.* 8, 17196–17205.

Malempati, S., and Hawkins, D. S. (2012). Rhabdomyosarcoma: review of the children's oncology group (COG) soft-tissue sarcoma committee experience and rationale for current COG studies. *Pediatr. Blood Cancer* 59, 5–10. doi:10.1002/pbc.24118

Marti, M., Montserrat, N., Pardo, C., Mulero, L., Miquel-Serra, L., Rodrigues, A. M., et al. (2013). M-cadherin-mediated intercellular interactions activate satellite cell division. *J. Cell Sci.* 126, 5116–5131. doi:10.1242/jcs.123562

Mashinchian, O., Pisconti, A., Le Moal, E., and Bentzinger, C. F. (2018). The muscle stem cell niche in health and disease. *Curr. Top. Dev. Biol.* 126, 23–65. doi:10.1016/bs.ctdb.2017.08.003

Masi, L., and Brandi, M. L. (2007). Calcitonin and calcitonin receptors. *Clin. Cases Min. Bone Metab.* 4, 117–122.

Mauro, A. (1961). Satellite cell of skeletal muscle fibers. *J. Biophys. Biochem. Cytol.* 9, 493–495. doi:10.1083/jcb.9.2.493

Millay, D. P., O'Rourke, J. R., Sutherland, L. B., Bezprozvannaya, S., Shelton, J. M., Bassel-Duby, R., et al. (2013). Myomaker is a membrane activator of myoblast fusion and muscle formation. *Nature* 499, 301–305. doi:10.1038/nature12343

Miller, P. J., and Hollenbach, A. D. (2007). The oncogenic fusion protein Pax3-FKHR has a greater post-translational stability relative to Pax3 during early myogenesis. *Biochim. Biophys. Acta* 1770, 1450–1458. doi:10.1016/j.bbagen.2007.06.016

Miwa, S., Yamamoto, N., Hayashi, K., Takeuchi, A., Igarashi, K., and Tsuchiya, H. (2020). Recent advances and challenges in the treatment of rhabdomyosarcoma. *Cancers (Basel)* 12, 1758. doi:10.3390/cancers12071758

Mohamed, A. D., Tremblay, A. M., Murray, G. I., and Wackerhage, H. (2015). The Hippo signal transduction pathway in soft tissue sarcomas. *Biochim. Biophys. Acta* 1856, 121–129. doi:10.1016/j.bbcan.2015.05.006

Mourikis, P., Gopalakrishnan, S., Sambasivan, R., and Tajbakhsh, S. (2012). Cell-autonomous Notch activity maintains the temporal specification potential of skeletal muscle stem cells. *Development* 139, 4536–4548. doi:10.1242/dev.084756

Murphy, M. M., Lawson, J. A., Mathew, S. J., Hutcheson, D. A., and Kardon, G. (2011). Satellite cells, connective tissue fibroblasts and their interactions are crucial for muscle regeneration. *Development* 138, 3625–3637. doi:10.1242/dev.064162

Nishikawa, K., Lindstedt, S. L., Hessel, A., and Mishra, D. (2020). N2A titin: signaling hub and mechanical switch in skeletal muscle. *Int. J. Mol. Sci.* 21, 3974. doi:10.3390/ijms21113974

Nusse, R. (2008). Wnt signaling and stem cell control. *Cell Res.* 18, 523–527. doi:10.1038/cr.2008.47

Nusse, R. (2012). Wnt signaling. *Cold Spring Harb. Perspect. Biol.* 4, a011163. doi:10.1101/cshperspect.a011163

Ognjanovic, S., Linabery, A. M., Charbonneau, B., and Ross, J. A. (2009). Trends in childhood rhabdomyosarcoma incidence and survival in the United States, 1975-2005. *Cancer* 115, 4218–4226. doi:10.1002/cncr.24465

Ohlendieck, K., Matsumura, K., Ionasescu, V. V., Towbin, J. A., Bosch, E. P., Weinstein, S. L., et al. (1993). Duchenne muscular dystrophy: deficiency of dystrophin-associated proteins in the sarcolemma. *Neurology* 43, 795–800. doi:10.1212/wnl.43.4.795

Olayioye, M. A., Neve, R. M., Lane, H. A., and Hynes, N. E. (2000). The ErbB signaling network: receptor heterodimerization in development and cancer. *EMBO J.* 19, 3159–3167. doi:10.1093/emboj/19.13.3159

Organ, S. L., and Tsao, M. S. (2011). An overview of the c-MET signaling pathway. *Ther. Adv. Med. Oncol.* 3, S7–S19. doi:10.1177/1758834011422556

Otto, A., Schmidt, C., Luke, G., Allen, S., Valasek, P., Muntoni, F., et al. (2008). Canonical Wnt signalling induces satellite-cell proliferation during adult skeletal muscle regeneration. *J. Cell Sci.* 121, 2939–2950. doi:10.1242/jcs.026534

Palacios, D., Mozzetta, C., Consalvi, S., Caretti, G., Saccone, V., Proserpio, V., et al. (2010). TNF/p38α/polycomb signaling to Pax7 locus in satellite cells links inflammation to the epigenetic control of muscle regeneration. *Cell Stem Cell* 7, 455–469. doi:10.1016/j.stem.2010.08.013

Parham, D. M., and Barr, F. G. (2013). Classification of rhabdomyosarcoma and its molecular basis. *Adv. Anat. Pathol.* 20, 387–397. doi:10.1097/PAP.0b013e3182a92d0d

Pawlikowski, B., Vogler, T. O., Gadek, K., and Olwin, B. B. (2017). Regulation of skeletal muscle stem cells by fibroblast growth factors. *Dev. Dyn.* 246, 359–367. doi:10.1002/dvdy.24495

Pedersen, B. K., and Febbraio, M. A. (2012). Muscles, exercise and obesity: skeletal muscle as a secretory organ. *Nat. Rev. Endocrinol.* 8, 457–465. doi:10.1038/nrendo.2012.49

Pillon, N. J., Bilan, P. J., Fink, L. N., and Klip, A. (2013). Cross-talk between skeletal muscle and immune cells: muscle-derived mediators and metabolic implications. *Am. J. Physiol. Endocrinol. Metab.* 304, E453–E465. doi:10.1152/ajpendo.00553.2012

Pisconti, A., Cornelison, D. D., Olguin, H. C., Antwine, T. L., and Olwin, B. B. (2010). Syndecan-3 and Notch cooperate in regulating adult myogenesis. *J. Cell Biol.* 190, 427–441. doi:10.1083/jcb.201003081

Pittman, R. N. (2000). Oxygen supply to contracting skeletal muscle at the microcirculatory level: diffusion vs. convection. *Acta Physiol. Scand.* 168, 593–602. doi:10.1046/j.1365-201x.2000.00710.x

Polesskaya, A., Seale, P., and Rudnicki, M. A. (2003). Wnt signaling induces the myogenic specification of resident CD45+ adult stem cells during muscle regeneration. *Cell* 113, 841–852. doi:10.1016/s0092-8674(03)00437-9

Price, F. D., von Maltzahn, J., Bentzinger, C. F., Dumont, N. A., Yin, H., Chang, N. C., et al. (2014). Inhibition of JAK-STAT signaling stimulates adult satellite cell function. *Nat. Med.* 20, 1174–1181. doi:10.1038/nm.3655

Purslow, P. P. (2020). The structure and role of intramuscular connective tissue in muscle function. *Front. Physiol.* 11, 495. doi:10.3389/fphys.2020.00495

Qaisar, R., and Larsson, L. (2014). What determines myonuclear domain size? *Indian J. Physiol. Pharmacol.* 58, 1–12.

Rahemi, H., Nigam, N., and Wakeling, J. M. (2015). The effect of intramuscular fat on skeletal muscle mechanics: implications for the elderly and obese. *J. R. Soc. Interface* 12, 20150365. doi:10.1098/rsif.2015.0365

Relaix, F., Bencze, M., Borok, M. J., Der Vartanian, A., Gattazzo, F., Mademtzoglou, D., et al. (2021). Perspectives on skeletal muscle stem cells. *Nat. Commun.* 12, 692. doi:10.1038/s41467-020-20760-6

Relaix, F., Rocancourt, D., Mansouri, A., and Buckingham, M. (2005). A Pax3/Pax7-dependent population of skeletal muscle progenitor cells. *Nature* 435, 948–953. doi:10.1038/nature03594

Relaix, F., and Zammit, P. S. (2012). Satellite cells are essential for skeletal muscle regeneration: the cell on the edge returns centre stage. *Development* 139, 2845–2856. doi:10.1242/dev.069088

Rodriguez Cruz, P. M., Cossins, J., Beeson, D., and Vincent, A. (2020). The neuromuscular junction in health and disease: molecular mechanisms governing synaptic formation and homeostasis. *Front. Mol. Neurosci.* 13, 610964. doi:10.3389/fnmol.2020.610964

Roman, W., Martins, J. P., and Gomes, E. R. (2018). Local arrangement of fibronectin by myofibroblasts governs peripheral nuclear positioning in muscle cells. *Dev. Cell* 46, 102–111. doi:10.1016/j.devcel.2018.05.031

Rossi, D., Pierantozzi, E., Amadsun, D. O., Buonocore, S., Rubino, E. M., and Sorrentino, V. (2022). The sarcoplasmic reticulum of skeletal muscle cells: a labyrinth of membrane contact sites. *Biomolecules* 12, 488. doi:10.3390/biom12040488

Rowland, L. A., Bal, N. C., and Periasamy, M. (2015). The role of skeletal-muscle-based thermogenic mechanisms in vertebrate endothermy. *Biol. Rev. Camb Philos. Soc.* 90, 1279–1297. doi:10.1111/brv.12157

Rozo, M., Li, L., and Fan, C. M. (2016). Targeting β1-integrin signaling enhances regeneration in aged and dystrophic muscle in mice. *Nat. Med.* 22, 889–896. doi:10.1038/nm.4116

Rudnicki, M. A., Braun, T., Hinuma, S., and Jaenisch, R. (1992). Inactivation of MyoD in mice leads to up-regulation of the myogenic HLH gene Myf-5 and results in apparently normal muscle development. *Cell* 71, 383–390. doi:10.1016/0092-8674(92)90508-a

Rudnicki, M. A., Schnegelsberg, P. N., Stead, R. H., Braun, T., Arnold, H. H., and Jaenisch, R. (1993). MyoD or Myf-5 is required for the formation of skeletal muscle. *Cell* 75, 1351–1359. doi:10.1016/0092-8674(93)90621-v

Rudolf, A., Schirwis, E., Giordani, L., Parisi, A., Lepper, C., Taketo, M. M., et al. (2016). β-Catenin activation in muscle progenitor cells regulates tissue repair. *Cell Rep.* 15, 1277–1290. doi:10.1016/j.celrep.2016.04.022

Saclier, M., Yacoub-Youssef, H., Mackey, A. L., Arnold, L., Ardjoune, H., Magnan, M., et al. (2013). Differentially activated macrophages orchestrate myogenic precursor cell fate during human skeletal muscle regeneration. *Stem Cells* 31, 384–396. doi:10.1002/stem.1288

Sambasivan, R., Yao, R., Kissenpfennig, A., Van Wittenberghe, L., Paldi, A., Gayraud-Morel, B., et al. (2011). Pax7-expressing satellite cells are indispensable for adult skeletal muscle regeneration. *Development* 138, 3647–3656. doi:10.1242/dev.067587

Sanes, J. R. (2003). The basement membrane/basal lamina of skeletal muscle. *J. Biol. Chem.* 278, 12601–12604. doi:10.1074/jbc.R200027200

Sanes, J. R., and Lichtman, J. W. (1999). Development of the vertebrate neuromuscular junction. *Annu. Rev. Neurosci.* 22, 389–442. doi:10.1146/annurev.neuro.22.1.389

Sastourne-Arrey, Q., Mathieu, M., Contreras, X., Monferran, S., Bourlier, V., Gil-Ortega, M., et al. (2023). Adipose tissue is a source of regenerative cells that augment the repair of skeletal muscle after injury. *Nat. Commun.* 14, 80. doi:10.1038/s41467-022-35524-7

Schmidt, M., Poser, C., Janster, C., and von Maltzahn, J. (2022). The hairpin region of WNT7A is sufficient for binding to the Frizzled7 receptor and to elicit signaling in myogenic cells. *Comput. Struct. Biotechnol. J.* 20, 6348–6359. doi:10.1016/j.csbj.2022.10.047

Schmidt, M., Poser, C., and von Maltzahn, J. (2020). Wnt7a counteracts cancer cachexia. *Mol. Ther. Oncolytics* 16, 134–146. doi:10.1016/j.omto.2019.12.011

Schmidt, M., Schuler, S. C., Huttner, S. S., von Eyss, B., and von Maltzahn, J. (2019). Adult stem cells at work: regenerating skeletal muscle. *Cell Mol. Life Sci.* 76, 2559–2570. doi:10.1007/s00018-019-03093-6

Schnoor, M., Cullen, P., Lorkowski, J., Stolle, K., Robenek, H., Troyer, D., et al. (2008). Production of type VI collagen by human macrophages: a new dimension in macrophage functional heterogeneity. *J. Immunol.* 180, 5707–5719. doi:10.4049/jimmunol.180.8.5707

Schuster-Gossler, K., Cordes, R., and Gossler, A. (2007). Premature myogenic differentiation and depletion of progenitor cells cause severe muscle hypotrophy in Delta1 mutants. *Proc. Natl. Acad. Sci. U. S. A.* 104, 537–542. doi:10.1073/pnas.0608281104

Schworer, S., Becker, F., Feller, C., Baig, A. H., Kober, U., Henze, H., et al. (2016). Epigenetic stress responses induce muscle stem-cell ageing by Hoxa9 developmental signals. *Nature* 540, 428–432. doi:10.1038/nature20603

Scrable, H., Cavenee, W., Ghavimi, F., Lovell, M., Morgan, K., and Sapienza, C. (1989). A model for embryonal rhabdomyosarcoma tumorigenesis that involves genome imprinting. *Proc. Natl. Acad. Sci. U. S. A.* 86, 7480–7484. doi:10.1073/pnas.86.19.7480

Sebire, N. J., and Malone, M. (2003). Myogenin and MyoD1 expression in paediatric rhabdomyosarcomas. *J. Clin. Pathol.* 56, 412–416. doi:10.1136/jcp.56.6.412

Senechal, C., Fujita, R., Jamet, S., Maiga, A., Dort, J., Orfi, Z., et al. (2022). The adhesion G-protein-coupled receptor Gpr116 is essential to maintain the skeletal muscle stem cell pool. *Cell Rep.* 41, 111645. doi:10.1016/j.celrep.2022.111645

Sethi, J. K., and Vidal-Puig, A. (2010). Wnt signalling and the control of cellular metabolism. *Biochem. J.* 427, 1–17. doi:10.1042/BJ20091866

Sharifi-Rad, M., Anil Kumar, N. V., Zucca, P., Varoni, E. M., Dini, L., Panzarini, E., et al. (2020). Lifestyle, oxidative stress, and antioxidants: back and forth in the pathophysiology of chronic diseases. *Front. Physiol.* 11, 694. doi:10.3389/fphys.2020.00694

Sharma, A., Oonthonpan, L., Sheldon, R. D., Rauckhorst, A. J., Zhu, Z., Tompkins, S. C., et al. (2019). Impaired skeletal muscle mitochondrial pyruvate uptake rewires glucose metabolism to drive whole-body leanness. *Elife* 8, e45873. doi:10.7554/eLife.45873

Shern, J. F., Chen, L., Chmielecki, J., Wei, J. S., Patidar, R., Rosenberg, M., et al. (2014). Comprehensive genomic analysis of rhabdomyosarcoma reveals a landscape of alterations affecting a common genetic axis in fusion-positive and fusion-negative tumors. *Cancer Discov.* 4, 216–231. doi:10.1158/2159-8290.CD-13-0639

Shirakawa, T., Toyono, T., Inoue, A., Matsubara, T., Kawamoto, T., and Kokabu, S. (2022). Factors regulating or regulated by myogenic regulatory factors in skeletal muscle stem cells. *Cells* 11, 1493. doi:10.3390/cells11091493

Singh, K., and Dilworth, F. J. (2013). Differential modulation of cell cycle progression distinguishes members of the myogenic regulatory factor family of transcription factors. *FEBS J.* 280, 3991–4003. doi:10.1111/febs.12188

Skapek, S. X., Ferrari, A., Gupta, A. A., Lupo, P. J., Butler, E., Shipley, J., et al. (2019). Rhabdomyosarcoma. *Nat. Rev. Dis. Prim.* 5, 1. doi:10.1038/s41572-018-0051-2

Soleimani, V. D., Punch, V. G., Kawabe, Y., Jones, A. E., Palidwor, G. A., Porter, C. J., et al. (2012). Transcriptional dominance of Pax7 in adult myogenesis is due to high-affinity recognition of homeodomain motifs. *Dev. Cell* 22, 1208–1220. doi:10.1016/j.devcel.2012.03.014

Sousa-Victor, P., Garcia-Prat, L., and Munoz-Canoves, P. (2018). New mechanisms driving muscle stem cell regenerative decline with aging. *Int. J. Dev. Biol.* 62, 583–590. doi:10.1387/ijdb.180041pm

Sousa-Victor, P., Gutarra, S., Garcia-Prat, L., Rodriguez-Ubreva, J., Ortet, L., Ruiz-Bonilla, V., et al. (2014). Geriatric muscle stem cells switch reversible quiescence into senescence. *Nature* 506, 316–321. doi:10.1038/nature13013

Stark, D. A., Karvas, R. M., Siegel, A. L., and Cornelison, D. D. (2011). Eph/ephrin interactions modulate muscle satellite cell motility and patterning. *Development* 138, 5279–5289. doi:10.1242/dev.068411

Stoveken, H. M., Hajduczok, A. G., Xu, L., and Tall, G. G. (2015). Adhesion G protein-coupled receptors are activated by exposure of a cryptic tethered agonist. *Proc. Natl. Acad. Sci. U. S. A.* 112, 6194–6199. doi:10.1073/pnas.1421785112

Stratton, M. R., Fisher, C., Gusterson, B. A., and Cooper, C. S. (1989). Detection of point mutations in N-ras and K-ras genes of human embryonal rhabdomyosarcomas using oligonucleotide probes and the polymerase chain reaction. *Cancer Res.* 49, 6324–6327.

Takada, Y., Ye, X., and Simon, S. (2007). The integrins. *Genome Biol.* 8, 215. doi:10.1186/gb-2007-8-5-215

Taylor, J. G. t., Cheuk, A. T., Tsang, P. S., Chung, J. Y., Song, Y. K., Desai, K., et al. (2009). Identification of FGFR4-activating mutations in human rhabdomyosarcomas that promote metastasis in xenotransplanted models. *J. Clin. Invest.* 119, 3395–3407. doi:10.1172/JCI39703

Taylor, L., Wankell, M., Saxena, P., McFarlane, C., and Hebbard, L. (2022). Cell adhesion an important determinant of myogenesis and satellite cell activity. *Biochim. Biophys. Acta Mol. Cell Res.* 1869, 119170. doi:10.1016/j.bbamcr.2021.119170

Tidball, J. G. (1995). Inflammatory cell response to acute muscle injury. *Med. Sci. Sports Exerc* 27, 1022–1032. doi:10.1249/00005768-199507000-00011

Tierney, M. T., Aydogdu, T., Sala, D., Malecova, B., Gatto, S., Puri, P. L., et al. (2014). STAT3 signaling controls satellite cell expansion and skeletal muscle repair. *Nat. Med.* 20, 1182–1186. doi:10.1038/nm.3656

Tintignac, L. A., Brenner, H. R., and Ruegg, M. A. (2015). Mechanisms regulating neuromuscular junction development and function and causes of muscle wasting. *Physiol. Rev.* 95, 809–852. doi:10.1152/physrev.00033.2014

Tonin, P. N., Scrable, H., Shimada, H., and Cavenee, W. K. (1991). Muscle-specific gene expression in rhabdomyosarcomas and stages of human fetal skeletal muscle development. *Cancer Res.* 51, 5100–5106.

Urciuolo, A., Quarta, M., Morbidoni, V., Gattazzo, F., Molon, S., Grumati, P., et al. (2013). Collagen VI regulates satellite cell self-renewal and muscle regeneration. *Nat. Commun.* 4, 1964. doi:10.1038/ncomms2964

Vasyutina, E., Lenhard, D. C., and Birchmeier, C. (2007a). Notch function in myogenesis. *Cell Cycle* 6, 1450–1453. doi:10.4161/cc.6.12.4372

Vasyutina, E., Lenhard, D. C., Wende, H., Erdmann, B., Epstein, J. A., and Birchmeier, C. (2007b). RBP-J (Rbpsuh) is essential to maintain muscle progenitor cells and to generate satellite cells. *Proc. Natl. Acad. Sci. U. S. A.* 104, 4443–4448. doi:10.1073/pnas.0610647104

Vasyutina, E., Stebler, J., Brand-Saberi, B., Schulz, S., Raz, E., and Birchmeier, C. (2005). CXCR4 and Gab1 cooperate to control the development of migrating muscle progenitor cells. *Genes Dev.* 19, 2187–2198. doi:10.1101/gad.346205

Verdijk, L. B., Koopman, R., Schaart, G., Meijer, K., Savelberg, H. H., and van Loon, L. J. (2007). Satellite cell content is specifically reduced in type II skeletal muscle fibers in the elderly. *Am. J. Physiol. Endocrinol. Metab.* 292, E151–E157. doi:10.1152/ajpendo.00278.2006

Vignaud, A., Hourde, C., Butler-Browne, G., and Ferry, A. (2007). Differential recovery of neuromuscular function after nerve/muscle injury induced by crude venom from Notechis scutatus, cardiotoxin from Naja atra and bupivacaine treatments in mice. *Neurosci. Res.* 58, 317–323. doi:10.1016/j.neures.2007.04.001

von Maltzahn, J. (2021). Regulation of muscle stem cell function. *Vitam. Horm.* 116, 295–311. doi:10.1016/bs.vh.2021.02.012

von Maltzahn, J., Bentzinger, C. F., and Rudnicki, M. A. (2011). Wnt7a-Fzd7 signalling directly activates the Akt/mTOR anabolic growth pathway in skeletal muscle. *Nat. Cell Biol.* 14, 186–191. doi:10.1038/ncb2404

von Maltzahn, J., Chang, N. C., Bentzinger, C. F., and Rudnicki, M. A. (2012). Wnt signaling in myogenesis. *Trends Cell Biol.* 22, 602–609. doi:10.1016/j.tcb.2012.07.008

von Maltzahn, J., Jones, A. E., Parks, R. J., and Rudnicki, M. A. (2013a). Pax7 is critical for the normal function of satellite cells in adult skeletal muscle. *Proc. Natl. Acad. Sci. U. S. A.* 110, 16474–16479. doi:10.1073/pnas.1307680110

von Maltzahn, J., Zinoviev, R., Chang, N. C., Bentzinger, C. F., and Rudnicki, M. A. (2013b). A truncated Wnt7a retains full biological activity in skeletal muscle. *Nat. Commun.* 4, 2869. doi:10.1038/ncomms3869

Wang, Y. X., Dumont, N. A., and Rudnicki, M. A. (2014). Muscle stem cells at a glance. *J. Cell Sci.* 127, 4543–4548. doi:10.1242/jcs.151209

Wang, Z., Grange, M., Wagner, T., Kho, A. L., Gautel, M., and Raunser, S. (2021). The molecular basis for sarcomere organization in vertebrate skeletal muscle. *Cell* 184, 2135–2150.e13. doi:10.1016/j.cell.2021.02.047

Webster, M. T., and Fan, C. M. (2013). c-MET regulates myoblast motility and myocyte fusion during adult skeletal muscle regeneration. *PLoS One* 8, e81757. doi:10.1371/journal.pone.0081757

Wei, Y., Qin, Q., Yan, C., Hayes, M. N., Garcia, S. P., Xi, H., et al. (2022). Single-cell analysis and functional characterization uncover the stem cell hierarchies and developmental origins of rhabdomyosarcoma. *Nat. Cancer* 3, 961–975. doi:10.1038/s43018-022-00414-w

Wen, Y., Bi, P., Liu, W., Asakura, A., Keller, C., and Kuang, S. (2012). Constitutive Notch activation upregulates Pax7 and promotes the self-renewal of skeletal muscle satellite cells. *Mol. Cell Biol.* 32, 2300–2311. doi:10.1128/MCB.06753-11

Willert, K., and Nusse, R. (2012). Wnt proteins. *Cold Spring Harb. Perspect. Biol.* 4, a007864. doi:10.1101/cshperspect.a007864

Wong, A., Garcia, S. M., Tamaki, S., Striedinger, K., Barruet, E., Hansen, S. L., et al. (2021). Satellite cell activation and retention of muscle regenerative potential after long-term denervation. *Stem Cells* 39, 331–344. doi:10.1002/stem.3316

Yamaguchi, M., Watanabe, Y., Ohtani, T., Uezumi, A., Mikami, N., Nakamura, M., et al. (2015). Calcitonin receptor signaling inhibits muscle stem cells from escaping the quiescent state and the niche. *Cell Rep.* 13, 302–314. doi:10.1016/j.celrep.2015.08.083

Yamamoto, M., Sakiyama, K., Kitamura, K., Yamamoto, Y., Takagi, T., Sekiya, S., et al. (2022). Development and regeneration of muscle, tendon, and myotendinous junctions in striated skeletal muscle. *Int. J. Mol. Sci.* 23, 3006. doi:10.3390/ijms23063006

Yartseva, V., Goldstein, L. D., Rodman, J., Kates, L., Chen, M. Z., Chen, Y. J., et al. (2020). Heterogeneity of satellite cells implicates DELTA1/NOTCH2 signaling in self-renewal. *Cell Rep.* 30, 1491–1503. doi:10.1016/j.celrep.2019.12.100

Yin, H., Price, F., and Rudnicki, M. A. (2013). Satellite cells and the muscle stem cell niche. *Physiol. Rev.* 93, 23–67. doi:10.1152/physrev.00043.2011

Yoshiko, A., Hioki, M., Kanehira, N., Shimaoka, K., Koike, T., Sakakibara, H., et al. (2017). Three-dimensional comparison of intramuscular fat content between young and old adults. *BMC Med. Imaging* 17, 12. doi:10.1186/s12880-017-0185-9

Yuan, B., and Ye, Q. (2021). Editorial: post-transcriptional and post-translational regulation of cancer metabolism. *Front. Cell Dev. Biol.* 9, 779157. doi:10.3389/fcell.2021.779157

Zhang, L., Kubota, M., Nakamura, A., Kaji, T., Seno, S., Uezumi, A., et al. (2021a). Dlk1 regulates quiescence in calcitonin receptor-mutant muscle stem cells. *Stem Cells* 39, 306–317. doi:10.1002/stem.3312

Zhang, L., Noguchi, Y. T., Nakayama, H., Kaji, T., Tsujikawa, K., Ikemoto-Uezumi, M., et al. (2019). The CalcR-PKA-yap1 Axis is critical for maintaining quiescence in muscle stem cells. *Cell Rep.* 29, 2154–2163. doi:10.1016/j.celrep.2019.10.057

Zhang, W., Liu, Y., and Zhang, H. (2021b). Extracellular matrix: an important regulator of cell functions and skeletal muscle development. *Cell Biosci.* 11, 65. doi:10.1186/s13578-021-00579-4

Zibat, A., Missiaglia, E., Rosenberger, A., Pritchard-Jones, K., Shipley, J., Hahn, H., et al. (2010). Activation of the hedgehog pathway confers a poor prognosis in embryonal and fusion gene-negative alveolar rhabdomyosarcoma. *Oncogene* 29, 6323–6330. doi:10.1038/onc.2010.368

Frontiers in
Molecular Neuroscience

Leading research into the brain's molecular structure, design and function

Part of the most cited neuroscience series, this journal explores and identifies key molecules underlying the structure, design and function of the brain across all levels.

Discover the latest Research Topics

See more →

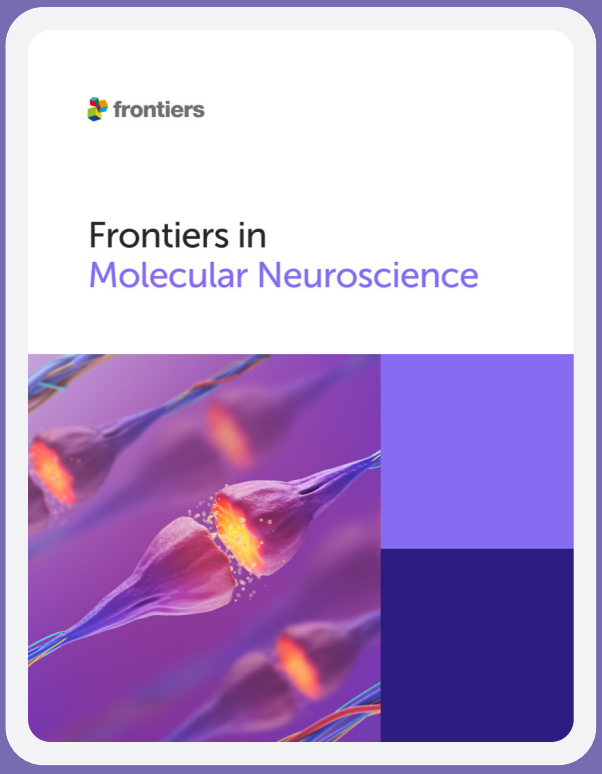

Frontiers

Avenue du Tribunal-Fédéral 34
1005 Lausanne, Switzerland
frontiersin.org

Contact us

+41 (0)21 510 17 00
frontiersin.org/about/contact